Copyright Warning & Restrictions

The copyright law of the United States (Title 17, United States Code) governs the making of photocopies or other reproductions of copyrighted material.

Under certain conditions specified in the law, libraries and archives are authorized to furnish a photocopy or other reproduction. One of these specified conditions is that the photocopy or reproduction is not to be "used for any purpose other than private study, scholarship, or research." If a, user makes a request for, or later uses, a photocopy or reproduction for purposes in excess of "fair use" that user may be liable for copyright infringement,

This institution reserves the right to refuse to accept a copying order if, in its judgment, fulfillment of the order would involve violation of copyright law.

Please Note: The author retains the copyright while the New Jersey Institute of Technology reserves the right to distribute this thesis or dissertation

Printing note: If you do not wish to print this page, then select "Pages from: first page # to: last page #" on the print dialog screen

ABSTRACT

REACTION MECHANISMS OF HYDROCARBON AND MERCURY SYSTEMS IN THE ATMOSPHERE AND IN COMBUSTION: A THEORETICAL STUDY OF THERMOCHEMICAL AND KINETIC PROPERTIES

by
Itsaso Auzmendi Murua

The continuing increase in the world population and the rapidly changing lifestyle and education of this population projects significant increases in energy requirements. Global warming is a worldwide major concern with a very serious potential stress on our climate threatening major changes to the environment. It is, without question, of major importance to improve the efficiency and optimize the current available combustion processes and fuel sources, to develop alternative fuels and to reduce the emissions of toxic pollutants.

The objective of this dissertation is to present thermochemical, kinetic and modeling results on two reference fuels (the land vehicle fuel isooctane and the jet fuel JP-10), on smaller cyclic alkanes and ethers, and on the oxidation of mercury by the addition of halogens, in atmospheric and combustion environments. As illustrated in the combustion models developed, a fundamental understanding of the processes can enable optimization, and lead to reductions in pollutant emissions.

Molecular geometries, vibration frequencies, internal rotor potentials and thermochemical properties ($\Delta_f H^o_{298,}$ S°(T) and $C°_p(T)$) are presented at different ab-initio, density functional theory (DFT) and composite calculation methods, with the use of several basis sets. Kinetic parameters are determined versus pressure and temperature for the chemically activated formation and unimolecular dissociation of the adducts, calculated via the use of multi-frequency quantum RRK analysis for the energy dependent rate constant with Master Equation analysis for fall off. The simulations for the determination of the

important reaction paths, identification of main products and determination of combustion characteristics at different process conditions are evaluated.

The thermochemical and kinetic properties developed during this work will aid in the optimization of the hydrocarbon fueled engine performance and other applications of the target fuels isooctane and JP-10. Thermochemical properties are developed for use in kinetics on oxidation and unimolecular dissociation of small cyclic alkanes and ethers for use in atmospheric and in combustion reaction mechanisms. Separately the understanding and developed kinetic and thermochemical parameters for mercury halides, and oxyhalides and the interactions of Hg and halides with NOx and SOx will help lead to a reduction of mercury emissions from power generating plants.

REACTION MECHANISMS OF HYDROCARBON AND MERCURY SYSTEMS IN THE ATMOSPHERE AND IN COMBUSTION: A THEORETICAL STUDY OF THERMOCHEMICAL AND KINETIC PROPERTIES

by
Itsaso Auzmendi Murua

A Dissertation
Submitted to the Faculty of
New Jersey Institute of Technology
in Partial Fulfillment of the Requirements for the Degree of
Doctor of Philosophy in Chemical Engineering

Otto H. York Department of
Chemical, Biological and Pharmaceutical Engineering

May 2013

.

APPROVAL PAGE

REACTION MECHANISMS OF HYDROCARBON AND MERCURY SYSTEMS IN THE ATMOSPHERE AND IN COMBUSTION: A THEORETICAL STUDY OF THERMOCHEMICAL AND KINETIC PROPERTIES

Itsaso Auzmendi Murua

Dr. Joseph W. Bozzelli, Dissertation Advisor — Date
Distinguished Professor of Chemistry and Environmental Science and Professor of Chemical Engineering, NJIT

Dr. Xianqin Wang, Committee Member — Date
Assistant Professor of Chemical Engineering, NJIT

Dr. Robert Barat, Committee Member — Date
Professor of Chemical Engineering, NJIT

Dr. Laurent Simon, Committee Member — Date
Associate Professor of Chemical Engineering, NJIT

Dr. Sumathy Raman, Committee Member — Date
Senior Researcher, Exxon Mobil, Annandale, NJ

.

BIOGRAPHICAL SKETCH

Author: Itsaso Auzmendi Murua

Degree: Doctor of Philosophy

Date: May 2013

Undergraduate and Graduate Education:

- Doctor of Philosophy in Chemical Engineering,
  New Jersey Institute of Technology, Newark, NJ, 2013

- Diploma in Chemical Engineering,
  University of the Basque Country, Bilbo, Spain, 2008
  Diploma Thesis: New Jersey Institute of Technology, Newark, NJ, 2008

Major: Chemical Engineering

Publications:

Itsaso Auzmendi-Murua, Sumit Charaya and Joseph W. Bozzelli, "Thermochemical properties of methyl substituted cyclic alkyl ethers and radicals for oxiranes, oxetanes and oxolanes: C–H bond energy trends with ring size and ether site" Journal of Physical Chemistry A, 117 (2): pp. 378-392, 2013.

Itsaso Auzmendi-Murua and Joseph W. Bozzelli, "Thermochemical properties and bond dissociation energies of C_3-C_5 cycloalkyl hydroperoxides and peroxy radicals: cycloalkyl radical + $^3O_2$ reaction thermochemistry," Journal of Physical Chemistry A, 116(28): pp. 7550-7563, 2012.

Itsaso Auzmendi-Murua, Jason M. Hudzik and Joseph W. Bozzelli, "Chemical activation of cyclic alkane and ether and tricyclodecane ring-opened diradicals with O_2: thermochemistry, reaction paths, kinetics," International Journal of Chemical Kinetics, 44(4): pp. 232-256, 2012.

Itsaso Auzmendi-Murua and Joseph W. Bozzelli, "Gas phase mercury conversion in H_2, O_2, chloro and bromo C_1-hydrocarbon and NO_x combustion effluent from use of an elementary kinetic mechanism," Combustion Science and Technology, 182: pp. 539-543, 2010.

Conferences:

Itsaso Auzmendi-Murua and Joseph W. Bozzelli, "Kinetic modeling of gas-phase mercury oxidation by halides (Cl, Br, I) in combustion effluents: importance of NOx and SOx," New Jersey Institute of Technology Dana Knox Student Research Showcase, Newark, NJ, 2013.

Itsaso Auzmendi-Murua, Alvaro Castillo and Joseph W. Bozzelli, "Study on density functional theory methods for the determination of mercury-halogen thermochemistry and kinetics," 245th American Chemistry Society National Meeting, New Orleans, LA, 2013.

Itsaso Auzmendi-Murua and Joseph W. Bozzelli, "Kinetic modeling of gas-phase mercury oxidation by halides (Cl, Br, I) in combustion effluents: importance of NOx and SOx," 245th American Chemistry Society National Meeting, New Orleans, LA, 2013.

Itsaso Auzmendi-Murua and Joseph W. Bozzelli, "Mercury oxidation via halogens (Cl, Br, I) under atmospheric conditions: thermochemistry and kinetics," 245th American Chemistry Society National Meeting, New Orleans, LA, 2013.

Itsaso Auzmendi-Murua and Joseph W. Bozzelli, "Thermochemical properties and bond dissociation energies of 3 – 5 member cyclic ether hydroperoxides and peroxy radicals: cyclic ether radical + $^3O_2$ reaction thermochemistry," 245th American Chemistry Society National Meeting, New Orleans, LA, 2013.

Itsaso Auzmendi-Murua and Joseph W. Bozzelli, "Thermochemistry and elementary reaction kinetic models for reactions of mercury with halogens, NOx and SOx: atmospheric and combustion environments," New Jersey Institute of Technology Chemical Engineering Department Seminar Session, Newark, NJ, 2013.

Itsaso Auzmendi-Murua and Joseph W. Bozzelli, "Kinetic modeling of gas-phase mercury oxidation by chlorine and bromine in combustion effluents during oxy-combustion," American Institute of Chemical Engineers Annual Meeting, Minneapolis, MN, 2011.

Itsaso Auzmendi-Murua, Suarwee Snitsiriwat and Joseph W. Bozzelli, "Thermochemistry, reaction paths and kinetics on the isooctane radical reactions with O_2: kinetic study at high pressures," American Institute of Chemical Engineers Annual Meeting, Minneapolis, MN, 2011.

Itsaso Auzmendi-Murua, Jason M. Hudzik and Joseph W. Bozzelli, "Chemical activation reaction of cyclic alkane ring-opened diradicals with molecular oxygen: Thermochemistry, reaction paths, kinetics," International Conference in Chemical Kinetics, Massachusetts Institute of Technology, Boston, MA, 2011.

Itsaso Auzmendi-Murua, Jason M. Hudzik and Joseph W. Bozzelli, "Chemical activation reaction of cyclic alkane ring-opened diradicals with molecular oxygen: thermochemistry, reaction paths, kinetics," 7th U.S. National Combustion Meeting, Georgia Institute of Technology, Atlanta, GA, 2011.

Itsaso Auzmendi-Murua and Joseph W. Bozzelli, "Kinetic modeling of gas-phase mercury oxidation by halides in combustion effluents: the importance of NOx," American Institute of Chemical Engineers Annual Meeting, Salt Lake City, UT, 2010.

Itsaso Auzmendi-Murua and Joseph W. Bozzelli, "Ambient temperature mercury oxidation thermochemistry and kinetics via chlorine and bromine," American Institute of Chemical Engineers Annual Meeting, Salt Lake City, UT, 2010.

Itsaso Auzmendi-Murua and Joseph W. Bozzelli, "Mercury (Hg^0) kinetics and reaction modeling with halogens under conditions of atmospheric chemistry and for removal of mercury from incinerator effluent: thermochemistry, oxidation with halogens, and effects of NO_x," New Jersey Institute of Technology Chemistry Department Seminar Session, Newark, NJ, 2010.

Itsaso Auzmendi-Murua and Joseph W. Bozzelli, "Kinetic modeling of gas-phase mercury oxidation by halides in combustion effluents: the importance of NO_x," 21st International Symposium on Gas Kinetics, Leuven, Belgium, 2010.

Itsaso Auzmendi-Murua and Joseph W. Bozzelli, "Detailed model for removal of mercury from incinerator effluent: oxidation with halogens and effects of NOx," New Jersey Institute of Technology Dana Knox Student Research Showcase, Newark, NJ, 2010.

Itsaso Auzmendi-Murua and Joseph W. Bozzelli, "Mercury oxidation thermochemistry and kinetics via chlorine and bromine under atmospheric conditions," Northeast Regional Meeting of the American Chemistry Society, Hartford, CT, 2009.

Itsaso Auzmendi-Murua and Joseph W. Bozzelli, "Elementary mechanism for gas phase mercury in H_2, O_2, mono chloro and bromo C_1 hydrocarbon, and chloro and bromo – NO_x combustion environments," Eastern States Section of the Combustion Institute, Fall Technical Meeting, University of Maryland, College Park, MD, 2009.

Itsaso Auzmendi-Murua and Joseph W. Bozzelli, "Elementary mechanism for gas phase mercury in H_2, O_2, mono chloro and bromo C_1 hydrocarbon, and chloro and bromo – NO_x combustion environments," 6th Mediterranean Combustion Meeting, Porticcio – Ajaccio, Corsica, France, 2009.

Itsaso Auzmendi-Murua and Joseph W. Bozzelli, "Gas phase mercury conversion in H_2, O_2, chloro and bromo C_1- hydrocarbon and NO_x combustion effluent from use of an elementary kinetic mechanism," 6th U.S. National Combustion Meeting, Ann Arbor, Michigan, 2009.

Itsaso Auzmendi-Murua and Joseph W. Bozzelli, "Study on gas phase mercury conversion in combustion flue (exit) environments," 61st Annual Research Conference of the Intercollegiate Council of the American Chemical Society Student Affiliate Chapters, North Jersey Section hosted by Fairleigh Dickinson University, Teaneck, NJ, 2009.

To my family,
amari, aitari, Lideri eta Ikerri,
for always giving me the strength, confidence, and support to adjust the sails

"The pessimist complains about the wind;
the optimist expects it to change;
the realist adjusts the sails."
William A. Ward

ACKNOWLEDGMENT

I would like to express my gratitude to my advisor, Prof. Joseph W. Bozzelli, for his guidance, supervision and patience, for sharing with me his knowledge and experience, and for always being so supportive.

I would also like to thank all the members in the Computational Chemistry Research Group: Dr. Rubik Asatryan, Dr. Alvaro Castillo, Anjani Gunturu, Jason Hudzik, Dr. Ponmile Oloyede, Suarwee Snitsiriwat, Suriyakit Yommee, and Heng Wang for all their help and friendliness during the five years that I have had the luck of being part of this group.

My sincere appreciation is extended to Prof. Barat, Prof. Simon, Prof. Wang, and Dr. Raman for serving on my committee.

I gratefully acknowledge all my American, Argentinian, Basque, Chinese, Finish, German, Indian, Italian, Iranian, Lebanese, Nigerian, Spanish, Swedish, Thai, and Turkish friends for making these five years unforgettable, not only for the academic knowledge acquired, but also for the personal growth experienced thanks to each of them. A special thanks to Gari, Julia and Olga, for being my family far from home.

I thank the Basque Government, for funding my studies in New Jersey Institute of Technology for the last four years.

Muchisimas gracias Iker por todo tu apoyo, porque incluso en la distancia, has sabido estar siempre a mi lado.

Azkenik, nere familiari eskerrik handienak, beraien deiekin, gutunekin eta bisitekin, beti nere ondoan egon izanagatik, eta nere buruan konfidantza edukitzen lagundu izanagatik, proiektu hau aurrera eramaten lagunduz.

TABLE OF CONTENTS

TABLE OF CONTENTS
(Continued)

TABLE OF CONTENTS
(Continued)

TABLE OF CONTENTS
(Continued)

Chapter **Page**

TABLE OF CONTENTS
(Continued)

LIST OF TABLES

LIST OF TABLES
(Continued)

LIST OF TABLES
(Continued)

LIST OF TABLES
(Continued)

LIST OF TABLES
(Continued)

Table **Page**

LIST OF TABLES
(Continued)

LIST OF TABLES
(Continued)

Table **Page**

LIST OF TABLES
(Continued)

LIST OF TABLES
(Continued)

Table **Page**

LIST OF SCHEMES

Table **Page**

LIST OF FIGURES

LIST OF FIGURES
(Continued)

Figure **Page**

LIST OF FIGURES
(Continued)

LIST OF FIGURES
(Continued)

Figure **Page**

LIST OF FIGURES
(Continued)

Figure **Page**

LIST OF FIGURES
(Continued)

Figure **Page**

LIST OF FIGURES
(Continued)

Figure **Page**

LIST OF FIGURES
(Continued)

Figure **Page**

LIST OF FIGURES
(Continued)

LIST OF FIGURES
(Continued)

Figure **Page**

LIST OF FIGURES
(Continued)

LIST OF SYMBOLS

$\Delta_f H^o_{298}$	Heat of formation
$\Delta_{rxn} H_{298}$	Heat of reaction
S^o	Standard entropy
Cp	Heat capacity
ΔG^o	Gibb's energy
T	Temperature
k_B	Boltzmann's constant
Ψ	Schrödinger wave functions
m	Mass
$V(x,y,z,t)$	Potential energy
E	Energy
$<S^2>$	Total spin
R	Gas constant
σ_i	Symmetry number
N_i	Number of molecules
D_i	Degeneracy
Q	Partition function
p_i	Number of discrete states
V	Volume
P	Pressure

LIST OF SYMBOLS

h	Planck's constant
n	Number of optical isomers
I	Moment of inertia
θ	Dihedral angle
k_f	Forward rate constant
k_r	Reverse rate constant
A	Pre-exponential Arrhenius factor
Ea	Activation Energy
ν	Frequency
r	Rate
K_c	Equilibrium constant
Z_{col}	Collision frequency
s	Number of oscillators
Y	Mass fraction
W	Molecular weight

CHAPTER 1

INTRODUCTION

Global demand for energy has increased in the last years due to the industrial development and the population growth. In 2010, the main sources of energy worldwide were oil (32.4%), coal (27.3%), natural gas (21.4%), biofuels/waste (10.0%), nuclear energy (5.7%) and hydro energy (2.3%). As a result of the decrease in the abundance of fossil fuels, and the increase in the regulations limiting the pollutants from combustion processes, it is significantly important to improve the efficiency of the available combustion processes, to develop alternative fuels, and to reduce the emissions of toxic pollutants produced in these combustion processes. In this context, there is an increased interest in developing a better understanding of the oxidation of large hydrocarbon fuels used in land vehicles and in aviation over a wide range of operating conditions, and of developing new technologies for the reduction of pollutants in the combustion flue gases.

The need of optimizing the combustion engines currently used in land vehicles has led to the development of the homogeneous charge compression ignition (HCCI) engines, which are considered as a promising engine for improved control of NOx and particulate emissions. In these engines, the autoignition process is strongly controlled by chemical kinetics of the peroxy radical chemistry, and therefore, it becomes important the construction of accurate models to describe the chemistry behind the auto-ignition behavior of different fuels. The accuracy of these models relies on the precision of thermochemical and kinetic properties of the reactant and intermediate species included in the model. The theoretical modeling and experimental studies for the development and

improvement of HCCI engines use isooctane (2,2,4- trimethylpentane) as one of the model fuel species, both as a neat fuel and as a major component in a primary reference fuel blend[1,2].

Apart from the importance of developing optimized fuels and combustion technologies for land vehicles, the current energy needs have led to the necessity of optimizing aircraft combustion processes, and of increasing the investigation and characterization of aviation fuels, as well as their combustion products. *Exo*-tricyclo[5.2.1.$0^{2,6}$]decane or *exo*-tetrahydrodicyclopentadiene (TCD, $C_{10}H_{16}$) is the principal component of the high-energy density hydrocarbon fuel commonly identified as JP-10. It is widely used in aircraft because of its appreciable density (0.94 g/cm^3), low freezing point (-79 °C) and the high volumetric energy content (39,434 MJ/m^3)[3]. The size and intricacy of the compound makes the analysis of its unimolecular decomposition and oxidation difficult. It is particularly advantageous to have an elementary reaction model for this fuel, because it is effectively, a single component fuel and its' chemical properties will not change from refinery to refinery as do other aviation and vehicle fuels. The model will be able to be improved, but it will not need to change for different fuel suppliers.

The determination of accurate thermochemical and kinetic properties of larger cyclic hydrocarbons such as TCD, requires to have very precise thermochemical and kinetic properties of the oxidation and unimolecular reactions of smaller cyclic alkanes. Recent studies have also shown that the formation of cyclic ethers is one of the main paths in the oxidation of hydrocarbons, such as isooctane[4], and in the oxidation of biomass derived alcohol fuels such as ethanol[5-92], propanol[5,10-17], butanol[5,17-29] and

pentanol[30-35]. Additionally, cyclic ethers can also be formed from atmospheric reactions of olefins and have also been linked to the formation of the secondary organic aerosol (SOA) in the atmosphere[36,37]. Current combustion mechanisms include the paths for the formation of the cyclic alkanes and ethers[38-45]. However, the oxidation and unimolecular dissociation reactions of these small cyclic alkanes are not currently included in the combustion reaction mechanisms. Therefore, it is of great importance both for combustion and atmospheric environments the determination of accurate thermochemical and kinetic properties of the oxidation and unimolecular dissociation of small cyclic alkanes and ethers.

As important as the above discussed optimization of the fuels currently used in the combustion processes, is the reduction of toxic emissions produced during these processes. The increase in the regulations limiting the pollutants from combustion processes has led to the need of optimizing the current air pollution control devices (APCD) available in electricity generating plants, and of developing new technologies for the reduction of the emissions to the atmosphere. Mercury emissions, $Hg^{o}(g)$, have become during the last years one of the major concerns for power generation, coal burning and incineration plants. Although mercury is present in coal and municipal solid wastes in only minute amounts, in the order of 0.1 ppm_w[46], 458.6 tons of mercury are emitted worldwide each year from power generating plants[47]. Once mercury is deposited on land or water, it can suffer several transformation reactions, ending up as methylmercury, CH_3Hg^+, (also dimethyl-mercury), an organic form of mercury, which is a potent neurotoxin[48,49]. Methylmercury in surface waters gets into the aquatic food chain and becomes stored in fish and shellfish muscle tissue, entering the human food chain

through fish consumption. Methylmercury is among the most highly bio-concentrated trace metals in the human food chain[50], and can cause damaging effects on the nervous system, toxicity to the kidneys, loss of hearing and abnormal behavior depending on the level of exposure[50]. Elemental mercury has been also observed to decrease along with the ozone in the Antarctic and Arctic early spring ozone hole events and its chemistry may be related to reactions with halogens and halogen oxides (e.g., Cl and ClO_x radicals)[51,52]. The study of the oxidation of mercury by halogens contributes to understand both the chemistry of its oxidation at atmospheric and combustion conditions.

Mercury can be present in the combustion flue gases as elemental mercury (Hg^o), oxidized mercury (Hg^{2+}), and mercury associated to particles (Hg_p). Elementary mercury is highly volatile, and it is not possible to eliminate it by using the usual air pollution control devices (scrubbers, electrostatic precipitators, fabric bags…). However, the oxidized mercury is water soluble, and has the tendency to associate to particles, and therefore, it can be eliminated by the pollutant control devices. Different techniques have been proposed for the elimination of mercury from the combustion flue gases, such as the addition of activated carbon, mercury control by corona discharge, and electro-catalytic oxidation technologies. The approach proposed in this work is the addition of halogens (chlorine, bromine and iodine) to the combustion gases, so that the elemental mercury (Hg^o) can be converted into the oxidized mercury ($HgCl_2$, $HgBr_2$, HgI_2), and therefore removed by the APCD.

During the last years, different attempts have been presented for the simultaneous elimination of mercury and NOx from combustion flue gases. One of the suggested solutions for the reduction of NOx emissions is oxicombustion, where the combustion is

performed with an oxidizer rich in O_2, instead of using air, and therefore reducing significantly the addition of N_2 into the system, and consequently also reducing the formation of NOx. Additionally, new technologies are being developed in the last years to reduce the SOx emissions, such as the removal of sulfur from coal and natural gas before burning it, and wet, dry and flue gas desulfurization (FGD) technologies[53]. However, not many studies have focused on determining the influence of the reduction of NOx and SOx emissions in the conversion of mercury by the addition of halogens.

The objective of this dissertation is to present thermochemical, kinetic and modeling results on two reference fuels (the land vehicle fuel isooctane and the jet fuel TCD), on smaller cyclic alkanes and ethers, and on the oxidation of mercury by halogens, in atmospheric and combustion environments.

CHAPTER 2

METHODOLOGY – THEORETICAL BACKGROUND

In Chapter 2, a detailed description of the calculation methods followed to compute the thermochemical and kinetic properties, as well as the procedures followed for the combustion chemistry modeling are presented.

2.1 Thermochemical Properties

The modeling of combustion processes requires accurate thermochemical property data - heats of formation ($\Delta_f H^o_{298}$), entropy (S^o) and heat capacities (Cp) as a function of temperature - for reactants, intermediates, final products and reaction transition states. These data allow the determination of the forward and reverse rate constants. Quantum chemical calculations provide the opportunity to accurately calculate these thermochemical properties.

2.1.1 Quantum Mechanics & Statistical Mechanics

Computational quantum mechanics calculations are used to obtain quantum mechanical energies for the target molecules. The electronic structure theory (quantum mechanics) is used to calculate molecular properties such as the energy of the molecular structure (spatial arrangement of atom or nuclei and electrons), energies and structure of transition states, molecular geometries, vibrational frequencies, rotational frequencies and moments of inertia. Quantum mechanical energies are based on 0 K electronic structures, which give quantized values of the energy and partition functions. To get other properties, and properties at other temperatures, statistical mechanics are needed.

Heisenberg's uncertainty principle indicates that the measurement changes the state of the system. In classical mechanics (macroscopic particles), the present state can be used to predict the future state of a system, by specifying all the forces acting on the system, the positions and the velocities. However, in quantum mechanics, it is possible to identify the probabilities and postulate the energy levels of particles, but it is not possible to exactly predict the future state of a quantum mechanical system.

Schrödinger communicated in four papers published in the first half of 1926, his wave equation and applied it to a number of problems (the hydrogen atom, the harmonic oscillator, the rigid rotator, the diatomic molecule, the hydrogen atom in an electric field). The wave equation enables to determine certain functions (Ψ) of the coordinates of a system and the time (Ψ = Schrödinger wave functions or probability amplitude functions). The wave function is a function of the particle's coordinates, and from that input, the state of the system can be deduced. The time dependent Schrödinger's wave function is:

$$-\frac{h^2}{8\pi^2 m}\left(\frac{\partial^2\Psi}{\partial x^2}+\frac{\partial^2\Psi}{\partial y^2}+\frac{\partial^2\Psi}{\partial z^2}\right)+V\Psi=-\frac{h}{2\pi i}\frac{\partial\Psi}{\partial t} \qquad (2.1)$$

where *m* is the mass of the particle, *h* is Planck's constant, $V(=V(x,y,z,t))$ is the potential energy of the system, $-\frac{h^2}{8\pi^2 m}\left(\frac{\partial^2\Psi}{\partial x^2}+\frac{\partial^2\Psi}{\partial y^2}+\frac{\partial^2\Psi}{\partial z^2}\right)$ is the kinetic energy term, and $V\Psi(=V(x,y,z,t)\Psi(x,y,z,t))$ is the potential energy term.

The equation gets simplified for a one dimensional system:

$$-\frac{h^2}{8\pi^2 m}\left(\frac{\partial^2\Psi(x,t)}{\partial x^2}\right)+V\Psi=-\frac{h}{2\pi i}\frac{\partial\Psi(x,t)}{\partial t} \qquad (2.2)$$

Given the initial state of the system (at time t_o), the partial derivative on the right hand side of the equation allow calculating the future state (wave function, Ψ).

The *x* coordinate cannot be specified using the wave function, but the wave function allows to determine the probability of finding the particle in a particular region of the *x* axis, since the square of the absolute value of a given wave function ($|\Psi|^2$) represents the probability distribution function (probability density) for the coordinates of the system in the state represented by the wave function, and $|\Psi|^2 dx$ is the probability.

The most common situation is a stationary state, where the state of the system is not changing with time. For this case, it is needed that the potential energy (*V*) is only a function of position (*V=V(x)*). The time dependent wave function can be defined as:

$$\Psi(x,t) = f(t)\psi(x) \tag{2.3}$$

$$\frac{\partial^2 \Psi(x,t)}{\partial x^2} = f(t)\frac{\partial^2 \psi(x,t)}{\partial x^2} \tag{2.4}$$

$$-\frac{h^2}{8\pi^2 m}\left(f(t)\frac{d^2\psi(x)}{dx^2}\right) + V(x) f(t)\psi(x) = -\frac{h}{2\pi i}\psi(x)\frac{\partial f(t)}{\partial t} \tag{2.5}$$

Rearranging:

$$-\frac{h^2}{8\pi^2 m}\frac{1}{\psi(x)}\left(f(t)\frac{d^2\psi(x)}{dx^2}\right) + V(x) = -\frac{h}{2\pi i}\frac{1}{f(t)}\frac{\partial f(t)}{\partial t} \tag{2.6}$$

Since the right hand side contains only functions dependent on time, and the left hand side contains only functions dependent on position, the only solution for the equation is that both sides are equal to a constant. This constant is defined as energy, *E*.

$$E = -\frac{h}{2\pi i}\frac{1}{f(t)}\frac{\partial f(t)}{\partial t} \tag{2.7}$$

$$E = -\frac{h^2}{8\pi^2 m}\frac{1}{\psi(x)}\left(\frac{d^2\psi(x)}{dx^2}\right) + V(x) \tag{2.8}$$

Therefore, the time independent Schrödinger's wave function is:

$$E\psi(x) = -\frac{h^2}{8\pi^2 m}\frac{d^2\psi(x)}{dx^2} + V(x)\psi(x) \tag{2.9}$$

The wave function requires three coordinates, or three quantum numbers, to describe the orbitals in which electrons can be found. The three coordinates that come from Schrödinger's wave equations are the principal (*n*), angular (*l*), and magnetic (*m*) quantum numbers. These quantum numbers describe the size, shape, and orientation in space of the orbitals on an atom. The principal quantum number (*n*) describes the size of the orbital. The angular quantum number (*l*) describes the shape of the orbital, and the magnetic quantum number (*m*), describes the orientation in space of a particular orbital.

The Schrödinger's equation can be solved exactly only for one electron atoms (H, He^+). For more complex systems (i.e., many electron atoms/molecules), some simplifying assumptions/approximations are needed.

2.1.2 Theoretical Methods and Basis Sets

The systems involving more than one electron require assumptions in order to obtain an approximate solution of the Schrödinger's equation. There are several different approaches for the determination of the electronic structures of the target molecules.

- *Ab initio methods* (from first principles): seek to derive a solution for the Schrödinger wave equation for the molecular system without parametrization (they use no experimental parameters in their computations). Their computations are based solely on the laws of quantum mechanics, on the values of a small number of physical constants (speed of light, masses and charges of electrons and

nuclei, Planck's constant), and a series of rigorous mathematical approximations. Some examples are: Hartree-Fock (Hartree-Fock, Restricted Open-Shell Hartree-Fock, Unrestricted Hartree-Fock), Post-Hartree-Fock (Møler-Plesset perturbation theory, Configuration Interaction, Coupled Cluster, Quadratic Configuration Interaction), and Multireference Methods.

- *Semi-empirical methods*: are based on the Hartree Forck (HF) formalism, but use many parameters derived from experimental data to simplify the computation. They solve an approximate form of the Schrödinger's equation that depends on having appropriate parameters available for the type of chemical system in question. It is very useful for the treatment of large molecules, where the full HF method without parametrization is too expensive. Some examples are: AM1, PM3 and MINDO/3.

- *Density Functional Theory (DFT) methods*: derives the properties of a many-electron system by using functionals (functions of another function, which in this case is the spatially dependent electron density, a physical characteristic of all molecules). Some examples are: B3LYP, M06-2X and B2PLYP.

- *Quantum Chemistry Composite methods*: combine methods with a high level of theory and a small basis set with methods that employ lower levels of theory with larger basis sets. Some examples are: G1, G2, G3, G3MP2B3 and CBS-QB3.

Basis sets are a set of functionals which are combined in linear combinations to create molecular orbitals. Most electronic structure theory calculations use linear combinations of Gaussian Type Orbital (GTO) functions, because they are the most efficient computationally (Slater Type Orbitals, STO, are computationally expensive).The main different types of basis-sets are:

- Pople-Style Basis Sets (X-YZG).

- Correlation-Consistent Basis Sets (cc-pVnZ): designed so that they have the unique property of forming a systematically convergent set. Calculations with a series of correlation consistent (cc) basis sets can lead to accurate estimates of the Complete Basis Set (CBS) limit.

2.1.2.1 Theoretical Methods used in this Study

- *B3LYP:* combines the three parameter Becke exchange functional, B3, with Lee-Yang- Parr's correlation functional, LYP[54], it is based on the Density Functional Theory.

- *B97-1:* a significant advance in Density Functional Theory was made in 1997 by Becke, who proposed to model exchange correlation functionals by a systematic procedure, and developed the B97 method. B97-1 was a modification by Hamprecht et al. and showed that the geometries calculated, including the geometries of a set of transition metal compounds, were improved over the BLYP functional[55].

- *BMK:* Boese and Martin's[56] τ-dependent hybrid Density Functional Theory based method. The method is rated highly in evaluations for both thermochemistry and barrier accuracy.

- *B1B95:* hybrid Density Functional Theory method, which employs Becke's exchange correlation functional[57]. It shows accurate thermochemistry in the G2 benchmarks of Pople et al.[58].

- *ωB97X:* long-range corrected (LC) hybrid functional developed by Chai et al. [59], which includes the short-range (SR) Hartree-Forck (HF) exchange.

- *B2PLYP:* based on a mixing of standard generalized gradient approximations (GGAs) for exchange by Becke (B) and for correlation by Lee, Yang, and Parr (LYP) with Hartree-Fock (HF) exchange and a perturbative second-order correlation part (PT2) that is obtained from the Kohn-Sham orbitals and eigenvalues[60].

- *M06:* hybrid meta exchange correlation functional, parametrized including both transition metals and nonmetals derived by Truhlar et al.[61].

- *M06-2X:* hybrid meta exchange correlation functional, it is a high nonlocality functional with double the amount of nonlocal exchange (2X), and it is parametrized only for nonmetals[61].

- *CBS-QB3 (Complete Basis Set):* multilevel chemistry model that predicts molecular energies with high accuracy and relatively low computational cost. It combines the results of several *ab initio* and Density Functional Theory individual methods and empirical correction terms to predict molecular energies with high accuracy and relatively low computational cost. It is based on B3LYP/CBSB7 calculations for the geometry optimization and frequencies, followed by a single point energy calculation at the CCSD(T)/6-31g+(d') and MP4SDQ/CBSB4 level of theory. It includes a total energy extrapolation to the infinite basis-set limit using pair natural-orbital energies at the MP2/CBSB3 level, and an additive correction at the CCSD(T) level of theory.

- *G3MP2B3 (G3MP2//B3LYP/6-31g(d)):* it is a variation of the Gaussian-3 (G3) method, that uses geometries and zero-point vibrational energy (ZPVE) scaled by unrestricted B3LYP/6-31g(d) calculations. The geometry optimization is followed by a series of high-level QCISD(T,FC)/6-31G(d) and MP2(FC)/G3MP2 large single point calculations.

- *CCSD(T):* coupled-cluster method that includes singles and doubles fully[62-65], and triples are calculated non-iteratively[66]. It uses basic Hartree–Fock molecular orbital method and constructs multi-electron wavefunctions using the exponential cluster operator to account for electron correlation (electron-electron interaction).

- *QCISD:* Quadratic Configuration Interaction (CI) calculation, including single and double substitutions[66].

2.1.2.2 Basis Sets used in this Study

- *6-31G(d,p) and 6-31G(2d,2p):* 6-31G is a split valence basis, where the core orbitals are a contraction of 6 primary Gaussian Type Orbitals (GTO), the inner part of the valence orbitals is a construction of 3 GTOs and the outer part of the valence represented by 1 GTO. The basis sets are polarized (split basis sets allow orbitals to change size, but not to change shape, and polarized basis sets remove this limitation). 6-31G(d,p) has a "d" set of polarization on heavy atoms, and a "p" set of polarization on hydrogen, whereas 6-31G(2d,2p) has "2d" sets of polarization on heavy atoms, and "2p" sets of polarization on hydrogen.

- *LANL2DZ:* includes the Los Alamos National Laboratory's Double Zeta (ζ) Effective Core Potential (ECP) for the sodium through bismuth elements, developed by Hay and Wadt[67]. The Douple Zeta means that the basis sets uses double the number of all basis functions. Effective Core Potentials (ECP, Pseudopotentials) are a useful means of replacing the core electrons in a calculation with an effective potential, thereby eliminating the need for the core basis functions, which usually require a large set of Gaussians to describe them.

- *SDD:* includes a Stuttgart/Dresden Double Zeta (ζ) Effective Core Potential (ECP) for the remainder of the elements after the first row[68-70].

- *Aug-cc-pVTZ-PP (AVTZ):* Augmented Correlation Consistent polarized valance only (V) basis set of Triple-Zeta (ζ) quality. It includes the use of small-core relativistic pseudopotentials (PP) for the inner electrons (in this work, Hg, Br and I). Developed by Peterson et al. for mercury[71].

2.1.2.3 Software used – Gaussian 03/09

All quantum chemical calculations have been performed within the Gaussian-03[72] and 09[73] software package.

2.1.3 Internal Rotational Potential

Conformational isomerism (rotational conformers) is a form of stereoisomerism in which the isomers can be interconverted exclusively by rotations about formally single bonds. The lowest energy conformer is the most stable, and therefore its identification becomes important for the determination of the thermochemical properties of the lowest energy conformer. In this work, rotational conformers related to the peroxide groups (R—OOH and RO—OH rotors), alkoxy groups (R—OH) and methyl groups (R—CH_3) are studied to determine the lowest energy conformer and to use the internal rotor potential for calculation of entropy and heat capacity contributions. Energy profiles for internal rotations were calculated to determine energies of the rotational conformers and interconversion barriers; these energy profiles allow calculation of contributions to entropy and heat capacity for the internal rotors. For internal rotor potentials, total energies as a function of the dihedral angles were computed at the B3LYP/6-31G(d,p) level of theory by scanning the torsion angles between 0^o and 360^o in steps of 10^o, while all remaining coordinates were fully optimized. All potentials are re-scanned when a lower energy conformer was found, relative to the initial low energy conformer, until the lowest energy conformer is found. The total energy corresponding to the most stable molecular conformer is set to zero and used as a reference point to plot the potential barriers. The most stable conformation of the molecular specie is used for the determination of the heat of formation, entropy and heat capacity of each of the species.

2.1.4 Work Reactions

Work reactions are hypothetical reactions used as a tool for the determination of the heats of formation of the target molecules. There are different methods available for the determination of the heat of formation of a given molecule:

- *Atomization reaction:* uses calculated values of $\Delta_f H^o$ of the atoms and the molecule at 0 K, experimental values of $\Delta_f H^o$ of the atoms at 0 K, thermal corrections (at 298 K) for the atoms from experiments, and thermal corrections for the molecule from the calculation.
- *Isodesmic reaction:* number of bonds of each given formal type is conserved, but the relationship among the bonds is altered. These reaction schemes help in the cancellation of systematic errors that arise in quantum chemical calculations due to the incomplete capture of the electron correlation energy[74,75].
- *Homodesmic reaction:* a subclass of isodesmic reactions, in which reactants and products contain equal numbers of carbon atoms in corresponding states of hybridization, and there is matching of the carbon-hydrogen bonds in terms of the number of hydrogen atoms joined to the individual carbon atoms.
- *Isogyric reaction:* a reaction in which the number of electron pairs is conserved.
- *Isogeitonic:* a reaction in which the groups are conserved.

Throughout this work, *isodesmic work reactions* are used for the determination of heats of formation. Each of the species is optimized at the selected level of theory, and the energy obtained is used to calculate the heat of reaction of the work reaction ($\Delta_{rxn}H_{298} = \Sigma E_{products} - \Sigma E_{reactants}$). The calculated heat of reaction of each work reaction ($\Delta_{rxn}H_{298}$) is used to calculate the heat of formation ($\Delta_f H^o_{298}$) of the target molecules ($\Delta_{rxn}H_{298} = \Sigma\Delta_f H^o_{298,products} - \Sigma\Delta_f H^o_{298,reactants}$), where the two products and one reactant are the reference molecules that have known, evaluated heats of formation from literature.

Take as an example the work reaction below, to determine the heat of formation

of the target molecule A, where B, C, and D are reference species:

$$\underset{\boldsymbol{\Delta_f H^o_{298,Target}}}{\boldsymbol{A}} + \underset{\Delta_f H^o_{298,B}}{B} \rightarrow \underset{\Delta_f H^o_{298,C}}{C} + \underset{\Delta_f H^o_{298,D}}{D}$$

The absolute enthalpy for each species in the work reaction (species A, B, C, and D) is calculated at a given level of theory in Gaussian and the heat of reaction, $\Delta_{rxn}H^o_{298}$, is calculated. Literature values for enthalpies of formation of the three reference compounds ($\Delta_f H^o_{298,B}$, $\Delta_f H^o_{298,C}$ and $\Delta_f H^o_{298,D}$) are used with the $\Delta_{rxn}H°_{298}$ to obtain the enthalpy of formation of the target molecule, $\boldsymbol{\Delta_f H^o_{298,Target}}$.

$$\Delta_{rxn}H°_{298\ \mathbf{calc}} = [(\text{energy C}) + (\text{energy D}) - (\text{energy B}) - (\text{energy A})] \times 627.51\ (\text{kcal/hartrees})$$

Using the calculated $\Delta_{rxn}H°_{298}$ and reference species to find the heat of formation of the target molecule:

$$\Delta_{rxn}H°_{298\ \mathbf{calc}} = (\Delta_f H^o_{298,C}) + (\Delta_f H^o_{298,D}) - (\Delta_f H^o_{298,B}) - \boldsymbol{(\Delta_f H^o_{298,A})}$$

The diradicals in the study were treated additionally, in order to account for the spin correction, by applying the spin-projection method developed by Yamaguchi et al.[76]. It is assumed that the singlet energy contamination arises only by the first higher multiplicity state. In most cases, the wavefunction for an open shell singlet is contaminated with a triplet, and therefore, the spin contamination has to be treated. The correction applied for the triplets is the following

$$\Psi_{(UB)} = c_S^1\phi + c_T^3\phi \tag{2.10}$$

$${}^1E_{(SC)} = {}^1E_{(UB)} + f_{SC}\left[{}^1E_{(UB)} - {}^3E_{(UB)}\right] \tag{2.11}$$

$$f_{SC} = \frac{{c_T}^2}{1-{c_S}^2} \approx \frac{{}^1\langle S^2\rangle}{{}^3\langle S^2\rangle - {}^1\langle S^2\rangle} \tag{2.12}$$

where $E_{(UB)}$ stands for the energy of an unrestricted B3LYP calculation, $E_{(SC)}$ for spin corrected energy, $<S^2>$ for the total spin of the diradical, and f_{SC} for factor of spin correction. If there is no contamination, $<S^2>$ should be s(s+1), where "s" is 1/2 times the number of unpaired electrons (0.75 for radicals, 2 for triplets and 0 for singlets). The energy of the contaminated singlet ($^1E_{(UB)}$) is corrected by adding the difference between the energy of the singlet and its corresponding triplet ($^1E_{(UB)}$-$^3E_{(UB)}$), multiplied by a correction factor (f_{SC}), which describes the degree of contamination of the singlet by the triplet. The correction factor is estimated from the spin values ($<S^2>$) of both the triplet and the singlet as shown in equation (2.12). The procedure followed for accounting for the spin contamination, involves optimizing the singlet and triplet diradicals and getting the corrections for temperature and enthalpies by a frequency calculation. From these calculations $^1E_{(UB)}$ (energy of the singlet), $^3E_{(UB)}$ (energy of the triplet), $^1<S^2>$ (total spin for the singlet, contaminated by the triplet) and $^3<S^2>$ (total spin of the triplet) are obtained. From equation (2.12) the correction factor is calculated, and from there the spin corrected energy of the singlet diradical, $^1E_{(SC)}$.

2.1.5 Bond Dissociation Enthalpies (BDE)

The bond dissociation enthalpies reflect the corresponding radical's stability and are used to estimate kinetics, and to determine heats of reaction for abstraction, elimination, beta scission and decomposition reactions. The C—H, R-OO—H, R-O—OH, R-O—H and C—C bond dissociation enthalpies are important in combustion modeling, in order to identify the unimolecular initiation and propagation reaction paths for each of the molecular species. The C—C bond dissociation enthalpies are very important for cyclic species, in order to determine whether the unimolecular dissociation reactions through

hydrogen abstraction or ring opening, or the oxidation with molecular oxygen $^3O_2$ will be the most important reaction paths.

Throughout this work, bond dissociation enthalpies are reported from the calculated heat of reaction ($\Delta_{rxn}H_{298}$) of the parent molecule and their radical corresponding to loss of H$^\bullet$, or $^\bullet$OH, where the enthalpies of parent molecule and product species are calculated in this study in conjunction with the value of 52.10 kcal mol^{-1} for H$^\bullet$ and 8.9 kcal mol^{-1} for $^\bullet$OH; the data correspond to the standard temperature at 298 K.

2.1.6 Population Analysis

The influence of the conformers to the heat of formation is determined through the population analysis. The rotational analysis identifies the different conformers for each of the species and the difference in energy between the lowest energy conformer and the rest of the conformers is determined. The Boltzmann distribution is applied to determine the fraction of each of the conformers at each temperature:

$$N_i = e^{-\Delta G_i/RT} \tag{2.13}$$

$$\Delta G_i = \Delta E_i + RT\ln(\sigma_i) \tag{2.14}$$

where ΔG_i is the Gibbs free energy, R is the gas constant, T is the absolute temperature, σ_i is the symmetry number,[83] and ΔE_i represents the difference between the energy of the conformer studied and the lowest energy configuration of the molecule:

$$\Delta E_i = E_i - E_{low} \tag{2.15}$$

The fraction is normalized to 1, including the lowest conformer, to determine the total fraction:

$$\frac{N_i}{N_{tot}} = \frac{D_i e^{-\Delta G_i/RT}}{\sum_{k=1}^{N_{conf}} D_k e^{-\Delta G_k/RT}} \tag{2.16}$$

$$\frac{N_i}{N_{tot}} = \frac{D_i e^{-(\Delta E_i + RT\ln(\sigma_i))/RT}}{\sum_{k=1}^{N_{conf}} D_k e^{-(\Delta E_k + RT\ln(\sigma_k))/RT}} = \frac{D_i e^{-\Delta E_i/RT} e^{-\ln(\sigma_i)}}{\sum_{k=1}^{N_{conf}} D_k e^{-\Delta E_k/RT} e^{-\ln(\sigma_k)}} \tag{2.17}$$

Assuming that all the conformers have the same symmetry:

$$\frac{N_i}{N_{tot}} = \frac{e^{-\ln(\sigma_i)} D_i e^{-\Delta E_i/RT}}{e^{-\ln(\sigma_i)} \sum_{k=1}^{N_{conf}} D_k e^{-\Delta E_k/RT}} = \frac{D_i e^{-\Delta E_i/RT}}{\sum_{k=1}^{N_{conf}} D_k e^{-\Delta E_k/RT}} \tag{2.18}$$

where N_i is the number of molecules in the ith conformation, N_{total} is the total number of molecules, N_{conf} is the number of conformations, D_i and D_k are the degeneracies of the ith and kth conformers, R is the gas constant, and T is the absolute temperature. The energy contribution of each of the conformers is calculated accounting for the calculated fraction and the value of the heat of formation of the lowest energy conformer at each temperature:

$$E_i(T) = \frac{N_i}{N_{tot}} \left[\Delta H_{f,lowest}(T) + \Delta E_i \right] \tag{2.19}$$

$$\Delta H_f(T) = \sum E_i(T) \tag{2.20}$$

The determination of the heat of formation of the lowest energy conformer at each of the temperatures follows the approach described below:

$$\mathbf{\Delta_f H^o, C_nH_mO_k\ (T)} = \Delta_f H^o_{,C_nH_mO_k}\ (298\ K) + [H\ (T) - H\ (298\ K)]_{C_nH_mO_k}$$

$$- n[H\ (T) - H\ (298\ K)]_C - m[H\ (T) - H\ (298\ K)]_{H_2} - k[H\ (T) - H\ (298\ K)]_{O_2}$$

where *[H (T) - H (298 K)]* for H_2, O_2 and C are added in order to account for the change in their heat capacity with temperature. These values have been obtained from the JANAF Thermochemical Tables[77]. *[H (T) - H (298 K)]*$_{C_nH_mO_k}$ values are obtained from the structural geometry of the molecule, calculated by SMCPS (see Section 2.1.7 below).

The rotational analysis of the studied species allows the identification of the different conformers (A, B, C…) and the difference in energy between the lowest energy conformer and the rest of the conformers is determined.

The isodesmic reactions provide the enthalpy of formation of the lowest energy configuration, and the rotor analysis provides the difference in energy of each of the other conformers with the lowest energy conformer.

2.1.7 Entropy and Heat Capacity

The entropy and heat capacity are derived from statistical mechanics principals[82]. The molar partition function (*Q*) for an assembly of identical molecules is:

$$Q = \sum_i p_i e^{-E_i/RT} \tag{2.21}$$

where p_i is the number of discrete states of the molecules which have the energy E_i in a system at thermal equilibrium *T* and volume *V*. For ideal gases the partition function can be factored into a product of partition functions for each of the degrees of freedom of the system. They have *3N* degrees of freedom, where *N* is the number of atoms in the molecule, ion, or radical; 3 translational degrees of freedom, 0 (for atoms), 2 (for linear molecules) or 3 (for non-linear molecules) rotational degrees of freedom, and the reminder internal vibrational degrees of freedom[82].

$$Q = Q_{trans} x Q_{rot} x Q_{vib} x Q_{elec} \tag{2.22}$$

Each of the thermodynamic properties depend on the logarithm or logarithmic derivative of the partition function and will thus receive additive contributions from each of the degrees of freedom[82]. The entropy calculation accounts for the contribution from the translations (S_{tran}), vibrations (S_{vib}), internal rotors ($S_{int,rot}$), hindered rotors ($S_{hind,rot}$), electronic contributions (S_{elec}), and the contribution of the optical isomers ($S_{opt,iso}$). The heat of capacity calculation accounts for the contribution from the translations ($C_{v,tran}$), vibrations ($C_{v,vib}$), internal rotors ($C_{v,rot}$), hindered rotors ($C_{v,hind,rot}$), and the electronic contributions ($C_{v,elec}$). The contribution of hindered rotors to the entropy and heat capacity are discussed in Section 2.1.8.

$$S = S_{tran} + S_{vib} + S_{\text{int},rot} + S_{hind,rot} + S_{elec} + S_{opt,iso} \tag{2.23}$$

$$S_{tran} = 37.0 + \frac{3}{2} R \ln\left(\frac{M_w}{40}\right) + \frac{3}{2} R \ln\left\{\frac{T}{298}\right\} \tag{2.24}$$

$$S_{vib} = R \ln\left(\frac{kT}{h\nu}\right) + R \tag{2.25}$$

$$S_{rot}^{linear} = 6.9 + R \ln\left(\frac{I}{\sigma_e}\right) + R \ln\left(\frac{T}{298}\right) \tag{2.26}$$

$$S_{rot}^{non-linear} = 11.5 + \frac{R}{2} \ln\left(\frac{I_m{}^3}{\sigma_e}\right) + \frac{3}{2} R \ln\left(\frac{T}{298}\right) \tag{2.27}$$

$$S_{rot}^{1D} = 4.6 + R \ln\left(\frac{I_r{}^{1/2}}{\sigma_i}\right) + \frac{R}{2} \ln\left(\frac{T}{298}\right) \tag{2.28}$$

$$S_{elec} \sim 0 \tag{2.29}$$

$$S_{opt,iso} = -R \ln(n) \tag{2.30}$$

$$C_p = C_{v,tran} + C_{v,vib} + C_{v,rot} + C_{v,hind,rot} + C_{v,elec} + R \tag{2.31}$$

$$C_{v,tran} = \frac{3}{2}R \tag{2.32}$$

$$C_{v,vib} = R\sum_i \left[\frac{x_i^{\,2} e^{x_i}}{\left(e^{x_i} - 1\right)^2} \right], \quad x_i = \frac{h\upsilon_i}{k_B T} \tag{2.33}$$

$$C_{v,rot}^{linear} = R \tag{2.34}$$

$$C_{v,rot}^{non-linear} = \frac{3}{2}R \tag{2.35}$$

$$C_{v,rot}^{1D} = \frac{R}{2} \tag{2.36}$$

$$C_{elec} \sim 0 \tag{2.37}$$

where R is the universal gas constant, Mw is the molecular weight, T is the temperature, P is the pressure, k_B is Boltzman's constant, h is Planck's constant, n is the number of optical isomers, I is the moment of inertia for a linear molecule about its center of mass, $I_m^{\,3}$ is the product of the three principal moments of inertia for a nonlinear molecule about the center of gravity, I_r is the reduced moment of inertia for the internal rotation, υ is the vibrational frequency (the moments of inertia and the frequencies are obtained from electronic structure theory calculations), σ_e is the external symmetry number of the molecule, and σ_e is the symmetry of the internal rotation.

2.1.7.1 Software used - SMCP

Entropy and heat capacity values as a function of temperature are determined from the calculated structures, moments of inertia, vibrational frequencies, internal rotor potentials, symmetry, electron degeneracy, number of optical isomers and the known mass of each molecule. The calculations use standard formulas from statistical mechanics

for the contributions of translation, vibrations and external rotation (TVR) using the SMCPS (Statistical Mechanics – Heat Capacity, *Cp*, and Entropy, *S*) program[78].

The program uses the rigid-rotor-harmonic approximation from the frequencies along with moments of inertia from the optimized B3LYP/6-31G(d,p) level.

2.1.8 Hindered Internal Rotors

The contributions to *S* and *Cp(T)* need to be separately calculated and incorporated into the thermodynamic properties for molecular species that have hindered internal rotors. One method to estimate the hinder rotor contributions is by using the vibration frequency for the torsion.

In this work, lower frequency vibrational modes that resemble torsions around single bonds were treated as hindered internal rotors, instead of treating them as harmonic oscillators. Energy profiles for internal rotations were calculated to determine energies of the rotational conformers and interconversion barriers along with contributions to entropy and heat capacity for the low barrier rotors.

2.1.8.1 Software used – Vibir and Rotator

Two different programs were used in this study for the determination of the influence of the hindered rotors for comparison: Vibir and Rotator[41].

- **Vibir:** it bases its calculations on the number of folds of the potential diagram, the moments of inertia of the rotor and the barrier height of the given rotor. It assumes a symmetrical internal rotation, and assumes the torsional potential has the simple form of a periodic cosine of barrier height V_o:

$$V\left(\theta, V_o\right) = \frac{V_o}{2}\left(1 - \cos\left(\sigma_{\text{int}}\theta\right)\right) \tag{2.38}$$

where σ_{int} is the rotational symmetry number.

The tables of Pitzer and Gwinn[79,80] are used to compute the contribution of the hindered rotor to the entropy and heat capacity:

$$x = \frac{V_o}{kT} \tag{2.39}$$

$$y = \sigma_{\text{int}} h \frac{1}{\left(8\pi^3 I_{\text{int}} kT\right)^2} \tag{2.40}$$

- **Rotator:** a relaxed rotational scan is done with dihedral angle increments of 10^o using B3LYP/6-31G(d,p) and the potential obtained is fitted to a truncated Fourier series expansion of the form in Equation (2.41) for the calculation of the contribution of the hindered rotor to the entropy and heat capacity[41].

$$V(\theta) = a_o + \sum_{n=1}^{10} a_n \cos(n\theta) + \sum_{n=1}^{10} b_n \sin(n\theta) \tag{2.41}$$

$$a_o = \frac{\sum_{i=1}^{m} f_i}{m} \tag{2.42}$$

$$a_n = \frac{\sum_{i=1}^{m} f_i \cos(n\theta)}{m} \tag{2.43}$$

$$b_n = \frac{\sum_{i=1}^{m} f_i \sin(n\theta)}{m} \tag{2.44}$$

It calculates the moment of inertia given the geometry of the studied rotor. It uses this potential to solve the 1-D Schrödinger equation in θ to calculate the energy levels, and therefore, the partition function of the hindered rotor. The program calculates the Hamiltonian matrix in the basis of the wave function of free internal rotation and performs the subsequent calculation of energy levels by direct diagonalization of the

Hamiltonian matrix. The contribution to entropy and heat capacity are determined according to standard expressions of statistical thermodynamics from the obtained partition functions. Rotator[41], accounts directly for contributions to entropy from the optical isomers. Coupling of the low barrier internal rotors with vibrations is not included.

2.1.9 Group Additivity Method

Group additivity is a straightforward and reasonably accurate calculation method to estimate thermodynamic properties of hydrocarbons and oxygenated hydrocarbons[81,82]. It is particularly useful for application to larger molecules and in codes or databases for the estimation of thermochemical properties in reaction mechanism generation.

Benson[81] realized that most molecular properties of larger molecules are composed of contributions due to groups. A group is defined as a polyvalent atom, in a molecule together with all of its ligands. According to his findings, the forces between atoms in the same or different molecules can be appreciated only over distances of the order of 1-3 Å, and therefore group additivity rules can be applied to these molecules. Benson and Buss[82] demonstrated that it is possible to make a hierarchical system of such additivity laws. The first approximation is the additivity of bond properties. For example for CH_3CH_2OH, $Cp(CH_3CH_2OH) = 5Cp(C—H) + Cp(C—O) + Cp(O—H)$. The second approximation is to treat the properties of a molecule as a linear sum of the contributions due to groups. The property of the molecule is therefore the sum of all atoms contributions. These bond properties contribute to the estimation of $\Delta H^o_{f,298}$, S^o_{298} and Cp_{298}. This method does not incorporate the nearest neighbor corrections and steric effects.

2.1.9.1 Software used - Therm

The program estimates the thermochemical properties by following the group additivity method. The code includes contributions for cyclization, gauche interactions, steric effects, repulsive and attractive effects for aromatic substituents.

The code only includes limited thermodynamic data to determine the interaction contributions. The importance of the interactions has to be recognized a priori, because otherwise, the resulting estimates will be less accurate than anticipated.

2.2 Kinetic Properties

Detailed combustion reaction mechanisms are comprised of many elementary chemical reaction steps, based upon fundamental thermochemical and kinetic principles. The accuracy of these combustion models depends on the precision of the thermochemical properties provided for the species involved in these reactions, and on the precision of the rate constants provided for each of the reactions in the model.

2.2.1 Transition State Theory

The Transition State Theory (TST) applies the principles of statistical mechanics and thermodynamics to a system in which activated complexes are effectively in equilibrium with reactant molecules. For the reaction:

$$A + B \rightarrow C$$

the reaction scheme is:

$$A + B \leftrightarrow AB^{\neq} \rightarrow C$$

where A and B are the reactants, C is the product and $AB^{\neq}$ is the transition state.

The method is based in two assumptions: (i) transition state species that originate as reactants are assumed to be in local equilibrium with reactants, and (ii) any system passing through the transition state does so only once (before the next collision or before it is stabilized or thermalized as reactant or product)[83].

2.2.1.1.Canonical Transition State Theory (CTST)

The transition state is a saddle point, where the potential energy rises in all directions except one (the reaction coordinate), as indicated in Figure 2.1.

The rate for the reaction A + B → C is:

$$r_A = k_f [A][B] = -\frac{d[A]}{dt} \rightarrow k_f = \frac{-d[A]/dt}{[A][B]} \tag{2.45}$$

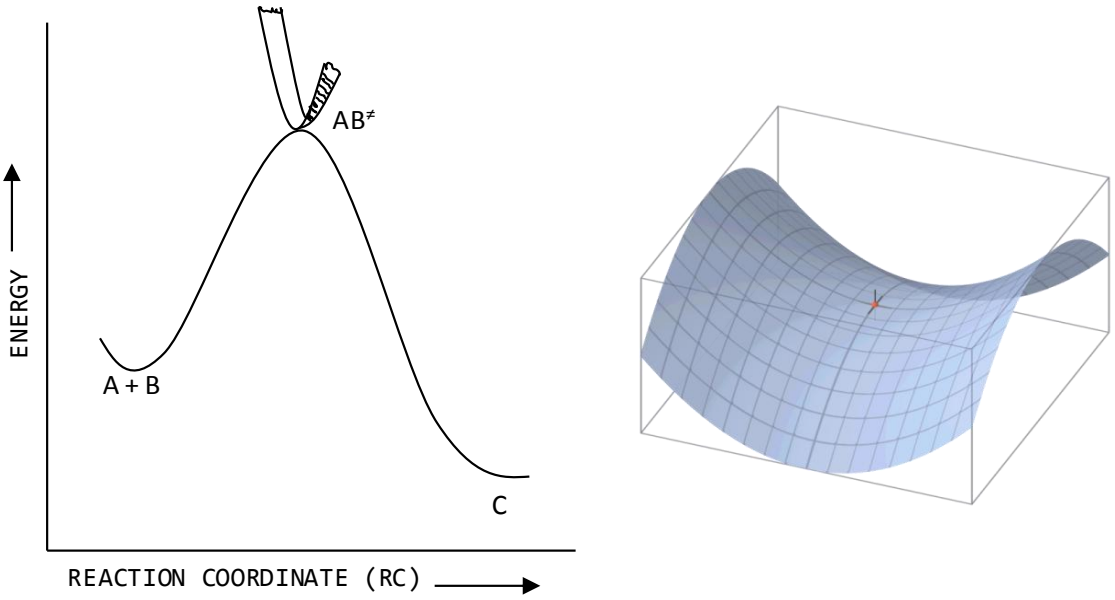

Figure 2.1 Canonical transition state theory

The rate constant is defined in the Arrhenius form as:

$$k_f = AT^n e^{(-Ea/RT)} \tag{2.46}$$

where *Ea* is the activation energy, *T* is the temperature, *n* is the temperature exponent, and *A* is the pre-exponential factor.

The statistical mechanic analysis assumes that the rate of the reaction is equal to the product of the frequency (ν_I) of the activated complex crossing the barrier and the concentration of the transition state complex.

$$-r_A = \nu_I \left[AB^{\neq} \right] \tag{2.47}$$

The transition state molecule and the reactants are in pseudo equilibrium at the top of the energy barrier. The equilibrium constant for the formation of the transition state is:

$$K_c^{\neq} = \frac{\left[AB^{\neq} \right]}{[A][B]} \tag{2.48}$$

The equilibrium constant is determined in statistical mechanics as:

$$K_c^{\neq} = \frac{Q^{\neq}}{Q_A Q_B} e^{-E_o/k_B T} \tag{2.49}$$

where Q_A and Q_B are the complete partition functions of the reactants A and B, and $Q^{\neq}$ is the partition function for the transition state structure. Rearranging:

$$k_f = \nu_I K_c^{\neq} = \frac{k_B}{hT} \frac{Q^{\neq}}{Q_A Q_B} e^{-E_o/k_B T} \tag{2.50}$$

The molar Gibbs standard free energy is calculated using the van t'Hoff relation:

$$\Delta G_o^{\neq} = -RT \ln(K_p^{\neq}) \tag{2.51}$$

$$K_p^{\neq} = e^{-\Delta G_o^{\neq}/RT} \tag{2.52}$$

The Gibbs standard free energy ($\Delta G_o^{\neq}$), from the electronic structure theory calculations and with the statistical mechanics, is expressed in terms of the standard enthalpy ($\Delta H_o^{\neq}$) and entropy changes ($\Delta S_o^{\neq}$) as:

$$\Delta G_o^{\neq} = \Delta H_o^{\neq} - T\Delta S_o^{\neq} \tag{2.53}$$

The relation between the pressure and concentration equilibrium constants is:

$$K_c^{\neq} = \frac{K_p^{\neq}}{\left(RT\right)^{\Delta n^{\neq}}} \tag{2.54}$$

where $\Delta n^{\neq}$ is the difference of molecules between the transition state and the reactants.

The rate constant is expressed as:

$$k_f = \frac{k_B T}{h} K_c^{\neq} = \frac{k_B T}{h} \frac{K_p^{\neq}}{\left(RT\right)^{\Delta n^{\neq}}} = \frac{k_B T}{h} \frac{e^{-\Delta G_o^{\neq}/RT}}{\left(RT\right)^{\Delta n^{\neq}}} = \frac{k_B T}{h} \frac{e^{-\left(\Delta H_o^{\neq} - T\Delta S_o^{\neq}\right)/RT}}{\left(RT\right)^{\Delta n^{\neq}}} \tag{2.55}$$

$$k_f = \frac{k_B T}{h} \exp\left(\frac{\Delta S_o^{\neq}}{R}\right) \exp\left(\frac{-\Delta H_o^{\neq}}{RT}\right) \left(RT\right)^{-\Delta n^{\neq}} \tag{2.56}$$

The reverse rate constant is determined from the thermochemical properties and the forward rate constant as:

$$K_C^{\neq} = \frac{k_f}{k_r} = \frac{A_f \exp\left(-E_f/RT\right)}{A_r \exp\left(-E_r/RT\right)} \tag{2.57}$$

2.2.1.2.Variational Transition State Theory (VTST)

The assumption of the transition state which states that any system passing through the transition state does so only once, depends on the location of the transition state. The transition state is not necessarily located at a saddle point, and it can be variationally defined as a point which fulfills the minimum-flux or maximum-free-energy-of-activation criteria[83] (see Figure 2.2).

There are different variational transition state theories (micronanonical, canonical, and improved canonical). In this work the canonical variational transition state theory approach is followed, where the position of the dividing surface is varied so as to minimize the rate constant at a given temperature.

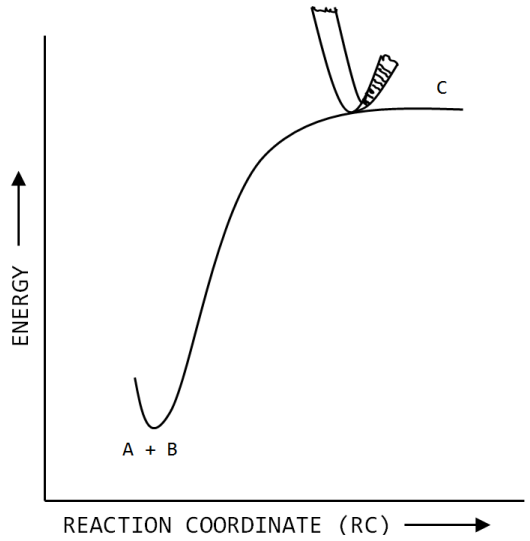

Figure 2.2 Variational transition state theory

The determination of the variational transition state requires a scan along the bond of interest, and the determination of the frequencies at each of these distances. Rate constants are determined (following the canonical transition state theory) from the reactant to each of these points (TST_i): $A + B \rightarrow TST_i \quad ; \quad k_i$. At each temperature, the distance that has the minimum rate constant is identified (resulting on the information of the minimum rate constant at each temperature), and the variational rate constant is determined from the fit of these rate constants to the Arrhenius equation (Equation 2.46).

2.2.2 Temperature and Pressure Dependence Models

Chemical reactions may be unimolecular (i.e., dissociation/isomerization) or bimolecular (i.e., chemically activated). Some of these reactions are “collisionless”, meaning that the intermediate complexes are so short-lived that they effectively do not suffer any collisions under conditions that are normally of interest. However, usually the intermediate complexes live long enough to suffer numerous collisions. All these reactions have both temperature and pressure dependence, and therefore require a theoretical description.

Molecules undergo thermal unimolecular reactions as a result of the energization by molecular collision. This molecular collision at a given temperature produces energized molecules with an equilibrium distribution of energy which enables the fraction of molecules energized into a particular energy range or quantum state. The energization methods other than by molecular collision, such as photoactivation and chemical activation, may produce a non- equilibrium situation in which molecules acquire energies far in excess of the average thermal energy. This amount of excess of energy contained in the energized adduct makes chemical activation reactions much more important in a particular system, and a much different treatment is required for the rate of conversion of the energized adduct to products (including back to reactant) which is very competing with the rate of its collisions to stabilization.

The pressure dependent reactions are: radical–radical recombination reactions, addition reactions of radicals to multiple bonds, insertions of species with empty orbitals into single bonds, elimination reactions, dissociation reactions, and isomerization reactions[84]. Chemical reaction events cause a change in molecular configuration at

constant energy. The rate coefficient for this process must be determined as a function of energy, *k(E)*, rather than the usual temperature.

2.2.2.1 Collision Models

There are different models for the determination of the energy transfer during the collisions:

- ***Strong Collision Assumption:*** it assumes that a single collision with a collider species completely activates AB or deactivates AB^*. This assumption leads to a bimodal energy distribution and ignores the fact that depending on the collision angle, relative velocities of the colliding species, and energy distribution in the colliders a wide range of interactions is possible.
- ***Modified Strong Collision Assumption:*** in real systems, not each collision leads to complete exchange of energy. The model assumes that only a fraction of all collisions is ‘‘strong’’ while the remaining collisions are elastic (no transfer of internal energy). A collision parameter (β_c) is introduced, which describes the fraction of ‘‘successful’’ collisions as a function of collider properties and the temperature.
- ***Master Equation:*** the model includes all possible states or energy levels of a molecule AB with AB^*. In a collision, energy can be transferred as translational, vibrational, and rotational energy. It assumes that collisions are independent events, and they depend only on the initial states of the two colliding partners. It defines a transition of a species AB from a state of energy E’ to a state of energy E as:

$$\frac{d\left[AB(E)\right]}{dt} = k(E,E')\left[AB(E')\right] \tag{2.58}$$

- ***Stochastic Approach:*** the model addresses the basic physical problem that chemical reactions are not continuous and that they may not be describable in a deterministic way. Instead, on a molecular level, reactions depend on randomly occurring collisions and the events can be seen as a ‘‘random walk’’ from one state to another. It is the most accurate method to describe complex chemical reactions.

2.2.2.2 Theories for the Determination of Temperature and Pressure Dependence

The different theories for the determination of the temperature and pressure dependence are described below.

- ***Lindemann Theory:*** it assumes for unimolecular reactions that a strong collision between the bath gas molecule (M) and the reactant AB, transfers enough energy to the reactants to reach a state above the reaction barrier (excitation step) .

$$AB + M \underset{k_{-1}}{\overset{k_1}{\rightleftarrows}} AB^* + M \tag{2.59}$$

$$AB^* \xrightarrow{k_2} A + B \tag{2.60}$$

The energized state AB* can:

- rearrange back to products A + B (reaction) or
- lose energy in a subsequent collision to re-form AB (deactivation)

The model assumes, that after some time, formation and destruction of AB* will be in balance:

$$\frac{d\left[AB^*\right]_{ss}}{dt} = 0 \tag{2.61}$$

$$\left[AB^*\right]_{ss} = \frac{k_1[M]}{k_{-1}[M] + k_2}[AB] \tag{2.62}$$

$$k_{uni} = \frac{k_1 k_2 [M]}{k_{-1}[M] + k_2} \tag{2.63}$$

$$[M] \to 0 \Rightarrow k_{uni} = k_o = k_1 [M] \tag{2.64}$$

$$[M] \to \infty \Rightarrow k_{uni} = k_\infty = \frac{k_1 k_2}{k_{-1}} \tag{2.65}$$

The Lindermann theory assumes that the time required to achieve the steady-state condition is negligible compared to the total reaction time, and that k_1, k_{-1} and k_2 do not depend on energy and can directly be calculated from kinetic collision theory. The theory shows that at the lower pressures, the rate of formation is linear with the pressure, at the higher pressures the rate of formation is independent of the pressure (high pressure limit), and at intermediate pressures, the dependence of the rate of formation with pressure is more complex (fall-off region) (see Figure 2.3.).

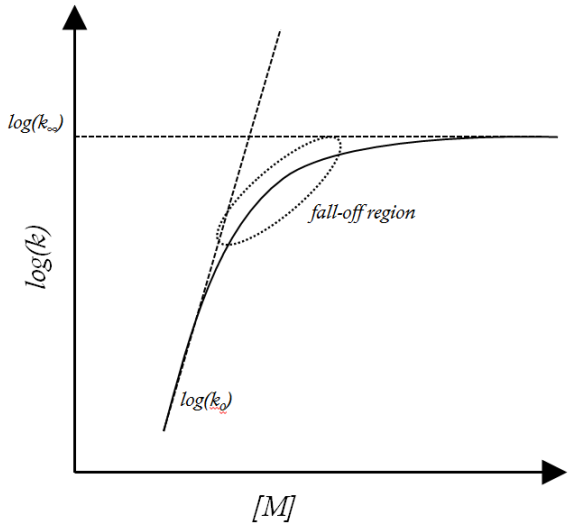

Figure 2.3 Schematic of the pressure dependence for a unimolecular reaction

Probability for AB species to obtain an energy greater than E_o is $exp(-E_o/RT)$.

$$k_1 = Z_{col} e^{(-E_o/RT)} \tag{2.66}$$

$$k_{-1} = Z_{col} \tag{2.67}$$

$$k_2 = \frac{k_\infty k_{-1}}{k_1} \tag{2.68}$$

where Z_{col} is the collision frequency:

$$Z_{col} = N_A \sigma_{AB} \sqrt{\frac{8k_B T}{\pi \mu_{AB}}} \tag{2.69}$$

This theory assumes that AB and AB* can be treated as different species. It can explain the occurrence of fall-off region, but it predicts its location to occur at higher pressures than experimentally observed.

- ***Hinshelwood-Lindemann Theory:*** in reality, AB* is the same species as AB with the difference that it contains additional internal energy, mainly stored in vibrational modes. A given amount of excess energy can be stored in many different combinations of vibrations (states) and the number of states increases rapidly with energy. The Hinshelwood-Lindermann model assumes that all vibrations are classical oscillators at equilibrium:

$$f(E) = \frac{(E/kT)^{s-1}}{(s-1)!} e^{-E/kT} \tag{2.70}$$

where s is the number of oscillators (vibration modes, each with frequency v).

$$k_1 = Z_{col} \frac{(E_o/kT)^{s-1}}{(s-1)!} e^{(-E_o/RT)} \tag{2.71}$$

Now the probability to find AB at the energy E depends on the number of oscillators (s) (on the size of the reacting molecule AB; larger species are more easily activated

to energies above E_o than small molecules). In general, the Hinshelwood–Lindemann model reproduces the location of the fall-off region well, but the shapes of fall-off curves are not accurately captured.

- ***Rice-Ramsperger-Kassel (RRK) Theory:*** the model suggests a modified reaction scheme[85,86]:

$$AB + M \underset{k_{-1}}{\overset{k_1}{\rightleftarrows}} AB^* + M \tag{2.72}$$

$$AB^* \xrightarrow{k_2} AB^{\neq} \tag{2.73}$$

$$AB^{\neq} \rightarrow A + B \tag{2.74}$$

The conversion of AB* to products is through a critical geometry $AB^{\neq}$. The model assumes that AB* and $AB^{\neq}$ have the same energy, E, with $E \geq E_o$. However, in AB* this energy is randomly distributed among all oscillators, whereas in $AB^{\neq}$ an amount $E_m \geq E_o$ is localized in the reactive mode. A single average frequency (ν) is assigned to all oscillators of AB.

- ***Quantum Rice-Ramsperger-Kassel (QRRK) Theory:*** the model represents the discrete-quantum version of the RRK Theory. Now the total distributable energy, E, is quantized by n quanta and the threshold energy, E_o, by m quanta ($n \geq m$). The model assumes that AB^o is initially at a certain temperature, and that at this temperature it has a given geometry, with certain vibrations and rotations. If the temperature of AB^o is increased (quanta added), it is needed to calculate the probability of how this quanta is distributed. The model calculates the probability that AB^o is exited to $AB^{\neq}$. The excess of energy can be stored in many different combinations of vibrations (states) - if the excess of energy is higher, the possible

combinations (states) are higher. The model calculates what fraction of molecules is in each bound of energy. One of the most significant pieces of information about collisional energy transfer at highly excited energy levels is the average energy removed per collision, $(\Delta E)_{down}$. For a given transition probability model, this quantity is the adjustable parameter used in fitting the experimental results. The single frequency versions of RRK and QRRK theories predict fall-off reasonably well. In the literature there are several ways to calculate the number of effective oscillators (Troe and Wagner[87], Golden[88], etc.), and Chang et al.[89] reported a three-frequency QRRK model, which is used in this work. In this model, the representative frequencies are obtained from fits to the *Cp(T)* values. The assumptions of the model are:

- Vibrational energy (E) of the reacting system is quantized
- *"s"* vibrational degrees of freedom of the adduct are considered as harmonic oscillators represented by a three reduced set of frequencies (v) and the energy E is divided into E/hv.

The determination of a reduced set of apparent frequencies (ω_i, ω_{ii}, ω_{iii}) is performed as:

$$C_{vib}(T) = B_i f(\theta/T)_i + B_{ii} f(\theta/T)_{ii} + B_{iii} f(\theta/T)_{iii} \tag{2.75}$$

where B_i, B_{ii}, and B_{iii} are the degeneracies, and:

$$f(\theta/T)_i = R\left(\frac{\theta_i}{T}\right)^2 \frac{\exp\left(\frac{\theta_i}{T}\right)}{\left(\exp\left(\frac{\theta_i}{T}\right)-1\right)^2} \tag{2.76}$$

The equations come from the statistical mechanics definition of the contribution to the heat capacity (*Cv*) of an ideal gas by harmonic oscillator of vibrational wavenumber:

$$(\theta)_i = \frac{hc\omega_i}{k} \tag{2.77}$$

$$B_{iii} = s - (B_i + B_{ii}) \tag{2.78}$$

A nonlinear molecule with no internal rotators has *(3n-6)* oscillators. Therefore, the $f(\theta/T)_i$ and B_i terms are determined by a nonlinear regression fit to the vibrational component of the *Cp(T)* data. The contributions from the external degrees of freedom are subtracted from the overall heat capacity, and the internal rotors are counted as half-vibrations.

- ***Rice-Ramsperger-Kassel-Markus (RRKM) Theory:*** it is the microcanonical version of the transition state theory, where the transition state ($AB^{\neq}$) is defined as the diving surface between reactants and products. The high pressure rate constant is calculated from the vibrational frequency distribution and moments of inertia of the transition state, and the pressure dependence of the rate constant is obtained by the resolution of the master equation. It is based on the accurate description of the geometry and degrees of freedom of the transition state.

2.2.3 Software Used

2.2.3.1 Determination of the High-Pressure Rate Constant – ThermKin

It calculates the rate constant from the information of the heat of formation and entropy of the reactants and the transition state.

$$k_f = \frac{k_B T}{h} \exp\left(\frac{\Delta S_o^{\neq}}{R}\right) \exp\left(\frac{-\Delta H_o^{\neq}}{RT}\right) (RT)^{-\Delta n^{\neq}} \quad (2.79)$$

2.2.3.2 Determination of k(E) and Fall-off – Chemaster, and ChemRate

- ***Chemaster:***

The program uses a multifrequency qRRK analysis for k(E) and Master Equation for fall-off for solving bimolecular reactions of the type described in Figure 2.4.

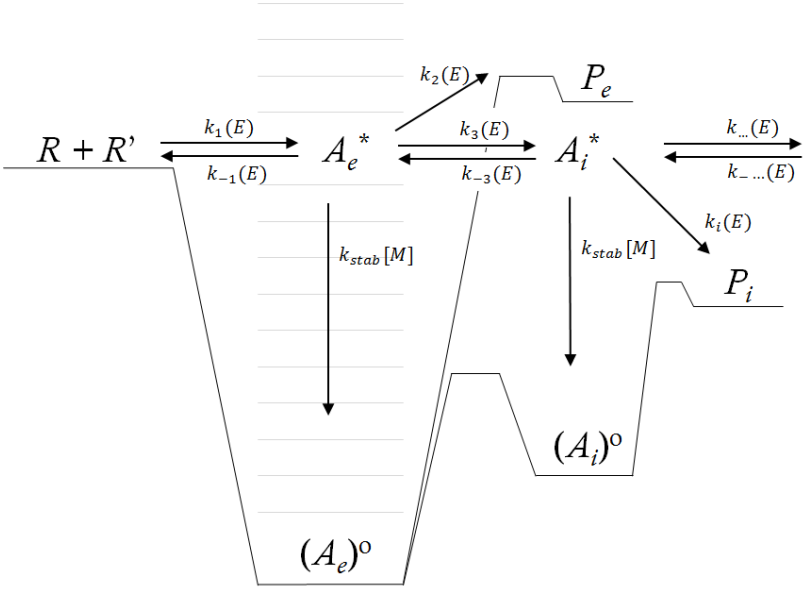

Figure 2.4 Schematic of the potential energy diagram for a bimolecular reaction

In Figure 2.4, A_i^* denotes an activated complex with energy of the new bond formed, A_i its stabilized adduct, and P_i denotes one of several product channels. The subscript *e* identifies the isomer formed directly by the initial reactants *R* and *R'*. Subsequent isomerizations can lead to other complexes that can dissociate to form various products, re-isomerize, or be collisionally de-energized to form stabilized adducts. The entrance isomer can also dissociate back to reactants, and this can

effectively be treated as another product channel. The model applies the steady-state assumption on the activated adducts.

The isomers formed can undergo dissociation reactions for the formation of several products *(P_1, P_2,…,P_N)*. The single-step isomer (A_i) dissociation to each of the products is represented as:

$$\begin{aligned} A_e &\rightarrow P_1 \\ &\rightarrow P_2 \\ &\rightarrow P_N \end{aligned}$$

The concentration of the activated complex A_i^* in the energy band $E \pm \Delta E/2$ is denoted as $\Delta C_i(E)$:

$$\frac{d[\Delta C_i(E)]}{dt} = \underbrace{k^{inp}[R][R']f(E,T)\delta_{i,e}}_{\text{production of Ai* from reactants}} + \underbrace{\sum_j \left(IS^T\right)_{i,j} \Delta C_i(E)}_{\text{production of Ai* from isomers}} - \Delta C_i(E)\left\{\underbrace{\sum_j IS_{i,j}}_{\text{loss of Ai* to isomers}} + \underbrace{\sum_m PD_{i,m}}_{\text{loss of Ai* to products}} + \underbrace{k_i^s(T)[M]}_{\text{loss of Ai* for stabilization}}\right\} \quad (2.80)$$

where k^{inp} is the input rate constant for the formation of the entrance isomer, $\delta_{i,e}$ is the delta function (the input channel is seen to enter the entrance well through the delta function), $f(E,T)$ is the product distribution resulting from the initial step, $IS_{i,j}$ is the isomerization matrix (contains the rate constants from isomer *i* to *j*), $PD_{i,m}$ is the product matrix (contains the rate constants from isomer *i* to product *m*), k_i^s is the stabilization rate for complex *i*, and *[M]* is the total concentration of the bath gas. A detailed description is included in reference[90].

While the qRRK-Master Equation code for the chemical activation analysis considers reaction of each of the chemically activated adducts (isomers) to all products, the Master Equation analysis for the stabilized isomer reactions is more limited. It

considers each of the single reaction steps out of the well that the stabilized isomer can undergo directly, but does not consider subsequent reactions of these first product(s).

The input parameters required by the software are: Lennard-Jones parameters, σ (collisional diameter) and ε (ε/k_B is the well-depth) for the adduct formed by the initial reaction and the bath gas, reduced sets of frequencies for each of the isomers, values of average energy transferred per collision (E_{down}), energy grid for the Master Equation (INT), energy where the integration stops (E_{head} = highest barrier + entered value), and high pressure rate constants for each reaction path (based on measured values, assigned by comparison to known rate constants, or theoretically calculated following the canonical or variational transition state theory).

- ***ChemRate***

The program contains a master equation solver so that rate constants for unimolecular reactions in the energy transfer region and chemical activation processes under steady and non-steady state conditions can be determined on the basis of the RRKM theory[91]. It calculates high pressure rate constants of all unimolecular reactions on the basis of transition state theory, determines specific rate constants on the basis of RRKM theory, treats multichannel reactions including chemical activation processes under equilibrium and non-equilibrium conditions, and calculates steady state rate constant as well as time-dependent rate constants.

2.3 Combustion Kinetic Modeling

The development of fundamental thermochemical and kinetic properties discussed in Sections 2.1 and 2.2 allow the assembling of elementary reaction mechanisms, used for the combustion kinetic modeling.

2.3.1 Application of Combustion Modeling

The goal of the combustion kinetic modeling is to model the chemical and thermodynamic behavior of a combustion process. As combustion technologies continue to evolve towards greater efficiency and reduced pollution, their development requires a comprehensive understanding of the combustion behavior of fuels. The kinetic modeling is one way to gain this knowledge through the examination of the pyrolysis and oxidation characteristics of fuels and can greatly increase the efficiency of studying a variety of combustion systems.

2.3.2 Software Used - ChemKin

ChemKin is a software that predicts the time-dependent chemical kinetics behavior of a homogeneous gas mixture in a closed system (the reacting mixture is treated as a closed system with no mass crossing the boundary).

Total mass of the mixture is constant:

$$m = \sum_{k=1}^{K} m_k \rightarrow \frac{dm}{dt} = 0 \tag{2.81}$$

where m_k is the mass of the k^{th} species, and K is the total number of species in the mixture.

The individual species are produced or destroyed according to:

$$\frac{dm_k}{dt} = V\omega_k W_k, k = 1, ..., K \Rightarrow \frac{dY_k}{dt} = v\omega_k W_k, k = 1, ..., K \quad (2.82)$$

where t is time, ω_k is the molar production rate of the k^{th} species by elementary reaction, Y_k $(=m_k/m)$ is the mass fraction of the k^{th} species, W_k is the molecular weight of the k^{th} species, V is the volume of the system, and v $(=V/m)$ is the specific volume.

Since in the systems studied in this work the temperature is known, the energy equation is unnecessary and the problem is completely defined by the equations above. The net chemical production rate (ω_k) of each species results from a competition between all the chemical reactions. Each reaction proceeds according to the law of mass action and the forward rate coefficients are in the modified Arrhenius form (Equation 2.46).

CHAPTER 3

OXIDATION OF SECONDARY ISOOCTANE

3.1 Overview

There is an increased interest in developing a better understanding of the oxidation of large hydrocarbon fuels over a wide range of operating conditions, due to the need to improve the efficiency and performance of currently operating engines and other combustors, and reduce levels of pollutant species emissions generated in the combustion processes. Isooctane (2,2,4- trimethylpentane) is used as one of the model fuel molecules in both modeling and experimental studies on spark and homogeneous charge compression ignition (HCCI) engines. It is used both as a neat fuel and as a major component in primary reference fuel blends[2,92-94].

Ignition kinetics and partial oxidation intermediate product profiles of isooctane have been studied using varied shock and flow experimental techniques and modeling performed with several kinetic models[92,95-100]. Experimental studies observe the importance of the formation of isooctane and substituted branched saturated cyclic ethers[101]. The chemical species used in these kinetic models typically used group additivity for thermochemical properties with bond dissociation enthalpies for intermediates from smaller molecule (model) reference chemical structures. Kinetic parameters involving reaction paths and rate constants were generally based on experimental data from less branched, smaller molecule reference species[96,97]. Isooctane is however a highly branched molecule (see Figure 3.1), and this branching may affect its thermochemistry and reaction barriers.

Thermochemical properties and kinetics of the secondary isooctane peroxide, the peroxy radical and the hydroperoxide alkyl radicals resulting from intramolecular H atom transfer reactions (isomerization) from the $^3O_2$ association reaction with the secondary isooctane radical are calculated in this study. Comparisons of the kinetic and thermochemical properties with literature on smaller, model systems and with estimation procedures are presented.

3.2 Thermochemical Properties

Structure and atom numbering nomenclature of the isooctane parent and the radical on the secondary carbon are illustrated in Figure 3.1.

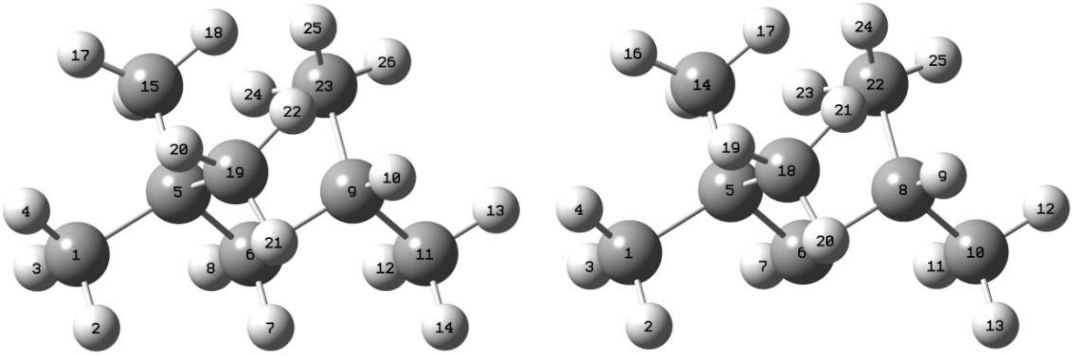

$(CH_3)_3CCH_2CH(CH_3)_2$ **$(CH_3)_3CCH^{\bullet}CH(CH_3)_2$**

c3cccc2 **c3cc$^{\bullet}$cc2**

Figure 3.1 Geometry and nomenclature for low energy conformers of isooctane and the secondary isooctane radical

The structure and atom numbering of the peroxy radical and its hydroperoxy alkyl radical isomers are illustrated in Figure 3.2.

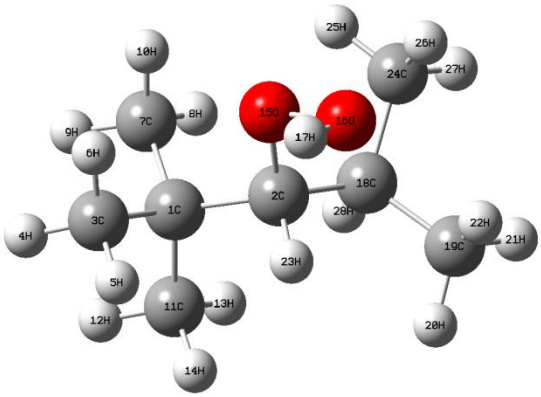

$(CH_3)_3CCH(OOH)CH(CH_3)_2$

c3ccqcc2

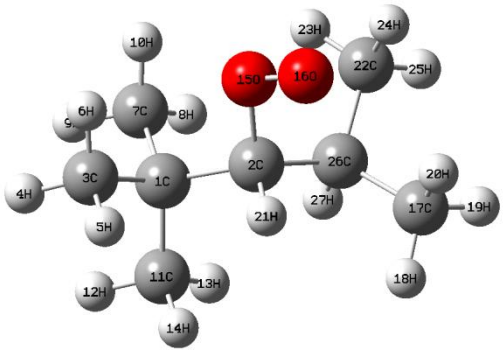

$(CH_3)_3CCH(OO^{\bullet})CH(CH_3)_2$

c3ccq$^{\bullet}$cc2

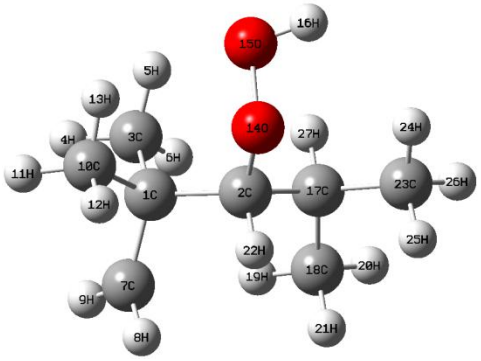

$(CH_3)_2(CH_2^{\bullet})CCH(OOH)CH(CH_3)_2$

c3$^{\bullet}$ccqcc2

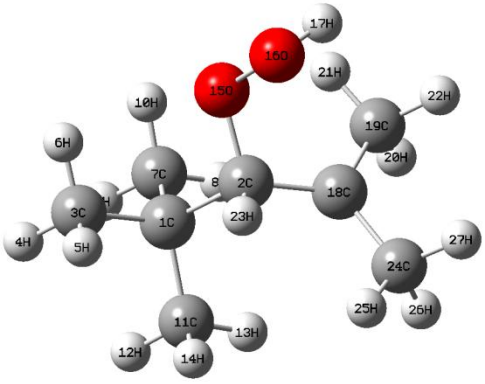

$(CH_3)_3CCH(OOH)C^{\bullet}(CH_3)_2$

c3ccqc$^{\bullet}$c2

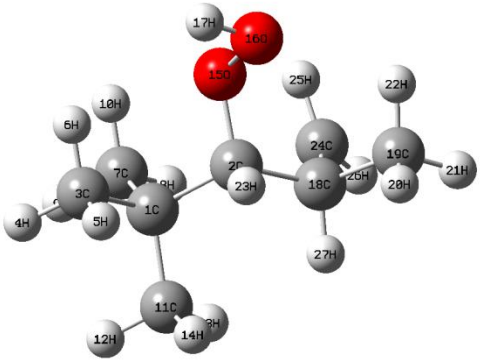

$(CH_3)_3CCH(OOH)CH(CH_3)(CH_2^{\bullet})$

c3ccqcc2$^{\bullet}$

Figure 3.2 Geometry and nomenclature for the optimized peroxy radical and its hydroperoxy alkyl radical isomers

The nomenclature used in the diagrams and figures for all the reactants and products is listed in Table 3.1.

Nomenclature	Species	Formula
c3cc•cc2	$(CH_3)_3CCH•CH(CH_3)_2$	C_8H_{17}
c3ccq•cc2	$(CH_3)_3CCH(OO•)CH(CH_3)_2$	$C_8H_{17}O_2$
c3•ccqcc2	$(CH_2•)(CH_3)_2CCH(OOH)CH(CH_3)_2$	$C_8H_{17}O_2$
c3ccqc•c2	$(CH_3)_3CCH(OOH)C•(CH_3)_2$	$C_8H_{17}O_2$
c3ccqcc2•	$(CH_3)_3CCH(OOH)CH(CH_3)(CH_2•)$	$C_8H_{17}O_2$
c3cco•cc2	$(CH_3)_3CCH(O•)CH(CH_3)_2$	$C_8H_{17}O$
c3c(c=o)cc2	$(CH_3)_3CC(=O)CH(CH_3)_2$	$C_8H_{16}O$
c=cc2	$CH_2=C(CH_3)_2$	C_4H_8
c(=o)cc2	$CH(=O)CH_2(CH_3)_2$	C_4H_9O
c2yoxtcc2	$(CH_3)_3C(CHCO)(CH_3)_2$	$C_8H_{16}O$
c=cmcqcc2	$CH_2=C(CH_3)CH(OOH)CH(CH_3)_2$	$C_7H_{14}O_2$
cq=cc2	$CH(OOH)=C(CH_3)_2$	C_4H_8O2
c3c•	$(CH_3)_3C•$	C_4H_9
c3cycocc2	$(CH_3)_3C(CHCO)(CH_3)_2$	$C_8H_{16}O$
c3cc=cc2	$(CH_3)_3CCH=C(CH_3)_2$	C_8H_{16}
c3cycccoc	$(CH_3)_3C(CHCHCH_2O)(CH_3)$	$C_8H_{16}O$
c=cc	$CH_2=CHCH_3$	C_3H_6
c3cc=o	$(CH_3)_3CCH(=O)$	$C_5H_{10}O$
c3ccqc=c	$(CH_3)_3CCH(OOH)CH=CH_2$	$C_7H_{14}O_2$

Table 3.1 Nomenclature of the reactants and products studied

Rotational conformers were studied to determine the lowest energy conformer for peroxy and hydroperoxy alkyl radicals. The existence of relatively low-energy rotation conformers with transitions through internal rotation barriers between the conformers usually has significant effects on the entropy[102]. Energy profiles for internal rotations were calculated to identify the lowest energy conformer, and determine energies of the different rotational conformers and interconversion barriers along with contributions to entropy and heat capacity for the low barrier rotors[103]. For the internal rotor potentials, the total energies as a function of the dihedral angles were computed at the B3LYP/6-

31G(d,p) level of theory. The resulting potential energy barriers for internal rotations in the stable hydroperoxide and the radicals are shown in Figures 3.3 to 3.5.

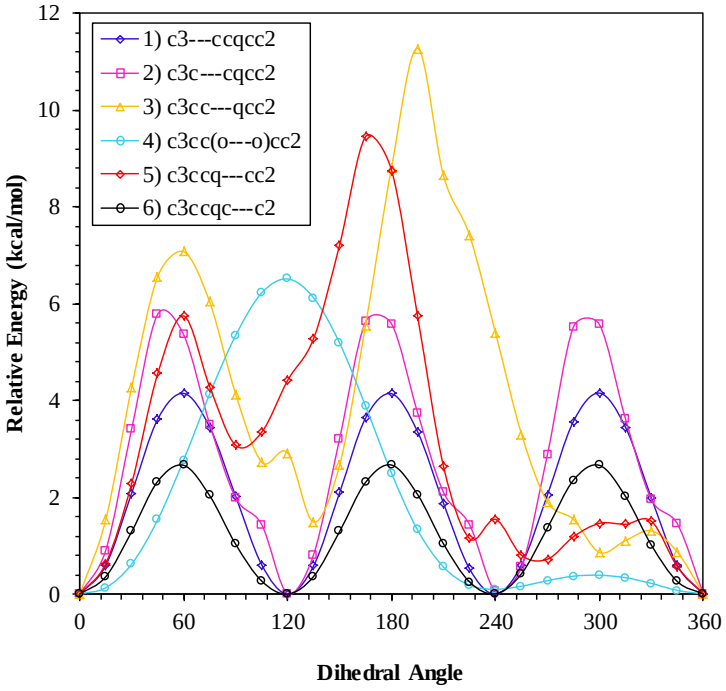

Figure 3.3 Potential energy profiles for internal rotations in c3ccqcc2

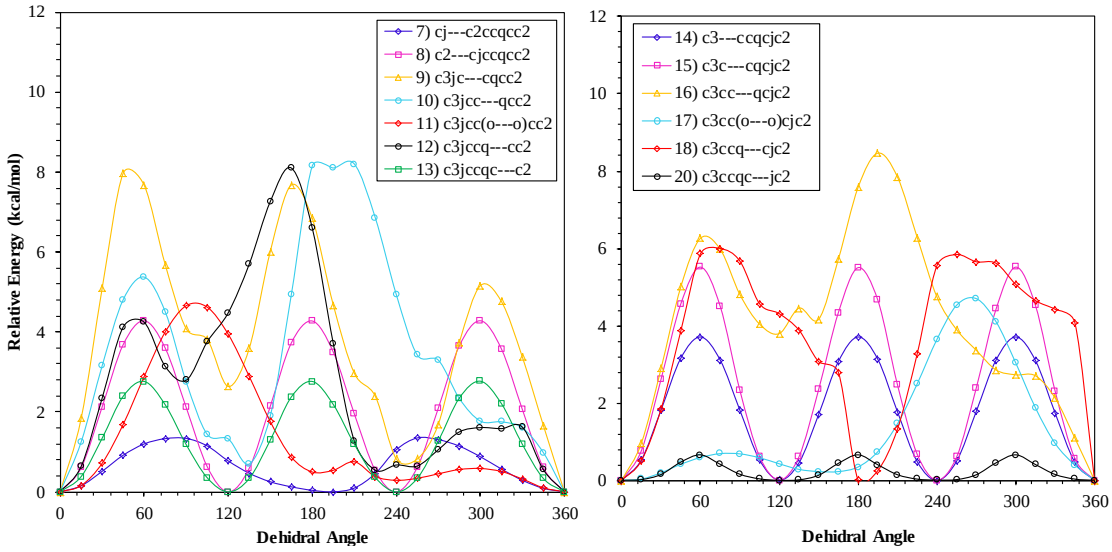

Figure 3.4 Potential energy profile for internal rotations in c3•ccqcc2 and c3ccqc•c2

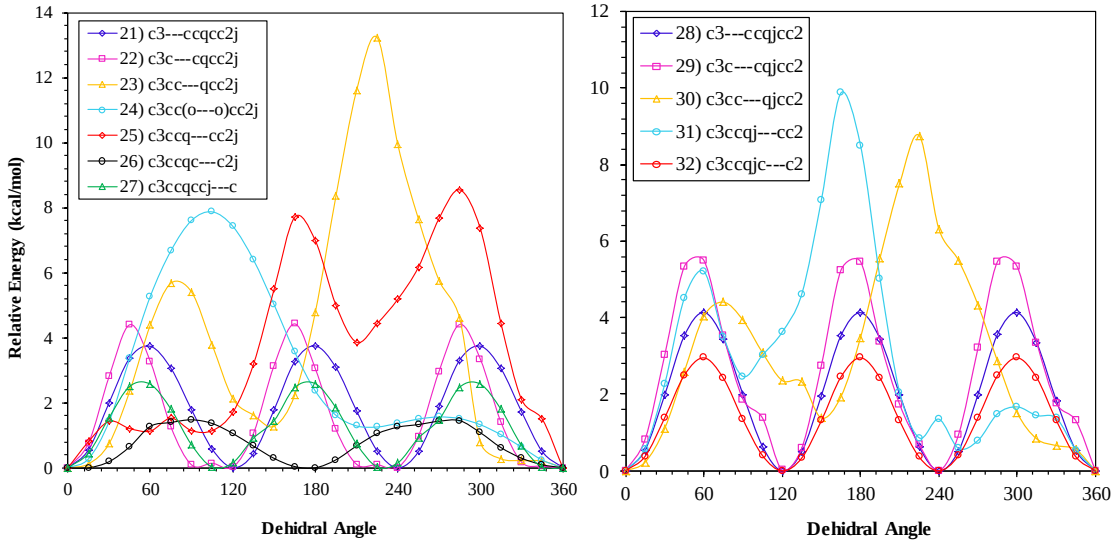

Figure 3.5 Potential energy profiles for internal rotations in c3ccqcc2• and c3ccq•cc2

The calculated rotational barriers are summarized in Table 3.2.

Table 3.2 Rotational barriers for the secondary isooctane hydroperoxide, the peroxy radical and the alkyl radicals

Scans	c3ccqcc2	c3•ccqcc2	c3ccqc•c2	c3ccqcc2•	c3ccq•cc2	Foldness
c•—c2ccqcc2	---	1.4	---	---	---	2
c3—ccqcc2	4.2	4.3	3.7	3.8	4.1	3
c3c—cqcc2	5.8	7.9	5.5	4.6	5.5	3
c3cc—qcc2	11.3	8.2	8.5	13.2	8.8	
c3cc(o—o)cc2	6.5	4.7	4.7	7.9	---	
c3ccq—cc2	9.5	8.1	6.0	8.5	9.9	2
c3ccqc—c2	2.7	2.8	0.7	2.6	2.9	3
c3ccqcc—c•	---	---	---	1.5	---	2

Units: kcal mol^{-1}

The rotational barriers of methyl groups in isooctane hydroperoxide and its radicals show three-fold symmetry with barriers near 3.0 kcal mol^{-1} for the CH_3 rotors on the isopropyl group $(CH_3)_3CCH(OOH)CH(CH_3)—(CH_3)$, while methyl rotors on the tertiary butyl are near 4.0 kcal mol^{-1} $(CH_3)—(CH_3)_2CCH(OOH)CH(CH_3)_2$. These are similar to the methyl rotor potentials in *n*-hydrocarbons.

When a radical site is located on one of the isopropyl methyl carbons of this secondary isooctane hydroperoxide the barrier decreases to 1.5 kcal mol^{-1} for $(CH_3)_3CCH(OOH)CH(CH_3)—(CH_2^{\bullet})$ and 1.4 kcal mol^{-1} for tertiary butyl methyls $(CH_2^{\bullet})—(CH_3)_2CCH(OOH)CH(CH_3)_2$. The rotational barrier of the CH_3 methyls on the isopropyl group $((CH_3)_3CCH(OOH)C^{\bullet}(CH_3)—(CH_3)$ decrease to 0.7 kcal mol^{-1} when the radical site is on the tertiary carbon, $((CH_3)_3CCH(OOH)C^{\bullet}(CH_3)_2)$,.

Rotational barriers of the tertiary-butyl group $((CH_3)_3C—CH(OOH)CH(CH_3)_2)$ exhibit three-fold symmetry with barriers of 4.5-6 kcal mol^{-1} and the barrier increases to 7.9 kcal mol^{-1}, when the radical site is located on a t-butyl methyl $(((CH_2^{\bullet})(CH_3)_2C—CH(OOH)CH(CH_3)_2)$.

The $(CH_3)_3CCH(OOH)—CH(CH_3)_2$ rotor in the isooctane hydroperoxide has two-fold symmetry with a 9 kcal mol^{-1} barrier, and the value decreases to 6 kcal mol^{-1} when the radical site is on the adjacent tertiary carbon $((CH_3)_3CCH(OOH)—C^{\bullet}(CH_3)_2)$. The rotational barrier for $(CH_3)_3CCH—(OOH)CH(CH_3)_2$ is 11.3 kcal mol^{-1} in isooctane hydroperoxide. It decreases to 3 kcal mol^{-1} for the alkyl hydroperoxide and the peroxy radicals, except for $(CH_3)_3CCH—(OOH)CH(CH_3)(CH_2^{\bullet})$, where this rotation barrier increases 2 kcal mol^{-1}.

The rotational barrier for $(CH_3)_3CCH(O—OH)CH(CH_3)_2$ is 6.5 kcal mol^{-1} and it is 4.7 kcal mol^{-1} for $(CH_3)_2(CH_2^{\bullet})CCH(O—OH)CH(CH_3)_2$ and $(CH_3)_3CCH(O—OH)C^{\bullet}(CH_3)_2$. However, the value is higher (7.9 kcal mol^{-1}) for $(CH_3)_3CCH(O—OH)CH(CH_3)(CH_2^{\bullet})$.

The molecular geometries of the lowest energy conformers are summarized in Appendix B. The vibrational frequencies of each of the calculated species are summarized in Appendix C.

Standard enthalpies of formation ($\Delta_f H^o_{298}$) were evaluated using work reactions with calculated energies, scaled zero point vibration energy (ZPVE), plus thermal enthalpy contributions (to 298 K) by B3LYP/6-31G(d,p) and CBS-QB3 levels of theory for each species[104,105]. Isodesmic work reactions were used to cancel systematic error and improve the accuracy of both the DFT and CBS-QB3 energy values. The standard enthalpies of formation at 298.15 K of the reference species used in these isodesmic work reactions are summarized in Appendix A. Example of work reactions used for the secondary isooctane peroxide are shown in Table 3.3.

Table 3.3 Example of work reactions for the peroxy radical from the secondary iso-octane radical

Work Reactions							$\Delta_f H^o_{298}$		
							B3LYP/ 6-31G(d,p)	**CBS-QB3**	**Group Additivity**[(a)]
c3ccq•cc2									
c3ccq•cc2	+	ccq	→	c3ccqcc2	+	ccq•	-42.77	-42.78	
c3ccq•cc2	+	c3cq	→	c3ccqcc2	+	c3cq•	-42.56	-42.63	
c3ccq•cc2	+	c2cq	→	c3ccqcc2	+	c2cq•	-43.08	-42.84	
						Ave.	**-42.80**	**-42.75**	-40.90
						σ	***0.26***	***0.10***	
						BDE	84.77	84.72	

Units: kcal mol^{-1}

(a) Introduction of gauche and 1,5 interactions

The influence of each conformer in the total heat of formation was determined for the species studied. Table 3.4 summarizes the heat of formation for the isooctane peroxy radicals studied at 298 K, with and without the influence of the rotational conformers.

Data in Table 3.4 illustrates that at temperatures above 400 K the contribution of rotational conformers becomes greater than 0.5 kcal mol^{-1}, and it is greater than 1 kcal mol^{-1} at temperatures above 1000 K.

Table 3.4 Influence of accounting for all the conformers, at 298 K

Species	$\Delta_f H°_{298}$		Diff
	Without accounting for all conformers	Accounting for all conformers	
c3ccqcc2	-75.47	-75.00	-0.47
c3ccq•cc2	-42.75	85.06	-0.34
c3•ccqcc2	-26.63	-26.32	-0.31
c3ccqc•c2	-31.00	-30.99	-0.01
c3ccqcc2•	-26.88	-26.21	-0.42

Units: kcal mol^{-1}

Appendix D contains all the work reactions used for the determination of the enthalpy of formation of the secondary isooctane peroxide radicals, and the products presented in the Potential Energy (PE) diagrams of Figures 3.6 to 3.9. The enthalpies of formation of the isooctane parent molecule and each of the isooctane alkyl radicals, as well as the bond dissociation enthalpies (BDE) for each of the radicals have been reported by Snitsiriwat and Bozzelli[106] and are summarized in Table 3.5.

Table 3.5 Enthalpies of formation at 298 K of the isooctane parent and radicals reported by Snitsiriwat and Bozzelli[106]

Species	$\Delta_f H°_{298}$	Bond Dissociation Enthalpy
c3cccc2$^{(*)}$	-54.40	---
c3•cccc2	-5.00	100.6
c3cccc2•	-5.18	100.5
c3cc•cc2	-9.03	96.4
c3ccc•c2	-12.30	93.1

Units: kcal mol^{-1}

CBS-QB3 calculations

$^{(*)}$ Experimental value[107] -53.54 ± 0.36 kcal mol^{-1}

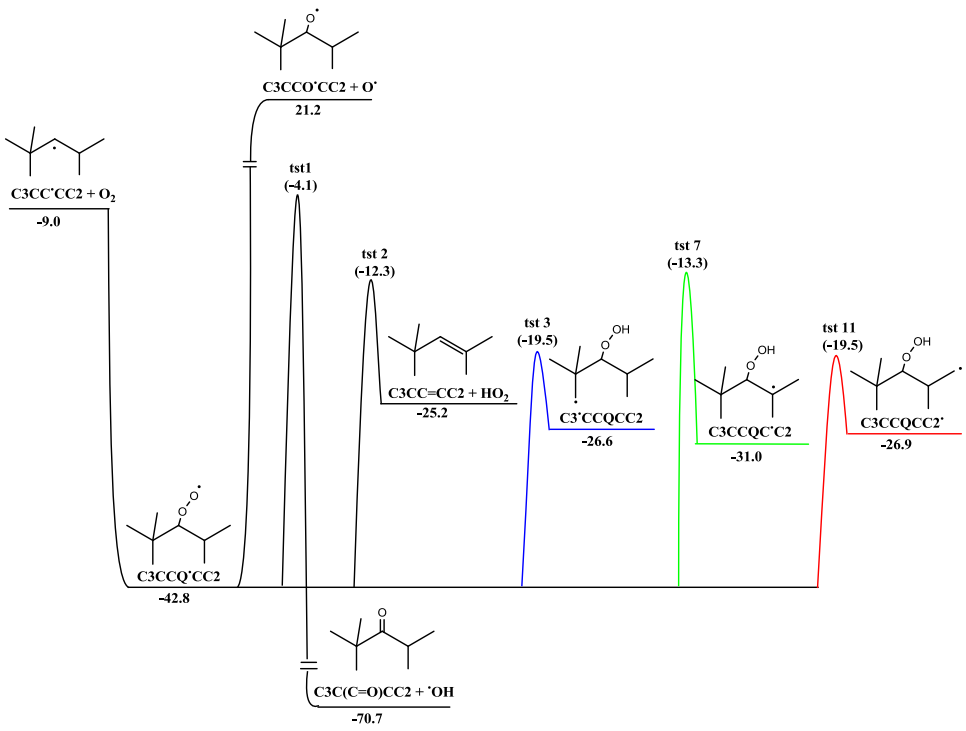

Figure 3.6 Potential energy diagram for the $(CH_3)_3CCH^{\bullet}CH(CH_3)_2 + {}^3O_2$ system, well 1. Units: kcal mol^{-1}, 298 K (CBS-QB3 level of theory)

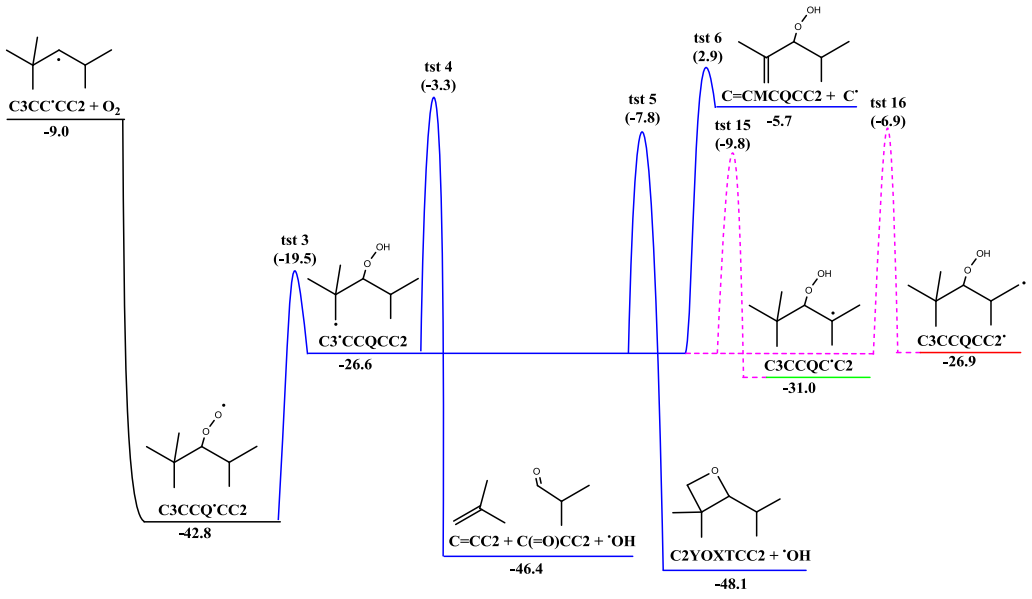

Figure 3.7 Potential energy diagram for the $(CH_3)_3CCH^{\bullet}CH(CH_3)_2 + {}^3O_2$ system, well 2. Units: kcal mol^{-1}, 298 K (CBS-QB3 level of theory)

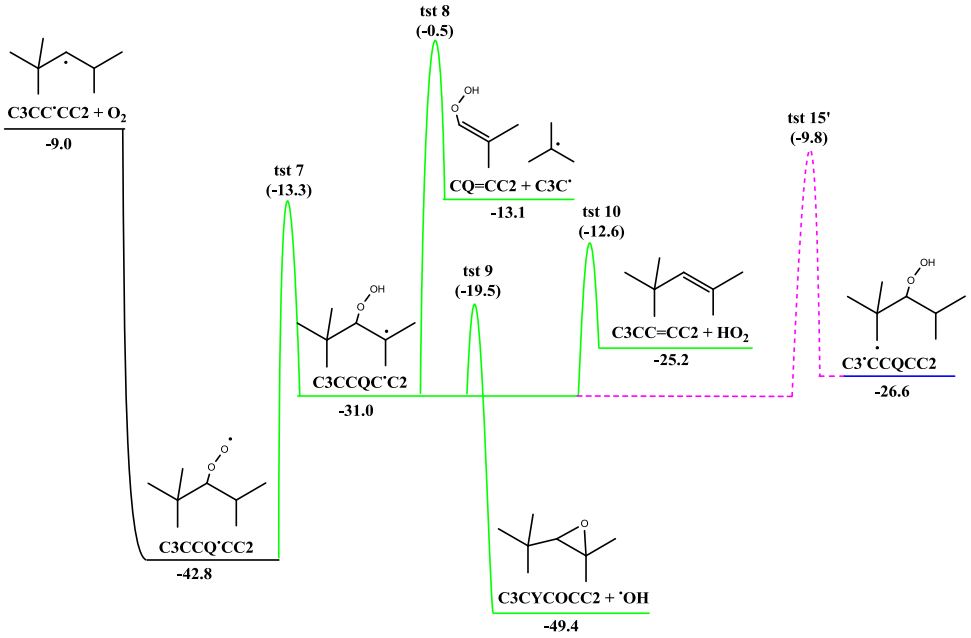

Figure 3.8 Potential energy diagram for the $(CH_3)_3CCH^{\bullet}CH(CH_3)_2 + {}^3O_2$ system, well 3. Units: kcal mol^{-1}, 298 K (CBS-QB3 level of theory)

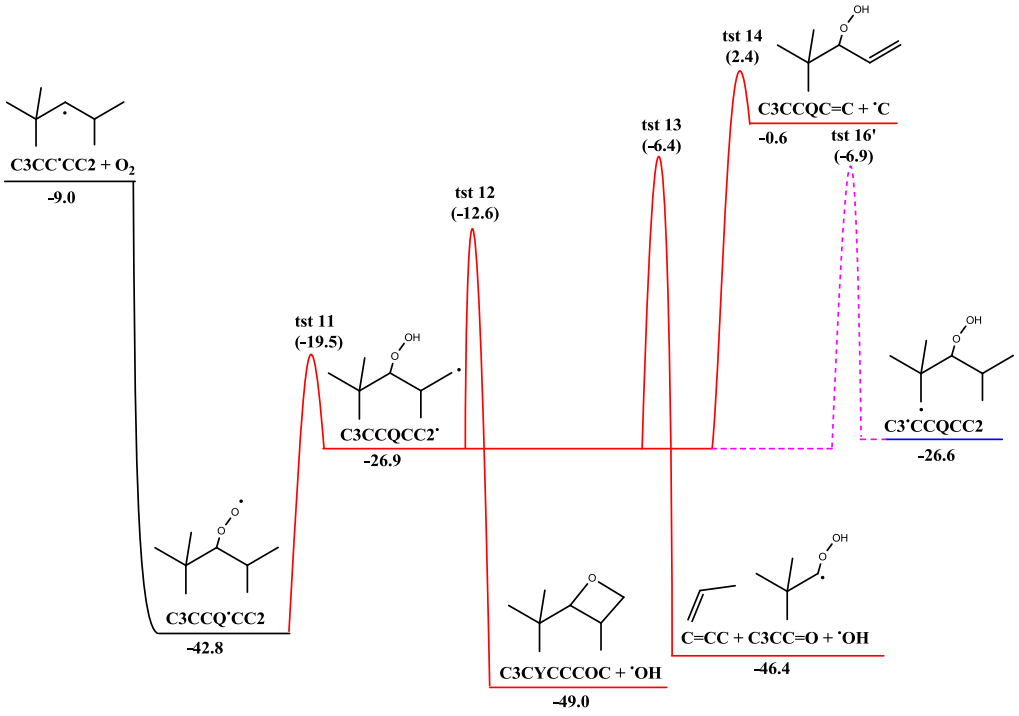

Figure 3.9 Potential energy diagram for the $(CH_3)_3CCH^{\bullet}CH(CH_3)_2 + {}^3O_2$ system, well 4. Units: kcal mol^{-1}. 298 K (CBS-QB3 level of theory)

The enthalpies of formation of the secondary isooctane peroxy radicals and the enthalpies of formation of the resulting products from the studied reaction channels are presented in Tables 3.6 and 3.7. The B3LYP calculations are in good agreement with the CBS-QB3 calculations when isodesmic work reactions are used. Enthalpies of the hydroperoxide and peroxy radical (at the CBS-QB3 level of theory) are -75.5 and -42.8 kcal mol^{-1}. The tertiary alkyl radical is -31.0 kcal mol^{-1}, which is 11.8 kcal mol^{-1} higher than the peroxy radical, and the primary methyl radicals on the tert-butyl and isopropyl groups are -26.6 and -26.8 kcal mol^{-1}, respectively, ~16 kcal mol^{-1} higher than the peroxy radical.

Table 3.6 Calculated enthalpies of formation at 298 K of the secondary isooctane hydroperoxide, the peroxy radical and the alkyl radicals

Species	$\Delta_f H^o_{298}$	
	B3LYP/ 6-31G(d,p)	**CBS-QB3**
c3ccqcc2	-74.13	-75.47
c3ccq•cc2	-42.80	-42.75
c3•ccqcc2	-26.96	-26.63
c3ccqc•c2	-31.94	-31.00
c3cccqc2•	-27.35	-26.88

Units: kcal mol^{-1}

The C—H bond dissociation enthalpies (BDE) are often used to reflect the corresponding radical's stability; they are also commonly used to estimate kinetic barriers for abstraction of the hydrogen atom by the radical pool species, and to determine the heat of reaction, $\Delta_{rxn}H^o_{298}$, for beta scission and decomposition reactions.

Table 3.7 Calculated enthalpies of formation at 298 K of the products from the studied reaction paths

Species	$\Delta_f H^o_{298}$	
	B3LYP/ 6-31G(d,p)	**CBS-QB3**
c3ccohcc2	-90.97	-92.17
c3cco˙cc2	-38.97	-38.39
c3cc=occ2	-81.28	-80.01
c=cmcqcc2	-38.38	-40.53
c3cc=cc2	-25.44	-25.73
c3cc=o	-60.46	-60.69
cq=cc2	-27.28	-25.38
c2yoxtcc2	-57.17	-57.62
c3cycccoc	-57.73	-58.50
c3cycocc2	-57.78	-58.91

Units: kcal mol^{-1}

Bond dissociation enthalpies are reported from the calculated heats of reaction ($\Delta_{rxn}H^o_{298}$) of the parent molecule and their radical corresponding to loss of hydrogen atoms, where the enthalpies of the parent molecule and the product radical were calculated in this study in conjunction with the value of 52.10 kcal mol^{-1} for the hydrogen atom; the data correspond to the standard temperature of 298.15 K. The individual bond dissociation enthalpy values are given in Table 3.8.

Table 3.8 Bond dissociation enthalpies, for C—H bonds

C—H bonds	Bond Dissociation Enthalpy	
	B3LYP/ 6-31G(d,p)	**CBS-QB3**
c3ccqcc2 → c3ccq˙cc2 + H	84.8	84.8
c3ccqcc2 → c3˙ccqcc2 + H	100.6	100.9
c3ccqcc2 → c3ccqc˙c2 + H	95.6	96.6
c3ccqcc2 → c3ccqcc2˙ + H	100.2	100.7

Units: kcal mol^{-1}

The ROO—H bond dissociation enthalpy is 84.8 kcal mol^{-1}. The H—ROOH bond dissociation enthalpy is 96.6 kcal mol^{-1} for the tertiary radical site on the hydroperoxide, which is 3.5 kcal mol^{-1} higher than on isooctane. The H—ROOH bond dissociation enthalpies on the methyl sites on the tert-butyl and isopropyl groups are 100.9 and 100.7 kcal mol^{-1}, respectively, similar to the primary bonds on isooctane. The RO—OH bond dissociation enthalpy is 46.0 kcal mol^{-1}.

Entropy and heat capacity contributions versus temperature were determined from the calculated structures, moments of inertia, non-torsion vibrational frequencies, internal rotor parameters, symmetry, electron degeneracy, number of optical isomers and the known mass of each molecule. The calculations used standard formulas from statistical mechanics for the contributions of translation, external rotation and vibrations using the "SMCPS"[78] program. Contributions from internal rotors were substituted for contributions from internal rotor torsion frequencies where barriers were determined to be low, using the Rotator code[11]. As example, the treatment of the rotors for the secondary isooctane hydroperoxide is summarized in Table 3.9.

Table 3.9 Rotor treatment example for the secondary isooctane hydroperoxide

Rotors		Barrier	Treatment
R1	(CH_3)—$(CH_3)_2CCH(OOH)CH(CH_3)_2$	4.2	Hindered Rotor
R2	$(CH_3)_3CCH(OOH)CH(CH_3)$—(CH_3)	2.7	Hindered Rotor
R3	$(CH_3)_3C$—$CH(OOH)CH(CH_3)_2$	5.8	Hindered Rotor
R4	$(CH_3)_3CCH(OOH)$—$CH(CH_3)_2$	9.5	Vibration
R5	$(CH_3)_3CCH($—$OOH)CH(CH_3)_2$	11.3	Vibration
R6	$(CH_3)_3CCH(O$—$OH)CH(CH_3)_2$	6.5	Hindered Rotor

Units: kcal mol^{-1}

Contributions from internal rotors from the Rotator code were substituted for torsion frequencies in the determination of the entropy, and heat capacities versus

temperature. Entropy and heat capacity calculations used structures and non-torsion frequencies from the B3LYP/6-31G(d,p) calculations. The results are summarized in Table 3.10, and Appendix E contains the values over a larger range of temperatures (5-5000 K). Appendix F also contains the thermochemical properties of the species calculated in this work in the NASA polynomial format for use in ChemKin.

Table 3.10 Ideal gas-phase thermochemical properties vs. temperature for the secondary isooctane hydroperoxide, the peroxy radical and the alkyl radicals

Species	S (298 K)	Cp(300)	Cp(400)	Cp(500)	Cp(600)	Cp(800)	Cp(1000)	Cp(1500)
c3ccqcc2	120.91	52.55	66.11	77.99	87.86	103.01	114.09	131.37
c3ccq˙cc2	114.74	53.35	67.00	78.71	88.30	102.79	113.27	129.44
c3˙ccqcc2	120.24	56.64	69.35	80.25	89.20	102.81	112.76	128.39
c3ccqc˙c2	121.61	53.30	66.17	77.53	86.96	101.35	111.80	127.99
c3cccqc2˙	120.91	52.53	66.11	77.99	87.86	103.01	114.09	131.37

Units: S(cal mol^{-1}) and Cp(kcal mol^{-1} K^{-1})

The thermochemical properties of the secondary isooctane hydroperoxide and corresponding radicals were also determined using group additivity (GA) for comparison purposes and calibration of the group additivity method[82]. Tables 3.11 and 3.12 summarize the groups used for the determination of each of the species, which includes Gauche and 1,5 interaction groups.

Table 3.11 Groups included for the determination of the secondary isooctane and the resulting peroxy radicals

c3ccqcc2		**Radicals**			
C/C/H3	5	**c3ccqc˙c2**		**c3ccq˙cc2**	
C/C4	1	Secondary radical	1	Alperox radical	1
C/C2/H/O	1	Rotors	5	Rotors	4
C/C3/H	1	Symmetry	729	Symmetry	729
O/C/O	1	**c3c˙ccqcc2**			
O/H/O	1	Primary radical	1		
Gauche	6	Rotors	5		
H/Repel/15	1	Symmetry	81		
OI	2	**c3ccqcc2˙**			
Rotors	5	Primary radical			
Symmetry	729	Rotors	5		
		Symmetry	243		

Table 3.12 Groups included for the determination of the resulting products

c3ccohcc2		**c3cco˙cc2**		**c3cc=occ2**	
C/C/H3	5	Alkoxy radical	1	C/C/H3	5
C/C4		Rotors	4	C/C3/CO	1
C/C2/H/O	1	Symmetry	729	CO/C2	1
O/C/H	1			C/C2/CO/H	1
C/C3/H	1			H/Repel/15	1
Gauche	6			Rotors	4
OI	1			Symmetry	729
H/Repel/15	1				
Rotors	4				
Symmetry	729				
c=cmcqcc2		**c3cc=cc2**		**c3cc=o**	
CD/H2	1	C/C/H3	5	C/C/H3	3
CD/C2	1	C/C3/CD	1	C/C3/CO	1
C/CD/H3	1	CD/C/H	1	CO/C/H	1
C/C/CD/H/O	1	CD/C2	1	Rotors	2
C/C3/H	1	Rotors	3	Symmetry	81
C/C/H3	2	Symmetry	729		
O/C/O	1				
O/H/O	1				
OI	1				
H/Repel/15	1				
Rotors	4				
Symmetry	27				
cq=cc2		**c2yoxtcc2**		**c3cycocc2**	
CD/H/O	1	C/C/H3	4	C/C/H3	5
CD/C2	1	C/C4	1	C/C4	1
C/CD/H3	2	C/C/H2/O	1	C/C2/H/O	1
O/CD/O	1	O/C2	1	C/C3/O	1
O/H/O	1	C/C3/H	1	O/C2	1
Rotors	2	C/C2/H/O	1	CY/C2O	1
Symmetry	9	OI	1	OI	1
		CY/C3O	1	Rotors	3
		Rotors	3	Symmetry	729
		Symmetry	81		
c3cyccoc					
C/C/H3	4				
C/C4	1				
C/C2/H/O	1				
C/C3/H	1				
C/C/H2/O	1				
O/C2	1				
CY/C3O	1				
OI	1				
Rotors	3				
Symmetry	243				

Comparisons of the group additivity calculations, and the heats of formation obtained by B3LYP/6-31G(d,p) and CBS-QB3 calculations are summarized in Table

3.13. A comparison of the entropy and heat capacity values obtained using group additivity and the results when using SMCPS / Rotator are also summarized in Table 3.14.

Table 3.13 Enthalpies of formation at 298 K obtained using B3LYP/6-31G(d,p) and CBS-QB3, and the values obtained with group additivity

Species	$\Delta_f H^o_{298}$				
	B3LYP/ 6-31G(d,p)	CBS-QB3	Group Additivity		
			No Interaction Terms	Interaction Terms Included	Interaction Terms
c3ccqcc2	-74.13	-75.47	-79.00	-75.10	6 Gauche 1 of 1,5 H-Interaction 2 optical isomers
c3ccq•cc2	-42.80	-42.75	-44.80	-40.90	6 Gauche 1 of 1,5 H-Interaction 2 optical isomers
c3•ccqcc2	-26.96	-26.63	-30.00	-26.10	6 Gauche 1 of 1,5 H-Interaction 2 optical isomers
c3ccqc•c2	-31.94	-31.00	-32.65	-29.75	6 Gauche 1 of 1,5 H-Interaction 2 optical isomers
c3cccqc2•	-27.35	-26.88	-30.00	-26.10	6 Gauche 1 of 1,5 H-Interaction 2 optical isomers

Units: kcal mol^{-1}

The data shows that the heat of formation values from group additivity are within 1-2.5 kcal mol^{-1} of the recommended CBS-QB3 data. The entropy and heat capacity values from group additivity are within 1 - 3.5 cal mol^{-1} K^{-1} of the data calculated using SMCPS and Rotator method for internal rotors. The accuracy of these parameters is important for the kinetics.

Table 3.14 Comparison between the entropy at 298 K and heat capacity at different temperatures obtained using SMCPS and Rotator, and the values obtained with group additivity

Species	S (298 K)	Cp(T)						
		300 K	400 K	500 K	600 K	800 K	1000 K	1500 K
c3ccqcc2								
Therm	119.89	53.77	68.00	80.40	90.35	105.46	116.47	132.93
SMCPS+Rotator	120.91	52.55	66.11	77.99	87.86	103.01	114.09	131.37
c3ccq•cc2								
Therm	117.37	51.72	65.16	76.85	86.26	100.74	111.50	127.85
SMCPS+Rotator	114.74	53.35	67.00	78.71	88.30	102.79	113.27	129.44
c3•ccqcc2								
Therm	123.17	53.00	66.67	78.49	87.95	102.30	112.73	128.06
SMCPS+Rotator	120.24	56.64	69.35	80.25	89.20	102.81	112.76	128.39
c3ccqc•c2								
Therm	124.33	52.27	65.37	77.30	86.96	101.71	112.02	127.70
SMCPS+Rotator	121.61	53.30	66.17	77.53	86.96	101.35	111.80	127.99
c3cccqc2•								
Therm	120.87	53.00	66.67	78.49	87.95	102.30	112.73	129.09
SMCPS+Rotator	120.91	52.53	66.11	77.99	87.86	103.01	114.09	131.37

Units: S(cal mol^{-1}) and Cp(kcal mol^{-1} K^{-1})

3.3 Kinetic Properties

Addition of molecular $^3O_2$ to the secondary radical forms a chemically activated secondary peroxy radical, 3-peroxy-isooctane $(CH_3)_3CCH(OO^•)CH(CH_3)_2$ with a well depth (chemical activation energy) of 33.7 kcal mol^{-1} (please see Figure 3.6, well 1). This peroxy radical adduct can undergo a number of intramolecular reactions before or after it is stabilized under combustion conditions. These intramolecular reactions include:

a) barrierless RO—O cleavage to form an alkoxy radical, $(CH_3)_3CCH(O^•)CH(CH_3)_2$, and an oxygen atom ($O^•$) with an energy of 64.0 kcal mol^{-1} relative to the stabilized peroxy radical and 29.3 kcal mol^{-1} relative to the initial reactant channel. Rate constants for

this simple molecular dissociation / association reaction are determined by variational transition state analysis.

b) intramolecular transfer of the hydrogen atom bonded to the secondary carbon (carbon of the peroxy radical group) to the peroxy radical (ipso carbon) and subsequent R$^{\bullet}$O—OH bond cleavage to form $(CH_3)_3CC(=O)CH(CH_3)_2$ plus $^{\bullet}$OH via tst1 has a barrier of 39.7 kcal mol^{-1}. This is 4.9 kcal mol^{-1} above the channel of the reactants.

c) molecular elimination of $HO_2^{\bullet}$ radical, where the H is from the tertiary carbon, to form isooctene (2-pentene, 2,4,4-trimethyl), $(CH_3)_3CCH=C(CH_3)_2$, via tst2. This has a barrier of 30.5 kcal mol^{-1}. The channel is 13.1 kcal mol^{-1} below the energy of the entrance channel and 20.6 kcal mol^{-1} above the energy of the stabilized peroxy adduct. This channel is a major path.

d) intramolecular transfer of a primary methyl hydrogen atom of the tert-butyl group to the peroxy radical via a 6 member ring transition state structure, tst3 (with a barrier of 23.3 kcal mol^{-1}). This channel is 17.5 kcal mol^{-1} below the energy of the entrance channel, and 16.2 kcal mol^{-1} above the energy of the stabilized peroxy radical. The symmetry of the t-butyl group results in a reaction degeneracy of 9. The resulting primary alkyl radical, $(CH_2^{\bullet})(CH_3)_2CCH(OOH)CH(CH_3)_2$, on the tert-butyl group, can undergo a number of further reactions (please see the PE diagram reaction channels in blue, well 2, Figure 3.7). These include:

   d.1) β-scission of the $(CH_2^{\bullet})(CH_3)_2C-CH(OOH)CH(CH_3)_2$ bond, and subsequent R$^{\bullet}$O—OH cleavage, to form $CH_2=C(CH_3)_2$, $CH(=O)CH_2(CH_3)_2$ and $^{\bullet}$OH via tst4 (with a barrier of 23.3 kcal mol^{-1}) relative to the alkyl radical. The final

products are 37.3 kcal mol^{-1} below the reactants, and 3.6 kcal mol^{-1} below the stabilized peroxy adduct.

d.2) dissociative ring closure to the four member ring ether $(CH_3)_2(CCH_2CH_2O)CH(CH_3)_2$ structure coupled with $^{\bullet}OH$ elimination via tst5 over a barrier of 18.8 kcal mol^{-1}. The final products are 39.0 kcal mol^{-1} below the entrance channel and 5.6 kcal mol^{-1} below the stabilized peroxy adduct.

d.3) β-scission (elimination) of a methyl from $(CH_3)-(CH_2^{\bullet})(CH_3)CCH(OOH)CH(CH_3)_2$ to form $CH_3^{\bullet}$ plus $CH_2=C(CH_3)CH(OOH)CH(CH_3)_2$ via tst6 (with a barrier of 29.3 kcal mol^{-1}). The products are 3.4 kcal mol^{-1} above the entrance channel and 37.1 kcal mol^{-1} above the stabilized peroxy adduct.

d.4) Two plausible intramolecular H-transfers (a.) from the tertiary alkyl radical to form $(CH_3)_3CCH(OOH)C^{\bullet}(CH_3)_2$ via tst15 (with a barrier of 16.8 kcal mol^{-1}) or (b.) from the primary alkyl radical to form $(CH_3)_3CCH(OOH)CH(CH_3)(CH_2^{\bullet})$ via tst16 over a barrier of 19.7 kcal mol^{-1}.

e) intramolecular transfer of a tertiary site hydrogen atom to the peroxy radical via a 5 member ring transition state structure, tst7 (with a barrier of 29.5 kcal mol^{-1}). The barrier is 4.2 and the product is 21.9 kcal mol^{-1} below the entrance channel, and 11.8 kcal mol^{-1} above the stabilized peroxy radical. The resulting tertiary alkyl radical $(CH_3)_3CCH(OOH)C^{\bullet}(CH_3)_2$ can undergo a number of reactions illustrated in the PE diagram reaction channels in green, well 3, Figure 3.8:

e.1) β-scission of the $(CH_3)_3C-CH(OOH)C^{\bullet}(CH_3)_2$ bond to form $CH(OOH)=C(CH_3)_2$ and $(CH_3)_3C^{\bullet}$ via tst8 (with a barrier of 30.5 kcal mol^{-1}).

e.2) dissociative ring closure to form a three member ether ring $(CH_3)_3C(CHCO)(CH_3)_2$ with $^{\bullet}OH$ elimination via tst9 over a barrier of 11.5 kcal mol^{-1}.

e.3) molecular elimination of $HO_2^{\bullet}$ to form isooctane $(CH_3)_3CC=C(CH_3)_2$ via tst10 (with a barrier of 18.4 kcal mol^{-1}).

e.4) intramolecular H-transfer to the primary alkyl radical $(CH_2^{\bullet})(CH_3)_2CCH(OOH)CH(CH_3)_2$ via tst15' (with a barrier of 19.2 kcal mol^{-1})

f) intramolecular hydrogen transfer of a primary site hydrogen atom on the isopropyl group to the peroxy radical via a 6 member ring transition state structure, tst11, with a barrier of 23.6 kcal mol^{-1}. The barrier for this channel is 17.8 kcal mol^{-1} below the reactants, and 15.9 kcal mol^{-1} above the stabilized peroxy radical. The resulting primary alkyl radical $(CH_3)_3CCH(OOH)CH(CH_3)(CH_2^{\bullet})$ can undergo a number of reactions illustrated in the PE diagram reaction channels in red for well 4 in Figure 3.9. these include:

f.1) dissociative ring closure to form the four member ether ring $(CH_3)_3C(CHCHCH_2O)(CH_3)$ structure plus $^{\bullet}OH$ elimination via tst12 over a barrier of 14.3 kcal mol^{-1}.

f.2) β-scission of the $(CH_3)_3CCH(OOH)—CH(CH_3)(CH_2^{\bullet})$ bond to form $CH_2=CHCH_3$ and $(CH_3)_3CC^{\bullet}H(OOH)$, via tst13, which has a barrier of 20.5 kcal mol^{-1}). This $(CH_3)_3CC^{\bullet}H(OOH)$ intermediate will rapidly undergo $RC^{\bullet}O—OH$ cleavage to form $(CH_3)_3CCH(=O)$ and $^{\bullet}OH$.

f.3) β-scission of the $(CH_3)_3CCH(OOH)CH(CH_2^{\bullet})—(CH_3)$ bond to form an hydroperoxide isoheptene $(CH_3)_3CCH(OOH)CH=CH_2$ and $CH_3^{\bullet}$ via tst14 over a barrier of 29.3 kcal mol^{-1}.

f.4) intramolecular H-transfer to $(CH_2^{\bullet})(CH_3)_2CCH(OOH)CH(CH_3)_2$, the primary alkyl radical, via tst16' with a barrier of 19.1 kcal mol^{-1}.

The formation of the tertiary hydroperoxide alkyl radical $(CH_3)_3CCH(OOH)C^{\bullet}(CH_3)_2$ (tst7, Ea=29.5 kcal mol^{-1}), has a higher barrier than the barriers for the formation of the primary alkyl hydroperoxides $(CH_2^{\bullet})(CH_3)_2CCH(OOH)CH(CH_3)_2$ and $(CH_3)_3CCH(OOH)CH(CH_3)(CH_2^{\bullet})$ (tst3, Ea=23.3 kcal mol^{-1} and tst11, Ea=23.6 kcal mol^{-1}, respectively). While the formation of the primary radical alkyl hydroperoxides have lower barriers, their further reaction has to overcome higher product formation barriers and the more favorable reverse reaction can result in a near equilibrium distribution of the isomers, depending on temperature and pressure.

However, after the higher barrier path hydroperoxide - tertiary alkyl radical is formed, low barrier reactions through tst9 and tst10 lead to the formation of a three member ether ring $(CH_3)_3C(CHCO)(CH_3)_2$ with elimination of an $^{\bullet}OH$ radical (Ea=11.5 kcal mol^{-1}), or the molecular elimination (β-scission) of $HO_2^{\bullet}$ to form isooctane, $(CH_3)_3CC=C(CH_3)_2$ (Ea=18.4 kcal mol^{-1}).

$^{\bullet}OH$ transfer reactions are not included in this study, since they have significantly higher barrier than the ether formation paths[108].

Figures 3.6 through 3.9 provide a detailed perspective of each of the alkyl radical-hydroperoxide wells in this system and Figure 3.10 represents the overall potential energy diagram for the system.

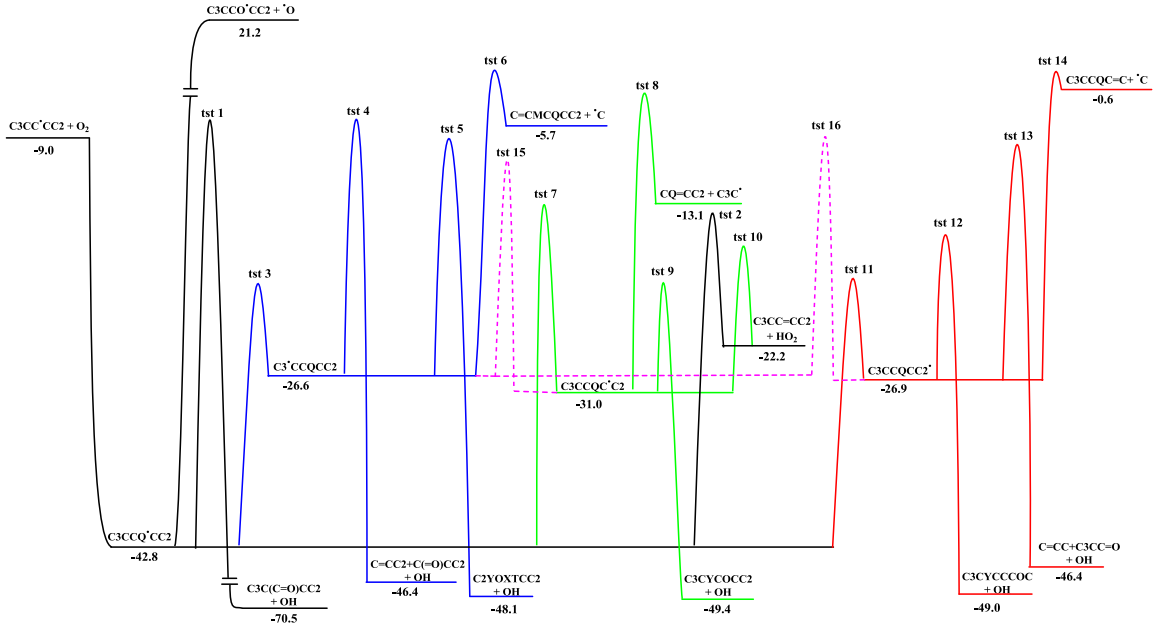

Figure 3.10 Potential energy diagram for the $(CH_3)_3CCH^{\bullet}CH(CH_3)_2 + {}^3O_2$ system. Units: kcal mol^{-1}, 298 K (CBS-QB3 level of theory)

High-pressure rate constant parameters have been calculated in the modified Arrhenius equation form: $k = AT^n \exp(-Ea/RT)$.

Classical canonical transition state theory was applied to determine the barriers of the transition state structures 1-16 for the determination of the rate constants. Table 3.15 summarizes the activation energies calculated.

Table 3.15 Calculated activation energies of the transition state structures from the studied reaction paths

Transition State Structures	Ea		Description
	B3LYP/ 6-31G(d,p)	CBS-QB3	
tst1	40.8	38.7	$O^{\bullet}$ elimination
tst2	26.2	30.5	$HO_2^{\bullet}$ elimination
tst3	24.3	23.3	Intramolecular H transfer
tst4	19.4	23.3	$^{\bullet}OH$ elimination and β-scission
tst5	16.3	18.8	$^{\bullet}OH$ elimination and cyclization
tst6	28.5	29.3	$CH_3^{\bullet}$ elimination
tst7	30.0	29.5	Intramolecular H transfer
tst8	26.5	30.5	β-scission
tst9	9.9	11.5	$^{\bullet}OH$ elimination and cyclization
tst10	14.6	18.4	$^{\bullet}OH$ elimination and β-scission
tst11	24.5	23.6	Intramolecular H transfer
tst12	12.6	14.3	$^{\bullet}OH$ elimination and cyclization
tst13	21.0	20.5	$^{\bullet}OH$ elimination and β-scission
tst14	28.2	29.3	$CH_3^{\bullet}$ elimination
tst15	14.8	16.8	Intramolecular H transfer
tst16	17.4	19.7	Intramolecular H transfer

Units: kcal mol^{-1}

The formation of $(CH_3)_3CCH(OO^{\bullet})CH(CH_3)_2$ ($(CH_3)_3CCH^{\bullet}CH(CH_3)_2 + {}^3O_2 \rightarrow (CH_3)_3CCH(OO^{\bullet})CH(CH_3)_2$) and the reverse of the decomposition reaction of $(CH_3)_3CCH(OO^{\bullet})CH(CH_3)_2$ to form $(CH_3)_3CCH(O^{\bullet})CH(CH_3)_2$ ($(CH_3)_3CCH(OO^{\bullet})CH(CH_3)_2 \rightarrow (CH_3)_3CCH(O^{\bullet})CH(CH_3)_2 + O^{\bullet}$) are barrier-less reactions, and variational transition state theory was applied for the determination of these rate constants. Figures 3.11 and 3.12 show the reaction potentials for the two simple dissociation reactions.

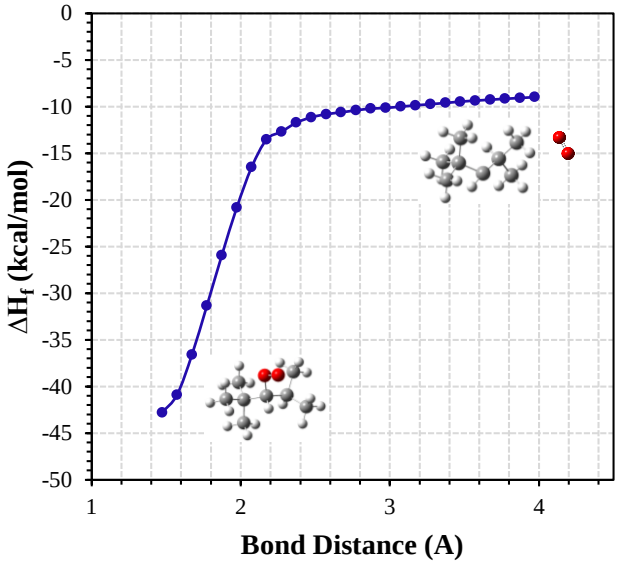

Figure 3.11 Reaction coordinate (dissociation curve) for the dissociation reaction $(CH_3)_3CCH(OO^{\bullet})CH(CH_3)_2 \rightarrow (CH_3)_3CCH^{\bullet}CH(CH_3)_2 + {}^3O_2$, as the C—O bond increases, calculated at UB3LYP/6-31G(d,p)

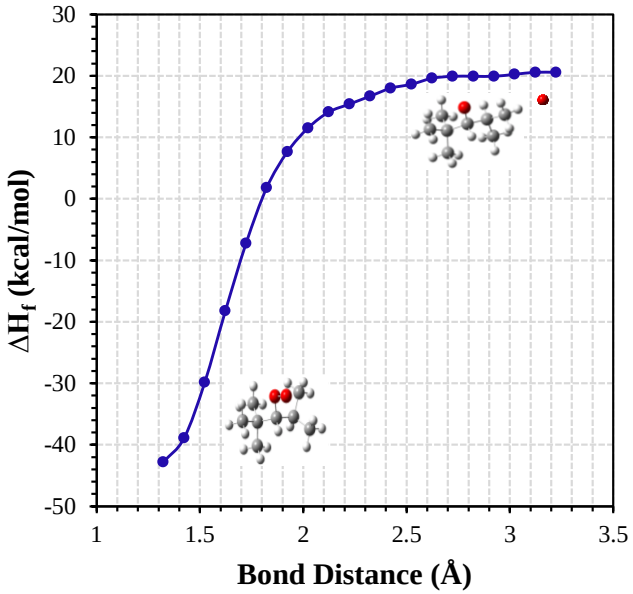

Figure 3.12 Reaction coordinate (dissociation curve) for the dissociation reaction $(CH_3)_3CCH(O^{\bullet})CH(CH_3)_2 + {}^{\bullet}OH \rightarrow (CH_3)_3CCH(OO^{\bullet})CH(CH_3)_2$, as the O—O bond increases, calculated at UB3LYP/6-31G(d,p)

High pressure rate constants were calculated from the thermochemical properties of the reactants, and the transition state structures. The high pressure rate constants calculated using these transition state structures are summarized in Table 3.16.

Table 3.16 Isooctane oxidation high pressure rate constants

Reactions	**A**	**n**	**Ea**
c3cc•cc2+O_2	2.83 10^{11}	0.2	-1.6
c3ccq•cc2 → c3cc•cc2+O_2	1.01 10^{18}	-1.1	38.6
c3ccq•cc2 → c3•ccqcc2	4.96 10^{11}	0.3	23.3
c3ccq•cc2 → c3ccqc•c2	5.39 10^{12}	0.1	30.3
c3ccq•cc2 → c3ccqcc2•	1.65 10^{10}	0.7	23.5
c3ccq•cc2 → c3cc=cc2 + HO_2•	1.84 10^{13}	-0.2	31.5
c3ccq•cc2 → c3cco•cc2 + •O	2.17 10^{12}	0.5	63.2
c3ccq•cc2 → c3cc=occ2 + •OH	6.70 10^{12}	0.3	39.6
c3•ccqcc2 → c3ccqc•c2	5.80 10^{10}	0.1	15.1
c3•ccqcc2 → c3ccqcc2•	1.17 10^{10}	1.0	18.5
c3•ccqcc2 → c=cmcqcc2 + •CH_3	1.49 10^{12}	0.3	30.0
c3•ccqcc2 → c2yoxtcc2 + •OH	9.28 10^{11}	-0.1	21.9
c3•ccqcc2 → c=cc2 + c=occ2 + •OH	2.53 10^{11}	0.0	23.6
c3ccqc• c2 → cq=cc2 + c3c•	7.81 10^{11}	0.6	28.5
c3ccqc•c2 → c3cc=cc2 + HO_2•	7.46 10^{11}	0.3	14.3
c3ccqc•c2 → c3cycocc2 + •OH	7.13 10^{13}	0.4	8.6
c3ccqcc2• → c3cycccoc + •OH	3.18 10^{11}	-0.1	15.5
c3ccqcc2• → c=cc + c3cc=o + •OH	7.97 10^{11}	0.1	20.9
c3ccqcc2• → c3ccqc=c + •CH_3	1.49 10^{12}	0.3	36.4

Units: A(mol cm^{-3} s^{-1}), Ea (kcal mol^{-1})

The reactions involving the primary alkyl radicals – $(CH_2•)(CH_3)_2CCH(OOH)CH(CH_3)_2$ and $(CH_3)_3CCH(OOH)CH(CH_3)(CH_2•)$ – have a degeneracy of 9 and 6, respectively due to the methyl groups. The degeneracy was included in the rate constants.

A comparison was carried out between the rate constants obtained in this study, and generic rate constants for model (smaller) systems in the literature[108,109]. The literature values tend to be slightly lower than the calculated values in this study, and this is due, in part, to lower bond dissociation enthalpies resulting in lower barriers. The lower bond dissociation enthalpies are probably due to release of some strain from the branching in the isooctane hydroperoxide/peroxy radical system. This data is summarized in Table 3.17 and comparisons of the rate constants are illustrated in Figures 3.13 to 3.16.

Table 3.17 Comparison of the high-pressure rate constants obtained in this study with literature values

Reactions	A	n	Ea	Ref.
c3ccq•cc2 → c3cc•cc2+O_2				
	1.01 x10^{18}	**-1.1**	**38.6**	**This work**
$RO_2^•$ → R•(s) + O_2	6.85 x10^{25}	-3.29	38.2	109
$RO_2^•$ → R•(s) + O_2	2.15 x10^{25}	-3.21	37.61	108
c3ccq•cc2 → c3cc=cc2 + $HO_2^•$				
	1.84 x10^{13}	**-0.2**	**31.5**	**This work**
$RO_2^•$ → olefin + $HO_2^•$	1.30 x10^{11}	0.5	31.0	109
$RO_2^•$ → olefin (st) + $HO_2^•$	7.06 x10^{12}	0.0	31.35	108
c3ccq•cc2 → c3cc=occ2 + •OH				
	6.7 x10^{12}	**0.3**	**39.6**	**This work**
COO• → C=O + •OH (1-3t rate)	4.87 x10^{5}	2.18	35.1	109
c3ccq•cc2 → c3•ccqcc2				
	4.96 x10^{11}	**0.3**	**23.3**	**This work**
1-5p rate-rule	1.46 x10^{8} *(1.62 x10^{7} x 9)*	1.23	21.5	109
1,5 H-shift, sp	3.53 x10^{12} *(3.92 x10^{11} x 9)*	0.0	22.57	108
1,5 H-shift, (1,5p)	4.5 x10^{8} *(5.01 x10^{7} x 9)*	1.1	21.9	110
c3ccq•cc2 → c3ccqcc2•				
	1.65 x10^{10}	**0.7**	**23.5**	**This work**
1-5p rate-rule	9.72 x10^{7} *(1.62 x10^{7} x 6)*	1.23	21.5	109
1,5 H-shift, sp	2.53 x10^{12} *(3.92 x10^{11} x 6)*	0.0	22.57	108
1,5 H-shift, (1,5p)	3.0 x10^{8} *(5.01 x10^{7} x 6)*	1.1	21.9	110
c3ccq•cc2 → c3ccqc•c2				
	5.39 x10^{12}	**0.1**	**30.3**	**This work**
1-4t rate-rule	2.52 x10^{7}	1.39	25.3	109
1,4 H-shift, st	5.41 x10^{11}	0.0	27.2	108
1,4 H-shift, (1,4t)	7.45 x10^{9}	0.6	27.3	110

Units: A(mol cm^{-3} s^{-1}), Ea (kcal mol^{-1})
R(s): secondary radical site

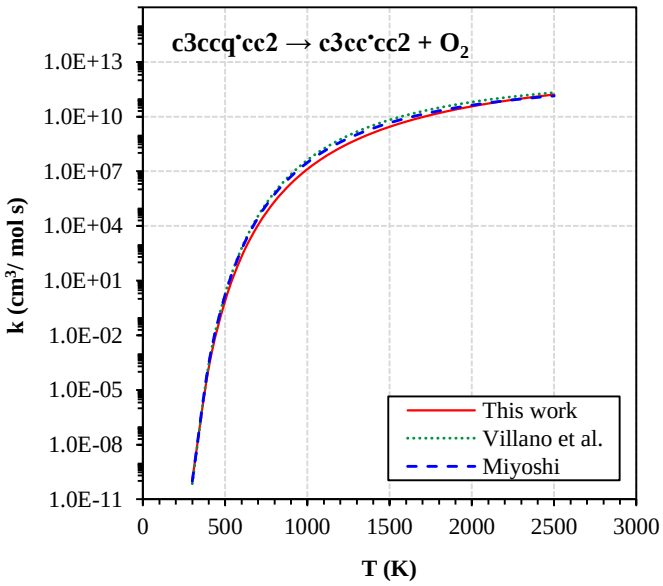

Figure 3.13 Comparison of the high-pressure rate constant of the dissociation reaction (c3ccq•cc2 → c3cc•cc2 + $^3O_2$) obtained in this work and the literature values[108,109]

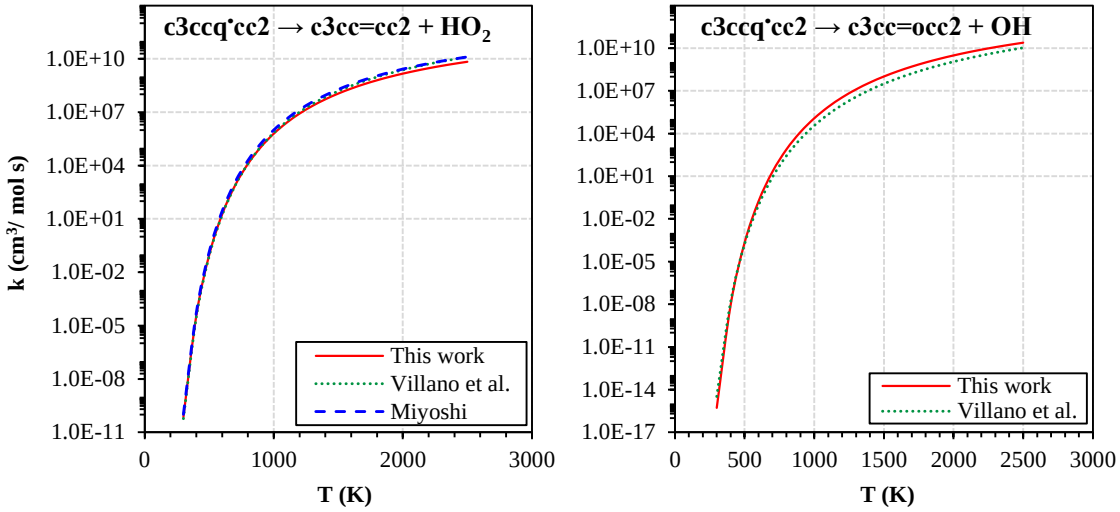

Figure 3.14 Comparison of the high-pressure rate constants of the $HO_2^•$ and $^•OH$ elimination reactions obtained in this work and the literature values[108,109]

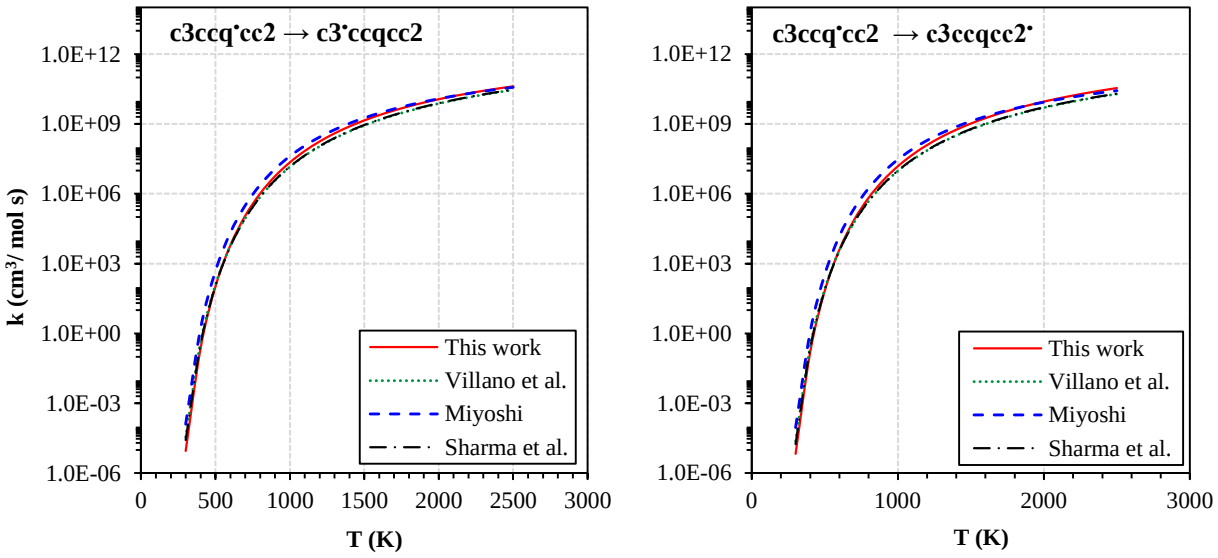

Figure 3.15 Comparison of the high-pressure rate constants for the intramolecular hydrogen transfers obtained in this work with literature values (c3ccq•cc2 → c3•ccqcc2, left, and c3ccq•cc2 → c3ccqcc2•, right)[108-110]

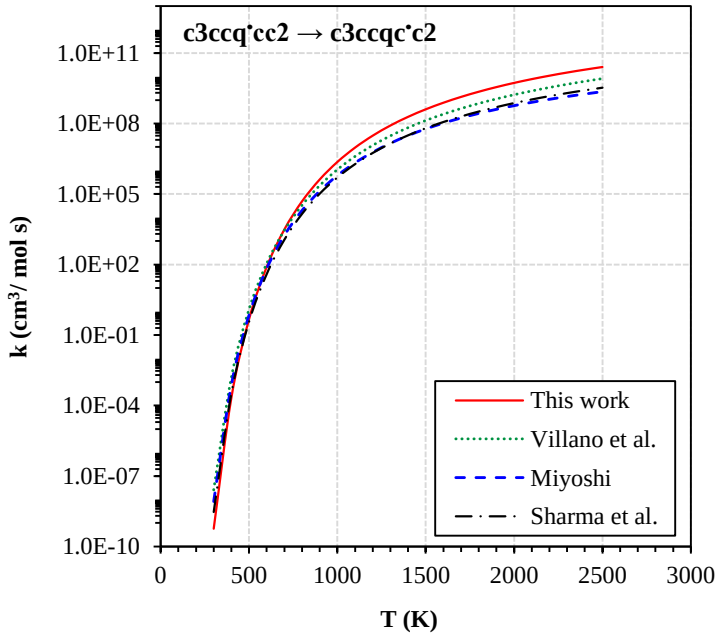

Figure 3.16 Comparison of the high-pressure rate constants for the intramolecular hydrogen transfers obtained in this work with literature values (c3ccq•cc2 → c3ccqc•c2)[108-110]

The variational transition state results for the molecular dissociation of the initial isooctane peroxy radical adduct reacting back to the secondary isooctane radical and $^3O_2$: $(CH_3)_3CCH(OO^{\bullet})CH(CH_3)_2 \rightarrow (CH_3)_3CCH^{\bullet}CH(CH_3)_2 + {}^3O_2$, ($k=1.01\ x10^{18}\ T^{1.1}\ e^{(-38.6/RT)}$) are in good agreement with the generic rules published by Miyoshi[108] ($k=2.15\ x10^{25}\ T^{-3.21}\ e^{(-37.6/RT)}$) and Villano et al.[109] ($k=6.85\ x10^{25}\ T^{-3.29}\ e^{(-38.2/RT)}$), as shown in Figure 3.13.

The direct molecular $HO_2^{\bullet}$ elimination of the isooctane peroxy radical to form isooctene, $(CH_3)_3CCH(OO^{\bullet})CH(CH_3)_2 \rightarrow (CH_3)_3CCH{=}C(CH_3)_2 + HO_2^{\bullet}$, is in good agreement with the generic rules available in the literature[108,109]. The results from this study ($k=1.84\ x10^{13}\ T^{-0.2}\ e^{(-31.5/RT)}$) show to have the same order of magnitude as the literature values ($k=1.30\ x10^{11}\ T^{0.5}\ e^{(-31.0/RT)}$)[109] and ($k=7.06\ x10^{12}\ e^{(-31.4/RT)}$)[108], Figure 3.14 (left).

The intramolecular transfer of the hydrogen atom bonded on the secondary (ipso) carbon to the peroxy oxygen radical and subsequent R$^{\bullet}$O—OH bond cleavage to form $(CH_3)_3CC(=O)CH(CH_3)_2$ plus $OH^{\bullet}$ ($k=6.7\ x10^{12}\ T^{0.3}\ e^{(-39.6/RT)}$) is in good agreement with the literature values ($k=4.87\ x10^{5}\ T^{2.18}\ e^{(-35.1/RT)}$)[109] as illustrated in Figure 3.14 (right).

A comparison of the intramolecular hydrogen transfer reactions to form the primary alkyl hydroperoxides is presented in Figure 3.15. The results from this study are in very good agreement with the generic rules presented by Villano et al.[109] and Miyoshi[108], and the values presented by Sharma et al.[110]. The values of Villano et al., Miyoshi and Sharma et al. are presented per hydrogen atom, and therefore for comparison with the results from this study, their pre-exponential factor (A) was multiplied by 9 for the tert-butyl methyls, and by 6 for the isopropyl methyls. The hydrogen transfer kinetic parameters for the formation of the primary radicals from this

study are $k=4.96\ x10^{11}\ T^{0.3}\ e^{(-23.3/RT)}$ and $k=1.65\ x10^{10}\ T^{0.7}\ e^{(-23.5/RT)}$, compared to $k=1.46\ x10^{8}\ T^{1.23}\ e^{(-21.5/RT)}$ and $k=9.72\ x10^{7}\ T^{1.23}\ e^{(-21.5/RT)}$ obtained by Villano et al.[109], $k=3.53\ x10^{12}\ e^{(-22.6/RT)}$ and $k=2.53\ x10^{12}\ e^{(-22.6/RT)}$ calculated by Miyoshi[108], and $k=4.50\ x10^{8}\ T^{1.1}\ e^{(-21.9/RT)}$ and $k=3.0\ x10^{8}\ T^{1.1}\ e^{(-21.9/RT)}$ determined by Sharma et al.[110]. The formation of the tertiary alkyl radical results on a rate constant of $k=5.39\ x10^{12}\ T^{0.1}\ e^{(-30.3/RT)}$, compared to the literature values[108-110] of $k=2.52\ x10^{7}\ T^{1.39}\ e^{(-25.3/RT)}$, $k=5.41\ x10^{11}\ e^{(-27.2/RT)}$ and $k=7.45\ x10^{9}\ T^{0.6}\ e^{(-27.3\ /RT)}$. Comparison of the intramolecular hydrogen transfer reaction to form the tertiary alkyl hydroperoxide is presented in Figure 3.16.

Kinetic parameters for the bimolecular chemical activation reactions, stabilization of each adduct (isomer) and for the subsequent unimolecular thermal dissociation reactions of the stabilized isomers were calculated by using a multifrequency quantum Rice-Ramsperger- Kassel (qRRK) analysis for $k(E)$ with the steady-state assumption on the energized adduct(s)[103]. The reduced set of three vibrational frequencies used to calculate the density of states are described in Table 3.18.

Table 3.18 Reduced frequencies of the isooctane oxidation system species

Species	Frequency	# Vibration Modes
c3ccq•cc2	1231.2	31.766
	3096.5	17.036
	1032.1	72.500
c3•ccqcc2	365.2	25.683
	1251.3	29.990
	3136.0	16.828
c3ccqc•c2	359.3	24.232
	1260.9	31.219
	3092.5	17.050
c3ccqcc2•	399.1	27.959
	1312.6	28.814
	3323.7	15.726

Units: cm^{-1}

The master equation model was used to calculate the collisional deactivation (or activation) of the energized adduct (for the chemical activation and the dissociation). It uses ΔE_{down} for the collisional deactivation with N_2 as the third body. The parameters used for the qRRK analysis are listed in Table 3.19. A detailed description of the method is included in reference[90].

Table 3.19 Parameters used in determination of the pressure and temperature collision effects on stabilization / activation kinetics

Parameters		
T_{range} (K)		300-2100
P_{range} (atm)		0.001-100
Bath gas	Species	N_2
	σ (A)	3.54
	e/k (K)	97.5
σ (A)		6.539
e/k (K)		584.0
ΔE_{down} (cal mol^{-1})		900
Integration interval (kcal)		1.0
E_{head} (kcal mol^{-1})		75

Figure 3.17 presents a comparison of the results for the secondary isooctane radical plus $^3O_2$ association by different high pressure rate constants from the literature[108,111] and this study for the formation of the adduct, and Table 3.20 summarizes the rate constants used. The results from this study ($k=2.83\ x10^{13}\ T^{0.15}\ e^{(1.61/RT)}$) show good agreement with the generic rule determined by Miyoshi ($k=3.49\ x10^{14}\ T^{-0.82}\ e^{(-0.54/RT)}$)[108]. The literature data from Chen et al.[111] represents the rate constant for the $^3O_2$ addition on a primary alkyl radical ($k=8.00\ x10^{13}T^{-0.44}$), which is a difference reaction system.

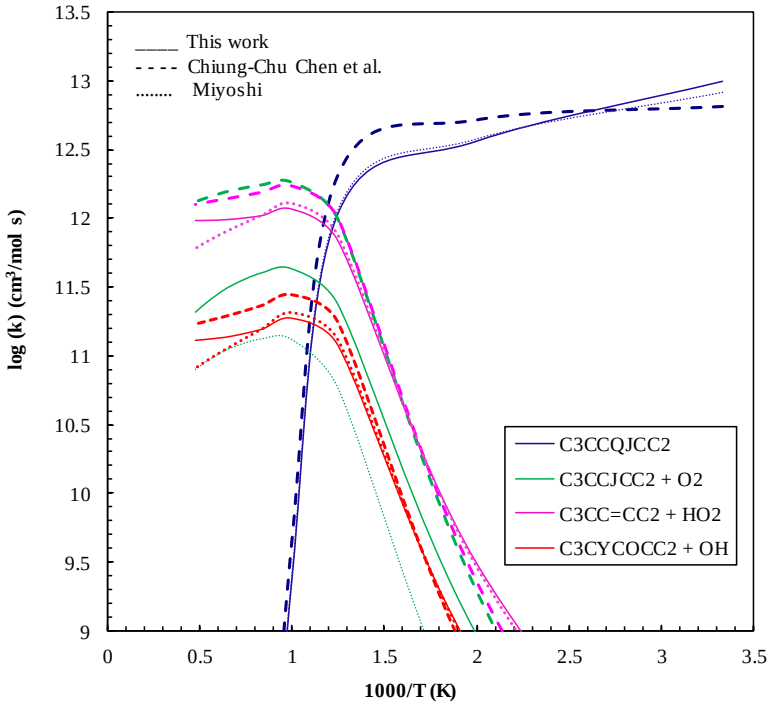

Figure 3.17 Comparison of the chemical activation results obtained using different rate constant values for the addition reaction $(CH_3)_3CCH^{\bullet}CH(CH_3)_2 + {}^3O_2 \rightarrow (CH_3)_3CCH(OO^{\bullet})CH(CH_3)_2$ at 1 atm, obtained using the variational transition state analysis in this work, and the one obtained by Miyoshi et al.[108] for the secondary radical + $^3O_2$ and by Chen et al.[111] for the n-propyl primary radical + $^3O_2$

Table 3.20 High-Pressure rate constants for $R^{\bullet} + O_2$

Reactions	**A**	**N**	**Ea**	**Ref.**
c3cc$^{\bullet}$cc2+O_2	**2.83 10^{13}**	**0.15**	**-1.61**	**This work**
$R^{\bullet}$(s) + O_2	3.49 10^{14}	-0.82	0.54	108
$R^{\bullet}$(p) + O_2	8.00 10^{13}	-0.44	0	111

$R^{\bullet}$(s) = secondary radical
$R^{\bullet}$(p) = primary radical

Rate constants to the different isomers and product sets versus temperature and pressure obtained by applying the qRRK / Master Equation analysis for the determination of chemical activation reaction of the secondary isooctane and $^3O_2$ are presented in Figures 3.18 to 3.20. All the calculated pressure and temperature dependent rate constants are summarized in Appendix F.

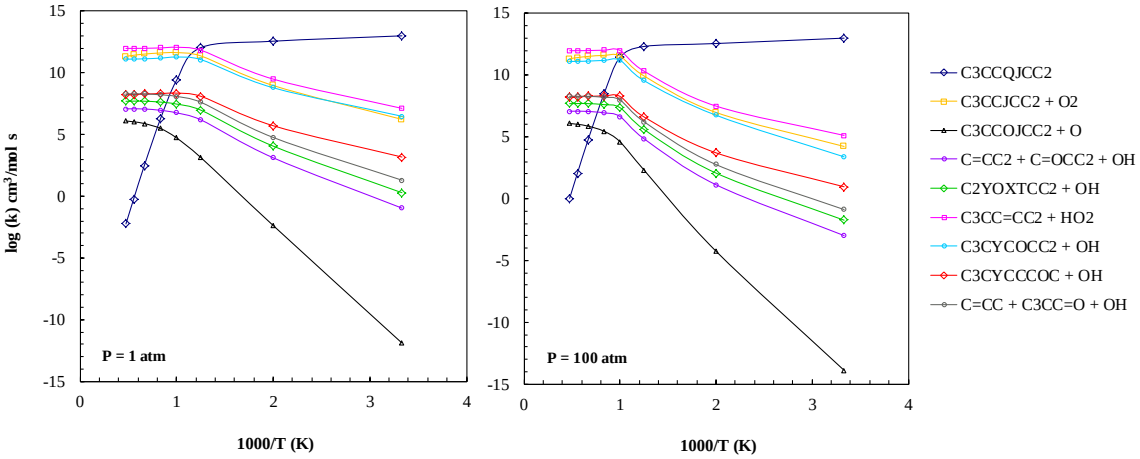

Figure 3.18 Calculated chemical activation rate constants vs. temperature at 1 atm (left) and 100 atm (right)

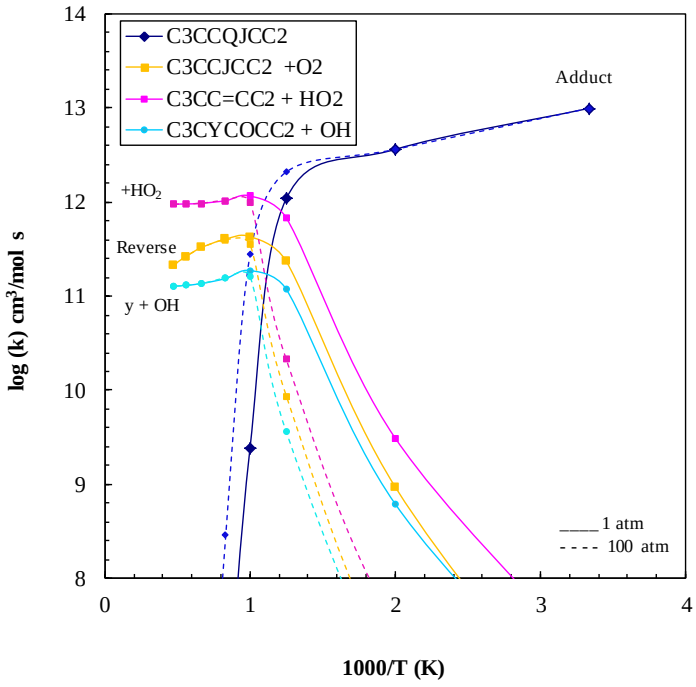

Figure 3.19 Comparison of the chemical activation rate constants vs. temperature at 1 atm and 100 atm

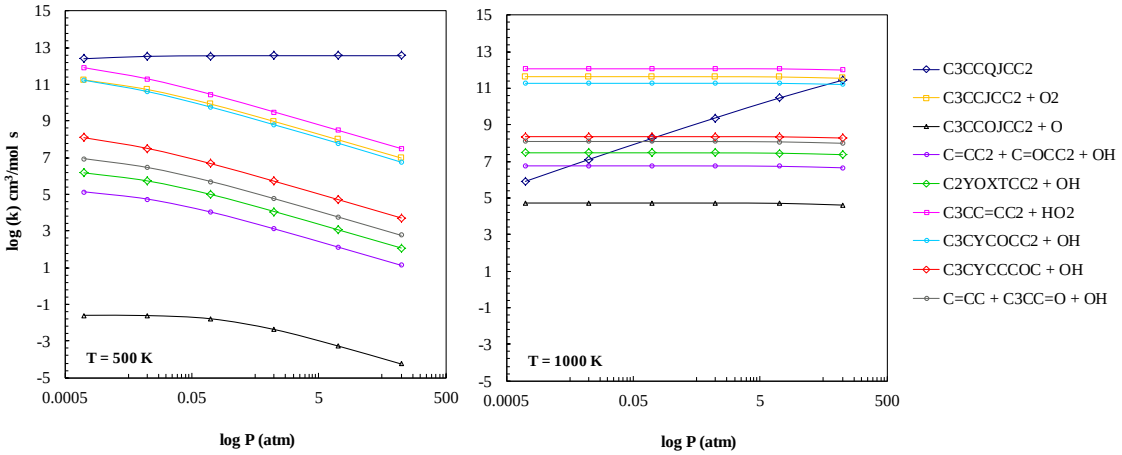

Figure 3.20 Calculated chemical activation rate constants vs. pressure at 500 K (right) and 1000 K (left)

Figure 3.18 provides the results of the chemical activation, representing the rate constants versus temperature for two different pressures (1 atm and 100 atm), and Figure 3.19 provides a comparison of these rate constants at the two studied pressures. Figure 3.20 represents the chemical activation rate constants versus pressure for two different temperatures (500 K and 1000 K). The results indicated in the figures, at both pressures, and the higher temperatures, show that the main forward reaction channel is the formation of $(CH_3)_3CCH=C(CH_3)_2$+ $HO_2^{\bullet}$, through transition state structures tst2 and tst10. The formation of the cyclic ether $(CH_3)_3C(CHCO)(CH_3)_2$ through transition state structure tst9 is the second more important channel, which proceeds from the intramolecular H transfer of the peroxy radical to form $(CH_3)_3CCH(OOH)C^{\bullet}(CH_3)_2$ through transition state structure tst7.

At high temperatures significant fraction of the initial energized peroxy radical adduct formed dissociates back to reactants (non reaction). At low temperatures the formation of the stabilized peroxy adduct is the dominant reaction channel and at high

temperatures. The formation of the cyclic ethers $(CH_3)_3C(CHCO)(CH_3)_2$, $(CH_3)_3C(CHCO)(CH_3)_2$, $(CH_3)_3C(CHCHCH_2O)(CH_3)$ plus $^{\bullet}OH$ radical, is also important.

The isomers formed by hydrogen transfer reactions from the energized and the stabilized peroxy radical can undergo dissociation reactions for the formation of several products *(P_1, P_2,…P_N)*. While the qRRK Master Equation code for the chemical activation analysis considers reaction of each of the chemically activated adducts (isomers) to all products, the Master Equation analysis for the stabilized isomer reactions is more limited. It considers each of the single reaction steps out of the well that the stabilized isomer can undergo directly, but does not consider subsequent reactions of these first product(s) , as described by Sheng et al.[90].

Figures 3.21 shows the temperature dependence of the rate constants obtained at 1 atm and 100 atm for the products (left) and the isomers (right). Figure 3.22 illustrates the pressure dependence of the rate constants at two different temperatures (500 K and 1000 K), for products (left) and isomers (right).

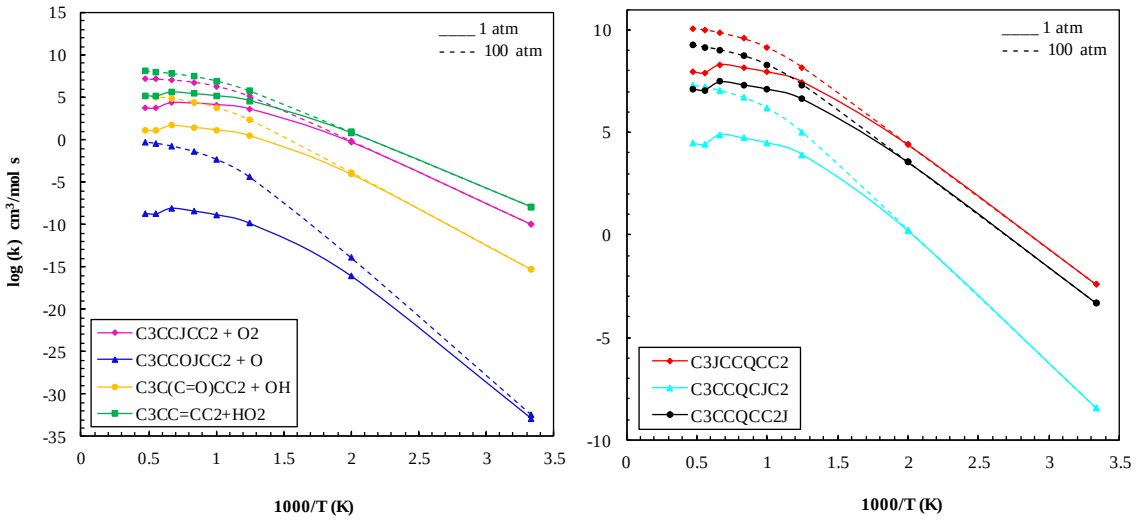

Figure 3.21 Calculated dissociation rate constants of $(CH_3)_3CCH(OO^{\bullet})CH(CH_3)_2$ vs. temperature at 1 atm and 100 atm to the different products (right) and isomers (left)

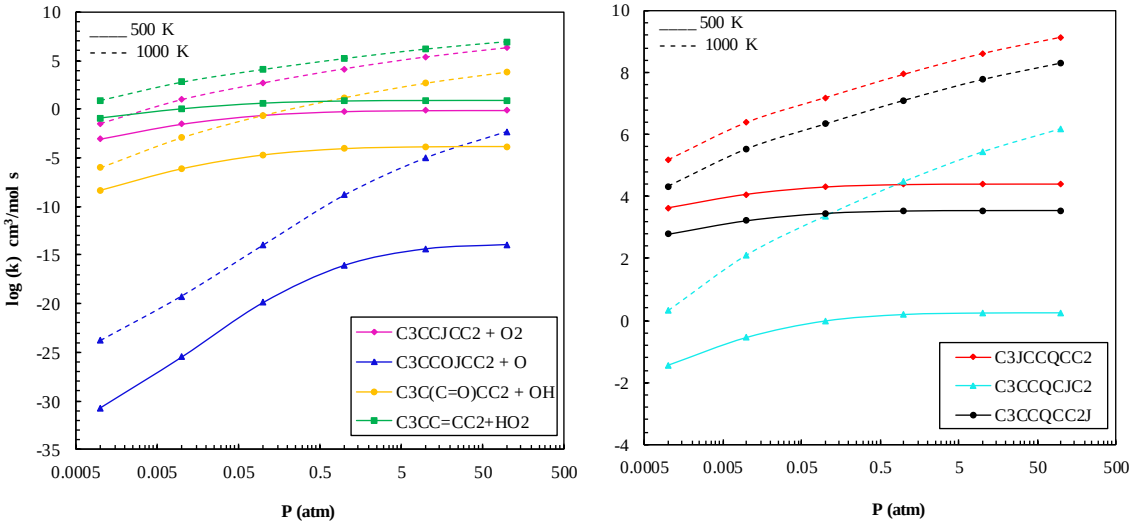

Figure 3.22 Calculated dissociation rate constants of $(CH_3)_3CCH(OO^{\bullet})CH(CH_3)_2$ vs. pressure at 500 K and 1000 K to form the different products (right) and isomers (left)

Figures 3.23 to 3.25 represent the dissociation rate constants for each of the studied isomers. At both pressures the dissociation of $(CH_3)_3CCH(OO^{\bullet})CH(CH_3)_2$ to form $(CH_3)_3CCH{=}C(CH_3)_2 + HO_2^{\bullet}$ and the cyclic ether $(CH_3)_3C(CHCHCH_2O)(CH_3) + {}^{\bullet}OH$ are the main reaction channels, through the lowest two transition state structures tst10 and tst9, respectively.

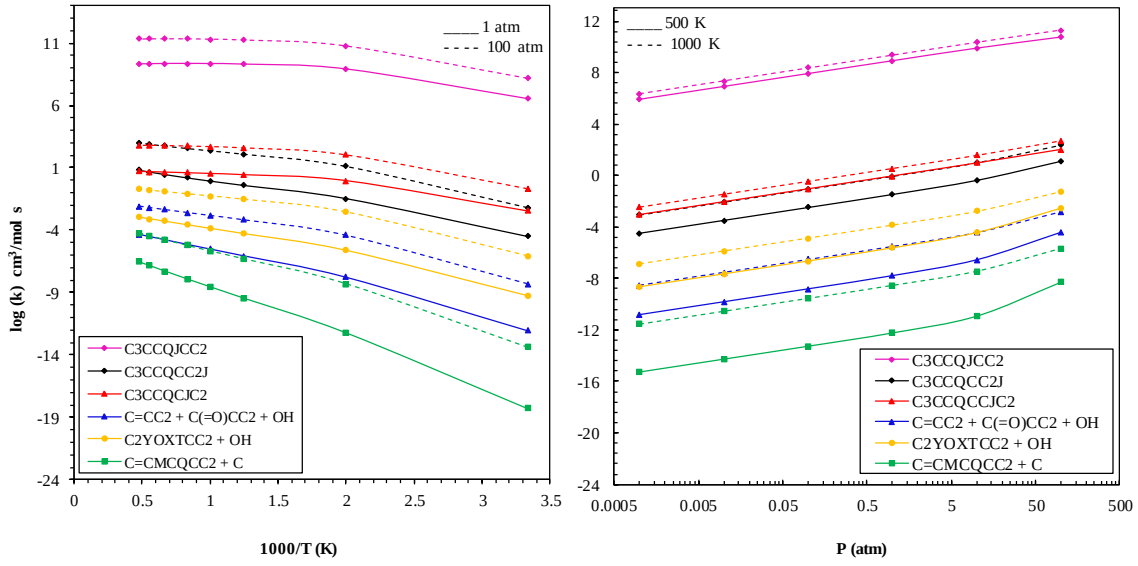

Figure 3.23 Calculated dissociation rate constants of $(CH_2^{\bullet})(CH_3)_2CCH(OOH)CH(CH_3)_2$ vs. temperature at 1 atm and 100 atm (right) and vs. pressure at 500 K and 1000 K (left)

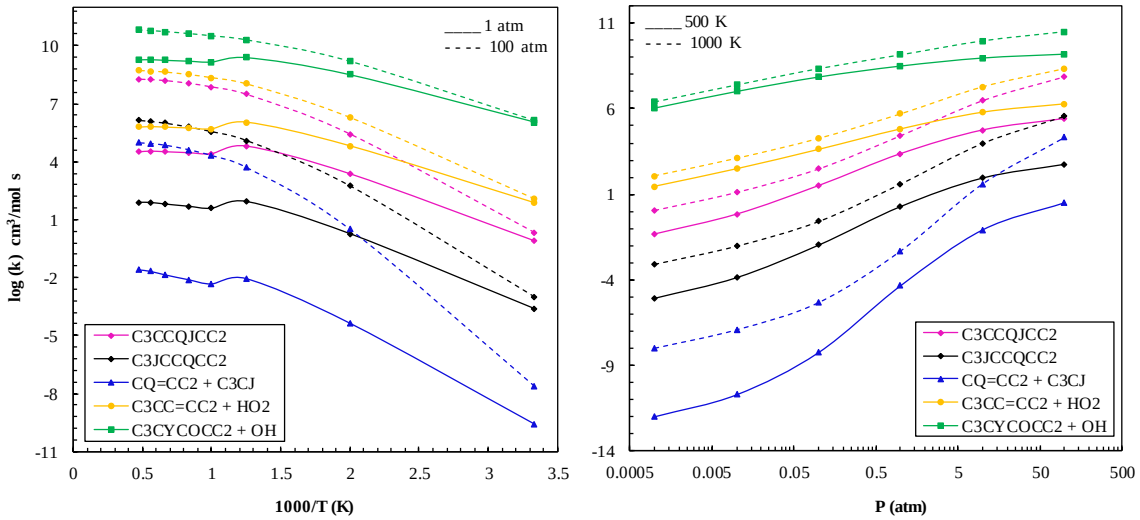

Figure 3.24 Calculated dissociation rate constants of $(CH_3)_3CCH(OOH)C^{\bullet}(CH_3)_2$ vs. temperature at 1 atm and 100 atm (right) and vs. pressure at 500 K and 1000 K (left)

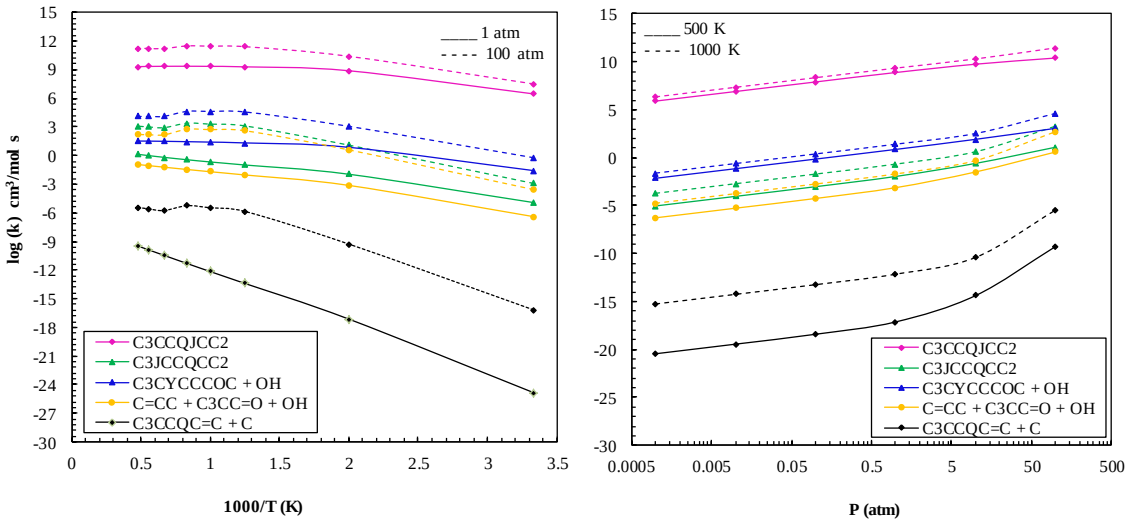

Figure 3.25 Calculated dissociation rate constants of $(CH_3)_3CCH(OOH)CH(CH_3)(CH_2^{\bullet})$ vs. temperature at 1 atm and 100 atm (right) and vs. pressure at 500 K and 1000 K (left)

3.4 Summary

Thermochemical parameters were determined at the B3LYP/6-31G(d,p) and CBS-QB3 level of theory for the secondary isooctane radical, the secondary isooctane hydroperoxide, the corresponding peroxy radical, and three hydroperoxy alkyl radical adducts. Thermochemical data was also determined for 10 product sets from unimolecular reactions of the adducts. Transition state structures and rate constants were determined for each of the reaction paths (illustrated in the potential energy diagram of Figure 3.10). The identified main reaction channels are summarized in Figure 3.26.

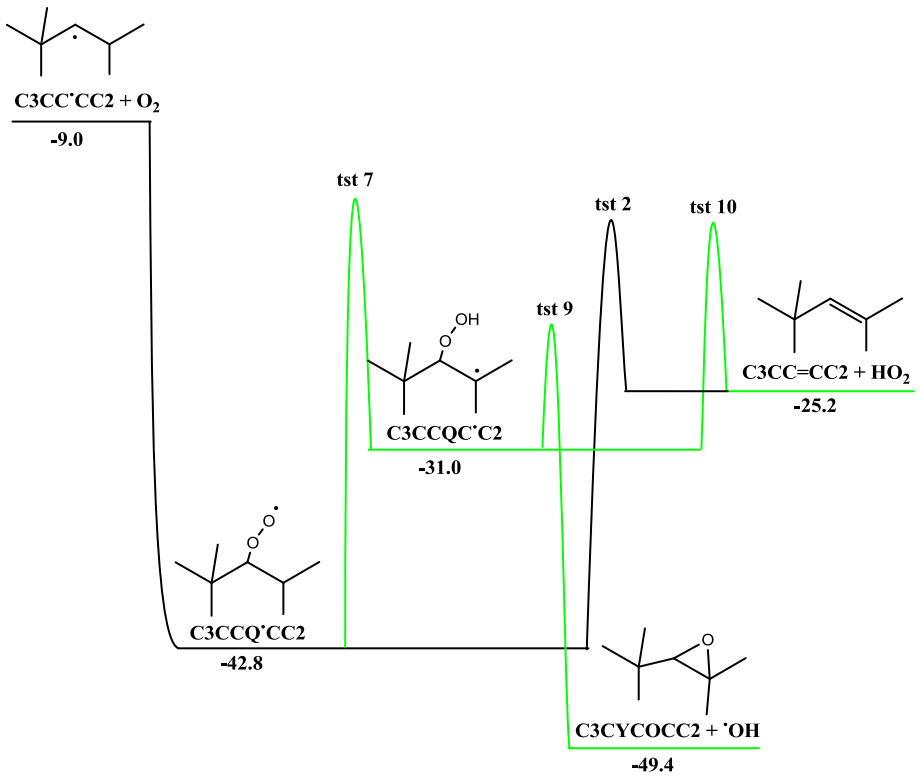

Figure 3.26 Potential energy diagram of the main products, isooctene + $HO_2^{\bullet}$ and $(CH_3)_3C(CHCO)(CH_3)_2 + {}^{\bullet}OH$

The kinetic analysis shows that at low and high pressures (in the range of 1-100 atm), and temperatures above 1000 K, the main reaction channels are the formation of

isooctene $(CH_3)_3CCH=C(CH_3)_2$ + $HO_2^{\bullet}$, through transition state structures tst2 and tst10, and the formation of the cyclic ether $(CH_3)_3C(CHCO)(CH_3)_2$ through transition state structure tst9 is the second more important channel, which proceeds from the intramolecular hydrogen transfer of the peroxy radical to form $(CH_3)_3CCH(OOH)C^{\bullet}(CH_3)_2$ through transition state structure tst7 (see Figure 3.25). At low temperatures (below 1000 K) the formation of the adduct - $(CH_3)_3CCH(OO^{\bullet})CH(CH_3)_2$ - is the dominant reaction channel.

The study highlights the importance of the formation of isooctane in the oxidation of isooctane at all temperatures. Moreover, this work notes that at low temperatures, the formation of the cyclic ethers - $(CH_3)_3C(CHCO)(CH_3)_2$, $(CH_3)_3C(CHCO)(CH_3)_2$, $(CH_3)_3C(CHCHCH_2O)(CH_3)$ - is important, and need to be well characterized and included in combustion mechanisms, as indicated also in experimental studies.

CHAPTER 4

UNIMOLECULAR DISSOCIATION AND OXIDATION OF TRICYCLODECANE

4.1 Overview

Exo-tricyclo[5.2.1.$0^{2,6}$]decane or *exo*-tetrahydrodicyclopentadiene (TCD, $C_{10}H_{16}$) is the principal component of the high-energy density hydrocarbon fuel commonly identified as JP-10. The structure of tricyclodecane with atom numbering is illustrated in Figure 4.1. TCD has good physical properties for a jet fuel with an appropriate density (0.94 g/cm^3), a low freezing point (-79 °C) and a volumetric energy content of 39,434 MJ/m^3.

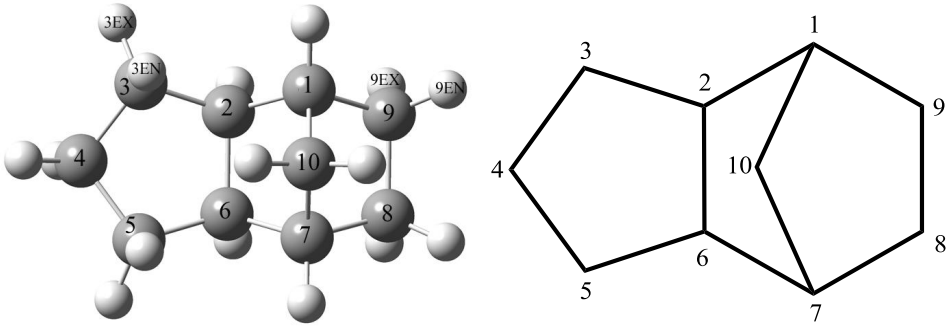

Figure 4.1 Schematic structure of tricyclodecane

A number of experimental and computational studies have been conducted in an effort to develop an improved understanding of JP-10 reaction chemistry[112-123]. Figure 4.2 illustrates the many different possible paths of decomposition and subsequent reaction with molecular oxygen $^3O_2$ that the TCD molecules can undergo in a combustion environment. The difficulty of the study of the pyrolysis and oxidation of JP-10 resides in the structural complexity of the TCD molecule.

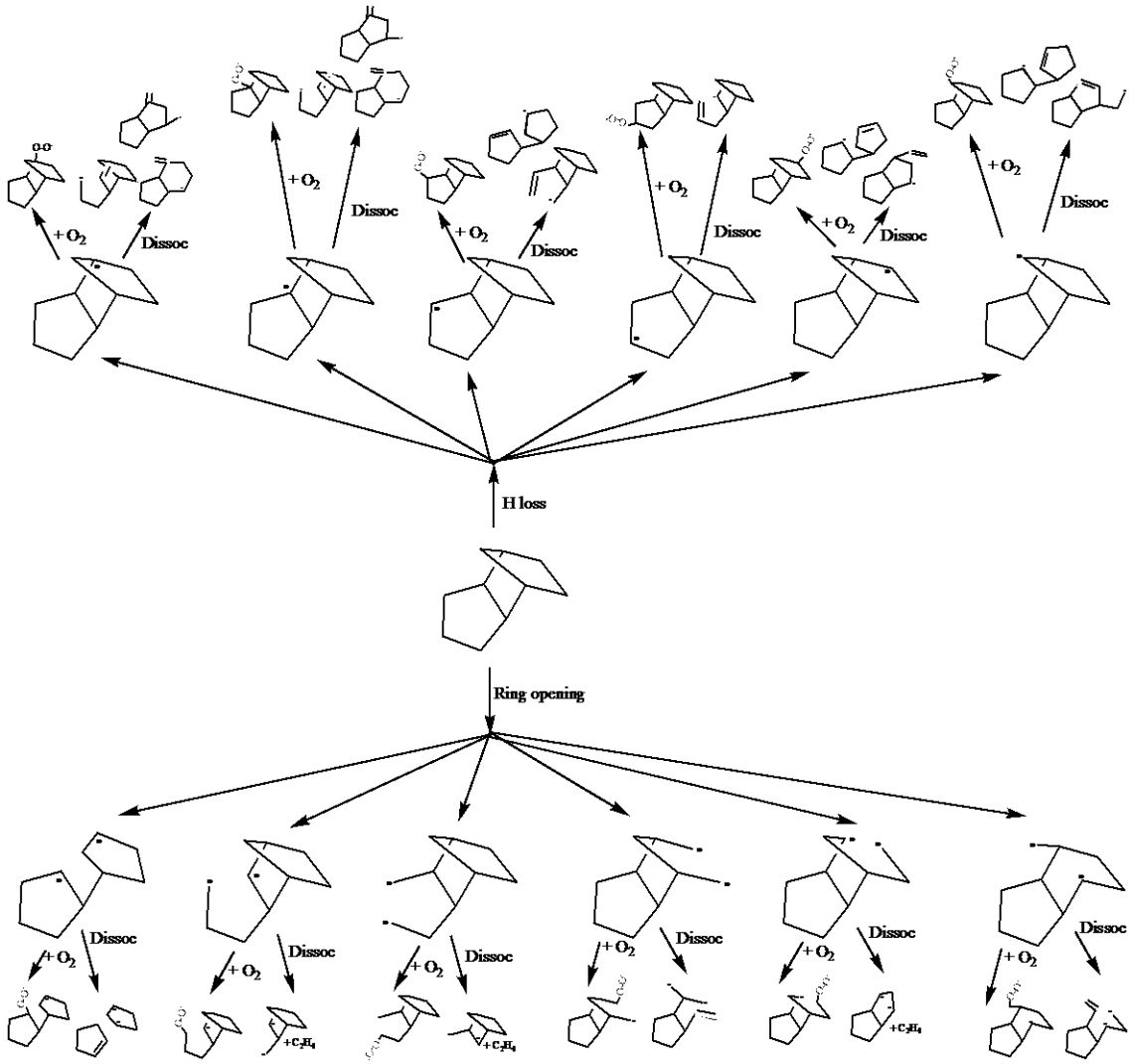

Figure 4.2 Ring opening, hydrogen loss, dissociation and oxidation paths of TCD

The initial unimolecular decomposition reactions of TCD at pre-combustion temperatures involve:

(i) Formation of single carbon site radicals in the ring via abstraction of hydrogen atoms on the TCD ring.

(ii) Generation of radicals formed via reactions with pool species.

At higher temperatures, the TCD decomposition reactions involve:

(i) Formation of diradicals with a radical on each of two carbon sites resulting from carbon – carbon bond cleavage, where the carbon – carbon bonds comprise links in the molecular ring system.

(ii) Formation of single carbon site radicals via simple dissociation loss of hydrogen atoms on the TCD ring, where these C—H bond dissociation enthalpies are 8 to 25 kcal mol^{-1} stronger than those of the carbon-carbon bond linkages. The larger differences in bond dissociation enthalpies between the stronger C—H and the C—C bonds is partially due to release of ring strain in cleavage of the carbon-carbon bonds.

Hudzik et al. have calculated the thermochemical properties of the parent TCD ring opening radicals and diradicals[124,125]. These active intermediates can undergo unimolecular dissociations, or association reactions with molecular oxygen, $^3O_2$, to form peroxy radicals. The reactions with molecular $^3O_2$ occur with effectively no activation energy and reasonably high pre-exponential factors. The thermochemistry of these oxidation reactions is needed to understand the kinetics of the initial TCD reactions, specifically the energetics (exothermicity – energy provided for subsequent reactions), reaction paths, the pressure dependence and the importance of the chemical activation reaction paths forming intermediate products.

Figure 4.3 illustrates the formation of a TCD alkyl radical and subsequent reaction of the alkyl radical with molecular $^3O_2$, resulting in the formation of a peroxy radical.

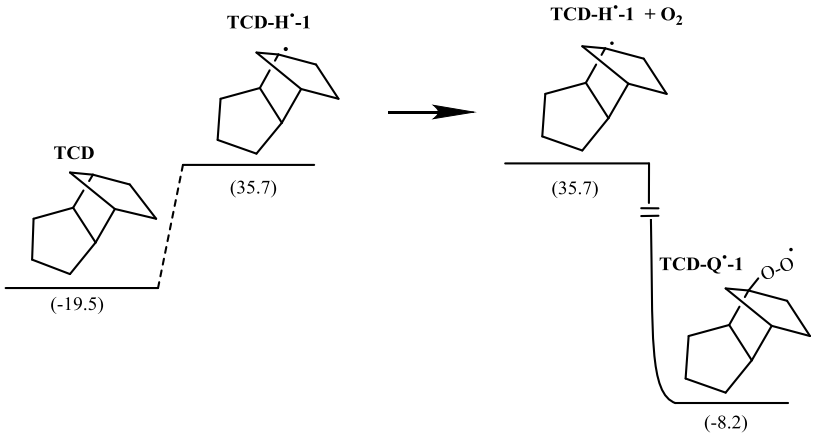

Figure 4.3 Example of hydrogen abstraction of TCD, and oxidation of formed alkyl radical with molecular oxygen $^3O_2$

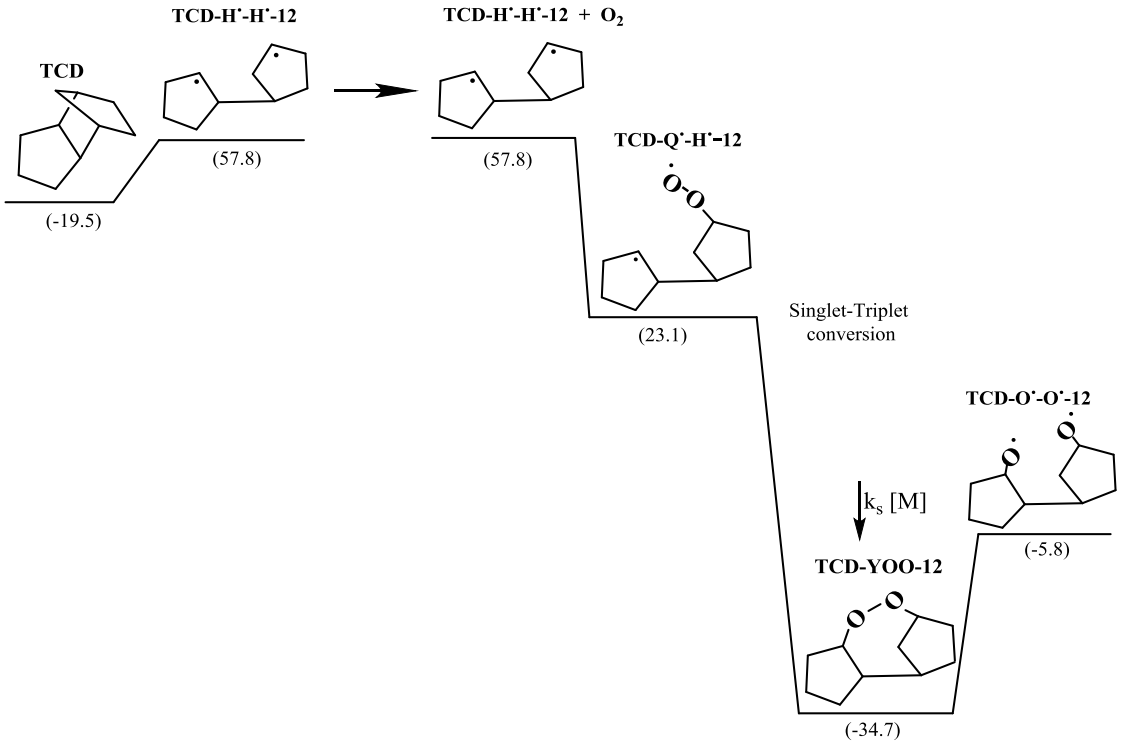

Figure 4.4 Example of ring opening of TCD, and oxidation of formed alkyl diradical with molecular oxygen $^3O_2$

Figure 4.4 shows the ring opening of the TCD parent molecule to form an alkyl diradical, and continued reaction of the diradical with molecular oxygen, $^3O_2$, resulting in

the formation of an alkyl/peroxy diradical. These alkyl/peroxy diradicals are initially triplets and can undergo triplet-singlet conversion, followed by a ring closure to form a cyclic peroxide. Under combustion conditions the cyclic peroxide will undergo rapid ring-opening via cleavage of the newly formed (weak) RO—OR' peroxide bond, which leads to the formation of a singlet di-alkoxy diradical.

Thermochemical properties of the peroxy radicals and the alkyl/peroxy diradicals resultant from the oxidation of TCD with the molecular oxygen, $^3O_2$, are investigated in this study. The alkoxy radicals and diradicals formed from the ring opening of the oxygenated cyclic species are also investigated. Properties are also determined for the oxygenated cyclic species formed from the ring closure of the peroxy diradicals.

Standard enthalpies of formation of each parent, radical and diradical are determined. Entropies ($S(T)$) and heat capacities ($C_p(T)$) are also determined for each species.

The schematic structure and nomenclature of the species studied during this study is presented in Schemes 4.1 to 4.7. The nomenclature used for the species is:

- TCD-OOH-m = TCD-Q-m = TCD-OOH-1 = TCD-Q-1 : indicates that hydroperoxide group is placed in carbon number 1 (carbon numbering corresponds to that in Figure 4.1)
- TCD-OOH-mn = TCD-Q-mn = TCD-OOH-12 = TCD-Q-12 : indicates the mn bond of TCD is cleaved (ring-opened), and that the hydroperoxide group is placed in carbon number 1 (carbon numbering corresponds to that in Figure 4.1)
- TCD-OOH-nm = TCD-Q-nm = TCD-OOH-21 = TCD-Q-21 :indicates the nm bond (= mn bond) is cleaved (ring-opened), and that the hydroperoxide group is placed in carbon number 2 (carbon numbering corresponds to that in Figure 4.1)
- TCD-OH-OH-nm = TCD-OH-OH-12 : indicates the nm bond ring-opened, and that the alcohol group is placed in carbon number 1 and 2 (carbon numbering corresponds to that in Figure 4.1)

TCD Hydroperoxides		
TCD-OOH-m	***TCD-OOH -mn***	***TCD-OOH -nm***
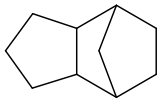 **TCD**	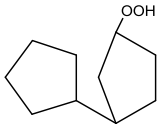 **TCD-OOH-12**	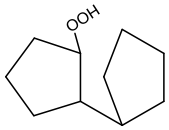 **TCD-OOH-21**
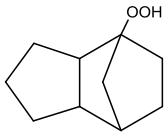 **TCD-OOH-1**	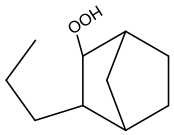 **TCD-OOH-23**	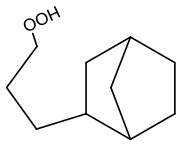 **TCD-OOH-32**
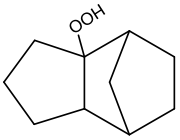 **TCD-OOH-2**	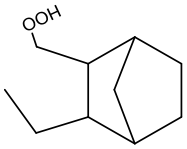 **TCD-OOH -34**	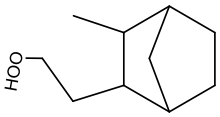 **TCD- OOH-43**
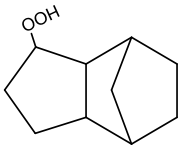 **TCD-OOH-3**	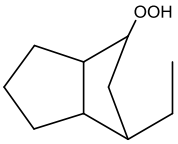 **TCD-OOH-19**	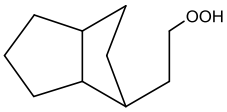 **TCD-OOH-91**
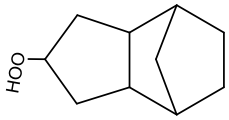 **TCD-OOH-4**	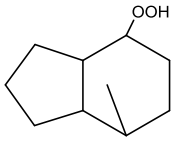 **TCD-OOH-1-10**	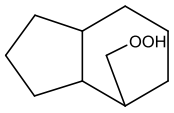 **TCD-OOH-10-1**
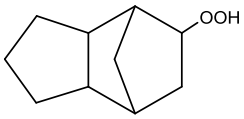 **TCD-OOH-9**	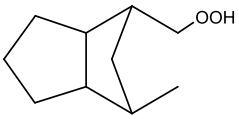 **TCD-OOH-98**	
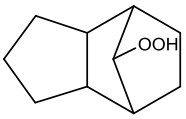 **TCD-OOH-10**	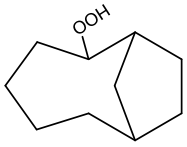 **TCD-OOH-26**	

Scheme 4.1 Studied tricyclodecane hydroperoxide structures

TCD Peroxy Radicals		
TCD-OO•-m	***TCD-OO•-mn***	***TCD-OO•-nm***
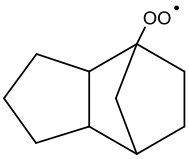 **TCD-OO•-1**	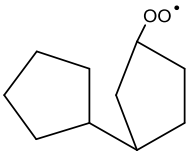 **TCD-OO•-12**	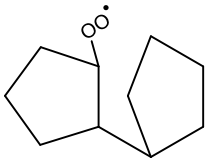 **TCD-OO•-21**
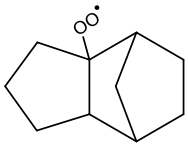 **TCD-OO•-2**	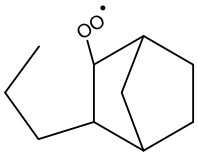 **TCD-OO•-23**	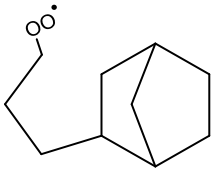 **TCD-OO•-32**
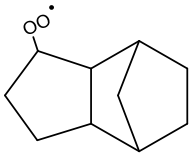 **TCD-OO•-3**	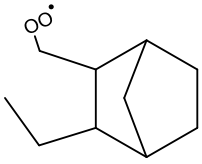 **TCD-OO•-34**	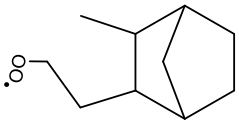 **TCD-OO•-43**
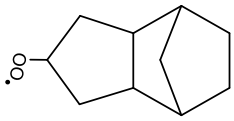 **TCD-OO•-4**	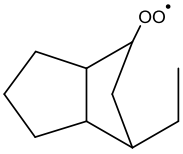 **TCD-OO•-19**	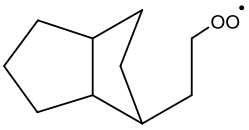 **TCD-OO•-91**
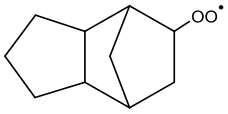 **TCD-OO•-9**	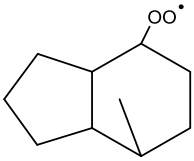 **TCD-OO•-1-10**	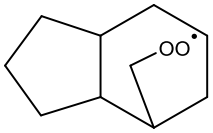 **TCD-OO•-10-1**
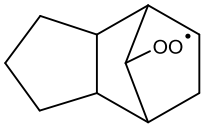 **TCD-OO•-10**	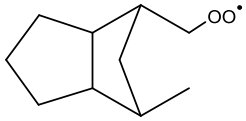 **TCD-OO•-98**	
	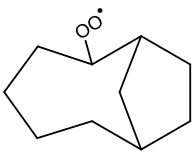 **TCD-OO•-26**	

Scheme 4.2 Studied tricyclodecane peroxy radical structures

TCD Alkyl/Peroxy Diradicals	
TCD-OO•-H•-mn	***TCD-OO•-H•-nm***
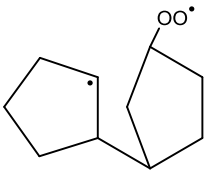 **TCD-OO•-H•-12**	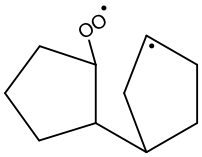 **TCD-OO•-H•-21**
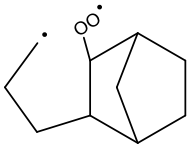 **TCD-OO•-H•-23**	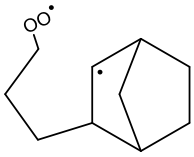 **TCD-OO•-H•-32**
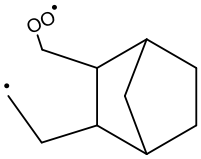 **TCD-OO•-H•-34**	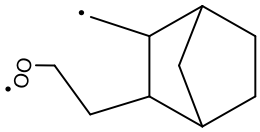 **TCD-OO•-H•-43**
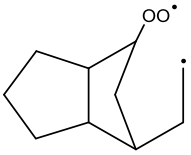 **TCD-OO•-H•-19**	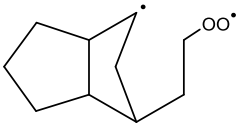 **TCD-OO•-H•-91**
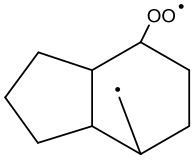 **TCD-OO•-H•-1-10**	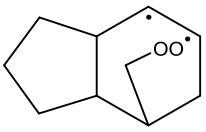 **TCD-OO•-H•-10-1**
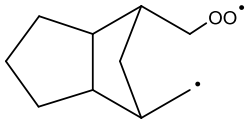 **TCD-OO•-H•-98**	
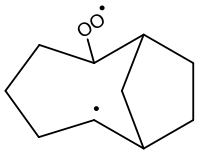 **TCD-OO•-H•-26**	

Scheme 4.3 Studied tricyclodecane alkyl peroxy diradical structures

TCD Alkoxides – TCD-OH-OH-mn			
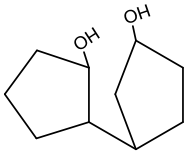	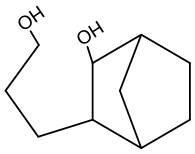	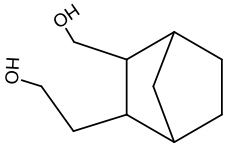	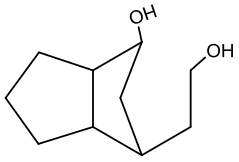
TCD-OH-OH-12	**TCD-OH-OH-23**	**TCD-OH-OH-34**	**TCD-OH-OH-91**
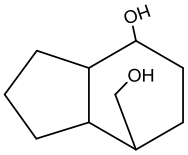	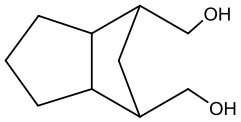	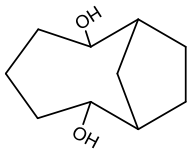	
TCD-OH-OH-1-10	**TCD-OH-OH-98**	**TCD-OH-OH-26**	

Scheme 4.4 Studied tricyclodecane alkoxide structures

TCD Alkoxy Radicals – TCD-OH-O˙-mn			
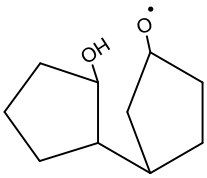	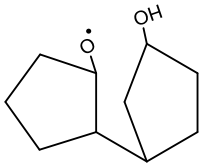	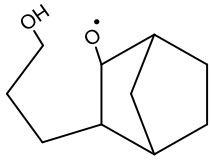	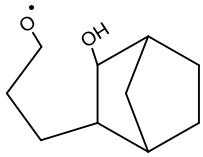
TCD-OH-O˙-12	**TCD-OH-O˙-21**	**TCD-OH-O˙-23**	**TCD-OH-O˙-32**
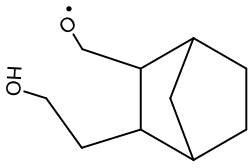	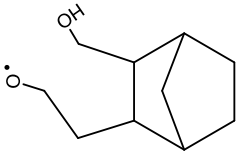	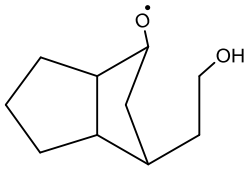	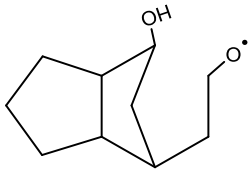
TCD-OH-O˙-34	**TCD-OH-O˙-43**	**TCD-OH-O˙-19**	**TCD-OH-O˙-91**
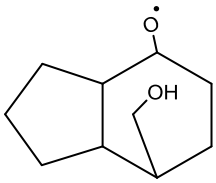	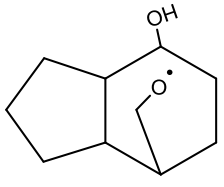	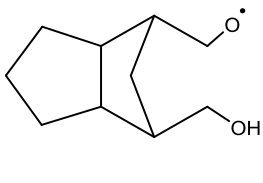	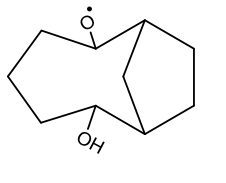
TCD-OH-O˙-1-10	**TCD-OH-O˙-10-1**	**TCD-OH-O˙-98**	**TCD-OH-O˙-26**

Scheme 4.5 Studied tricyclodecane alkoxy radical structures

TCD Dialkoxy Diradicals – TCD-O˙-O˙-mn

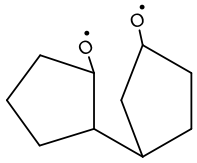

TCD-O˙-O˙-12

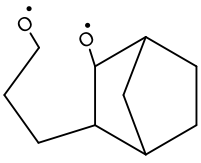

TCD-O˙-O˙-23

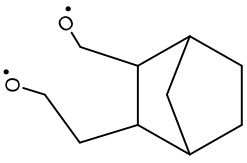

TCD-O˙-O˙-34

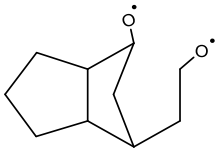

TCD-O˙-O˙-91

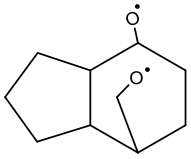

TCD-O˙-O˙-1-10

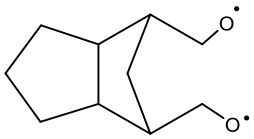

TCD-O˙-O˙-98

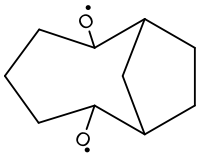

TCD-O˙-O˙-26

Scheme 4.6 Studied tricyclodecane dialkoxy diradical structures

TCD Oxygenated Cyclic – TCD-YOO-mn

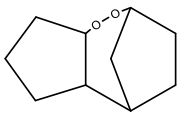

TCD-YOO-12

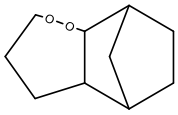

TCD-YOO-23

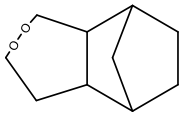

TCD-YOO-34

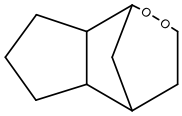

TCD-YOO-91

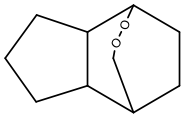

TCD-YOO-10-1

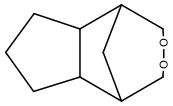

TCD-YOO-98

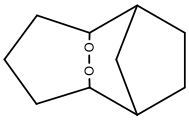

TCD-YOO-26

Scheme 4.7 Studied tricyclodecane oxygenated cyclic structures

4.2 Thermochemical Properties

The calculations for enthalpies of formation on the *TCD hydroperoxides, alcohols, peroxy and alkoxy radicals* were all performed at the B3LYP-6-31G(d,p) level using three different types of work reactions. The calculations for enthalpies of formation on the *TCD peroxy and alkoxy diradicals* were performed at the B3LYP-6-31G(d,p) level using three different approaches described below. The optimized geometries for each of the calculated structures are presented in Appendix H.

The hydroperoxide or alcohol group can be placed in two different positions for each of the TCD sites, as described in the example in Figure 4.5 for the peroxides and in Figure 4.6 for the alcohols. All the possible sites of the OOH and OH groups were studied to calculate the energies and find the lowest energy conformer.

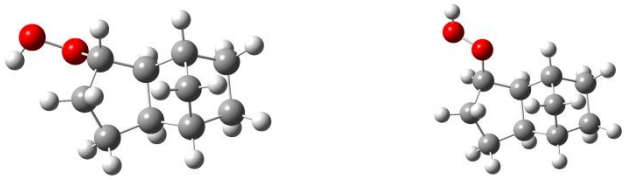

TCD-OOH-3-a **TCD-OOH-3-b**

Figure 4.5 Representation of two sites for the OOH group on TCD-OOH-3

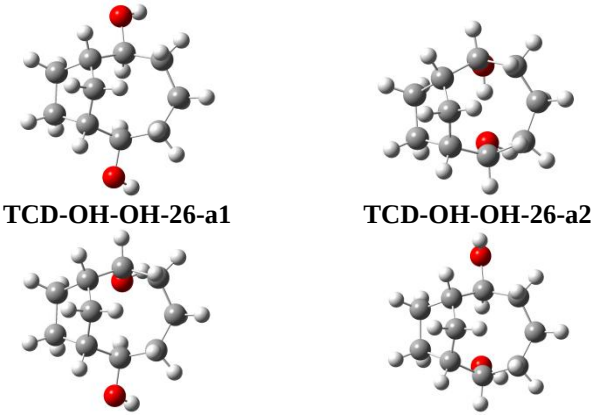

TCD-OH-OH-26-a1 **TCD-OH-OH-26-a2**

TCD-OH-OH-26-b1 **TCD-OH-OH-26-b2**

Figure 4.6 Representation of different sites for the OH groups on TCD-OOH-26

The work reaction methods for the parent hydroperoxides are described in Scheme 4.8. The 3 to 5 member cyclic hydroperoxide species used for reference species are from a previous study[126], and were calculated using CBS-QB3 and G3MP2B3 levels of theory.

TCD-Q-m

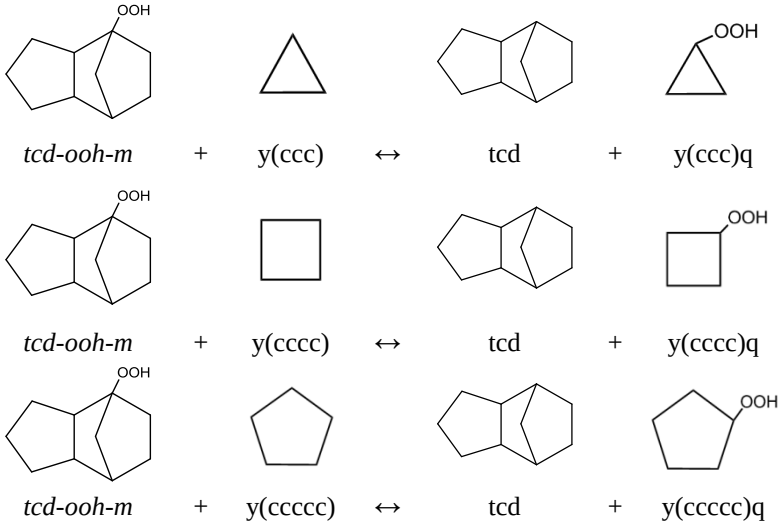

tcd-ooh-m + y(ccc) ↔ tcd + y(ccc)q

tcd-ooh-m + y(cccc) ↔ tcd + y(cccc)q

tcd-ooh-m + y(ccccc) ↔ tcd + y(ccccc)q

TCD-Q-mn

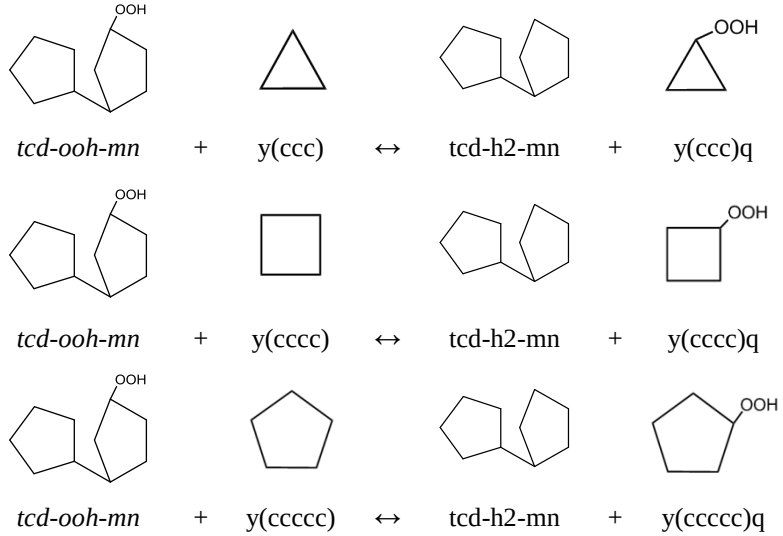

tcd-ooh-mn + y(ccc) ↔ tcd-h2-mn + y(ccc)q

tcd-ooh-mn + y(cccc) ↔ tcd-h2-mn + y(cccc)q

tcd-ooh-mn + y(ccccc) ↔ tcd-h2-mn + y(ccccc)q

Scheme 4.8 Example of work reactions used for the hydroperoxide species

The TCD parent molecule and the ring opened parent molecules used as reference in the work reactions were also from a previous study[123,124] at the B3LYP/6-31G(d,p), B3LYP/6-31G(2d,2p), CBS-QB3 and G3MP2B3 levels of theory. The average values of the CBS-QB3 and G3MP2B3 calculations reported were used as reference for the work reactions in this study.

TCD-Q$^{\bullet}$-m						
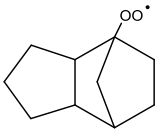	+	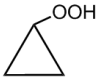	↔	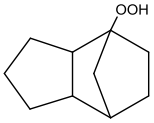	+	
tcd-oo$^{\bullet}$-m	+	y(ccc)q	↔	tcd-ooh-m	+	y(ccc)q$^{\bullet}$
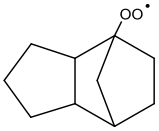	+	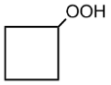	↔	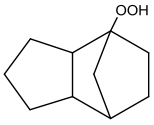	+	
tcd-oo$^{\bullet}$-m	+	y(cccc)q	↔	tcd-ooh-m	+	y(cccc)q$^{\bullet}$
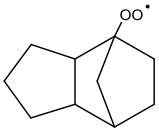	+	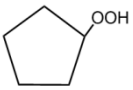	↔	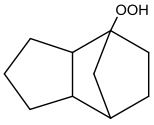	+	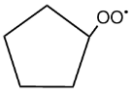
tcd-oo$^{\bullet}$-m	+	y(ccccc)q	↔	tcd-ooh-m	+	y(ccccc)q$^{\bullet}$
TCD-Q$^{\bullet}$-mn						
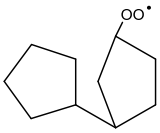	+	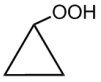	↔	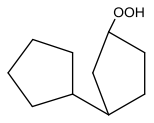	+	
tcd-oo$^{\bullet}$-mn	+	y(ccc)q	↔	tcd-ooh-mn	+	y(ccc)q$^{\bullet}$
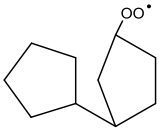	+	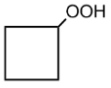	↔	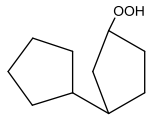	+	
tcd-oo$^{\bullet}$-mn	+	y(cccc)q	↔	tcd-ooh-mn	+	y(cccc)q$^{\bullet}$
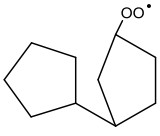	+	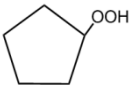	↔	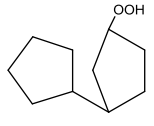	+	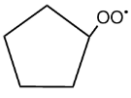
tcd-oo$^{\bullet}$-mn	+	y(ccccc)q	↔	tcd-ooh-mn	+	y(ccccc)q$^{\bullet}$

Scheme 4.9 Example of work reactions used for the peroxy radicals

The determination for the properties of the *TCD peroxy radicals* used three work reactions, as indicated in Scheme 4.9. The 3 to 5 member cyclic hydroperoxide and peroxy radical species used in these work reactions are from reference[126] at the CBS-QB3 and G3MP2B3 level of theory.

Table 4.1 Summary of C—H bond dissociation enthalpies (BDE) for the triplet and singlet TCD alkyl diradicals calculated by Hudzik et al.[125]

Species	***C—H BDE***		**Species**	***C—H BDE***	
	Triplet	***Singlet***		***Triplet***	***Singlet***
TCD-H•-H-12 → TCD-H•-H•-12 + H•	96.5	96.8	TCD-H•-H-21 → TCD-H•-H•-12 + H•	96.0	96.3
TCD-H•-H-23 → TCD-H•-H•-23 + H•	101.3	101.7	TCD-H•-H-32 → TCD-H•-H•-23 + H•	98.9	99.2
TCD-H•-H-34 → TCD-H•-H•-34 + H•	100.8	100.8	TCD-H•-H-43 → TCD-H•-H•-34 + H•	100.7	100.7
TCD-H•-H-19 → TCD-H•-H•-19 + H•	100.9	100.8	TCD-H•-H-91 → TCD-H•-H•-19 + H•	98.0	97.9
TCD-H•-H-1-10 → TCD-H•-H•-1-10 + H•	99.9	100.0	TCD-H•-H-10-1 → TCD-H•-H•-1-10 + H•	95.4	95.5
TCD-H•-H-26 → TCD-H•-H•-26 + H•	96.9	94.4			
TCD-H•-H-98 → TCD-H•-H•-98 + H•	101.5	100.8			

Units: kcal mol^{-1}

Three methods were used in the determination of the enthalpies of formation for the *TCD alkyl / peroxy diradicals.*

1) B3LYP/6-31G(d,p) calculations with three work reactions involving linear *diradical reference species* as indicated in Scheme 4.10.
2) B3LYP/6-31G(d,p) calculations with three work reactions involving cyclic *radical reference species* as indicated in Scheme 4.11.
3) The heat of formation of the peroxy radicals calculated in this work, and the C—H bond dissociation enthalpies for the TCD alkyl radicals calculated by using G3MP2B3 and CBS-QB3 from Hudzik et al.[125] (data listed in Table 4.1) and reaction scheme illustrated in Scheme 4.12.

TCD-OO•-H•-mn						
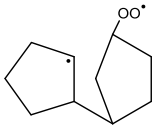	+	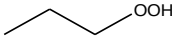	↔	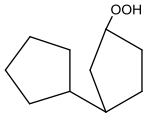	+	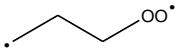
tcd-oo•-h•-mn	+	ccccooh	↔	tcd-ooh-mn	+	c•cccoo•
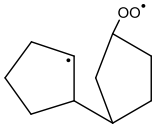	+	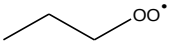	↔	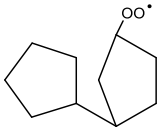	+	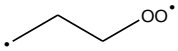
tcd-oo•-h•-mn	+	ccccoo•	↔	tcd-oo•-mn	+	c•cccoo•
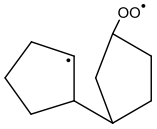	+	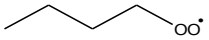	↔	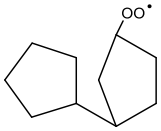	+	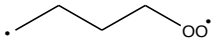
tcd-oo•-h•-mn	+	cccccoo•	↔	tcd-oo•-mn	+	c•ccccoo•

Scheme 4.10 Example of work reactions used for the alkyl peroxy diradicals (method 1)

TCD-OO•-H•-mn						
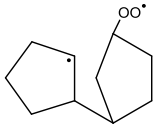	+		↔	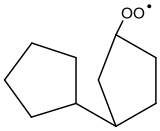	+	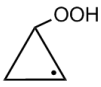
tcd-oo•-h•-mn	+	y(ccc)q	↔	tcd-oo•-mn	+	y(c•cc)q
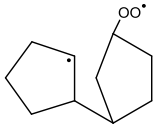	+	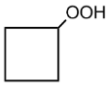	↔	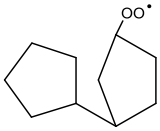	+	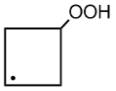
tcd-oo•-h•-mn	+	y(cccc)q	↔	tcd-oo•-mn	+	y(c•ccc)q
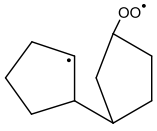	+	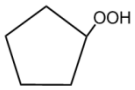	↔	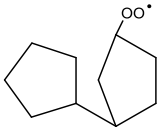	+	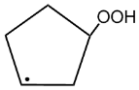
tcd-oo•-h•-mn	+	y(ccccc)q	↔	tcd-oo•-mn	+	y(c•cccc)q

Scheme 4.11 Example of work reactions used for the alkyl peroxy diradicals (method 2)

TCD-OO•-H•-mn				
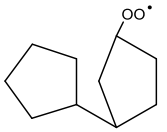		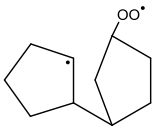		H•
tcd-oo•-mn	↔	*tcd-oo•-h•-mn*	+	H

Scheme 4.12 Example of calculation method used for the alkyl peroxy diradicals (method 3)

The first and second methods used work reactions with reference species (cyclic, linear -hydroperoxide, -peroxy radical and -diradical) enthalpies from the literature[126]. The TCD hydroperoxide parent molecules and peroxy radicals calculated in this work were used in these two schemes as reference species. The third approach used the C—H bond dissociation enthalpies for the calculation of the heats of formation of the TCD peroxy diradicals[125], as indicated below and in Scheme 4.12.

$$[\text{tcd-oo}^{\bullet}\text{-mn}] = \mathbf{[tcd\text{-}oo^{\bullet}\text{-}h^{\bullet}\text{-}mn]} + [H^{\bullet}]$$

$$\Delta_{rxn}H^{o}_{298\ calc} = \Delta H^{\circ}_{298\ C\text{—}H\ BDE}{}^{125} = \mathbf{\Delta_f H^{o}_{298}\,(tcd\text{-}oo^{\bullet}\text{-}h^{\bullet}\text{-}mn)} + \Delta_f H^{o}_{298}\,(H^{\bullet}) - \Delta_f H^{o}_{298}\,(\text{tcd-oo}^{\bullet}\text{-mn})$$

The triplet TCD alkyl-peroxy diradicals were determined by the use of the C—H bond dissociation enthalpies for the triplet TCD dialkyl diradicals calculated by Hudzik et al.[125], and the singlet TCD alkyl-peroxy diradicals were calculated by the use of C—H bond dissociation enthalpies for the singlet dialkyl diradicals calculated by Hudzik et al. [125] (summarized in Table 4.1).

The heats of formation of the *TCD alcohols* and *TCD alkoxy radicals* were calculated with three work reactions for each species as indicated in Scheme 4.13 and Scheme 4.14, respectively.

TCD-OH-OH-mn

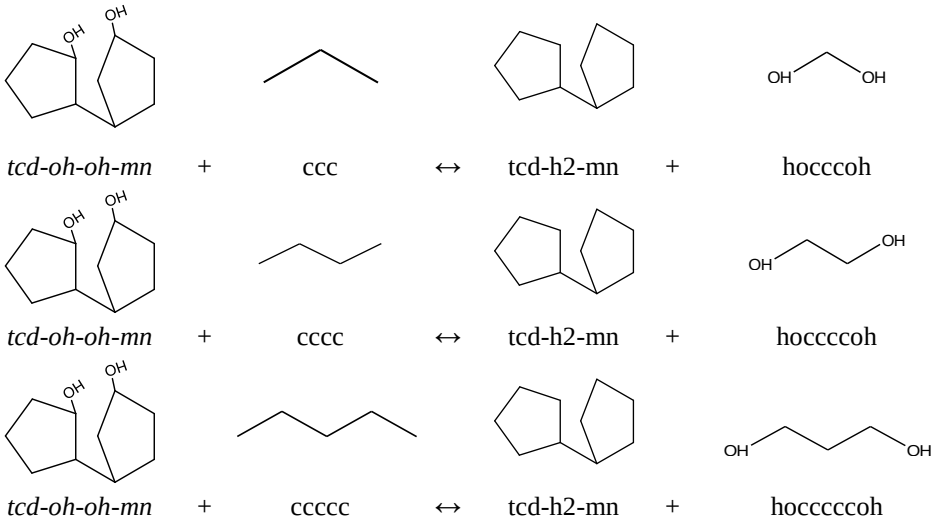

tcd-oh-oh-mn + ccc ↔ tcd-h2-mn + hocccoh

tcd-oh-oh-mn + cccc ↔ tcd-h2-mn + hocccccoh

tcd-oh-oh-mn + ccccc ↔ tcd-h2-mn + hoccccccoh

Scheme 4.13 Example of work reactions used for the alcohols

The 3 to 5 member cyclic alkanes used in these work reactions as reference are from the literature[126]. The TCD parent molecule and the ring opened TCD parent molecules used in these work reactions as reference were calculated by CBS-QB3 and G3MP2B3 level of theory[125]. The linear di-alcohols and alkoxy radicals used as reference in the work reactions were calculated in this work. The TCD alcohol parent molecules calculated in this work were used as reference species for the determination of the TCD alkoxy radicals.

TCD-O•-OH-mn

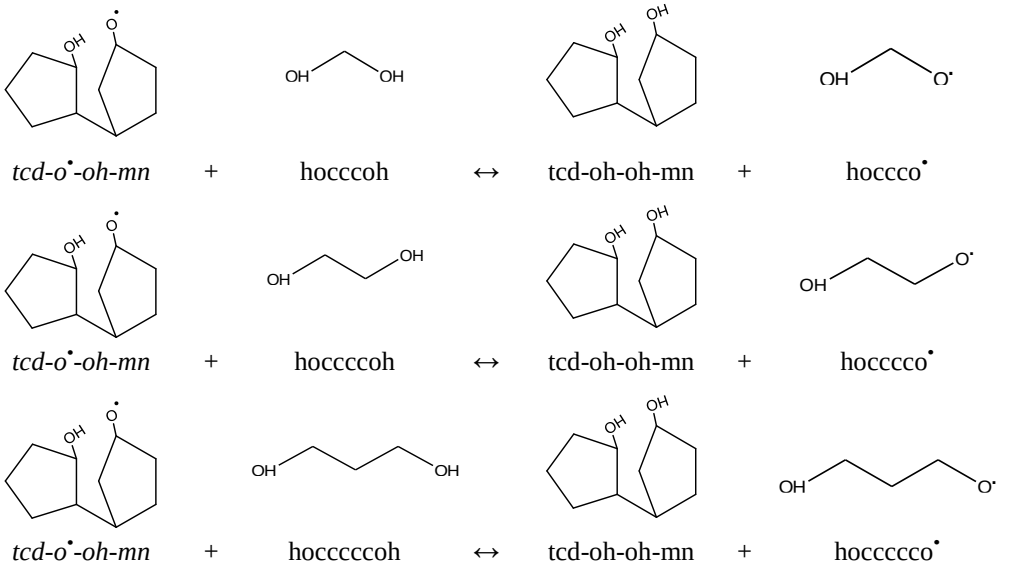

TCD-OH-O•-mn

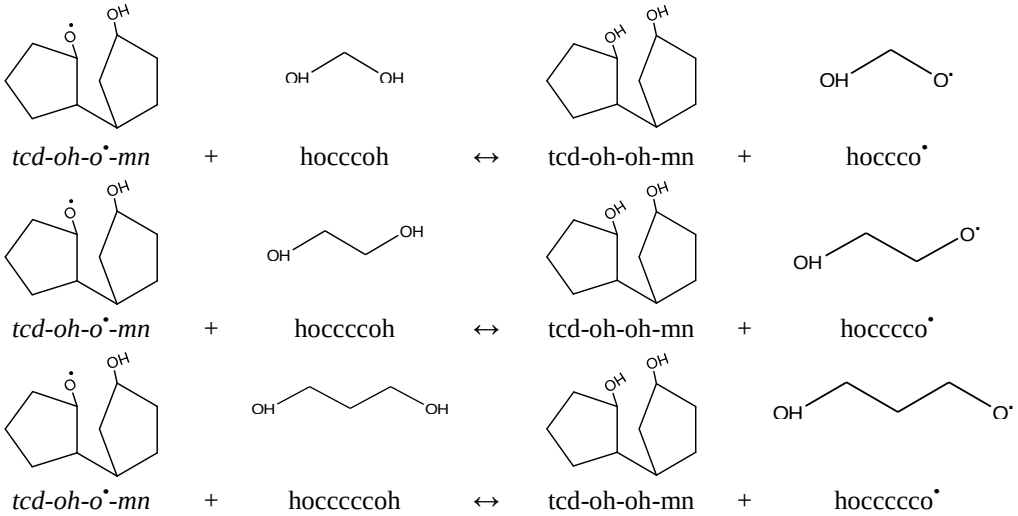

Scheme 4.14 Example of work reactions used for the alkoxy radicals

Three methods were used for the determination of the *TCD dialkoxy diradical enthalpies*:

1) B3LYP-6-31G(d,p) calculations with one set of three of work reactions involving linear *diradical reference species* as shown in Scheme 4.15.
2) B3LYP-6-31G(d,p) calculations with two sets of three work reactions (a total of 6 work reactions) involving two linear *radical reference species* (single radical sites) as illustrated in Scheme 4.16.
3) The third method for the di-alkoxy radicals used the standard enthalpy of formation for the TCD alkoxy radical and the calculated bond dissociation enthalpy for loss of the H atom on the remaining hydroxyl group of the di-alcohol, with data from Table 4.2 and method illustrated in Scheme 4.17.

Table 4.2 O—H bond dissociation enthalpies (BDE) used for the determination of the triplet and singlet dialkoxy diradicals

	TCD-O•-O•-mn						**BDE**	
Triplets	**a)**	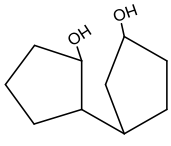	tcd-oh-oh-mn	↔	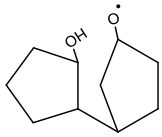 tcd-o•-oh-mn	+ H•	***12***	104.61
							23	104.20
							34	104.72
							91	104.29
							26	108.78
							98	103.11
							1-10	103.10
	b)	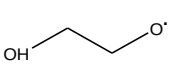	hocccco•	↔	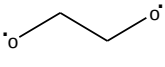 •occcco• (t)	+ H•	104.07	
Singlets		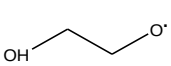	hocccco•	↔	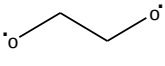 •occcco• (s)	+ H•	104.95	

Units: kcal mol^{-1}

TCD-O•-O•-mn

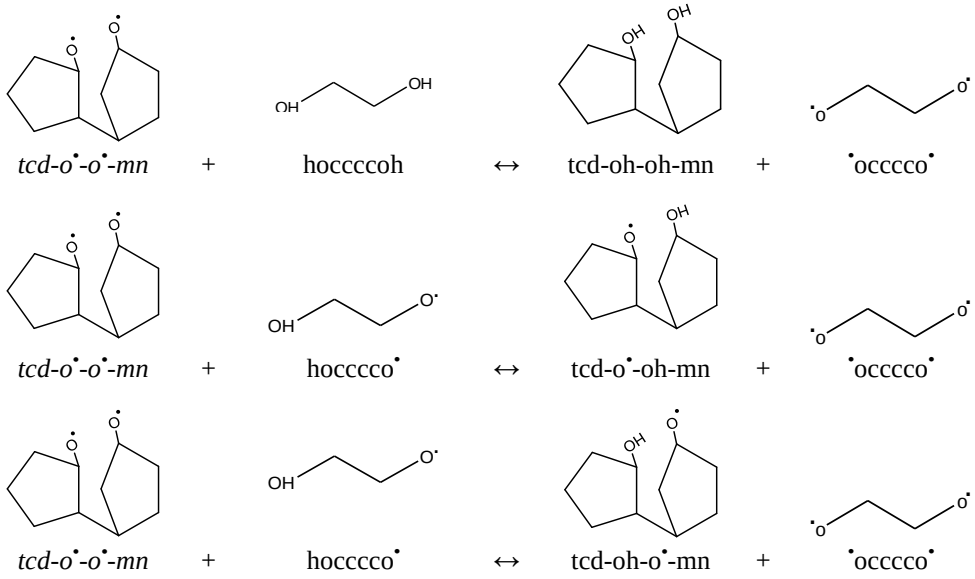

Scheme 4.15 Example of work reactions used for the dialkoxy diradicals (method 1)

The third method used the O—H bond dissociation enthalpies for the calculation of the heats of formation of the TCD alkoxy diradicals, as indicated below:

$$[\text{tcd-o}^{\bullet}\text{-oh-mn}] \leftrightarrow \mathbf{[tcd\text{-}o^{\bullet}\text{-}o^{\bullet}\text{-}mn]} + [H^{\bullet}]$$

$$\Delta_{rxn}H°_{298\ calc} = \Delta H°_{298\ C—H\ BDE} = \mathbf{\Delta_f H°_{298}\,(tcd\text{-}o^{\bullet}\text{-}o^{\bullet}\text{-}mn)} + \Delta_f H°_{298}\,(H^{\bullet}) - \Delta_f H°_{298}\,(\text{tcd-o}^{\bullet}\text{-oh-mn})$$

The calculation of enthalpies for the triplet diradicals used the O—H bond dissociation enthalpies calculated from the TCD alkoxy radicals (section (a) in Table 4.2) and the O—H bond dissociation enthalpies calculated from the C_4 member triplet linear dialkoxy diradicals (section (b) in Table 4.2). The O—H bond dissociation enthalpy calculated from the C_4 membered singlet dialkoxy diradical was used for the determination of the singlet diradicals.

TCD-O•-O•-mn

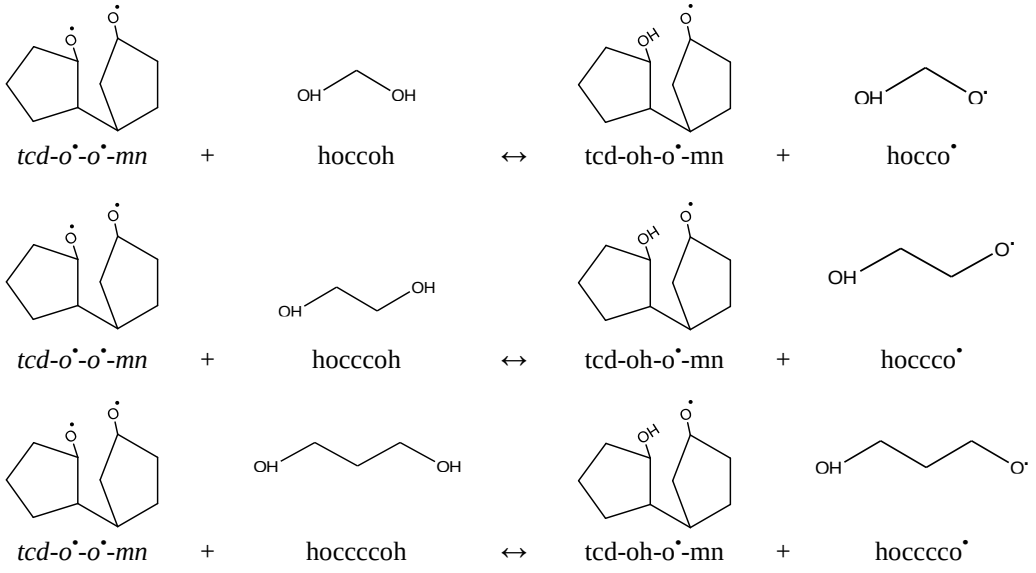

Scheme 4.16 Example of work reactions used for the dialkoxy diradicals (method 2)

TCD-O•-O•-mn

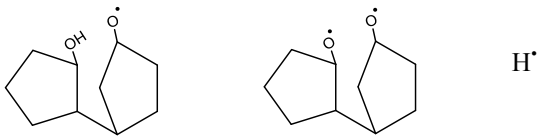

tcd-o•-oh-mn ↔ *tcd-o•-o•-mn* + H

Scheme 4.17 Example of calculation method used for the dialkoxy diradicals (method 3)

The determination of the oxygenated cyclic species, used B3LYP/6-31G(d,p) calculations coupled with three work reactions as indicated in Scheme 4.18, with 3 to 5 member cyclic alkanes and 5 to 7 member oxygenated cyclic species used as references. The TCD parent molecule used in these work reactions as reference is from the literature[123] and is calculated at the CBS-QB3 level of theory.

TCD-YOO-mn

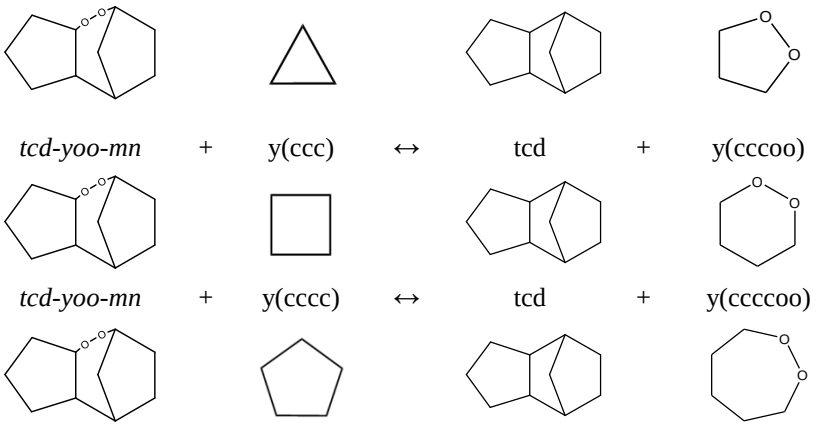

tcd-yoo-mn + y(ccc) ↔ tcd + y(cccoo)

tcd-yoo-mn + y(cccc) ↔ tcd + y(ccccoo)

tcd-yoo-mn + y(ccccc) ↔ tcd + y(cccccoo)

Scheme 4.18 Example of work reactions used for the oxygenated cyclic species

Appendix I includes all the work reactions used for the determination of the heats of formation for each of the species, including the conformers.

Tables 4.3 to 4.10 summarize the heats of formation of the species calculated during this study, as well as the OO—H, O—H and R—OOH bond dissociation enthalpies (BDE) for the radical species.

Table 4.3 Heat of formation of the TCD hydroperoxides

Species	$\Delta H°_{f\,298}$	**Species**	$\Delta H°_{f\,298}$	**Species**	$\Delta H°_{f\,298}$
TCD-Q-1	-41.25	TCD-Q-12	-53.85	TCD-Q-21	-52.59
TCD-Q-2	-41.97	TCD-Q-23	-46.36	TCD-Q-32	-45.88
TCD-Q-3	-40.66	TCD-Q-34	-46.41	TCD-Q-43	-45.94
TCD-Q-4	-40.65	TCD-Q-19	-53.79	TCD-Q-91	-50.46
TCD-Q-9	-40.30	TCD-Q-1-10	-52.88	TCD-Q-10-1	-48.81
TCD-Q-10	-39.21	TCD-Q-26	-47.82		
		TCD-Q-98	-52.45		

Units: kcal mol^{-1}

Table 4.4 Heat of formation and bond dissociation enthalpies (BDE) of the TCD peroxy radicals

Species	$\Delta H°_{f\,298}$	**Species**	$\Delta H°_{f\,298}$	**Species**	$\Delta H°_{f\,298}$
TCD-Q$^{\bullet}$-1	-8.19	TCD-Q$^{\bullet}$-12	-21.23	TCD-Q$^{\bullet}$-21	-20.07
BDE	*85.16*	*BDE*	*84.72*	*BDE*	*84.62*
TCD-Q$^{\bullet}$-2	-10.04	TCD-Q$^{\bullet}$-23	-13.70	TCD-Q$^{\bullet}$-32	-11.47
BDE	*85.03*	*BDE*	*84.69*	*BDE*	*85.20*
TCD-Q$^{\bullet}$-3	-8.19	TCD-Q$^{\bullet}$-34	-13.35	TCD-Q$^{\bullet}$-43	-12.32
BDE	*84.57*	*BDE*	*85.11*	*BDE*	*85.66*
TCD-Q$^{\bullet}$-4	-7.75	TCD-Q$^{\bullet}$-19	-22.02	TCD-Q$^{\bullet}$-91	-17.14
BDE	*85.00*	*BDE*	*84.01*	*BDE*	*85.42*
TCD-Q$^{\bullet}$-9	-7.53	TCD-Q$^{\bullet}$-1-10	-20.34	TCD-Q$^{\bullet}$-10-1	-15.56
BDE	*84.88*	*BDE*	*84.64*	*BDE*	*85.35*
TCD-Q$^{\bullet}$-10	-6.04	TCD-Q$^{\bullet}$-26	-16.47		
BDE	*85.27*	*BDE*	*84.45*		
		TCD-Q$^{\bullet}$-98	-19.35		
		BDE	*85.20*		

Units: kcal mol^{-1}

Table 4.5 Heat of formation of the TCD alkyl/peroxy diradicals (triplet and singlet)

Species	$\Delta H°_{f\,298}$							
	Triplets				Singlets			
	S^2	Appr. 1 (Sch. 10)	Appr. 2(*) (Sch. 11)	Appr. 3 (Sch. 11)	S^2	Appr. 1 (Sch. 10)	Appr. 2(*) (Sch. 11)	Appr. 3 (Sch. 11)
TCD-Q•-H•-12	*(2.0072)*	20.31	23.85	23.17	*(1.0071)*	21.03	23.85	23.47
TCD-Q•-H•-21	*(2.0072)*	21.37	24.75	23.87	*(1.0057)*	21.85	24.67	24.17
TCD-Q•-H•-23	*(2.0071)*	32.84	36.24	35.50	*(0.9788)*	32.42	35.26	35.90
TCD-Q•-H•-32	*(2.0068)*	30.52	34.32	35.33	*(1.0025)*	30.86	34.11	35.65
TCD-Q•-H•-34	*(2.0068)*	32.71	36.10	35.35	*(1.0049)*	33.19	36.02	35.35
TCD-Q•-H•-43	*(2.0070)*	34.26	37.65	36.28	*(0.9421)*	33.68	36.51	36.28
TCD-Q•-H•-19	*(2.0070)*	25.23	28.61	26.78	*(1.0038)*	25.63	28.45	26.68
TCD-Q•-H•-91	*(2.0071)*	24.50	27.99	28.66	*(0.9419)*	24.04	26.86	28.66
TCD-Q•-H•-1-10	*(2.0069)*	25.25	28.62	27.46	*(1.0036)*	25.69	28.50	27.56
TCD-Q•-H•-10-1	*(2.0070)*	24.99	28.36	27.74	*(1.0012)*	25.1	28.03	27.84
TCD-Q•-H•-26	*(2.0073)*	22.93	25.98	28.33	*(1.0012)*	23.22	25.70	25.83
TCD-Q•-H•-98	*(2.0067)*	27.53	30.90	30.05	*(1.0034)*	27.90	27.53	29.35

Units: kcal mol^{-1}

(*) Recommended values

Table 4.6 Heat of formation of the TCD alcohols

Species	$\Delta H°_{f\,298}$
TCD-OH-OH-12	-110.99
TCD-OH-OH-23	-105.24
TCD-OH-OH-34	-99.83
TCD-OH-OH-91	-107.32
TCD-OH-OH-26	-104.65
TCD-OH-OH-98	-107.39
TCD-OH-OH-1-10	-106.02

Units: kcal mol^{-1}

Table 4.7 Heat of formation and bond dissociation enthalpies (BDE) of the TCD alkoxy radicals

Species	$\Delta H°_{f\,298}$	Species	$\Delta H°_{f\,298}$
TCD-OH-O•-12	-58.48	TCD-OH-O•-21	-58.31
BDE	*104.61*	*BDE*	*104.78*
TCD-OH-O•-23	-53.14	TCD-OH-O•-32	-50.07
BDE	*104.20*	*BDE*	*107.27*
TCD-OH-O•-34	-47.21	TCD-OH-O•-43	-47.09
BDE	*104.72*	*BDE*	*104.84*
TCD-OH-O•-91	-55.13	TCD-OH-O•-19	-55.63
BDE	*104.29*	*BDE*	*103.79*
TCD-OH-O•-26	-47.73	TCD-OH-O•-62	-48.13
BDE	*108.78*	*BDE*	*108.38*
TCD-OH-O•-98	-56.38	TCD-OH-O•-89	-55.14
BDE	*103.11*	*BDE*	*104.34*
TCD-OH-O•-1-10	-54.93	TCD-OH-O•-10-1	-54.95
BDE	*103.10*	*BDE*	*103.08*

Units: kcal mol^{-1}

Table 4.8 Heat of formation of the TCD dialkoxy diradicals (triplet and singlet)

Species	$\Delta H°_{f\,298}$								
	Triplets					Singlets			
	S^2	Appr. 1 (Sch. 10)	Appr. 2(*) (Sch. 11)	Appr. 3 (Sch. 12)		S^2	Appr. 1 (Sch. 10)	Appr. 2(*) (Sch. 11)	Appr. 3 (Sch. 12)
				a)	b)				
TCD-O•-O•-21	*(2.0070)*	-6.35	-5.77	-6.72	-6.34	*(1.0060)*	-6.56	-5.79	-5.36
TCD-O•-O•-23	*(2.0075)*	0.65	1.64	2.03	1.9	*(0.9851)*	0.57	1.15	2.78
TCD-O•-O•-34	*(2.0060)*	5.10	5.90	5.53	4.88	*(1.0041)*	5.45	5.85	5.76
TCD-O•-O•-91	*(2.0068)*	-4.11	-3.12	-3.44	-3.66	*(1.0047)*	-3.60	-3.01	-2.78
TCD-O•-O•-26	*(2.0071)*	5.70	8.05	8.55	3.84	*(1.0069)*	5.18	7.11	4.72
TCD-O•-O•-98	*(2.0066)*	-4.71	-3.72	-4.13	-3.17	*(1.0023)*	-4.95	-4.36	-2.29
TCD-O•-O•-1-10	*(2.0072)*	-4.26	-3.36	-3.95	-2.98	*(1.0049)*	-3.47	-3.40	-2.10

Units: kcal mol^{-1}

(*) Recommended values

Table 4.9 R—OOH bond dissociation enthalpies (BDE)of the TCD hydroperoxides

Species	*BDE*	Species	*BDE*	Species	*BDE*
TCD-Q-1	79.9	TCD-Q-12	70.2	TCD-Q-21	69.44
TCD-Q-2	73.42	TCD-Q-23	67.21	TCD-Q-32	67.23
TCD-Q-3	70.01	TCD-Q-34	67.56	TCD-Q-43	67.19
TCD-Q-4	70.6	TCD-Q-19	68.24	TCD-Q-91	67.91
TCD-Q-9	70.35	TCD-Q-1-10	67.83	TCD-Q-10-1	68.36
TCD-Q-10	74.66	TCD-Q-26	67.87		
		TCD-Q-98	69.2		

Units: kcal mol^{-1}

Table 4.10 Heat of formation of the TCD oxygenated cyclic species

Species	$\Delta H°_{f\,298}$
TCD-YOO-12	-34.66
TCD-YOO-23	-38.04
TCD-YOO-34	-37.59
TCD-YOO-19	-45.09
TCD-YOO-26	-49.00
TCD-YOO-98	-45.94
TCD-YOO-1-10	-42.51

Units: kcal mol^{-1}

The OO—H bond dissociation enthalpies calculated for the different positions of tricyclodecane are in the range of 84.5-85.5 kcal mol^{-1}, similar of that for cyclopentane, y(ccccc)q$^{\bullet}$ (85.1 kcal mol^{-1})[38-45], and for the linear alkanes (85.9, 85.6, 84.7 and 85.4 kcal mol^{-1} for the $CH_3OO^{\bullet}$, $CH_3CH_2OO^{\bullet}$, $CH_3CH_2CH_2OO^{\bullet}$ and $CH_3CH_2CH_2CH_2OO^{\bullet}$, respectively, and 85.1 kcal mol^{-1} for $(CH_3)_2CHOO^{\bullet}$)[127]. The O—H bond dissociation enthalpies determined for the tricyclodecane dialcohols are ~104.5 kcal mol^{-1} for all positions, except for TCD-OH-OH-98 and TCD-OH-OH-1-10, where the bond dissociation enthalpies are ~1.5 kcal mol^{-1} smaller (103.1 kcal mol^{-1}), and for TCD-OH-OH-26, where the bond dissociation enthalpy is ~4 kcal mol^{-1} larger (108.8 and 108.4 kcal mol^{-1} for TCD-OH-O$^{\bullet}$-26 and TCD-OH-O$^{\bullet}$-62, respectively). TCD-OH-OH-26 has

hydrogen bonding between the two OH groups (see Figure 4.7), which results in stronger O—H bond dissociation enthalpies.

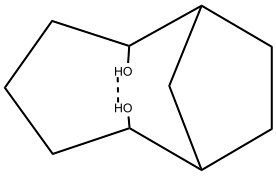

Figure 4.7 Structure of TCD-OH-OH-26

For comparison, the five member ring cyclic alcohol[38-45], y(ccccc)oh, has a bond dissociation enthalpy of 105.1 kcal mol^{-1} and $CH_3CH_2O^{\bullet}$ has a bond dissociation enthalpy[127] of 105.0 kcal mol^{-1} and 105.1 kcal mol^{-1} for $(CH_3)_2CHO^{\bullet}$.

The R—OOH bond dissociation enthalpies presented in Table 4.9 show that for the R—OOH bond dissociation enthalpies for the TCD-$Q^{\bullet}$-m species are ~70 kcal mol^{-1} for all cases except for TCD-$Q^{\bullet}$-2 and TCD-$Q^{\bullet}$-10, where the bond dissociation enthalpies are 73.4 and 74.7 kcal mol^{-1}, respectively, and for TCD-$Q^{\bullet}$-1, where the bond dissociation enthalpy is 79.9 kcal mol^{-1}. The results for the R—OOH bond dissociation enthalpies for the TCD-$Q^{\bullet}$-mn species indicate that the values are in the order of ~67-70 kcal mol^{-1}. The R—OOH bond dissociation enthalpies for the linear alkanes are 69.0, 70.5, 70.0 and 69.3 for $CH_3OO^{\bullet}$, $CH_3CH_2OO^{\bullet}$, $CH_3CH_2CH_2OO^{\bullet}$ and $CH_3CH_2CH_2CH_2OO^{\bullet}$, respectively[127].

The second and third approach followed for the determination of the heat of formation of the TCD alkyl-peroxy diradicals represent good agreement between the results, while the first approach results in values that are ~2-3 kcal mol^{-1} lower for the heat of formation. However, for the TCD dialkoxy diradicals, all three approaches show good agreement. The heats of formation determined by approach 2 are recommended, since the work reactions used are isodesmic, and are considered to result in a better cancellation of the systematic error.

Table 4.11 Entropy (S^o, 298 K) and heat capacity (Cp(T)) for the studied systems

Species	S^o	Cp						
	298 K	300 K	400 K	500 K	600 K	800 K	1000 K	1500 K
TCD-OOH-1	94.03	43.36	59.94	74.49	86.43	104.23	116.74	135.44
TCD-OOH-2	94.16	43.41	60.05	74.63	86.57	104.34	116.82	135.47
TCD-OOH-3	94.44	42.74	59.47	74.19	86.24	104.16	116.71	135.45
TCD-OOH-4	95.68	42.94	59.58	74.25	86.28	104.18	116.74	135.47
TCD-OOH-9	95.11	42.85	59.51	74.19	86.22	104.14	116.70	135.44
TCD-OOH-1-10	95.29	43.01	59.58	74.20	86.22	104.11	116.68	135.43
TCD-OO•-1	93.71	41.25	57.44	71.68	83.37	100.75	112.91	130.90
TCD-OO•-2	93.73	41.28	57.54	71.80	83.48	100.83	112.96	130.93
TCD-OO•-3	94.23	40.68	57.05	71.45	83.24	100.72	112.91	130.92
TCD-OO•-4	94.46	40.70	57.07	71.45	83.24	100.72	112.92	130.93
TCD-OO•-9	94.83	40.71	57.03	71.40	83.18	100.67	112.88	130.91
TCD-OO•-1-10	95.02	40.89	57.11	71.43	83.19	100.66	112.85	130.88
TCD-OOH-12	106.29	47.29	64.02	79.07	91.64	110.71	124.31	144.81
TCD-OOH-21	107.90	47.37	64.02	79.05	91.60	110.66	124.25	144.76
TCD-OOH-23	101.15	47.66	64.43	79.41	91.89	110.82	124.33	144.77
TCD-OOH-32	103.94	46.87	63.74	78.88	91.49	110.60	124.22	144.75
TCD-OOH-34	103.14	47.64	64.29	79.24	91.74	110.71	124.26	144.75
TCD-OOH-43	102.37	47.62	64.31	79.28	91.78	110.74	124.29	144.76
TCD-OOH-19	102.84	47.74	64.37	79.31	91.79	110.76	118.08	144.80
TCD-OOH-91	102.43	44.77	61.24	76.04	88.40	107.10	120.38	140.22
TCD-OOH-1-10	101.66	47.58	64.11	79.01	91.49	110.52	124.13	144.69
TCD-OOH-10-1	102.49	46.78	63.40	78.44	91.06	110.27	124.00	144.67
TCD-OOH-26	98.54	46.54	63.39	78.50	91.13	110.33	124.03	144.67
TCD-OOH-98	105.16	47.84	64.33	79.22	91.70	110.70	124.29	124.29
TCD-OO•-12	105.94	45.19	61.56	76.30	88.61	107.25	120.49	140.28
TCD-OO•-21	108.25	45.32	61.62	76.33	88.62	107.23	120.46	140.24
TCD-OO•-23	101.03	45.61	62.00	76.66	88.88	107.37	120.51	140.23
TCD-OO•-32	103.64	44.80	61.36	76.20	88.55	107.21	120.44	140.23
TCD-OO•-34	102.57	45.55	61.88	76.54	88.76	107.29	120.46	140.21
TCD-OO•-43	102.23	45.56	61.92	76.59	88.81	107.33	120.49	140.23
TCD-OO•-19	102.63	45.77	62.02	76.63	88.83	107.35	120.52	140.26
TCD-OO•-91	105.04	46.84	63.62	78.73	91.35	110.51	124.17	144.75
TCD-OO•-1-10	102.43	45.58	61.72	76.28	88.49	107.06	120.31	140.15
TCD-OO•-10-1	102.55	44.73	61.03	75.76	88.11	106.87	120.20	140.14
TCD-OO•-26	98.06	44.43	60.92	75.72	88.10	106.86	120.20	140.13
TCD-OO•-98	104.96	45.75	61.92	76.51	88.73	107.28	120.49	140.26
TCD-OO•-H•-12	110.38	43.69	59.23	73.20	85.22	103.50	116.04	135.08
TCD-OO•-H•-21	112.69	43.82	59.29	73.23	85.22	103.48	116.00	135.04
TCD-OO•-H•-23	103.64	44.83	60.64	74.75	86.48	104.21	116.77	135.57
TCD-OO•-H•-32	108.08	43.3	59.03	73.10	85.16	103.45	115.99	135.03
TCD-OO•-H•-34	105.18	44.78	60.52	74.63	86.36	104.13	116.72	135.55
TCD-OO•-H•-43	104.84	44.79	60.56	74.68	86.41	104.17	116.75	135.57
TCD-OO•-H•-19	105.24	45.00	60.66	74.72	86.43	104.18	116.78	135.6
TCD-OO•-H•-91	109.48	45.34	61.29	75.63	87.96	106.76	119.72	139.55
TCD-OO•-H•-1-10	105.04	44.81	60.35	74.37	86.09	103.9	116.57	135.49
TCD-OO•-H•-10-1	106.99	43.23	58.69	72.66	84.72	103.12	115.75	134.94
TCD-OO•-H•-26	102.50	42.93	58.59	72.62	84.70	103.11	115.75	134.93
TCD-OO•-H•-98	107.57	44.98	60.56	74.60	86.33	104.12	116.75	135.60

Units: S (cal mol^{-1}) ; Cp (cal mol^{-1} K^{-1})

Table 4.11 Entropy (S^o, 298 K) and heat capacity (Cp(T)) for the studied systems (continued)

Species	S^o	Cp						
	298 K	300 K	400 K	500 K	600 K	800 K	1000 K	1500 K
TCD-OH-OH-12	103.87	47.36	64.23	79.31	91.84	110.76	124.23	144.60
TCD-OH-OH-23	98.67	46.40	63.52	78.75	91.38	110.44	123.99	144.48
TCD-OH-OH-34	103.73	47.20	63.94	78.98	91.52	110.51	124.04	144.50
TCD-OH-OH-91	102.04	47.25	64.02	79.06	91.60	110.59	124.12	144.56
TCD-OH-OH-26	97.33	46.72	63.68	78.80	91.39	110.44	124.01	144.51
TCD-OH-OH-98	105.68	47.40	63.97	78.94	91.48	110.49	124.05	144.53
TCD-OH-OH-1-10	96.91	45.74	62.76	78.00	90.71	109.96	123.67	144.36
TCD-OH-O˙-12	102.77	46.31	62.83	77.48	89.62	107.89	120.85	140.31
TCD-OH-O˙-21	104.78	46.43	62.87	77.49	89.62	107.89	120.85	140.32
TCD-OH-O˙-23	98.05	45.68	62.55	77.38	89.60	107.94	120.92	140.38
TCD-OH-O˙-32	98.39	45.77	62.46	77.20	89.39	107.72	120.72	140.24
TCD-OH-O˙-34	101.07	46.30	62.75	77.41	89.58	107.91	120.91	140.39
TCD-OH-O˙-43	101.07	46.30	62.75	77.41	89.58	107.91	120.91	140.39
TCD-OH-O˙-19	100.77	45.95	62.36	77.01	89.20	107.60	120.65	140.24
TCD-OH-O˙-91	99.97	45.81	62.42	77.18	89.43	107.86	120.90	140.42
TCD-OH-O˙-26	94.77	44.97	61.76	76.61	88.91	107.44	120.56	140.20
TCD-OH-O˙-98	101.05	45.87	62.30	77.02	89.27	107.74	120.83	140.40
TCD-OH-O˙-1-10	97.35	45.50	62.04	76.78	89.04	107.56	120.69	140.32
TCD-OH-O˙-10-1	100.11	45.90	62.35	77.03	89.24	107.68	120.76	140.35
TCD-O˙-O˙-12	101.31	45.33	61.53	75.87	87.73	105.51	118.05	136.72
TCD-O˙-O˙-23	96.59	44.70	61.25	75.77	87.71	105.56	118.12	136.79
TCD-O˙-O˙-34	99.61	45.32	61.45	75.80	87.69	105.53	118.11	136.8
TCD-O˙-O˙-91	98.51	44.83	61.12	75.57	87.54	105.48	118.10	136.83
TCD-O˙-O˙-26	93.31	43.99	60.46	75.00	87.02	105.06	117.76	136.61
TCD-O˙-O˙-98	99.59	44.89	61.00	75.41	87.38	105.36	118.03	136.81
TCD-O˙-O˙-1-10	95.88	44.52	60.74	75.17	87.15	105.18	117.89	136.73
TCD-YOO-12	90.87	41.37	58.22	73.08	85.32	103.61	116.45	135.49
TCD-YOO-23	91.02	41.26	58.09	72.96	85.21	103.53	116.39	135.46
TCD-YOO-34	90.36	41.02	57.91	72.83	85.12	103.50	116.39	135.49
TCD-YOO-91	90.51	41.19	58.04	72.92	85.19	103.54	116.41	135.49
TCD-YOO-26	89.06	41.04	57.88	72.75	85.01	103.38	116.28	135.41
TCD-YOO-98	90.17	40.86	57.71	72.64	84.96	103.40	116.34	135.48
TCD-YOO-1-10	90.73	41.05	57.69	72.50	84.78	103.23	116.20	135.40

Units: S (cal mol^{-1}) ; Cp (cal mol^{-1} K^{-1})

Entropy and heat capacity contributions as a function of temperature were determined from the calculated structures, moments of inertia, vibrational frequencies, symmetry, electron degeneracy, number of optical isomers and the known mass of each molecule. Entropy and heat capacity calculations were performed using B3LYP/6-31G(d,p), the results are summarized in Table 4.11, and Appendix J includes the entropy

and heat capacity values versus temperature (5 K ≤ T ≤ 5000 K). Appendix K includes the thermochemical properties of all the species studied in the NASA polynomial format for use in ChemKin.

4.3 Kinetic Properties

Initial unimolecular decomposition reaction of TCD involves formation of diradicals with one radical on each of two carbon sites resulting from carbon – carbon bond cleavage, as discussed in Section 4.2. Single carbon site radicals are also formed on TCD via loss of hydrogen atoms on the TCD ring. These radicals and diradicals can undergo unimolecular dissociation reactions, or molecular oxygen $^3O_2$ will also react with these radical sites. Figure 4.8 shows a representation of the studied reaction paths.

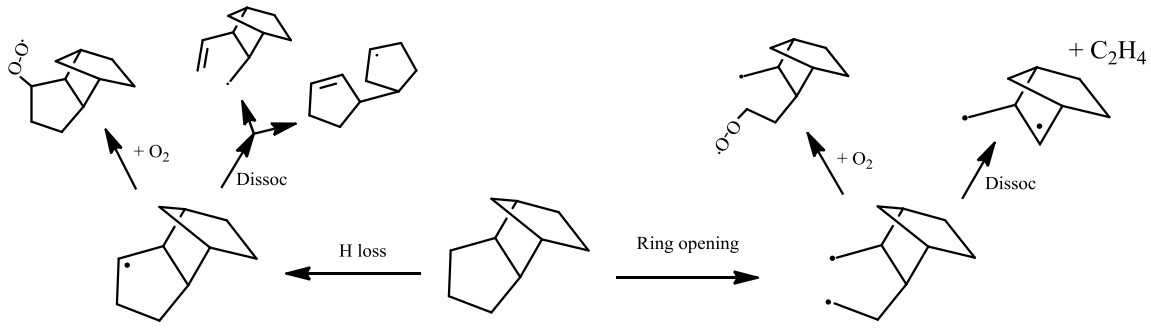

Figure 4.8 Ring opening, hydrogen loss, dissociation and oxidation examples of TCD

The systems studied are listed in Table 4.12. The nomenclature used for each of the species, is illustrated in Table 4.13. Thermochemical properties of all the species calculated are discussed in Section 4.2., and the thermochemical properties of all the reactants, products, and intermediate species included in the kinetic analysis, are included in Appendix K in the NASA polynomial format.

Table 4.12 Systems included in the TCD kinetic study

Studied systems	Studied systems
TCD → H loss → Dissociation	***TCD → Ring Opening → Dissociation***
TCD → TCD- H•-3 → Dissociation	TCD → TCD- H•- H•-1-9 → Dissociation
TCD → TCD- H•-4 → Dissociation	TCD → TCD- H•- H•-1-10 → Dissociation
TCD → TCD- H•-9 → Dissociation	
TCD → H loss → + O_2	***TCD → Ring Opening → + O_2***
TCD → TCD- H•-3 → + O_2	TCD → TCD- H•- H•-1-9 → + O_2
TCD → TCD- H•-4 → + O_2	TCD → TCD- H•- H•-1-10 → + O_2
TCD → TCD- H•-9 → + O_2	

Table 4.13 Species included in the TCD kinetic study

Nomenclature	Schematic	Formula	Nomenclature	Schematic	Formula
TCD		$C_{10}H_{16}$	VCCMjCV2	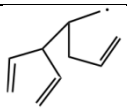	$C_{10}H_{15}$
TCD-Hj-3		$C_{10}H_{15}$	VCBIY221j	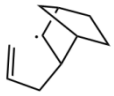	$C_{10}H_{15}$
TCD-Hj-4		$C_{10}H_{15}$	VCVYC5j	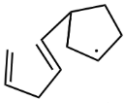	$C_{10}H_{15}$
TCD-Hj-9	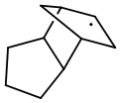	$C_{10}H_{15}$	VCCMjCV2	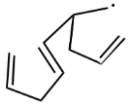	$C_{10}H_{15}$
TCD-Hj-Hj-1-2	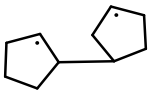	$C_{10}H_{15}$	YC6Ej		C_6H_9
TCD-Hj-Hj-1-9	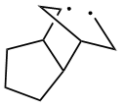	$C_{10}H_{16}$	VCVV		C_7H_{10}
TCD-Hj-Hj-1-10	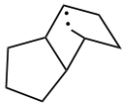	$C_{10}H_{16}$	VCjV		C_5H_7
YC5EYC5jS		$C_{10}H_{15}$	YC5jYC5E3	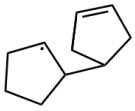	$C_{10}H_{15}$
YC5ECMjCV	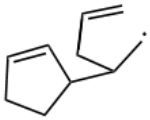	$C_{10}H_{15}$	YC5YC5jV	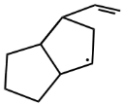	$C_{10}H_{15}$
YC5Ej1		C_5H_7	YC5E		C_5H_8
VCV		C_5H_8	YC5Ej2		C_5H_7

Table 4.13 Species included in the TCD kinetic study (continued)

Nomenclature	Schematic	Formula	Nomenclature	Schematic	Formula
YC5DE		C_5H_6	VYC5CjV	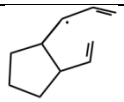	$C_{10}H_{15}$
VVCj		C_5H_7	VCjCCCVV		$C_{10}H_{15}$
VBIY221Cj	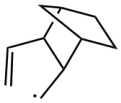	$C_{10}H_{15}$	CjCVV		C_6H_9
YC5jCV2	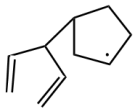	$C_{10}H_{15}$	YC5YC5V	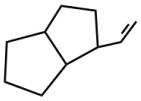	$C_{10}H_{16}$
TCD-Qj-3	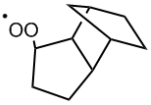	$C_{10}H_{15}O_2$	YC5Y5E1CC	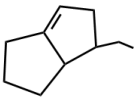	$C_{10}H_{16}$
TCD-Oj-3		$C_{10}H_{15}O$	YC5Y5E2CC	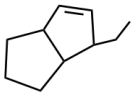	$C_{10}H_{16}$
TCD-Q-3-Hj-4	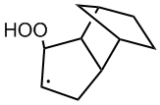	$C_{10}H_{15}O_2$	YC5YC5jj		C8H12
TCD-D-34		$C_{10}H_{14}$	YC8DE		C8H12
TCD-DO-3	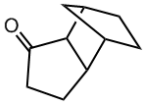	$C_{10}H_{14}O$	YC6DE13		C_6H_8
TCD-Qj-4	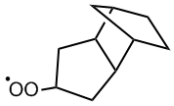	$C_{10}H_{15}O_2$	YC5(V)CMjCj	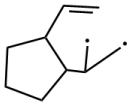	$C_{10}H_{16}$
TCD-Oj-4	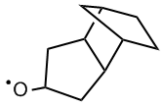	$C_{10}H_{15}O$	YC5jV	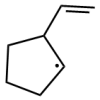	C_7H_{11}
TCD-Q-4-Hj-5	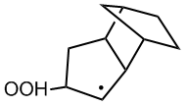	$C_{10}H_{15}O_2$	YC5EV	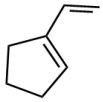	C_7H_{10}
TCD-D-45	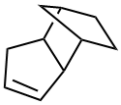	$C_{10}H_{14}$	VVCCCj		C_7H_{11}
TCD-DO-4	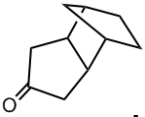	$C_{10}H_{14}O$	VVCj		C_5H_7
TCD-Qj-9	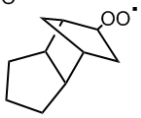	$C_{10}H_{15}O_2$	YC6ECj	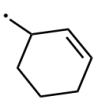	C_7H_{11}

Table 4.13 Species included in the TCD kinetic study (continued)

Nomenclature	Schematic	Formula	Nomenclature	Schematic	Formula
TCD-Oj-9	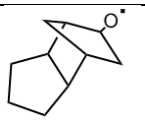	$C_{10}H_{15}O$	BI340V	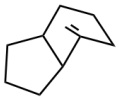	$C_{10}H_{16}$
TCD-Q-9-Hj-8	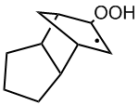	$C_{10}H_{15}O_2$	BI340E1M	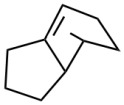	$C_{10}H_{16}$
TCD-D-89		$C_{10}H_{14}$	BI340E2M	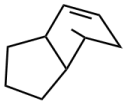	$C_{10}H_{16}$
TCD-DO-9	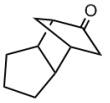	$C_{10}H_{14}O$	YC6V		C_7H_{10}
TCD-Qj-Hj-1-2	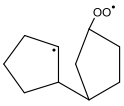	$C_{10}H_{16}O_2$	YC5jYC5E2	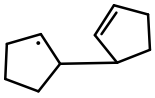	$C_{10}H_{15}$
TCD-yoo-1-2	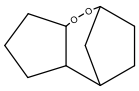	$C_{10}H_{16}O_2$	YC5OjPNj=O	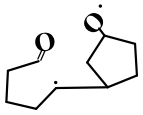	$C_{10}H_{16}O_2$
TCD-Oj-Oj-1-2	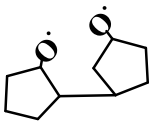	$C_{10}H_{16}O_2$	YC5=OYC5OH	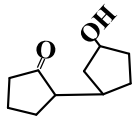	$C_{10}H_{16}O_2$
O=C9jMj=O	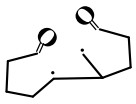	$C_{10}H_{16}O_2$	Y5OjPN=Oj	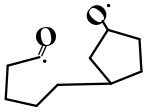	$C_{10}H_{16}O_2$
CjCCHO		C_3H_5O	VCjCCCCHO	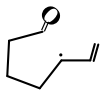	$C_7H_{11}O$
VCMjCCCHO		$C_7H_{11}O$	YC5YC5E1	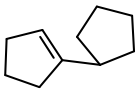	$C_{10}H_{16}$
YC5E		C_5H_8	YC5YC5E2	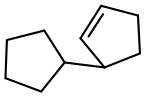	$C_{10}H_{16}$
YC5-Hj-Hj		C_5H_8	YC5YC5E3	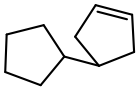	$C_{10}H_{16}$
TCD-Qj-Hj-1-9		$C_{10}H_{16}O_2$	TCD-Qj-Hj-1-10	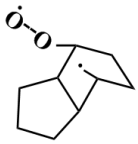	$C_{10}H_{16}O_2$

Table 4.13 Species included in the TCD kinetic study (continued)

Nomenclature	Schematic	Formula	Nomenclature	Schematic	Formula
TCD-yoo-1-9	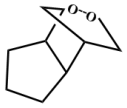	$C_{10}H_{16}O_2$	TCD-yoo-1-10	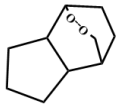	$C_{10}H_{16}O_2$
TCD-Oj-Oj-1-9	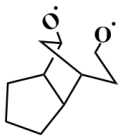	$C_{10}H_{16}O_2$	TCD-Oj-Oj-1-10	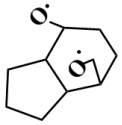	$C_{10}H_{16}O_2$
YC5jC(CC=O)CCOj	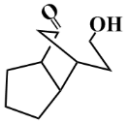	$C_{10}H_{16}O_2$	YC5jC(COj)C3=O	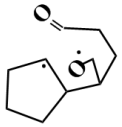	$C_{10}H_{16}O_2$
YC5jC(CC=O)Cj	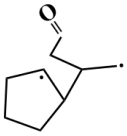	$C_9H_{14}O$	YC5jCjC3=O	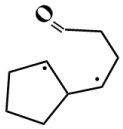	$C_9H_{14}O$
BIY330=OCCOH	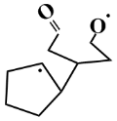	$C_{10}H_{16}O_2$	YC5YC6(=O)COH	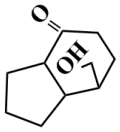	$C_{10}H_{16}O_2$
CjC=C equal C=CCj		C_3H_5	C=CCC=C		C_5H_8
Cj=CC=C		C_4H_5	C=CC=C		C_4H_6

High-pressure rate constant parameters have been taken from the literature or have been estimated from rate rules. Table 4.14 summarizes the literature references for each set of rate constants.

Table 4.14 Sets of reactions considered for each system, and references for high-pressure rate constant parameters

Reactions	Reference
1. Intramolecular H transfer to form olefins	[123, 128]
2. β-scissions to form olefins	[129]
3. C–H rupture	[130]
4. Chemical activation with molecular oxygen	This work

Approximately five collisions (A = 9 x10^{13} cm^3 mol^{-1} s^{-1}) and a small barrier (Ea=1.5 kcal mol^{-1}) was estimated for the electronic state crossing, collision of diradical with bath gas or chemical activation of diradical in association reaction with $^3O_2$, as there

is ~35 kcal mol^{-1} of chemical activation here. The intramolecular hydrogen transfer reactions were estimated from literature calculations on four to six membered ring-opened systems[128] at the CBS-QB3 level, and a computational study on the thermal decomposition of tricyclodecane[123]. The rate constants for the unimolecular beta-scission reactions were estimated from a literature evaluation of experimental data on beta-scission reactions of hydrocarbons[129]. For the C–H rupture reactions, rate constants were estimated from high-pressure rate constants calculated by Dean et al.[130]. Kinetic parameters for the bimolecular chemical activation reactions and the subsequent unimolecular thermal dissociation reactions to adducts and product sets were calculated by using a multifrequency quantum Rice-Ramsperger- Kassel (qRRK) analysis for $k(E)$ with the steady-state assumption on the energized adduct(s). For the study, reduced sets of frequencies were used. The parameters used for the QRRK analysis are listed in Table 4.15, and Table 4.16 includes the reduced frequencies used for the kinetic analysis. A detailed description of the code is shown in the reference[89]. The high-pressure limiting rate constant for all the diradical + $^3O_2$ reactions were estimated as 1.5 x10^{13} independent of temperature.

Table 4.15 Parameters for the determination of the pressure and temperature dependence of rate constants

Parameters		
T_{range} (K)		300-2400
P_{range} (atm)		0.001-100
Bath gas	Species	N_2
	σ (A)	3.54
	e/k (K)	97.5
σ (A)		5.32
e/k (K)		608.8
ΔE_{down} (cal mol^{-1})		900.
Integration interval (kcal)		0.5
E_{head} (kcal mol^{-1})		65

Table 4.16 Reduced frequencies for species

Species	Frequencies (cm^{-1})	# Vibration Modes
TCD- H•-3	438.4	19.094
	1235.2	36.343
	3026.3	16.563
TCD- H•-4	337.1	32.325
	785.9	32.908
	4000.0	5.767
TCD- H•-9	329.1	31.180
	777.8	33.549
	3999.8	5.771
TCD- H•- H•-1-2	327.0	32.430
	799.3	33.387
	4000.0	5.682
TCD- H•- H•-1-9	558.2	24.584
	1416.7	32.546
	3479.3	13.869
TCD- H•- H•-1-10	472.4	24.053
	1335.9	38.258
	3259.2	15.189

There are a number of reactions that are not included in this mechanism analysis. These include:

- Abstraction and association reactions by radical pool species on the reactants and intermediates. These are omitted because their concentration is several orders of magnitude below that of the reactive $^3O_2$ moiety, where the oxygen association has a high pre-exponential factor and no barrier.
- Intramolecular hydrogen transfer of the ROO• peroxy radicals where the barrier is relatively high (above 20 kcal mol^{-1}).
- HO_2 and H_2O molecular elimination reactions from the peroxy radicals and peroxides, where high barriers reduce their importance.
- Further reactions of initial products to complete oxidation.

The decomposition of TCD is started by a hydrogen abstraction by radical pool species, or the ring opening of one of the C–C bonds in the parent TCD molecule. Table

4.17 summarizes the bond dissociation enthalpies to form the alkyl radicals, calculated by Hudzik et al.[124] at the CBS-QB3 level of theory.

Table 4.17 C─H bond dissociation enthalpies of the TCD parent molecule to form the radicals

Species	***C—H BDE***
TCD-H•-1	107.2
TCD-H•-2	100.1
TCD-H•-3	**98.0**
TCD-H•-4	**98.5**
TCD-H•-9	**98.7**
TCD-H•-10	104.1

Units kcal mol^{-1}

Results show that C─H bonds in the position 3, 4 and 9 are the weakest bonds, and therefore, these were the systems studied throughout this work.

The C─C bond energies from the literature[125] calculated at the CBS-QB3 level of theory, for the ring opening of the TCD parent molecule for the formation of the singlet diradicals are summarized in Table 4.18.

Table 4.18 C─C bond dissociation enthalpies of the TCD parent molecule to form the diradicals

Species	***C—C BDE***
TCD-H•-H•-1-2	***70.4***
TCD-H•-H•-2-3	73.3
TCD-H•-H•-3-4	78.5
TCD-H•-H•-2-6	75.4
TCD-H•-H•-1-10	***68.9***
TCD-H•-H•-1-9	***70.0***
TCD-H•-H•-9-8	76.8

Units kcal mol^{-1}

The results in Table 4.18 show that C─C bonds 1-10, 1-9 and 1-2 are the weakest bonds. Therefore, 1-2, 1-10 and 1-9 are the systems studied throughout the study. The rate constants estimated for each of the systems are summarized in Appendix L.

Figure 4.9 and 4.10 represent the potential energy diagrams for the hydrogen loss of the parent TCD to form the alkyl radicals (Figure 4.9) and the C─C ring opening of the parent TCD to form the diradicals (Figure 4.10).

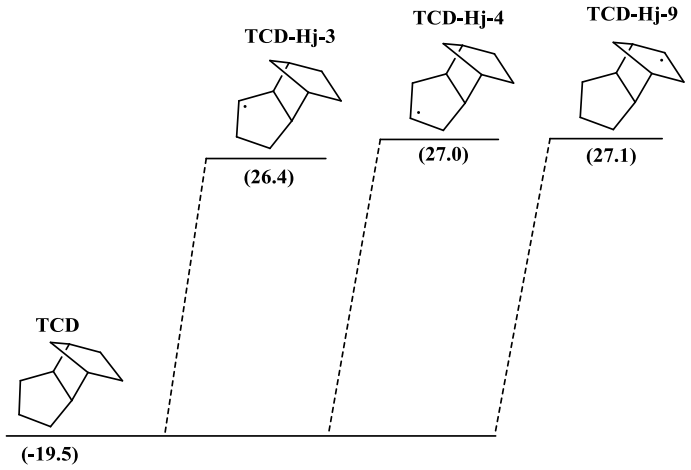

Figure 4.9 TCD hydrogen loss to TCD-H•-3, TCD-H•-4, and TCD-H•-9. All values are at 298 K. Units: kcal mol^{-1}. j = represents a radical site

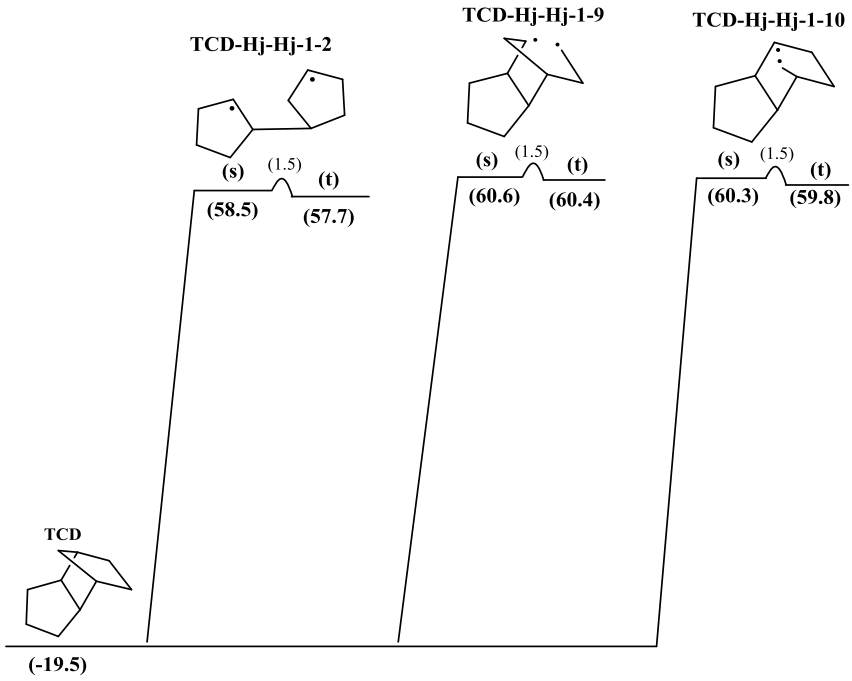

Figure 4.10 TCD ring-opening to TCD-H•-H•-1-2, TCD-H•- H•-1-9 and TCD-H•- H•-1-10. All values are at 298 K. Units: kcal mol^{-1}. j = represents a radical site

Figures 4.11 to 4.13 represent the dissociation of the alkyl radicals formed by the hydrogen loss of the parent TCD. Both intramolecular H transfer and the β-scission reactions were considered.

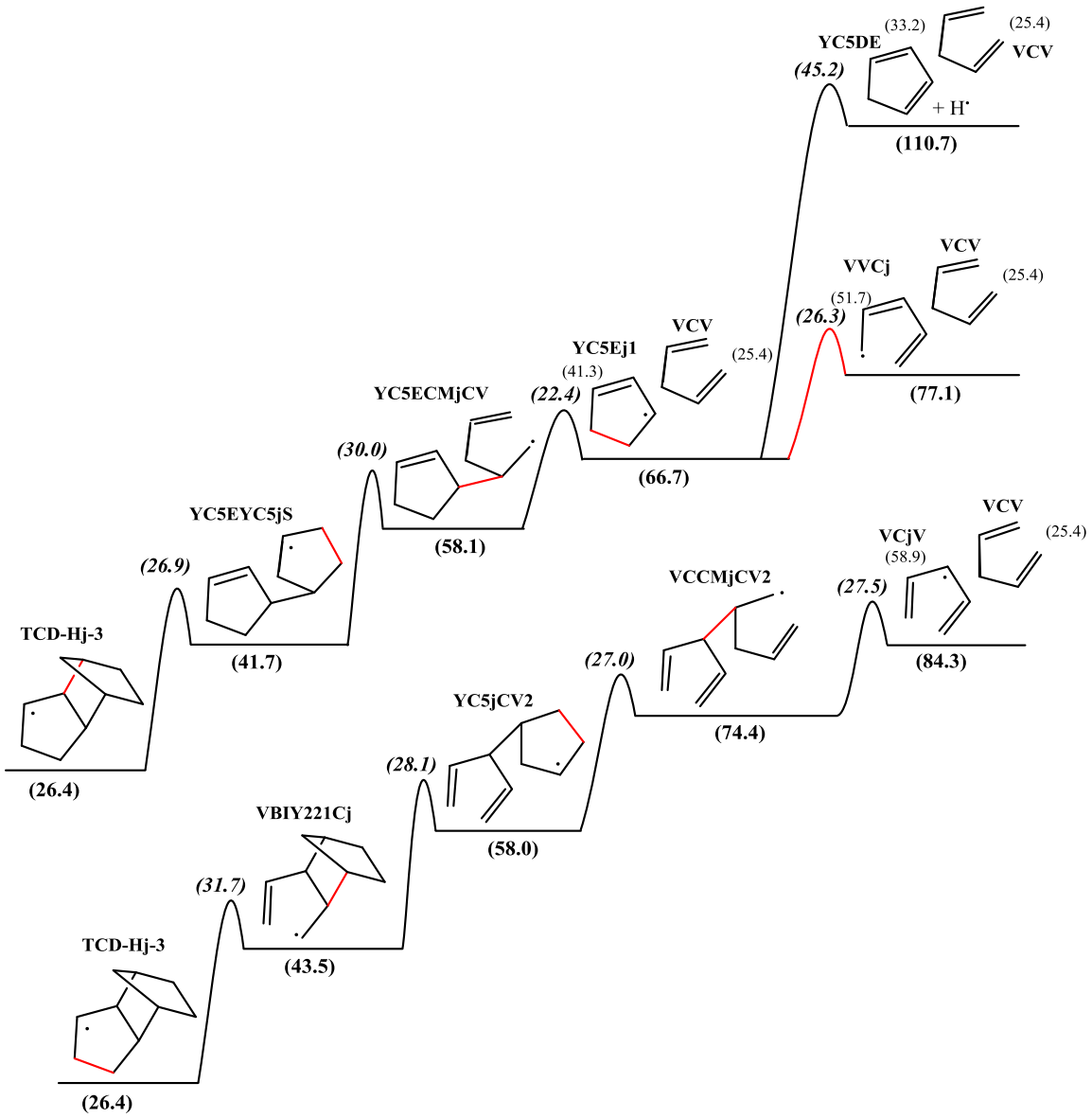

Figure 4.11 TCD hydrogen loss TCD-H$^{\bullet}$-3 dissociation potential energy diagram. All values are at 298 K. Units: kcal mol^{-1}. j = represents a radical site

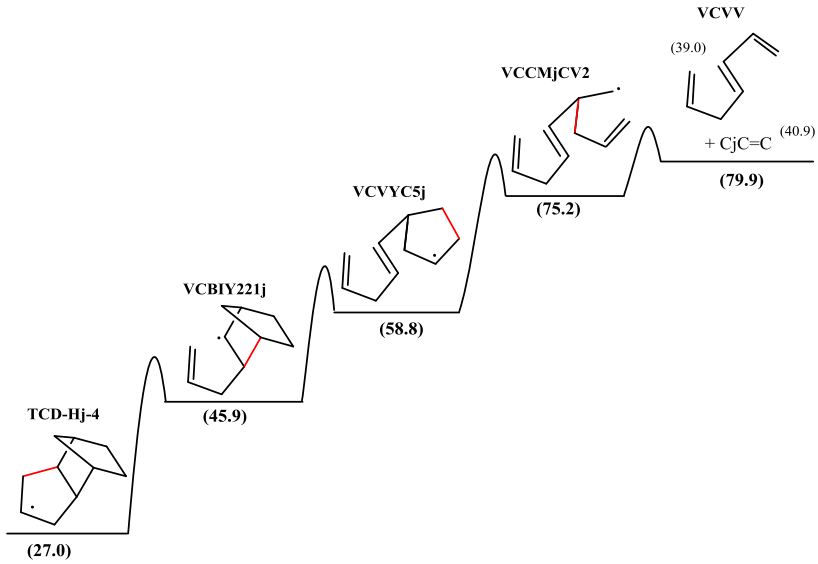

Figure 4.12 TCD hydrogen loss TCD-H•-4 dissociation potential energy diagram. All values are at 298 K. Units: kcal mol^{-1}. j = represents a radical site

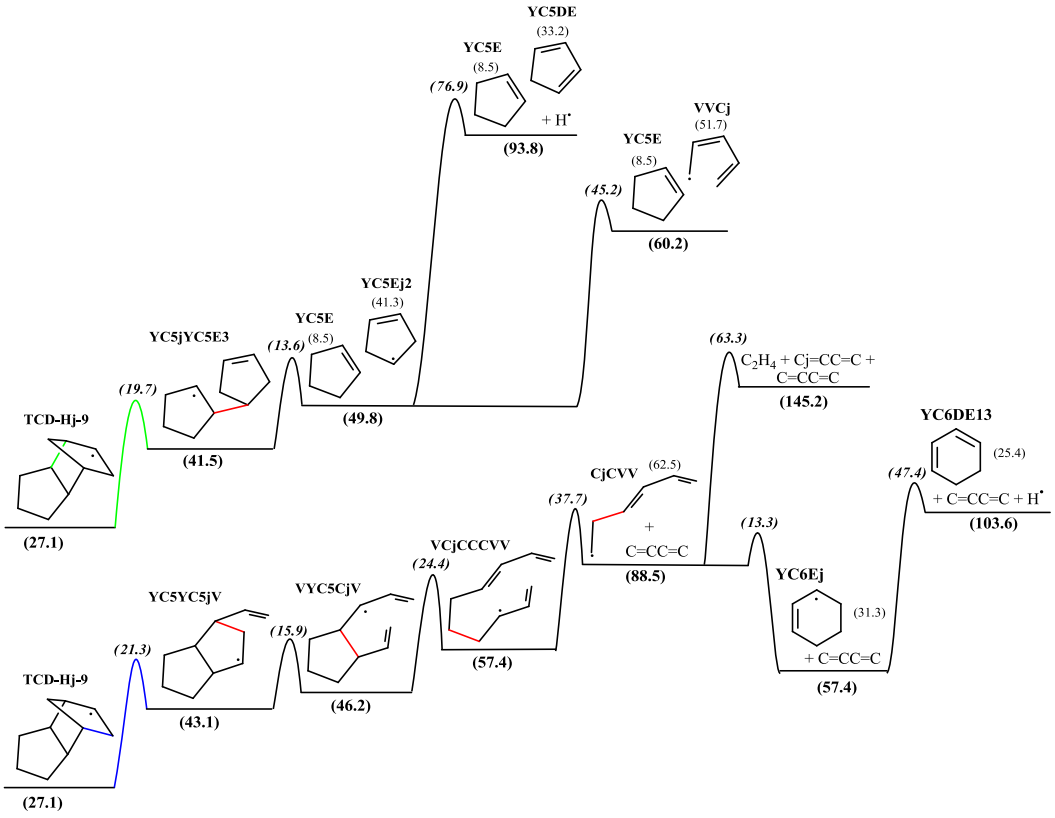

Figure 4.13 TCD hydrogen loss TCD-H•-9 dissociation potential energy diagram. All values are at 298 K. Units: kcal mol^{-1}. j = represents a radical site

Figures 4.14, 4.17 and 4.20 represent the $^3O_2$ addition to the alkyl radicals formed, leading to the formation of the peroxy radical, that can undergo:

(a) a barrierless RO—O cleavage to form an alkoxy radical and an oxygen atom ($O^{\bullet}$).
(b) intramolecular transfer of a secondary hydrogen atom of the ring to the peroxy radical to form an alkyl hydroperoxide.
(c) molecular elimination of $HO_2^{\bullet}$ radical, where the H is from a secondary carbon in the ring to form a cyclic olefin.
(d) intramolecular transfer of the hydrogen atom bonded to a secondary carbon to the peroxy oxygen radical and subsequent $R^{\bullet}O$—OH bond cleavage to form cyclic ketone plus $OH^{\bullet}$.

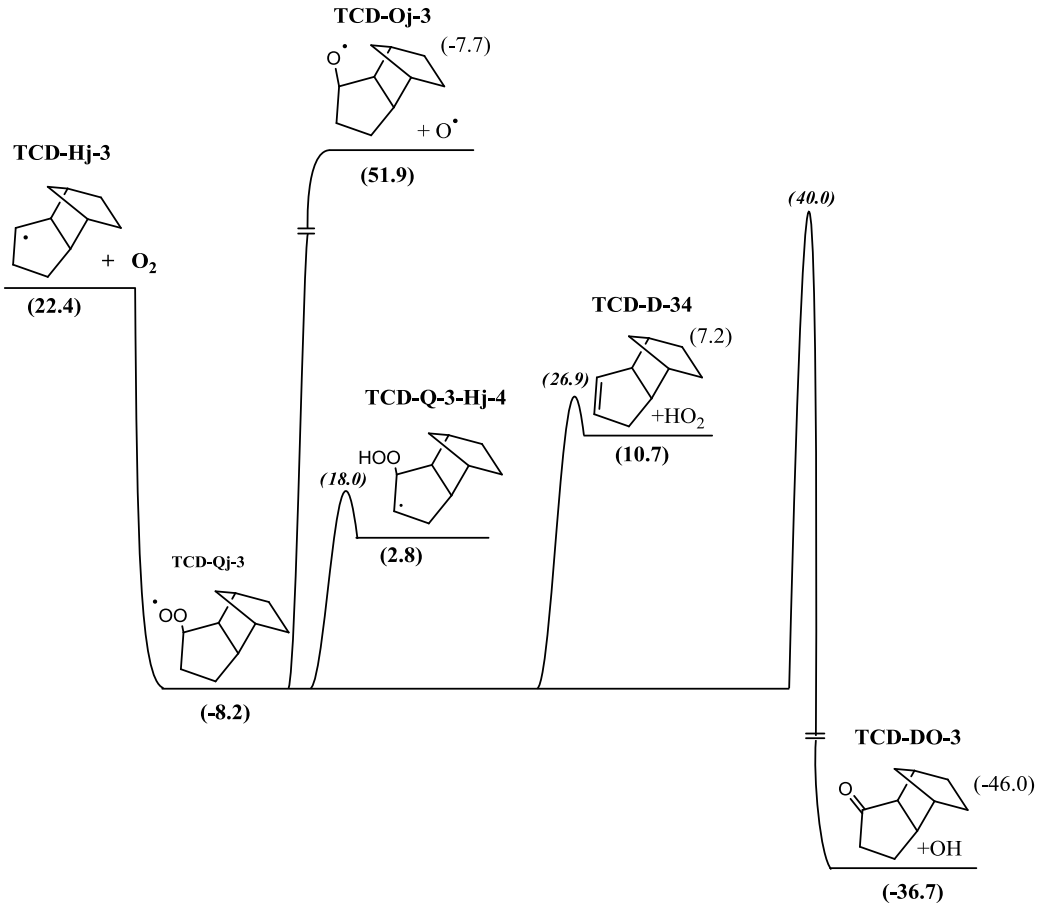

Figure 4.14 TCD hydrogen loss TCD-H$^{\bullet}$-3 oxidation with $^3O_2$ potential energy diagram. All values are at 298 K. Units: kcal mol^{-1}. j = represents a radical site

For each of the systems, the chemical activation figures are represented, for two different pressures (1 atm and 100 atm) and temperatures (500 K and 1000 K) in Figures 4.15 and 4.16 for radical 3, Figures 4.18 and 4.19 for radical 4, and Figures 4.21 and 4.22 for radical 9.

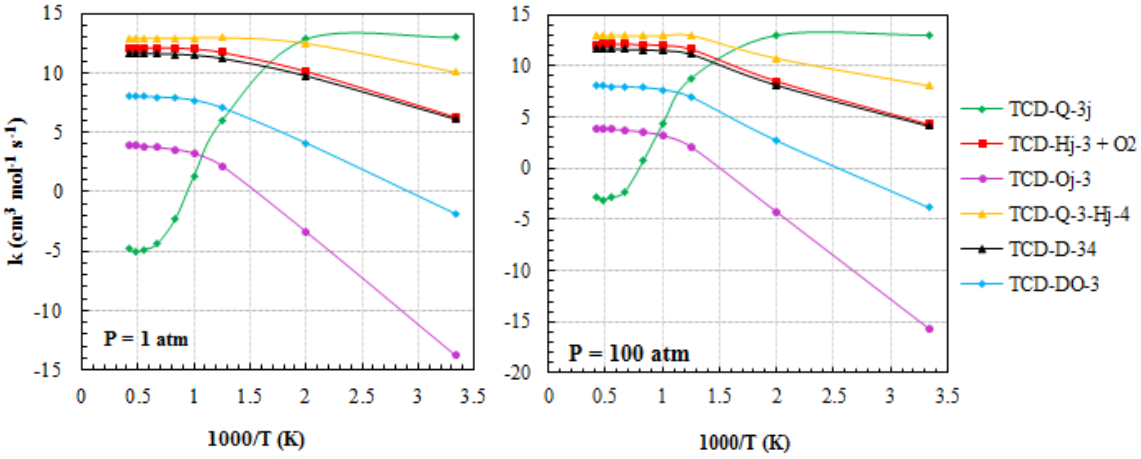

Figure 4.15 Chemical activation calculation of TCD-H•-3 oxidation with $^3O_2$ at a constant pressure of 1 atm (left) and 100 atm (right)

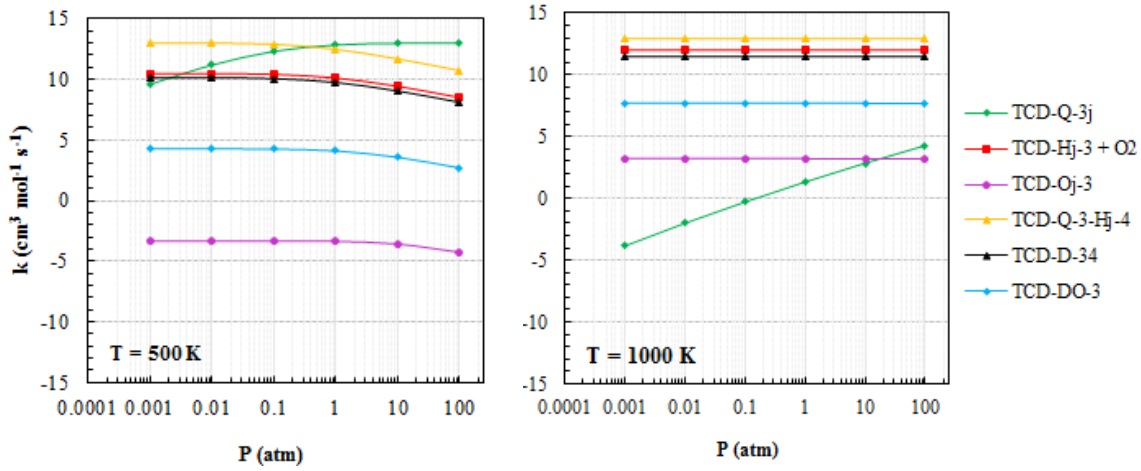

Figure 4.16 Chemical activation calculation of TCD-H•-3 oxidation with $^3O_2$ at a constant temperature of 500 K (left) and 1000 K (right)

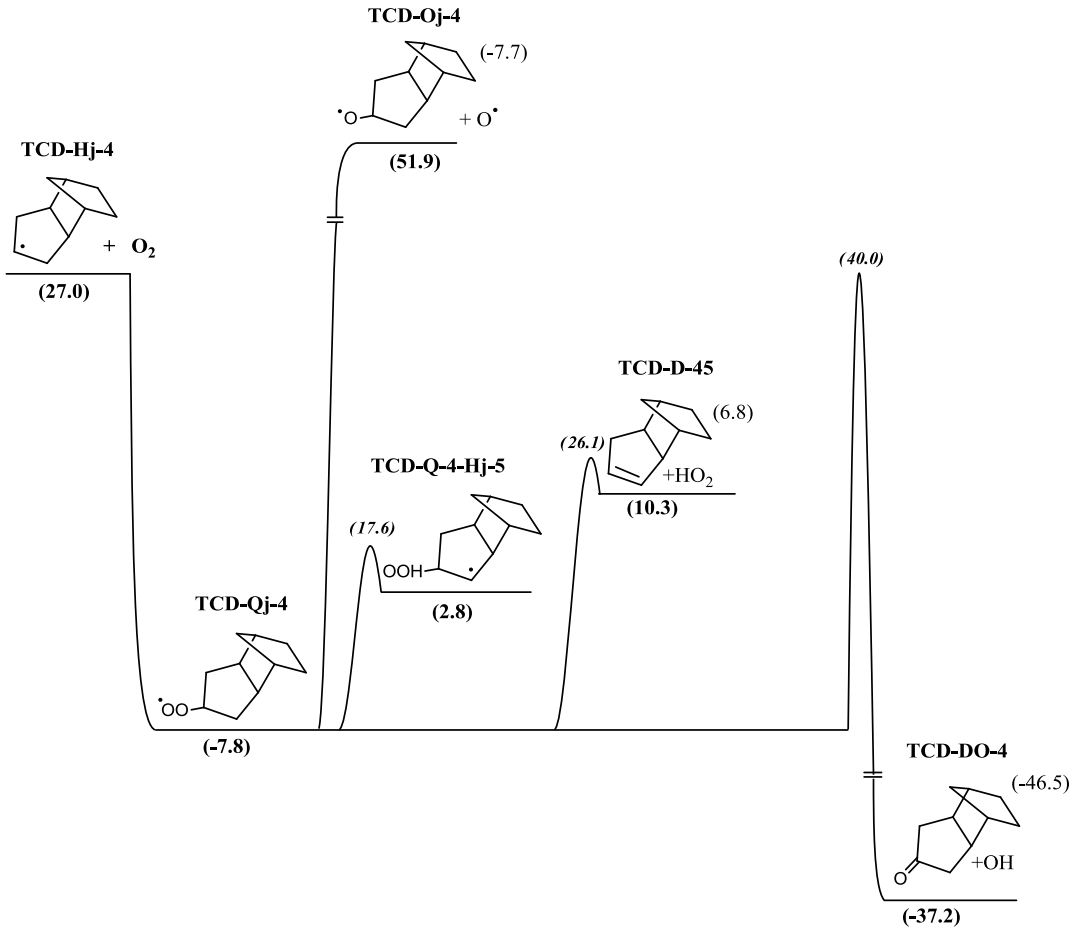

Figure 4.17 TCD hydrogen loss TCD-H•-4 oxidation with $^3O_2$ potential energy diagram. All values are at 298 K. Units: kcal mol^{-1}. j = represents a radical site

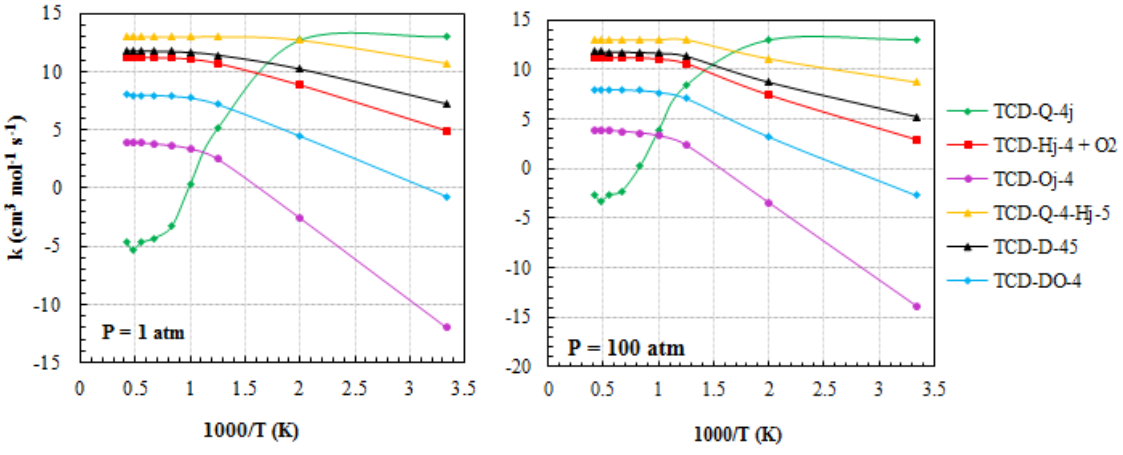

Figure 4.18 Chemical activation calculation of TCD-H•-4 oxidation with $^3O_2$ at a constant pressure of 1 atm (left) and 100 atm (right)

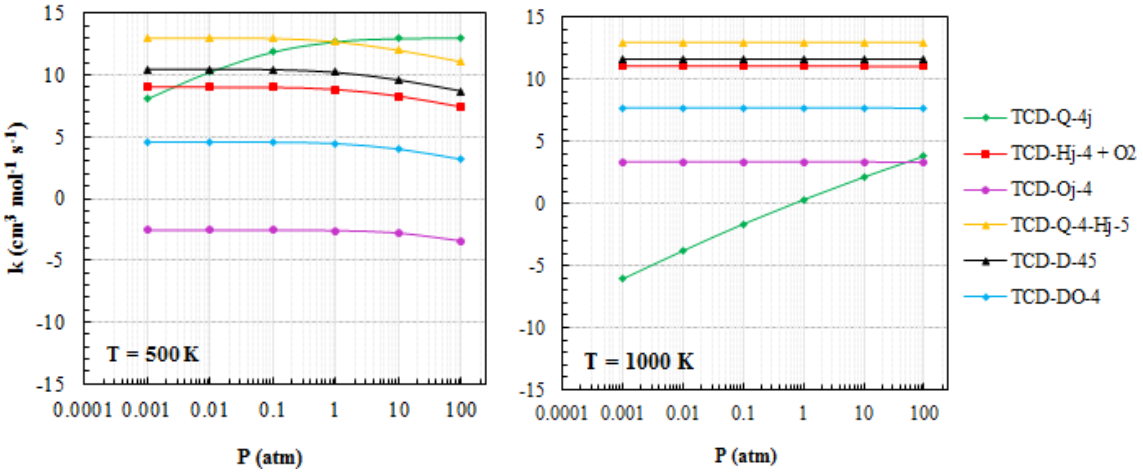

Figure 4.19 Chemical activation calculation of TCD-H•-4 oxidation with $^3O_2$ at a constant temperature of 500 K (left) and 1000 K (right)

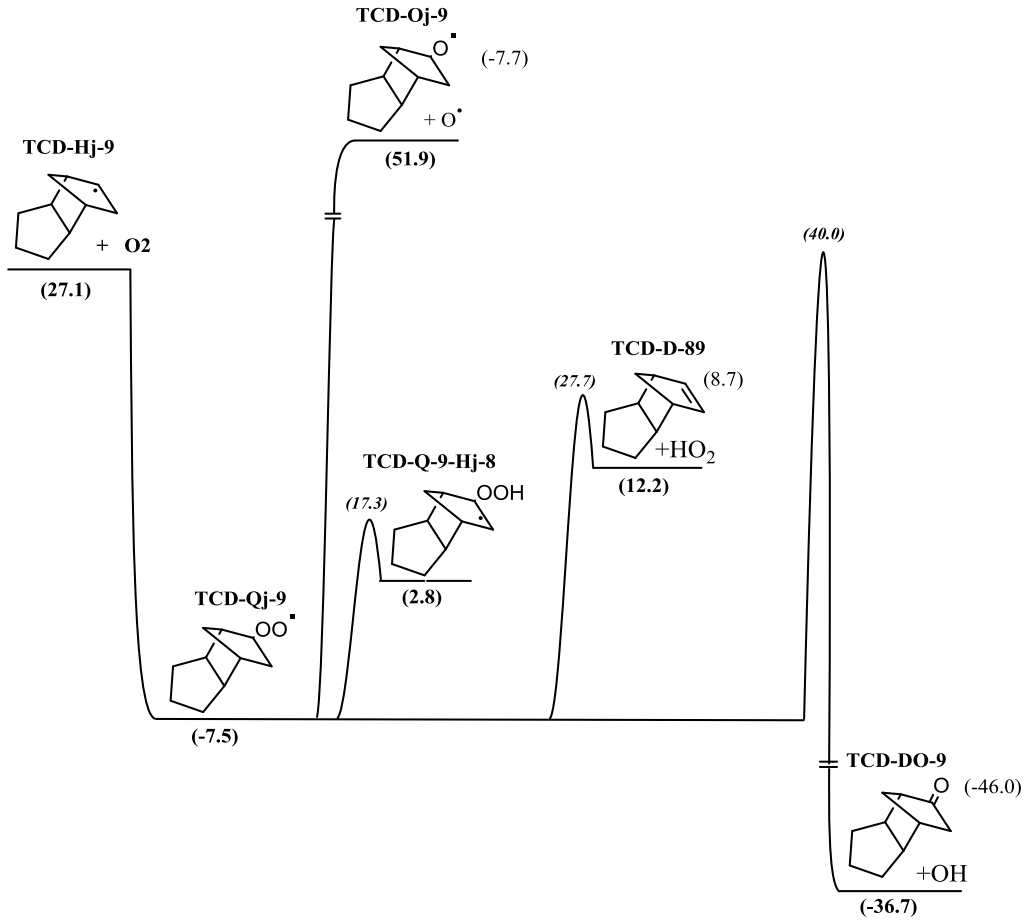

Figure 4.20 TCD hydrogen loss TCD-H•-9 oxidation with $^3O_2$ potential energy diagram. All values are at 298 K. Units: kcal mol^{-1}. j = represents a radical site

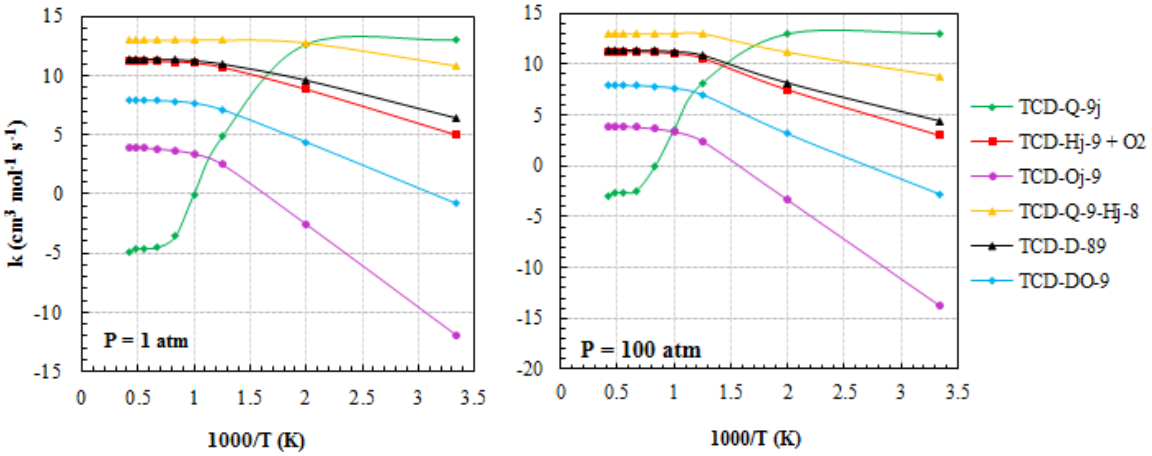

Figure 4.21 Chemical activation calculation of TCD-H•-9 oxidation with $^3O_2$ at a constant pressure of 1 atm (left) and 100 atm (right)

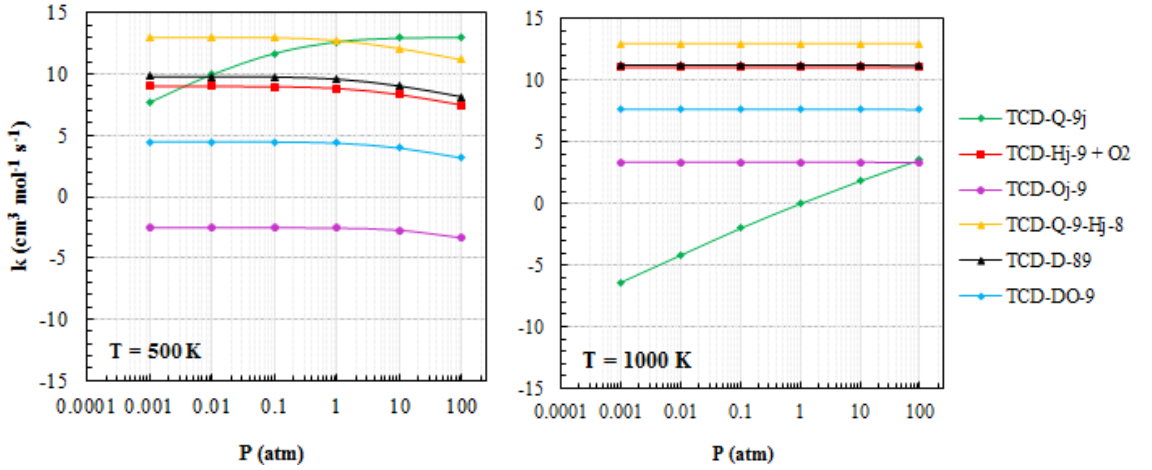

Figure 4.22 Chemical activation calculation of TCD-H•-9 oxidation with $^3O_2$ at a constant temperature of 500 K (left) and 1000 K (right)

Figures 4.23, 4.24 and 4.25 represent the dissociation of the alkyl diradical formed via the ring opening of the parent TCD (C─C bonds 1-2,1-9, and 1-10, respectively). Both intramolecular H transfer and *β*-scission reactions have been considered.

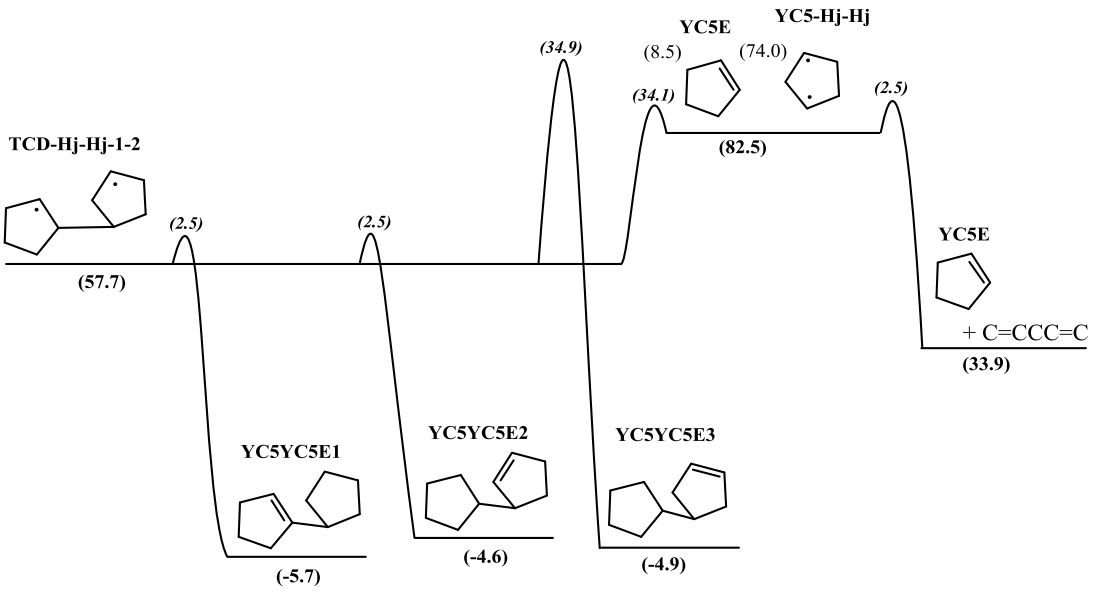

Figure 4.23 TCD ring-opened TCD-H•-H•-1-2 dissociation potential energy diagram. All values are at 298 K. Units: kcal mol^{-1}. j = represents a radical site

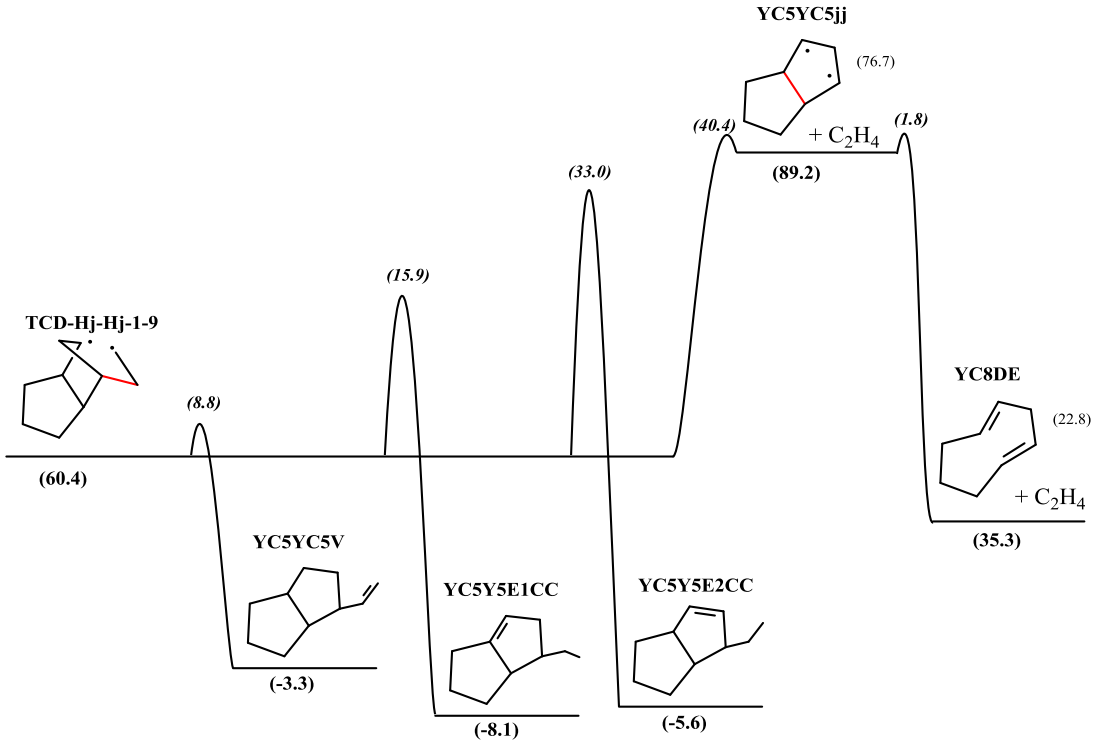

Figure 4.24 TCD ring-opened TCD-H•-H•-1-9 dissociation potential energy diagram. All values are at 298 K. Units: kcal mol^{-1}. j = represents a radical site

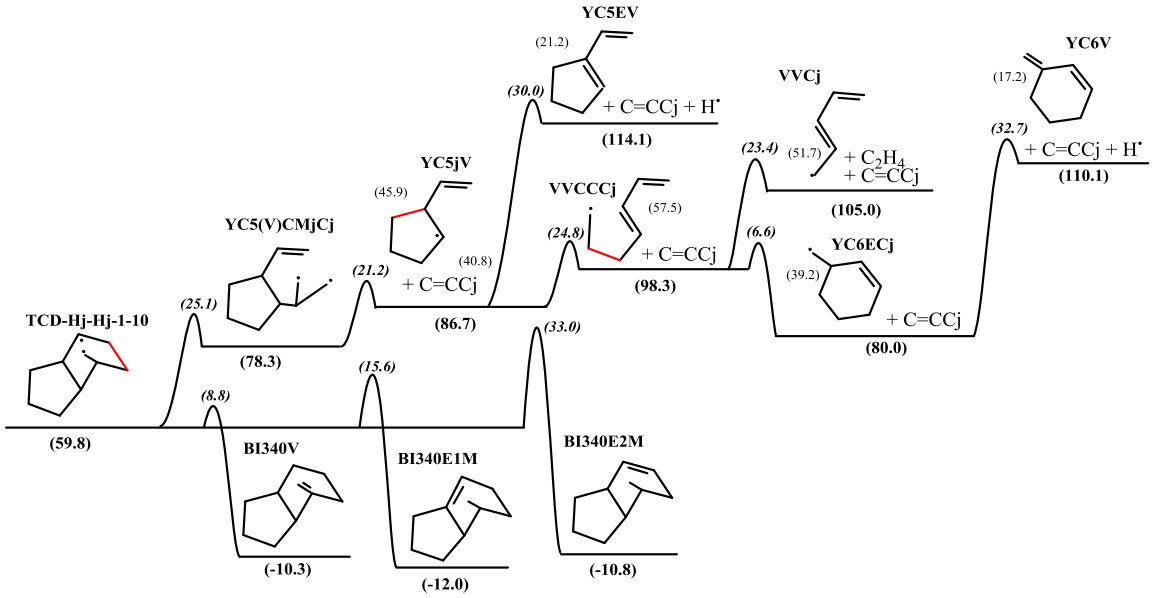

Figure 4.25 TCD ring-opened TCD-H•-H•-1-10 dissociation potential energy diagram. All values are at 298 K. Units: kcal mol^{-1}. j = represents a radical site

Figures 4.26, 4.29 and 4.32 represent the $^3O_2$ addition to the alkyl diradical formed via the ring opening of the parent TCD (C─C bonds 1-2, 1-9 and 1-10, respectively), leading to the formation of the peroxy radical, that can undergo:

(a) triplet–singlet conversion via electronic state crossing, collision of diradical with bath gas, or chemical activation of diradical with molecular gas.

(b) molecular elimination of $HO_2^•$ radical, where the H is from a secondary carbon in the ring to form a cyclic olefin with an alkyl radical site.

(c) ring closure of the singlet peroxy diradical that will result in the formation of a oxygenated ring. This ring can undergo low-energy ring opening through the RO─OR bond, resulting in a dialkoxy radical. The dialkoxy diradical can undergo: (i) intramolecular hydrogen transfer to form a cyclic alkene bonded to a cyclic alkoxide, and (ii) decomposition through β-scission reactions.

For each of the systems, the chemical activation figures are represented, for two different pressures (1 atm and 100 atm) and temperatures (500 K and 1000 K) in Figures 4.27 and 4.28 for diradical 1-2, Figures 4.30 and 4.31 for diradical 1-9, and Figures 4.33 and 4.34 for diradical 1-10.

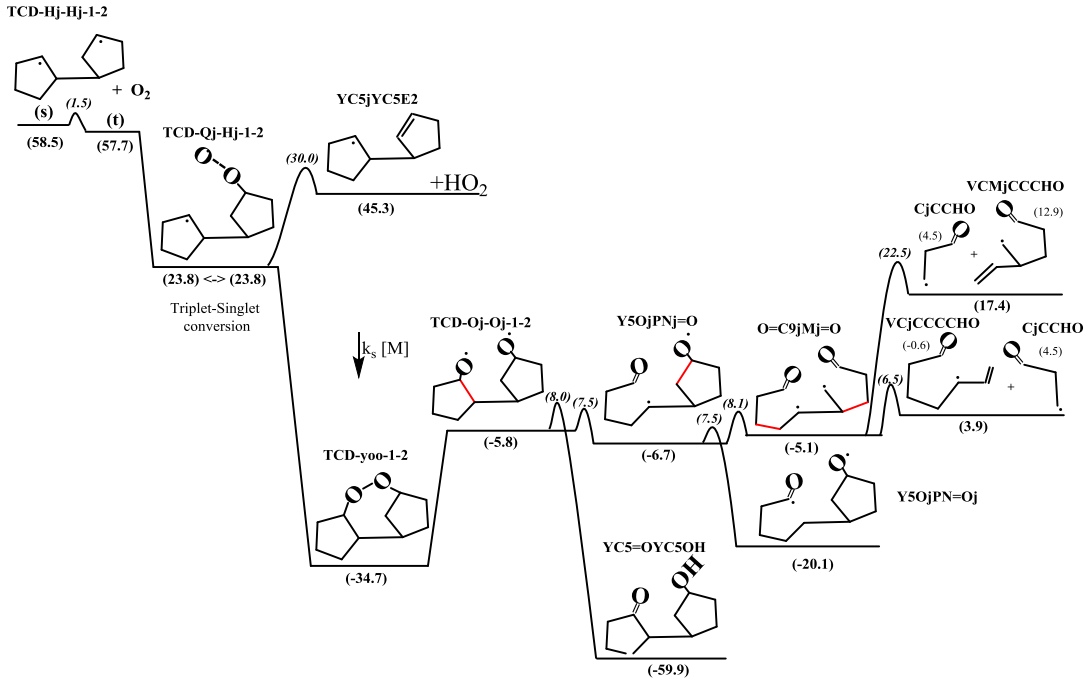

Figure 4.26 TCD ring-opened TCD-H•-H•-1-2 oxidation with $^3O_2$ potential energy diagram. All values are at 298 K. Units: kcal mol^{-1}. j = represents a radical site

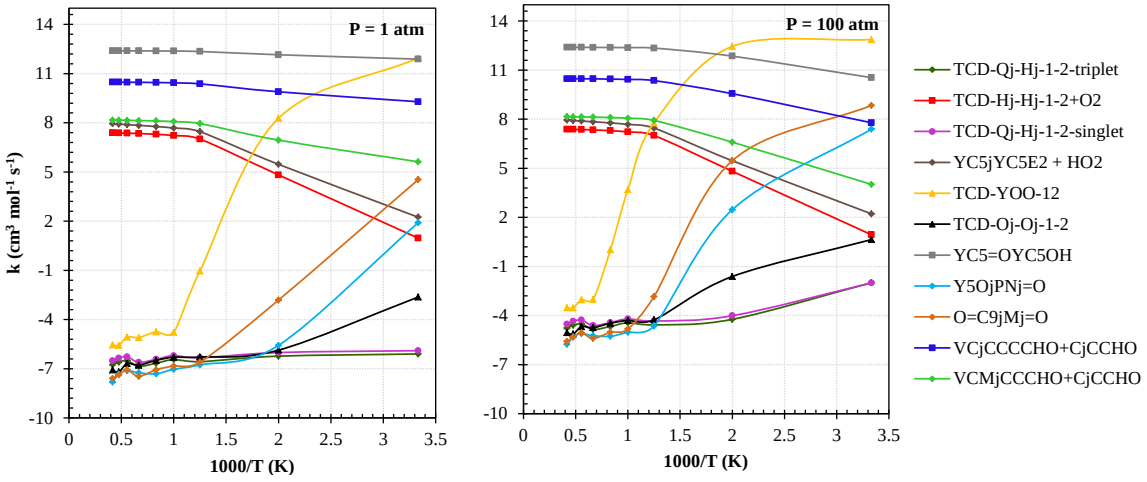

Figure 4.27 Chemical activation calculation of TCD-H•-H•-1-2 oxidation with $^3O_2$ at a constant pressure of 1 atm (left) and 100 atm (right)

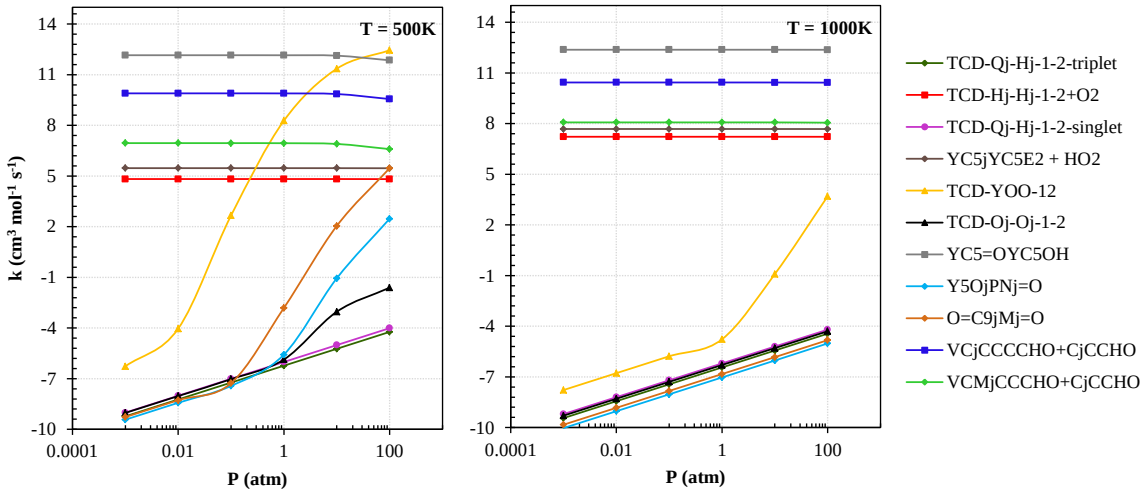

Figure 4.28 Chemical activation calculation of TCD-H•-H•-1-9 oxidation with $^3O_2$ at a constant temperature of 500 K (left) and 1000 K (right)

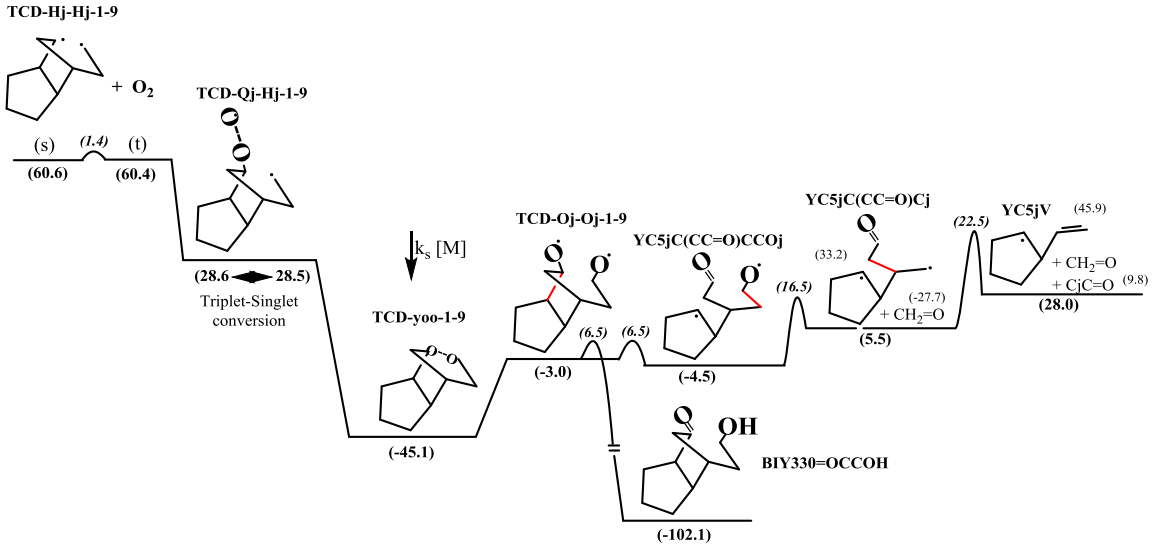

Figure 4.29 TCD ring-opened TCD-H•-H•-1-9 oxidation with $^3O_2$ potential energy diagram. All values are at 298 K. Units: kcal mol^{-1}. j = represents a radical site

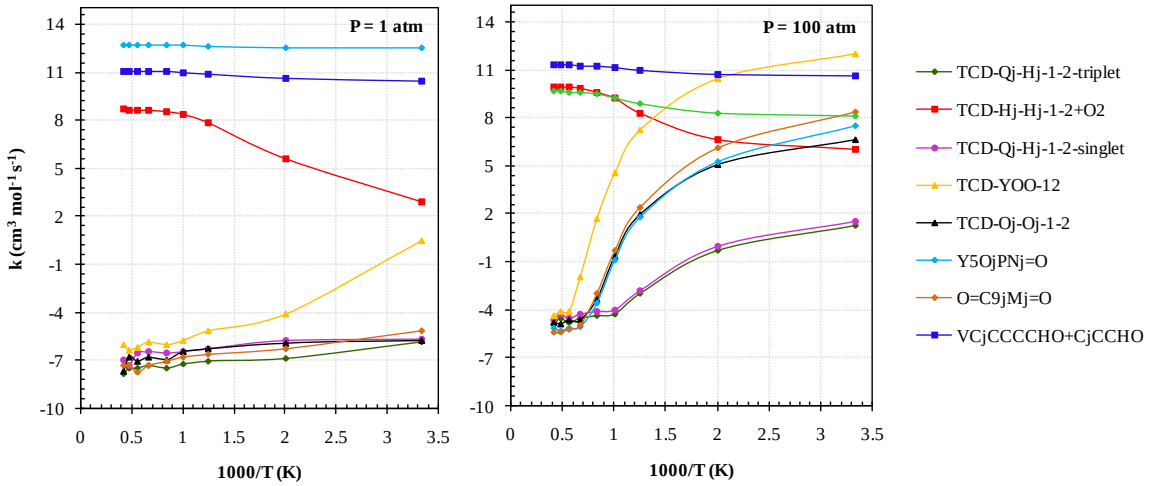

Figure 4.30 Chemical activation calculation of TCD-H•-H•-1-9 oxidation with $^3O_2$ at a constant pressure of 1 atm (left) and 100 atm (right)

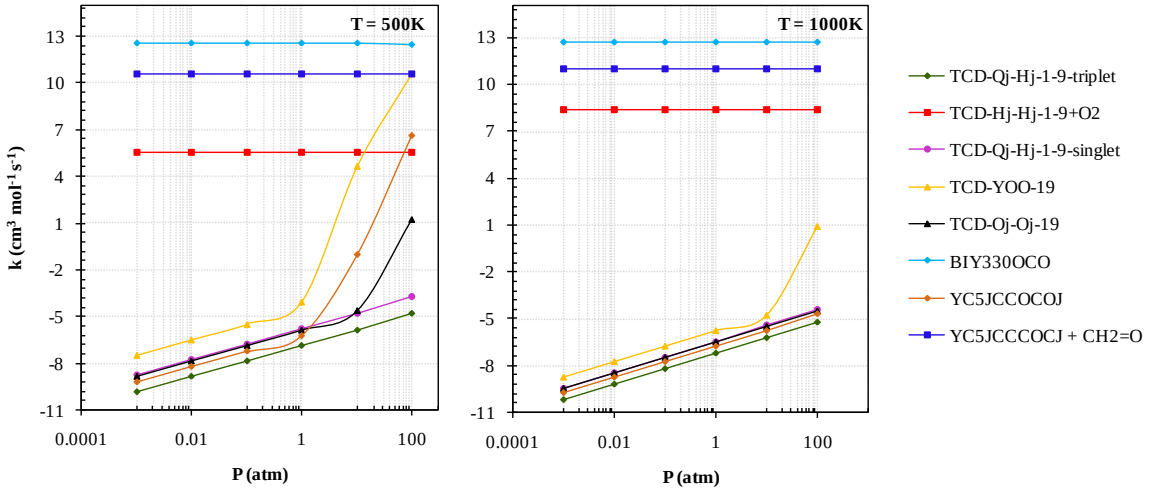

Figure 4.31 Chemical activation calculation of TCD-H•-H•-1-9 oxidation with $^3O_2$ at a constant temperature of 500 K (left) and 1000 K (right)

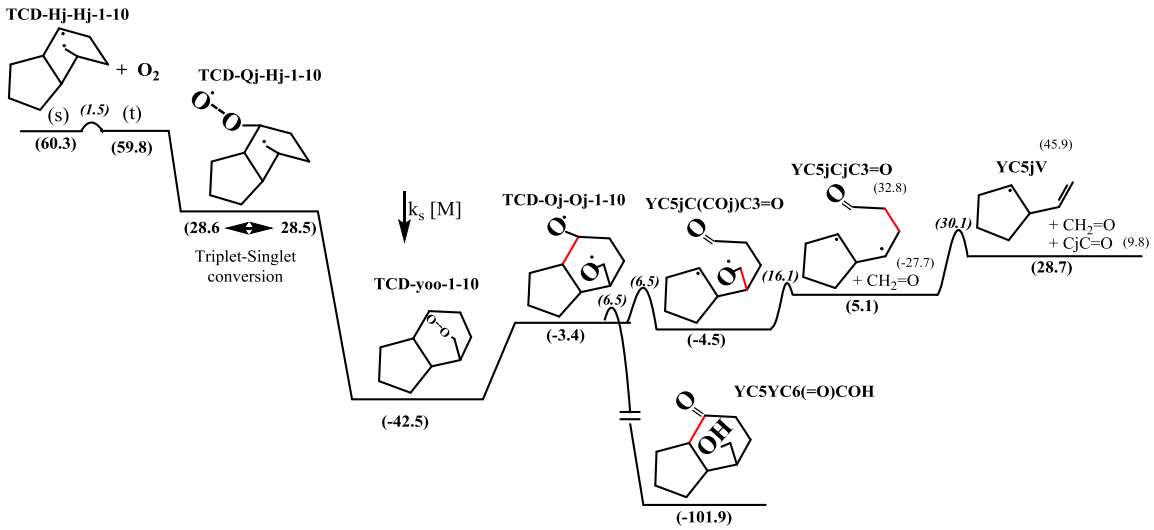

Figure 4.32 TCD ring-opened TCD-H•-H•-1-10 oxidation with $^3O_2$ potential energy diagram. All values are at 298 K. Units: kcal mol^{-1}. j = represents a radical site

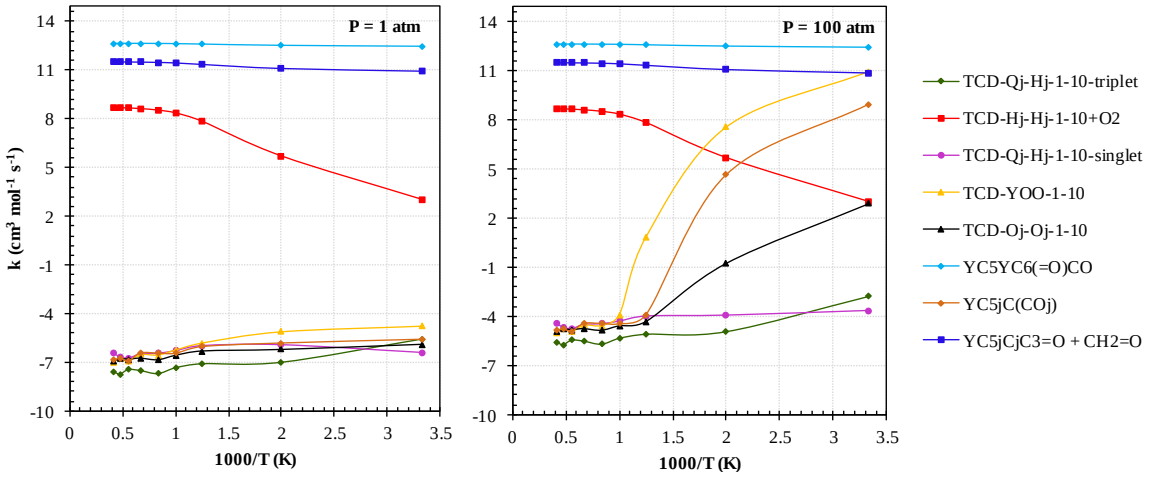

Figure 4.33 Chemical activation calculation of TCD-H•-H•-1-10 oxidation with $^3O_2$ at a constant pressure of 1 atm (left) and 100 atm (right)

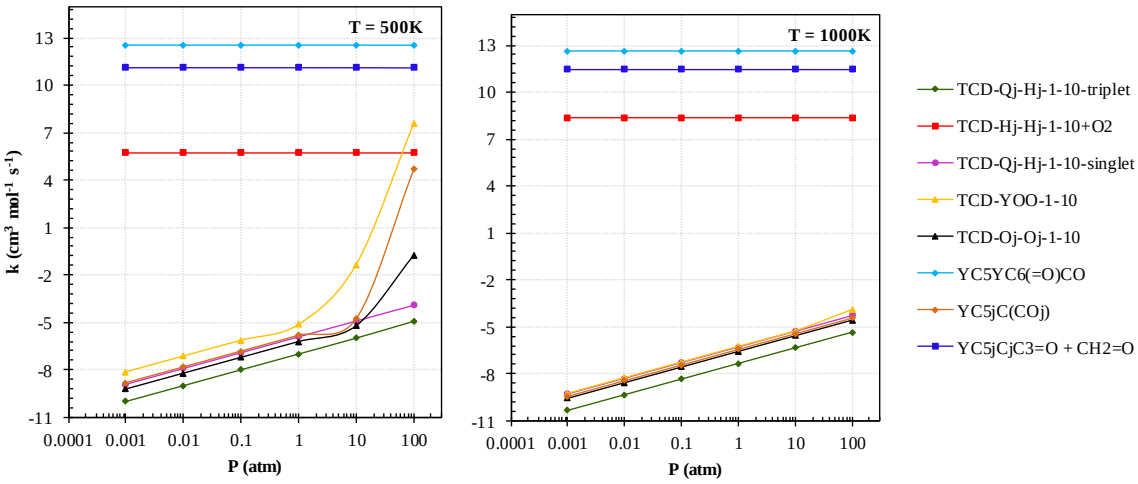

Figure 4.34 Chemical activation calculation of TCD-H•-H•-1-10 oxidation with $^3O_2$ at a constant temperature of 500 K (left) and 1000 K (right)

4.4 Summary

The enthalpies of formation, entropies and heat capacities of TCD hydroperoxides, peroxy radicals, alkyl/peroxy diradicals, TCD dialkohols, dialkoxy radicals, dialkoxy diradicals and oxygenated cyclic species resultant from the oxidation of TCD were determined in this study, at the B3LYP/6-31G(d,p) Density Functional Theory level of theory in conjunction with a series of work reactions. The OO—H, O—H and R—OOH bond dissociation enthalpies are presented for the different positions of the tricyclodecane hydroperoxides and dialcohols. Results show that the bond dissociation enthalpies are similar of that for cyclopentane, and for the linear alkanes, expect for TCD-OH-OH-98, TCD-OH-OH-1-10, TCD-OH-OH-26, TCD-OOH-1, TCD-OOH-2 and TCD-OOH-10, where the bond dissociation enthalpies are ±4 kcal mol^{-1} versus the values for cyclopentane, and the linear alkanes. The accuracy of these bond dissociation enthalpies is important for the construction of fundamental reaction mechanisms.

Rate constants have been estimated for the unimolecular dissociation of the radicals and diradicals resultant from the C–H bond cleave and C–C ring opening of the parent TCD molecule. Rate constants are presented also for the chemical activation of the radicals/diradicals with molecular oxygen $^3O_2$. Results show that at the low temperatures and higher pressures, the formation of oxygenated cyclic species becomes important. At high temperatures, the intramolecular hydrogen transfer reactions and beta-scission reactions are dominant.

The calculated thermochemical and kinetic properties were incorporated in a reaction mechanism, where further reactions of initial intermediates and products to complete oxidation are included, with the aim of determining the pyrolysis and oxidation characteristics of the jet fuel JP-10.

CHAPTER 5

UNIMOLECULAR DISSOCIATION AND OXIDATION OF CYCLIC ALKANES AND ETHERS

5.1 Overview

Current commercial fuels are blends of linear/branched/cyclic alkanes, alkenes, and aromatics, as represented in Figure 5.1. Cyclic alkanes are present in significant amounts in many commercial fuels: diesel fuels contain up to 27% of cycloalkanes, most common commercial aviation fuels (Jet A and Jet A-1) contain around 20% of cycloalkanes, whereas gasoline contains only around 3% of cycloalkanes[128].

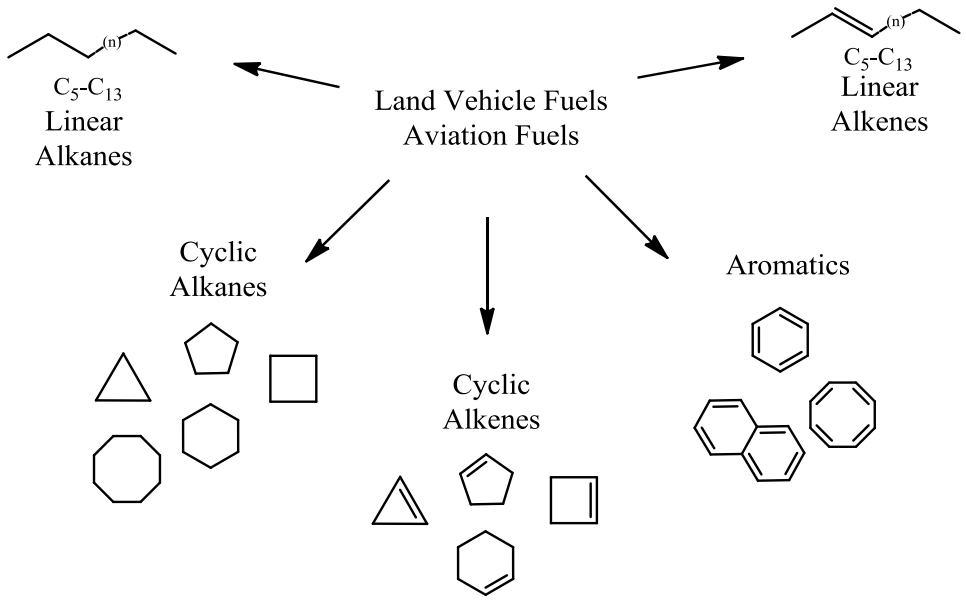

Figure 5.1 Composition of land vehicle and aviation fuels

The need to optimize aircraft combustion processes, has led during the last years to an increase in the investigation and characterization of aviation fuels, which have large

concentrations of cyclic components. One of the jet fuels of interest is JP-10 (discussed in Chapter 4). The main component of JP-10 is tricyclodecane (TCD) formed of three bonded cyclopentane rings. In order to determine the thermochemical properties of the oxidation of larger cyclic hydrocarbons, such as TCD, it is of great importance to have accurate thermochemical and kinetic properties of the oxidation and unimolecular reactions of smaller cyclic alkanes.

Additionally, cyclic ethers are formed in the initial reactions of alkyl radicals with $^3O_2$ in combustion and pre-combustion processes that occur at moderate temperatures. Experimental data of Jones et al.[131] show that the vapor-phase oxidation of C_6-C_{16} hydrocarbons yields 11-25 wt % heterocyclic oxygenates as products. From the oxidation of *n*-hexane, the cyclic ether fraction contained 59% oxolanes (five-membered rings, tetrahydrofurane, THF), 35% oxetanes (four-membered rings), and 6% oxiranes (three-membered rings). From n-heptane, the cyclic ether fraction contained 68% oxolanes, 26% oxetanes, and 6% oxiranes. Moderate-temperature (580-600 K) oxidation of primary reference fuels *n*-heptane and isooctane (2,2,4-trimethylpentane)[132,133] at pressures as high as 40 bar yielded, 10 and 60% cyclic ethers, respectively. An example of the formation paths of cyclic ethers from the oxidation of isooctane is illustrated in Figure 5.2.

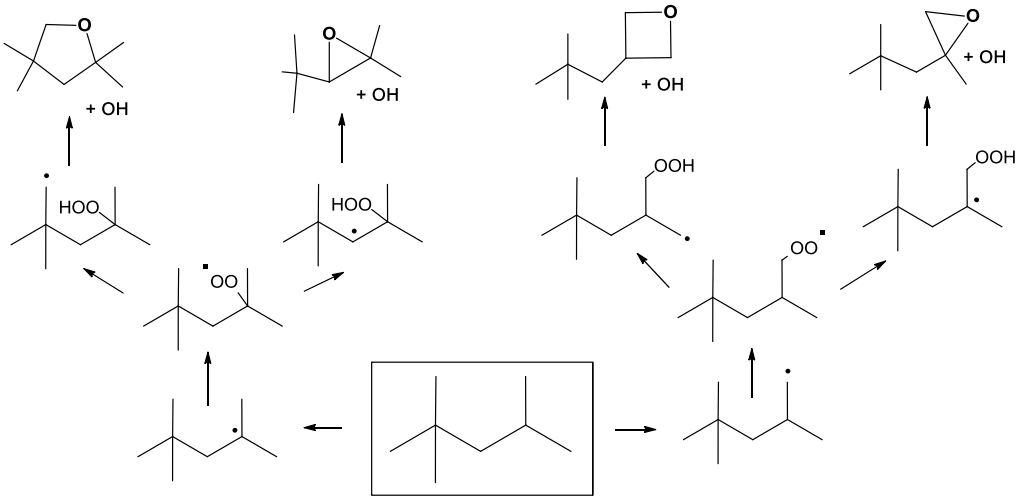

Figure 5.2 Important initial reaction paths in oxidation of isooctane form cyclic ethers

The initial reaction of a hydrocarbon radical with $^3O_2$ forms a peroxy radical with typically 25 to 50 kcal mol^{-1} of initial, chemical-activation energy. The energized and the stabilized peroxy adduct can undergo an intramolecular hydrogen atom transfer reaction forming a hydroperoxyalkyl radical. The formed carbon alkyl radical site has a low reaction barrier for intramolecular addition to the oxygen atom adjacent to the carbon of the hydroperoxy group (carbon-oxygen bond formation). This forms the cyclic ether and cleaves the weak (45 kcal mol^{-1}) RO—OH bond. Formation of the stronger C—O sigma bond is exothermic and the accompanying generation of OH radical results in propagation and sometimes in generation of multi radical products, resulting in chain-branching. The thermochemistry of the cyclic alkane and ether intermediates formed in this oxidation process is important to understanding their further reactions in the combustion systems.

Additionally, the theoretical and modeling investigation of the oxidation of biomass derived alcohol fuels such as ethanol[6,134], propanol[12,15,17], butanol[17,21,24,27,29,135] and pentanol[30,136] have also shown the formation of cyclic ethers to be important. Figure

5.3 illustrates the reaction paths for the formation of cyclic ethers from the oxidation of isopentanol.

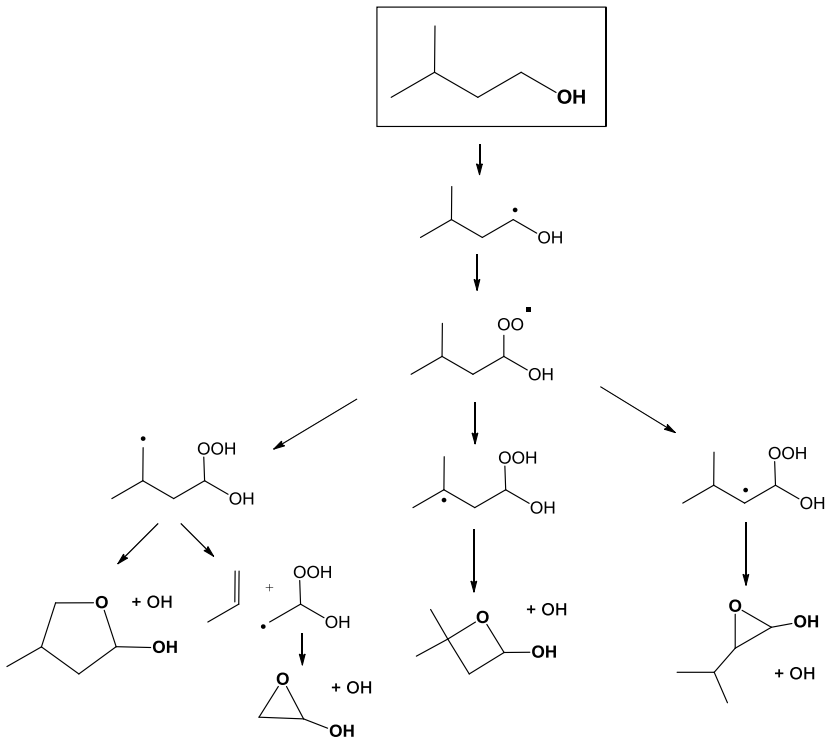

Figure 5.3 Initial reaction paths in oxidation of isopentanol form cyclic ethers

Cyclic ethers can also be formed from atmospheric reactions of olefins, following the steps: (i) $^{\bullet}$OH addition, (ii) O_2 association, (iii) loss of NO_2 by reaction with NO, (iv) cyclization by $O^{\bullet}$ addition to the secondary л bond, which forms the cyclic ether. A potential energy path diagram for the formation of cyclic ethers from the oxidation of isoprene is illustrated in Figure 5.4. Cyclic ethers have also been linked to the formation of the secondary organic aerosol (SOA) in the atmosphere[36,37].

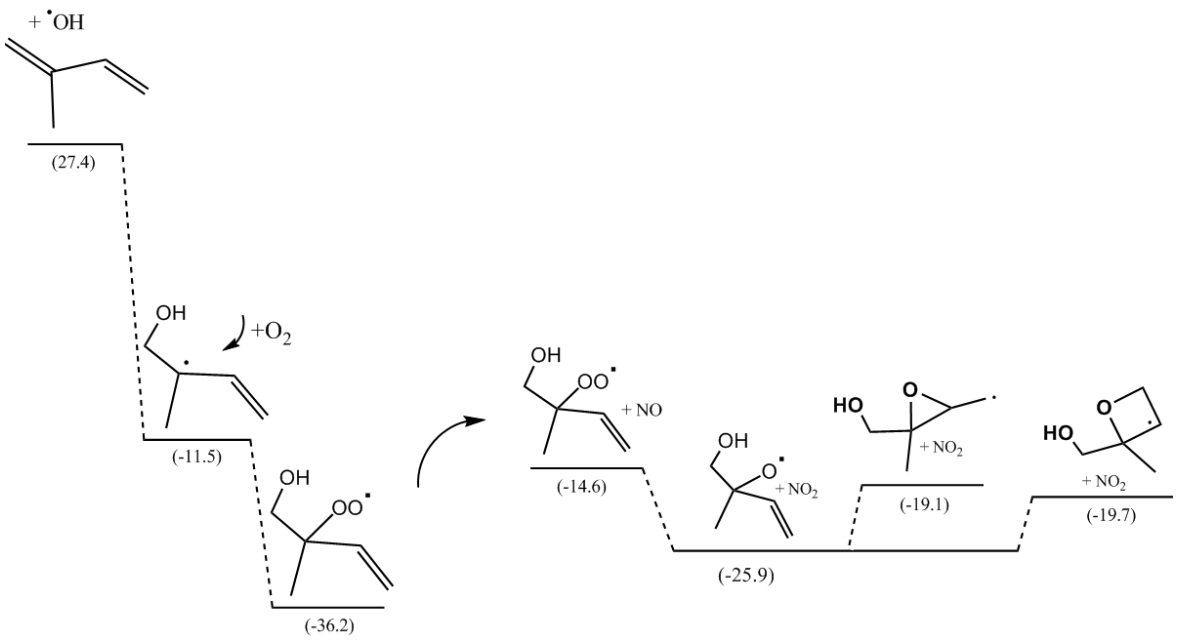

Figure 5.4 Oxidation of isoprene leading to formation of cyclic ethers. Units: kcal mol^{-1}

Once the cyclic alkanes and ethers are formed, they can undergo several further reactions, these include: (i) a C—C bond cleavage that leads to the formation of a diradical, which subsequently can undergo unimolecular decomposition reactions, or react with a molecular oxygen, $^3O_2$, to form a peroxy diradical, (ii) undergo loss of a hydrogen atom by abstraction, which leads to the formation of an alkyl radical. These radicals can further react by unimolecular decomposition reactions (beta scission), or react with molecular oxygen, $^3O_2$, under lean conditions, and at low and intermediate temperatures, to form a peroxy radical, that can isomerize through an intramolecular hydrogen-atom transfer reaction forming hydroperoxyalkyl radicals, R•OOH, as illustrated in Figure 5.5 for the cyclic ethers. Ring opening reactions of strained 3 to 5 member cyclic alkanes or ethers resulting in formation of diradicals can occur at lower, more moderate combustion temperatures, than bond cleavage in non-strained

hydrocarbons because of the release of ring strain, which results from the lower C—C bond energies.

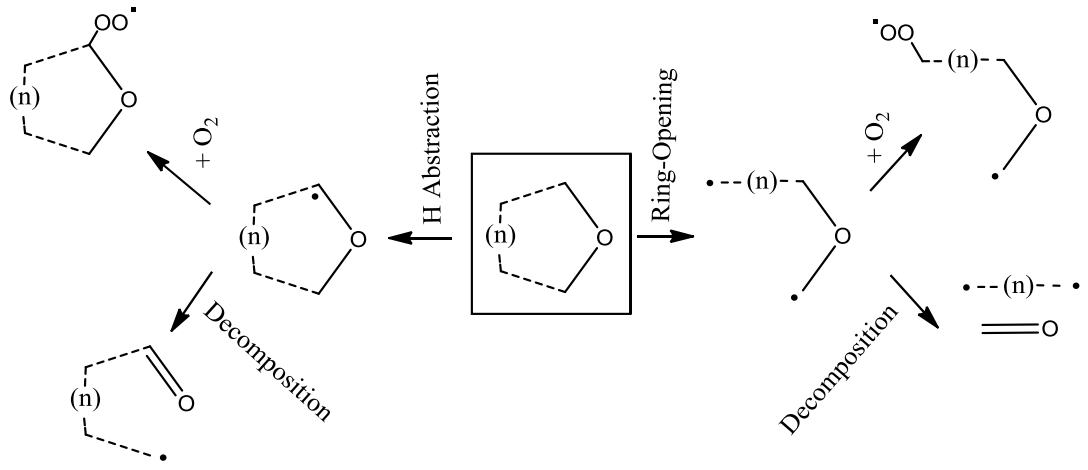

Figure 5.5 Unimolecular decomposition and oxidation paths of cyclic ethers

Several studies have focused on the development of the thermochemical properties and chemical kinetic models for cyclohexane[137-143], and several studies have covered the C_7-C_9 single rings[45,144-146]. However, there are few studies on rings below C_6 and over C_9. Sirjean et al. have studied thermochemistry and kinetics of ring opening reactions of cyclic alkanes using high level computational chemistry calculations on both singlet and triplet[42,128,147]. In 2008, they published a study of the gas-phase unimolecular decomposition of C_3-C_7 cyclic alkyl radicals at the CBS-QB3 level[42] and they further studied the gas-phase reactions of cyclopentyl- and cyclohexyl- peroxy radicals at the CBS-QB3 level[147]. Additionally, there are a number of studies on the thermochemistry of cyclic ethers[148,149]. Ruzsinszky et al., with the aim of improving the rapid estimation of basis set error and correlation energy from partial charges method (REBECEP), calculated the heats of formation of several oxygenated hydrocarbons, including oxirane

and oxolane (-12.6 and -44.0 kcal mol^{-1}, respectively)[150]. Wijaya et al. published data on the thermochemical properties of cyclic ethers at the BH&HLYP level of theory (-12.61, -19.65 and -44.58 kcal mol^{-1}, respectively for oxirane, oxetane, and oxolane)[44]. Bozzelli et al.[151] also published data on oxetane (-19.24 kcal mol^{-1}) at the B3LYP/6-31G(d,p) level of theory with the use of isodesmic work reactions. Agapito et al.[152] studied bond dissociation enthalpies on oxolane at the CBS-Q level. Their calculated C—H bond dissociation enthalpies of oxolane are: 93.1 kcal mol^{-1} leading to the α-furanyl and 97.9 kcal mol^{-1} leading to β-furanyl.

Combustion models include the formation of cyclic alkanes and ethers[38-45], but to our knowledge, there are no studies on the unimolecular dissociation and oxidation reactions of the cyclic alkyl radicals and diradicals formed from the cyclic alkane and ethers. Additionally, there is not available literature data for the thermochemical properties and the C—H, O—H and O—OH bond dissociation enthalpies of the cyclic alkane and ether hydroperoxides, alcohols, peroxy, alkoxy and alkyl radicals.

The goal of the present work is to develop the thermochemistry of peroxy and hydroperoxy-alkyl radicals formed by the cyclic alkane and ether radical plus $^3O_2$ reactions ($yC^{\bullet}_3$-$yC^{\bullet}_5$ + $^3O_2$ and $yC^{\bullet}_2O$-$yC^{\bullet}_4O$ + $^3O_2$, y represents cyclic), and of the diradicals formed from the ring opening of the cyclic alkane and ethers, using computational chemistry. Additionally, the aim is to determine the importance of the reactions of the cyclic alkanes and ethers both in combustion processes and in atmospheric chemistry.

5.2 $^3O_2$ Addition to yC3-yC5 Cyclic Alkanes: Thermochemical Properties

Tables 5.1 to 5.3 represent the schematic structure and the nomenclature of the studied systems (*q* represents –OOH, *y* represents cyclic).

Three membered rings		
 **y(ccc)** **y($CH_2CH_2CH_2$)**	 **y(c$^{\bullet}$cc)** **y($CH^{\bullet}CH_2CH_2$)**	
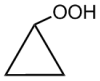 **y(ccc)q** **y(CH_2CH_2CH)OOH**	 **y(ccc)q$^{\bullet}$** **y(CH_2CH_2CH)OO$^{\bullet}$**	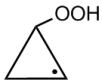 **y(c$^{\bullet}$cc)q** **y($CH^{\bullet}CH_2CH$)OOH**

Table 5.1 Nomenclature and structures of the C_3 cycloalkanes

Four membered rings		
 **y(cccc)** **y($CH_2CH_2CH_2CH_2$)**	 **y(c$^{\bullet}$ccc)** **y($CH^{\bullet}CH_2CH_2CH_2$)**	
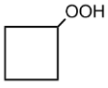 **y(cccc)q** **y($CH_2CH_2CH_2CH$)OOH**		
 **y(cccc)q$^{\bullet}$** **y($CH_2CH_2CH_2CH$)OO$^{\bullet}$**	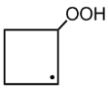 **y(c$^{\bullet}$ccc)q** **y($CH^{\bullet}CH_2CH_2CH$)OOH**	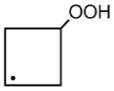 **y(cc$^{\bullet}$cc)q** **y($CH_2CH^{\bullet}CH_2CH$)OOH**

Table 5.2 Nomenclature and structures of the C_4 cycloalkanes

Five membered rings		
 **y(ccccc)** **$y(CH_2CH_2CH_2CH_2CH_2)$**	 **$y(c^{\bullet}cccc)$** **$y(CH^{\bullet}CH_2CH_2CH_2CH_2)$**	
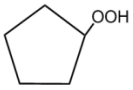 **y(ccccc)q** **$y(CH_2CH_2CH_2CH_2CH)OOH$**		
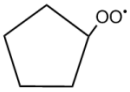 **y(ccccc)$q^{\bullet}$** **$y(CH_2CH_2CH_2CH_2CH)OO^{\bullet}$**	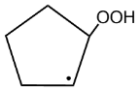 **$y(c^{\bullet}cccc)q$** **$y(CH^{\bullet}CH_2CH_2CH_2CH)OOH$**	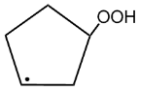 **$y(cc^{\bullet}ccc)q$** **$y(CH_2CH^{\bullet}CH_2CH_2CH)OOH$**

Table 5.3 Nomenclature and structures of the C_5 cycloalkanes

The optimized geometries of each of the species are summarized in Appendix M, and the vibrational frequencies are summarized in Appendix N.

The hydroperoxide group can be placed in two different positions for cyclobutane and cyclopentane - equatorial (a) and axial (b) - resulting in a difference in energy of ~1 kcal mol^{-1} for the cyclobutane peroxide and ~0.5 kcal mol^{-1} for the cyclopentane, see Figure 5.6.

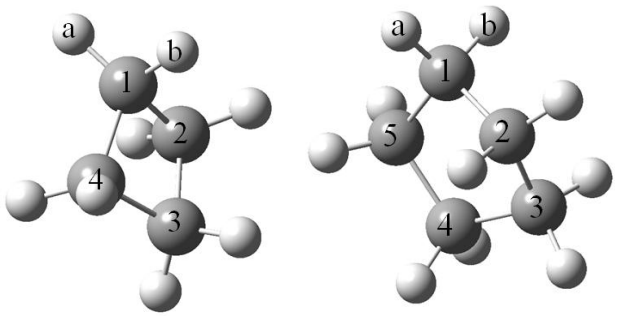

y(cccc) **y(ccccc)**

Figure 5.6 Two sites, equatorial and axial, (see a and b above, respectively) for the OOH group on cyclobutane and cyclopentane

The dihedral angles for carbons in the cyclobutyl and cyclopentyl ring hydroperoxides are summarized in Table 5.4 (the numbering of the atoms corresponds to that in Figure 5.6).

Table 5.4 Dihedral angles in cyclobutyl and cyclopentyl hydroperoxides

Species	Dihedral	(°)	
		Equatorial (a)	Axial (b)
y(cccc)	D(1,2,3,4)	18.4131	
y(ccccc)	D(1,5,4,3) D(5,1,2,3)	38.2160 3.52413	
y(cccc)q	D(1,2,3,4)	18.8845	14.2094
y(ccccc)q	D(1,5,4,3) D(5,1,2,3)	41.2877 9.20701	35.6058 6.3377

Calculations performed at the B3LYP/6-31G(d,p) level, in conjunction with the determination of internal rotation potentials (see Appendix O) were used to identify the lowest energy configuration, and work reactions for the cancelation of the systematic error were used to determine enthalpy of formation values. The results are summarized in Table 5.5.

Table 5.5 Example differences in heats of formation at 298 K of peroxide site conformers in cyclobutyl and cyclopentyl hydroperoxides (see discussion below)

Species	$\Delta H°_{f\,298}$	Species	$\Delta H°_{f\,298}$
y(cccc)q-a	-17.72	y(ccccc)q-a	-41.67
y(cccc)q-b	-16.79	y(ccccc)q-b	-41.14

Units: kcal mol^{-1}

The rotational analysis was performed to determine the lowest energy conformer. Appendix O contains the figures of the rotational analysis for each of the studied species. The calculated rotational barrier heights are summarized in Table 5.6.

The rotational barriers of the ring- hydroperoxide group (y—ooh = H-C-O-O dihedral angle) have near three fold symmetry, and maxima at 4 to 5.5 kcal mol^{-1}, for all cases. The y—$OO^{\bullet}$ peroxy radical rotors have lower barriers at ~ 2 kcal mol^{-1}. The rotational barriers about the y-O—OH bonds are ~5-6 kcal mol^{-1} in all the peroxides.

Table 5.6 Rotational barriers for cyclic alkanes

Species	O—OH	C—OOH
y(ccc)q	5.05	4.61
y(cccc)q	5.84	4.82
y(ccccc)q	5.97	5.93
y(ccc)q$^{\bullet}$	---	2.05
y(cccc)q$^{\bullet}$	---	2.16
y(ccccc)q$^{\bullet}$	---	2.39
y(c$^{\bullet}$cc)q	4.79	4.03
y(c$^{\bullet}$ccc)q	5.90	5.57
y(cc$^{\bullet}$cc)q	5.88	5.42
y(c$^{\bullet}$cccc)q	6.04	5.43
y(cc$^{\bullet}$ccc)q	6.13	5.54

Units: kcal mol^{-1}

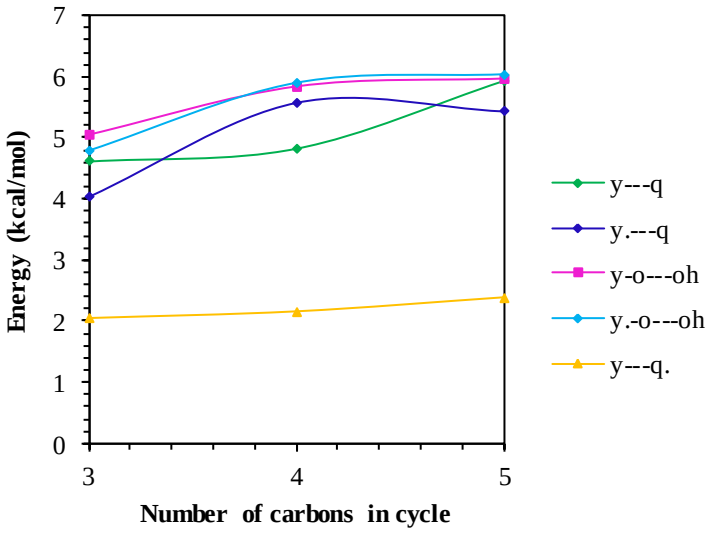

The geometry of the lowest energy conformer is determined from the rotational scans; the low energy structures are illustrated in Figure 5.7.

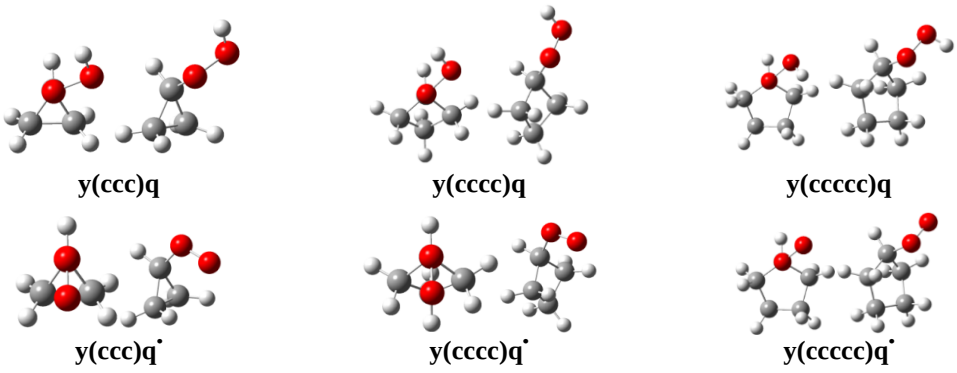

Figure 5.7 Geometry of the lowest energy conformers, position of the OOH group

All hydroperoxides and hydroperoxyalkyl radicals, have the OOH group in the gauche position. However, in the case of the peroxy radicals, for cylopentane, the $OO^{\bullet}$ group is in the gauche position, but cyclopropane and cyclobutane have the $OO^{\bullet}$ group in the *anti* position. Table 5.7 summarizes the differences in energy between the *gauche* and *anti* structures. The *gauche* and *anti* positions correspond to the H-C-O-O structure.

Table 5.7 Differences in energy between the *gauche* and *anti* structures

Species	**$\Delta_f H^o_{298}$ (anti - gauche)**
y(ccc)q	3.14
y(cccc)q	0
y(ccccc)q	0.63
y(ccc)q$^{\bullet}$	-1.26
y(cccc)q$^{\bullet}$	-1.26
y(ccccc)q$^{\bullet}$	0.63
y(c$^{\bullet}$cc)q	1.88
y(c$^{\bullet}$ccc)q	0
y(cc$^{\bullet}$cc)q	0
y(c$^{\bullet}$cccc)q	1.26
y(cc$^{\bullet}$ccc)q	1.88

Units: kcal mol^{-1}

Appendix P summarizes the work reactions used for the determination of the heats of formation (see work reactions in Table 5.8 as example) and Appendix A contains the heats of formation of the reference species used in the work reactions. The enthalpies of formation obtained at the B3LYP(6-31G(d,p) and 6-31G(2d,2p)), CBS-QB3 and G3MP2B3 levels of theory plus use of work reactions are summarized in Table 5.9 to 5.11.

Table 5.8 Example of work reactions and calculated $\Delta_f H^o_{298}$ for the cyclopropyl peroxy radical vs. calculation method

Work Reactions	$\Delta_f H^o_{298}$							
	B3LYP							
	6-31G(d,p)	6-31G(2d,2p)	CBS-QB3	G3MP2B3	Average DFT	Average ab initio	Average methods	Therm
y(ccc)q								
y(ccc)q$^{\bullet}$ + ccq = y(ccc)q + ccq$^{\bullet}$	26.77	26.59	27.25	27.32				
y(ccc)q$^{\bullet}$ + ccqc = y(ccc)q + ccq$^{\bullet}$c	26.82	26.71	27.32	27.37				
y(ccc)q$^{\bullet}$ + c3cq = y(ccc)q + c3cq$^{\bullet}$	27.30	27.19	27.57	27.59				
Aver.	26.96	26.83	27.38	27.43	26.90	27.41	***27.15***	22.87
BDE	86.60	86.47	87.02	87.07			*86.69*	86.3
σ							*0.30*	

Units: kcal mol^{-1}

Results for the cyclopropylhydroperoxide and its derivatives show good agreement between all the methods, except in the case of y(ccc)q, where there is a difference of ~1.5 kcal mol^{-1} between the values obtained by B3LYP and higher level (CBS-QB3 and G3MP2B3) values. The average value obtained from CBS-QB3 and G3MP2B3 is recommended, -7.54 kcal mol^{-1}. The heat of formation and bond dissociation enthalpy calculated for the cyclopropyl carbon radical are in good agreement to the ones calculated by Sirjean et al.[42] and Bach et al. [153].

Table 5.9 Calculated enthalpies of formation at 298 K of the cyclopropylhydroperoxide and its derivatives

Species		$\Delta H°_{f\,298}$								
		B3LYP		CBS-QB3	G3MP2B3	Average DFT	Average ab initio (*)	Average methods	Group Additivity	Literature
		6-31G(d,p)	6-31G(2d,2p)							
y(ccc)q		-9.08	-9.03	-7.57	-7.51	-9.06	**-7.54**	*-8.30*	-11.33	
	σ							*0.88*		
y(c˙cc)		69.81	69.86	69.87	69.61	69.83	**69.74**	*69.79*	66.94	69.5[42]
	BDE	109.17	109.22	109.23	108.97	*109.19*	***109.10***	*109.15*	106.3	109.5[153]
	σ							*0.12*		
y(ccc)q˙		26.96	26.83	27.38	27.42	26.90	**27.41**	*27.15*	22.87	
	BDE	86.60	86.47	87.02	87.07	86.53	***87.04***	*86.79*	86.30	
	σ							*0.30*		
y(c˙cc)q		49.87	49.84	50.22	50.00	49.86	**50.11**	*49.98*	42.87	
	BDE	109.51	109.48	109.85	109.63	109.49	***109.74***	*109.62*	106.3	
	σ							*0.17*		

Units: kcal mol^{-1}

Standard deviation (σ) does not include the error of the reference species; Group Additiivty values prior to this study.

(*) Recommended value

Table 5.10 Calculated enthalpies of formation at 298 K of the cyclobutylhydroperoxide and its derivatives

Species		$\Delta H°_{f\,298}$								
		B3LYP								
		6-31G(d,p)	6-31G(2d,2p)	CBS-QB3	G3MP2B3	Average DFT	Average ab initio(*)	Average methods	Group Additivity	Literature
y(cccc)q		-17.72	-17.77	-17.35	-17.36	-17.75	**-17.36**	*-17.55*	-17.28	
	σ							*0.23*		
y(c˙ccc)		54.47	54.46	54.91	54.85	54.47	**54.88**	*54.68*	53.14	54.0[42]
	BDE	99.95	99.94	100.39	100.33	99.95	***100.36***	*100.16*	98.45	100.9[153]
	σ							*0.24*		
y(cccc)q˙		15.60	15.58	16.00	16.02	15.59	**16.01**	*15.80*	16.92	
	BDE	85.26	85.24	85.65	85.67	85.25	***85.66***	*85.45*	86.30	
	σ							*0.24*		
y(c˙ccc)q		31.36	31.28	31.86	31.72	31.32	**31.79**	*31.55*	29.07	
	BDE	101.01	100.93	101.37	101.21	100.97	***101.44***	*101.21*	98.45	
	σ							*0.31*		
y(cc˙cc)q		31.09	31.10	31.34	31.30	31.09	**31.32**	*31.21*	29.07	
	BDE	100.74	100.75	101.00	100.96	100.75	***100.98***	*100.86*	98.45	
	σ							*0.13*		

Units: kcal mol^{-1}

Standard deviation (σ) does not include the error of the reference species

(*) Recommended value

The coupled calculation/work reaction methods on enthalpies and bond dissociation enthalpies on the cyclobutylhydroperoxide and its derivatives exhibit good agreement between DFT and the higher calculation levels. Differences for this C_4 system shows the average DFT versus ab initio enthalpies and bond dissociation enthalpies are within 0.5 kcal mol^{-1} or less. The cyclic alkyl radical y(cc˙ccq) is found to be more stable than y(c˙cccq), by 0.34 kcal mol^{-1}. The heat of formation and bond dissociation enthalpy calculated for the cyclobutyl radical are in good agreement to the ones calculated by Sirjean et al.[42] and Bach et al.[153].

Table 5.11 Calculated enthalpies of formation at 298 K of the cyclopentylhydroperoxide and its derivatives

Species		$\Delta H°_{f\,298}$								
		B3LYP								
		6-31G(d,p)	6-31G(2d,2p)	CBS-QB3	G3MP2B3	Average DFT	Average ab initio(*)	Average methods	Group Additivity	Literature
y(ccccc)q		-41.67	-41.69	-42.23	-42.20	-41.68	**-42.21**	*-41.95*	-42.81	
	σ							*0.31*		
y(c˙cccc)		26.79	26.84	26.10	26.07	26.81	**26.09**	*26.45*	26.61	25.7[42]
	BDE	97.15	97.20	96.46	96.43	97.17	***96.45***	*96.81*	98.45	97.2[153]
	σ							*0.42*		
y(ccccc)q˙		-9.03	-9.03	-9.00	-8.97	-9.03	**-8.99**	*-9.01*	-8.61	-11.7[147], -8.0 [(a)]
	BDE	85.02	85.01	85.05	85.07	85.02	***85.06***	*85.04*	86.3	
	σ							*0.03*		
y(c˙cccc)q		3.54	3.73	3.75	3.72	3.63	**3.74**	*3.69*	3.54	4.3[147], 3.5 [(a)]
	BDE	97.59	97.77	97.80	97.77	97.68	***97.78***	*97.73*	98.45	
	σ							*0.10*		
y(cc˙ccc)q		3.39	3.45	3.33	3.26	3.42	**3.29**	***3.36***	3.54	3.7[147], -0.7 [(a)]
	BDE	97.44	97.50	97.38	97.31	97.47	***97.34***	*97.41*	98.45	
	σ							*0.04*		

Units: kcal mol^{-1}

Standard deviation (σ) does not include the error of the reference species

[(a)] Thergas[154] calculations

[(*)] Recommended value

The calculations on enthalpies and bond dissociation enthalpies on the cyclopentylhydroperoxide and its derivatives show good agreement between DFT and the higher calculation levels. Results also agree with literature data with one exception, the y(ccccc)q˙ where there is a discrepancy of ~2.5 kcal mol^{-1} versus the values of Sirjean et al.[147] , obtained at the CBS-QB3 level of theory. The secondary carbon radical in the 4 member ring, y(cc˙ccc)q is slightly more stable than the carbon radical adjacent to the peroxy group, y(c˙cccc)q, by 0.33 kcal mol^{-1}. The heat of formation and bond dissociation

enthalpy calculated for the cyclopentyl radical are in good agreement to the ones calculated by Sirjean et al.[42,147] and Bach et al.[153].

The C—H bond dissociation enthalpies, along with the corresponding radical's stability, help to predict specific carbon sites where bond cleavage will occur in abstraction and decomposition reactions. Bond dissociation enthalpies are reported from the calculated $\Delta_f H^o_{298}$ of parent molecule and their radical corresponding to loss of hydrogen atoms, where the enthalpies of parent molecule and product species are calculated in this study in conjunction with the value of 52.10 kcal mol^{-1} for the hydrogen atom; the data correspond to the standard temperature of 298.15 K. The individual bond dissociation enthalpy values are given in Table 5.12.

Results show that the hydroperoxide - alkyl radicals (R$^{\bullet}$COOH) and the alkyl radicals (R$^{\bullet}$) have differences in C–H bond dissociation enthalpies of ~0.6-1.3 kcal mol^{-1} relative to C—H bonds on the respective non hydroperoxide ring systems.

Table 5.12 C–H and ROO—H bond dissociation enthalpies for each of the calculated systems

Species	Bond Dissociation Enthalpies
y(c$^{\bullet}$cc)	109.10
y(c$^{\bullet}$ccc)	100.36
y(c$^{\bullet}$cccc)	96.45
y(ccc)q$^{\bullet}$	87.04
y(cccc)q$^{\bullet}$	85.66
y(ccccc)q$^{\bullet}$	85.04
y(c$^{\bullet}$cc)q	109.74
y(c$^{\bullet}$ccc)q	101.44
y(cc$^{\bullet}$cc)q	100.98
y(c$^{\bullet}$ccc)q	97.78
y(cc$^{\bullet}$ccc)q	97.34

Units: kcal mol^{-1}

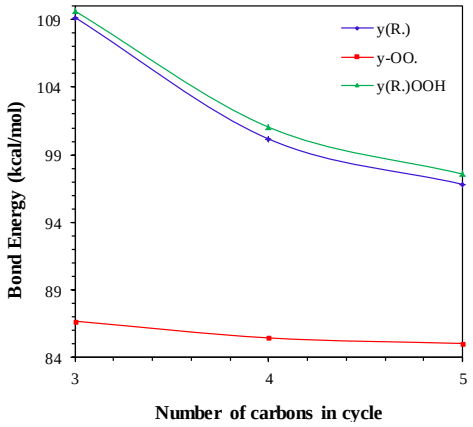

Overall the C—H bond dissociation enthalpies are higher for carbons in smaller rings. In the case of alkyl radicals (C–H bond dissociation enthalpy to form y(c•cc), y(c•ccc) and y(c•cccc) are 109.10, 100.36 and 96.45 kcal mol^{-1}, respectively, where a normal secondary C–H bond in an alkane such as n-butane is 98.5 kcal mol^{-1}). The high bond energies in these non hydroperoxide $C_3 - C_5$ cyclic alkanes have been previously reported and the values from this study are in good agreement with respected, published values as shown in the tables.

There is a smaller difference in the case of the peroxy radicals (ROO–H). Bond dissociation enthalpy for y(ccc)q•, y(cccc)q• and y(ccccc)q• are 87.04, 85.66 and 85.04 kcal mol^{-1}, respectively, where conventional alkyl-OO—H bonds are 86.5 kcal mol^{-1}.

The heats of formation and O—H bond dissociation enthalpies were calculated for 3 to 5 member cyclic alkane alcohols at the CBS-QB3 level of theory. Results of the heats of formation and the bond dissociation enthalpies are summarized in Table 5.13.

Table 5.13 Heat of formation of cyclic alcohols and alkoxides

Species	$\Delta H^o_{f,298}$	Species	$\Delta H^o_{f,298}$	BDE
 **y(ccc)oh**	-24.64	 **y(ccc)o•**	16.07	*92.8*
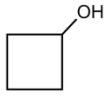 **y(cccc)oh**	-34.50	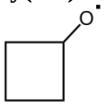 **y(cccc)o•**	18.40	*105.0*
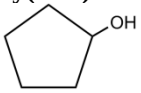 **y(ccccc)oh**	-58.91	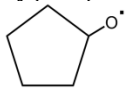 **y(ccccc)o•**	-5.91	*105.1*

Units: kcal mol^{-1}

The O—OH bond dissociation enthalpies were calculated for each of the systems, summarized in Table 5.14.

Table 5.14 Summary of the O—OH bond energies of cyclic alkanes

Bonds	BDE
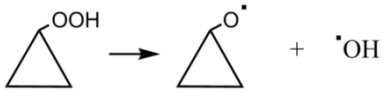 **y(ccc)ooh → y(ccc)o• + •oh**	*32.5*
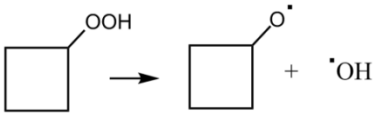 **y(cccc)ooh → y(cccc)o• + •oh**	*43.6*
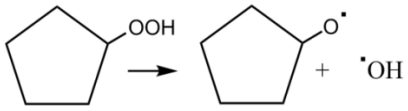 **y(ccccc)ooh → y(ccccc)o• + •oh**	*45.2*

Units: kcal mol^{-1}

The O—H and O—OH bond dissociation enthalpies are comparable to those of linear alcohols for four and five member cyclic alcohols, but the values are ~11.5 kcal mol^{-1} lower for cyclopropanol.

The $R^{\bullet}$ + $^{3}O_2$ well-depth is an important factor in kinetics for the chemical activation analysis of these association reactions. Table 5.15 summarizes the well-depths for each of the systems. The well-depth increases significantly with ring strain in these three cyclic species ($R^{\bullet}$ + $^{3}O_2$ well-depth for cyclopropyl, cyclobutyl and cyclopentyl are 42.33, 38.87 and 35.08 kcal mol^{-1}, respectively). Figures 5.8 to 5.10 illustrate the initial intramolecular H atom transfer reaction energy diagrams for the three studied systems. The heat of formation value indicated is the average of the CBS-QB3 and G3MP2B3 level methods used.

Table 5.15 $R^{\bullet}$ + $^3O_2$ (chemical activation) well-depths for each of the systems studied

System	Well-Depth
y(c$^{\bullet}$cc) + O_2	42.33
y(c$^{\bullet}$ccc) + O_2	38.87
y(c$^{\bullet}$cccc) + O_2	35.08

Units: kcal mol^{-1}

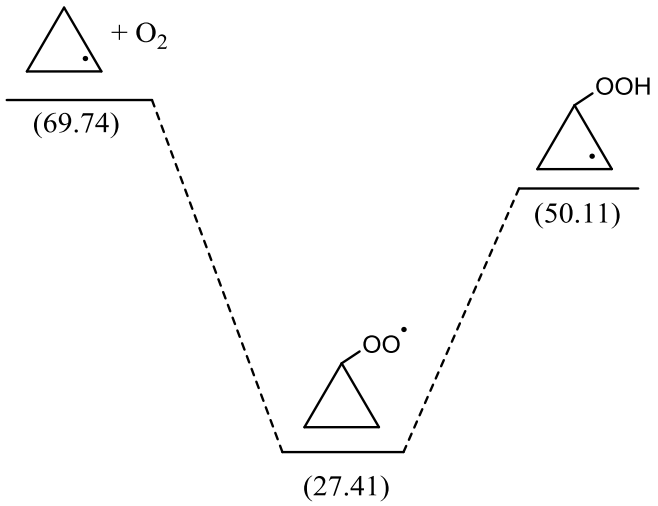

Figure 5.8 Potential energy diagram for cyclopropyl + $^3O_2$, at 298 K

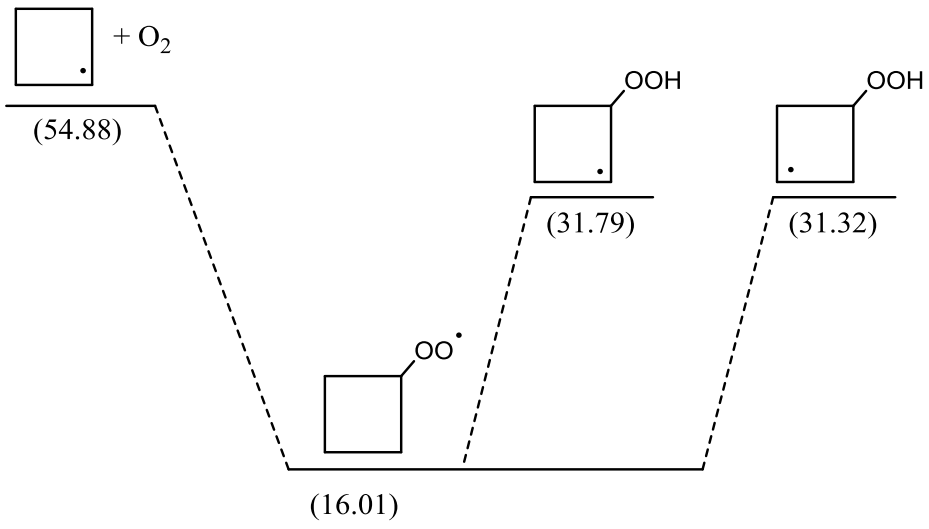

Figure 5.9 Potential energy diagram for cyclobutyl + $^3O_2$, at 298 K

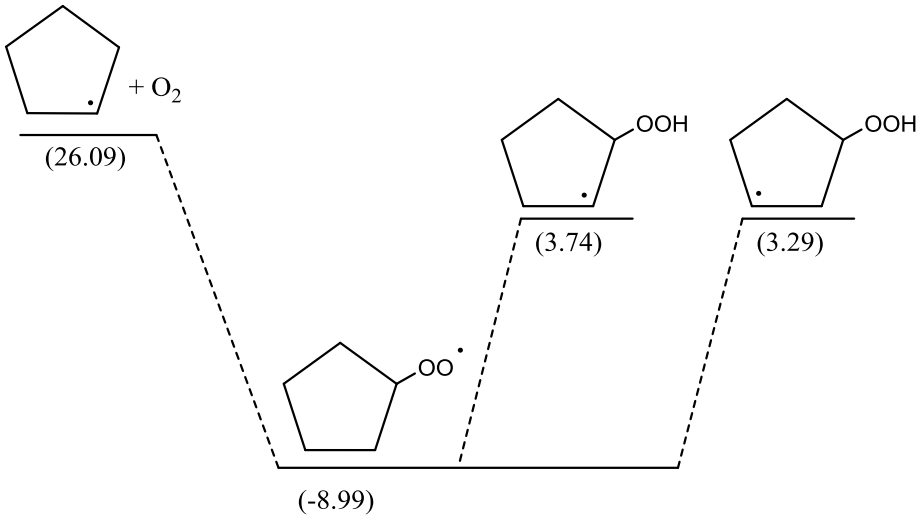

Figure 5.10 Potential energy diagram for cyclopentyl + $^3O_2$, at 298 K

Entropy and heat capacity values are summarized in Table 5.16. Appendix Q summarizes the entropy and heat capacity values versus temperature (5-5000 K).

Table 5.16 Entropy and heat capacity values versus temperature

Species	S° (298 K)	C°$_p$(T)						
		300 K	400 K	500 K	600 K	800 K	1000 K	1500 K
y(ccc)q	77.44	21.55	27.43	32.36	36.19	41.57	45.28	51.02
y(c˙cc)	60.99	12.20	16.06	19.47	22.27	26.52	29.64	34.57
y(ccc)q˙	76.43	19.51	24.36	28.68	32.21	37.44	41.13	46.75
y(c˙cc)q	79.32	22.39	27.34	31.28	34.30	38.63	41.68	46.48
y(cccc)q	82.86	24.99	32.27	38.69	43.96	51.80	57.35	65.75
y(c˙ccc)	66.05	15.69	21.39	26.53	30.82	37.38	42.15	49.46
y(cccc)q˙	81.85	22.94	29.63	35.66	40.66	48.19	53.53	61.56
y(c˙ccc)q	85.14	25.65	32.32	38.08	42.73	49.56	54.33	61.52
y(cc˙cc)q	85.63	25.98	32.61	38.33	42.95	49.72	54.46	61.60
y(ccccc)q	90.07	31.51	40.55	48.56	55.15	65.02	72.02	82.63
y(c˙cccc)	70.32	19.44	26.91	33.69	39.39	48.15	54.50	64.19
y(ccccc)q˙	86.14	27.30	35.64	43.21	49.54	59.16	66.02	76.36
y(c˙cccc)q	88.49	30.21	38.53	45.79	51.73	60.57	66.81	76.27
y(cc˙ccc)q	88.61	30.01	38.59	45.98	51.96	60.80	67.02	76.41

Units: S (cal mol^{-1}), Cp (cal mol^{-1} K^{-1})

A comparison has been made between the values obtained by group additivity calculations, and the average of the heats of formation obtained when CBS-QB3 and G3MP2B3 calculations have been applied, summarized in Table 5.17. Similarly, Table 5.18 includes a comparison of the entropy values obtained by group additivity calculations, and the SMCPS calculations, where both the effect of the internal rotors, treated as harmonic oscillators, and hindered rotors is included.

Table 5.17 Comparison between the $\Delta_f H^o_{298}$ obtained using the average of the values from CBS-QB3 and G3MP2B3 calculations, and the values obtained using groups previously available

Species	$\Delta_f H^o_{298}$	
	Average ab initio	**Group Additivity**
y(ccc)q	***-7.54***	-11.33
y(c˙cc)	***69.74***	66.94
y(ccc)q˙	***27.41***	22.87
y(c˙cc)q	***50.11***	42.87
y(cccc)q	***-17.36***	-17.28
y(c˙ccc)	***54.88***	53.14
y(cccc)q˙	***16.01***	16.92
y(c˙ccc)q	***31.79***	29.07
y(cc˙cc)q	***31.32***	29.07
y(ccccc)q	***-42.21***	-42.81
y(c˙cccc)	***26.09***	26.61
y(ccccc)q˙	***-8.99***	-8.61
y(c˙cccc)q	***3.74***	3.54
y(cc˙ccc)q	***3.29***	3.54

Units: kcal mol^{-1}

Table 5.18 Comparison between the $S^{o}(298)$ obtained from SMCPS calculations, and the values obtained using groups previously available

Species	S°	
	SMPS	**Group Additivity**
y(ccc)q	***77.44***	76.25
y(c•cc)	***60.99***	60.30
y(ccc)q•	***73.43***	76.47
y(c•cc)q	***79.32***	80.69
y(cccc)q	***82.86***	83.51
y(c•ccc)	***66.05***	66.18
y(cccc)q•	***81.85***	83.73
y(c•ccc)q	***85.14***	87.95
y(cc•cc)q	***85.63***	87.95
y(ccccc)q	***90.07***	87.95
y(c•cccc)	***70.32***	68.62
y(ccccc)q•	***86.14***	86.17
y(c•cccc)q	***88.49***	90.39
y(cc•ccc)q	***88.61***	90.39

Units: kcal mol^{-1}

Appendix R summarizes the available groups utilized, as well as the groups developed for the determination of each of the species (the ones in bold indicate the generated group). A set of new and several revised groups have been developed in order to include them in codes used for group additivity calculations (such as Therm). Table 5.19 summarizes the groups that have been developed.

Table 5.19 Groups developed in this study and previously determined groups used

Group	$\Delta_f H^o_{298}$ (*)	S°(298)	C°$_p$(T)							Ref.
			300	400	500	600	800	1000	1500	
Developed groups										
Stable groups										
CY/C3/Q	31.32	33.23	-3.36	-3.14	-3.01	-2.74	-2.85	-3.21	2.68	
CY/C4/Q	26.43	29.23	-5.42	-5.25	-4.93	-4.32	-3.69	-3.48	3.21	
CY/C5/Q	6.51	27.02	-4.40	-3.92	-3.31	-2.48	-1.54	-1.15	5.89	
Radical groups										
CY/C3J	109.10	0.69	-1.17	-2.12	-2.96	-3.67	-4.77	-5.54	-6.65	
CY/CJ3/Q	109.74	1.88	0.85	-0.08	-1.08	-1.88	-2.94	-3.60	-4.55	
CY/C3/QJ	87.04	-1.01	-2.04	-3.07	-3.68	-3.98	-4.13	-4.15	-4.28	
CY/C4J	100.36	-1.51	-1.29	-1.95	-2.64	-3.27	-4.33	-5.09	-6.14	
CY/CJ4/Q	101.44	2.28	0.65	0.05	-0.61	-1.22	-2.24	-3.02	-4.23	
CY/CJS4/Q	100.98	2.77	0.99	0.35	-0.36	-1.01	-2.08	-2.89	-4.16	
CY/C4/QJ	85.66	-1.01	-2.05	-2.63	-3.03	-3.30	-3.61	-3.82	-4.19	
CY/C5J	96.45	0.32	-0.49	-1.33	-2.17	-2.93	-4.14	-4.98	-6.06	
CY/CJ5/Q	97.78	-1.58	-1.29	-2.03	-2.76	-3.42	-4.46	-5.21	-6.36	
CY/CJS5/Q	97.34	-1.46	-1.50	-1.96	-2.58	-3.19	-4.22	-5.00	-6.22	
CY/C5/QJ	85.06	-3.94	-4.21	-4.91	-5.35	-5.61	-5.86	-6.00	-6.28	
Known groups										
C/C2/H2	-4.93	9.42	5.50	6.95	8.25	9.35	11.07	12.34	14.20	[81]
C/C2/H/O	-7.20	-11.00	4.80	6.64	8.10	8.73	9.81	10.40	11.51	[155]
O/C/O	-5.50	8.54	3.90	4.31	4.60	4.84	5.32	5.80		[155]
O/H/O	-16.30	27.83	5.21	5.72	6.17	6.66	7.15	7.61	8.43	[155]
CY/C3	27.53	32.04	-3.13	-2.67	-2.32	-2.11	-1.92	-1.84	-1.38	[156]
CY/C4	26.51	29.88	-5.02	-4.46	-3.83	-3.31	-2.57	-2.12	-1.20	[156]
CY/C5	5.91	22.90	-7.57	-6.51	-5.39	-4.43	-3.06	-2.22	-0.75	[156]

Units: kcal mol^{-1}

(*) It represents $\Delta_f H^o_{298}$ for the stable groups, and Bond Dissociation Enthalpy for the radical groups

5.3 $^3O_2$ Addition to yC2O-yC4O Cyclic Ethers: Thermochemical Properties

Tables 5.20 to 5.22 illustrate the cyclic ether structures studied, along with the nomenclature used for each of the species (*q* represents –OOH, *y* represents cyclic).

The nomenclature used for the position identification of the peroxy groups is:

- q_{eth} (or $q_{eth}^{\bullet}$) represents a hydroperoxide group (or peroxy radical group) bonded to a carbon in the ring adjacent to the ether oxygen.
- q_{sec} (or $q_{sec}^{\bullet}$) represents a hydroperoxide group (or peroxy radical group) bonded to a carbon in the ring that is NOT adjacent to an ether oxygen.

Table 5.20 Nomenclature and structures of the yC_2O cyclic ethers (y=cyclic ; q= OOH)

Three membered rings – yC_2O		
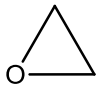	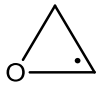	
y(cco) **y(CH_2CH_2O)** **Oxirane**	**y($c^{\bullet}co$)** **y($CH^{\bullet}CH_2O$)** **Alkyl Oxirane**	
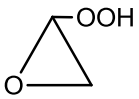	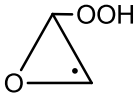	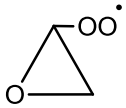
y(cco)-q_{eth} **y(CH_2CHO)-OOH** **Oxirane Hydroperoxide**	**y($c^{\bullet}co$)-q_{eth}** **y($CH^{\bullet}CHO$)-OOH** **Alkyl Oxirane Hydroperoxide**	**y(cco)-$q_{eth}^{\bullet}$** **y(CH_2CHO)-$OO^{\bullet}$** **Oxirane Peroxy**

Table 5.21 Nomenclature and structures of the yC_3O cyclic ethers (y=cyclic ; q= OOH)

Four membered rings – yC_3O		
 **y(ccco)** **y($CH_2CH_2CH_2O$)** **Oxetane**	 **y(c˙cco)** **y(CH˙CH_2CH_2O)** **Alkyl Oxetane**	 **y(cc˙co)** **y(CH_2CH˙CH_2O)** **Alkyl Oxetane**
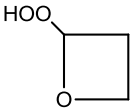 **y(ccco)-q_{eth}** **y(CH_2CH_2CHO)-OOH** **Oxetane Hydroperoxide**	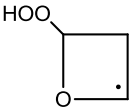 **y(c˙cco)-q_{eth}** **y(CH˙CH_2CHO)-OOH** **Alkyl Oxetane Hydroperoxide**	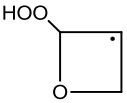 **y(cc˙co)-q_{eth}** **y(CH_2CH˙CHO)-OOH** **Alkyl Oxetane Hydroperoxide**
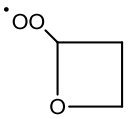 **y(ccco)-q_{eth}˙** **y(CH_2CH_2CHO)-OO˙** **Oxetane Peroxy**		
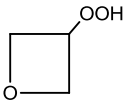 **y(ccco)-q_{sec}** **y(CH_2CHCH_2O)-OOH** **Oxetane Hydroperoxide**	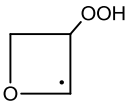 **y(c˙cco)-q_{sec}** **y(CH˙$CHCH_2O$)-OOH** **Alkyl Oxetane Hydroperoxide**	
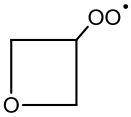 **y(ccco)-q_{sec}˙** **y(CH_2CHCH_2O)-OO˙** **Oxetane Peroxy**		

Table 5.22 Nomenclature and structures of the yC_4O cyclic ethers (y=cyclic ; q= OOH)

Five membered rings – yC_4O		
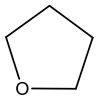	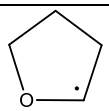	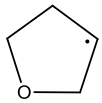
y(cccco) **$y(CH_2CH_2CH_2CH_2O)$** **Oxolane** **Tetrahydrofuran (THF)**	**$y(c^{\bullet}ccco)$** **$y(CH^{\bullet}CH_2CH_2CH_2O)$** **Alkyl Oxolane**	**$y(cc^{\bullet}cco)$** **$y(CH_2CH^{\bullet}CH_2CH_2O)$** **Alkyl Oxolane**
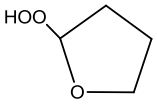	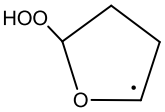	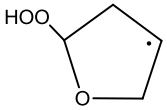
$y(cccco)\text{-}q_{eth}$ **$y(CH_2CH_2CH_2CHO)\text{-}OOH$** **Oxolane Hydroperoxide**	**$y(c^{\bullet}ccco)\text{-}q_{eth}$** **$y(CH^{\bullet}CH_2CH_2CHO)\text{-}OOH$** **Alkyl Oxolane Hydroperoxide**	**$y(cc^{\bullet}cco)\text{-}q_{eth}$** **$y(CH_2CH^{\bullet}CH_2CHO)\text{-}OOH$** **Alkyl Oxolane Hydroperoxide**
	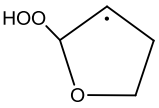	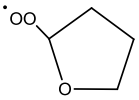
	$y(ccc^{\bullet}co)\text{-}q_{eth}$ **$y(CH_2CH_2CH^{\bullet}CHO)\text{-}OOH$** **Alkyl Oxolane Hydroperoxide**	**$y(cccco)\text{-}q_{eth}^{\bullet}$** **$y(CH_2CH_2CH_2CHO)\text{-}OO^{\bullet}$** **Oxolane Peroxy**
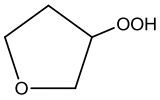	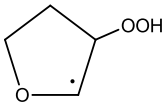	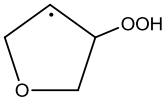
$y(cccco)\text{-}q_{sec}$ **$y(CH_2CHCH_2CH_2O)\text{-}OOH$** **Oxolane Hydroperoxide**	**$y(c^{\bullet}ccco)\text{-}q_{sec}$** **$y(CH^{\bullet}CHCH_2CH_2O)\text{-}OOH$** **Alkyl Oxolane Hydroperoxide**	**$y(ccc^{\bullet}co)\text{-}q_{sec}$** **$y(CH_2CHCH^{\bullet}CH_2O)\text{-}OOH$** **Alkyl Oxolane Hydroperoxide**
	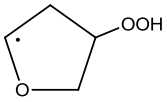	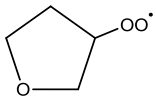
	$y(cccc^{\bullet}o)\text{-}q_{sec}$ **$y(CH_2CHCH_2CH^{\bullet}O)\text{-}OOH$** **Alkyl Oxolane Hydroperoxide**	**$y(cccco)\text{-}q_{sec}^{\bullet}$** **$y(CH_2CHCH_2CH_2O)\text{-}OO^{\bullet}$** **Oxolane Peroxy**

Rotational conformers related to the peroxide group (R—OOH and RO—OH rotors) were studied to determine the lowest energy conformer of each parent and radical. The resulting internal rotor potentials were also used for calculation of entropy and heat capacity contributions. Appendix S summarizes the geometries for each of the molecules studied, and Appendix T summarizes the frequencies.

The potential energies for internal rotor potentials were computed at the B3LYP/6-31G(d,p) level of theory. Appendix U contains the figures for the rotational analysis performed for each of the species studied.

Table 5.23 summarizes the rotational barriers of all the systems studied. The rotational barriers of the ring- hydroperoxide group (yC—OOH = H-C-O-O dihedral angle) have near three fold symmetry, and a barrier of 5.1 to 11.0 kcal mol^{-1}. The barrier is significantly higher when the peroxy, OOH, group is adjacent to the oxygen in the ring (q_{eth}). The barriers for 3, 4 and 5 member cyclics with the peroxy group adjacent to the ether oxygen are 8.2, 10.8 and 8.2 kcal mol^{-1}, respectively. When the peroxy group is bonded to a secondary carbon in the ring (q_{sec}), not adjacent to the ether oxygen, the barriers for the 4 and 5 member cyclics are 5.1 and 5.6 kcal mol^{-1}, respectively. The rotational barriers of the ring- peroxy radical group (yC—$OO^{\bullet}$ = H-C-O-$O^{\bullet}$ dihedral angle) have lower barriers than the yC—OOH rotors in all cases. The peroxy radical rotors are ~3 kcal mol^{-1} lower in the case of y(cco)q_{eth}, y(ccco)q_{sec}, and y(cccco)q_{sec}, and ~6-6.5, kcal mol^{-1} lower in the case of y(ccco)q_{eth}, and y(cccco)q_{eth}.

The rotational barriers about the yC-O—OH bonds range from 4.7 to 9.4 kcal mol^{-1}. In the 4 member ring, the barrier is 4.7 kcal mol^{-1} higher when the peroxy group is bonded to an ether carbon in the ring (q_{eth}) compared to when the peroxy group is bonded to a normal secondary carbon, non-ether carbon, in the ring (q_{sec}). In the 5 member ring, the same barrier (~6.5 kcal mol^{-1}) is observed both when the peroxy group is adjacent to an ether carbon in the ring (q_{eth}), and when it is on a non-ether carbon in the ring (q_{sec}).

Table 5.23 Rotational barriers for the cyclic ether system

Species	yC—Q	yC-(O—OH)	Species	yC—Q	yC-(O—OH)	Species	yC—Q
y(cco)q$_{eth}$	8.2	7.3	**y(c˙co)q**$_{eth}$	9.4	7.1	**y(cco)q**$_{eth}$˙	5.4
y(ccco)q$_{eth}$	10.8	9.4	**y(c˙cco)q**$_{eth}$	11.0	8.6	**y(ccco)q**$_{eth}$˙	4.1
			y(cc˙co)q$_{eth}$	10.9	7.2		
y(ccco)q$_{sec}$	5.1	4.7	**y(c˙cco)q**$_{sec}$	6.7	6.6	**y(ccco)q**$_{sec}$˙	2.2
y(cccco)q$_{eth}$	8.2	6.6	**y(c˙ccco)q**$_{eth}$	9.8	7.4	**y(cccco)q**$_{eth}$˙	2.4
			y(cc˙cco)q$_{eth}$	8.1	6.5		
			y(ccc˙co)q$_{eth}$	8.8	6.7		
y(cccco)q$_{sec}$	5.6	6.4	**y(c˙ccco)q**$_{sec}$	6.2	6.7	**y(cccco)q**$_{sec}$˙	2.4
		---	**y(ccc˙co)q**$_{sec}$	5.2	7.3		
			y(cccc˙o)q$_{sec}$	5.8	7.6		

Units: kcal mol^{-1}

Enthalpies of formation ($\Delta_f H^o_{298}$) were evaluated using calculated energies at the B3LYP/6-31G(d,p), B3LYP/6-31G(2d,2p), CBS-QB3 and G3MP2B3 levels of theory plus use of isodesmic work reactions[157,158]. The standard enthalpies of formation at 298.15 K of the reference species used in the reactions are summarized in Appendix A.

Appendix V summarizes the heats of formation obtained from each of the work reactions, for all methods. The standard enthalpies of formation calculated are shown in Table 5.24, 5.25 and 5.26.

Table 5.24 Calculated enthalpies of formation at 298 K of oxirane and its derivatives

Species		$\Delta H^{o}_{f,298}$							
		B3LYP		CBS-QB3	G3MP2B3	Average DFT	Average Composite	Average Methods	Literature
		6-31G(d,p)	6-31G(2d,2p)						
y(cco)		-12.35	-12.01	-12.63	-12.80	-12.18	**-12.72**	*-12.45*	*-12.58*[77], *-12.6*[150], *-12.61*[159], *-13.20*[44]
	σ	*0.57*	*0.44*	*0.32*	*0.29*	*0.24*	*0.12*	*0.35*	
y(cco)q$_{eth}$		-40.48	-40.31	-39.04	-39.12	-40.39	**-39.08**	*-39.74*	
	σ	*1.04*	*1.01*	*0.02*	*0.02*	*0.11*	*0.06*	*0.76*	
y(c˙co)		39.40	39.39	39.88	39.49	39.39	**39.69**	*39.54*	*35.8±1.5*[160]
	BDE	*104.22*	*104.21*	*104.70*	*104.31*	*104.21*	***104.51***	*104.36*	*100.5±1.5*[160]
	σ	*0.55*	*0.58*	*0.06*	*0.06*	*0.00*	*0.28*	*0.23*	
y(cco)q$_{eth}$˙		-0.57	-0.81	-0.71	-0.82	-0.69	**-0.77**	*-0.73*	
	BDE	*90.61*	*90.37*	*90.47*	*90.36*	*90.49*	***90.41***	*90.45*	
	σ	*0.12*	*0.18*	*0.23*	*0.22*	*0.17*	*0.08*	*0.11*	
y(c˙co)q$_{eth}$		12.66	12.49	13.31	12.99	12.57	**13.15**	*12.96*	
	BDE	*103.84*	*103.67*	*104.49*	*104.17*	*103.75*	***104.33***	*104.04*	
	σ	*0.36*	*0.38*	*0.32*	*0.24*	*0.12*	*0.23*	*0.36*	
y(cc˙o)q$_{eth}$		15.06	14.97	15.97	15.87	15.02	**15.92**	15.47	
		106.2	*106.2*	*107.2*	*107.1*	*106.2*	***107.1***	*106.7*	
		0.13	*0.03*	*0.26*	*0.20*	*0.06*	*0.07*	*0.52*	

Units: kcal mol^{-1}

(*) Standard deviation (σ) does not include the error of the reference species

BDE = Bond Dissociation Enthalpy

Average DFT = Average between 6-31G(d,p) and 6-31G(2d,2p)

Average Composite = average between CBS-QB3 and G3MP2B3

Table 5.25 Calculated enthalpies of formation at 298 K of oxetane and its derivatives

Species		$\Delta H^{o}_{f,298}$							
		B3LYP							
		6-31G(d,p)	6-31G(2d,2p)	CBS-QB3	G3MP2B3	Average DFT	Average Composite	Average Methods	Literature
y(ccco)		-19.77	-18.83	-19.46	-18.86	-19.30	**-19.16**	*-19.23*	*-19.25*[161], *-19.24*[151], *-19.65*[44]
	σ	*0.57*	*0.44*	*0.32*	*0.29*	*0.07*	*0.18*	*0.13*	
y(ccco)q_{eth}		-51.60	-51.55	-51.10	-51.12	-51.58	**-51.11**	*-51.34*	
	σ	*1.04*	*1.01*	*0.02*	*0.02*	*0.04*	*0.02*	*0.27*	
y(ccco)q_{sec}		-40.47	-40.49	-39.90	-39.97	-40.48	**-39.94**	-40.21	
	σ	*1.04*	*1.01*	*0.02*	*0.02*	*0.01*	*0.05*	*0.31*	
y(c˙cco)		24.65	24.60	24.56	24.62	24.63	**24.59**	*24.61*	
	BDE	*95.49*	*95.44*	*95.40*	*95.46*	*95.47*	***95.43***	*95.45*	
	σ	*0.55*	*0.58*	*0.06*	*0.06*	*0.03*	*0.04*	*0.04*	
y(cc˙co)		31.01	31.10	30.80	30.93	*31.05*	**30.87**	*30.96*	
	BDE	*101.85*	*101.94*	*101.64*	*101.77*	*101.89*	***101.71***	*101.80*	
	σ	*0.55*	*0.58*	*0.06*	*0.06*	*0.06*	*0.09*	*0.13*	
y(ccco)q_{eth}˙		-12.59	-12.65	-13.21	-13.44	-12.62	**-13.32**	*-12.97*	
	BDE	*90.62*	*90.56*	*90.00*	*89.77*	*90.59*	***89.89***	*90.24*	
	σ	*0.42*	*0.41*	*0.36*	*0.37*	*0.04*	*0.16*	*0.42*	
y(c˙cco)q_{eth}		-4.66	-4.81	-4.88	-4.93	-4.73	**-4.91**	*-4.82*	
	BDE	*98.55*	*98.40*	*98.33*	*98.28*	*98.48*	***98.30***	*98.39*	
	σ	*0.12*	*0.09*	*0.09*	*0.09*	*0.10*	*0.04*	*0.12*	
y(cc˙co)q_{eth}		1.11	1.21	0.60	0.55	*1.16*	**0.57**	*0.87*	
	BDE	*104.32*	*104.42*	*103.81*	*103.76*	*104.37*	***103.78***	*104.08*	
	σ	*0.34*	*0.36*	*0.30*	*0.29*	*0.07*	*0.04*	*0.34*	
y(ccco)q_{sec}˙		-5.06	-5.17	-5.43	-5.53	*-5.12*	**-5.48**	*-5.30*	
	BDE	*86.98*	*86.87*	*86.61*	*86.51*	*86.92*	***86.56***	*86.74*	
	σ	*0.22*	*0.20*	*0.19*	*0.19*	*0.07*	*0.07*	*0.22*	
y(c˙cco)q_{sec}		2.23	2.20	2.38	2.38	*2.21*	**2.38**	*2.30*	
	BDE	*94.27*	*94.24*	*94.42*	*94.42*	*94.25*	***94.42***	*94.34*	
	σ	*0.10*	*0.10*	*0.08*	*0.08*	*0.02*	*0.00*	*0.10*	

Units: kcal mol^{-1}

(*) Standard deviation (σ) does not include the error of the reference species

BDE = Bond Dissociation Enthalpy

Average DFT = Average between 6-31G(d,p) and 6-31G(2d,2p)

Average Composite = average between CBS-QB3 and G3MP2B3

Table 5.26 Calculated enthalpies of formation at 298 K of oxolane and its derivatives

Species		$\Delta H^{o}_{f,298}$							
		B3LYP							
		6-31G(d,p)	6-31G(2d,2p)	CBS-QB3	G3MP2B3	Average DFT	Average Composite	Average Methods	Literature
y(cccco)		-44.51	-43.93	-44.30	-43.63	-44.22	**-43.97**	-44.09	*-44.03*[162], *-44.0*[150], *-44.58*[44]
	σ	*0.57*	*0.44*	*0.32*	*0.29*	*0.08*	*0.03*	*0.06*	
y(cccco)q_{eth}		-75.60	-75.20	-75.65	-75.62	-75.40	**-75.63**	*-75.52*	
	σ	*1.04*	*1.01*	*0.02*	*0.02*	*0.28*	*0.02*	*0.21*	
y(cccco)q_{sec}		-66.07	-65.81	-66.49	-66.52	*-65.94*	**-66.50**	-66.22	
	σ	*1.04*	*1.01*	*0.02*	*0.02*	*0.18*	*0.02*	*0.34*	
y(c˙ccco)		-2.18	-1.99	-2.01	-2.02	-2.08	**-2.02**	-2.05	*-4.3±1.5*[160]
	BDE	*93.58*	*93.77*	*93.75*	*93.74*	*96.68*	***93.74***	*93.71*	*93.1*[152], *92.1±1.6*[160]
	σ	*0.55*	*0.58*	*0.06*	*0.06*	*0.14*	*0.01*	*0.09*	
y(cc˙cco)		2.50	2.72	2.47	2.55	2.61	**2.51**	2.56	
	BDE	*98.26*	*98.48*	*98.23*	*98.31*	*98.37*	***98.27***	*98.32*	*97.9*[152]
	σ	*0.55*	*0.58*	*0.06*	*0.06*	*0.16*	*0.06*	*0.11*	
y(cccco)q_{eth}˙		-38.65	-38.84	-39.05	-39.16	-38.75	**-39.10**	-38.93	
	BDE	*89.08*	*88.89*	*88.68*	*88.57*	*88.98*	***88.63***	*88.80*	
	σ	*0.22*	*0.19*	*0.18*	*0.18*	*0.13*	*0.08*	*0.22*	
y(c˙ccco)q_{eth}		-31.09	-31.28	-30.70	-30.78	-31.19	**-30.74**	-30.96	
	BDE	*96.64*	*96.45*	*97.03*	*96.95*	*96.54*	***96.99***	*96.77*	
	σ	*0.27*	*0.29*	*0.23*	*0.20*	*0.13*	*0.06*	*0.27*	
y(cc˙cco)q_{eth}		-28.67	-28.66	-28.62	-28.64	-28.67	**-28.63**	-28.65	
	BDE	*99.06*	*99.07*	*99.11*	*99.09*	*99.06*	***99.10***	*99.08*	
	σ	*0.02*	*0.02*	*0.01*	*0.01*	*0.01*	*0.02*	*0.02*	
y(ccc˙co)q_{eth}		-27.88	-27.74	-27.88	-27.87	-27.81	**-27.88**	-27.84	
	BDE	*99.85*	*99.99*	*99.85*	*99.86*	*99.92*	***99.85***	*99.89*	
	σ	*0.07*	*0.06*	*0.03*	*0.03*	*0.09*	*0.01*	*0.07*	

Units: kcal mol^{-1}

(*) Standard deviation (σ) does not include the error of the reference species

BDE = Bond Dissociation Enthalpy

Average DFT = Average between 6-31G(d,p) and 6-31G(2d,2p)

Average Composite = average between CBS-QB3 and G3MP2B3

Table 5.26 Calculated enthalpies of formation at 298 K of oxolane and its derivatives (continued)

Species		$\Delta H^o_{f,298}$							
		B3LYP							
		6-31G(d,p)	6-31G(2d,2p)	CBS-QB3	G3MP2B3	Average DFT	Average ab initio(*)	Average methods	Literature
y(cccco)$q_{sec}^{\bullet}$		-32.24	-32.24	-32.32	-32.36	-32.24	**-32.34**	-32.29	
	BDE	*86.36*	*86.36*	*86.28*	*86.24*	*86.36*	***86.26***	*86.31*	
	σ	*0.06*	*0.06*	*0.05*	*0.05*	*0.00*	*0.03*	*0.06*	
y(c$^{\bullet}$ccco)q_{sec}		-26.66	-26.55	-26.20	-26.01	-26.61	**-26.11**	-26.36	
	BDE	*91.94*	*92.05*	*92.40*	*92.59*	*91.99*	***92.49***	*92.24*	
	σ	*0.30*	*0.28*	*0.26*	*0.27*	*0.08*	*0.13*	*0.30*	
y(ccc$^{\bullet}$co)q_{sec}		-18.84	-18.78	-18.59	-18.54	-18.81	**-18.57**	-18.69	
	BDE	*99.76*	*99.82*	*100.01*	*100.06*	*99.79*	***100.03***	*99.91*	
	σ	*0.14*	*0.13*	*0.12*	*0.12*	*0.04*	*0.03*	*0.14*	
y(cccc$^{\bullet}$o)q_{sec}		-24.22	-24.30	-23.81	-23.83	-24.26	**-23.82**	-24.04	
	BDE	*94.38*	*94.30*	*94.79*	*94.77*	*94.34*	***94.78***	*94.56*	
	σ	*0.25*	*0.27*	*0.22*	*0.21*	*0.06*	*0.02*	*0.25*	

Units: kcal mol^{-1}
Standard deviation (σ) does not include the error of the reference species
(*) Recommended value

The calculated results for oxirane, oxetane and oxolane parent ethers (-12.72, -19.16, -43.97 kcal mol^{-1}, respectively) show good agreement with the available literature data, in all cases within ~ 0.5 kcal mol^{-1}. The available literature data for the oxirane radical[160] is 4 kcal mol^{-1} lower than the value calculated in this study, and for the oxolane radical the calculation from this study is 2.3 kcal mol^{-1} lower than the value presented by Luo[160], and 0.6 kcal mol^{-1} lower than the value presented by Agapito et al.[152].

The heats of formation and bond dissociation enthalpies are not reported for peroxide carbon sites for oxetane and oxolane. Zhu and Bozzelli[163] report that the C—H bonds on carbon sites of peroxides are ~3-5 kcal mol^{-1} weaker than the C—H bonds on corresponding non peroxide carbon sites. The loss of a H$^{\bullet}$ atom at these sites results in a RC$^{\bullet}$OOH intermediate that is not stable; it rapidly dissociates into a lactone and $^{\bullet}$OH

(propiolactone, $\Delta H^{o}_{f,298}$ = -68.4 kcal mol^{-1}, is formed from the oxidation of oxetane[164], and butyrolactone, $\Delta H^{o}_{f,298}$ = -87.0 kcal mol^{-1} is formed from the oxidation of oxolane[165]). The heat of formation for the oxirane alkyl hydroperoxide with the radical site in the peroxide carbon is 2.77 kcal mol^{-1} higher ($\Delta H^{o}_{f,298}$ =15.92 kcal mol^{-1}) than the heat of formation of the oxirane alkyl hydroperoxide with the radical site in the non-peroxide carbon ($\Delta H^{o}_{f,298}$ =13.15 kcal mol^{-1}). Once the radical on the peroxide carbon is formed, it can also further react to form lactone and $^{\bullet}$OH (acetolactone $\Delta H^{o}_{f,298}$ =-47.3 kcal mol^{-1})[166].

The results for all the cyclic ethers also show good agreement between the Density Functional Theory (B3LYP) and higher level composite methods (CBS-QB3 and G3MP2B3). The higher level composite methods present a higher consistency between the values obtained, and the average value of the CBS-QB3 and G3MP2B3 calculations (indicated in bold in the tables) is recommended.

Table 5.27 represents the uncertainties calculated for each of the methods used, accounting for the uncertainty from the work reactions, and the uncertainty of the reference species used in the respective work reactions, and assuming the work reactions cancel the systematic error. Appendix AA contains an explanation of the calculation method for the uncertainties.

Table 5.27 Calculated uncertainties for each method

Parameters	B3LYP/ 6-31G(d,p)	B3LYP/ 6-31G(2d,2p)	CBS-QB3	G3MP2B3
Uncertainty from method	2.07	2.04	0.12	0.12
Uncertainty from reference species	0.75	0.75	0.75	0.75
RMS	±1.56	±1.54	±0.54	±0.54

Table 5.28 represents a summary of the heats of formation ($\Delta H^{\circ}_{f\ 298}$) and bond dissociation enthalpies (BDE) recommended for each of the systems studied.

Table 5.28 Summary of recommended $\Delta H^{o}_{f,298}$ and BDE values for the studied species

Species		$\Delta H^{o}_{f,298}$	C—H BDE	Species		$\Delta H^{o}_{f,298}$	C—H BDE
y(cco)		-12.72		**y(cccco)**		-43.97	
y(cco)q$_{eth}$		-39.08		**y(cccco)q$_{eth}$**		-75.63	
y(c˙co)		39.69	104.51	**y(cccco)q$_{sec}$**	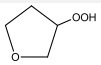	-66.50	
y(cco)q$_{eth}$˙		-0.77	90.41	**y(c˙ccco)**		-2.02	93.74
y(c˙co)q$_{eth}$		13.15	104.33	**y(cc˙cco)**		2.51	98.27
y(cc˙o)q$_{eth}$		15.92	107.10	**y(cccco)q$_{eth}$˙**		-39.10	88.63
y(ccco)		-19.16		**y(c˙ccco)q$_{eth}$**		-30.74	96.99
y(ccco)q$_{eth}$		-51.11		**y(cc˙cco)q$_{eth}$**		-28.63	99.10
y(ccco)q$_{sec}$		-39.94		**y(ccc˙co)q$_{eth}$**		-27.88	99.85
y(c˙cco)		24.59	95.43	**y(cccco)q$_{sec}$˙**		-32.34	86.26
y(cc˙co)		30.87	101.71	**y(c˙ccco)q$_{sec}$**	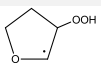	-26.11	92.49
y(ccco)q$_{eth}$˙		-13.32	89.89	**y(ccc˙co)q$_{sec}$**	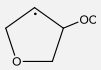	-18.57	100.03
y(c˙cco)q$_{eth}$		-4.91	98.30	**y(cccc˙o)q$_{sec}$**	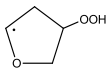	-23.82	94.78
y(cc˙co)q$_{eth}$		0.57	103.78				
y(ccco)q$_{sec}$˙		-5.48	86.56				
y(c˙cco)q$_{sec}$		2.38	94.42				

Units: kcal mol^{-1}

The C—H bond dissociation enthalpies are important fundamental properties that reflect the corresponding radical's stability and serve to identify specific carbon sites where C—H bond cleavage will occur in abstraction of H atoms from carbon sites and in elimination (beta scission) reactions. Bond dissociation enthalpies are reported from the calculated $\Delta_f H^o_{298}$ of parent molecule and their radical corresponding to loss of hydrogen atoms, where the enthalpies of parent molecule and product species are calculated in this study in conjunction with the value of 52.10 kcal mol^{-1} for the hydrogen atom at 298.15 K. Table 5.29 provides a comparison of the secondary C–H bond dissociation enthalpies for cyclic alkanes and ethers, at different positions of the rings. Table 5.29 lists C—H bond dissociation enthalpies for different carbon ring sites:

- Group 1) Cyclic ether, radical site is in non-ether carbon
- Group 2) Cyclic ether, radical site is in ether-carbon
- Group 3) Cyclic ether peroxide, peroxy group is in ether carbon, radical site is in non-ether carbon
- Group 4) Cyclic ether peroxide, peroxy group is in ether carbon, radical site is in ether carbon
- Group 5) Cyclic ether peroxide, peroxy group is in non-ether carbon, radical site is in non-ether carbon
- Group 6) Cyclic ether peroxide, peroxy group is in non-ether carbon, radical site is in ether carbon

Figure 5.11 illustrates a comparison of the results obtained for the C—H bond dissociation enthalpies.

Table 5.29 Comparison of secondary C─H bond dissociation enthalpies for yC_2O-yC_4O cyclic ethers

Bond Dissociated	C—H Bond Dissociation Enthalpies			
	yC_2O	**yC_3O**	**yC_4O**	**Linear Alkanes/Ethers**
No peroxy group				
(1) 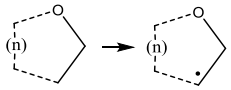		101.7	98.3	*99.12*[b] *($CH_3CH^{\bullet}CH_3$)*
(2) 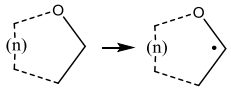	104.5	95.4	93.7	*95.01*[c] *($CH_3CH^{\bullet}OCH_3$)*
Cyclic Alkanes	*109.1*[a]	*100.4*[a]	*96.5*[a]	
Peroxy group bonded to ether carbon (q_{eth})				
(3) 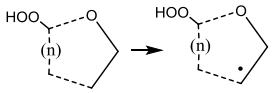		103.8 (q_{eth})	99.1 (q_{eth}) 99.9 (q_{eth})	
(4) 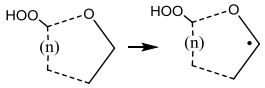	104.3 (q_{eth})	98.3 (q_{eth})	97.0 (q_{eth})	
Cyclic Alkane Peroxides		*101.0*[a]	*97.4*[a]	
Peroxy group bonded to non-ether carbon (q_{sec})				
(5) 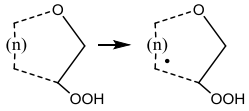			100.0 (q_{sec})	
(6) 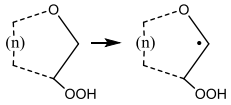		94.4 (q_{sec})	94.8 (q_{sec}) 92.5 (q_{sec})	
Cyclic Alkane Peroxides	*109.7*[a]	*101.4*[a]	*97.8*[a]	

a) Ref. [38-45], b) Ref. [167], c) Ref. [168]

Units: kcal mol^{-1}

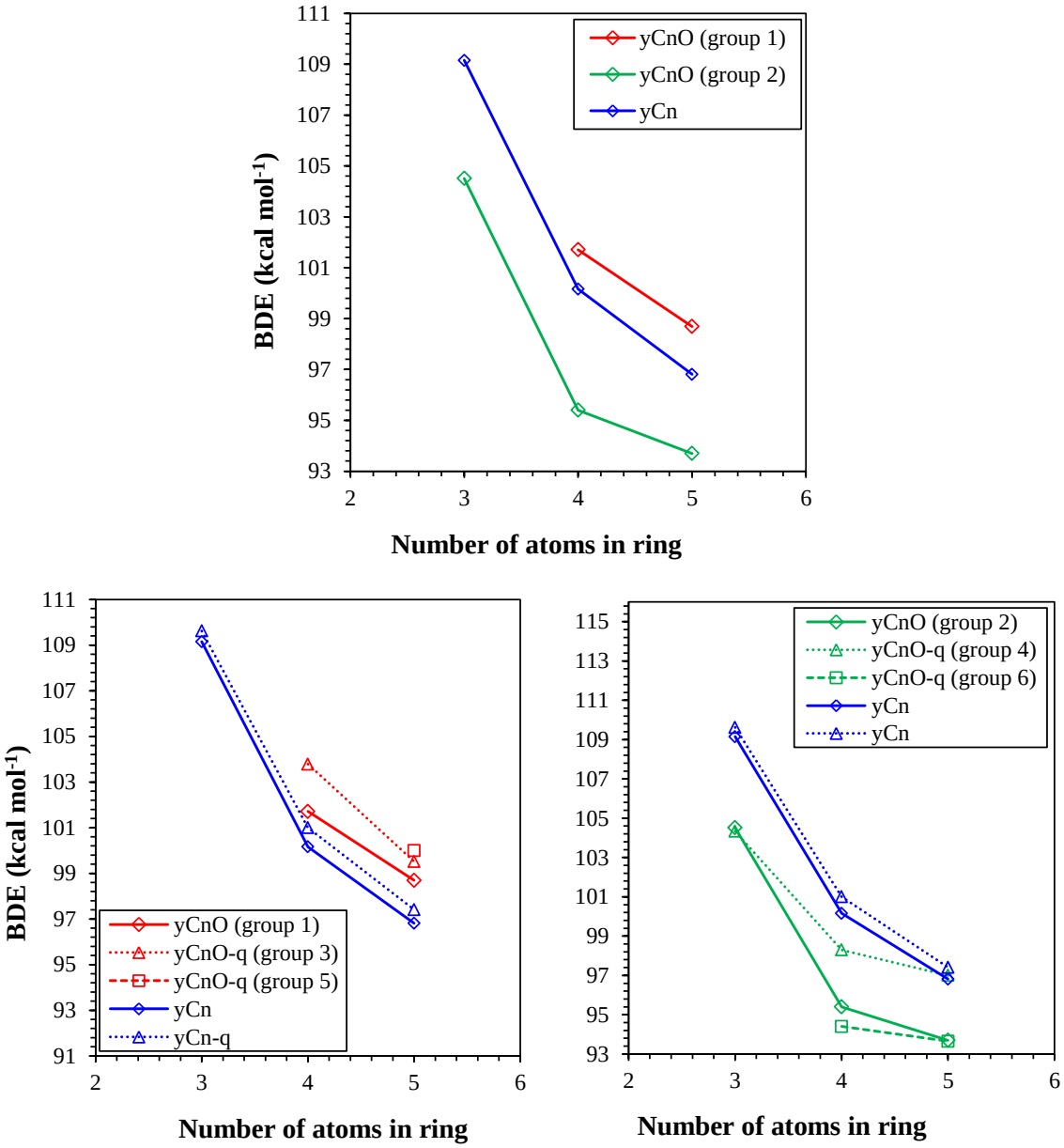

Figure 5.11 Comparison of C—H bond dissociation enthalpies for yC_2O-yC_4O cyclic ethers

Radical sites for cyclic ethers on non-ether carbon sites (group 1) are 4.6 and 6.3 kcal mol^{-1} higher (for oxetane and oxolane, respectively) versus ether carbon sites (group 2). The trend is similar of that observed between linear alkanes and ethers, where the C—H bond dissociation enthalpies are ~4 kcal mol^{-1} higher in linear alkanes. C—H bond

dissociation enthalpies on cyclic ethers on non-ether carbon sites (group 1) are 1.3-1.8 kcal mol^{-1} higher than the C—H bond dissociation enthalpies for cyclic alkanes, which implies that non-ether carbon sites in cyclic ethers are more stable, and therefore less reactive than the carbon sites in cyclic alkanes.

Non-ether carbon site C—H bond dissociation enthalpies of cyclic ethers without peroxy groups (group 1) are 0.8-2.1 kcal mol^{-1} lower versus cyclic ethers with the peroxy group in the ether position (group 3), and 1.7 kcal mol^{-1} lower versus cyclic ethers with the peroxy group in the non-ether position (group 5). Non-ether carbon site C—H bond dissociation enthalpies of cyclic ethers with the peroxy group in the ether position (group 3) are ~0.1-0.5 kcal mol^{-1} lower versus cyclic ethers with the peroxy group in the non-ether position (group 5). Therefore, the presence of the peroxy group in the ring (when bonded both in the ether carbon and non-ether carbons) increases the C—H bond dissociation enthalpies, making the carbons in non-ether positions more stable. The non-ether carbon site C—H bond dissociation enthalpy for the oxolane hydroperoxide, with the peroxy group in the ether carbon, is 0.8 kcal mol^{-1} higher when the radical site is adjacent to the carbon bonded to the peroxy group, which implies that the peroxy group stabilizes the radical site.

Ether carbon site C—H bond dissociation enthalpies of cyclic ethers without peroxy groups (group 2) are 2.9-3.4 kcal mol^{-1} lower versus cyclic ethers with the peroxy group in the ether position (group 4), and 1.0-1.2 kcal mol^{-1} higher versus cyclic ethers with the peroxy group in the non-ether position (group 6). Ether carbon site C—H bond dissociation enthalpies of cyclic ethers with the peroxy group in the ether position (group 4) are ~3.9-4.5 kcal mol^{-1} higher versus cyclic ethers with the peroxy group in the non-

ether position (group 6). Hence, the presence of the peroxy group bonded to the ether carbon in the ring increases the C—H bond dissociation enthalpies, making the carbons in the ether positions more stable. However, the presence of the peroxy group bonded to the non-ether carbon in the ring decreases the C—H bond dissociation enthalpies, making the carbons in the ether positions more reactive. The ether carbon site C—H bond dissociation enthalpy for the oxolane hydroperoxide, with the peroxy group in the ether carbon, is 2.3 kcal mol^{-1} lower when the radical site is adjacent to the carbon bonded to the peroxy group, which implies that the peroxy group reduces the stability.

In all cases, the C—H bond dissociation enthalpies decrease with increasing number of carbons in the ring, and for 5 member rings, the bonds are similar to linear alkanes and ethers (99.12 kcal mol^{-1} for $CH_3CH^{\bullet}CH_3$[167] and 95.01 kcal mol^{-1} for $CH_3CH^{\bullet}OCH_3$[168]).

Table 5.30 summarizes the OO—H peroxy bond dissociation enthalpies for the cyclic alkanes and ethers (see Figure 5.12, left). OO—H bond dissociation enthalpies on cyclic ethers with the peroxy group bonded to the non-ether carbon are 3.33 and 2.37 kcal mol^{-1} lower (for oxetane and oxolane, respectively) versus cyclic ethers with the peroxy group bonded to the ether carbon. The OO—H bonds for cyclic alkanes are ~1 kcal mol^{-1} lower compared to the bonds in the cyclic ethers, with the peroxy group bonded to the non-ether carbon. Hence, the presence of the ether oxygen in the ring stabilizes the cyclic hydroperoxides, especially when the peroxy group is bonded to the ether carbon. The trend is similar of that observed between linear alkanes and ethers, where the OO—H bond dissociation enthalpies are ~2.5 kcal mol^{-1} higher in linear alkanes. In all cases, the OO—H bond dissociation enthalpies decrease with increasing number of carbons in the

ring (for ether carbons 90.4, 89.9 and 88.6 kcal mol^{-1} for y(cco)$q_{eth}^{\bullet}$, y(ccco)$q_{eth}^{\bullet}$ and y(cccco)$q_{eth}^{\bullet}$, respectively, and for secondary carbons: 86.56 and 86.26 kcal mol^{-1} for y(ccco)$q_{sec}^{\bullet}$ and y(cccco)$q_{sec}^{\bullet}$, respectively), and for 5 member rings, the bonds are similar to linear alkanes (85.1 kcal mol^{-1} for $(CH_3)_2CHOO^{\bullet}$[127]).

Table 5.30 Comparison of peroxy bond dissociation enthalpies (OO—H) for yC_2O-yC_4O cyclic ethers

Bond Dissociated	OO—H Bond Dissociation Enthalpies			
	yC_2O	**yC_3O**	**yC_4O**	**Linear Alkanes/Ethers**
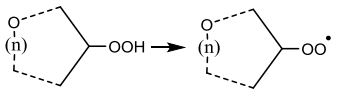		86.6 (q_{sec})	86.3 (q_{sec})	*85.1*[b] *($(CH_3)_2CHOO^{\bullet}$)*
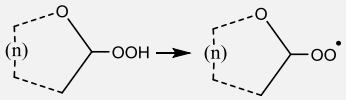	90.4	89.9 (q_{eth})	88.6 (q_{eth})	
Cyclic Alkane Peroxides	*87.0*[a]	*85.7*[a]	*85.1*[a]	

a) Ref. [38-45], b) Ref. [127], c) Group Additivity
Units: kcal mol^{-1}

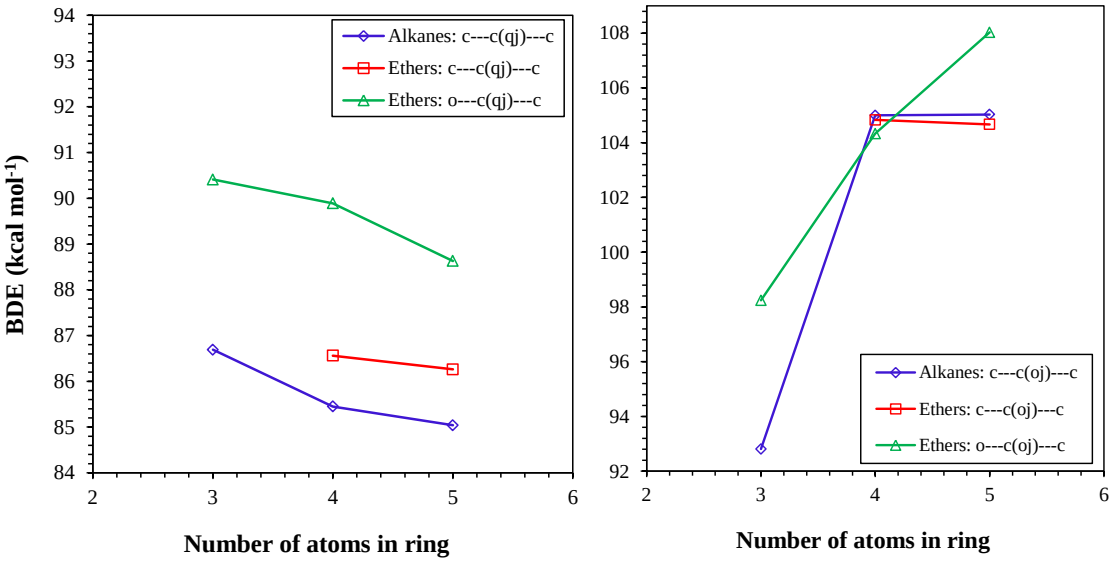

Figure 5.12 Comparison of OO—H (left) and O—H (right) bond dissociation enthalpies for yC_2O-yC_4O cyclic ethers (j=radical site)

Table 5.31 summarizes the heats of formation for the cyclic ether alcohol and alkoxides. Table 5.32 provides a comparison of the O—H peroxy bond dissociation enthalpies for the cyclic alkanes and ethers (see Figure 5.12, right).

Table 5.31 Heat of formation of cyclic ether alcohols and alkoxides

Species	$\Delta_f H°_{298}$	Species	$\Delta_f H°_{298}$	BDE
 **y(cco)oh$_{eth}$**	-59.23	 **y(cco)o$_{eth}^{\bullet}$**	-11.26	*98.24*
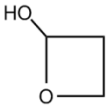 **y(ccco)oh$_{eth}$**	-67.13	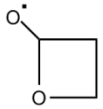 **y(ccco)o$_{eth}^{\bullet}$**	-14.90	*104.33*
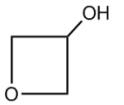 **y(ccco)oh$_{sec}$**	-57.43	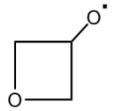 **y(ccco)o$_{sec}^{\bullet}$**	-4.49	*104.83*
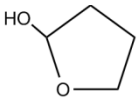 **y(cccco)oh$_{eth}$**	-92.52	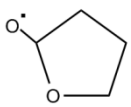 **y(cccco)o$_{eth}^{\bullet}$**	-36.59	108.03
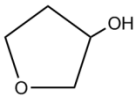 **y(cccco)oh$_{sec}$**	-81.75	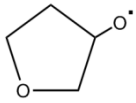 **y(cccco)o$_{sec}^{\bullet}$**	-29.18	104.67

Units: kcal mol^{-1}

Table 5.32 Comparison of alkoxy bond dissociation enthalpies (O—H) for yC$_2$O-yC$_4$O cyclic ethers

Bond Dissociated	O—H Bond Dissociation Enthalpies			
	yC$_2$O	**yC$_3$O**	**yC$_4$O**	**Linear Alkanes/Ethers**
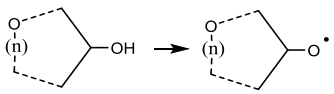		104.8	104.7	*105.1*[b] *((CH$_3$)$_2$CHO$^{\bullet}$)*
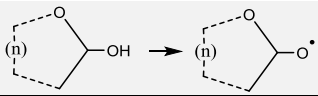	98.2	104.3	108.0	
Cyclic Alkane Alcohols	*92.8*[a]	*105.0*[a]	*105.1*[a]	

Units: kcal mol^{-1}

a) Ref. [38-45], b) Ref.[160]

The O—H bond dissociation enthalpy for oxetane with the alcohol group bonded to the non-ether carbon is only 0.5 kcal mol^{-1} higher versus oxetane with the alcohol group bonded to the ether carbon. The O—H bond is 3.4 kcal mol^{-1} lower for oxolane with the alcohol group bonded to the non-ether carbon versus oxolane with the alcohol group bonded to the ether carbon. In the five member ring, the OH group is significantly closer to the ether oxygen than in the 4 member ring, hence causing the O—H to be stronger in the 5 member ring, and therefore it causes the oxolane with the alcohol group in ether carbon to be more stable. The O—H bonds for cyclic alkanes are only ~0.5 kcal mol^{-1} lower compared to the bonds in the cyclic ethers, with the alcohol group bonded to the non-ether carbon, so they have similar reactivity. The O—H bond dissociation enthalpies increase with increasing number of carbons in the ring for the species with the alcohol group in the ether carbon (98.3, 104.3 and 108.0 kcal mol^{-1} for $y(cco)o_{eth}^{\bullet}$, $y(ccco)o_{eth}^{\bullet}$ and $y(cccco)o_{eth}^{\bullet}$, respectively). The O—H bonds are similar for the species with the alcohol group in the non-ether carbon (104.8 and 104.7 kcal mol^{-1} for $y(ccco)o_{sec}^{\bullet}$ and $y(cccco)o_{sec}^{\bullet}$, respectively), and similar to those of linear alkanes (105.1 kcal mol^{-1} for $(CH_3)_2CHO^{\bullet}$)[160].

The O—OH bond dissociation enthalpies are reported from the calculated $\Delta H_f^o{}_{298}$ of parent hydroperoxide molecule and their alkoxy radical corresponding to loss of $^{\bullet}OH$, where the enthalpies of parent molecule and radicals are calculated in this study in conjunction with the value of 8.9[169] kcal mol^{-1} for $^{\bullet}OH$ at 298.15 K. Table 5.33 provides a comparison between the O—OH bond energies for cyclic alkanes and ethers (see Figure 5.13).

Table 5.33 Comparison of O—OH bond dissociation enthalpies for yC_3-yC_5 cyclic alkanes and yC_2O-yC_4O cyclic ethers

Bond Dissociated	O—OH Bond Dissociation Enthalpies			
	yC_2O	**yC_3O**	**yC_4O**	**Linear Alkanes/Ethers**
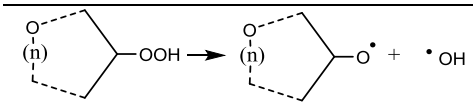		44.4	46.2	*44.9* [b] *($(CH_3)_2CHO^{\bullet}$)*
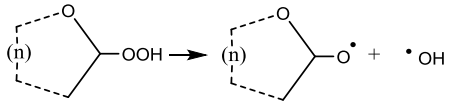	36.7	45.1	47.9	
Cyclic Alkanes	*32.5* [a]	*43.6* [a]	*45.2* [a]	

Units: kcal mol^{-1}

a) Ref. [38-45], b) Ref.[160]

O—OH bond dissociation enthalpies for cyclic ethers with the peroxy group bonded to the non-ether carbon are 0.7 and 1.7 kcal mol^{-1} lower (for oxetane and oxolane, respectively) versus cyclic ethers with the peroxy group bonded to the ether carbon. The O—OH bonds for cyclic alkanes are ~1 kcal mol^{-1} lower compared to the bonds in the cyclic ethers with the peroxy group bonded to the non-ether carbon. Therefore, the hydroperoxides with the OOH group bonded to the ether carbon are more stable than the hydroperoxides with the OH bonded to the non-ether carbon, and to the cyclic alkane hydroperoxides. The O—OH bond dissociation enthalpies increase with increasing number of carbons in the ring for the species with the alcohol group in the ether carbon (36.7, 45.1 and 47.9 kcal mol^{-1} for $y(cco)q_{eth}$, $y(ccco)q_{eth}$ and $y(cccco)q_{eth}$, respectively). The O—OH bonds for oxetane and oxolane with the peroxy group in the non-ether carbon (44.4 and 46.2 kcal mol^{-1} for $y(ccco)o_{sec}^{\bullet}$ and $y(cccco)o_{sec}^{\bullet}$, respectively) are similar to those of linear alkanes (44.9 kcal mol^{-1} for $(CH_3)_2CHO^{\bullet}$)[160].

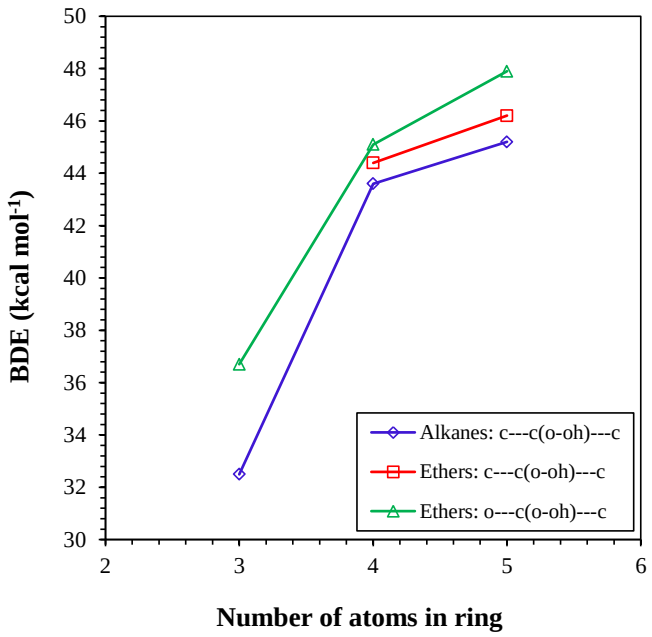

Figure 5.13 Comparison of O—OH bond dissociation enthalpies for yC_2O-yC_4O cyclic ethers (j=radical site)

The $R^{\bullet} + {}^3O_2$ well-depth is an important factor in kinetics for the chemical activation analysis for these association reactions. Table 5.34 summarizes the well-depths for each of the ether systems, and Figure 5.14 illustrates the results obtained.

Table 5.34 $R^{\bullet} + {}^3O_2$ (chemical activation) well-depths for each of the systems studied

System	Well-Depth
$y(c^{\bullet}co) + O_2$	40.46
$y(c^{\bullet}cco) + O_2$	37.91
$y(cc^{\bullet}co) + O_2$	36.35
$y(c^{\bullet}ccco) + O_2$	37.08
$y(cc^{\bullet}cco) + O_2$	34.85

Units: kcal mol^{-1}

The well-depth increases with ring strain in these three cyclics; $R^{\bullet} + {}^3O_2$ well-depth for $yC^{\bullet}_2O$ (oxirane), $yC^{\bullet}_3O$ (oxetane) and $yC^{\bullet}_4O$ (oxolane) are 40.5, 37.9/36.3

(q_{eth}/q_{sec}) and 37.1/34.9 (q_{eth}/q_{sec}) kcal mol^{-1}, respectively (compared to the $R^{\bullet} + {}^3O_2$ well-depth for $yC^{\bullet}_3$, $yC^{\bullet}_4$ and $yC^{\bullet}_5$ are 42.3, 38.9 and 35.1 kcal mol^{-1}, respectively).

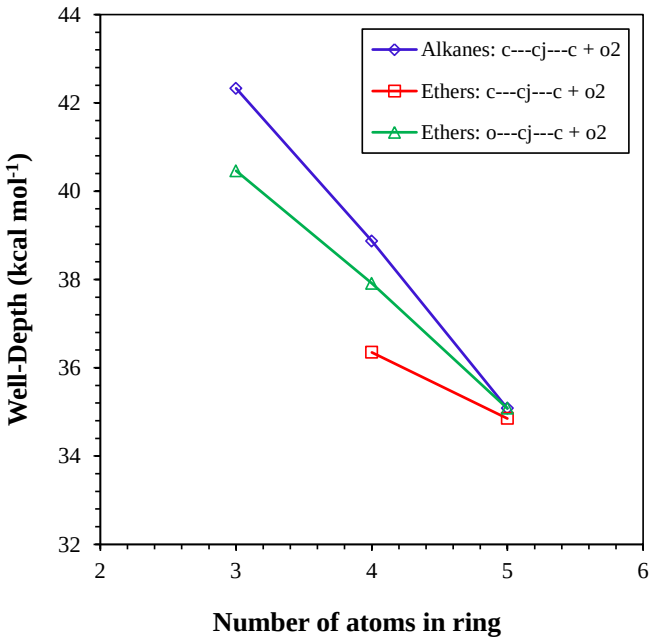

Figure 5.14 Comparison of $R^{\bullet} + {}^3O_2$ well-depths for yC_2O-yC_4O cyclic ethers (j=radical site)

Figures 5.15 to 5.17 illustrate the initial intramolecular H atom transfer reaction energy diagrams for the three studied systems. The heat of formation value indicated is the average of the CBS-QB3 and G3MP2B3 level methods used.

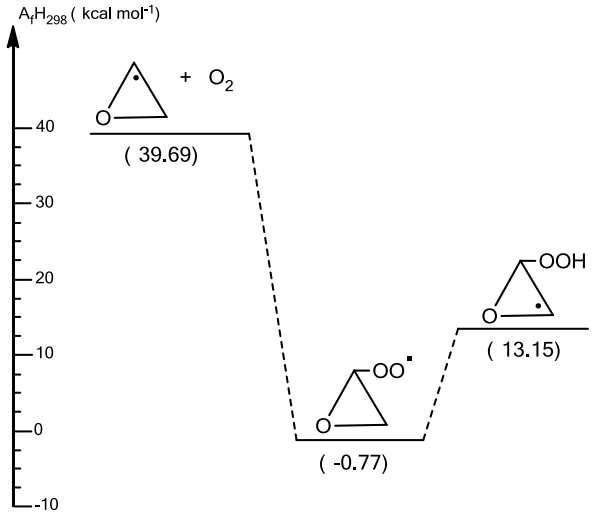

Figure 5.15 Potential energy diagram for alkyl oxirane + $^3O_2$, at 298 K

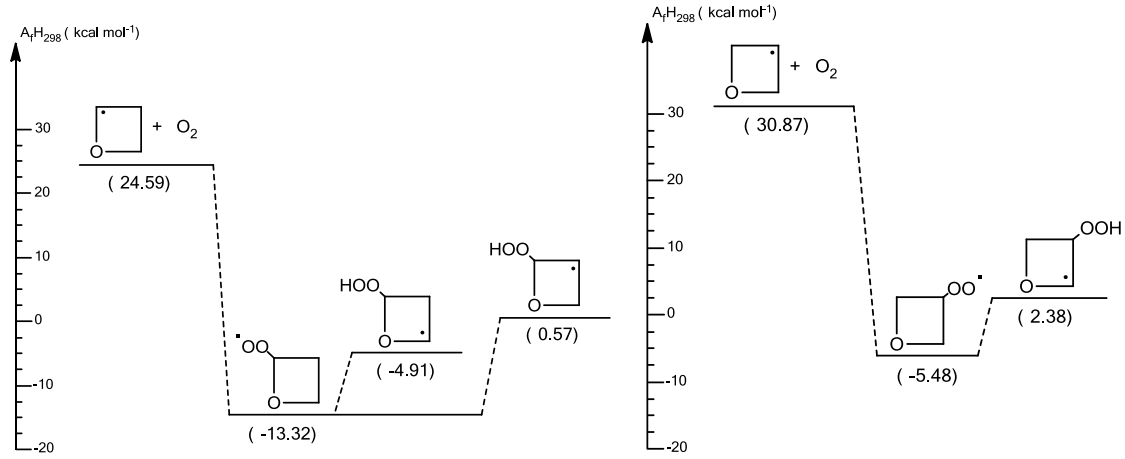

Figure 5.16 Potential energy diagram for alkyl oxetane + $^3O_2$, at 298 K

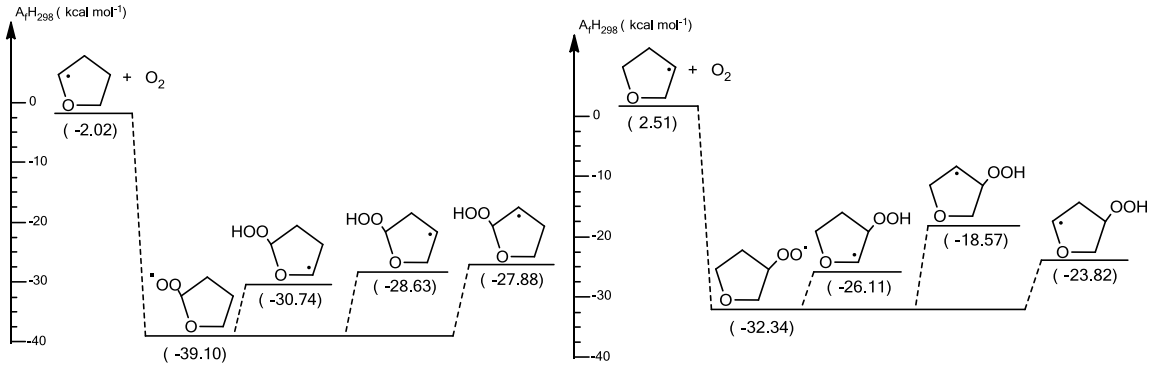

Figure 5.17 Potential energy diagram for alkyl oxolane + $^3O_2$, at 298 K

Entropy and heat capacity values were obtained from SMCPS and Rotator calculations. Table 5.35 summarizes the entropy (S^o, 298 K) and heat capacity (Cp(T)) values obtained for the studied systems. Lowest energy geometries, frequencies, rotation barriers and moments of inertia used for the determination of the entropy and heat capacity, as well as the entropy and heat capacity values for each of the studied systems versus temperature are summarized in Appendix W.

Table 5.35 Entropy (S^o, 298 K) and heat capacity (Cp(T)) for the studied cyclic ether systems

Species	S^o	Cp						
	298 K	300 K	400 K	500 K	600 K	800 K	1000 K	1500 K
y(cco)	59.30	11.22	14.58	17.69	20.31	24.30	27.18	31.59
y(c˙co)	58.95	11.02	13.88	16.38	18.34	20.95	22.47	24.22
y(cco)q_{eth}	74.13	20.90	25.62	29.41	32.22	35.98	38.46	42.20
y(cco)q_{eth}˙	72.53	17.63	21.56	24.88	27.53	31.33	33.91	37.68
y(c˙co)q_{eth}	75.75	20.31	24.41	27.75	30.23	33.43	35.35	38.02
y(ccco)	67.08	14.94	20.05	24.83	28.89	35.13	39.62	46.41
y(c˙cco)	64.72	15.03	19.73	23.94	27.43	32.67	36.39	42.00
y(cc˙co)	66.21	15.84	20.37	24.46	27.87	33.02	36.69	42.21
y(ccco)q_{eth}	75.85	23.86	31.09	37.16	41.86	48.23	52.26	57.91
y(ccco)q_{eth}˙	79.86	21.61	27.13	32.09	36.16	42.17	46.34	52.45
y(c˙cco)q_{eth}	77.84	24.80	31.20	36.20	39.98	45.12	48.46	53.23
y(cc˙co)q_{eth}	79.02	25.14	31.60	36.74	40.58	45.65	48.83	53.33
y(ccco)q_{sec}	81.63	22.94	29.14	34.59	39.03	45.52	49.98	56.57
y(ccco)q_{sec}˙	80.89	20.92	26.58	31.63	35.78	41.91	46.16	52.38
y(c˙cco)q_{sec}	79.73	26.12	31.70	36.02	39.34	44.10	47.40	52.42
y(cccco)	72.66	19.03	25.89	32.28	37.70	46.06	52.08	61.18
y(c˙ccco)	70.05	19.26	25.68	31.46	36.29	43.62	48.86	56.78
y(cc˙cco)	71.23	19.82	26.11	31.82	36.61	43.90	49.12	56.96
y(cccco)q_{eth}	80.57	29.12	37.69	44.87	50.54	58.61	64.05	72.11
y(cccco)q_{eth}˙	85.57	25.38	32.71	39.28	44.73	52.89	58.61	67.10
y(c˙ccco)q_{eth}	82.85	28.14	36.63	43.55	48.84	56.06	60.81	67.78
y(cc˙cco)q_{eth}	84.33	30.24	37.88	44.12	48.99	55.93	60.64	67.66
y(ccc˙co)q_{eth}	83.24	30.14	37.95	44.26	49.19	56.14	60.83	67.76
y(cccco)q_{eth}	85.66	27.82	35.67	42.59	48.25	56.68	62.58	71.41
y(cccco)q_{eth}˙	85.64	25.31	32.67	39.26	44.73	52.92	58.66	67.16
y(c˙ccco)q_{eth}	87.40	29.18	36.32	42.44	47.37	54.59	59.61	67.12
y(ccc˙co)q_{eth}	87.96	28.73	35.79	41.91	46.89	54.25	59.39	67.07
y(cccc˙o)q_{eth}	84.82	28.49	35.81	42.02	47.02	54.34	59.45	67.08

Units: S (cal mol^{-1}) ; Cp (cal mol^{-1} K^{-1})

Table 5.36 Groups developed for cyclic ethers, and previous determined groups used

Group	$\Delta_f H°_{298}$ (*)	S° (298)	C°p(T) 300	400	500	600	800	1000	1500	Ref.
Developed groups										
Stable groups										
CY/C2O	26.68	31.02	-2.16	-2.82	-2.61	-2.35	-2.32	-2.08	2.33	
CY/C3O	25.17	29.38	-3.94	-4.30	-3.72	-3.12	-2.56	-1.98	2.95	
CY/C4O	5.29	25.54	-5.35	-5.41	-4.52	-3.66	-2.70	-1.86	3.52	
CY/C2O/Q	30.02	31.35	-1.85	-2.06	-2.17	-2.06	-2.31	-2.93	-0.01	
CY/C3O/Qe	22.92	23.65	-4.39	-3.54	-2.67	-1.77	-1.13	-1.47	1.50	
CY/C3O/Qs	28.46	27.98	-4.35	-4.93	-4.58	-3.86	-3.38	-3.09	1.57	
CY/C4O/Qe	3.33	18.95	-4.63	-3.89	-3.21	-2.44	-1.82	-2.02	1.50	
CY/C4O/Qs	6.83	22.59	-4.97	-5.35	-4.83	-3.99	-3.29	-2.83	2.21	
Radical groups										
CY/CJ2O	104.51	-0.35	-0.20	-0.70	-1.31	-1.97	-3.35	-4.71	-11.97	
CY/CJ2O/Qe	104.33	1.62	-0.59	-1.21	-1.66	-1.99	-2.55	-3.11	-4.18	
CY/C2O/QeJ	90.41	-1.60	-3.27	-4.06	-4.53	-4.69	-4.65	-4.55	-4.52	
CY/C3JO-e	95.43	-2.36	0.09	-0.32	-0.89	-1.46	-2.46	-3.23	-4.41	
CY/C3JO-s	101.71	-0.87	0.90	0.32	-0.37	-1.02	-2.11	-2.93	-4.20	
CY/CJ3O-e/Qe	98.30	1.99	0.94	0.11	-0.96	-1.88	-3.11	-3.80	-4.68	
CY/CJ3O-s/Qe	103.78	3.17	1.28	0.51	-0.42	-1.28	-2.58	-3.43	-4.58	
CY/CJ3O-e/Qs	94.42	-1.90	3.18	2.56	1.43	0.31	-1.42	-2.58	-4.15	
CY/C3O/QeJ	89.89	4.01	-2.25	-3.96	-5.07	-5.70	-6.06	-5.92	-5.46	
CY/C3O/QsJ	86.56	-0.74	-2.02	-2.56	-2.96	-3.25	-3.61	-3.82	-4.19	
CY/C4JO-e	93.74	-2.61	0.23	-0.21	-0.82	-1.41	-2.44	-3.22	-4.40	
CY/C4JO-s	98.27	-1.43	0.79	0.22	-0.46	-1.09	-2.16	-2.96	-4.22	
CY/CJ4O-e/Qe	96.99	2.28	-0.98	-1.06	-1.32	-1.70	-2.55	-3.24	-4.33	
CY/CJ4O-s/Qe	99.10	3.76	1.12	0.19	-0.75	-1.55	-2.68	-3.41	-4.45	
CY/CJ4O-s2/Qe	99.85	2.67	1.02	0.26	-0.61	-1.35	-2.47	-3.22	-4.35	
CY/CJ4O-e2/Qs	92.49	1.74	1.36	0.65	-0.15	-0.88	-2.09	-2.97	-4.29	
CY/CJ4O-s/Qs	100.03	2.30	0.91	0.12	-0.68	-1.36	-2.43	-3.19	-4.34	
CY/CJ4O-e/Qs	94.78	-0.84	0.67	0.14	-0.57	-1.23	-2.34	-3.13	-4.33	
CY/C4O/QeJ	88.63	5.00	-3.74	-4.98	-5.59	-5.81	-5.72	-5.44	-5.01	
CY/C4O/QsJ	86.26	-0.02	-2.51	-3.00	-3.33	-3.52	-3.76	-3.92	-4.25	
Known groups										
C/C2/H2	-4.93	9.42	5.50	6.95	8.25	9.35	11.07	12.34	14.20	36
C/C2/H/O	-7.20	-11.00	4.80	6.64	8.10	8.73	9.81	10.40	11.51	155
C/C/H2/O	-8.10	9.80	4.99	6.85	8.30	9.43	11.11	12.33	12.33	155
C/C/H/O2	-16.00	-12.07	5.25	7.10	8.81	9.55	10.31	11.05	11.05	155
O/C/O	-5.50	8.54	3.90	4.31	4.60	4.84	5.32	5.80		155
O/H/O	-16.30	27.83	5.21	5.72	6.17	6.66	7.15	7.61	8.43	155
O/C2	-23.20	8.68	3.40	3.70	3.70	3.80	4.40	4.60	4.60	155

Units: kcal mol^{-1}

(*) It represents $\Delta_f H°(298)$ for the stable groups, and bond dissociation enthalpy for the radical groups

The thermodynamic properties of the studied species have been determined using group additivity. A set of new groups have been developed in order to include them in

codes used for group additivity calculations. Table 5.36 summarizes the groups that have been developed, and Appendix X summarizes the description of the groups.

5.4 Unimolecular Dissociation and Chemical Activation of Ring-Opened 3 to 5 Member Ring Cyclic Alkanes and Ethers

The calculated reaction systems are presented in Table 5.37.

Table 5.37 Nomenclature of studied cyclic alkane and ether systems

a)		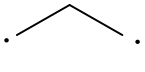	**d)**		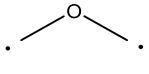
	y(ccc) **y($CH_2CH_2CH_2$)**	**c˙cc˙** **CH_2˙CH_2CH_2˙**		**y(cco)** **y(CH_2CH_2O)**	**c˙oc˙** **CH_2˙OCH_2˙**
b)		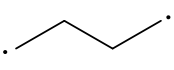	**e)**		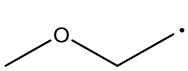
	y(cccc) **y($CH_2CH_2CH_2CH_2$)**	**c˙ccc˙** **CH_2˙$CH_2CH_2CH_2$˙**		**y(ccco)** **y($CH_2CH_2CH_2O$)**	**c˙occ˙** **CH_2˙OCH_2CH_2˙**
c)		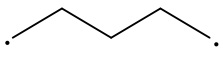			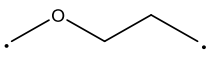
	y(ccccc) **y($CH_2CH_2CH_2CH_2CH_2$)**	**c˙cccc˙** **CH_2˙$CH_2CH_2CH_2CH_2$˙**			**c˙occc˙** **CH_2˙$OCH_2CH_2CH_2$˙**
			f)		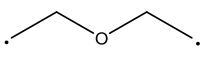
				y(cccco) **y($CH_2CH_2CH_2CH_2O$)**	**c˙cocc˙** **CH_2˙$CH_2OCH_2CH_2$˙**

An example of the calculation method is presented in Table 5.38 for the butan-1,4-yl diradical. The calculated enthalpies of formation of the diradicals resultant of the ring opening of cyclobutane - $y(CH_2CH_2CH_2CH_2) \rightarrow CH_2^{\bullet}CH_2CH_2CH_2^{\bullet}$- and its reaction with molecular oxygen, as well as the work reactions used, determined at different levels of theory for comparison are summarized in Table 5.38. The B3LYP/6-31G(d,p) level calculations were used for remaining species.

Table 5.38 Thermochemical properties- standard enthalpies for $CH_2^{\bullet}CH_2CH_2CH_2^{\bullet}$

Work Reactions	$\Delta_f H^o_{298}$						
	B3LYP 6-31G(d,p)	**BMK 6-31G(d,p)**	**B1B95 6-31G(d,p)**	**Average methods**	**Via Bond Energies**	**GA**	**Lit.**
$c^{\bullet}ccc^{\bullet}$ + cc = $cccc^{\bullet}$ + $cc^{\bullet}$	67.18	67.52	67.54				
$c^{\bullet}ccc^{\bullet}$ + ccc = $cccc^{\bullet}$ + $ccc^{\bullet}$	67.38	67.80	67.66				
$c^{\bullet}ccc^{\bullet}$ + cccc = $cccc^{\bullet}$ + $cccc^{\bullet}$	67.02	67.55	67.58				
$c^{\bullet}ccc^{\bullet}$ + ccccc = $cccc^{\bullet}$ + $ccccc^{\bullet}$	67.11	67.94	67.83				
Ave.	67.17	67.70	67.65	***67.51***	67.51	67.74	67.43[170]
σ				*0.29*			

Units: kcal mol^{-1}

The nomenclature of the diradicals and intermediates studied are summarized in Table 5.39, and the calculated enthalpies of formation of the diradicals and the intermediates formed are summarized in Table 5.40.

Table 5.39 Nomenclature of the diradicals and intermediate species included in the reaction mechanisms

Species	Formula	Species	Formula
$c^{\bullet}c^{\bullet}$	CH_2CH_2	**$o^{\bullet}ccco^{\bullet}$**	$OCH_2CH_2CH_2O$
$c^{\bullet}cc^{\bullet}$	$CH_2CH_2CH_2$	**$c^{\bullet}occo^{\bullet}$**	$CH_2OCH_2CH_2$
$c^{\bullet}ccc^{\bullet}$	$CH_2CH_2CH_2CH_2$	**$o^{\bullet}coco^{\bullet}$**	OCH_2OCH_2O
$c^{\bullet}cccc^{\bullet}$	$CH_2CH_2CH_2CH_2CH_2$	**$o^{\bullet}cocco^{\bullet}$**	$OCH_2OCH_2CH_2O$
$c^{\bullet}ccq^{\bullet}$	$CH_2CH_2CH_2OO$	**$o^{\bullet}coccco^{\bullet}$**	$OCH_2OCH_2CH_2CH_2O$
$c^{\bullet}cccq^{\bullet}$	$CH_2CH_2CH_2CH_2OO$	**$o^{\bullet}ccocco^{\bullet}$**	$OCH_2CH_2OCH_2CH_2O$
$c^{\bullet}ccccq^{\bullet}$	$CH_2CH_2CH_2CH_2CH_2OO$	**y(ccc)**	$y(CH_2CH_2CH_2)$
$o^{\bullet}ccco^{\bullet}$	$OCH_2CH_2CH_2O$	**y(cccc)**	$y(CH_2CH_2CH_2CH_2)$
$o^{\bullet}cccco^{\bullet}$	$OCH_2CH_2CH_2CH_2O$	**y(ccccc)**	$y(CH_2CH_2CH_2CH_2CH_2)$
$o^{\bullet}ccccco^{\bullet}$	$OCH_2CH_2CH_2CH_2CH_2O$	**y(ccccoo)**	$y(CH_2CH_2CH_2CH_2OO)$
$o^{\bullet}cc^{\bullet}$	OCH_2CH_2	**y(cccccoo)**	$y(CH_2CH_2CH_2CH_2OO)$
$c^{\bullet}oc^{\bullet}$	CH_2OCH_2	**y(cco)**	$y(CH_2CH_2O)$
$c^{\bullet}occ^{\bullet}$	$CH_2OCH_2CH_2$	**y(ccco)**	$y(CH_2CH_2CH_2O)$
$c^{\bullet}cocc^{\bullet}$	$CH_2CH_2OCH_2CH_2$	**y(cccco)**	$y(CH_2CH_2CH_2CH_2O)$
$c^{\bullet}occc^{\bullet}$	$CH_2OCH_2CH_2CH_2$	**y(coo)**	$y(CH_2OO)$
$c^{\bullet}ocq^{\bullet}$	CH_2OCH_2OO	**y(ccoo)**	$y(CH_2CH_2OO)$
$c^{\bullet}occq^{\bullet}$	$CH_2OCH_2CH_2OO$	**y(cocoo)**	$y(CH_2OCH_2OO)$
$c^{\bullet}coccq^{\bullet}$	$CH_2CH_2OCH_2CH_2OO$	**y(coccoo)**	$y(CH_2OCH_2CH_2OO)$
$c^{\bullet}occcq^{\bullet}$	$CH_2OCH_2CH_2CH_2OO$	**y(cocco)**	$y(CH_2OCH_2CH_2O)$
$o^{\bullet}co^{\bullet}$	OCH_2O	**y(ccoccoo)**	$y(CH_2CH_2OCH_2CH_2OO)$
$o^{\bullet}cco^{\bullet}$	OCH_2CH_2O	**y(coccoo)**	$y(CH_2OCH_2CH_2CH_2OO)$

Table 5.40 Thermochemistry: cyclics and the diradicals

Species	$\Delta_f H^o_{298}$ B3LYP/6-31G(d,p)	GA	Species	$\Delta_f H^o_{298}$ B3LYP/6-31G(d,p)	GA
c˙c˙	77.19	67.74	**o˙ccco˙**	0.64	6.99
c˙cc˙	72.24	72.67	**c˙occo˙**	7.85	13.66
c˙ccc˙	67.17	67.74	**o˙coco˙**	-31.30	-25.54
c˙cccc˙	62.49	62.81	**o˙cocco˙**	-35.60	-26.51
c˙ccq˙	38.42	38.17	**o˙coccco˙**	-37.46	-31.44
c˙cccq˙	32.93	33.24	**o˙ccocco˙**	-32.13	-27.48
c˙ccccq˙	26.38	28.31	**y(ccc)**	12.74	
o˙ccco˙	5.75	6.99	**y(cccc)**	6.62	
o˙cccco˙	3.51	2.06	**y(ccccc)**	-18.26	
o˙ccccco˙	-1.77	-2.87	**y(ccccoo)**	-36.63	-30.84
o˙cc˙	43.98	44.76	**y(cccccoo)**	-47.49	
c˙oc˙	47.75	54.80	**y(cco)**	-12.63	
c˙occ˙	40.88	46.50	**y(ccco)**	-18.62	
c˙cocc˙	39.38	38.20	**y(cccco)**	-43.67	
c˙occc˙	35.93	41.57	**y(coo)**	-4.47	
c˙ocq˙	9.69	12.97	**y(ccoo)**	-4.81	
c˙occq˙	5.47	12.00	**y(cocoo)**	-58.16	
c˙coccq˙	3.48	3.70	**y(coccoo)**	-64.18	
c˙occcq˙	-0.42	7.07	**y(cocco)**	-73.18	
o˙co˙	20.07	12.89	**y(ccoccoo)**	-71.09	
o˙cco˙	7.91	11.92	**y(coccoo)**	-77.48	

Units: kcal mol^{-1}

Tables 5.41 and 5.42 summarize the heat release for the ring opening of the cyclic alkanes and ethers.

Table 5.41 Summary of the ring opening of cyclic alkanes

C—C Bond Dissociation	**C—C Bond Energy**
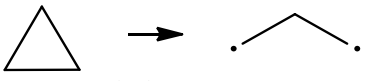 **y(ccc) → c˙cc˙**	59.5
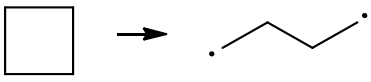 **y(cccc) → c˙ccc˙**	60.6
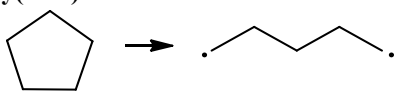 **y(ccccc) → c˙cccc˙**	80.8

Units: kcal mol^{-1}

Table 5.42 Summary of the ring opening of cyclic ethers

C—C Bond Dissociation	C—C Bond Energy
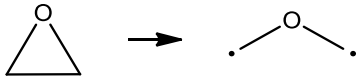	60.7
y(cco) → c˙oc˙	
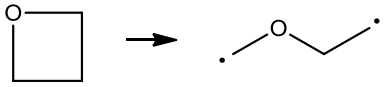	59.5
y(ccco) → c˙occ˙	
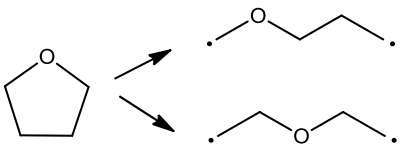	79.6 83.1
y(cccco) →	**c˙occc˙** **c˙cocc˙**

Units: kcal mol^{-1}

Table 5.43 summarizes the type of reactions studied:

Table 5.43 Set of reactions considered for each system

Reactions
1. Unimolecular reactions of the diradical: · Intramolecular H transfer to form an olefin · β-scissions to form olefins · Further reactions of radicals products with $^3O_2$
2. Chemical activation of the diradicals with the molecular oxygen
3. Reactions of stabilized intermediates: · β-scissions to form olefins · Ring-closure · Intramolecular H transfer to form an olefin

High-pressure rate constant parameters were taken from the literature or from calculated transition state structures and energies, as summarized in Table 5.44.

Table 5.44 References for the high pressure rate constant parameters included in the reaction mechanism

Reactions		Ref.
1.	Intramolecular H transfer to form olefins	128,170
2.	β-scissions to form olefins	171
3.	C─H rupture	130
4.	Chemical activation with molecular oxygen	This work

Approximately five collisions (A = 9 x10^{13} cm^3 $mol^{-1}s^{-1}$) and a small barrier (Ea=1.5 kcal mol^{-1}) were estimated, for the electronic state crossing, collision of diradical with bath gas or chemical activation of diradical in association reaction with $^3O_2$.

The intramolecular hydrogen transfer reactions were estimated from literature calculations on four to six membered ring-opened systems[128] at the CBS-QB3 level, and a computational study on the thermal decomposition of tricyclodecane[153]. The rate constants for the unimolecular beta-scission reactions were estimated from a literature evaluation of experimental data on beta-scission reactions of hydrocarbons[171]. For the C─H rupture reactions, rate constants were estimated from high-pressure rate constants calculated by Dean et al. [130].

Kinetic parameters for the bimolecular chemical activation reactions and the subsequent unimolecular thermal dissociation reactions to adducts and product sets were calculated by using a multifrequency quantum Rice-Ramsperger- Kassel (qRRK) analysis for $k(E)$ with the steady-state assumption on the energized adduct(s). Both the forward and reverse paths are included for adducts. Reverse directions of products are incorporated in the subsequent mechanism analysis using ChemKin[172].

Table 5.45 Parameters for the determination of the pressure and temperature dependence of rate constants

Parameters		
T_{range} (K)		300-2400
P_{range} (atm)		0.001-100
Bath gas	Species	N_2
	σ (A)	3.54
	e/k (K)	97.5
σ (A)		4.34
e/k (K)		366.9
ΔE_{down} (cal mol^{-1})		900
Integration interval (kcal)		1.0
E_{head} (kcal mol^{-1})		75

The current version of the qRRK computer code utilizes a reduced set of three vibrational frequencies that accurately reproduce the molecule (adduct) heat capacity data. For the study, reduced sets of 3n-6 frequencies were used for the partition functions. The parameters used for the qRRK analysis are listed in Table 5.45 and 5.46.

Table 5.46 Reduced frequencies for ring opened cyclic alkane and ethers

Species	**Frequencies (cm^{-1})**	**# Vibration Modes**
c˙cc˙	574	7.51
	1556	7.99
	3666	5.00
c˙cc˙	505.1	10.18
	1470.3	12.36
	3505.4	6.95
c˙cccc˙	476.9	13.02
	1442.8	16.71
	3423.5	8.77
c˙oc˙	426.7	4.88
	1299.4	6.23
	3260.3	3.89
c˙occ˙	395.9	7.76
	1271.2	10.18
	3132.4	6.06
c˙occc˙	373.0	10.34
	1283.4	14.55
	3091.7	8.11
c˙cocc˙	387.7	10.65
	1262.1	14.25
	3085.2	8.11

The high-pressure limiting rate constant for all the diradical + $^3O_2$ reactions was estimated to be 1.5 x10^{13} independent of temperature. For the primary radicals + $^3O_2$ reaction Sheng et al.[173] calculated (vtst) a high pressure limit of 2.94 .10^{13} $T^{-0.44}$, which was used as part of the base for this assumption.

The results from the chemical activation analysis and from analysis of dissociation of important intermediates formed in the oxidation system along with unimolecular reactions of the diradicals were input to a ChemKin reaction mechanism.

This mechanism was utilized to evaluate the forward reactions of the diradical(s) and to evaluate the importance of the oxidation paths versus the different unimolecular dissociation, isomerization, and intramolecular H atom transfers which are illustrated in the diradical reaction path potential curves. It also provides time profiles of the reaction products.

There are a number of reactions that were not included in this mechanism analysis. These include:

- Abstraction and association reactions by radical pool species on the reactants and intermediates. These were omitted because their concentration is several orders of magnitude below that of the reactive $^3O_2$ moiety, where the oxygen association has a high pre-exponential factor and no barrier.
- Intramolecular hydrogen transfer of the ROO$^{\bullet}$ peroxy radicals where the barrier is relatively high (above 20 kcal mol^{-1}).
- HO_2 and H_2O molecular elimination reactions from the peroxy radicals and peroxides, where high barriers reduce their importance.
- Further reactions of initial products to complete oxidation.

Table 5.47 below summarizes the number of reaction and number of species for the elementary reaction mechanisms built for each of the studied systems.

Table 5.47 Cyclic alkane and ether elementary reaction mechanisms

Systems		Number of Reactions	Number of Species
y(ccc)	→ **c˙cc˙**	9	13
y(cccc)	→ **c˙ccc˙**	10	15
y(ccccc)	→ **c˙cccc˙**	15	19
y(cco)	→ **c˙oc˙**	10	16
y(ccco)	→ **c˙occ˙**	11	13
y(cccco)	→ **c˙occc˙**	16	14
	→ **c˙cocc˙**	16	14

The initial concentrations used for the modeling of all the systems are summarized in Table 5.48:

Table 5.48 Initial concentrations for all the cyclic alkane and ether systems

Species (1 atm)	Initial concentration (%)
Diradical	0.001
N_2	0.86
O_2	0.14

The ratio N_2:O_2 = 0.86:0.14 was chosen as an estimate of reduced O_2 presence in internal engine combustion. Figure 5.18 shows the influence of using 86% of N_2 and 14% of O_2 instead of using the standard ratio 79% of N_2 and 21% of O_2. As expected, at both temperatures, the gas mixture with the higher concentration of O_2 leads to a higher formation of the oxidation product, y($CH_2CH_2CH_2CH_2O$). The formation of this five membered cyclic ether results from the chemical activated reaction of the diradical formed from the ring-opening of cyclopentane, with molecular oxygen.

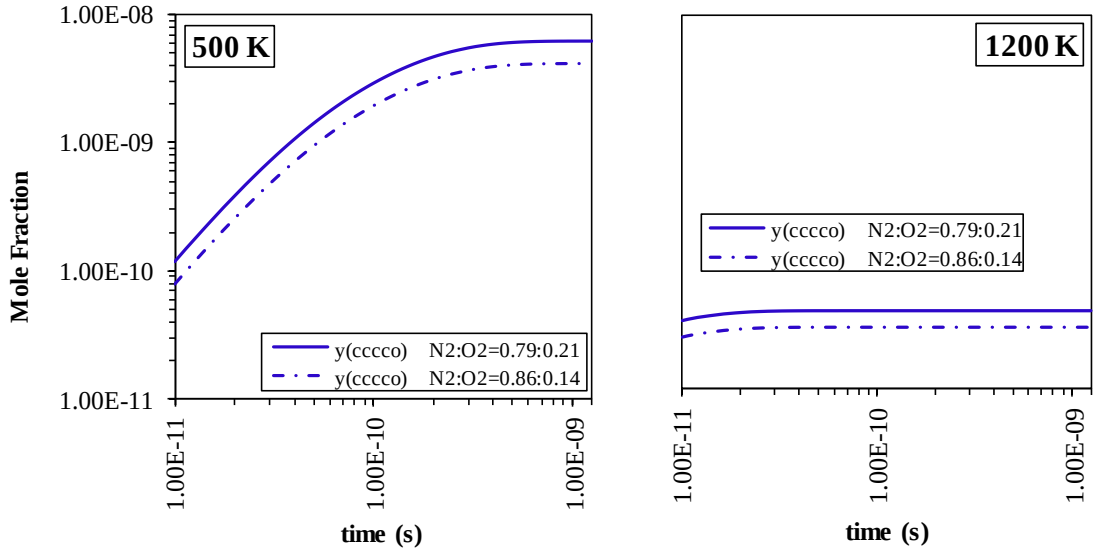

Figure 5.18 Comparison of the mole fraction of y($CH_2CH_2CH_2CH_2O$) versus time using two different N_2:O_2 compositions for the gas mixture, at 500 K and 1200 K

Figure 5.19 shows the potential energy diagram of the diradical resulting from the ring opening of cyclopropane. The β-scission of $CH_2^{\bullet}CH_2CH_2^{\bullet}$ to ethylene plus $^1CH_2$ is ~ 41.67 kcal mol^{-1} endothermic. In all cases the diradicals formed from the ring opening readily reform to the respective cyclic parents via simple association reactions. These association reactions are rapid, they occur with low or no barrier and relatively high pre-expoential factors. However the target of this study is the evaluation of the important forward reaction paths, and these reverse reactions are not included in this analysis.

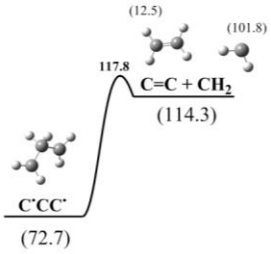

Figure 5.19 Potential energy diagram of diradical dissociation of $CH_2^{\bullet}CH_2CH_2^{\bullet}$. All values are at 298 K. Units kcal mol^{-1}

Figure 5.20 represents the chemical activation of $CH_2^{\bullet}CH_2CH_2^{\bullet}$ with molecular oxygen. The first step consists on the formation of the peroxy adduct. $CH_2^{\bullet}CH_2CH_2OO^{\bullet}$(t), that can undergo triplet-singlet conversion via electronic state crossing, collision of diradical with bath gas or chemical activation of diradical with molecular gas. The ring closure of the singlet peroxy diradical results on the formation of a five member ring y($CH_2CH_2CH_2OO$). This ring can undergo low energy ring opening through the RO─OR bond resulting in a di-alkoxy radical $O^{\bullet}CH_2CH_2CH_2O^{\bullet}$, that can react through low energy β-scission reactions leading to oxygenated products.

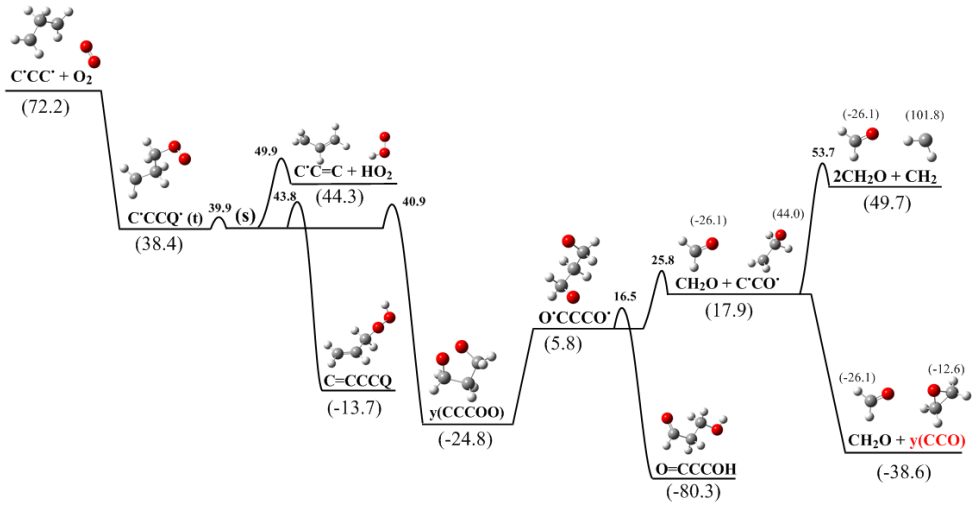

Figure 5.20 y($CH_2CH_2CH_2$) ring opening $CH_2^{\bullet}CH_2CH_2^{\bullet}$ + O_2 potential energy diagram. All values are at 298 K. Units kcal mol^{-1}

Figure 5.21 summarizes the chemical activation results of the ring opened diradical from cyclopropane with $^3O_2$ at 1 atm and 1000 K. The only important oxidation channel is the formation of the peroxy adduct and its dissociation to a formaldehyde + c$^{\bullet}$co$^{\bullet}$, the dissociation of the adduct back to the initial diradical + $^3O_2$ is a non-reaction.

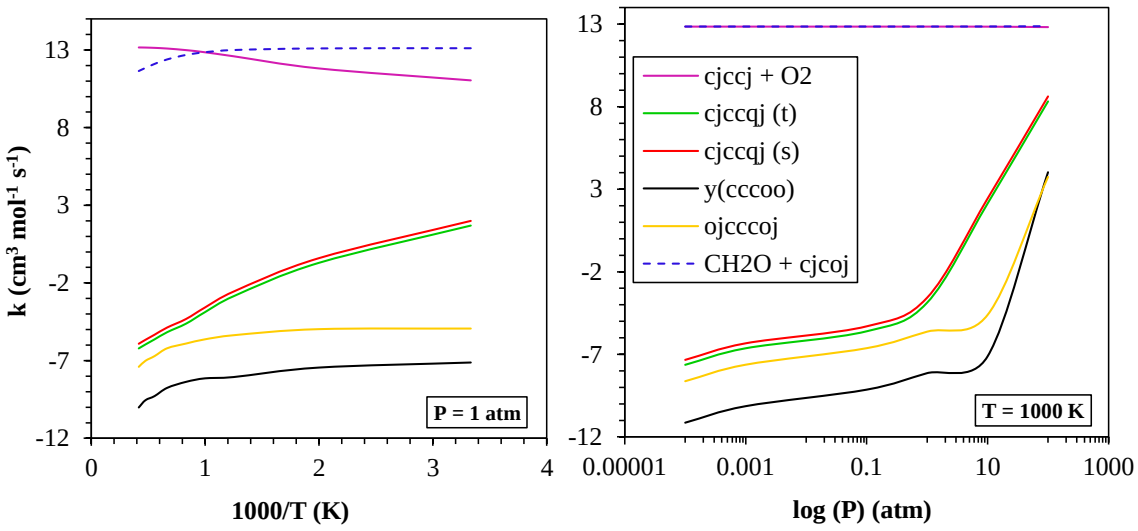

Figure 5.21 Chemical activation plot of rate constants vs. T at 1 atm and vs. P at 1000 K for $CH_2^{\bullet}CH_2CH_2^{\bullet}$ + $^3O_2$ (does not include unimolecular reactions of the diradical) j=radical site

ChemKin modeling, concentration of products versus reaction time, for oxidation and unimolecular reactions on the ring opened diradical from cyclopropane is illustrated in Figure 5.22 for temperatures of 500 K and 1200 K. Results indicate that the main reaction path is the ring closure for the formation of the cyclic ether y($CH_2CH_2CH_2O$) plus a formaldehyde. At higher temperatures, the formation of ethylene becomes important.

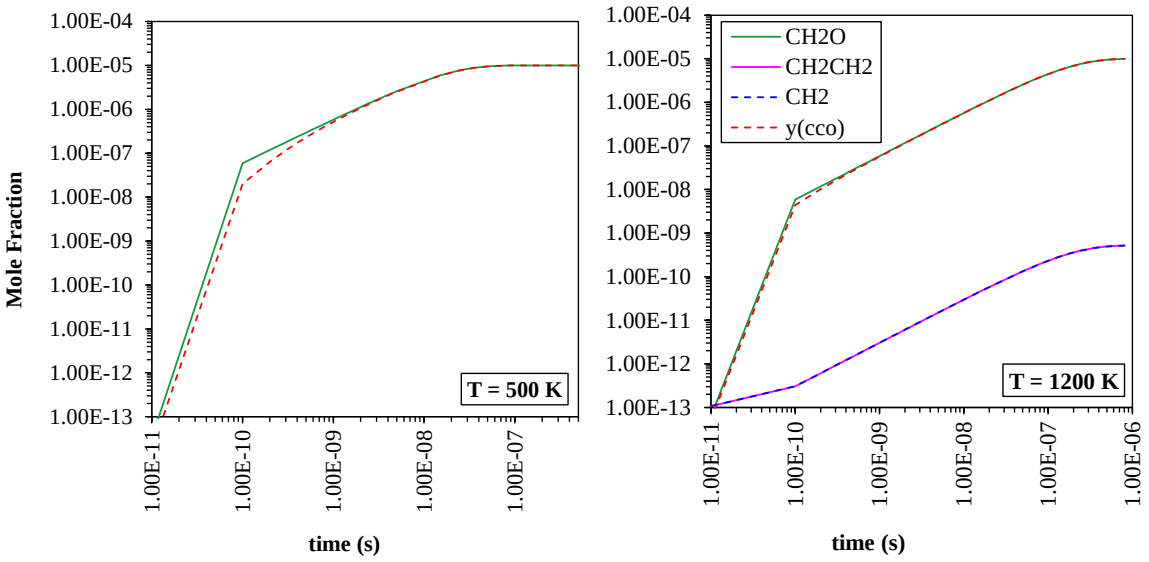

Figure 5.22 ChemKin modeling of unimolecular and oxidation reactions of $CH_2^{\bullet}CH_2CH_2^{\bullet}$ at 1 atm. (CH_2CH_2 and CH_2 are overlapped at 1200 K)

A potential energy diagram for reactions of the diradical resulting from the ring opening of cyclobutane is presented in Figure 5.23. The intramolecular H transfer to form a stable olefin from $CH_2^{\bullet}CH_2CH_2CH_2^{\bullet}$ is 67.51 kcal mol^{-1} exothermic with a barrier of 16.44 kcal mol^{-1}. This results in formation of butene, whereas the β-scission reaction leads to the formation of two ethelenes, with a lower barrier[1] of 3.03 kcal mol^{-1}.

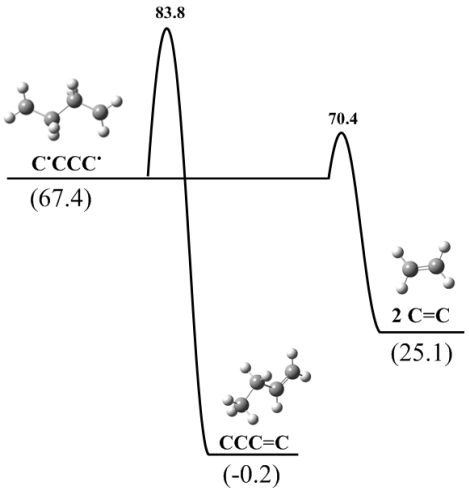

Figure 5.23 Potential energy diagram of diradical dissociation and intramolecular H transfer of $CH_2^{\bullet}CH_2CH_2CH_2^{\bullet}$. All values are at 298 K. Units kcal mol^{-1}

Figure 5.24 representes the chemical activation of $CH_2^{\bullet}CH_2CH_2CH_2^{\bullet}$ with molecular oxygen, following the same reaction path presented for the three member cyclic alkane system.

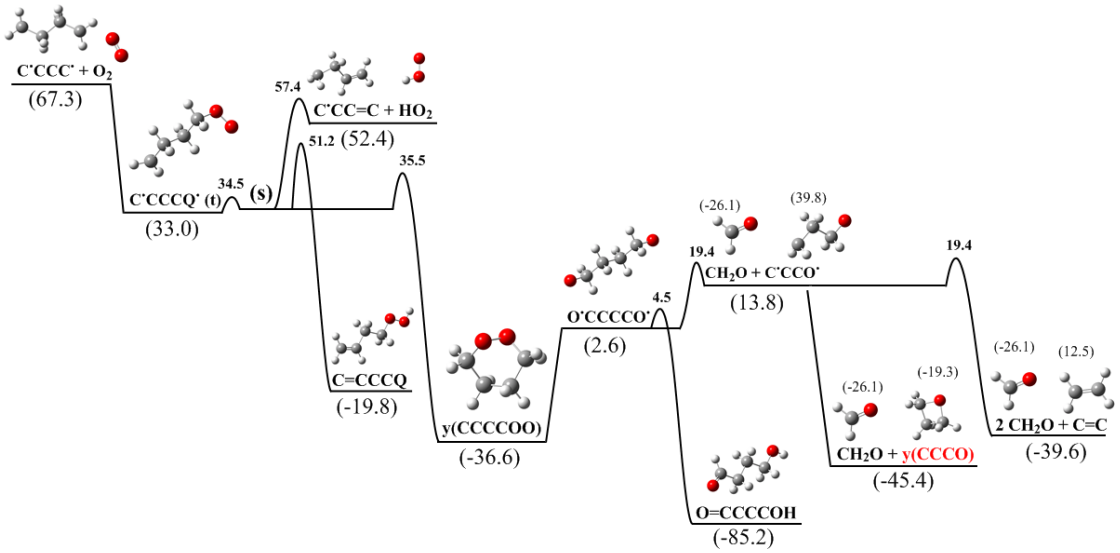

Figure 5.24 y($CH_2CH_2CH_2CH_2$) ring opening $CH_2^{\bullet}CH_2CH_2CH_2^{\bullet}$ ring opened + $^3O_2$ potential energy diagram. All values are at 298 K. Units kcal mol^{-1}

Figure 5.25 summarizes the chemical activation results of the ring opened diradical from cyclobutane reaction with $^3O_2$. The only important oxidation channel is formation of the peroxy adduct and its dissociation to one formaldehyde plus $CH_2^{\bullet}CH_2CH_2O^{\bullet}$, and the dissociation of the adduct back to the initial diradical + $^3O_2$. The $CH_2^{\bullet}CH_2CH_2O^{\bullet}$ can cyclize or react to ethylene plus CH_2O.

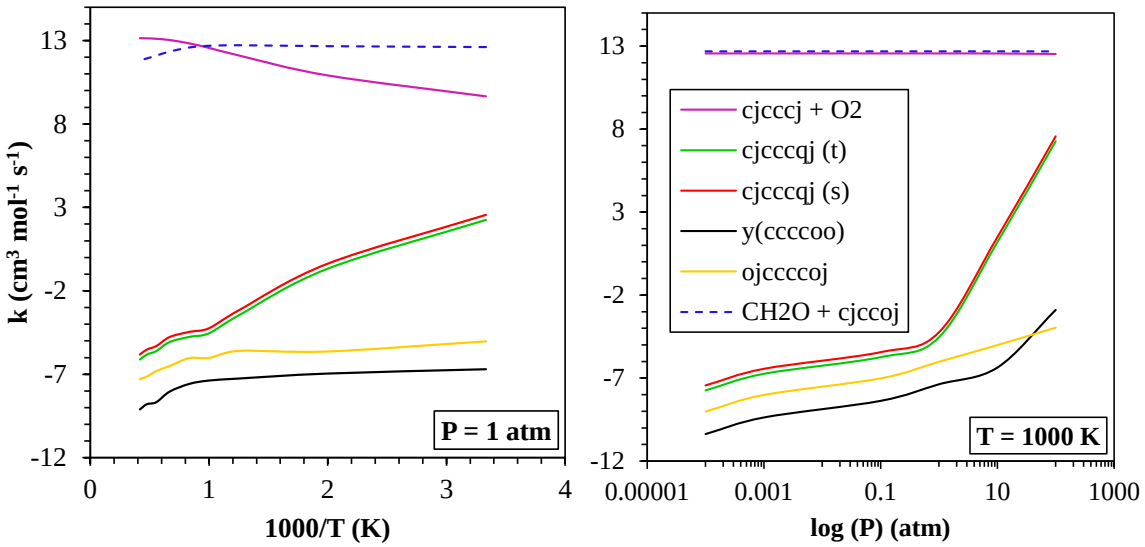

Figure 5.25 Chemical activation plot of rate constants vs. T at 1 atm and vs. P at 1000 K for $CH_2^{\bullet}CH_2CH_2CH_2^{\bullet}$ + $^3O_2$ (does not include unimolecular reactions of the diradical). j=radical site

The ChemKin modeling of concentration of products versus reaction time, for oxidation and unimolecular dissociation on the ring opened diradical from cyclobutane is illustrated in Figure 5.26 for temperatures of 500 K and 1200 K. The results at both temperatures show that unimolecular dissociation to two ethylene moieties is the most important channel. Oxidation to two formaldehyde plus ethylene at 500 K is next most important, while intramolecular H transfer to form butene is more important at 1200 K. The formation of oxitane y($CH_2CH_2CH_2O$) has some importance at 500 K, but becomes negligible at 1200 K.

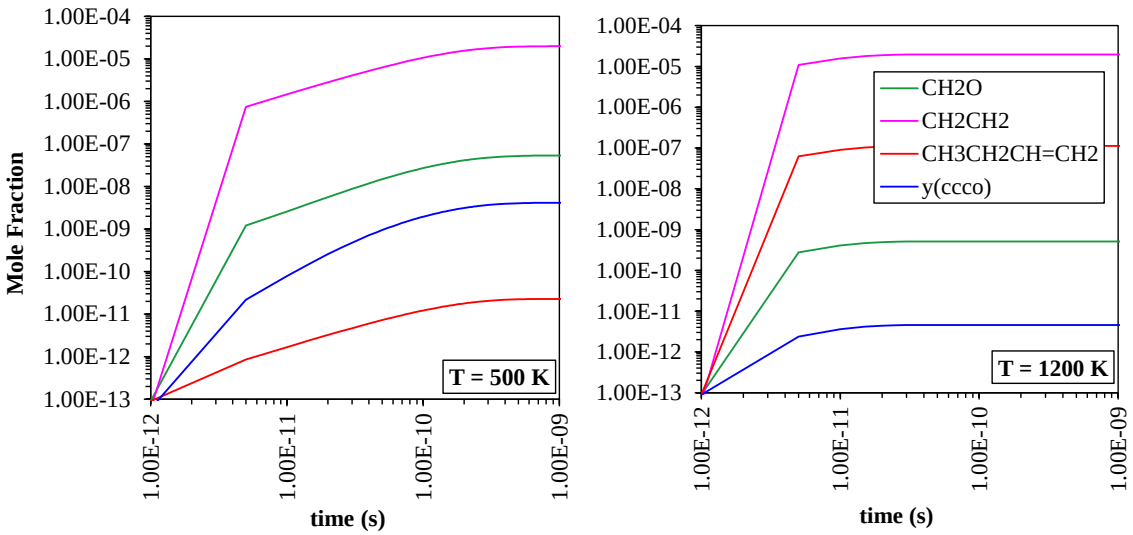

Figure 5.26 ChemKin modeling of unimolecular and oxidation reactions of $CH_2^{\bullet}CH_2CH_2CH_2^{\bullet}$ at 1 atm (CH_2CH_2 is dominant at both temperatures)

The dissociation of the $CH_2^{\bullet}CH_2CH_2CH_2CH_2^{\bullet}$ diradical from the ring opening of the cycopentane is illustrated in Figure 5.27. Intramolecular H transfer results on the formation of pentene, through a lower barrier[1] (7.76 kcal mol^{-1}) than in the case of $CH_2^{\bullet}CH_2CH_2CH_2^{\bullet}$. The β-scission reaction results in the endothermic formation of two ethelenes and the diradical $^1CH_2$, or the formation of one ethelene and the ring closure to form cyclopropane, thought a barrier[1] of 26.16 kcal mol^{-1}.

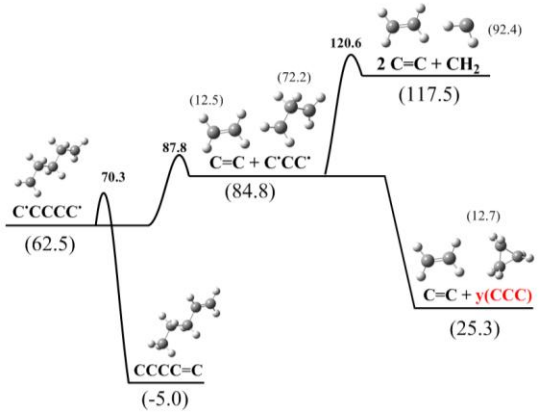

Figure 5.27 Potential energy diagram of diradical dissociation and intramolecular H transfer of $CH_2^{\bullet}CH_2CH_2CH_2CH_2^{\bullet}$. All values are at 298 K. Units kcal mol^{-1}

Figure 5.28 represents the chemical activation of $CH_2^{\bullet}CH_2CH_2CH_2CH_2^{\bullet}$ with molecular oxygen, following similar reaction paths to those described for the propane ring opened alkane + $^3O_2$ system above.

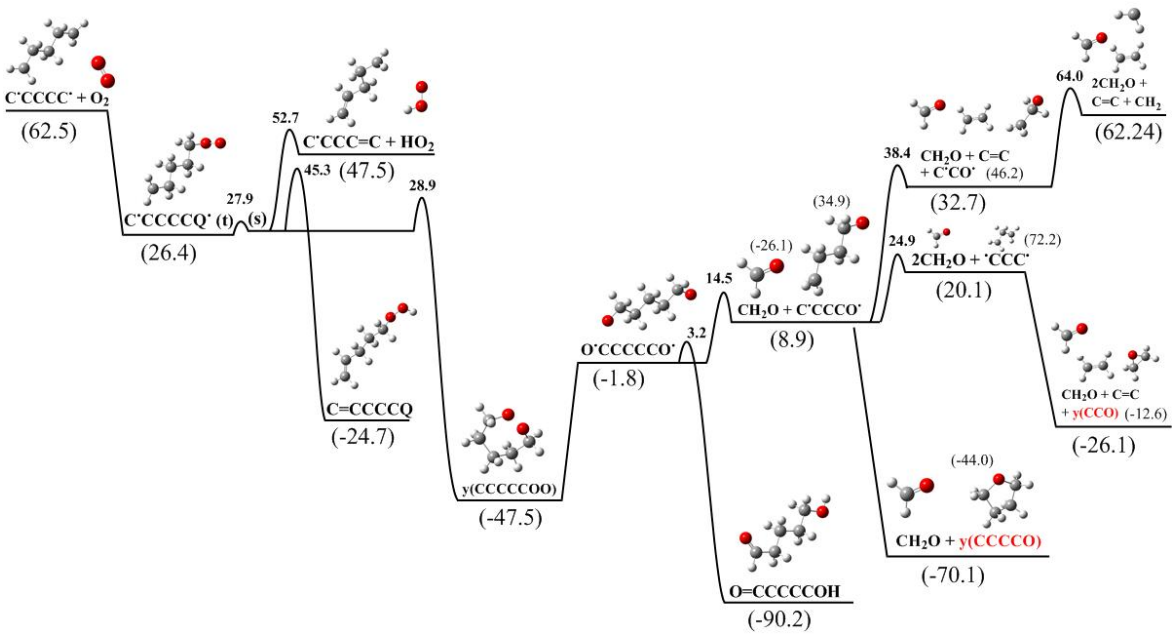

Figure 5.28 y($CH_2CH_2CH_2CH_2CH_2$) ring opening $CH_2^{\bullet}CH_2CH_2CH_2CH_2^{\bullet}$ ring opened + $^3O_2$ potential energy diagram. All values are at 298 K. Units kcal mol^{-1}

Figure 5.29 illustrates the results for the chemical activation analysis on the ring opened diradical from cyclopentane with $^3O_2$. The important oxidation channel is formation of the peroxy adduct and its dissociation to a formaldehyde + $CH_2^{\bullet}CH_2CH_2CH_2O^{\bullet}$, where the dissociation of the adduct back to the initial diradical + $^3O_2$ is a not reaction. The $CH_2^{\bullet}CH_2CH_2CH_2O^{\bullet}$ diradical can undergo ring closure to tetrahydrofuran, intramolecular H atom transfer to form 1 butene 4-ol for dissociate to formaldehyde plus $CH_2^{\bullet}CH_2CH_2^{\bullet}$.

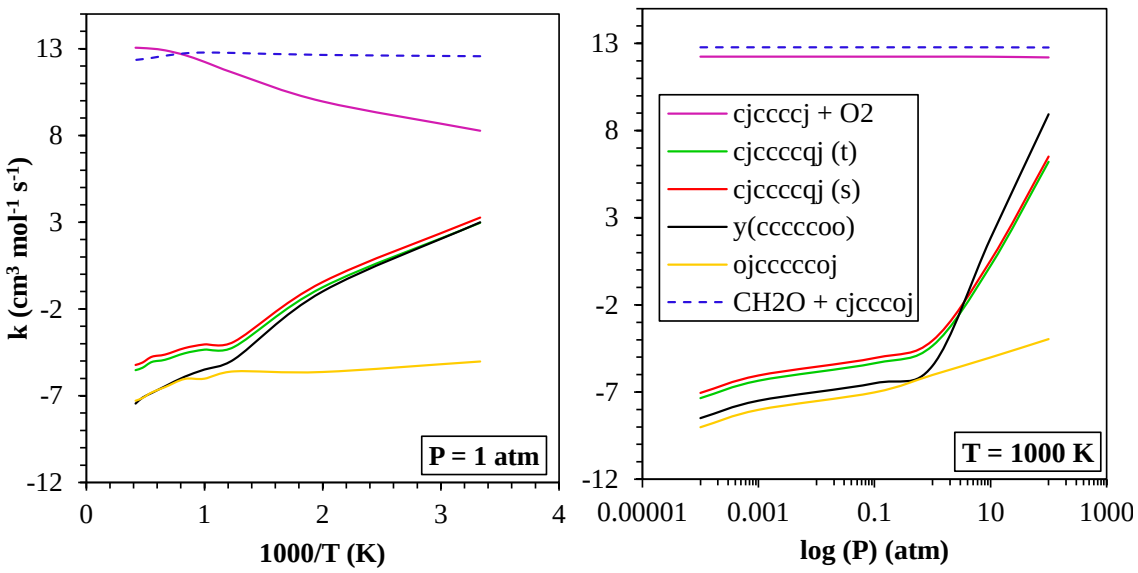

Figure 5.29 Chemical activation plot of rate constants vs. T at 1 atm and vs. P at 1000 K for $CH_2^{\bullet}CH_2CH_2CH_2CH_2^{\bullet}$ + $^3O_2$ (does not include unimolecular reactions of the diradical). j=radical site

ChemKin modeling for concentration of products versus reaction time with the oxidation and unimolecular dissociation reactions of the ring opened diradical from cyclopentane is illustrated in Figure 5.30 for temperatures of 500 K and 1200 K. At low temperatures, results indicate that the unimolecular dissociation of the diradical via the intramolecular hydrogen transfer for the formation of pentene, and the β-dissociation followed by the ring closure to form cyclopropane are the main reaction paths. The reaction from the chemical activation of the diradical with molecular oxygen resulting in formation of two formaldehydes plus ethylene and singlet diradical $^1CH_2$ is also important. At higher temperatures, the intramolecular H transfer to form pentene is the dominant reaction path.

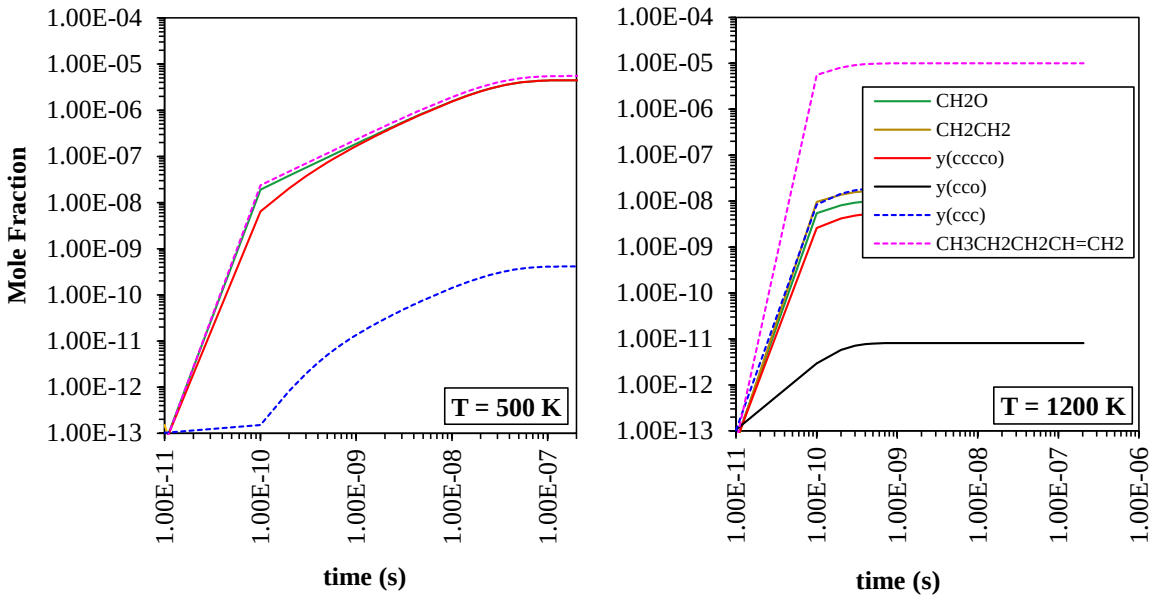

Figure 5.30 ChemKin modeling of unimolecular and oxidation reactions of $CH_2\dot{C}H_2CH_2CH_2\dot{C}H_2$ at 1 atm

At 500 K pentene, y($CH_2CH_2CH_2CH_2O$) and ch_2o are major product and overlap. At 1200 K pentene is major product and CH_2O, CH_2CH_2, y($CH_2CH_2CH_2CH_2O$) and y($CH_2CH_2CH_2$) are similar.

Figures 5.31 and 5.32 represent the unimolecular dissociation of the three member cyclic ether ring opened diradicals and the chemical activation of the diradical with molecular oxygen, respectively.

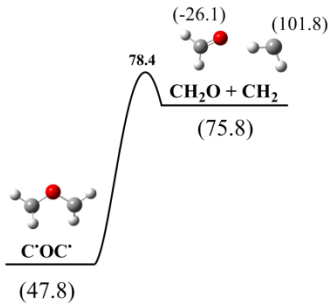

Figure 5.31 Potential energy diagram of diradical dissociation $CH_2\dot{O}CH_2\dot{}$. All values are at 298 K. Units kcal mol^{-1}

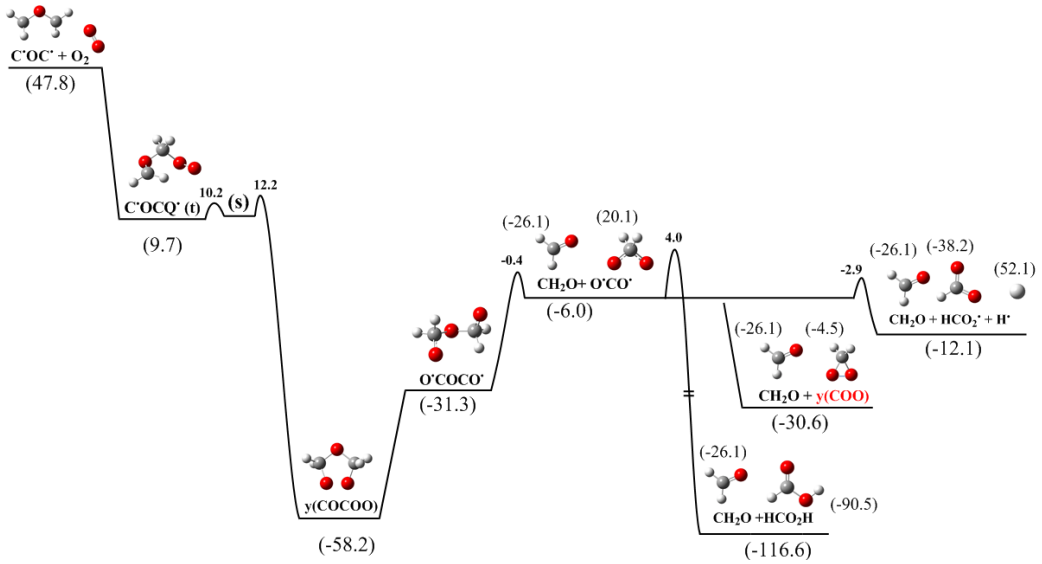

Figure 5.32 y(CH_2CH_2O) ring opening CH_2˙OCH_2˙ ring opened + $^3O_2$ potential energy diagram. All values are at 298 K. Units kcal mol^{-1}

Figure 5.33 summarizes the chemical activation results of the ring opened diradical from the three membered cyclic ether with $^3O_2$. The important oxidation channel is formation of the peroxy adduct and its dissociation to a formaldehyde + O˙CH_2O˙, which will form HCO_2H or HCO_2˙ + H.

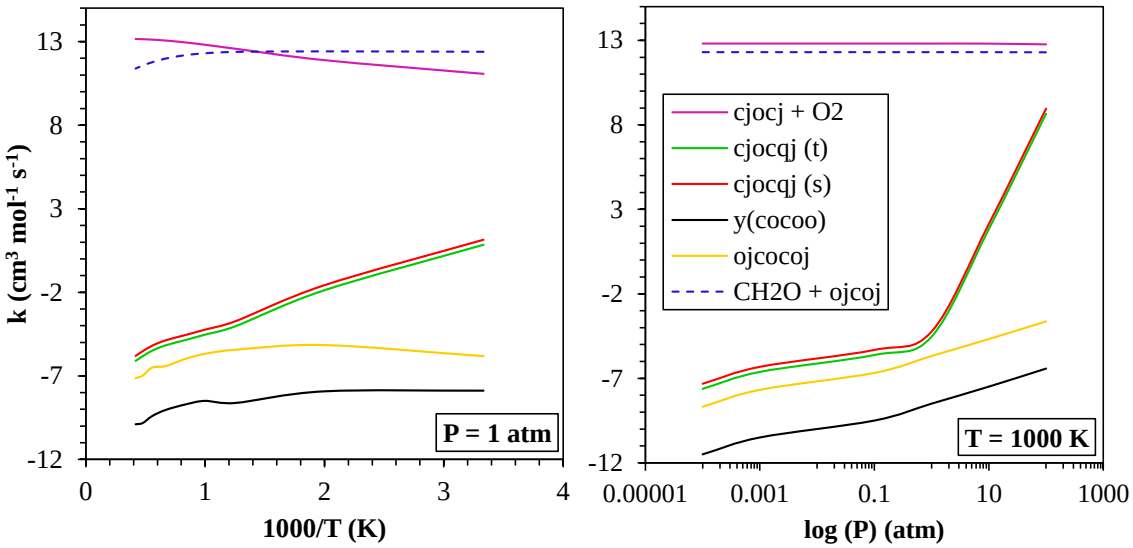

Figure 5.33 Chemical activation plot of rate constants vs. T at 1 atm and vs. P at 1000 K for CH_2˙OCH_2˙+ $^3O_2$. (does not include unimolecular reactions of the diradical). j=radical site

ChemKin modeling, concentration of products versus reaction time, for oxidation and unimolecular dissociation on the ring opened diradical from three members cyclic ether is illustrated in Figure 5.34 for temperatures of 500 and 1200 K.

At both temperatures, results indicate that the formation of formaldehyde and $HCO_2^{\bullet}$, through a C–H rupture for hydrogen elimination. At lower temperatures, the ring closure resulting on y(CH_2OO) has some importance, but this di-oxirane ring is unstable and dissociates to $HCO_2^{\bullet}$ with only a 28 kcal mol^{-1} barrier. The dioxirane is not important at higher temperatures. The unimolecular β-scission of the diradical takes some importance at higher temperatures, resulting on the formation of a formaldehyde and the singlet diradical $^1CH_2$.

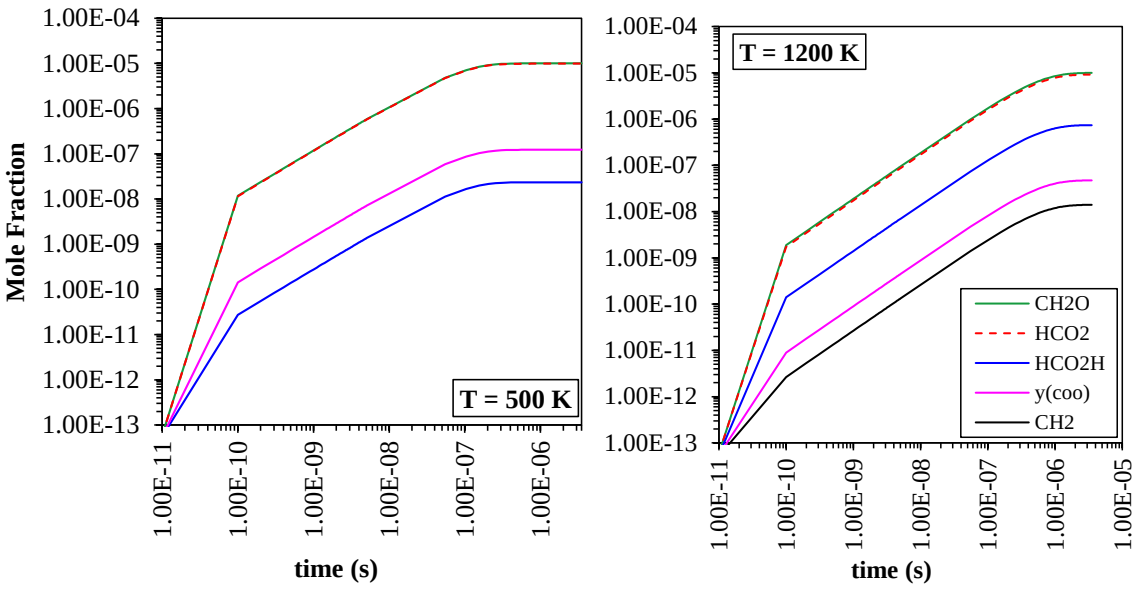

Figure 5.34 ChemKin modeling of unimolecular and oxidation reactions of $CH_2^{\bullet}OCH_2^{\bullet}$ at 1 atm (CH_2O and $HCO_2^{\bullet}$ are dominant and overlap at both temperatures)

Figures 5.35 and 5.36 represent the unimeolcuar dissociation of the four membered cyclic ether ring opened diradical, and the chemical activation of the diradical with molecular oxygen, respectively.

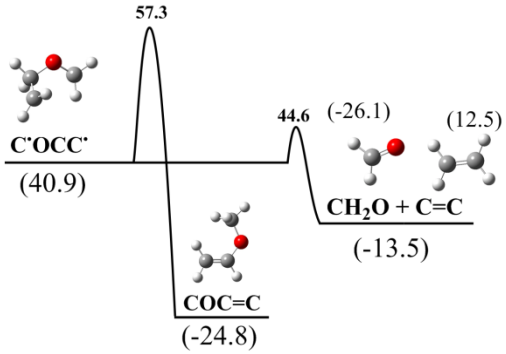

Figure 5.35 Potential energy diagram of diradical dissociation and intramolecular H transfer of CH_2˙OCH_2CH_2˙. All values are at 298 K. Units kcal mol^{-1}

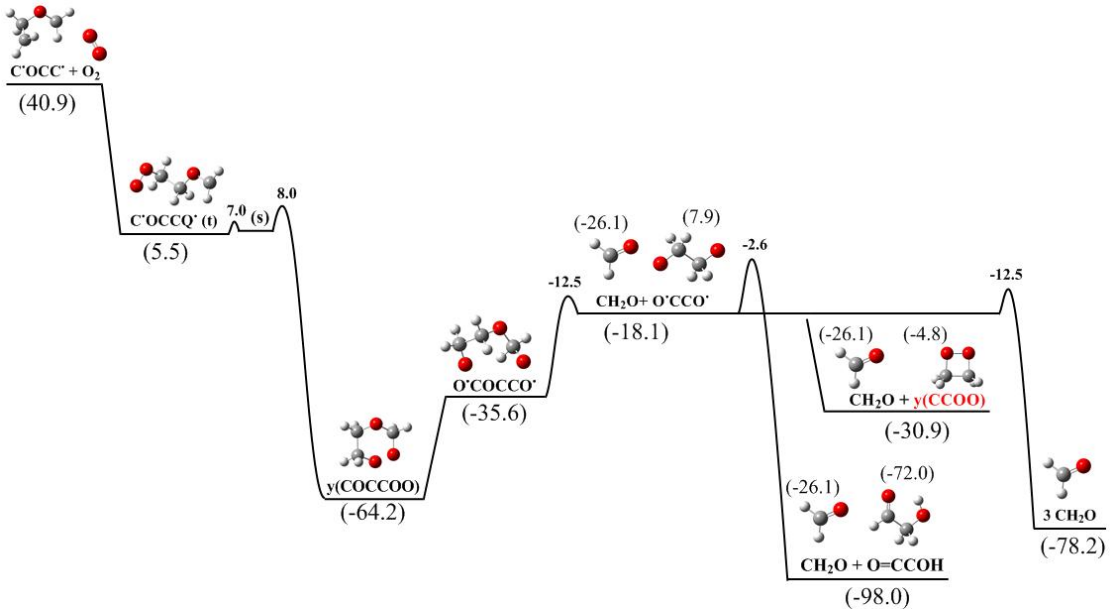

Figure 5.36 y($CH_2CH_2CH_2O$) ring opening CH_2˙OCH_2CH_2˙ ring opened + $^3O_2$ potential energy diagram. All values are at 298 K. Units kcal mol^{-1}

Figure 5.37 illustrates the chemical activation results of the ring opened diradical from the four membered cyclic ether with $^3O_2$. The most important oxidation channel is formation of the peroxy adduct and its dissociation to a formaldehyde + $O^{\bullet}CH_2CH_2O^{\bullet}$.

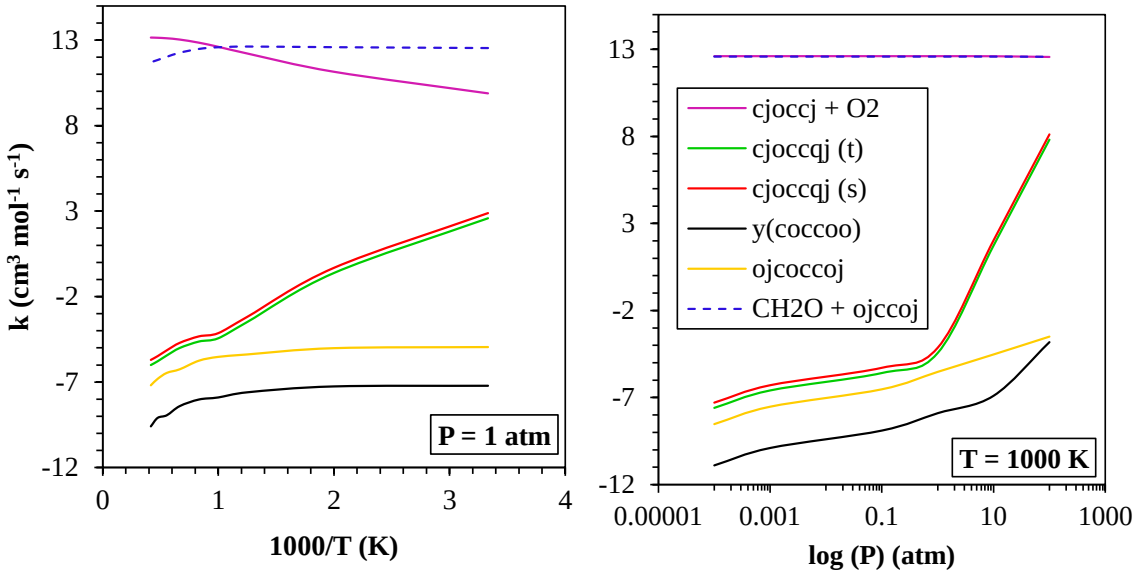

Figure 5.37 Chemical activation plot of rate constants vs. T at 1 atm and vs. P at 1000 K for $CH_2^{\bullet}OCH_2CH_2^{\bullet}$ + $^3O_2$. (does not include unimolecular reactions of the diradical). j=radical site

ChemKin modeling of concentration versus reaction time, for oxidation and unimolecular dissociation on the ring opened diradical from four membered cyclic ether is illustrated in Figure 5.38 for temperatures of 500 K and 1200 K.

At all temperatures the unimolecular dissociation via β-scissions for the formation of a formaldehyde plus ethylene is the most important reaction path. At lower temperatures the ring closure of the stabilized intermediate $O^{\bullet}CH_2CH_2O^{\bullet}$ resultant from the chemical activation has some importance, although it is negligible at higher temperatures. The unimolecular intramolecular hydrogen transfer for the formation of

$CH_3OCH=CH_2$ has some importance at both temperatures, whereas the intramolecular hydrogen transfer of the intermediare diradical $O\cdot CH_2CH_2O\cdot$ for the formation of $O=CHCH_2OH$ is not important.

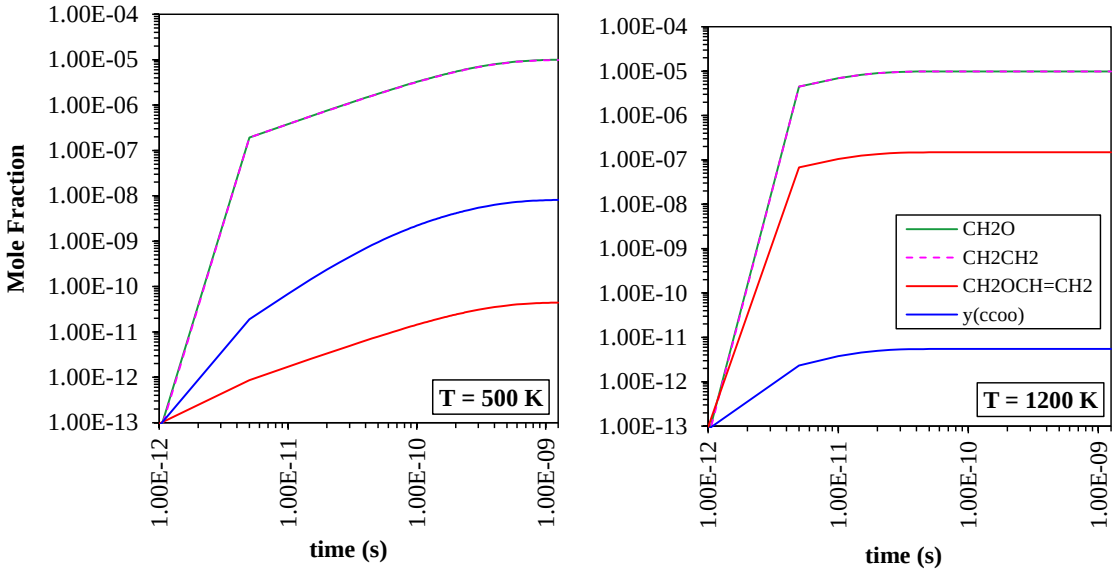

Figure 5.38 ChemKin modeling of unimolecular and oxidation reactions of $CH_2\dot{O}CH_2CH_2\dot{}$ at 1 atm. At both temperatures CH_2O and CH_2CH_2 are dominant and overlap

In the case of the ring opening of the five membered cyclic ether, two different diradicals can be formed depending on the C—C bond that is opened, as indicated in Figure 5.39. Cleavage of the carbon—carbon bond adjacent to the ether link is 3.5 kcal mol^{-1} lower in energy (weaker) and is favored.

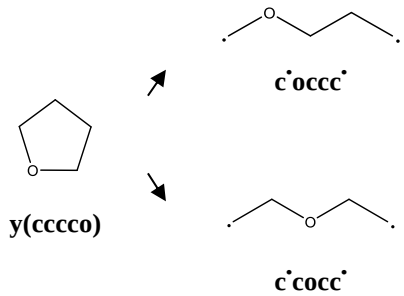

Figure 5.39 Ring opening of $y(CH_2CH_2CH_2CH_2O)$ to two different diradicals, $CH_2\dot{O}CH_2CH_2CH_2\dot{}$ and $CH_2\dot{C}H_2OCH_2CH_2\dot{}$

The dissociation of these two diradicals formed from the ring opening of the five membered ether (tetrahydrofuran) are illustrated in Figure 5.40.

Intramolecular H transfer can result in two products: $CH_3OCH_2CH{=}CH_2$ and $CH_3CH_2OCH{=}CH_2$. For the diradical, subsequent β-scission reactions will result in the formation of ethylene, CH_2O and $^1CH_2$ in both cases; alternately a first β-scission reaction followed by the ring-closure results in formation of cyclopropane or in a three member cyclic ether depending on the first β-scission path.

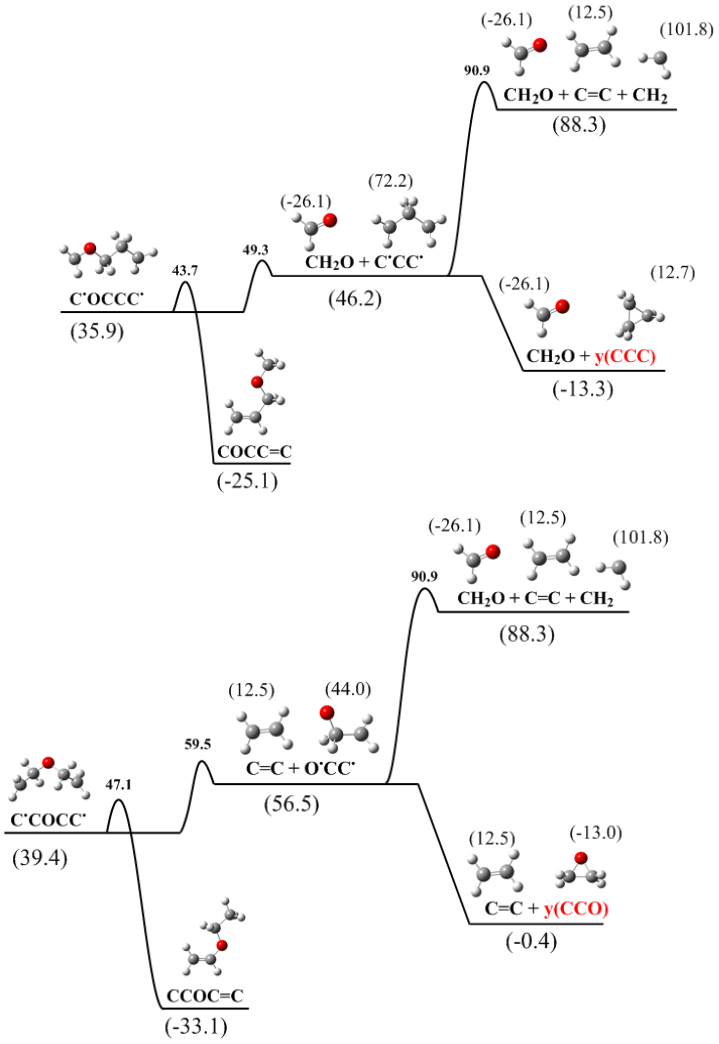

Figure 5.40 Potential energy diagram of diradical dissociation and intramolecular H transfer of $CH_2^{\bullet}OCH_2CH_2CH_2^{\bullet}$ and $CH_2^{\bullet}CH_2OCH_2CH_2^{\bullet}$. All values are at 298 K. Units kcal mol^{-1}

Figure 5.41 represents the chemical activation of $CH_2^{\bullet}OCH_2CH_2CH_2^{\bullet}$ and $CH_2^{\bullet}CH_2OCH_2CH_2^{\bullet}$ with molecular oxygen, following the reaction path presented for the ether systems presented above.

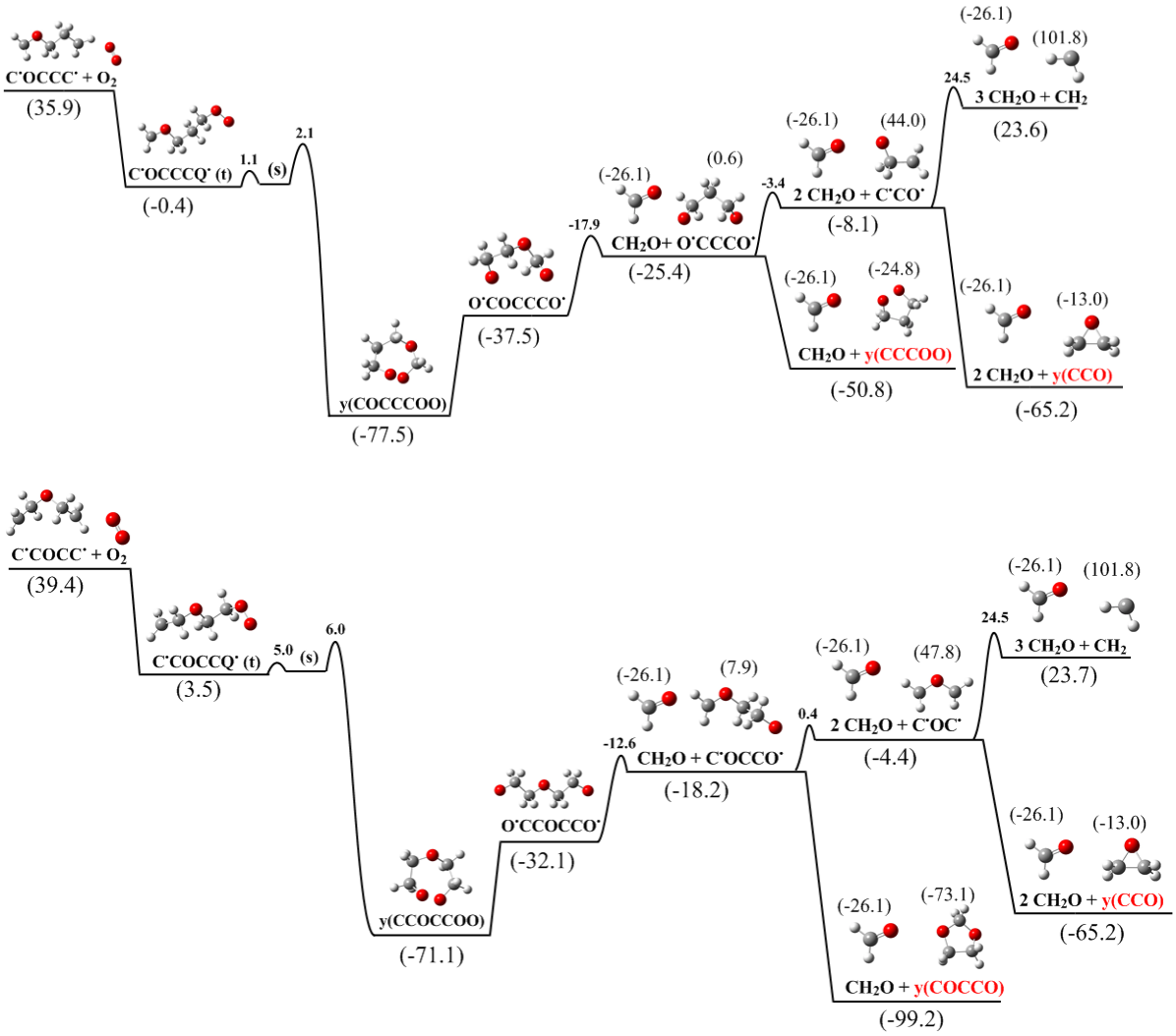

Figure 5.41 y($CH_2CH_2CH_2CH_2O$) ring opening $CH_2^{\bullet}OCH_2CH_2CH_2^{\bullet}$ and $CH_2^{\bullet}CH_2OCH_2CH_2^{\bullet}$ ring opened + $^3O_2$ potential energy diagram. All values are at 298 K. Units kcal mol^{-1}

Figures 5.42 and 5.43 show the chemical activation results of the ring opened diradical from the five membered cyclic ether with $^3O_2$. The most important oxidation

channel is formation of the peroxy adduct and its dissociation to a formaldehyde + $O^{\bullet}CH_2CH_2CH_2O^{\bullet}$ (first case), and formaldehyde + $CH_2^{\bullet}OCH_2CH_2O^{\bullet}$ (second case).

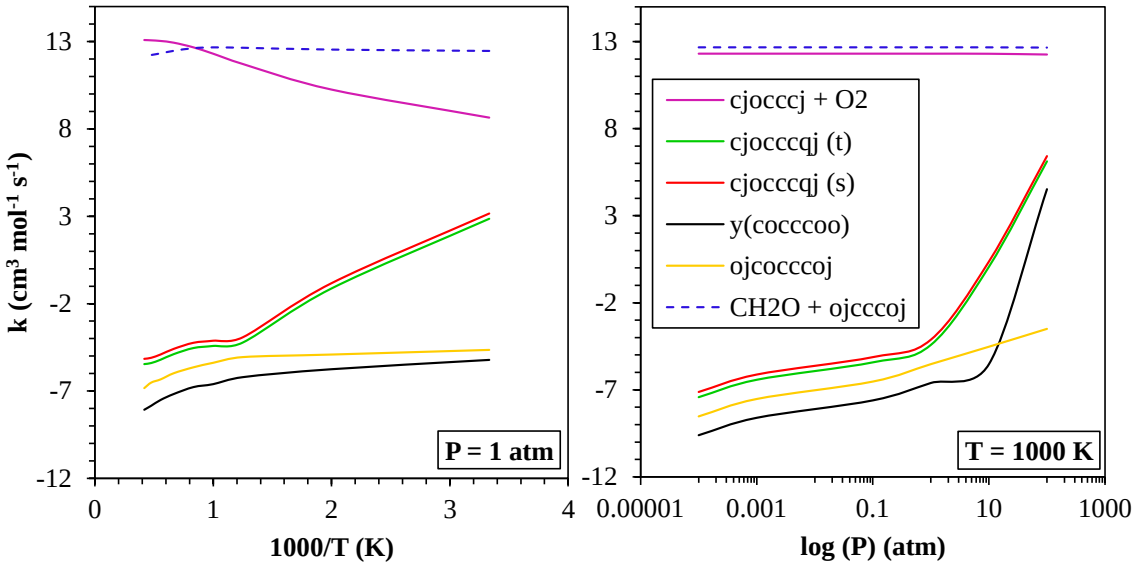

Figure 5.42 Chemical activation plot of rate constants vs. T at 1 atm and vs. P at 1000 K for $CH_2^{\bullet}OCH_2CH_2CH_2^{\bullet}$ + $^3O_2$ (does not include unimolecular reactions of the diradical). j=radical site

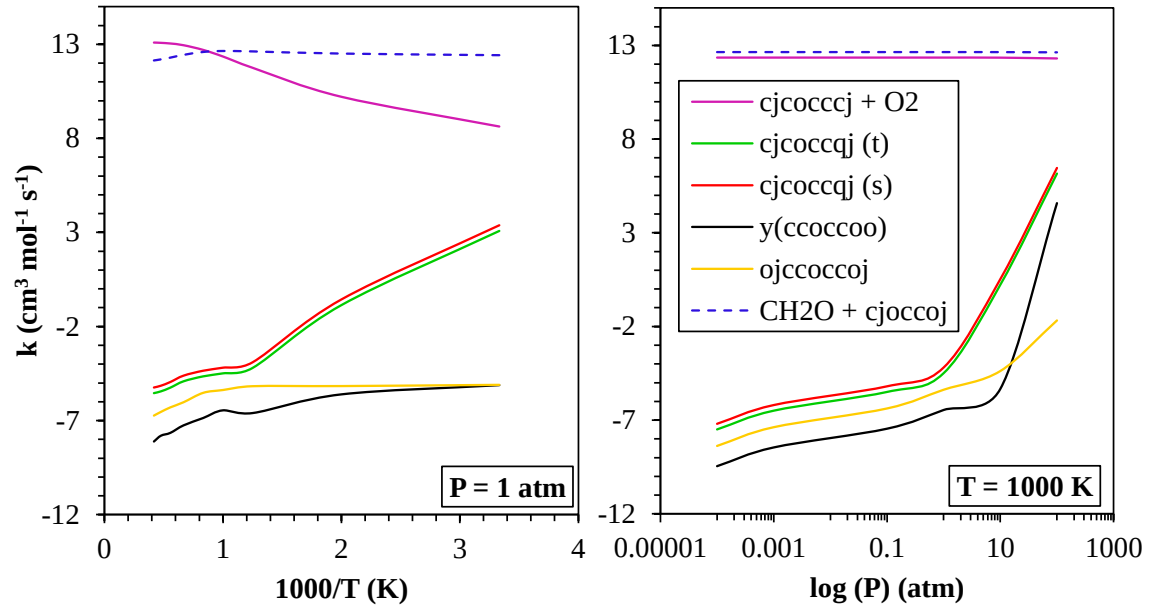

Figure 5.43 Chemical activation plot of rate constants vs. T at 1 atm and vs. P at 1000 K for $CH_2^{\bullet}CH_2OCH_2CH_2^{\bullet}$ + $^3O_2$ (does not include unimolecular reactions of the diradical). j=radical site

ChemKin modeling of concentration versus reaction time, for oxidation and unimolecular dissociation and unimolecular reactions of the ring opened diradical from the five membered cyclic ether is illustrated in Figures 5.44 and 5.45 for temperatures of 500 K and 1200 K.

The formation of $CH_3OCH_2CH=CH_2$ through the unimolecular intramolecular H transfer is the dominant reaction path at both temperatures for the first case. At 500 K, the reaction to formaldehyde and ring closure to form y($CH_2CH_2CH_2OO$) resultant from the chemical activation of the diradical wth molecular oxygen is the second most important reaction path. However, at 1200 K the ring closure resultant from the unimolecular dissociation of the diradical to form two formaldehyde plus cyclopropane becomes the dominant path.

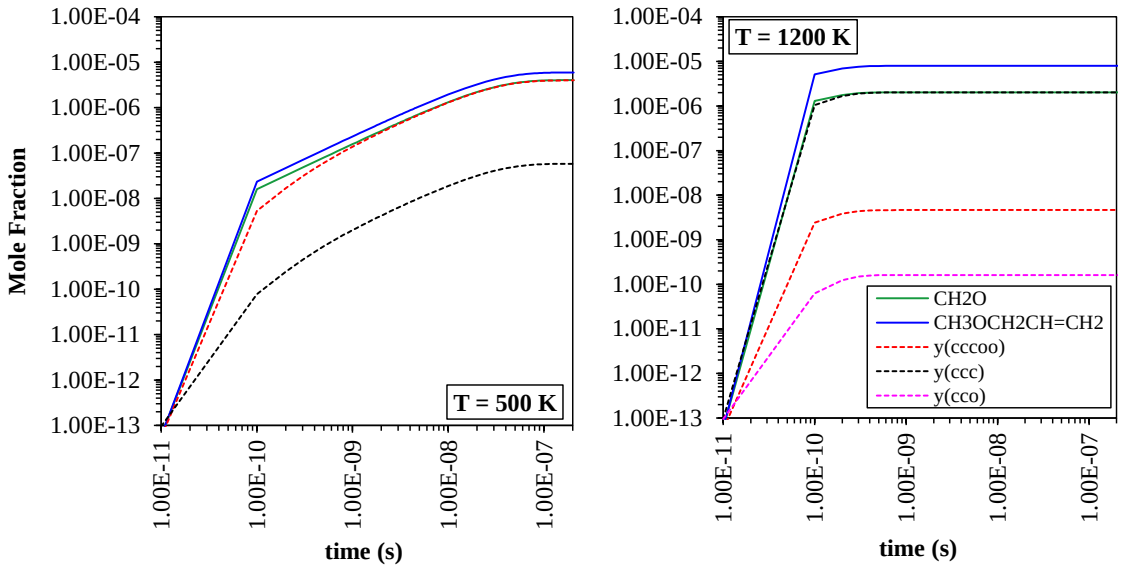

Figure 5.44 ChemKin modeling of unimolecular and oxidation reactions of $CH_2\dot{O}CH_2CH_2CH_2\dot{}$ at 1 atm. At 500 K $CH_2OCH_2CH=CH_2$, CH_2O and y($CH_2CH_2CH_2OO$) are dominant and overlap. At 1200 K CH_2O and y($CH_2CH_2CH_2$) overlap

At both temperatures, the intramolecular H transfer resulting on the formation of $CH_3CH_2OCH{=}CH_2$ is the dominant reaction path for the second case. At low temperatures, the reaction path for the formation of formaldehyde and ring closure to form y($CH_2OCH_2CH_2O$) resultant from the chemical activation of the diradical wth molecular oxygen is the second most important reaction path. However, at higher temperatures the ring closure resultant from the unimolecular dissociation of the diradical to form formaldehyde plus the three memebered cyclic ether becomes the dominant reaction path.

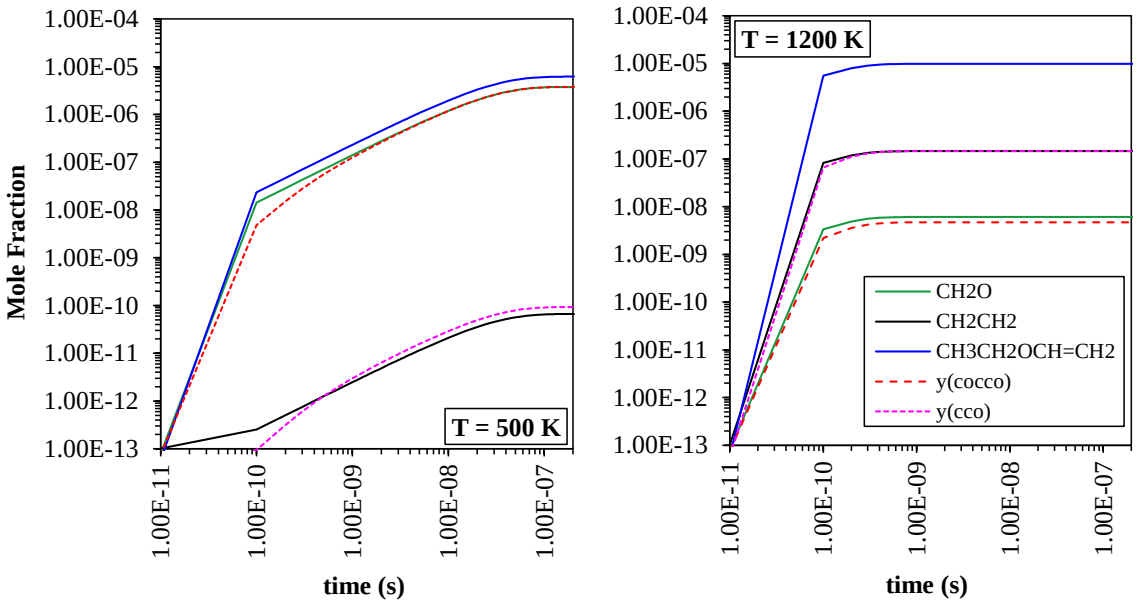

Figure 5.45 ChemKin modeling of unimolecular and oxidation reactions of $CH_2{\cdot}CH_2OCH_2CH_2{\cdot}$ at 1 atm. At 500 K $CH_3CH_2OCH{=}CH_2$, CH_2O and y($CH_2OCH_2CH_2O$) are dominant and overlap. At 1200 K CH_2CH_2 and y(CH_2CH_2O) overlap

Appendix Y contains the thermochemical properties of the cyclic alkane and ether systems studied. Appendix Z summarizes the mechanisms used for the study of the

importance of the unimolecular dissociation and oxidation reactions of the ring opened 3 to 5 cyclic alkanes and ethers.

5.5 Summary

Thermochemical properties, enthalpies of formation, entropy, S°(T) and heat capacity, $C°_p(T)$, values, bond dissociation enthalpies and $R^{\bullet} + {}^3O_2$ well-depths are presented for the 3 to 5 cyclic alkanes and ethers, their corresponding alkyl radicals, peroxy radicals, and hydroperoxyalkyl radicals.

Additionally, the thermochemical properties for ring opening, unimolecular dissociations and oxidation reactions of parent and intermediate radicals for C_3 - C_5 cyclic alkanes, C_2 to C_4 cyclic ethers were calculated. Kinetics for unimolecular dissociation, oxidation and intramolecular H atom transfer are assembled and implemented in detailed mechanisms to evaluate importance of unimolecular dissociation versus oxidation of the radicals. Kinetics include ${}^3O_2$ association with the initially formed diradicals, spin state change estimated by collision or chemical activation, with ring closure of the alkyl - peroxy diradical and subsequent cleavage of the weak RO–OR' peroxy bond amplifying the exothermicity (chemical activation energy) of the peroxy bond formation.

C—H bond dissociation enthalpies on cyclic ethers on non-ether carbon sites are 1.3-1.8 kcal mol^{-1} higher than the C—H bond dissociation enthalpies for cyclic alkanes, which implies that non-ether carbon sites in cyclic ethers are more stable, and therefore less reactive than the carbon sites in cyclic alkanes. The presence of the peroxy group (when bonded both in the ether carbon and non-ether carbons) in the ring increases the

C—H bond dissociation enthalpies, making the carbons in non-ether positions more stable. The presence of the peroxy group bonded to the ether carbon in the ring increases the C—H bond dissociation enthalpies, making the carbons in the ether positions more stable. However, the presence of the peroxy group bonded to the non-ether carbon in the ring decreases the C—H bond dissociation enthalpies, making the carbons in the ether positions more reactive. In all cases, the C—H bond dissociation enthalpies decrease with increasing number of carbons in the ring, and for 5 member rings, the bonds are similar to linear alkanes and ethers.

The presence of the ether oxygen in the ring stabilizes the cyclic hydroperoxides (OO—H bonds get stronger), especially when the peroxy group is bonded to the ether carbon. The hydroperoxides with the OOH group bonded to the ether carbon are more stable than the hydroperoxides with the OOH bonded to the non-ether carbon, and to the cyclic alkane hydroperoxides. The O—H bonds for cyclic alkanes are only ~0.5 kcal mol^{-1} lower compared to the bonds in the cyclic ethers, with the alcohol group bonded to the non-ether carbon, so they have similar reactivity. The well-depths $R^{\bullet} + {}^{3}O_2$ are lower for cyclic ethers than for cyclic alkanes, and decrease with decreasing ring strain for both cyclic alkanes and ethers.

The results of the kinetics for the 3 to 5 cyclic alkane and ether systems show that unimolecular-low energy β-scission reactions and intramolecular H abstraction reactions are important at all temperatures and dominate at high temperatures, bi-molecular oxidation reactions have some importance at lower to moderate temperatures (up to 1000 K), and cyclization reactions to smaller ring intermediates are important at low to moderate temperatures, low energy unimolecular reactions are the dominant paths, when

they are available, when association reaction with $^3O_2$ occurs, reactions show near complete conversion to oxidized products with competition from reaction back to $^3O_2$ + radical at higher temperatures. This reverse reaction allows the diradical to reform, then further react via all channels open to it, the addition of $^3O_2$ to the diradicals, at higher pressures results in stabilization of intermediates (e.g. $CH_2^{\bullet}CH_2CH_2CH_2OO^{\bullet}$, y($CH_2CH_2CH_2CH_2OO$), $O^{\bullet}CH_2CH_2CH_2CH_2O^{\bullet}$ for the alkane diradicals and $CH_2^{\bullet}OCH_2CH_2OO^{\bullet}$, y($CH_2OCH_2CH_2OO$), $O^{\bullet}CH_2OCH_2CH_2O^{\bullet}$ for the diradical from cyclic ethers). Intermediates react to lower energy products CH_2O and $CH_2=CH_2$ for the alkane systems and to CH_2O and unsaturated oxygenated alkenes (e.g. $CH_3CH_2OCH=CH_2$) from the cyclic ethers.

CHAPTER 6

OXIDATION OF MERCURY BY HALOGENS (Cl, Br, I) AT ATMOSPHERIC CONDITIONS

6.1 Overview

The adverse effects of mercury in the environment have been known for years; however, it has only been in recent years that regulation of mercury has been significantly implemented. In March 2005 US EPA regulated mercury emissions from coal-fired power plants, when issuing the Clean Air Mercury Rule (CAMR), which created the first performance standards and established permanent, declining caps in mercury emissions. On December 21, 2011, EPA announced standards to limit mercury emissions from electricity generating plans[174]. In January 2013, 140 nations adopted the first legally binding international treaty to set enforceable limits on emissions of mercury, and exclude, phase out or restrict some products that contain mercury.

Although mercury is present in coal and municipal solid wastes in only minute amounts, on the order of 0.1 ppm_w[46], 458.6 tons of mercury are emitted worldwide each year from power generating plants, 63.1 tons being emitted in North America and 241.1 tons in Asia and Oceania as of 2009[47]. Mercury is among the most highly bio-concentrated trace metals in the human food chain[50]. Once mercury is deposited on land or into water, it is transformed by micro-organisms into methyl-mercury ($[CH_3Hg]^+$) and dimethyl-mercury ($Hg(CH_3)_2$), an organic form of mercury, which is a potent neurotoxin[48,49]. Elemental mercury, $Hg^o(g)$, is also observed to decrease along with the early spring ozone hole events in the Antarctic and Arctic areas, and its chemistry may

likely be related to reactions with halogens and halogen oxides, e.g. chlorine atoms and ClO_x radicals[51,52].

There are several early experimental studies focused on the halogenation chemistry of mercury under ambient or near ambient conditions. In 1936 Richard A. Ogg et al.[175] performed experiments at 1 atm and 383 K to study the oxidation reactions between Hg and Br_2. They used a dish of liquid Hg under a fluorescent screen, on which the ascending Hg vapor was detected as a dark shadow. In order to demonstrate the oxidation of the mercury by the halogens, they introduced a small dish of liquid bromine above the mercury, which resulted in the disappearance of the shadow in the screen interpreted as reaction of Hg with Br_2. They proposed two different mechanisms. The first one involving the reactions:

$$Hg + Br_2 \rightarrow HgBr + Br \quad (6.1)$$

$$HgBr + Br_2 \rightarrow HgBr_2 + Br \quad (6.2)$$

The second mechanism involved only an association:

$$Hg + Br_2 \rightarrow HgBr_2 \quad (6.3)$$

Ogg et al. concluded that the mechanism involving reactions (6.1) and (6.2) play no appreciable role, and that the observed mercury-bromine reaction is due to the association (insertion) reaction (6.3). They provided upper and lower limits for the velocity constant 10^7 cm^3 mol^{-1} s^{-1} and $l0^5$ cm^3 mol^{-1} sec^{-1}, respectively. They assumed that the reaction occurs only on collision with a third body, concluding a rate constant of 4×10^{10} cm^6 mol^{-2} s^{-1}.

In 1949 P'Yankov et al.[176] published experimental results studying the reaction of Hg and Cl_2 at 1 atm, using a gas flow reactor. Gaseous chlorine was flowed over a pool

of liquid mercury, with Cl/Hg ratios ranging from 2 to 16. Analysis of solids formed versus mercury vapor in products were performed downstream separately. P'Yankov reported the reaction was too fast to measure and that the ratio Cl/Hg in the solid product was less than stoichiometric. He concluded that the main product was Hg_2Cl_2, but that the $HgCl_2$ concentration increased slowly when increasing the Hg/Cl ratio (with ratios of $HgCl_2$ to total product of 7.3 at reacting Cl/Hg ratio of 2).

Menke et al.[177] presented experimental results, where mercury vapor was generated by bubbling dry air through mercury, and chlorine gas was introduced from a chlorine cylinder. Both flows were combined in a quartz mixing tube under flow conditions. The resulting gases of the reaction between the mercury and chlorine flowed through a UV flameless atomic absorption mercury vapor analyzer and then to an impinger with a scrubbing solution of $KMnO_4$ and H_2SO_4. They reported that even at low (0.5 ppm Cl_2) chlorine concentrations, the chlorine and mercury vapor react to form significant quantities of a reaction product. They suggested the product may be $HgCl_2$.

Hall et al.[178] published experimental results for total mercury plus elemental concentrations obtained as products from a small-scale propane-fired flue gas generator. Hg oxidation was studied with and without Cl_2 present. Vaporized elemental mercury was added to the propane flame at a concentration of 150 μg m^{-3} and with 8% excess of oxygen, studying the percentage of mercury oxidized after 0.8 seconds in the furnace and the duct (T>773 K) with and without adding chlorine to the reaction system. Hall et al. did not report any rate constants. The reactions proposed were:

$$Hg(g) + ½\ O_2(g) \leftrightarrow HgO(g) \quad (6.4)$$

$$HgO(g) \leftrightarrow HgO(s) \quad (6.5)$$

$HgO\ (g,s) + 2HCl(g) \leftrightarrow HgCl_2\ (g) + H_2O(g)$ (6.6)

$2HCl(g) + ½\ O_2(g) \leftrightarrow Cl_2(g) + H_2O(g)$ (6.7)

$Hg(g) + Cl_2(g) \leftrightarrow HgCl_2(g)$ (6.8)

$2Hg(g) + Cl_2(g) \leftrightarrow Hg_2Cl_2(s)$ (6.9)

$Hg_2Cl_2(s) \leftrightarrow Hg(g) + HgCl_2(g)$ (6.10)

Fontijn et al.[179] published higher temperature experimental data on the rate constants for the reaction between Cd and Cl_2, using an industrial grade quartz reaction tube, under a wide range of Cl_2 concentrations (18-1487 ppm), and pressure (8-80 $x10^{-3}$ atm) and temperature (466-875 K) conditions. They stated that there was no experimental evidence for association or insertion reactions, and that the products of the reaction most likely would be CdCl + Cl. In their conclusions, they report that similar considerations could be used to predict the behavior of the 12 metals, suggesting that the reaction $Hg+Cl_2 \rightarrow HgCl+Cl$ would not proceed at measurable rates under normal combustion conditions, and they do not discuss a direct insertion reaction of Cl_2 in mercury. The findings below are in agreement with Fontijn et. al.

Using Menke et al.'s experimental results[177], Schroeder et al.[180] calculated a rate constant, providing an upper limit of 2.4 $x10^8$ $cm^3mol^{-1}s^{-1}$ (at $[Cl_2(g)]$ = 4.4 and 10.3 mg m^{-3}; R.H. = 13%) for the reaction $Hg+Cl_2$. However, they stated that the variation of the rate constant with chlorine concentration and humidity shows that the actual reaction is not entirely described by $Hg+Cl_2 \rightarrow HgCl_2$.

Experimental data on Hg conversion with chlorine present at concentrations as low as 10 ppm in a flow reactor at 1 atm, where a natural gas flame was used as the source of combustion effluent reactants, was published by Kramlich et al. in 2000[181].

They indicated that the product of the direct reaction could be $HgCl_2$, and provided a rate constant of 3.4 $x10^9$ $cm^3mol^{-1}s^{-1}$, for temperatures between 293 and 973 K, indicating that the conversion was independent of the temperature in the range of temperature indicated. One year later Edwards et al.[182] constructed a reaction mechanism that they simulated with ChemKin[172], to compare model results with experimental data. The Edwards et al. mechanism used Kramlich et al.'s [181] experimental rate constants above with no activation energy for the insertion reaction of mercury in molecular chlorine, k = 3.4 $x10^9$(exp(0.0/RT)) $cm^3mol^{-1}s^{-1}$.

Ariya et al.[183,184] performed experiments to study the oxidation of mercury by chlorine, bromine and iodine, at 1 atm and 298±1 K, in which reactants and products were monitored using three different detection techniques (cold-vapor atomic absorption spectroscopy, mass spectroscopic detection after separation on a gas chromatograph, and direct sampling from the reaction chamber into the mass spectrometer). Reactions of mercury with molecular halogens were studied using 0.5-10 ppm of mercury and 10-50 ppm Cl_2 and Br_2 and 130 ppm I_2. Reaction products (Hg^0, $HgCl_2$, $HgBr_2$, HgI_2) were pre-concentrated and then measured by a direct probe (using a mass spectrometer), by a derivatization (based on the quantitative transformation of $HgCl_2$, $HgBr_2$ and HgI_2 to the more volatile organo-mercury compound n-Bu_2Hg), and by analyzing the butyl-Hg with ICP-MS. They stated that for $Hg+X_2$ (X=Cl,Br,I) reactions, the major products identified were $HgCl_2$, $HgBr_2$, and HgI_2. They reported rate constants for the following reactions:

$Hg + Cl_2 \rightarrow$ Products $(1.6\pm0.2)\ x10^6$ $cm^3\ mol^{-1}\ s^{-1}$

$Hg + Cl \rightarrow$ Products $(6.0\pm0.2)\ x10^{12}$ $cm^3\ mol^{-1}\ s^{-1}$

$Hg + Br_2 \rightarrow$ Products $(5.4\pm0.2)\ x10^7$ $cm^3\ mol^{-1}\ s^{-1}$ (upper limit)

$Hg + Br \rightarrow Products$ $(1.9\pm0.2)\ x10^{12}$ $cm^3\ mol^{-1}\ s^{-1}$

$Hg + I_2 \rightarrow Products$ $(7.6\pm0.58)\ x10^{4}$ $cm^3\ mol^{-1}\ s^{-1}$ (upper limit)

Chang et al. carried out vapor phase experiments[185,186] to study the oxidation of mercury by chlorine and bromine at 297±1 K and 1 atm. They used cold vapor atomic absorption spectrophotometer, absorption spectrometry, a Pyrex reactor and a vacuum system. They used three sizes of reactors with different surface-to-volume ratios (190, 380, and 960 cm^3) to determine the contribution of the surface. They also studied difference in loss of Hg using pulsed vs. continuous source of the absorption (Hg line) for evaluation of photo induced reactions. In 2005 they published[186] a rate constant for the oxidation reaction of mercury by Cl_2, and indicated that the gas-phase reaction of Hg and Cl_2 can be regarded as a three-body reaction ($Hg + Cl_2 + M \rightarrow HgCl_2 + M$). In 2007 they published[185] their experimental calculations for the oxidation of mercury by bromine under atmospheric conditions where the kinetics changed with both surface to volume ratio and with pulsed versus continuous source operation. Their pulsed light source data might be an excitation of the Hg having a significant, acceleration effect on the kinetics.

Yan et al.[187,188] reported experimental data for the oxidation of mercury by chlorine, bromine, iodine, bromine chloride and iodine chloride at 1 atm and 373 K. Starting with an initial concentration of mercury of 0.16 ppm, almost no oxidation of mercury is observed when using 10 ppm of Cl_2. Yan et al. reported a rate constant 1.39 $x10^7$ $cm^3\ mol^{-1}\ s^{-1}$ for reaction of Hg with BrCl, and 3.43 $x10^7$ $cm^3\ mol^{-1}\ s^{-1}$ for reaction of Hg with ICl, but they do not report a numerical rate constant for Cl_2, Br_2 and I_2. However, they do report plots with the oxidation of Hg by Cl_2, Br_2 and I_2 addition (experimental C/C_o versus time). The experimental data (plot) provided by Yan et al. is

extracted for the 10 ppm concentrations of Br_2 and Cl_2, and 5.1 ppm for I_2. Using the experimental data from their plot, the data from Yan et al. was interpreted, and a rate constant was calculated as indicated below.

$$\frac{d[Hg]}{dt} = -k[X_2][Hg] \Rightarrow [X_2] = Cl_2, Br_2, I_2 \tag{6.11}$$

assuming [X] is constant, let $k' = k[X_2]$:

$$\frac{d[Hg]}{dt} = -k'[Hg] \tag{6.12}$$

$$\ln[Hg/Hg_o] = -k't \rightarrow k' = \frac{-\ln[Hg/Hg_o]}{t} \tag{6.13}$$

A numerical value for the rate constant was estimated as 2.62 x10^7 cm^3 mol^{-1} s^{-1}, when using 10 ppm Br_2, with no Cl_2 present. An upper limit rate constant for Cl_2 can be estimated by assuming Yan et al. [187] could observe conversion above 5% for Cl_2 reaction with no Br_2 present. Using the 5 % maximum conversion assumption a rate constant for Hg reaction with Cl_2 at 373 K as less than or equal to 1.67 x10^6 cm^3 mol^{-1} s^{-1} is estimated. A numerical value for the rate constant was estimated as 1.20 x10^8 cm^3 mol^{-1} s^{-1}, when using 5.1 ppm I_2, with no Cl_2 present.

Goodsite et al.[190] studied the oxidation of Hg to $HgBr_2$ under conditions relevant to the troposphere using computational chemistry (at B3LYP/CEP-121G level of theory). They provided rate constants for the reactions Hg+Br→HgBr and HgBr+Br→$HgBr_2$, but they did not report details on Hg association with or insertion to Br_2.

Hg + Br → HgBr k = 6.6 10^{11} (T/298 K)$^{-2.37}$ $cm^3mol^{-1}s^{-1}$ (180-400 K)

HgBr + Br → $HgBr_2$ k = 1.5 10^{14} (T/298 K)$^{-0.57}$ $cm^3mol^{-1}s^{-1}$ (180-400 K)

The manuscript by Goodsite et al.[190] also provided data for the oxidation of mercury with iodine.

$Hg + I \rightarrow HgI$ $\quad k = 2.4\ 10^{11}\ (T/298\ K)^{-2.37}\ cm^3mol^{-1}s^{-1}$ (180-400 K)

In 2005 Peterson et al.[52] carried out high level icMRCI+Q theoretical calculations for the insertion reaction, $Hg+Br_2 \leftrightarrow HgBr_2$, by microcanonical variational transition state theory. They used a multireference configuration interaction calculation with a series of correlation consistent basis sets up to quadruple-ζ quality with subsequent extrapolation to the complete basis set limit. They reported a high value for the activation energy at 27.2 kcal mol^{-1} and a rate constant of 1.65 $x10^{-7}$ $cm^3mol^{-1}s^{-1}$ at 298 K. Peterson et al. reported the following kinetic parameters by quasiclassical trajectory calculations on the potential surfaces for the reactions of mercury and bromine at this temperature:

$HgBr + Br \rightarrow Hg + Br_2$ $\quad k = 2.34\ x10^{13}\ cm^3\ mol^{-1}\ s^{-1}$ (abstraction reaction)[a]

$HgBr + Br \rightarrow HgBr_2$ $\quad k = 1.79\ x10^{13}\ cm^3\ mol^{-1}\ s^{-1}$ (recombination reaction)[a]

$HgBr + Br \rightarrow HgBr + Br$ $\quad k = 2.39\ x10^{13}\ cm^3\ mol^{-1}\ s^{-1}$ (exchange reaction)[a]

$Hg + Br_2 \rightarrow HgBr_2$ $\quad k = 1.65\ x10^{-7}\ cm^3\ mol^{-1}\ s^{-1}$ (insertion reaction)[b (**)]

[a] Calculated by QCT

[b] Calculated by variational transition state

(**) Reported value is 2.74 10^{-31} $cm^3\ mol^{-1}\ s^{-1}$, but we interpret the units as $cm^3molecule^{-1}s^{-1}$. The value has been converted to $cm^3\ mol^{-1}\ s^{-1}$.

That same year, Peterson et al.[191] published on the energetics of I_2, HgI and HgI_2 but no kinetic parameters were reported.

The research group of Wilcox[192], evaluated the reaction kinetics on $Hg+Cl_2$ reacting through a linear Hg—Cl-Cl complex to HgCl + Cl products, using a basis set that employs a relativistic compact effective potential, B3LYP/RCEP60 VDZ of the Stevens et al. group[193] and transition state theory. They calculated a rate constant of

$6.0x10^{13}exp(-43.3$ kcal mol^{-1} /RT) $cm^3mol^{-1}s^{-1}$. In a more recent paper[194], Wilcox et al. studied the reaction between Hg and Br_2 to products HgBr + Br at the same level of theory; they reported a rate constant of 1.15 $x10^{15}$ exp(-30.1/RT) cm^3 mol^{-1} sec^{-1} . These reactions are endothermic by 33 and 29.5 kcal mol^{-1} respectively. They do not report on the insertion reaction, but comment that the direct insertion reaction is not likely to occur because of the high activation energy.

Liu et al.[195], recently discussed different computational methods and basis sets for the study of the reaction mechanism of Hg/O and Hg/Cl interactions; they concluded that QCISD/RCEP28DVZ is the most accurate method. Using this level of theory, they calculated activation energies by thermal energy calibration (including zero-point energy calibration), and evaluated kinetic parameters at temperatures (298 K, 600 K, 1000 K, and 1500 K) by transition state theory. They provided the rate expressions for several reactions involving mercury. For the direct insertion reaction of mercury in molecular chlorine, they estimated an activation energy of 39.49 kcal mol^{-1} and a pre-exponential factor of 1.04 10^{14} $cm^3mol^{-1}s^{-1}$. They indicate use of transition state theory and provide a transition state structure for the insertion reaction; but do not present any other calculation details. This data are compared further below.

The implications of computational studies by the research groups of Peterson[52], Wilcox[192,194] and Liu[195] all infer a sequence of reactions forming the stable HgX_2 (X=Cl, Br, I) that does not involve a direct reaction of Hg + X_2 to form HgX_2. They all suggest a reaction sequence that requires radical halogen species.

$$Hg + X + (M) \rightarrow HgX + (M) \quad (6.14)$$

$$Hg + X_2 \rightarrow HgX + X \quad (6.15)$$

$$HgX + X_2 \rightarrow HgX_2 + X \quad (6.16)$$

It is appropriate to emphasize that the bond energies of Hg—Cl, Hg—Br and Hg—I are very weak (24.9, 13.5 and 8.3 kcal mol^{-1}, respectively, gas phase). These important intermediates are borderline stable at atmospheric conditions and unstable at combustion and incinerator effluent temperatures. The enthalpy of formation and bond energies of each of the species are summarized in Table 6.1.

Table 6.1 Enthalpies of formation and bond dissociation enthalpies at 298 K (gas phase). HgX_2 bond energies are for the HgX—X bond, second Hg—X bond in structure

Species	$\Delta_f H°(298)$	Bond Energy	Ref.
Hg	14.67		77
Cl	28.99		77
Br	26.74		77
I	25.52		77
Cl_2	0.00	57.98	77
Br_2	7.39	46.09	77
I_2	14.92	-36.12	77
HgCl	18.75	24.91	51
HgBr	24.88	16.53	51
HgI	31.90	-8.29	77
$HgCl_2$	-34.96	82.70	51
$HgBr_2$	-20.42	72.62	51
HgI_2	-3.86	-61.28	77

Units: kcal mol^{-1}

The possible reactions between mercury and the halogens are summarized in Table 6.2, each with the corresponding heat of reaction.

Table 6.2 Enthalpies of reaction of the studied Hg/Cl, Hg/Br and Hg/I reactions

Reactions	ΔH_{rxn}		
	Cl	**Br**	**I**
$Hg + X \leftrightarrow HgX$	-24.91	-13.53	-8.29
$HgX + X_2 \leftrightarrow HgX_2 + X$	-24.72	-25.95	-25.16
$Hg + X_2 \leftrightarrow HgX + X$	33.07	29.56	27.83
$HgX + X \leftrightarrow HgX_2$	-82.70	-72.04	-61.28
$Hg + X_2 \leftrightarrow HgX_2$	-49.63	-42.48	-33.45

Units: kcal mol^{-1}

The reactions Hg + X → HgX are exothermic (-24.9, -13.5 and -8.3 kcal mol^{-1}, respectively, for Cl, Br and I), and could occur at atmospheric temperature, but require an initial reaction of halogen atoms. The reactions of Hg with Cl_2, Br_2 and I_2 to the corresponding HgX + X are endothermic (33.1, 29.6 and 27.8 kcal mol^{-1}, respectively, for Cl, Br and I) and will not occur at atmospheric conditions, unless Hg or the halogens are in an excited state. The insertion reactions of Hg with halogen molecules to HgX_2 are exothermic (-49.6, -42.5 and -33.5 kcal mol^{-1}, respectively), but are predicted to have significant barriers (39.5 and 27.2 kcal mol^{-1} for chlorine and bromine, respectively), which preclude HgX_2 formation under atmospheric conditions (see Table 6.3).

Table 6.3 Rate constants from theoretical literature calculations for Hg + X_2, at 298 K

Reactions	**Activation Energy**	**Rate constant**	**Ref.**
$Hg+Cl_2 \leftrightarrow HgCl_2$	39.49	1.13 $x10^{-15}$	[195]
$Hg+Br_2 \leftrightarrow HgBr_2$	27.2	1.65 $x10^{-7}$ (*)	[52]

Units: Ea (kcal mol^{-1}) and rate constant (cm^3 $mol^{-1}s^{-1}$)

(*) Reported value is 2.7 $x10^{-31}$ $cm^3mol^{-1}s^{-1}$, we assume units are $cm^3molecule^{-1}s^{-1}$

Therefore, it is difficult to justify the formation of HgX_2 observed by experimental studies under atmospheric conditions with the current available literature thermochemical and kinetic data. There are three scenarios that could justify the loss of Hg observed experimentally: (i) the conversion of mercury occurs through heterogeneous reactions on the walls of the reactor, (ii) there is a source of halogen atoms in the experiments, (iii) the insertion reaction: Hg + X_2 → HgX_2 is more important than previously predicted. A number of the earlier studies also infer that a direct Hg + X_2 → HgX_2 path may occur[52,192,194,195], but there are uncertainties on the height of the barriers.

In the above atmospheric temperature and pressure lab environments, the presence of atom sources is usually not considered for experiments that did not have such a source. If there would be a source or reaction to form the Cl, Br or I atoms, the reactions Hg + X → HgX could rapidly happen. Once HgCl, HgBr or HgI is formed, it is sufficiently long lived that further reactions with halogen molecules or atoms can form the more stable $HgCl_2$, $HgBr_2$ and HgI_2. The reaction of HgX with halogen atoms to form HgX_2 is exothermic (-82.7, -72.0 and -61.3 kcal mol^{-1} for Cl, Br and I, respectively). The HgX reactions with halogen molecules to form HgX_2 + X are also exothermic (-24.7, -25.9 and -25.2 kcal mol^{-1} for Cl, Br and I systems, respectively). The exothermicity comes from the stronger XHg—X bond relative to the Hg—X bonds.

A detailed reaction mechanism for the description of the atmospheric oxidation of mercury, based on fundamental principles of thermochemistry and statistical mechanics is assembled in this work. The constructed mechanism is used for comparison with the available literature experimental data. Further calculations on the direct insertion reaction ($Hg + X_2 \rightarrow HgX_2$) are performed, since the reactions present some uncertainties. A number of calculation methods and several basis sets are used for comparison.

6.2 Thermochemical Properties

The thermochemical properties, heats of formation, entropies and heat capacities (T) were determined from evaluation of literature data, from the published values by the research groups of Peterson[51,205], Goodsite[190], and Dibble, and from calculations from this study. Enthalpies of atoms are from NIST[77]. Table 6.1 summarizes the heats of formation and bond dissociation enthalpies (at 298 K) of the species used in these reaction systems,

including the literature reference. Table 6.4 provides data on the entropy and heat capacity versus temperature for each of the species.

Table 6.4 Enthalpies of formation and bond dissociation enthalpies at 298 K (gas phase)

Species	$\Delta_f H^o_{298}$	S^o_{298}	Cp(300)	Cp(400)	Cp(500)	Cp(600)	Cp(800)	Cp(1000)	Cp(1500)
Hg	14.67	41.82	4.97	4.97	4.97	4.97	4.97	4.97	4.97
Cl	28.99	39.50	5.32	5.32	5.32	5.32	5.32	5.32	5.32
Br	26.74	41.80	5.08	5.08	5.08	5.08	5.08	5.08	5.08
I	25.52	43.21	4.97	4.97	4.97	4.97	4.97	4.97	5.00
Cl_2	0.00	53.30	8.12	8.37	8.58	8.73	8.88	8.96	9.07
Br_2	7.39	58.65	8.62	8.77	8.86	8.91	8.97	9.01	9.08
I_2	14.92	62.31	8.96	8.96	8.96	8.99	9.06	9.10	9.45
HgCl	18.75	62.14	8.71	8.84	8.93	8.99	9.05	9.10	9.22
HgBr	24.90	64.59	8.84	8.86	8.89	8.90	8.92	8.93	8.94
HgI	31.90	67.10	9.06	9.15	9.22	9.29	9.42	9.54	9.84
$HgCl_2$	-34.96	73.76	13.20	13.49	13.64	13.72	13.80	13.84	13.88
$HgBr_2$	-20.42	74.21	14.79	14.80	14.81	14.82	14.84	14.85	14.88
HgI_2	-3.86	80.36	14.89	14.89	14.89	14.89	14.89	14.89	14.89
tst($HgCl_2$)	59.74	75.38	11.65	11.77	11.82	11.85	11.88	11.90	11.91
tst($HgBr_2$)	61.95	79.80	11.79	11.85	11.87	11.89	11.90	11.91	11.92
tst(HgI_2)	66.96	82.81	11.84	11.87	11.89	11.90	11.91	11.92	11.92

Units: kcal mol^{-1} for $\Delta_f H^o_{298}$ and cal K^{-1} for S^o_{298} and Cp(T)

Transition state structures and energies were calculated, at several levels of theory; the transition state data is used primarily for pre-exponential kinetic factors. Thermochemical properties for the species involved in the direct insertion reaction were obtained using the B3LYP, ωB97X, B2PLYP, M06 and M06-2X levels of theory, and three different basis sets, LANL2DZ, SDD and aug-cc-pVTZ-PP (AVTZ). Single point calculations were performed at the higher level CCSD(T) level, with the use of the aug-cc-pVTZ-PP (AVTZ) basis set.

6.3 Kinetic Properties

Association, insertion and addition reactions have been treated as chemical activation reactions with quantum Rice Ramsperger Kassel analysis for k(E) and Master Equation analysis for fall-off (pressure/temperature dependent stabilization of the energized adduct)[42]. Unimolecular dissociation reactions are also treated with qRRK k(E) / ME analysis. Kinetics of these small molecules (several atom species, example HgCl, $HgCl_2$, etc.) are in the low pressure or fall-off kinetic regions with strong functions of temperature and pressure in the kinetics. Input rate expressions for the qRRK analysis are from work of Peterson[52], Goodsite[190] and Wilcox[192,194] groups and this study.

The chemical activation kinetics for $Hg + X_2 \rightarrow HgX_2$ insertion reactions were estimated from the theoretical calculations in this study. The barriers needed to fit the experimental rate constants are also calculated. Temperature and pressure dependence of the rate constants were calculated with the Chemaster Code[173]. Table 6.5 summarizes the parameters used for the determination of the qRRK k(E) / ME analysis, and the figures with the pressure and temperature dependence of the rate constants. Figures 6.1 to 6.3 represent the temperature and pressure dependence of the studied reactions.

Table 6.5 Parameters used in the determination of the pressure and temperature dependence of rate constants

Parameters		**Hg+Cl_2**	**Hg+Br_2**	**Hg+I_2**
T_{range} (K)		300-2000	300-2000	300-2000
P_{range} (atm)		0.001-10	0.001-10	0.001-10
Bath gas	Species	N_2	N_2	N_2
	σ (A)	3.62	3.62	3.62
	ε /k_B (K)	97.5	97.5	97.5
σ (A)		5.73	5.08	5.08
ε/k_B (K)		733.8	686.2	686.2
ΔE_{down} (cal mol^{-1})		830	830	830
$\Delta E_{average}$ (cal mol^{-1})		300	300	300
Integration interval (kcal)		0.5	0.5	0.5
E_{head} (kcal mol^{-1})		75	75	75

E_{head} = energy above highest barrier to which the calculation determines the fraction of active complex for k(E)
k_B = Boltzman constant
σ = collision diameter
ε = potential well depth

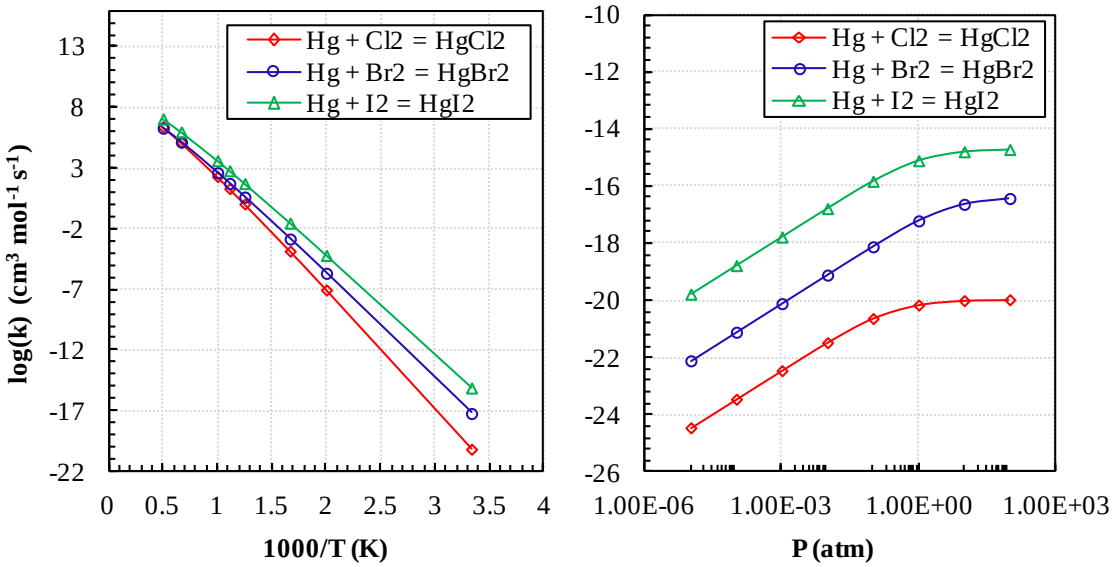

Figure 6.1 log (k) vs. temperature at 1 atm for Hg + X_2 ↔ HgX_2 (left) and log (k) vs. pressure at 300 K for Hg + X_2 ↔ HgX_2 (right)

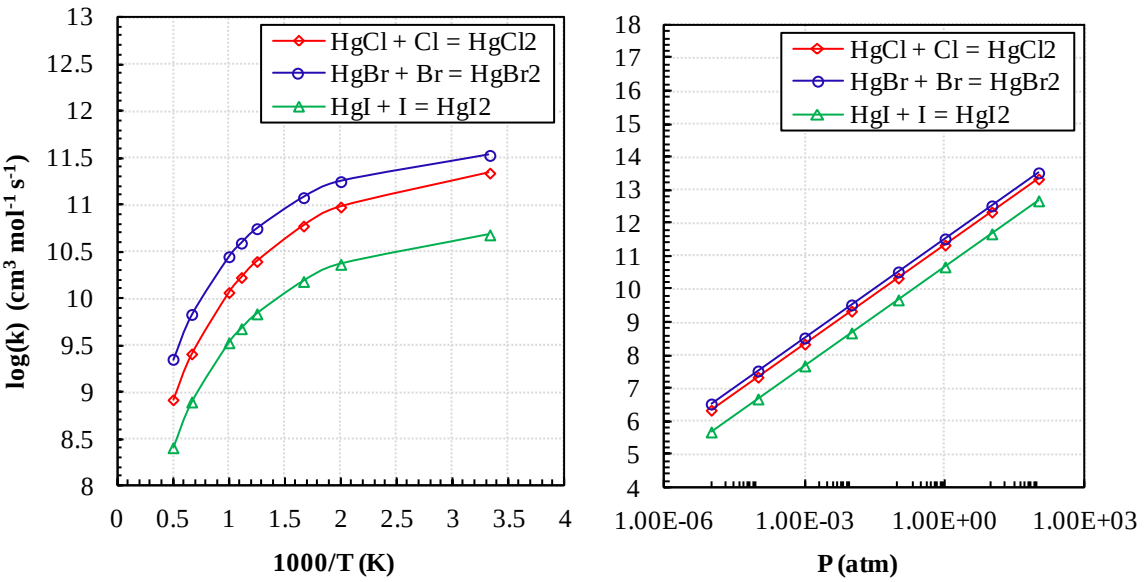

Figure 6.2 log (k) vs. temperature at 1 atm for HgX + X↔ HgX_2 (left) and log (k) vs. pressure at 300 K for HgX + X↔ HgX_2 (right)

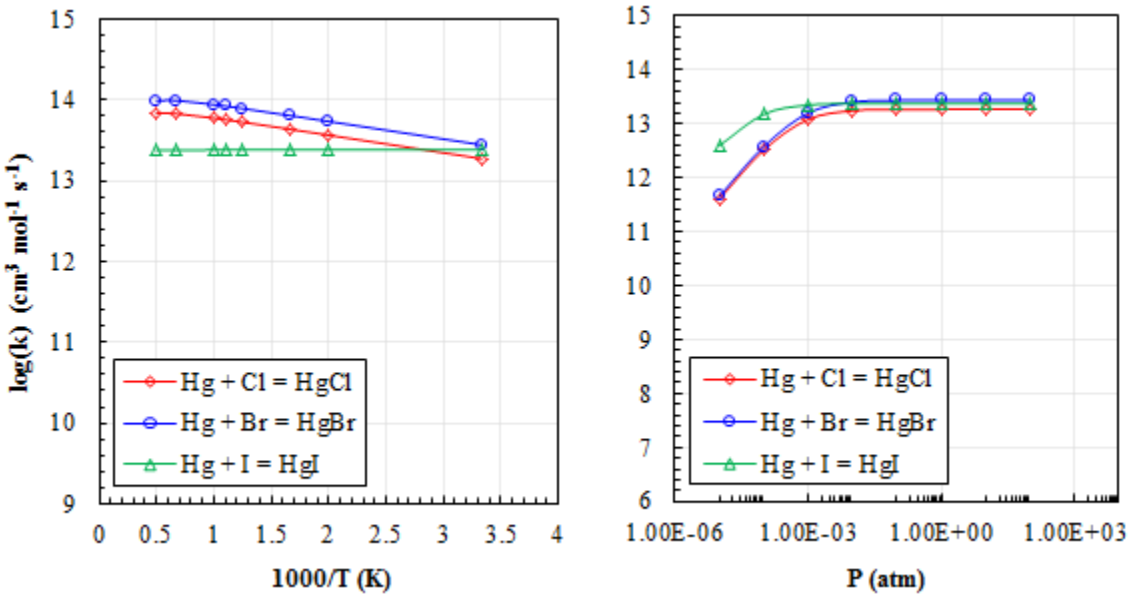

Figure 6.3 log (k) vs. temperature of at 1 atm for Hg + X ↔ HgX (left) and log (k) vs. pressure at 300 K for Hg + X_2 ↔ HgX (right)

The rate constant for the reaction $HgBr_2$ →Hg+Br_2 was calculated by ChemRate[91] in order to check the consistency of the Chemaster calculations. Results show good

agreement between the results obtained by ChemRate and Chemaster. Figure 6.4 shows the comparison. The results obtained for the temperature dependence are in excellent agreement, and the results for the pressure dependence show very good agreement at high pressures, but show a difference of less than an order of magnitude at the lower pressures.

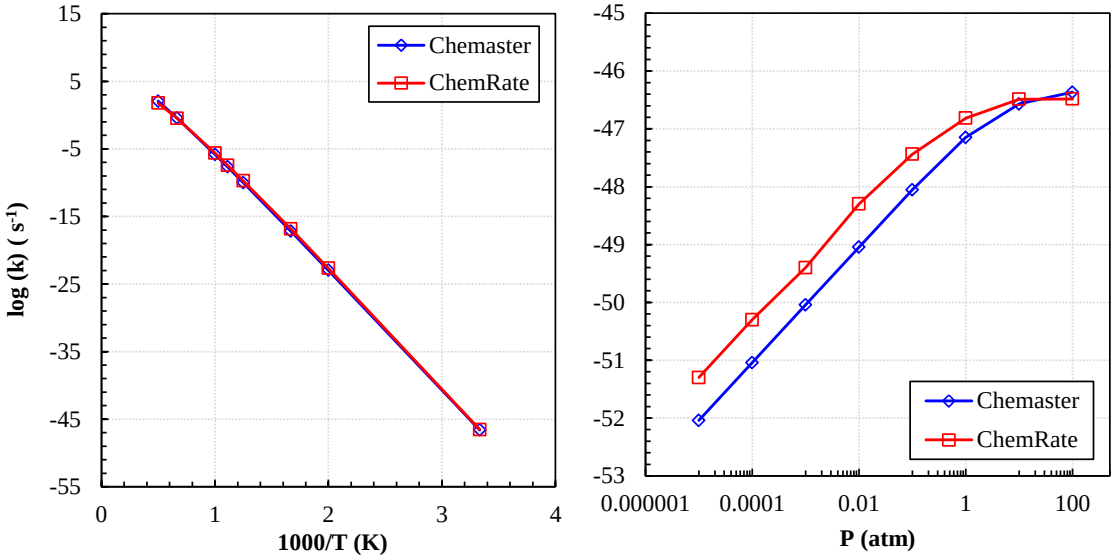

Figure 6.4 Comparison between the results obtained by Chemaster and ChemRate for the rate constant of the reaction $HgBr_2 \rightarrow Hg + Br_2$

6.4 Kinetic Modeling and Results

The reactions accepted for the oxidation of Hg by chlorine, bromine and iodine are (where X = Cl, Br, I):

$Hg + X \rightarrow HgX$	(exothermic by 24.9, 13.5, 8.3 kcal mol^{-1} for Cl, Br, and I, but needs atom source)
$HgX + X \rightarrow HgX_2$	(exothermic by 82.7, 72.0, 61.3 kcal mol^{-1} for Cl, Br and I, but needs atom source)
$HgX + X_2 \rightarrow HgX_2+X$	(exothermic by 24.2, 25.9, 25.2 kcal mol^{-1} for Cl, BR and I, but needs atom source to form HgX)

$Hg + X_2 \rightarrow HgX + X$ (endothermic by 33.1, 29.6, 27.8 kcal mol-1 for Cl, Br and I, plus has a high barrier of 43.3, 30.1, 27.7 kcal mol^{-1} for Cl, Br, I)

In 2002 Ariya et al.[183,184] published tubular flow reactor experimental results for the oxidation of mercury by chlorine, bromine, and iodine at atmospheric conditions (1 atm, 298 K). They followed the loss of mercury for reaction under conditions of different halogen concentrations. Chang et al.[185,186] also published experimental results on the low temperature oxidation of mercury (1 atm, 296 K) by both chlorine and bromine, obtained by measuring the concentration of Hg^o as a function of time in Pyrex flasks by a mercury cold vapor atomic absorption spectrophotometer and a vacuum system for gas handling. Yan et al.[187,188] published experimental results for the oxidation of mercury by chlorine, bromine, iodine, BrCl and ICl at 1 atm and 373 K, by in situ monitoring of the concentration of Hg^o in the reactor (a stainless steel cylinder) as a function of time by a mercury cold vapor atomic adsorption spectrophotometer. These experiments did not have any planned atom sources to initiate the reaction ($X_2 \rightarrow X + X$ is endothermic by 57.9 kcal mol^{-1} for X=Cl, 46.1 kcal mol^{-1} for X=Br, and 36.1 kcal mol^{-1} for X=I, at the low temperatures studied X_2 will not dissociate.). Yet they report loss of Hg and/or HgX_2 formation and with the data observed, they report rate constants for the reaction of Hg with X_2 to form HgX_2.

One possible source for formation of HgX_2 is an insertion reaction (the reaction $Hg + X_2 \rightarrow HgX + X$ is sufficiently endothermic to limit its consideration). Table 6.3 summarizes the theoretically calculated barriers and rate constants reported in the literature for the insertion reaction ($Hg + X_2 \rightarrow HgX_2$, Ea=39.5 and 27.2 kcal mol^{-1} for chlorine and bromine, respectively). Table 6.6, 6.7 and 6.8 present a summary of the

reported experimental data on rate constants for the reactions of mercury with molecular chlorine, bromine and iodine, respectively ($Hg + X_2 \rightarrow HgX_2$).

Table 6.6 Rate constants from experimental conversion of Hg ($Hg + Cl_2$) from the literature

Conditions	Rate constant	Ref.
$Hg + Cl_2 \leftrightarrow HgCl_2$		
----	2.4×10^8	180
293-973 K 1 atm	3.4×10^9	181
298 K 1 atm	$(1.6 \pm 0.2) \times 10^6$	183
297 K 1 atm	$(1.7 \pm 0.2) \times 10^5$	186
373 K 1 atm	1.67×10^6	187

Units: $cm^3\ mol^{-1}\ s^{-1}$

Table 6.7 Rate constants from experimental conversion of Hg ($Hg + Br_2$) from the literature

Conditions	Rate constant	Ref.
$Hg + Br_2 \leftrightarrow HgBr_2$		
383 K 1 atm	4×10^{10}	175
298 K 1 atm	$(5.4 \pm 0.2) \times 10^7$	183
296 K 1 atm	$(3.6 \pm 0.5) \times 10^7$	185
373 K 1 atm	2.62×10^7	187

Units: $cm^3\ mol^{-1}\ s^{-1}$

Table 6.8 Rate constants from experimental conversion of Hg (Hg + I_2) from the literature

Conditions	Rate constant	Ref.
$Hg + I_2 \leftrightarrow HgI_2$		
296±2 K 1 atm	(7.6±0.3) $x10^4$ (upper limit)	184
373 K 1 atm	1.20 $x10^8$	188

Units: $cm^3\ mol^{-1}\ s^{-1}$

Tables 6.9, 6.10 and 6.11 summarize the reactions and rate constants from the literature for the oxidation of mercury by chlorine, bromine and iodine, respectively.

Table 6.9 Elementary rate constants from the literature for reactions of Hg and HgCl with chlorine

Reactions	A	n	Ea	Ref.
$Hg + Cl \leftrightarrow HgCl$	2.4 $x10^8$ 1.95 $x10^{13}$	1.4 0.0	-14400 0	203 182
$HgCl + Cl_2 \leftrightarrow HgCl_2 + Cl$	1.39 $x10^{14}$	0.0	1000	203
$Hg + Cl_2 \leftrightarrow HgCl + Cl$	1.39 $x10^{14}$ 6.15 $x10^{13}$	0.0 0.0	34000 43300	201 192
$HgCl + Cl \leftrightarrow HgCl_2$	2.19 $x10^{18}$ 1.95 $x10^{13}$	0.0 0.0	3100 0	203 182

Units: A ($cm^3\ mol^{-1}\ sec^{-1}$) and Ea ($kcal\ mol^{-1}$)

Table 6.10 Elementary rate constants from the literature for reactions of Hg and HgBr with bromine

Reactions	A	n	Ea	Ref.
$Hg + Br \leftrightarrow HgBr$	6.63 $x10^{11}$ 2.75 $x10^{11}$	0.0 0.0	0 -1620	190 192
$HgBr + Br_2 \leftrightarrow HgBr_2 + Br$	1.11 $x10^{14}$	0	60	198
$Hg + Br_2 \leftrightarrow HgBr + Br$	1.15 $x10^{15}$	0.0	30100	192
$HgBr + Br \leftrightarrow HgBr_2$	1.51 x 10^{14}	0.0	0	190

Units: A ($cm^3\ mol^{-1}\ sec^{-1}$) and Ea ($kcal\ mol^{-1}$)

Table 6.11 Elementary rate constants from the literature for reactions of Hg with iodine

Reactions	A	n	Ea	Ref.
Hg + I ↔ HgI	2.41 x10^{11}	-2.38	0.0	[190]

Units: A (cm^3 mol^{-1} sec^{-1}) and Ea (kcal mol^{-1})

There are only 2 possible reactions between Hg and the molecular halogens: Hg + X_2 → HgX_2 and Hg + X_2 → HgX + X.

The bond dissociation reaction XHg—X, HgX—X and Hg—XX (X=Cl,Br,I) are barrierless (as indicated in Figures 6.5, 6.6 and 6.7), and several rate constants for the reaction Hg + X_2 → HgX + X have been reported in the literature[52,192,194].

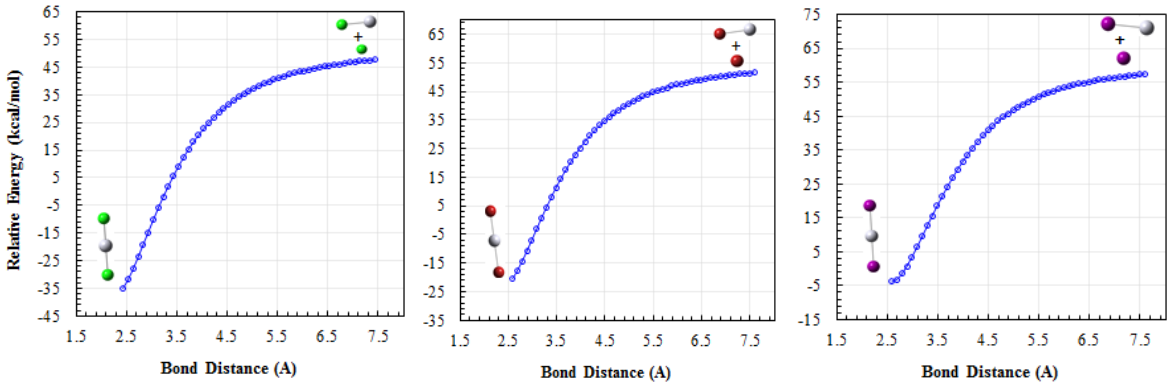

Figure 6.5 Potential energy diagram for the ClHg—Cl (left), BrHg—Br (middle) and IHg—I (right) bonds

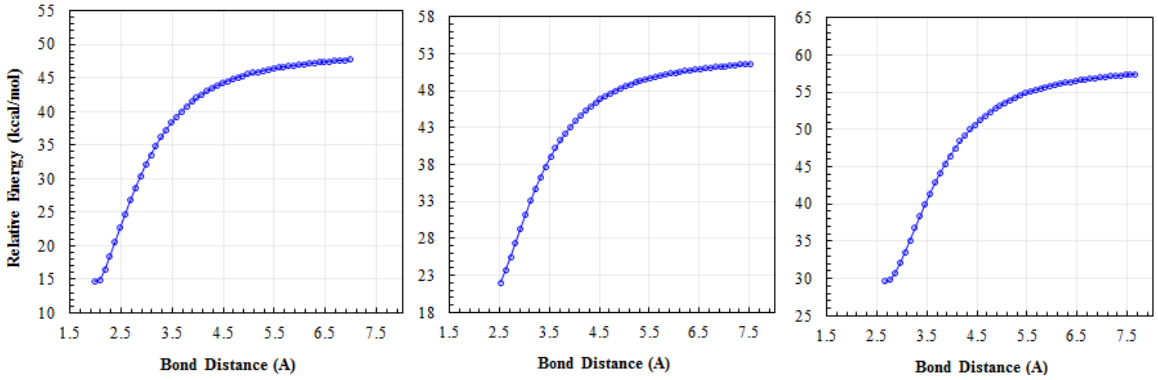

Figure 6.6 Potential energy diagram for the HgCl—Cl (left), HgBr—Br (middle) and HgI—I (right) bonds

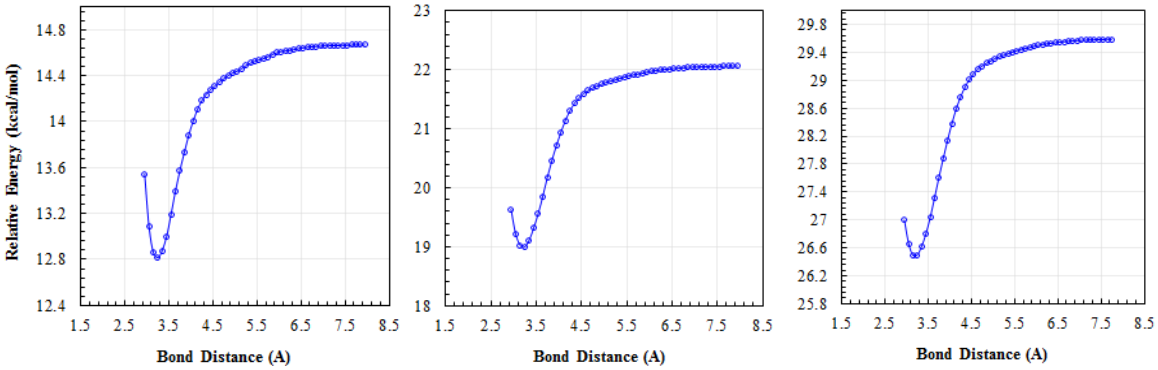

Figure 6.7 Potential energy diagram for the Hg—ClCl (left) and Hg—BrBr (middle) and Hg—II (right) bonds

At atmospheric conditions, the reaction $Hg + X_2 \rightarrow HgX + X$ is not important, and will not result in loss of Hg. Therefore, the only possible reaction at atmospheric conditions is $Hg + X_2 \rightarrow HgX_2$.

The data from the several sets of experiments performed by Ariya et al.[183,184], Chang et al.[185,186] and Yan et al.[187,188] for chlorine bromine and iodine was modeled. The ChemKin code[172] was used to set up and solve the differential equations for the mechanisms. For the modeling, detailed reaction mechanisms were used with reactions that follow thermodynamics and that are fully reversible, where the rate constants were taken from the literature. Tables 6.12, 6.13 and 6.14 present a summary of the literature experimental data used for comparison in this modeling study.

Table 6.12 Rate constants from literature experimental data for $Hg + Cl_2$

Conditions	Rate constants	Ref.
$Hg + Cl_2 \rightarrow$ Products		
1 atm 298±1 K 0.5-10 ppm Hg 10-50 ppm Cl_2	$(1.6\pm0.2) \times 10^{6}$	183
1 atm 296 K 0.16 ppm Hg 242 ppm Cl_2	$(1.7\pm0.2) \times 10^{5}$	186
1 atm 373 K 0.16 ppm Hg 10 ppm Cl_2	1.67×10^{6}	187

Units: $cm^3\ mol^{-1}\ s^{-1}$

Table 6.13 Rate constants from literature experimental data for $Hg + Br_2$

Conditions	Rate constants	Ref.
$Hg + Br_2 \rightarrow$ Products		
1 atm 298±1 K 0.5-10 ppm Hg 10-50 ppm Br_2	$(5.4\pm0.2) \times 10^{7}$ (upper limit)	183
1 atm 297±1 K 0.2 ppm Hg 13 ppm Br_2	$(3.6\pm0.5) \times 10^{7}$	185
1 atm 373 K 0.16 ppm Hg 10 ppm Br_2	2.62×10^{7}	187

Units: $cm^3\ mol^{-1}\ s^{-1}$

Table 6.14 Rate constants from literature experimental data for Hg + I_2

Conditions	Rate constants	Ref.
Hg + I_2 → Products		
1 atm 373 K 0.16 ppm Hg 5.1 ppm I_2	1.20 x10^8	188

Units: cm^3 mol^{-1} s^{-1}

The sub-mechanisms used for comparison with the literature experimental data are summarized in Tables 6.15, 6.16 and 6.17, for chlorine, bromine and iodine, respectively.

Table 6.15 Reactions and rate constants from the literature for the conversion of Hg by chlorine

Reactions	A	n	Ea	Ref.
Cl + Cl ↔ Cl_2	5.79 x10^{14}	0.0	-1600	206
Hg + Cl ↔ HgCl	2.4 x10^8	1.4	-14400	203
HgCl + Cl_2 ↔ $HgCl_2$ + Cl	1.39 x10^{14}	0.0	1000	203
Hg + Cl_2 ↔ HgCl + Cl	6.15 x10^{13}	0.0	43300	192
HgCl + Cl ↔ $HgCl_2$	2.19 x10^{18}	0.0	3100	203

Units: A (cm^3 mol^{-1} sec^{-1}) and Ea (cal mol^{-1})

Table 6.16 Reactions and rate constants from the literature for the conversion of Hg by bromine

Reactions	A	n	Ea	Ref.
Br + Br ↔ Br_2	1.48 x10^{14}	0	-1700	207
Hg + Br ↔ HgBr	2.75 x10^{11}	0.0	-1620	192
HgBr + Br_2 ↔ $HgBr_2$ + Br	1.11 x10^{14}	0	60	198
Hg + Br_2 ↔ HgBr + Br	1.15 x10^{15}	0.0	30100	192
HgBr + Br ↔ $HgBr_2$	1.51 x 10^{14}	0.0	0	190

Units: A (cm^3 mol^{-1} sec^{-1}) and Ea (cal mol^{-1})

Table 6.17 Reactions and rate constants from the literature for the conversion of Hg by iodine

Reactions	A	n	Ea	Ref.
$I + I \leftrightarrow I_2$	2.00×10^{14}	0.0	-1143	207
$Hg + I \leftrightarrow HgI$	1.86×10^{17}	-2.38	0.0	190
$HgI + I_2 \leftrightarrow HgI_2 + I$	1.48×10^{16}	0.0	0.0	(*)
$Hg + I_2 \leftrightarrow Hg I + I$	8.68×10^{18}	0.0	27796	(*)
$HgI + I \leftrightarrow HgI_2$	3.66×10^{10}	0.0	0.0	(*)

Units: A (cm^3 mol^{-1} sec^{-1}) and Ea (cal mol^{-1})
(*) This work

Figures 6.8 to 6.13 represent the comparison between the experimental data and the model results using the available rate constants in the literature.

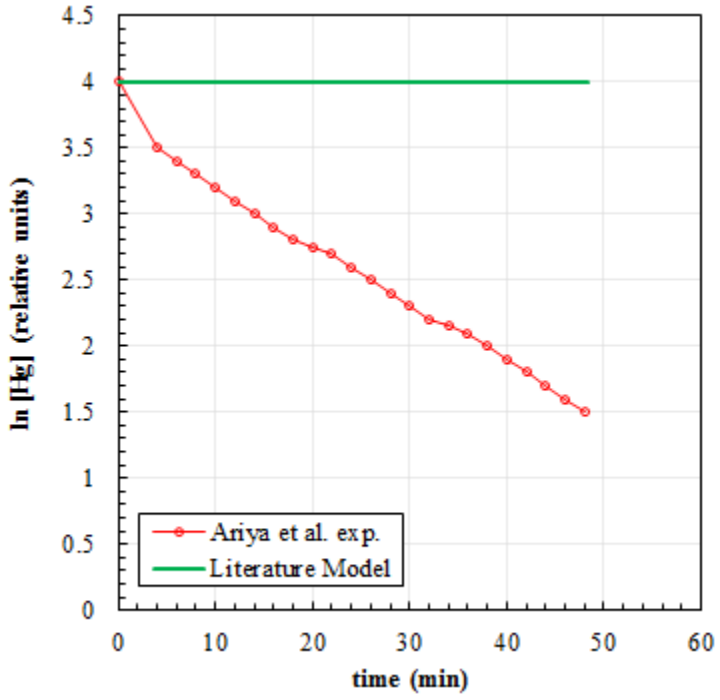

Figure 6.8 Hg loss by reaction with Cl_2; solid green line is kinetics from elementary reaction mechanism from the literature; red circles are Ariya et al.'s[183] experimental data, at 1 atm and 298 K, with initial Hg of 1 ppm and 10 ppm Cl_2

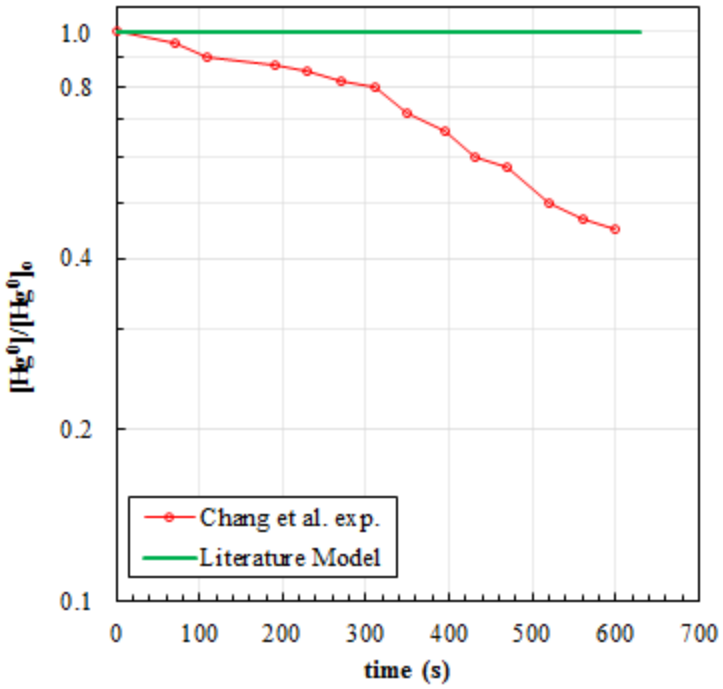

Figure 6.9 Hg loss by reaction with Cl_2; solid green line is kinetics from elementary reactions from the literature; red circles are Chang et al.'s[186] experimental data, at 1 atm and 296 K, with initial Hg of 0.2 ppm and 242 ppm Cl_2.

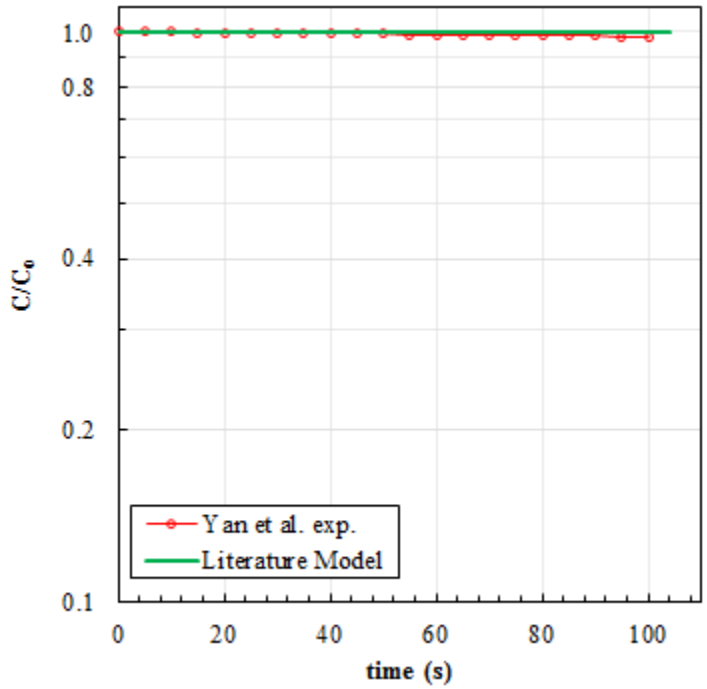

Figure 6.10 Hg loss by reaction with Cl_2; solid green line is kinetics from elementary reactions from the literature; red circles are Yan et al.'s[187] experimental data, at 1 atm and 373 K, with initial Hg of 0.16 ppm and 10 ppm Cl_2.

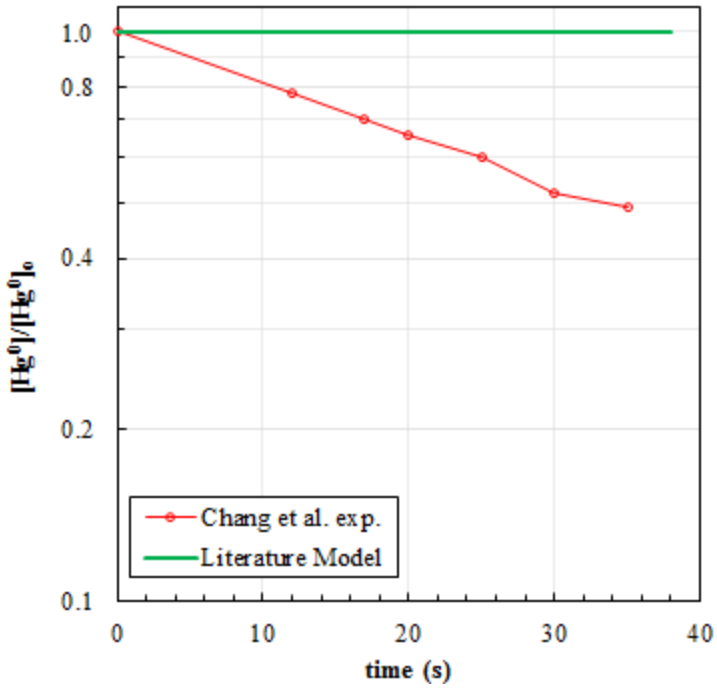

Figure 6.11 Hg loss by reaction with Br_2; solid green line is kinetics from elementary reactions from the literature; red circles are Chang et al.'s[185] experimental data, at 1 atm and 297 K, with initial Hg of 0.2 ppm and 13 ppm Br_2.

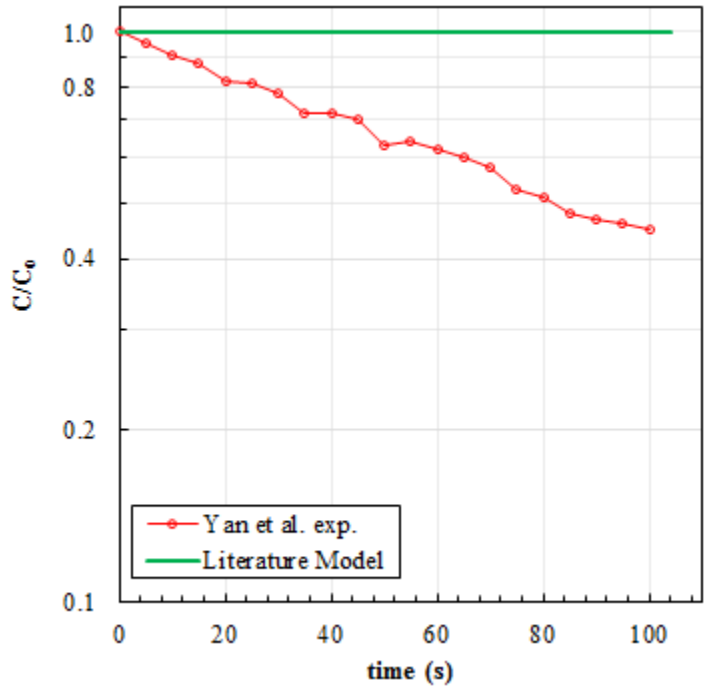

Figure 6.12 Hg loss by reaction with Br_2; solid green line is kinetics from elementary reactions from the literature; red circles are Yan et al.'s[187] experimental data, at 1 atm and 373 K, with initial Hg of 0.16 ppm and 10 ppm Br_2.

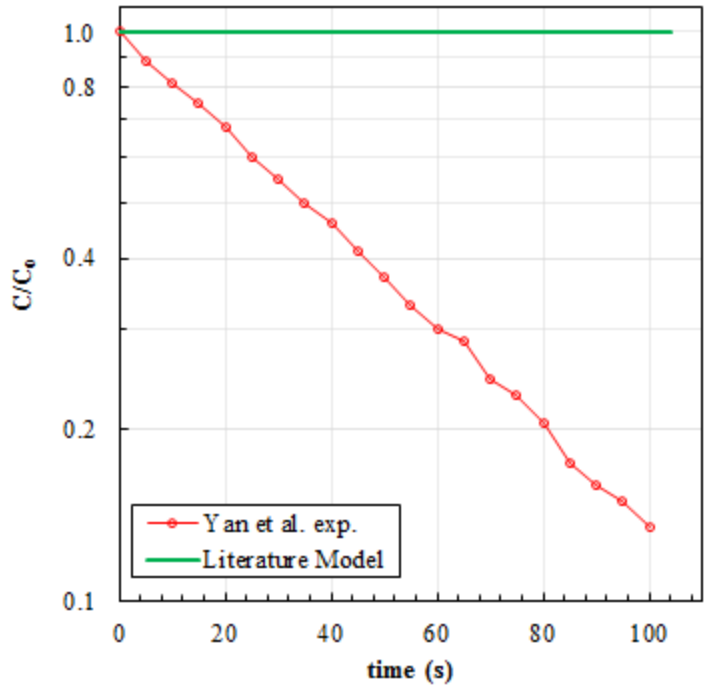

Figure 6.13 Hg loss by reaction with I_2; solid green line is kinetics from elementary reactions from literature; red circles are Yan et al.'s[188] experimental data, at 1 atm and 373 K, with initial Hg of 0.16 ppm and 5.1 ppm I_2.

In trying to reproduce the experimental results with the rate constants and sub-mechanisms proposed in the literature (summarized in Table 6.15 for Cl_2, Table 6.16 for Br_2, and Table 6.17 for I_2), effectively no conversion of mercury is found and no agreement with the experimental data is obtained under atmospheric conditions. The computational results indicate that experimental results cannot be explained by the mechanisms built by using the rate constants in the literature (Table 6.15, 6.16 and 6.17) with thermodynamically consistent reverse reactions.

In order to explain the experimentally observed mercury loss, the insertion reaction ($Hg + X_2 \rightarrow HgX_2$) is further studied, and the influence of a source of halogen atoms in the reaction systems is considered in this study.

In this section the insertion reactions of mercury into chlorine, bromine and iodine molecules forming HgX_2 are further considered; these reactions are overall exothermic, as an option to reproduce (explain) the experimental results.

Using computational chemistry studies, a nonlinear Cl—Hg—Cl complex as found, that can react directly to $HgCl_2$. The chemically activated $HgCl_2$* formed from this insertion can also undergo dissociation to HgCl + Cl. A similar complex and reaction system was also obtained for bromine and iodine, where $HgBr_2$ and HgI_2 are formed through a nonlinear X—Hg—X intermediate (X=Br,I). Two different transition states were found for the insertion reaction of mercury into chlorine and bromine, (i) symmetric and (ii) non-symmetric. The symmetric transition states are found to have a lower barrier than the non-symmetric transition states. However, in order to determine the symmetric transition states, the symmetry of the two X—Hg—X bond lengths was needed to be forced (frozen). Only the non-symmetric transition state was found for the insertion reaction of mercury into iodine. The non-symmetric transition states are optimized structures and were used for the kinetic calculations.

Different levels of theory were used for the determination of the rate constants for comparison and for the selection of the most accurate method. Tables 6.18 and 6.19 summarize the geometries and frequencies obtained for the Hg-Cl system at the different levels of theory, Tables 6.20 and 6.21 represent the data for the Hg-Br system, and Tables 6.22 and 6.23 represent the data for the Hg-I system for the ground state and the transition state.

Table 6.18 Calculated frequencies (cm^{-1}) for chlorine species and comparison to available literature data

Species	Ref.	Level of theory						
		B3LYP/ LanL2dz	B3LYP/ sdd	B3LYP/ AVTZ	wB97X/ AVTZ	B2PLYP/ AVTZ	M06 / AVTZ	M06 -2X/ AVTZ
$HgCl_2$	*100*[a]	68	83	98	103	102	99	98
	313[b], *366*[c]	290	314	338	362	353	352	344
	376[c], *413*[d]	347	379	392	411	407	404	392
Cl_2	*559.71*[e]	468	471	539	597	552	573	576
TS ClHgCl (sym)				-212	-326	-242	-237	-314
				121	148	124	140	139
				198	159	233	185	214
TS ClHgCl (non-sym)		-162	-210	-262	-396	-160	-277	-349
		99	110	107	133	121	117	127
		238	236	223	246	2	226	245

[a] Ref. [208]. [b] Ref. [209]. [c] Ref. [210] [d] Ref. [77] [e] Ref. [211]

Table 6.19 Calculated bond lengths (Å) and bond angles (º) for chlorine species and comparison to available literature data

Species	bond length/ bond angle	Ref.	Level of theory						
			B3LYP/ LanL2dz	B3LYP/ sdd	B3LYP/ AVTZ	wB97X/ AVTZ	B2PLYP/ AVTZ	M06 / AVTZ	M06 -2X/ AVTZ
$HgCl_2$	***r(ClHg)***	*2.25*[a], *2.44*[b]	2.44	2.37	2.29	2.26	2.27	2.28	2.28
	θ(ClHgCl)	*180*[a]	180.00	180.00	180.00	180.00	180.00	180.00	180.00
Cl_2	***r(ClCl)***	*1.99*[c]	2.22	2.23	2.02	1.96	2.01	2.00	2.00
TS ClHgCl (sym)	***r(ClHg)***				2.79	2.79	2.67	2.78	2.74
	r(HgCl)				2.79	2.79	2.67	2.78	2.74
	θ(ClHgCl)				55.53	54.65	56.74	55.47	55.56
TS ClHgCl (non-sym)	***r(ClHg)***		3.01	2.83	2.76	2.71	2.65	2.73	2.73
	r(HgCl)		2.85	2.80	2.70	2.65	2.64	2.69	2.66
	θ(ClHgCl)		53.78	57.76	54.87	56.87	61.14	57.31	57.25

[a] Ref. [212]. [b] Ref. [213]. [c] Ref.[211].

Table 6.20 Calculated frequencies (cm^{-1}) for bromine species and comparison to available literature data

Species	Ref.	Level of theory						
		B3LYP/ LanL2dz	B3LYP/ sdd	B3LYP/ AVTZ	wB97X/ AVTZ	B2PLYP/ AVTZ	M06 / AVTZ	M06 -2X/ AVTZ
$HgBr_2$	*68*[a], *71.6*[b]	46	59	65	69	68	65	66
	222[c], *229*[d], *226.9*[b]	179	200	207	225	218	212	212
	297.8[e], 302.5[b]	244	272	276	295	288	282	275
Br_2	*325.3*[f]	270	281	317	347	326	331	345
TS BrHgBr (sym)	*-189.4*[g]			-128	-172	-149	-130	-184
	55.7[g]			88	79	100	106	106
	152.6[g]			134	123	150	115	125
TS BrHgBr (non-sym)		-122	-149	-178	-273	-148	-189	-222
		71	69	80	96	102	84	94
		146	143	149	169	162	149	167

[a] Ref. [214]. [b] Ref. [52]. [c] Ref. [215]. [d] Ref. [216]. [e] Ref. [205]. [f] Ref. [217]. [g] Ref. [52].

Table 6.21 Calculated bond lengths (Å) and bond angles (º) for bromine species and comparison to available literature data

Species	bond length/ bond angle	Ref.	Level of theory						
			B3LYP/ LanL2dz	B3LYP/ sdd	B3LYP/ AVTZ	wB97X/ AVTZ	B2PLYP/ AVTZ	M06 / AVTZ	M06 -2X/ AVTZ
$HgBr_2$	***r(BrHg)***	*2.404*[a], *2.37*[b]	2.58	2.48	2.42	2.39	2.40	2.42	2.41
	θ(BrHgBr)	*180*[a]	179.40	179.46	180.00	180.00	180.00	180.00	180.00
Br_2	***r(BrBr)***	*2.28*[c], *2.288*[a]	2.51	2.45	2.32	2.28	2.30	2.29	2.28
TS BrHgBr (sym)	***r(BrHg)***	*2.85*[a]			2.90	2.98	2.80	2.94	2.88
	r(HgBr)	*2.85*[a]			2.90	2.98	2.80	2.94	2.88
	θ(BrHgBr)	*55.74*[a]			60.47	58.64	61.27	60.21	59.57
TS BrHgBr (non-sym)	***r(BrHg)***		3.03	2.96	2.88	2.81	2.80	2.84	2.84
	r(HgBr)		3.08	2.92	2.80	2.75	2.75	2.80	2.80
	θ(BrHgBr)		58.86	61.66	62.54	64.48	65.62	62.85	62.84

[a] Ref. [52]. [b] Ref. [218]. [c] Ref. [214].

Table 6.22 Calculated frequencies (cm^{-1}) for iodine species and comparison to available literature data

Species	Ref.	Level of theory						
		B3LYP/ LanL2dz	B3LYP/ sdd	B3LYP/ AVTZ	wB97X/ AVTZ	B2PLYP / AVTZ	M06 / AVTZ	M06 -2X/ AVTZ
HgI_2	*51*[c], *53.7*[i], *63*[d]	68	47	49	52	52	50	49
	155[e], *156*[c], *158*[f], *163.7*[i]	290	143	148	161	156	150	152
	235[c], *237.5*[g], *240.5*[i]	346	220	220	236	230	224	221
I_2	*214.5*[a], *218.1*[b,i]	468	185	212	233	219	218	234
TS IHgI (non-sym)		-162	-121	-146	-242	-55	-151	-183
		99	62	70	83	19	77	81
		238	107	112	128	30	113	128

[a] Ref. [219], [b] Ref. [220], [c] Ref. [221], [d] Ref. [222], [e] Ref. [223], [f] Ref. [215], [g] Ref. [224], [h] Ref. [225], [i] Ref. [191]

Table 6.23 Calculated bond lengths (Å) and bond angles (º) for iodine species and comparison to available literature data

Species	bond length/ bond angle	Ref.	Level of theory						
			B3LYP/ LanL2dz	B3LYP/ sdd	B3LYP/ AVTZ	wB97X/ AVTZ	B2PLYP / AVTZ	M06 / AVTZ	M06 -2X/ AVTZ
HgI_2	***r(IHg)***	*2.5*[d,e]	2.44	2.66	2.61	2.58	2.59	2.62	2.59
	θ(IHgI)	*180.0*[b]	180.00	180.00	180.00	180.00	180.00	180.00	180.00
I_2	***r(II)***	*2.66*[a,b,e], *2.67*[c]	2.22	2.85	2.70	2.66	2.69	2.69	2.66
TS IHgI (non-sym)	***r(IHg)***		3.26	3.19	3.09	3.01	4.11	3.03	3.06
	r(HgI)		3.20	3.05	2.94	2.89	4.10	2.95	2.87
	θ(IHgI)		63.95	67.28	68.43	67.51	73.60	69.04	67.17

[a] Ref. [219], [b] Ref. [220], [c] Ref. [191], [d] Ref. [221], [e] Ref. [191]

Tables 6.24, 6.25 and 6.26 represent the energetics (enthalpy of reaction and activation energy) for each level of theory for Cl_2, Br_2, and I_2, respectively.

Table 6.24 Reaction enthalpies and activation energies for $Hg + Cl_2 \rightarrow HgCl_2$

		Level of theory							
Parameter	**Ref.**	**B3LYP/ LanL2dz**	**B3LYP/ sdd**	**B3LYP/ AVTZ**	**wB97X/ AVTZ**	**B2PLYP/ AVTZ**	**M06 / AVTZ**	**M06 -2X/ AVTZ**	**CCSD(T)/ AVTZ**
$Hg + Cl_2 \rightarrow HgCl_2$									
ΔHrxn	*-49.63*[a]	-54.96	-51.71	-44.18	-55.34	-46.82	-47.21	-49.10	-47.93
ΔH_{calc}-ΔH_{exp}		*5.33*	*2.08*	*5.45*	*5.71*	*2.81*	*2.42*	*0.53*	*1.70*
Ea (Sym TS)	*39.49*[b]	---	---	29.95	30.18	35.18	32.38	39.01	
Ea (Non-sym TS)		13.81	14.89	37.33	44.22	38.28	37.90	**45.07**	

Units: kcal mol^{-1}
[a] Ref. [77]. [b] Ref. [195].

Table 6.25 Reaction enthalpies and activation energies for $Hg + Br_2 \rightarrow HgBr_2$

		Level of theory							
Parameter	**Ref.**	**B3LYP/ LanL2dz**	**B3LYP/ sdd**	**B3LYP/ AVTZ**	**wB97X/ AVTZ**	**B2PLYP/ AVTZ**	**M06 / AVTZ**	**M06 -2X/ AVTZ**	**CCSD(T)/ AVTZ**
$Hg + Br_2 \rightarrow HgBr_2$									
ΔHrxn	*-42.48*[a]	-42.87	-41.41	-35.98	-46.11	-39.31	-34.56	-42.51	-41.86
ΔH_{calc}-ΔH_{exp}		*0.39*	*1.07*	*6.5*	*3.63*	*3.17*	*7.92*	*0.03*	*0.62*
Ea (Sym TS)	*27.2*[b]	---	---	25.66	35.61	30.28	24.27	33.18	
Ea (Non-sym TS)		15.19	24.81	33.35	46.38	34.98	33.03	**39.89**	

Units: kcal mol^{-1}
[a] Ref. [77]. [b] Ref. [52].

Table 6.26 Reaction enthalpies and activation energies for $Hg + I_2 \rightarrow HgI_2$

Parameter	Ref.	Level of theory							
		B3LYP/ LanL2dz	**B3LYP/ sdd**	**B3LYP/ AVTZ**	**wB97X/ AVTZ**	**B2PLYP/ AVTZ**	**M06 / AVTZ**	**M06 -2X/ AVTZ**	**CCSD(T)/ AVTZ**
$Hg + I_2 \rightarrow HgI_2$									
ΔHrxn	*-33.45*[a]	-34.58	-34.41	-26.65	-36.17	-30.15	-25.28	-32.78	-32.96
ΔH_{calc}-ΔH_{exp}		*-1.14*	*-0.96*	*6.80*	*-2.72*	*3.30*	*8.17*	*0.66*	*0.49*
Ea (Non-symm TS)		18.13	24.81	31.48	42.89	57.20	28.90	**37.37**	

Units: kcal mol^{-1}

[a] Ref. [77]

For all chlorine, bromine and iodine calculations the, M06-2X/AVTZ calculation method shows excellent agreement with the experimental data, for the geometry, the frequencies, and enthalpies of reaction. The M06-2X/AVTZ level of theory was selected for the determination of the kinetics. Table 6.27 includes the high pressure rate constants calculated at the M06-2X/AVTZ level of theory for the insertion reactions.

Table 6.27 High pressure limit rate constants for the insertion reactions

Reactions	A	n	α	Ea
$Hg + Cl_2 \rightarrow HgCl_2$	1.66 x10^{10}	1.20	0	45513
$Hg + Br_2 \rightarrow HgBr_2$	2.83 x10^{10}	1.06	0	40438
$Hg + I_2 \rightarrow HgI_2$	2.37 x10^{10}	1.06	0	38020

Units: A (cm^3 mol^{-1} sec^{-1}) and Ea (cal mol^{-1})

The barriers obtained at this level of theory are 45.1, 39.9 and 37.4 kcal mol^{-1} for chlorine, bromine and iodine, respectively. The symmetric barriers obtained by the forced calculations are in good agreement with the available literature data: 39.49 kcal mol^{-1} (chlorine) and 27.2 kcal mol^{-1} (bromine), compared to the calculations from this study,

39.01 kcal mol^{-1} (chlorine) and 33.18 kcal mol^{-1} (bromine)[52,195]. Table 6.28 summarizes the pressure dependence of the rate constants calculated.

Table 6.28 Rate constants for the insertion reactions from 0.01 atm to 100 atm

Reactions	**A**	**n**	**α**	**Ea**
$Hg + Cl_2 \rightarrow HgCl_2$				
0.01 atm	4.14×10^{21}	-3.64	0	46746
0.1 atm	9.14×10^{22}	-3.74	0	47108
1 atm	1.44×10^{24}	-3.78	0	47953
10 atm	6.34×10^{23}	-3.39	0	48604
100 atm	9.00×10^{20}	-2.30	0	48384
$Hg + Br_2 \rightarrow HgBr_2$				
0.01 atm	7.03×10^{18}	-3.01	0	41861
0.1 atm	7.07×10^{19}	-3.01	0	41877
1 atm	7.03×10^{20}	-3.01	0	42005
10 atm	2.69×10^{21}	-2.89	0	42424
100 atm	3.44×10^{20}	-2.36	0	42744
$Hg + I_2 \rightarrow HgI_2$				
0.01 atm	2.55×10^{19}	-3.02	0	39389
0.1 atm	2.71×10^{20}	-3.03	0	39466
1 atm	2.33×10^{21}	-3.01	0	39835
10 atm	1.68×10^{21}	-2.68	0	40328
100 atm	8.33×10^{18}	-1.76	0	40224

Units: A (cm^3 mol^{-1} sec^{-1}) and Ea (cal mol^{-1})

Figure 6.14 illustrates the potential energy diagram for the Hg + Cl_2 reaction system. It also shows a higher energy reaction for dissociation [226] of the energized $HgCl_2$ complex into HgCl + Cl. Data in the figure include the activation energy obtained at the different computational methods. Figures 6.15 and 6.16 illustrate the same for the bromine and iodine systems, respectively.

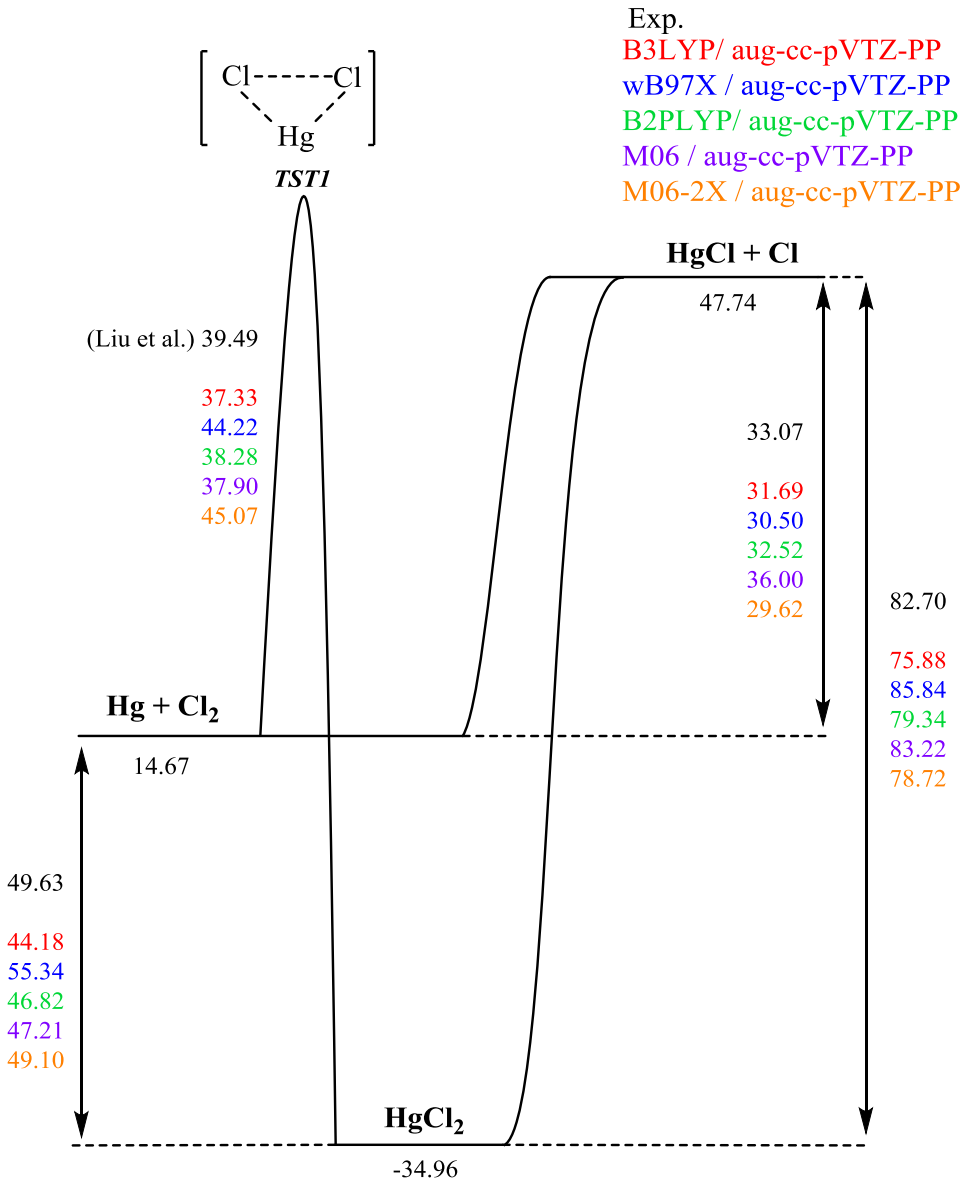

Figure 6.14 Potential energy diagram or the reaction Hg + Cl_2

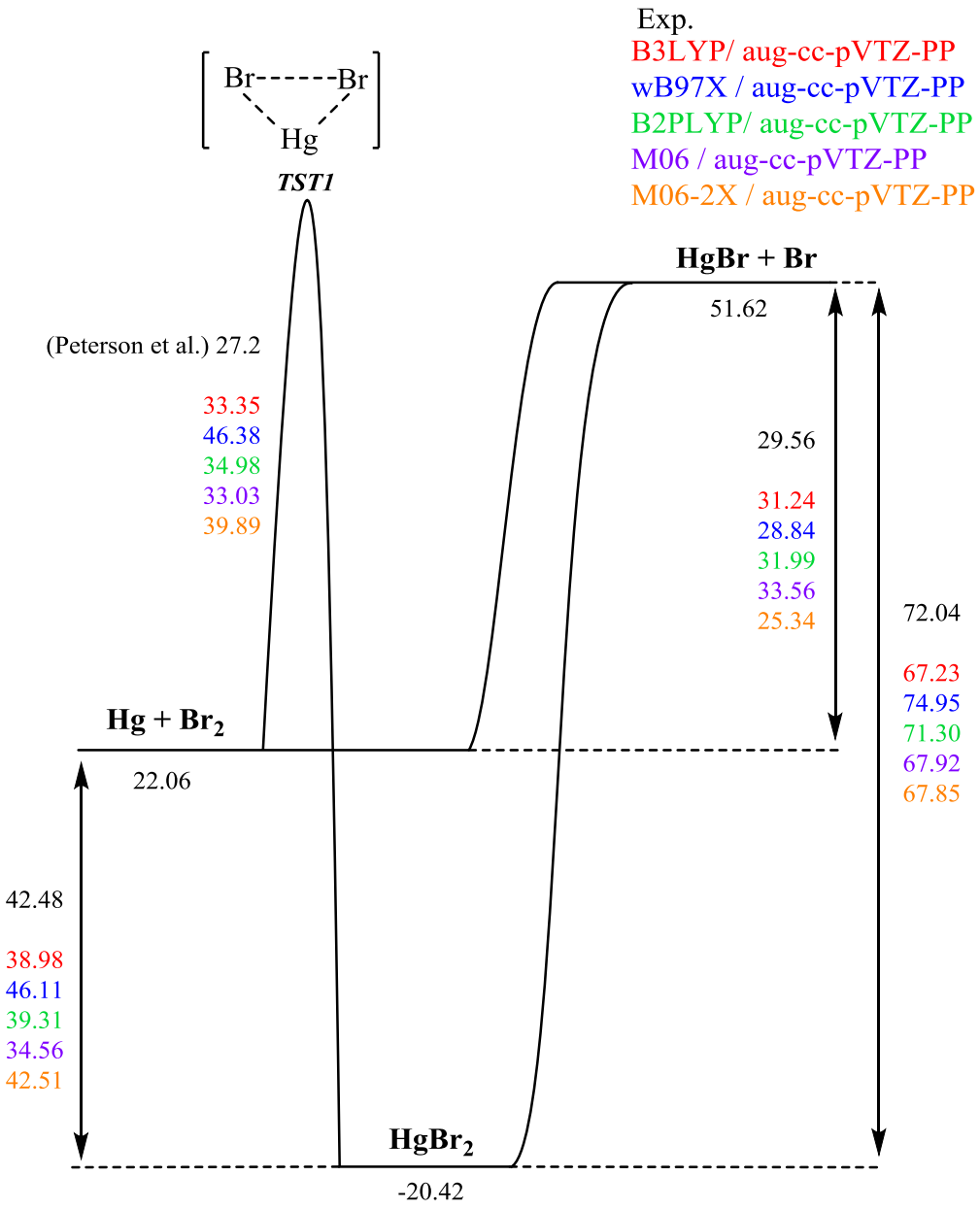

Figure 6.15 Potential energy diagram for insertion of Hg + Br_2

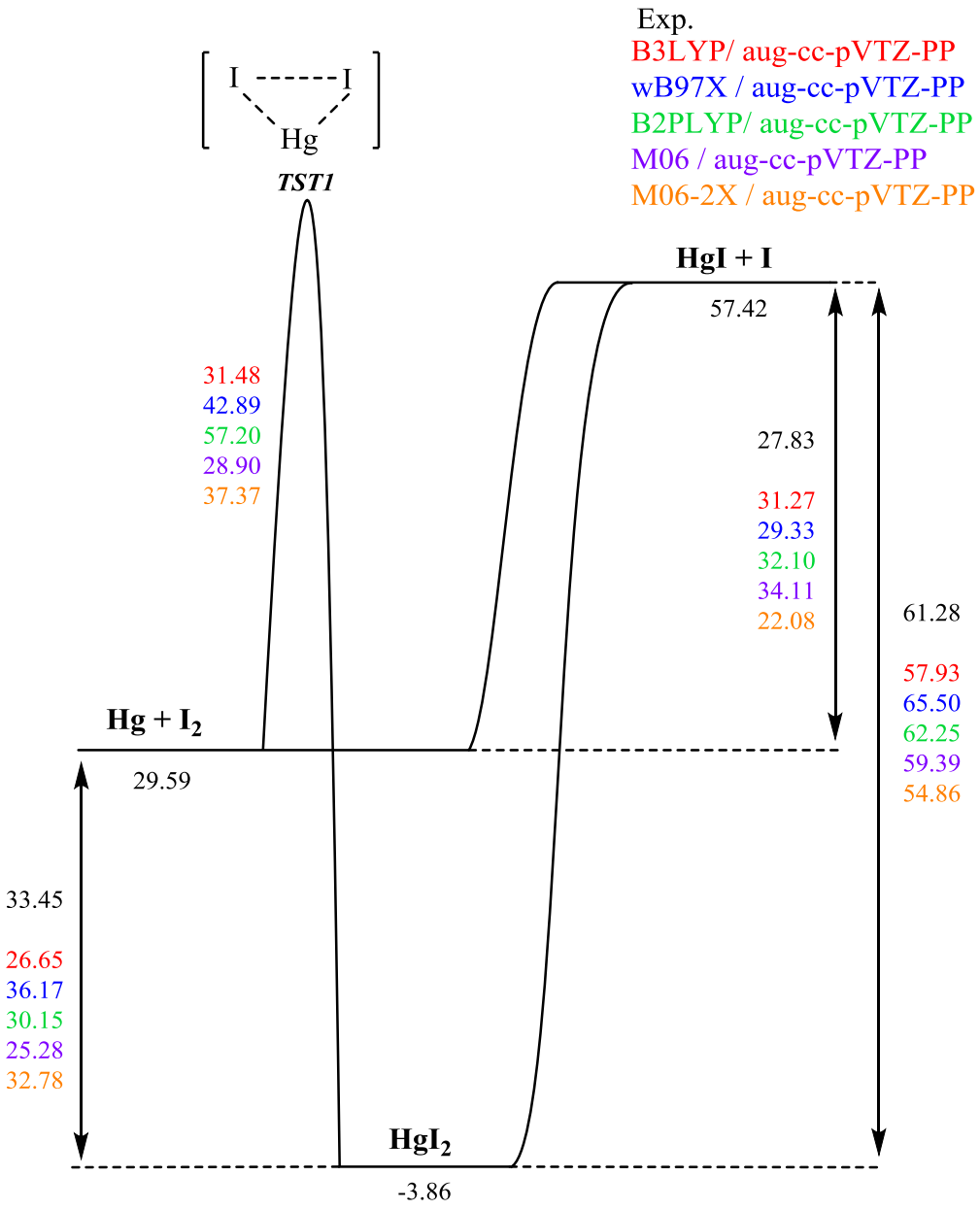

Figure 6.16 Potential energy diagram or the reaction Hg + I_2

The influence of including the insertion reactions in the model is modeled (using the rate constants calculated in this study). The inclusion of the calculated transition state rate constants to the mechanism described in Table 6.15, 6.16 and 6.17 does not result in any conversion of mercury, as indicated in Figures 6.17 to 6.22.

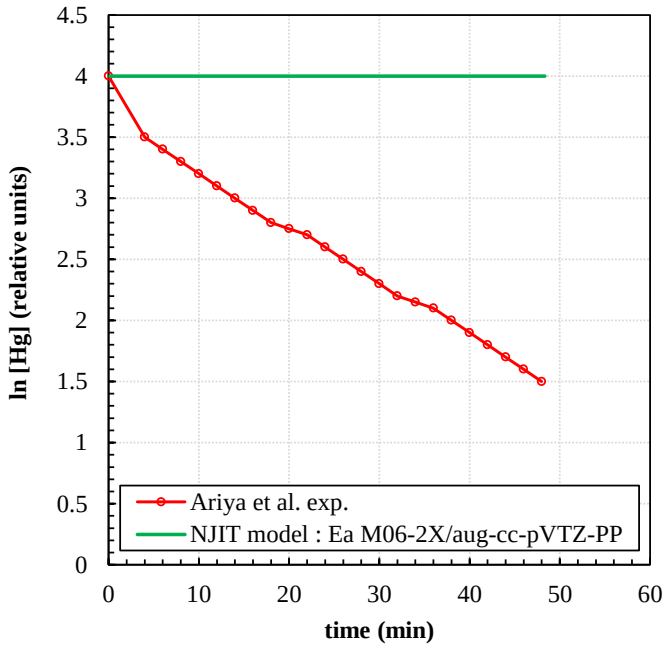

Figure 6.17 Hg loss by reaction with Cl_2 (1 ppm Hg, 10 ppm Cl_2 at 298 K and 1 atm); solid green line is kinetics from elementary reactions from the literature, red circles are Ariya et al.'s[183] experimental data.

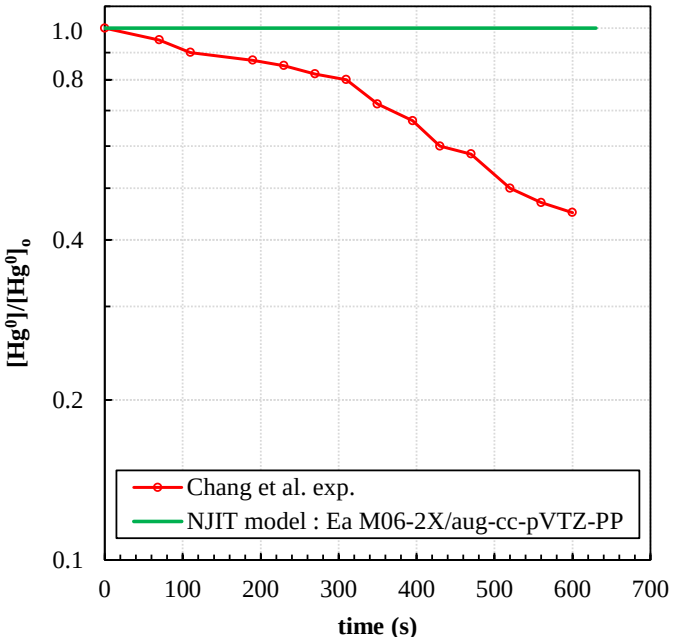

Figure 6.18 Hg loss by reaction with Cl_2 (0.2 ppm Hg, 242 ppm Cl_2 at 297 K and 1 atm); solid green line is kinetics from elementary reactions from the literature, red circles are Chang et al.'s[186] experimental data.

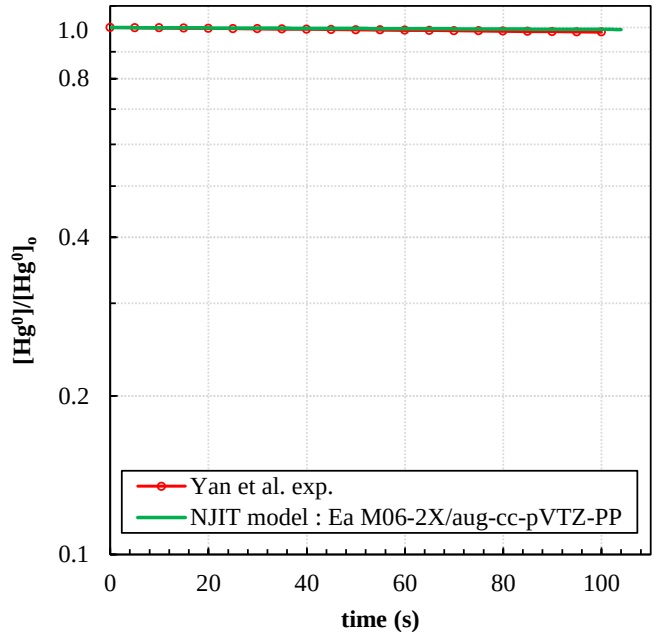

Figure 6.19 Hg loss by reaction with Cl_2 (0.16 ppm Hg, 10 ppm Cl_2 at 373 K and 1 atm); solid green line is kinetics from elementary reactions from the literature, red circles are Yan et al.'s[187] experimental data.

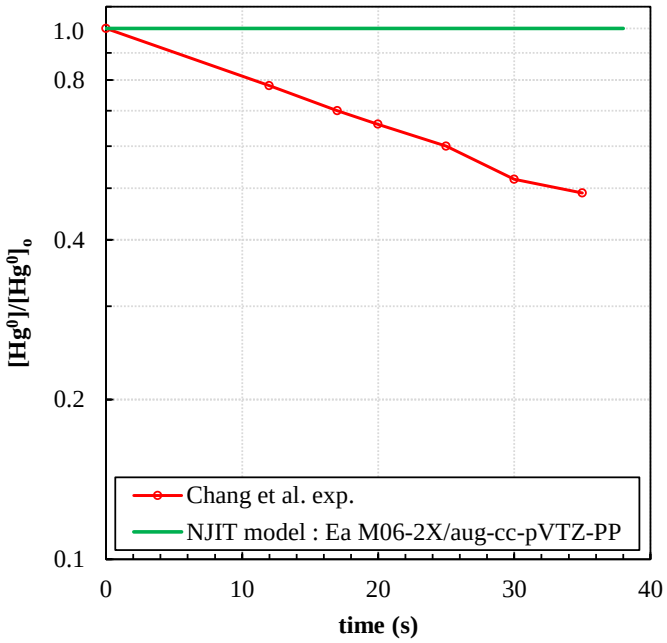

Figure 6.20 Hg loss by reaction with Br_2 (0.2 ppm Hg, 13 ppm Br_2 at 296 K and 1 atm); solid green line is kinetics from elementary reactions from the literature, red circles are Chang et al.'s[185] experimental data.

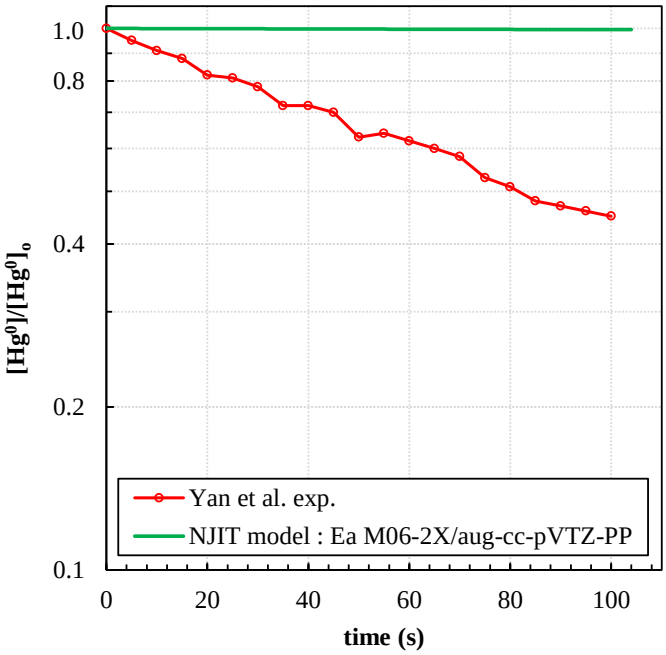

Figure 6.21 Hg loss by reaction with Br_2 (0.16 ppm Hg, 10 ppm Br_2 at 373 K and 1 atm); solid green line is kinetics from elementary reactions from the literature, red circles are Yan et al.'s[187] experimental data.

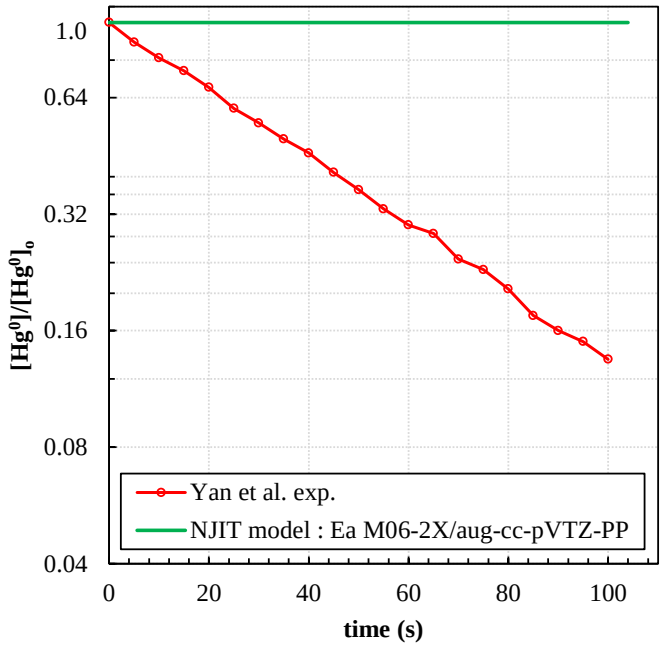

Figure 6.22 Hg loss by reaction with I_2 (0.16 ppm Hg, 5.1 ppm I_2 at 373 K and 1 atm); solid green line is kinetics from elementary reactions from the literature, red circles are Yan et al.'s[188] experimental data.

The mercury conversion data observed in the literature are used to empirically calculate an energy barrier (Ea_{fit}) for the reaction $Hg + X_2 \rightarrow HgX_2$ that would explain the experiments.

$$k = AT^n \exp\left(-Ea/RT\right) \Rightarrow Ea_{fit} = -RT \ln\left(\frac{k_{exp}}{A_{th}T^{n_{th}}}\right) \quad (6.17)$$

where R is the universal gas constant, k_{exp} is the rate constant from the literature, A_{th} is the pre-exponential factor calculated theoretically at the M06-2X/AVTZ level of theory, n_{th} is the temperature power calculated at the M06-2X/AVTZ level of theory, and Ea_{fit} is the activation energy that would be needed to fit the experimental rate constants at the given temperature the experiments were performed. The activation energy obtained to fit Ariya et al.'s experimental rate constant for the reaction $Hg + Cl_2 \rightarrow HgCl_2$ is 9.5 kcal mol^{-1}, an Ea value of 10.8 kcal mol^{-1} was needed to fit Chang et.'s experimental rate constant, and an Ea value of 12.1 kcal mol^{-1} to fit Yan et al's experimental rate constant. The activation energy calculated to fit Ariya et al.'s experimental rate constant for the reaction $Hg + Br_2 \rightarrow HgBr_2$ is 7.3 kcal mol^{-1}, an Ea value of 7.5 kcal mol^{-1} was needed to fit Chang et al.'s experimental data, and an Ea value of 9.8 kcal mol^{-1} to fit Yan et al.'s experimental data. The activation energy determined to fit Yan et al.'s experimental rate constant for the reaction $Hg + I_2 \rightarrow HgI_2$ is 8.6 kcal mol^{-1}. Table 6.29 summarizes the results obtained for the activation energies (the activation energies needed to fit the experimental rate constants and the activation energies calculated theoretically at the M06-2X/AVTZ level of theory).

Table 6.29 Activation energies needed to fit the experimental data

Reactions	Ea	Ref.
$Hg + Cl_2 \rightarrow HgCl_2$	9.5	Ariya et al.
	10.8	Chang et al.
	12.1	Yan et al.
	45.07	Theoretical
$Hg + Br_2 \rightarrow HgBr_2$	7.3	Ariya et al.
	7.5	Chang et al.
	9.8	Yan et al.
	39.89	Theoretical
$Hg + I_2 \rightarrow HgI_2$	8.6	Yan et al.
	37.37	Theoretical

Units: kcal mol^{-1}

The activation energy values obtained from the fits to the three experiments are similar for chlorine, bromine and iodine. The empirical fit values are, however, on the order of 30 kcal mol^{-1} lower than the barriers calculated theoretically (45.1, 39.9 and 37.4 kcal mol^{-1} for chlorine, bromine and iodine, respectively) and also similarly lower than the values calculated by other researchers with higher level calculation methods.

It is not justified to use the empirically calculated values in an insertion reaction to explain the atmospheric mercury conversion. The rate constants calculated at the M06-2X/AVTZ level of theory (summarized in Table 6.27) are recommended.

Chang et al.'s experiments are carried out at room temperature, where they add Cl_2 to Hg in order to study the Hg loss. At room temperature, Cl_2 does not dissociate to Cl. However, in the experiments they use a mercury light source to detect Hg atoms in a spherical bulb that could result in excited Hg* and reactions of Hg* with Cl_2 could result in dissociation of Cl_2 molecules to Cl atoms or insertion reaction. Their results also show that the use of a lower flux (pulsed) light source results in a significant decrease in Hg^0 loss relative to the continuous light source supporting an light or an Hg* interaction.

Ariya et al. mention that in order to prevent the dissociation of I_2, the reaction is studied in a completely darkened chamber, and they also note the formation of particulate matter, which may infer heterogeneous reactions.

An added modeling study was performed to evaluate the possible effect of the presence of halogen atoms in the reaction systems as an initiation mechanism, and to evaluate the concentration of atoms needed to explain the data. To test this case presence of Cl atoms was included in the reaction system for the ChemKin modeling, using the sub-mechanism that includes the insertion reaction calculated at the M06-2X/AVTZ level of theory. In the absence of Cl atoms, no conversion of Hg (initial concentration 0.16 ppm) is observed. However, when Cl atoms are added, the conversion of Hg starts, and from the modeling results it is concluded that ~7.5 $x10^{-5}$ ppb Cl would be necessary to obtain ~45% conversion of mercury observed at Chang et al.'s experiments, and ~ 10^{-3} ppb are necessary to obtain total conversion of mercury, at the conditions of the experiment: 0.16 ppm Hg, 10 ppm Cl_2 at 373 K and 1 atm. Table 6.30 and Figure 6.23 illustrate the results of these calculations.

Table 6.30 Conversion of Hg versus Cl atom concentration, with initially 0.16 ppm Hg, and 10 ppm Cl_2 at 297 K and 1 atm

Cl_2/Cl concentration	**10 ppm Cl_2 0 ppb Cl**	**10 ppm Cl_2 1.0 $x10^{-6}$ ppb Cl**	**10 ppm Cl_2 1.0 $x10^{-5}$ ppb Cl**	**10 ppm Cl_2 1.0 $x10^{-4}$ ppb Cl**	**10 ppm Cl_2 1.0 $x10^{-3}$ ppb Cl**
$[Hg]/[Hg]_0$	1.0	0.993	0.879	0.264	0.0

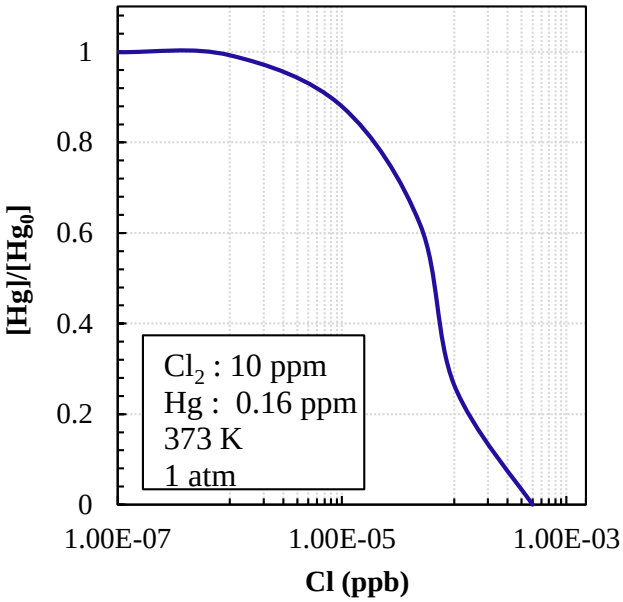

Figure 6.23 Conversion of Hg versus Cl atom concentration, with initially 0.16 ppm Hg, and 10 ppm Cl_2 at 373 K and 1 atm

This modeling is also performed for bromine and iodine, to study the influence of atomic bromine and iodine in the reaction system. The bromine mechanism including the insertion reaction calculated at M06-2X/AVTZ level of theory has been used. Results indicate that higher concentrations of Br atoms are needed to affect conversion relative to chlorine. As in the case of chlorine, no conversion is obtained in the absence of bromine atoms, ~10^{-1} ppb would be necessary to obtain ~45% conversion of mercury observed at Chang et al.'s experiments, and a total conversion is obtained when ~1 ppb Br atoms are added to the reaction system. Table 6.31 and Figure 6.24 represent the results of these calculations.

Table 6.31 Conversion of Hg versus Br atom concentration, with initially 0.16 ppm Hg, and 10 ppm Br_2 at 296 K and 1 atm

Br_2/Br concentration	**10 ppm Br_2 0 ppb Br**	**10 ppm Br_2 1.0 10^{-2} ppb Br**	**10 ppm Br_2 1.0 x10^{-1} ppb Br**	**10 ppm Br_2 1.0 10^{-0} ppm Br**
$[Hg]/[Hg]_0$	1.0	0.921	0.449	0.0

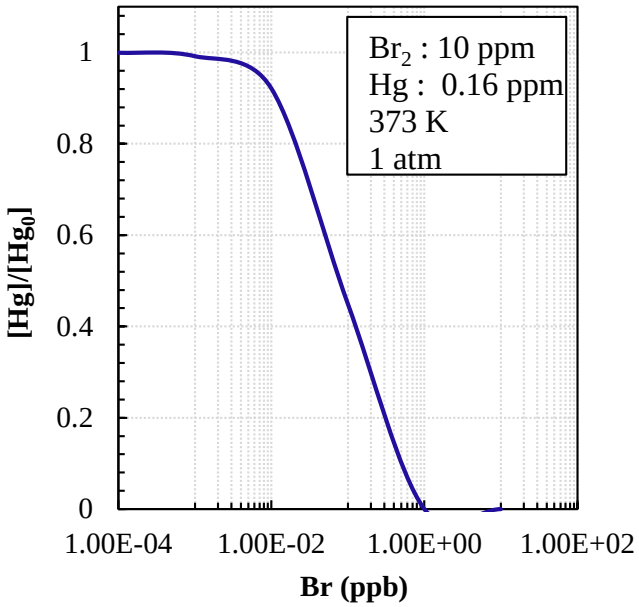

Figure 6.24 Conversion of Hg versus Br atom concentration, with initially 0.16 ppm Hg, and 10 ppm Br_2 at 373 K and 1 atm

The iodine mechanism including the insertion reaction calculated at M06-2X/AVTZ level of theory was used. Results indicate that higher concentrations of I atoms are needed to effect conversion relative to chlorine and bromine. As in the case of chlorine and bromine, no conversion is obtained in the absence of iodine atoms, ~5 $x10^{-1}$ ppb would be necessary to obtain ~15% conversion of mercury observed at Yan et al.'s experiments, and total conversion is obtained when ~10^2 ppb I atoms are added to the reaction system. Table 6.32 and Figure 6.25 represent the results of these calculations. Modeling results confirm that very small concentrations of X atoms (~10^{-5} – 10^2 ppb) serve to reproduce the experimental mercury loss observed.

Table 6.32 Conversion of Hg versus I atom concentration, with initially 0.16 ppm Hg, and 10 ppm I_2 at 373 K and 1 atm

I_2/I concentration	**10 ppm I_2 0 ppb I**	**10 ppm I_2 1.0 10^{-1} ppb I**	**10 ppm I_2 1.0 $x10^{-0}$ ppb I**	**10 ppm I_2 1.0 10^1 ppb I**	**10 ppm I_2 1.0 10^2 ppb I**
$[Hg]/[Hg]_0$	1.0	0.955	0.69	0.166	0.0

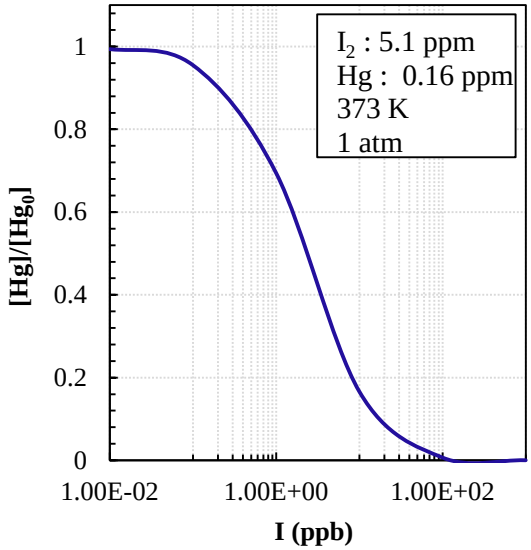

Figure 6.25 Conversion of Hg versus I atom concentration, with initially 0.16 ppm Hg, and 5.1 ppm I_2 at 373 K and 1 atm

6.5 Summary

A fundamentally based reaction mechanism and kinetic parameters found in the literature do not predict any significant formation of HgX_2 or loss of Hg under atmospheric conditions relative to that observed in the experimental studies.

The same complete lack of conversion occurs when trying to reproduce the experimental data using the rate constants developed in this study (with thermodynamically consistent reverse reactions with pressure dependence for the chemical activation and dissociation reactions are incorporated), when the insertion reactions ($Hg + X_2 \rightarrow HgX_2$) are included.

Theory support that the insertion reaction mechanism has a high barrier, and therefore the inclusion of these reactions in the elementary reaction mechanism does not result on the oxidation of mercury.

Modeling results confirm that if the experiments had a source of X atoms, the reactions $Hg + X \rightarrow HgX$ and $HgX + X \rightarrow HgX_2$ dominate the Hg oxidation, and the experimentally observed mercury loss could be justified.

CHAPTER 7

OXIDATION OF MERCURY BY HALOGENS (Cl, Br, I) IN COMBUSTION EFFLUENTS: INFFLUENCE OF COMBUSTION PROCESSES

7.1 Overview

The toxicity of mercury has been well known for years, and the increase of its emissions to the atmosphere is getting apparent in the last years. A study conducted in 2009 determined that 2479 tons of mercury are emitted worldwide every year[227], from which 1289 tons are emitted from industrial processes, 459 tons from power generating plants, 586 tons from biomass burning, 76 tons from transportation and 72 tons from residential sources. The increase of mercury emissions in Asia from coal burning and artisanal goal mining[228] since the 1950's is the most significant[227,228].

The increasing concern on the toxicity of mercury has led many countries to implement regulations on the power generating and waste incineration plants for the control of mercury emissions. Mercury is present in the combustion flue gases as elemental mercury (Hg^o), oxidized mercury (Hg^{2+}), and mercury associated to particles (Hg_p). Elementary mercury is highly volatile, and it is not feasible to capture it by using the usual air pollution control devices (scrubbers, electrostatic precipitators, fabric bags…). However, the oxidized mercury is water soluble and has the tendency to associate to particles, and these forms can be eliminated by the air pollutant control devices. Figure 7.1 represents a schematic view of the usual control devices in a power generation plant.

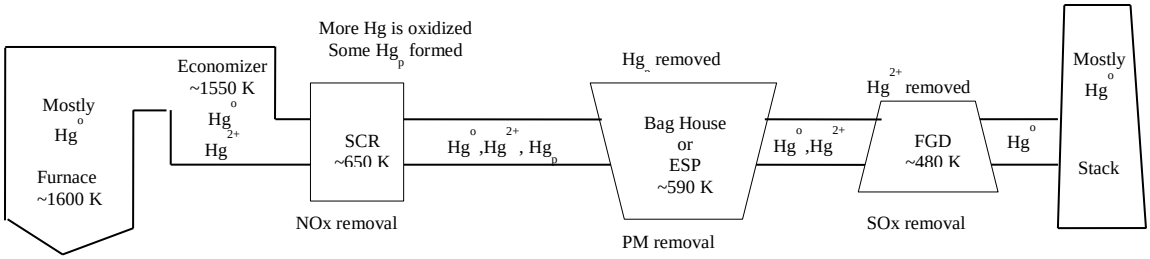

Figure 7.1 Schematic structure of air pollution control devices in a power generating plant

In the combustion chamber, mercury is present mainly as elemental mercury (Hg^o), with some oxidized mercury (Hg^{2+}) and mercury associated to particles (Hg_p). After the economizer, the selective catalytic reduction (SCR) or selective noncatalytic reduction (SNCR) systems aim to remove nitrogen oxides (NOx) from the combustion effluent, but they additionally succeed in oxidizing part of the elemental mercury into the oxidized Hg^{2+}, and part of the Hg^{2+} will also deposit in the particulate matter that is present. The goal of fabric filters (bag houses) or electrostatic precipitators (ESP) is the elimination of the particulate matter, and therefore, part of the mercury that is associated with the particles is eliminated in this step. The flue-gas desulfurization (FGD) targets the removal of sulfur oxides (SOx), and additionally succeeds to remove most of the oxidized mercury that is still present in the system. However, only a small fraction of the elemental mercury is removed through the air pollutant control devices.

A number of power generating plants have started incorporating specific mercury removal technologies[229,230]. The most common technology is the injection of activated carbon, which promotes the attachment of mercury to the carbon particles. The injection of bromine to the flue gases has also been tested in power plants[230], where bromine was proven to be effective at oxidizing mercury. The disadvantage of adding halogens is that they can cause corrosion problems, increase of halogen content in fly ash, and can

increase the emissions of halogens from air pollution control devices (APCD)[231], and therefore this must be accounted. Alternative techniques have also been proposed over the last years, such as mercury control by corona discharge[232], circulating fluid bed for mercury and fine particulate control[233], and electro-catalytic oxidation (ECO)[234] technologies. The approach followed in this work consists of the addition of halogens (chlorine, bromine and iodine) to the combustion gases (added directly in the furnace), so that the elemental mercury (Hg^o) is converted into the oxidized mercury ($HgCl_2$, $HgBr_2$, HgI_2), and therefore removed by the air pollution control devices available in most power generating plants.

Different approaches have been presented for the elimination of NOx from combustion flue gases during the last years. One of the suggested solutions for the reduction of NOx emissions is oxi-combustion, where the combustion is performed with an oxidizer rich in O_2, instead of using air, reducing significantly the addition of N_2 in the system, and therefore decreasing the concentration of NOx in the flue gases. There are, however a few studies that have focused on determining the influence of the reduced NOx emissions in the conversion of mercury by the addition of halogens and these are discussed just below. Technologies are also continuing on removal of sulfur from coal and natural gas in order to reduce the SOx emissions. It is therefore of value to determine the influence of the concentration of NOx and SOx in the speciation of mercury.

The goal of this study is to construct an elementary reaction mechanism to describe the oxidation of mercury by the addition of halogens in combustion effluents, as well as to determine the influence of the process conditions in the efficiency of oxidizing mercury.

The earliest mechanism for Hg^0 oxidation in a flue-gas stream was proposed by Hall et al.[235]; but it did not incorporate kinetic and thermochemical details. The formulation of a homogeneous, gas phase, mercury reaction mechanism started with a reaction scheme published by Widmer et al.[202,236]. The mechanism consisted of an eight step elementary reaction sequence for the formation of $HgCl_2$ from Hg^0 and chlorine-containing species. Sliger et al.[237,238] studied the reactions of Hg^0 with HCl at various concentrations and temperatures, and developed a model that incorporated a reaction set using H_2, O_2, CO, CO_2 plus an additional reaction set of 18 equations involving Cl, Cl_2, HCl, ClO (chlorine monoxide), and HOCl. Senior et al.[201] included kinetic parameters for the homogeneous oxidation of elemental mercury by chlorine, using reactions from the literature. A later paper by Edwards et al.[239] extended the model proposed by Sliger et al.[237] by including more chlorination pathways, calculating new rate constants for some of the reactions, and including Hg reactions involving HgO. In addition to the eight-step reaction set, the authors added: (i) a sub-mechanism that described chlorine chemistry with nitrogen oxides (NOx) chemistry, (ii) a moist CO oxidation sub-mechanism and (iii) a H/N/O sub-mechanism. The total mechanism included 102 elementary chemical reactions.

Xu et al.[204] listed, for the first time, the reactions along with the rate constants calculated from computational chemistry and transition state theory, used in their model. Their mechanism included Widmer et al.'s[202,236] Hg reactions, and they included 6 additional reactions containing HgO. Their work resulted in an oxidation model of 107 reactions and 30 species. Krishnakumar et al.[240] performed an evaluation of the available literature mechanisms, concluding that the Qiu mechanism predicted Hg oxidation in

several experimental systems and conditions fairly accurately although it did not provide the best agreement in all cases. Over the last years, the University of Utah has conducted several experimental studies on the oxidation of mercury by the addition of chlorine and bromine, as well as the influence of NOx and SOx on the conversion of mercury[196,241,242]. Ghorishi et al.[243] and Helble et al.[244] have also studied the influence of the sulfur oxides on the mercury oxidation.

Several groups have worked on the development of the thermochemical and kinetic properties of mercury reactions with chlorine[183,186,189,192,245,246], bromine[51,52,185,189,191,194,205,247] and iodine[188,191] at atmospheric and combustion conditions, that have been incorporated in the reaction mechanisms.

The elementary reaction mechanism developed in this study (203 species and 957 reactions) is targeted to model and provide evaluation of conditions needed for conversion of elemental mercury into its oxidized form ($HgCl_2$, $HgBr_2$, HgI_2), trends in the chemistry of mercury in a coal combustion environment, and the influence of nitrogen oxides (NOx), sulfur oxides (SOx), the addition of vapor water (H_2O), the use of different temperature profiles and the fuel/air equivalence ratio (CH_4 is the studied fuel) in the speciation of mercury.

7.2 Thermochemical Properties

The thermochemical properties, heats of formation, entropies and heat capacities (T) were determined from evaluation of literature values, and for new species, the thermochemical properties were calculated by use of computational chemistry with Density Functional Theory (DFT) based M06-2X/aug-cc-pVTZ-PP (AVTZ)[61] (Augmented Correlation Consistent basis sets of Triple-ζ quality)[248,249] for mercury

species and the DFT-based multilevel schemes G3[250], CBS-QB3[251], and CBS-APNO[252] for non-mercury species. All calculations were performed by the Gaussian 03 and 09 suite of programs[73] in conjunction of isodesmic work reactions for the determination of the enthalpies of formation[104]. Entropy and heat capacity contributions versus temperature were determined from the calculated structures, moments of inertia, non-torsion vibrational frequencies, internal rotor parameters, symmetry, electron degeneracy, number of optical isomers and the known mass of each molecule. The calculations used standard formulas from statistical mechanics for the contributions of translation, external rotation and vibrations using the SMCPS code[78].

The bond distance and frequencies of NO, SO, HgCl, and HgBr, have been studied in several experimental and theoretical studies. In this work, several levels of theory were tested to determine the most appropriate methods for the determination of the enthalpies of formation and heats of reactions of the mercury-halogen-nitrogen oxide systems. Table 7.1 summarizes the results obtained for NO, SO, HgCl and HgBr at the different levels of theory. Results show that CBS-QB3 presents good accuracy for the determination of nitrogen oxides. B2PLYP/AVTZ and M06-2X/AVTZ are the most accurate methods for the mercury-halogen systems. They both also show good agreement with the literature experimental data of NO and SO.

CBS-QB3 (for halogen-NOx and halogen-SOx species), and B2PLYP/AVTZ and M06-2X/AVTZ (for mercury-halogen-NOx and mercury-halogen-SOx species) levels of theory were selected for the determination of the enthalpies of formation. The less expensive B3LYP/LANL2DZ and B3LYP/SDD calculations were performed for comparison.

Table 7.1 Bond length (Å) and frequencies (cm^{-1}) for NO, HgCl, and HgBr and several levels of theory

Level of Theory	NO		SO		HgCl		HgBr	
	Bond	**Freq.**	**Bond**	**Freq.**	**Bond**	**Freq.**	**Bond**	**Freq.**
CBS-QB3 (B3LYP/6-31G(2d,d,p))	1.15	1988.3	1.50	1121.9	---	---	---	---
B3LYP/LANL2DZ	1.20	1770.5	1.63	950.3	2.61	229.0	2.78	141.5
B2PLYP/LANL2DZ	1.21	1749.5	1.67	807.0	2.56	251.4	2.72	156.9
ωB97X/LANL2DZ	1.19	1866.4	1.61	1029.5	2.55	265.8	2.70	167.9
M06/LANL2DZ	1.19	1832.3	1.62	992.3	2.57	247.9	2.74	152.8
M06-2X/LANL2DZ	1.18	1871.6	1.61	1026.7	2.54	269.0	2.70	170.8
B3LYP/SDD	1.20	1771.4	1.62	959.0	2.55	231.2	2.69	143.3
B2PLYP/SDD	1.21	1749.6	1.66	815.0	2.52	251.8	2.65	157.2
ωB97X/SDD	1.19	1867.3	1.59	1042.8	2.50	261.8	2.63	163.7
M06/SDD	1.19	1832.8	1.60	1004.8	2.55	220.1	2.67	150.8
M06-2X/SDD	1.18	1872.5	1.59	1047.3	2.51	268.8	2.63	173.4
B3LYP/AVTZ	1.15	1968.3	1.50	1145.2	2.46	240.9	2.61	155.8
B2PLYP/AVTZ	***1.15***	***1891.1***	***1.51***	***1080.1***	***2.42***	***262.3***	***2.56***	***168.7***
ωB97X/AVTZ	1.14	2040.0	1.48	1227.3	2.40	279.9	2.56	172.1
M06/AVTZ	1.14	2017.6	1.49	1195.7	2.45	246.0	2.64	134.0
M06-2X/AVTZ	***1.14***	***2066.0***	***1.48***	***1224.2***	***2.41***	***274.3***	***2.55***	***181.6***
Lit.	*1.154*[1]	*1904.2*[2]	1.481[253]	1150.8[220]	*2.36*[253], *2.50*[213]	*292.61*[220], *298.97*[222]	*2.49*[254], *2.62*[220]	*188.3*[220], *218*[225], *220*[223]

The enthalpies of formation, reaction enthalpies and bond dissociation enthalpies of mercury-halogen, halogen-nitrogen oxide, mercury-halogen-nitrogen oxide, halogen-sulfur oxide, and mercury-halogen-sulfur oxide systems are presented in this section. The determination of the heats of formation used isodesmic work reactions. The standard enthalpies of formation at 298.15 K of the reference species used in these reactions are summarized in Appendix A. The work reactions used for the determination of the heats of formation of each of the species are summarized in Appendix AD.

Figures 7.2 to 7.6 illustrate the schematic representation and the nomenclature of the molecules studied in this work. Appendix AB includes the specifications of the optimized geometries and Appendix AC includes the frequencies of each of the species.

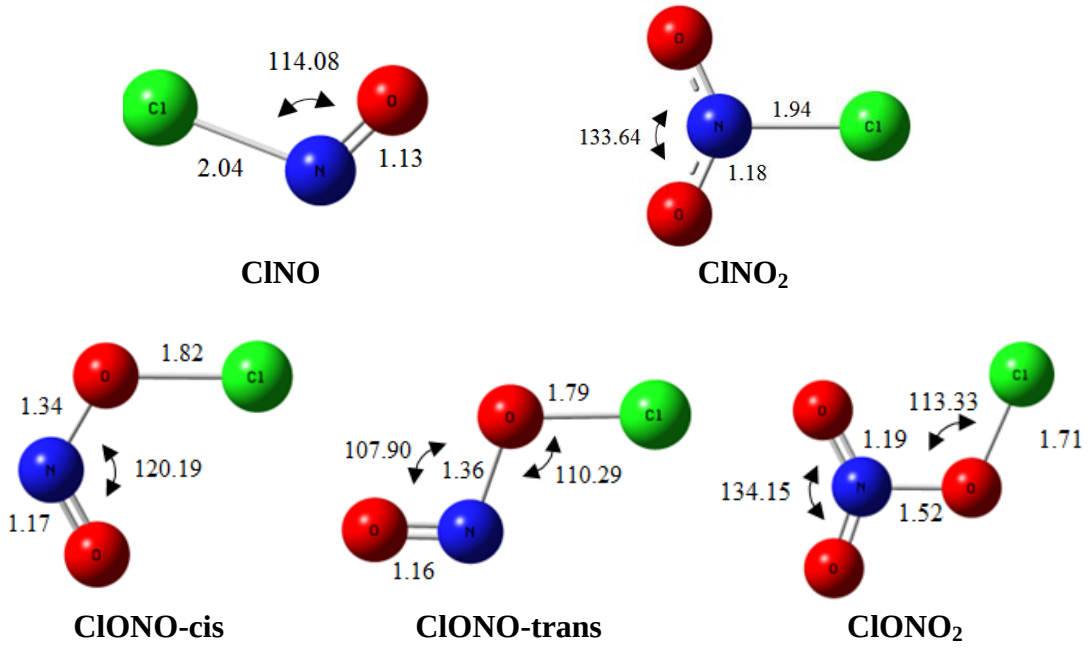

Figure 7.2 Structure and nomenclature of the chlorine nitrogen oxides studied

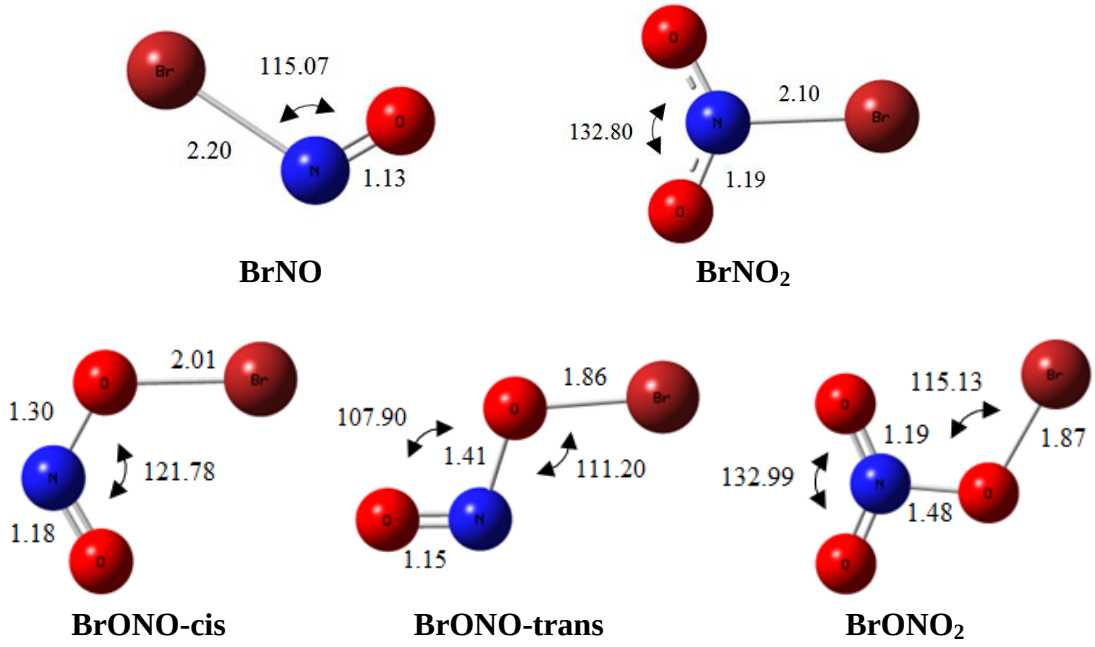

Figure 7.3 Structure and nomenclature of the bromine nitrogen oxides studied

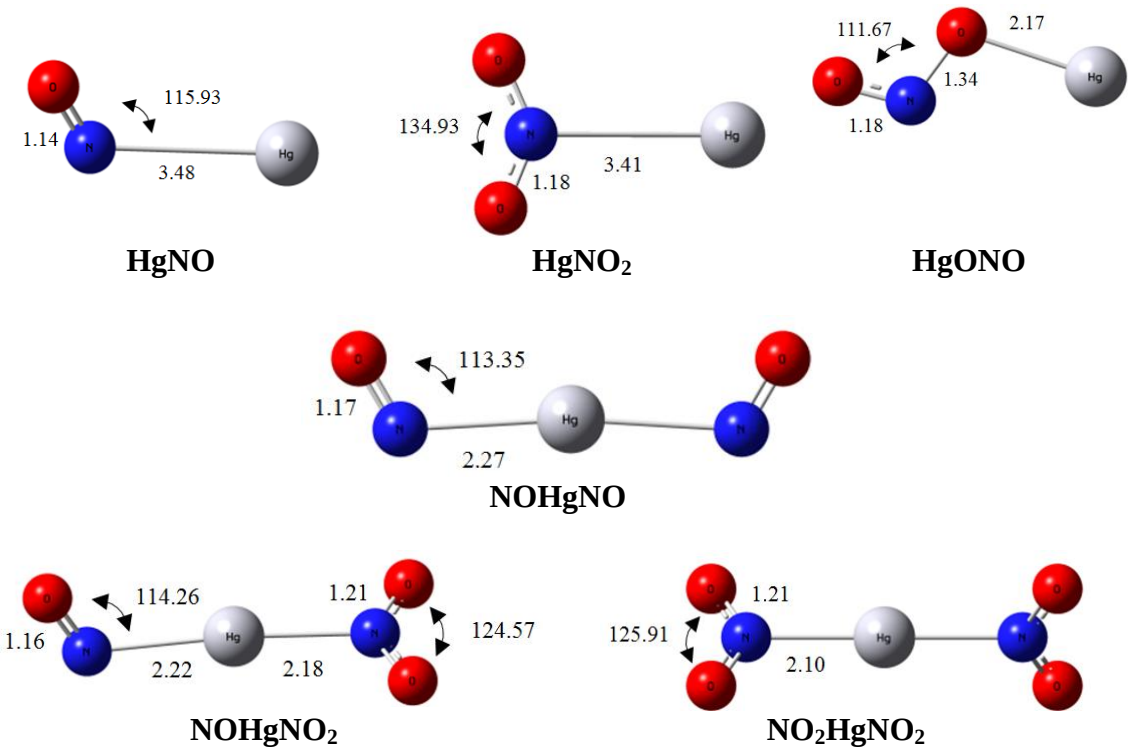

Figure 7.4 Structure and nomenclature of the mercury nitrogen oxides studied

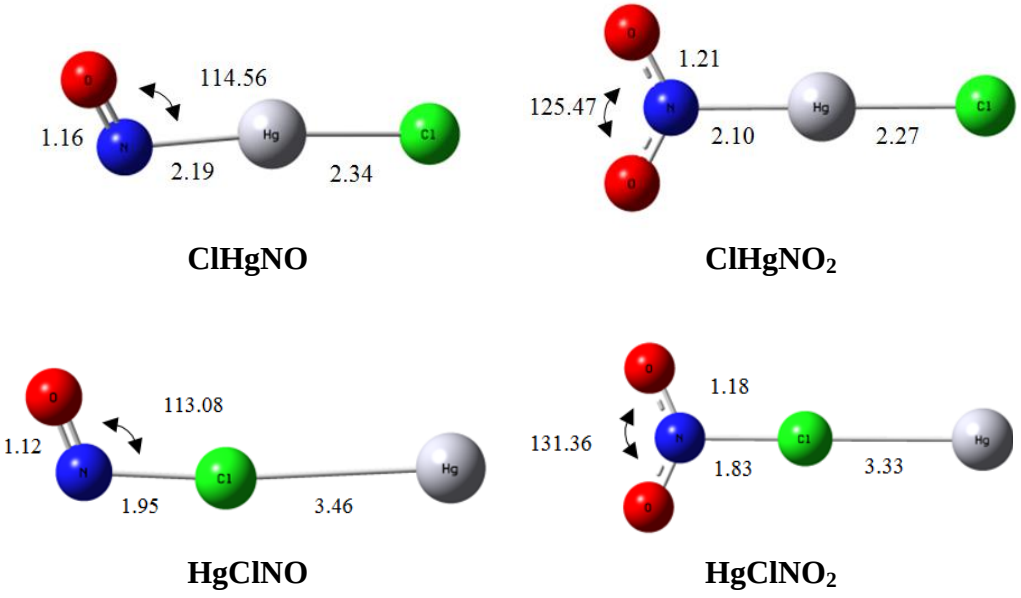

Figure 7.5 Structure and nomenclature of mercury chloride nitrogen oxides studied

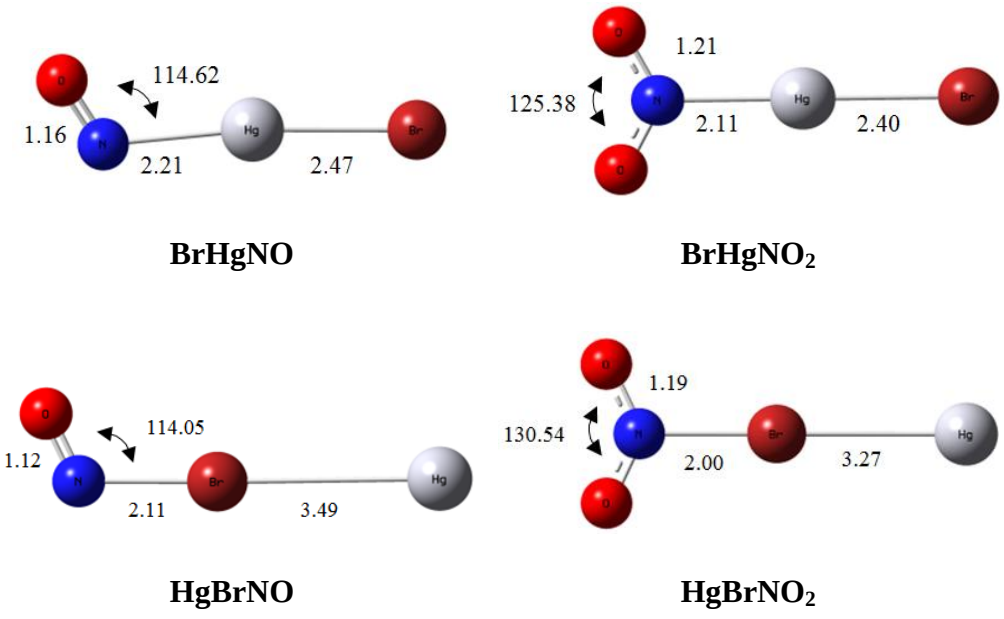

BrHgNO **$BrHgNO_2$**

HgBrNO **$HgBrNO_2$**

Figure 7.6 Structure and nomenclature of the mercury bromide nitrogen oxides studied

The calculated heats of formation of chlorine–nitrogen oxide species are summarized in Table 7.2, calculated at the different levels of theory, in conjunction with work reactions. The table also provides available literature data for comparison.

Table 7.2 Calculated enthalpies of formation of chlorinated nitrogen oxide molecules

Species	$\Delta_f H°_{298}$					
	CBS-QB3 (*)	B3LYP/ LANL2DZ	B3LYP/ SDD	B2PLYP/ AVTZ	M06-2X/ AVTZ	Ref.
ClO	24.10	30.25	29.49	24.64	24.54	24.19[77]
HCl	-21.81	-24.59	-23.54	-21.31	-20.76	-22.06[255]
HOCl	-18.06	-15.28	-16.33	-18.56	-19.11	-17.81[77]
ClNO	12.15	7.24	6.52	10.10	13.14	12.36[77]
$ClNO_2$	2.34	-0.07	-1.08	-0.54	2.24	2.99[77]
ClONO-cis	15.52	6.40	5.21	11.74	15.50	---
ClONO-trans	17.33	14.03	12.83	15.71	18.88	---
$ClONO_2$	6.42	0.87	1.30	5.38	8.35	---

Units: kcal mol^{-1}
(*) Recommended

Results show that CBS-QB3 is in good agreement (± <0.5 kcal mol^{-1}) with the literature data for all the studied species. The M06-2X/AVTZ is also shown to be in good agreement with the experimental data (±<1 kcal mol^{-1}). The B2PLYP/AVTZ is shown to have a difference of ±0.5-3.5 kcal mol^{-1} compared to the literature data. The less expensive B3LYP/LANL2DZ and B3LYP/SDD methods show agreement at ± 2 kcal mol^{-1} for HCl and HOCl; but the results are not in good agreement for the chlorinated nitrogen oxides. The results obtained using CBS-QB3 in conjunction with the work reactions are recommended.

The heats of formation of bromine–nitrogen oxide species are summarized in Table 7.3, calculated at the different levels of theory, in conjunction with work reactions. Table 7.3 provides also available literature data for comparison.

Table 7.3 Calculated enthalpies of formation of brominated nitrogen oxide molecules

Species	$\Delta_f H°_{298}$					
	CBS-QB3 (*)	**B3LYP/ LANL2DZ**	**B3LYP/ SDD**	**B2PLYP/ AVTZ**	**M06-2X/ AVTZ**	**Ref.**
BrO	30.30	32.55	32.70	29.00	29.73	30[256]
HBr	-8.67	-12.58	-14.18	-8.76	-9.46	-8.67[255]
HOBr	-16.32	-13.34	-11.38	-16.06	-15.18	-19.0[255]
BrNO	21.27	15.57	15.25	17.97	20.81	19.60[257]
$BrNO_2$	10.83	6.26	5.97	5.86	8.99	---
BrONO-cis	19.77	7.50	7.86	13.84	18.16	---
BrONO-trans	21.99	15.58	15.77	18.59	22.58	---
$BrONO_2$	8.63	7.33	7.62	7.48	8.94	---

Units: kcal mol^{-1}
(*) Recommended

CBS-QB3 results show very good agreement for BrO and HBr. The enthalpy of formation obtained for HOBr is 3 kcal mol^{-1} higher compared to the available literature

data, and 2 kcal mol^{-1} higher for BrNO. Results from the M06-2X/AVTZ calculation method are also in very good agreement with the experimental data. The B2PLYP/AVTZ method is ~1 - 2 kcal mol^{-1} higher compared to the literature values. The less expensive B3LYP/LANL2DZ and B3LYP/SDD do not show good agreement for the brominated nitrogen oxides. The results obtained using CBS-QB3 in conjunction with the work reactions are recommended.

Table 7.4 summarizes the reaction enthalpies for chlorinated and brominated nitrogen oxide species, calculated at the CBS-QB3 level of theory.

Table 7.4 Calculated reaction enthalpies of chlorinated and brominated nitrogen oxide molecules (X=Cl,Br) at the CBS-QB3 level of theory

Species	$\Delta_{rxn}H°_{298}$	
	Cl	**Br**
X + NO → XNO	-38.4	-27.1
X + NO_2 → XNO_2	-34.6	-23.8
X + NO_2 → XONO-cis	-21.4	-14.9
X + NO_2 → XONO-trans	-19.6	-12.7
X + NO_3 → XONO_2	-39.6	-35.1
XO + NO → XONO-cis	-30.3	-31.8
XO + NO → XONO-trans	-28.4	-29.6
XO + NO_2 → XONO_2	-25.7	-29.3

Units: kcal mol^{-1}

Results show that the bonds are relatively weak: X—ONO 21.4 kcal mol^{-1} for chlorine and 14.9 kcal mol^{-1} for bromine for the *cis* position, and 19.6 kcal mol^{-1} for chlorine and 12.7 kcal mol^{-1} for bromine for the *trans* position, X—NO is 38.4 kcal mol^{-1} for chlorine and 27.1 kcal mol^{-1} for bromine, X—NO_2 is 34.6 kcal mol^{-1} for chlorine and 23.8 kcal mol^{-1} for bromine, and the strongest bond is X—ONO_2, 39.6 kcal mol^{-1} for chlorine and 35.1 kcal mol^{-1} for bromine. XO—NO 30.3 kcal mol^{-1} for chlorine and 31.8 kcal mol^{-1} for bromine for the *cis* position, and 28.4 kcal mol^{-1} for chlorine and 29.6 kcal

mol^{-1} for bromine for the *trans* position, XO—NO_2 is 25.7 kcal mol^{-1} for chlorine and 29.3 kcal mol^{-1} for bromine (X=Cl, Br).

Results in this study show that the chlorine-nitrogen oxide bonds are stronger than the bromine-nitrogen oxide bonds by: ~10 kcal mol^{-1} for X—NO and X—NO_2, ~6 kcal mol^{-1} for X—ONO-cis/trans and ~4 kcal mol^{-1} for X—ONO_2. However, the XO—NO bonds are ~1.5 kcal mol^{-1} for bromine-nitrogen oxides, and the XO—NO_2 bond is 3.6 kcal mol^{-1}; stronger for bromine, than for chlorine.

Table 7.5 summarizes the literature bond dissociation enthalpies for HgCl, HgBr, $HgCl_2$, and $HgBr_2$, for comparison. The Hg—Cl bond dissociation enthalpy is 13.5 kcal mol^{-1} weaker than the Cl—NO bond, and the Hg—Br bond dissociation enthalpy is 10.5 kcal mol^{-1} weaker than the Br—NO bond.

Table 7.5 Literature reaction enthalpies of mercury chloride/bromide molecules (X=Cl,Br)

Species	$\Delta_{rxn}H°_{298}$	
	Cl	**Br**
X + Hg → HgX	-24.9	-16.5
X + HgX → HgX_2	-82.7	-72.6

Units: kcal mol^{-1}

Table 7.6 summarizes the enthalpies of formation of the mercury nitrogen oxide systems, calculated at the B3LYP/LANL2DZ, B3LYP/SDD, B2PLYP/AVTZ and M06-2X/AVTZ levels of theory, in conjunction with work reactions (summarized in Appendix AD).

Table 7.6 Calculated enthalpies of formation of mercury nitrogen oxide molecules

Species	$\Delta_f H°_{298}$			
	B3LYP/ LANL2DZ	**B3LYP/ SDD**	**B2PLYP/ AVTZ**	**M06-2X/ AVTZ (*)**
HgNO	43.93	40.96	36.88	33.87
$HgNO_2$	29.69	28.09	22.49	24.81
HgONO	37.70	39.75	44.00	39.40
NOHgNO	80.22	77.94	---	98.11
$NOHgNO_2$	45.29	43.52	57.30	55.38
NO_2HgNO_2	15.95	14.23	27.28	20.24

Units: kcal mol^{-1}
(*) Recommended

Results for chlorinated and brominated nitrogen oxides show that M06-2X/AVTZ is in very good agreement with the available literature data. In our previous study on the atmospheric mercury oxidation by the addition of chlorine, bromine and iodine[22] (see Chapter 6), it was shown that M06-2X/AVTZ accurately calculates the frequencies, geometries and energetics of the mercury halogen systems. Therefore, the values obtained with the M06-2X/AVTZ level of theory in conjunction with work reactions are recommended to use. B3LYP/LANL2DZ and B3LYP/SDD are ~10 kcal mol^{-1} high for most cases, and B2PLYP/AVTZ is ~3 kcal mol^{-1} high for all systems. Results show that NOHgNO and $NOHgNO_2$ are extremely unstable ($\Delta_f H°_{298}$ = 98.11 and 55.38 kcal mol^{-1}, respectively), and will not have relevance at atmospheric and combustion conditions.

Table 7.7 summarizes the reaction enthalpies calculated for the mercury-nitrogen oxide systems at the M06-2X/AVTZ levels of theory.

Table 7.7 Calculated reaction enthalpies of mercury nitrogen oxide molecules at the M06-2X/AVTZ level of theory

Species	$\Delta_{rxn}H°_{298}$	
Hg + NO → HgNO	-2.4	~ Stable
Hg + NO_2 → $HgNO_2$	2.2	Unstable
Hg + NO_2 → HgONO	16.8	Unstable
HgNO + NO → NOHgNO	42.7	Unstable
HgNO + NO_2 → $NOHgNO_2$	13.6	Unstable
$HgNO_2$ + NO → $NOHgNO_2$	9.0	Unstable
$HgNO_2$ + NO_2 → NO_2HgNO_2	-12.5	Stable

Units: kcal mol^{-1}

Results show that Hg—NO_2, Hg—ONO, NO—HgNO, NO—$HgNO_2$ and NOHg—NO_2 bonds are endothermic, and therefore will not form. Hg—NO has a very weak bond, ~2 kcal mol^{-1}. NO_2—$HgNO_2$ has the strongest bond dissociation enthalpy (12.5 kcal mol^{-1}). NO_2—$HgNO_2$ has a bond distance of 2.1 Å, whereas the Hg—NO_2 bond is 3.4 Å.

Tables 7.8 and 7.9 summarize the enthalpies of formation of the chlorinated and brominated mercury nitrogen oxide systems, respectively, calculated at the B3LYP/LANL2DZ, B3LYP/SDD, B2PLYP/AVTZ and M06-2X/AVTZ levels of theory, in conjunction with work reactions.

Table 7.8 Calculated enthalpies of formation of chlorinated mercury nitrogen oxide molecules

Species	$\Delta_fH°_{298}$			
	B3LYP/ LANL2DZ	**B3LYP/ SDD**	**B2PLYP/ AVTZ**	**M06-2X/ AVTZ (*)**
ClHgNO	22.26	19.23	27.82	28.98
$ClHgNO_2$	-10.01	-11.87	-5.48	-7.81
HgClNO	23.51	22.67	23.27	25.18
$HgClNO_2$	11.00	11.57	13.72	15.49

Units: kcal mol^{-1}
(*) Recommended

Table 7.9 Calculated enthalpies of formation of brominated mercury nitrogen oxide molecules

Species	$\Delta_f H°_{298}$			
	B3LYP/ LANL2DZ	**B3LYP/ SDD**	**B2PLYP/ AVTZ**	**M06-2X/ AVTZ**
BrHgNO	32.16	29.75	35.67	35.93
$BrHgNO_2$	0.09	-1.20	2.65	-1.00
HgBrNO	32.36	30.67	31.38	34.03
$HgBrNO_2$	19.36	19.16	20.52	22.39

Units: kcal mol^{-1}

The results obtained by the M06-2X/AVTZ of theory in conjunction with work reactions are recommended, as indicated above.

The enthalpies of reaction of the mercury – halogen – nitrogen oxide species are summarized in Table 7.10, calculated at the M06-2X/AVTZ level of theory.

Table 7.10 Calculated reaction enthalpies of chlorinated and brominated mercury nitrogen oxide molecules (X=Cl,Br) at the M06-2X/AVTZ level of theory

Species	$\Delta_{rxn}H°_{298}$	
	Cl	**Br**
Addition Reactions		
$HgX + NO \rightarrow XHgNO$	-11.4	-10.6
$HgX + NO_2 \rightarrow XHgNO_2$	-34.5	-33.8
$HgX + NO \rightarrow HgXNO$	-15.2	-12.5
$HgX + NO_2 \rightarrow HgXNO_2$	-11.2	-10.4
$X + HgNO \rightarrow XHgNO$	-33.9	-24.7
$X + HgNO_2 \rightarrow XHgNO_2$	-61.6	-52.5
$Hg + XNO \rightarrow HgXNO$	-2.6	-1.5
$Hg + XNO_2 \rightarrow HgXNO_2$	-1.4	-1.3
Insertion Reactions		
$Hg + XNO \rightarrow XHgNO$	1.2	0.5
$Hg + XNO_2 \rightarrow XHgNO_2$	-24.7	-24.8
$X + HgNO \rightarrow HgXNO$	-37.7	-26.6
$X + HgNO_2 \rightarrow HgXNO_2$	-38.3	-29.2

Units: kcal mol^{-1}

Dibble et al. determined the bond dissociation enthalpies of XHg—NO and XHg—NO_2 at the CCSD(T)/aug-cc-pVTZ-PP level of theory (11.7 and 35.6 kcal mol^{-1}, respectively, for bromine, and 13.0 and 36.6 kcal mol^{-1}, respectively, for chlorine)[258]. There is good agreement between their data and the data presented in this work at the M06-2X/aug-cc-pVTZ-PP level of theory (10.6 and 33.8 kcal mol^{-1}, respectively, for bromine, and 11.4 and 34.5 kcal mol^{-1}, respectively, for chlorine). The Cl—$HgNO_2$ and Br—$HgNO_2$ bonds (~50-60 kcal mol^{-1}) are significantly stronger than the rest of the bonds, but for its formation, $HgNO_2$ is needed, which is extremely unstable ($Hg+NO_2 \rightarrow HgNO_2$, $\Delta_{rxn}H°_{298}$=2.2 kcal mol^{-1}). ClHg—NO_2 and BrHg—NO_2 are relatively strong too (~34 kcal mol^{-1}), as well as Cl—HgNO and Br—HgNO (~25-34 kcal mol^{-1}).

Table 7.10 summarizes also the heats of reaction for the insertion reactions (~38 and ~28 kcal mol^{-1} for chlorine and bromine, respectively).

Figures 7.7 to 7.11 show the schematic representation and the nomenclature of the molecules studied in this work. Appendix AB includes the specifications of the optimized geometries and Appendix AC includes the frequencies of each of the species.

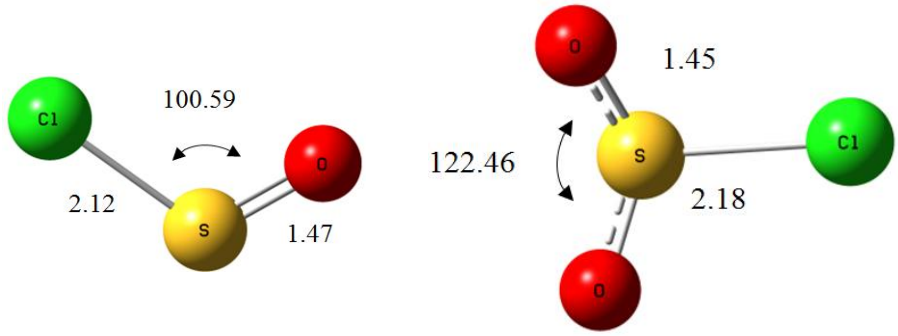

ClSO **$ClSO_2$**

Figure 7.7 Structure and nomenclature of the chlorine sulfur oxides studied

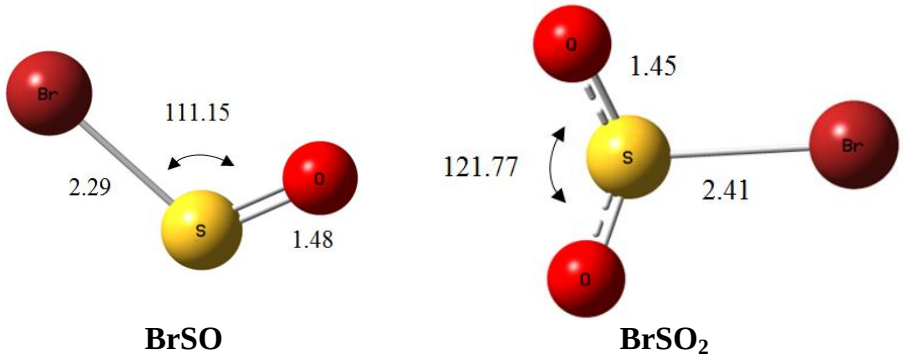

Figure 7.8 Structure and nomenclature of the bromine sulfur oxides studied

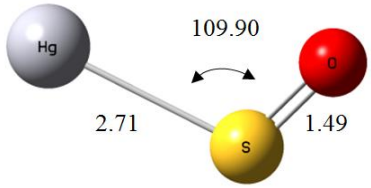

Figure 7.9 Structure and nomenclature of the mercury sulfur oxides studied

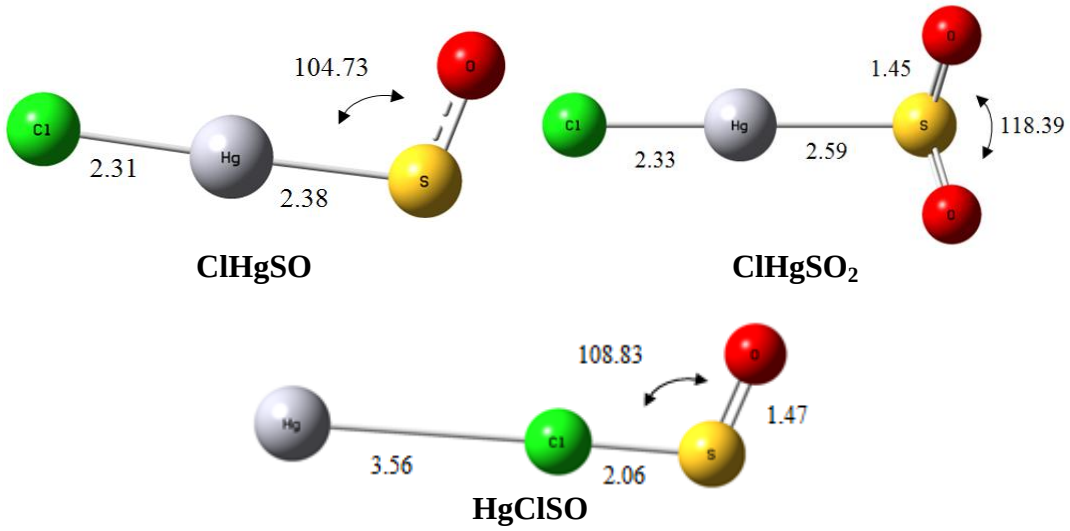

Figure 7.10 Structure and nomenclature of the mercury chloride sulfur oxides studied

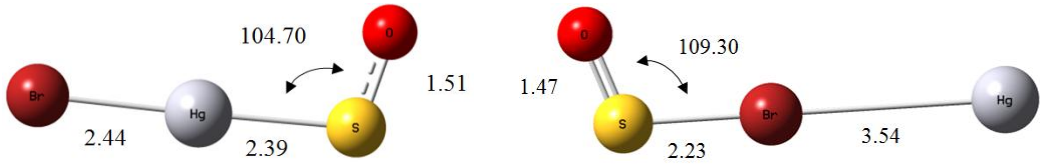

BrHgSO **HgBrSO**

Figure 7.11 Structure and nomenclature of the mercury bromide nitrogen oxides studied

Table 7.11 summarizes the heats of formation calculated for the chlorinated and brominated sulfur oxides at the different levels of theory.

Table 7.11 Calculated enthalpies of formation of chlorinated and brominated sulfur oxide molecules

Species	$\Delta_f H°_{298}$					
	CBS-QB3 (*)	**B3LYP/ LANL2DZ**	**B3LYP/ SDD**	**B2PLYP/ AVTZ**	**M06-2X/ AVTZ**	**Ref.**
ClSO	-24.58	-16.25	-17.39	-24.78	-22.53	*-24.50*[259]
$ClSO_2$	-57.47	-56.28	-58.69	-57.96	-56.29	*-53.95*[260], *-63.13*[261], *-49.65*[262]
BrSO	-14.15	-8.15	-10.04	-14.91	-12.91	
$BrSO_2$	-48.50	-41.65	-47.51	-50.47	-48.93	*-49.80*[260]

Units: kcal mol^{-1}
(*) Recommended

The heats of formation calculated at the CBS-QB3, B2PLYP/AVTZ and M06-2X/AVTZ levels of theory are in good agreement (±2.3 kcal mol^{-1} for ClSO, ±1.3 kcal mol^{-1} for $ClSO_2$, ±2 kcal mol^{-1} for BrSO and ±1.5 kcal mol^{-1} for $BrSO_2$, respectively). Results summarized in Table 7.11 show that CBS-QB3 is the most accurate level of theory among the studied methods to calculate the energetics of halogen-SOx species. The calculations performed at the CBS-QB3 level of theory are recommended (-24.58

kcal mol^{-1} for ClSO, -57.47 kcal mol^{-1} for $ClSO_2$, -14.15 kcal mol^{-1} for BrSO and -48.50 kcal mol^{-1} for $BrSO_2$).

Table 7.12 summarizes the X—SOx (X=Cl, Br) bond dissociation enthalpies, calculated at the CBS-QB3 level of theory.

Table 7.12 Calculated reaction enthalpies of chlorinated and brominated sulfur oxide molecules (X=Cl,Br) at the CBS-QB3 level of theory

Species	$\Delta_{rxn}H°_{298}$	
	Cl	**Br**
X + SO → XSO	-54.8	-42.1
X + SO_2 → XSO_2	-15.5	-4.3

Units: kcal mol^{-1}

The results show that the chlorinated sulfur oxides are more stable than the brominated sulfur oxides by 11-12 kcal mol^{-1}, and that ClSO and BrSO are more unstable than $ClSO_2$ and $BrSO_2$ by ~38 kcal mol^{-1}.

The bond dissociation enthalpies for the halogenated mercury species are summarized in Table 7.5. Compared to the chlorinated and brominated sulfur oxides, results show that XSOx species are more stable than HgX species. The X—SO bond dissociation enthalpies are 54.8 and 42.1 kcal mol^{-1} for chlorine and bromine, respectively (see Table 7.12), these are more stable than the X—NO bond dissociation enthalpies, 38.4 and 27.1 kcal mol^{-1} for chlorine and bromine, respectively (see Table 7.4). The X—SO_2 BDE's, are 15.5 and 4.3 kcal mol^{-1} for chlorine and bromine, respectively (see Table 7.12), results show that these are more unstable than the X—NO_2 BDE's, 34.6 and 23.8 kcal mol^{-1} for chlorine and bromine, respectively (see Table 7.4).

The calculated heats of formation of HgSO at the different levels of theory are summarized in Table 7.13. Table 7.14 summarizes the Hg—SOx bond dissociation enthalpies at the M06-2X/AVTZ level of theory.

Table 7.13 Calculated enthalpies of formation of the mercury nitrogen oxide

Species	$\Delta_f H°_{298}$			
	B3LYP/ LANL2DZ	**B3LYP/ SDD**	**B2PLYP/ AVTZ**	**M06-2X/ AVTZ (*)**
HgSO	27.07	26.87	33.68	36.74

Units: kcal mol^{-1}
(*) Recommended

Table 7.14 Calculated reaction enthalpies of the mercury nitrogen oxide at the M06-2X/AVTZ level of theory

Species	$\Delta_{rxn} H°_{298}$
Hg + SO → HgSO	20.9

Units: kcal mol^{-1}

No bonding is found for the formation of HgSO, $HgSO_2$, HgOSO, or $HgOSO_2$. The formation of Hg—SO is endothermic by 20.9 kcal mol^{-1}, and $HgSO_2$ is a loose complex identified but separated by distances of 4.3 Å. The formation of HgSO, $HgSO_2$, HgOSO, and $HgOSO_2$ are not relevant at atmospheric or combustion environments.

Starting with either HgCl or HgBr association with SO or SO_2 is found, forming X-Hg-SO and X-Hg-SO_2. Table 7.15 summarizes the heats of formation of the chlorinated and brominated mercury sulfur oxide molecules.

Table 7.15 Calculated enthalpies of formation of chlorinated and brominated mercury sulfur oxide molecules

Species	$\Delta_f H°_{298}$			
	B3LYP/ LANL2DZ	**B3LYP/ SDD**	**B2PLYP/ AVTZ**	**M06-2X/ AVTZ (*)**
ClHgSO	-20.92	-23.41	-13.03	-14.38
$ClHgSO_2$	-71.61	-67.65	-56.91	-59.81
HgClSO	-11.48	-10.81	-11.61	-9.94
BrHgSO	-9.46	-11.64	-4.36	-6.60
HgBrSO	-0.20	0.01	-0.85	0.37

Units: kcal mol^{-1}
(*) Recommended

The levels of theory B2PLYP/AVTZ and M06-2X/AVTZ are in very good agreement for all the molecules (±1-3 kcal mol^{-1}). B3LYP calculations with the smaller LANL2DZ and SDD basis sets show to have good agreement for HgClSO and HgBrSO (all the results are within ~1.5 kcal mol^{-1}), but show lower enthalpies of formation by ~10 kcal mol^{-1} for the rest of the species. From the calculations of bond distances, and frequencies performed to determine the accuracy of the levels of theory, it was concluded that M06-2X/AVTZ is the method that presents the best agreement with the literature theoretical and experimental data. Therefore, the heats of formation calculated at the M06-2X/AVTZ level of theory are recommended (-14.38 kcal mol^{-1} for ClHgSO, -59.81 kcal mol^{-1} for $ClHgSO_2$, -9.94 kcal mol^{-1} for HgClSO, -6.60 kcal mol^{-1} for BrHgSO and -59.24 kcal mol^{-1} for HgBrSO). Table 7.16 summarizes the bond dissociation enthalpies for the chlorinated and brominated mercury sulfur oxide molecules calculated at the M06-2X/AVTZ level of theory.

Table 7.16 Calculated reaction enthalpies of chlorinated and brominated mercury sulfur oxide molecules (X=Cl,Br) at the M06-2X/AVTZ level of theory

Species	$\Delta_{rxn}H°_{298}$	
	Cl	**Br**
Addition Reactions		
$HgX + SO \rightarrow XHgSO$	-34.3	-32.7
$HgX + SO_2 \rightarrow XHgSO_2$	-7.6	---
$HgX + SO \rightarrow HgXSO$	-29.9	-25.7
$X + HgSO \rightarrow XHgSO$	-80.1	-70.1
$Hg + XSO \rightarrow HgXSO$	0	-0.2
Insertion Reactions		
$Hg + XSO \rightarrow XHgSO$	-4.5	-7.1
$Hg + XSO_2 \rightarrow XHgSO_2$	-17.0	---
$X + HgSO \rightarrow HgXSO$	-75.7	-63.1

Units: kcal mol^{-1}

Table 7.16 summarizes also the heats of reaction for the insertion reactions, where $X + HgSO \rightarrow HgXSO$ is shown to be highly exothermic (63-75 kcal mol^{-1}). X—$HgSO_2$, XHg—SO and HgX—SO bonds are relatively strong (~25-35 kcal mol^{-1}). Results indicate, that once HgX intermediates are formed, they can further react with the SO and SO_2 present in the combustion effluents, to form XHgSO and $XHgSO_2$. Results show that X—HgSO bonds are significantly stronger (~70-80 kcal mol^{-1}) than the rest of the bonds. However, as discussed above, the formation of HgSO is not relevant at atmospheric and combustion effluents.

The entropy and heat capacity values for each of the systems studied are summarized in Table 7.17 for the nitrogen oxide species, and in Table 7.18 for the sulfur oxide species. Appendix AE includes the values of the entropy and heat capacity for 5-5000 K.

Table 7.17 Entropy and heat capacity versus temperature for the studied nitrogenated species

Species	$\Delta_f H^o_{298}$	S^o_{298}	Cp(T)						
			300 K	400 K	500 K	600 K	800 K	1000 K	1500 K
ClNO	24.54	61.05	8.94	9.35	9.70	10.01	10.51	10.87	11.37
BrNO	30.30	63.50	9.02	9.42	9.75	10.04	10.54	10.89	11.38
$ClNO_2$	2.34	64.97	10.90	12.21	13.28	14.13	15.33	16.07	16.99
$BrNO_2$	10.83	67.44	11.12	12.37	13.40	14.23	15.40	16.12	17.01
ClONO-cis	15.52	65.47	11.89	13.23	14.19	14.91	15.87	16.46	17.17
BrONO-cis	19.77	67.63	11.93	13.28	14.24	14.96	15.92	16.49	17.20
ClONO-trans	17.33	65.50	12.13	13.36	14.25	14.93	15.86	16.44	17.16
BrONO-trans	21.99	67.96	12.36	13.53	14.39	15.05	15.94	16.50	17.19
$ClONO_2$	6.42	68.49	13.75	15.95	17.62	18.87	20.53	21.53	22.71
$BrONO_2$	8.63	70.95	14.00	16.14	17.77	18.99	20.62	21.59	22.74
HgNO	43.93	71.37	9.92	9.99	10.11	10.28	10.64	10.93	11.38
$HgNO_2$	29.69	81.41	12.72	13.42	14.11	14.72	15.67	16.29	17.08
HgONO	37.70	72.37	12.66	13.69	14.51	15.15	16.04	16.58	17.24
NOHgNO	80.22	82.09	18.26	19.15	19.87	20.50	21.46	22.11	22.96
$NOHgNO_2$	45.29	86.41	20.67	22.27	23.59	24.68	26.27	27.29	28.55
NO_2HgNO_2	15.95	88.50	22.78	25.19	27.17	28.76	31.02	32.42	34.11
ClHgNO	22.26	75.62	14.53	15.18	15.65	16.03	16.58	16.94	17.41
BrHgNO	32.16	78.18	14.74	15.31	15.74	16.09	16.62	16.97	17.42
$ClHgNO_2$	-10.01	79.28	16.88	18.29	19.38	20.23	21.42	22.14	23.01
$BrHgNO_2$	0.09	81.82	17.18	18.48	19.51	20.33	21.47	22.18	23.02
HgClNO	23.51	81.50	14.47	15.06	15.49	15.85	16.40	16.79	17.31
HgBrNO	32.36	84.74	14.71	15.22	15.61	15.94	16.46	16.83	17.33
$HgClNO_2$	11.00	85.04	16.33	17.86	19.03	19.95	21.21	21.98	22.92
$HgBrNO_2$	19.36	86.56	16.76	18.16	19.26	20.12	21.32	22.06	22.96

Units: S(cal mol^{-1}) and Cp(kcal $mol^{-1} K^{-1}$)

Table 7.18 Entropy and heat capacity versus temperature for the studied sulfur species

Species	$\Delta_f H^o_{298}$	S^o_{298}	Cp(T)						
			300 K	400 K	500 K	600 K	800 K	1000 K	1500 K
ClSO	-24.58	63.90	9.54	10.10	10.52	10.84	11.23	11.45	11.70
BrSO	-57.47	66.40	9.70	10.21	10.61	10.90	11.27	11.48	11.71
$ClSO_2$	-14.15	68.73	12.86	14.04	14.93	15.58	16.41	16.88	17.41
$BrSO_2$	-48.50	71.66	13.08	14.16	15.00	15.62	16.43	16.89	17.41
HgSO	36.74	70.90	10.05	10.41	10.72	10.98	11.31	11.50	11.72
ClHgSO	-14.38	74.56	13.28	14.02	14.51	14.85	15.25	15.46	15.69
BrHgSO	-59.81	76.70	13.50	14.15	14.59	14.90	15.28	15.48	15.70
$ClHgSO_2$	-9.94	82.31	16.89	18.00	18.86	19.50	20.34	20.81	21.36
HgClSO	-6.60	79.55	13.05	13.75	14.26	14.63	15.09	15.35	15.64
HgBrSO	0.37	80.89	13.34	13.95	14.40	14.73	15.15	15.39	15.66

Units: S(cal mol^{-1}) and Cp(kcal mol^{-1} K^{-1})

Appendix AF includes the thermochemical properties of all the species included in the developed mechanism, in the NASA polynomial format.

7.3 Kinetic Properties

The rate constants were obtained from evaluation of literature values, and in the absence of actual rate data for the gas-phase reactions of mercury, Arrhenius constants ($k = AT^n \exp(-Ea/RT)$) were determined from the canonical transition state theory. Some kinetic parameters were estimated from similar reactions (generic reactions) and the known thermochemistry. Kinetics of small molecules in these system (several atoms species, example HgCl, $HgCl_2$, etc.) are in the low pressure or fall-off kinetic regions with strong functions of temperature and pressure in the kinetics. Therefore, association, dissociation and addition reactions were treated as chemical activation reactions with

quantum Rice Ramsperger Kassel (qRRK) analysis for k(E) and master equation for fall-off[103,263].

7.4 Reaction Mechanism

The mechanism developed in this study has been divided into 8 sub-mechanisms as described in Table 7.19. The mechanism incorporates elementary reaction kinetics and thermochemistry for: (1) mercury reaction with halogens (Cl, Br, I), hydroxides, nitrogen oxides (NOx) and sulfur oxides (SOx) with reactions taken from the literature[51,52,183,189-192,194,205] and developed during this study, (2) bromine reactions with hydroxides, nitrogen oxides (NOx), sulfur oxides (SOx) and C_1-C_2 hydrocarbons taken from the literature[264,265] and developed in this study, (3) chlorine reactions with hydroxides, nitrogen oxides (NOx), sulfur oxides (SOx) and C_1-C_2 hydrocarbons taken from the literature[264,266-268] and developed in this study, (4) iodine reactions with hydroxides, nitrogen oxides (NOx), and C_1-C_2 hydrocarbons hydrocarbons taken from the literature[264], (5) chlorine-bromine-iodine reactions taken from the literature[264], (6) hydroxide reactions (H_2, O_2) developed by Asatryan et al.[269], (7) nitrogen oxidation reactions developed by Bozzelli et al.[270], and (8) sulfur oxidation reactions developed by the University of Leeds[271]. Hydrocarbon reactions do not include molecular weight growth. The overall elementary reaction mechanism consists of 203 species and 957 reactions.

Table 7.19 Sub-mechanisms, number of reactions and species included in the elementary reaction mechanism

	Submechanism	# Species	# Reactions	Refs
1	**Mercury-Halogen-Hydroxide-NOx-SOx**	48	96	
	Mercury-Bromine			192,194, (*)
	Mercury-Bromine Hydroxide			51,52,191
	Mercury-Chlorine			192
	Mercury-Chlorine Hydroxide			183,189
	Mercury-Iodine			(*)
	Mercury-Chlorine-Bromine-Iodine			(*)
	Mercury-Hydroxide			(*)
	Mercury-NO_x			(*)
	Mercury-NO_x-Halogen			(*)
	Mercury-SO_x			(*)
	Mercury-SO_x-Halogen			(*)
2	**Bromine**	52	69	
	Bromine-Hydroxide			283, 77
	Bromine-NO_x			283, 77
	Bromine-SO_x			(*)
	Bromo-Methane oxidation			283, 77
3	**Chlorine**	59	234	
	Chlorine-Hydroxide			267,269-271
	Chlorine-NO_x			267,269-271
	Chlorine-SO_x			(*)
	Chloro-Methane oxidation			267,269-271
4	**Iodine**	26	40	
	Iodine-Hydroxide			283, 77
	Iodine-NO_x			283, 77
	Iodine-Methane oxidation			283, 77
5	**Halogens**	11	14	
	Bromine-Chlorine-Iodine			283, 77
6	**H_2/O_2**	10	21	
				269
7	**Nitrogen Oxidation / NO / NOx**	74	372	
				270
8	**Sulfur Oxidation / SO / SOx**	23	111	
				271

(*) Developed in this study

7.5 Kinetic Modeling Results

The ChemKin Collection[172] was used to set up and solve the differential equations for the developed mechanism. Rate constants for the reverse reactions are determined from the thermochemistry and the forward rate constants (reactions are thermodynamically consistent). The Aurora ChemKin package was used for the simulation of the initial combustion of natural gas. Figure 7.12 represents a schematic view of the simulation model used for the combustion of natural gas and air in the combustion chamber.

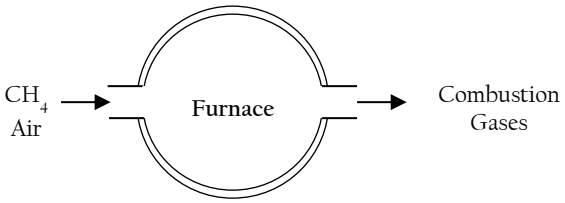

Figure 7.12 Schematic view of the simulation model for the combustion chamber

The Plug ChemKin package[172] was used to model the addition of the halogens in the furnace, and the cooling process until the combustion effluent arrives to the exhaust. Figure 7.13 represents a schematic view of the model. Different temperature profiles were used.

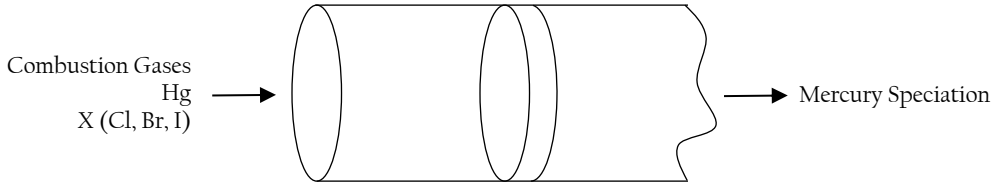

Figure 7.13 Schematic view of the simulation model for the addition of halogens and mercury in the furnace, plus the cooling process until the exhaust

The initial concentrations and temperature profiles were taken from the experimental studies carried out in the University of Utah[196,241,242] for comparison of the modeling results of this study with their experiment data. A natural-gas-fired combustor was used in their experiments. The initial natural gas and air concentrations used are summarized in Table 7.20. The initial concentrations and the concentration ranges used for the modeling of the combustion flue gases to study the oxidation of mercury are summarized in Table 7.21.

Table 7.20 Initial concentration of the natural gas and air burned in the combustion chamber

Species	Concentration (%)
CH_4	8
C_2H_6	0.4
C_3H_8	0.1
CO_2	0.1
O_2	19.2
N_2	72.2

Table 7.21 Initial concentrations of the combustion effluent

Species	Concentration
H_2	0.6 %
O_2	1.9 %
OH	0.6 %
H_2O	16.5 %
CO	1.4 %
CO_2	7.8 %
N_2	70.9 %
NOx	0-60 ppmv
SOx	0-400 ppmv
Cl	0-500 ppmv
Br	0-40 ppmv
I	0-30 ppmv

The conversion of mercury was determined as:

$$Hg(\%) = \frac{Hg_o - Hg_f}{Hg_o} 100 \tag{7.1}$$

where Hg_o is the initial mole fraction of mercury in the combustion flue gases, and Hg_f is the final mole fraction of mercury in the combustion flue gases.

The Utah Low Quench Temperature Profile, LQ (10-14-6), starts at 1181 K, achieves a maximum temperature of 1367 K and has a slow cooling rate of 210 K per second to obtain the final temperature of 617 K. The Utah High Quench Temperature Profile, HQ (12-14-6), starts at a slightly lower temperature of 1009 K, increases the temperature until the maximum of 1366 K, and has a faster cooling rate of 440 K/s, until it obtains the final temperature of 590 K. The 1600-600 K Temperature Profile, FQ6 (16-6), starts at 1600 K, and has a faster cooling rate, 660 K/s, to reach the final temperature of 600 K. The 1400-400 K Temperature Profile, FQ4 (10-14-4), starts at 1009 K, increases the temperature to a maximum of 1366 K, and after remaining for ~1 sec at the maximum temperature, cools down at 660 K/s, to a final temperature of 370 K. The 1400-400 K Long Temperature Profile, FQ13 (10-14-4), starts at 1009 K, increases the temperature to a maximum of 1366 K, and after remaining for ~2 sec at the maximum temperature, cools down at 660 K/s, to a final temperature of 370 K The temperature profiles studied are represented in Figure 7.14.

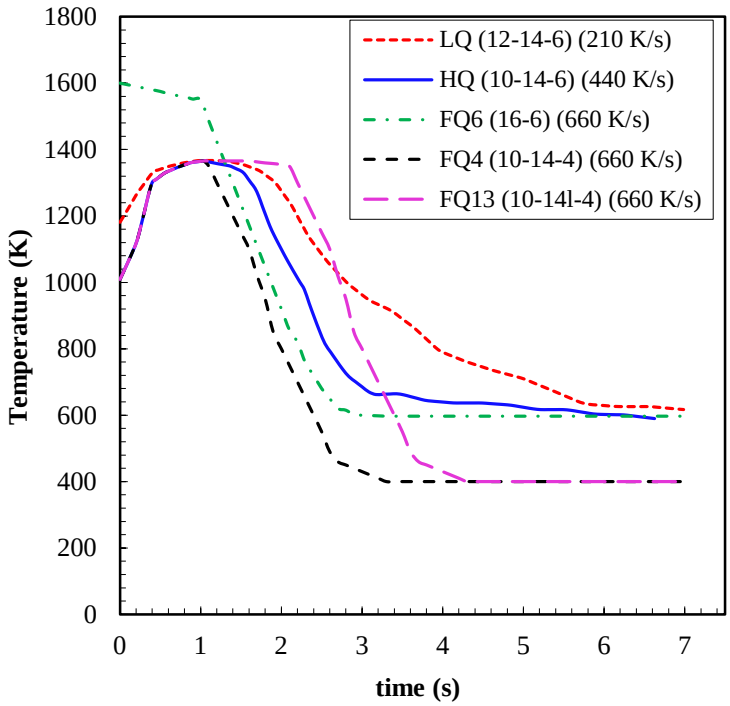

Figure 7.14 Temperature profiles used in Hg conversion mechanism runs

Simulations were carried out at the selected five quench temperature profiles, in order to determine the influence of the temperature profile on the oxidation of mercury by chlorine, bromine and iodine. The concentration of the halogens was varied, 0- 500 ppm for chlorine (HCl), 0- 40 ppm for bromine (HBr), and 0-30 ppm for iodine (HI) for each of the temperature profiles. Figures 7.15 to 7.17 illustrate the oxidation of mercury obtained when the halogens (chlorine, bromine and iodine, respectively) are added to the system, for each of the temperature profiles. The conversion is calculated as indicated in equation (7.1).

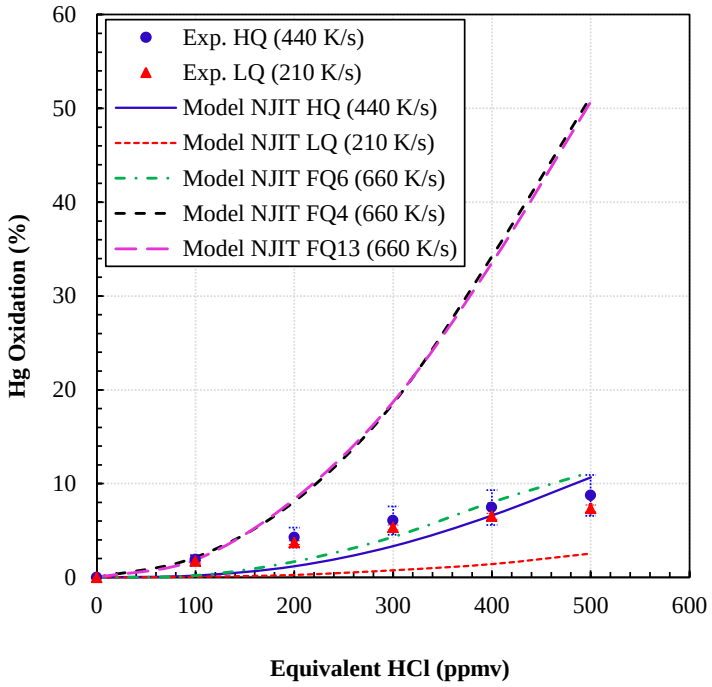

Figure 7.15 Mercury oxidation by the addition of chlorine

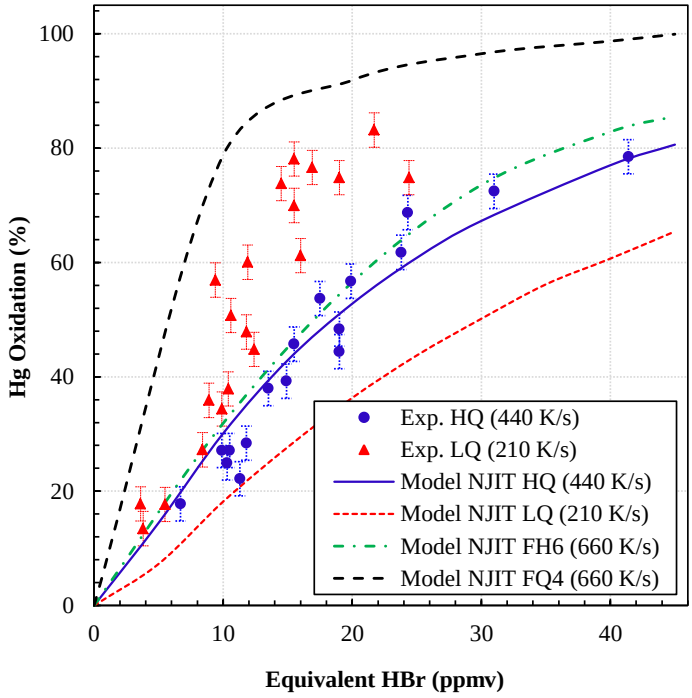

Figure 7.16 Mercury oxidation by the addition of bromine

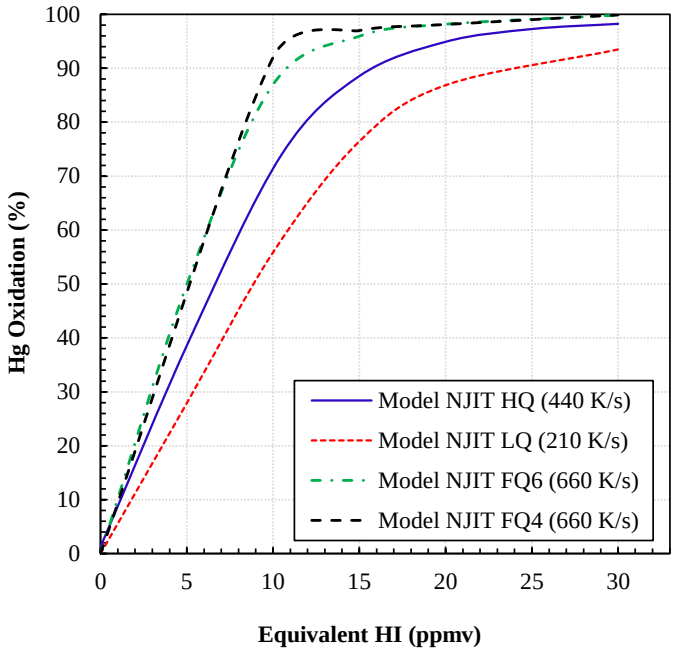

Figure 7.17 Mercury oxidation by the addition of iodine

Results show that the higher temperature quench rate provides a higher conversion of mercury compared to the lower temperature quench profile for all the halogens, and that the temperature profile (FQ6) that has the fastest quench (660 K/s) and finishes at the lowest temperature (370 K) provides the highest conversion of mercury for all chlorine, bromine and iodine addition. Calculation results indicate that the longer stay at the higher temperatures (temperature profile FQ13 compared to FQ4) does not result in a higher conversion of mercury. All temperature profiles have a high temperature region (1400-1600 K), which is necessary for the formation of the radical pool, so that mercury reacts with the atomic halogen (Hg + X → HgX). However, the higher quench temperature profile (FQ4, 660 K/s) has a longer residence time at the lower temperatures (370 K), which is necessary to keep some of the concentration of the unstable HgX species, so that HgX can further react to form the much more stable HgX_2. Figures 7.18 and 7.19 illustrate the concentration of HgCl and $HgCl_2$, respectively versus time for the

different temperature profiles. The calculation results show that the formation of HgCl starts as soon as the system starts quenching, as well as the formation of $HgCl_2$. The conversion of mercury stops when the system achieves the stable low temperature.

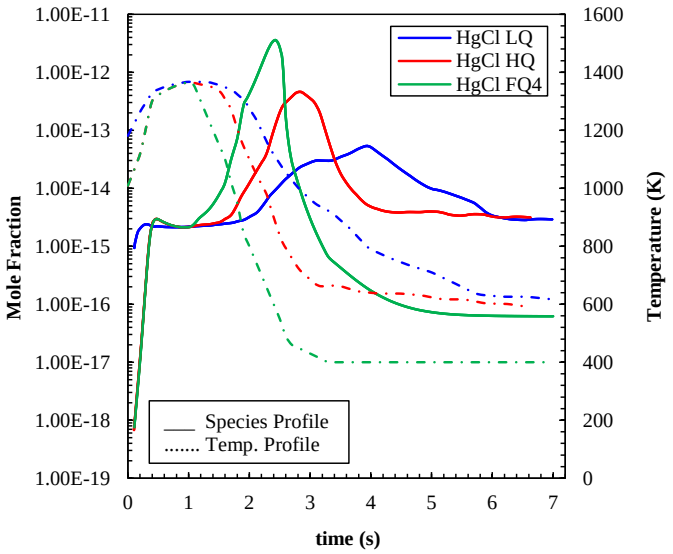

Figure 7.18 Mole fraction of HgCl versus time for initial NO of 30 ppm, and Cl of 500 ppm, for each of the temperature profiles

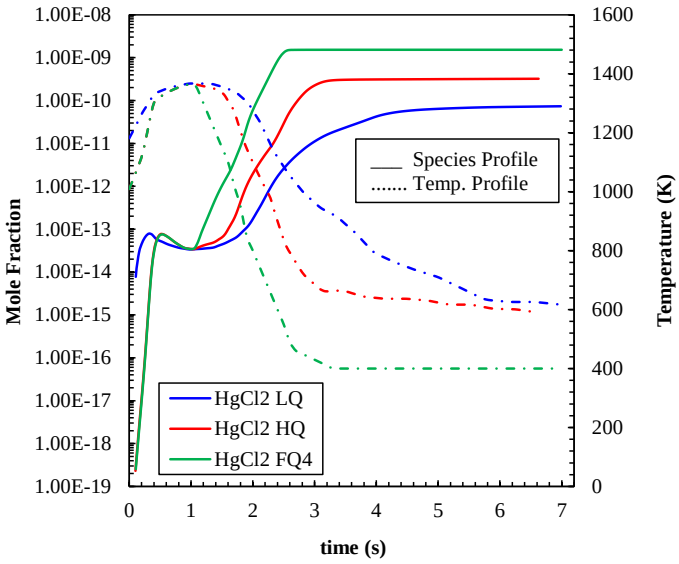

Figure 7.19 Mole fraction of HgCl versus time for initial NO of 30 ppm, and Cl of 500 ppm, for each of the temperature profiles

Table 7.22 summarizes the heats of reaction for the mercury halogen reactions discussed (Hg—X bond are very weak, 24.9, 13.5 and 8.3 kcal mol^{-1} for chlorine, bromine and iodine, respectively, whereas the XHg—X bonds are significantly stronger, 82.7, 72.0 and 61.3 kcal mol^{-1} for chlorine, bromine and iodine, respectively).

Table 7.22 Enthalpies of reaction of the studied Hg/Cl, Hg/Br and Hg/I reactions

Reactions	ΔH_{rxn}		
	Cl	**Br**	**I**
Hg + X ↔ HgX	-24.91	-13.53	-8.29
HgX + X_2 ↔ HgX_2 + X	-24.72	-25.95	-25.16
Hg + X_2 ↔ HgX + X	33.07	29.56	27.83
HgX + X ↔ HgX_2	-82.70	-72.04	-61.28
Hg + X_2 ↔ HgX_2	-49.63	-42.48	-33.45

Units: kcal mol^{-1}

Additionally, the species mole fraction profiles for hydrogen atom (H) and hydroxide (OH) (see Figures 7.20 and 7.21, respectively), show that the higher quench temperature profile leads to a decrease in their concentration, which means that less chlorine reacts with free hydrogen atoms, and there is more free chlorine available to oxidize mercury.

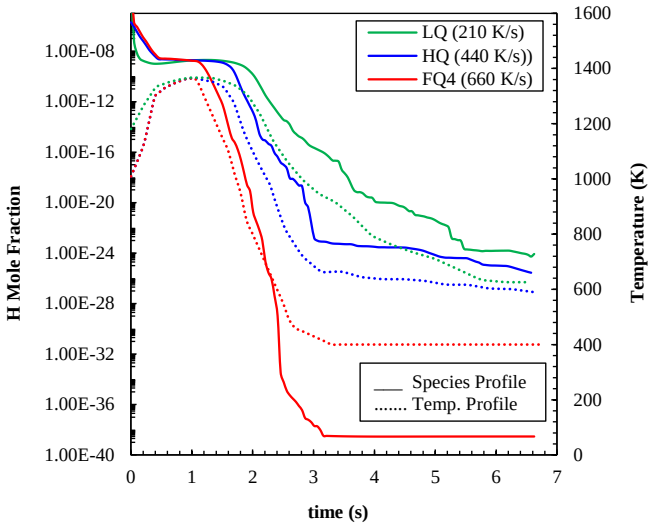

Figure 7.20 Mole fraction of hydrogen atom (H) versus time for initial NO of 30 ppm, and Cl of 500 ppm

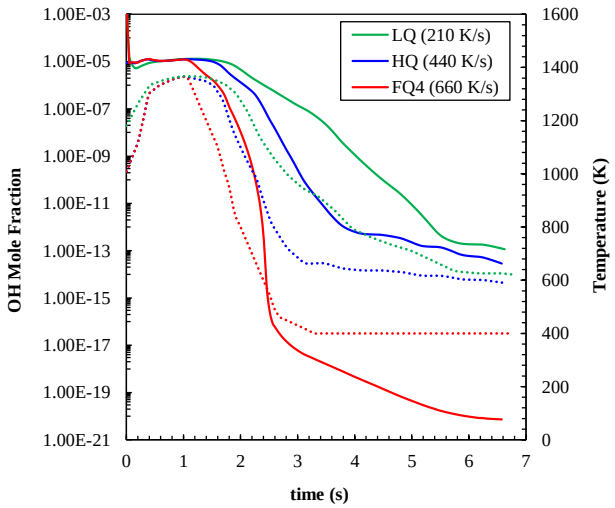

Figure 7.21 Mole fraction of hydroxide (˙OH) versus time for initial NO of 30 ppm and Cl of 500 ppm

The profile of the mole fraction of ClO versus time (see Figure 7.22) shows that higher quench temperature profiles lead to the formation of lower concentrations of ClO, which results on having more free chlorine in the system to convert mercury into its oxidized form.

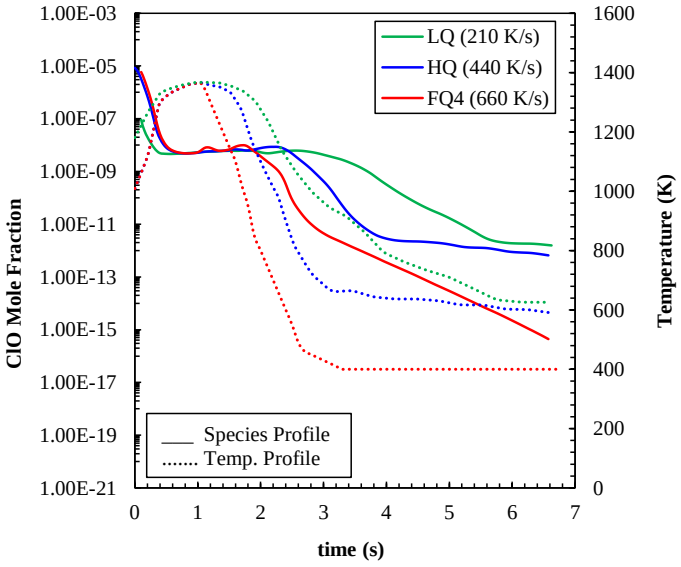

Figure 7.22 Mole fraction of ClO versus time for initial NO of 20 ppm, and Cl of 500 ppm

The results obtained from the simulations for chlorine and bromine were compared with the experimental results obtained by Van Otten et al.[242] in Figures 7.15 and 7.16, respectively. Results for chlorine (see Figure 7.15) show reasonable agreement for the high quench temperature profile, but the mercury conversion predicted by the mechanism developed in this study for the lower temperature profile is lower than that obtained experimentally. Results for bromine (see Figure 7.16) show good agreement for the high quench temperature profile, but the modeling results predict that the lower quench temperature profile results in a lower conversion of mercury (as for chlorine), whereas their experimental results show that the lower quench temperature profile, results in a higher conversion of mercury.

The concentration of HCl in the flue gas is usually in the order of 1-150 ppmv depending on the type of coal burned (bituminous or sub-bituminous). However, the concentration of iodine and bromine in the flue gases is much lower (0-3 ppm). Figure 7.23 shows a comparison between the conversion obtained by the addition of chlorine, bromine and iodine for the high quench temperature profile.

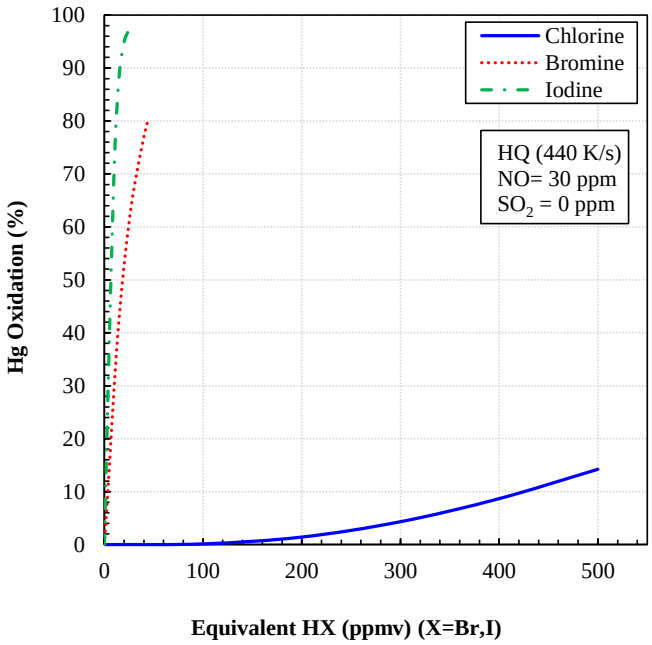

Figure 7.23 Mercury oxidation by the addition of chlorine, bromine and iodine

Results indicate that iodine and bromine are significantly more efficient for the conversion of mercury, than chlorine. The addition of significantly smaller concentrations of bromine and iodine would result in almost total conversion of mercury.

The Hg—Cl and ClHg—Cl bonds are stronger than the correspondent bonds for bromine and iodine (Hg—X bond 24.9, 13.5 and 8.3 kcal mol^{-1} for chlorine, bromine and iodine, respectively, and XHg—X bonds 82.7, 72.0 and 61.3 kcal mol^{-1} for chlorine, bromine and iodine, respectively). However, results indicate that chlorine is much less effective when oxidizing mercury. Figures 7.24 to 7.29 show the profiles of the mole fraction of the mercury and halogen species versus time. Figure 7.24, 7.26 and 7.28 show that mercury is oxidized mainly to $HgCl_2$, $HgBr_2$ and HgI_2, which was expected, since these species are much more stable than HgCl, HgBr and HgI.

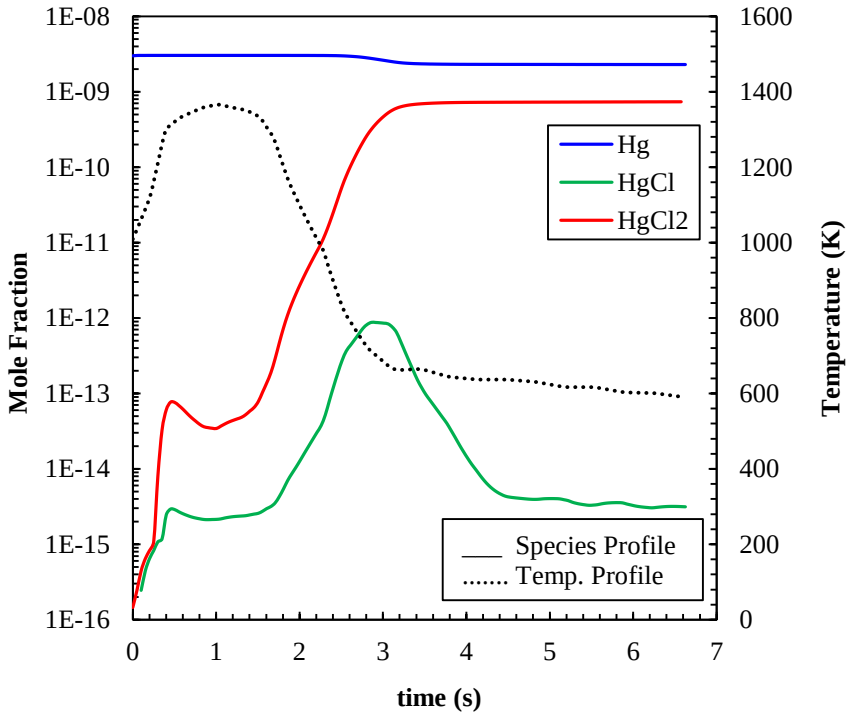

Figure 7.24 Mole fraction of Hg, HgCl and $HgCl_2$ vs. time for initial NO of 30 ppm, and Cl of 500 ppm

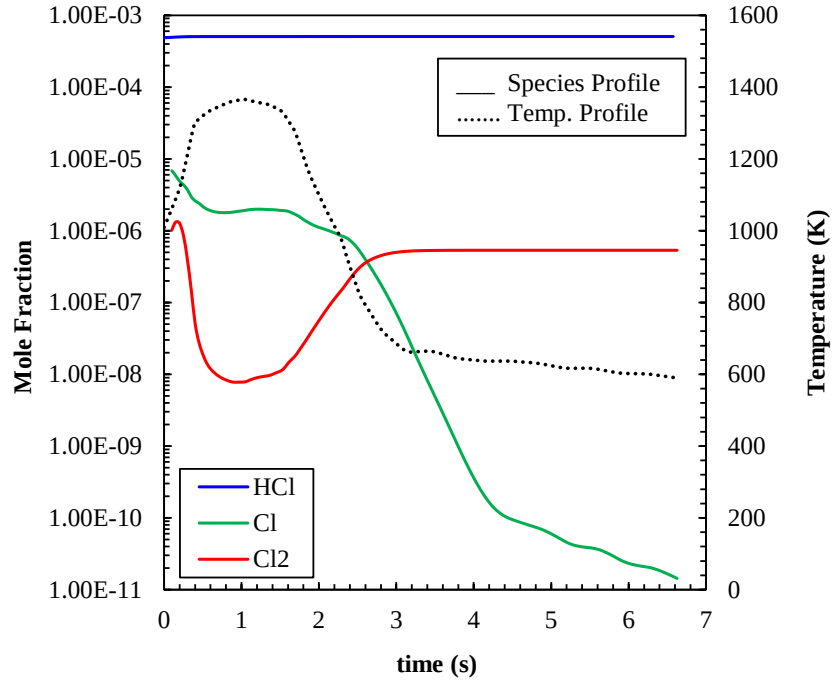

Figure 7.25 Mole fraction of HCl, Cl and Cl_2 vs. time for initial 30 ppm NO and 500 ppm Cl

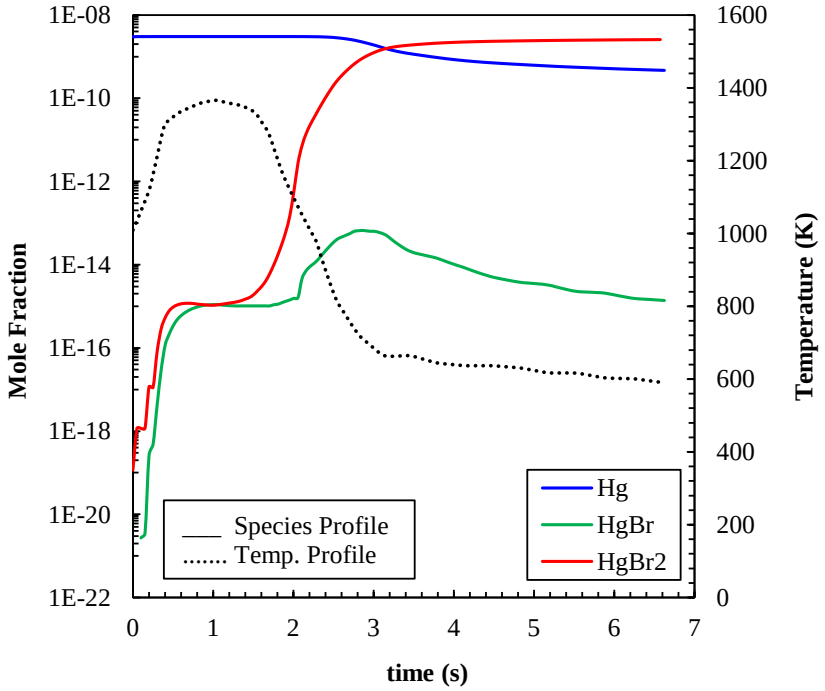

Figure 7.26 Mole fraction of Hg, HgBr and $HgBr_2$ vs. time for initial 30 ppm NO and 40 ppm Br

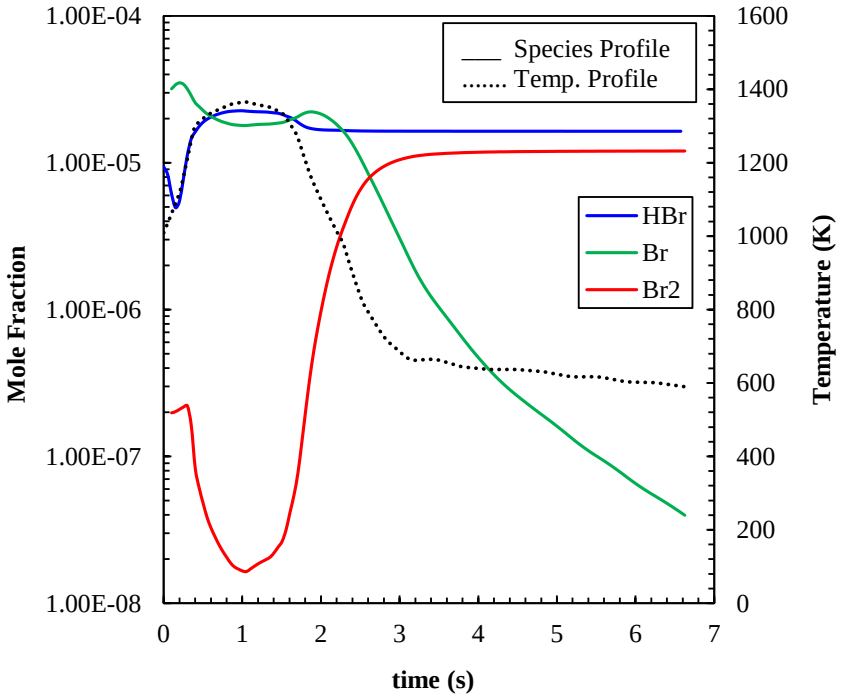

Figure 7.27 Mole fraction of HBr, Br and Br_2 vs. time for initial NO of 30 ppm and Br of 40 ppm

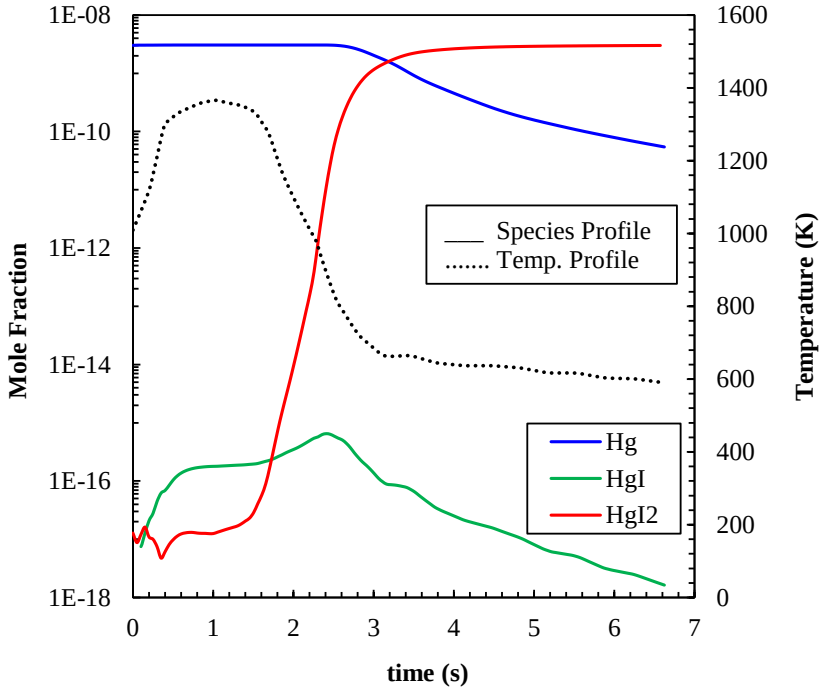

Figure 7.28 Mole fraction of Hg, HgI and HgI_2 vs. time for initial NO of 30 ppm and I of 30 ppm

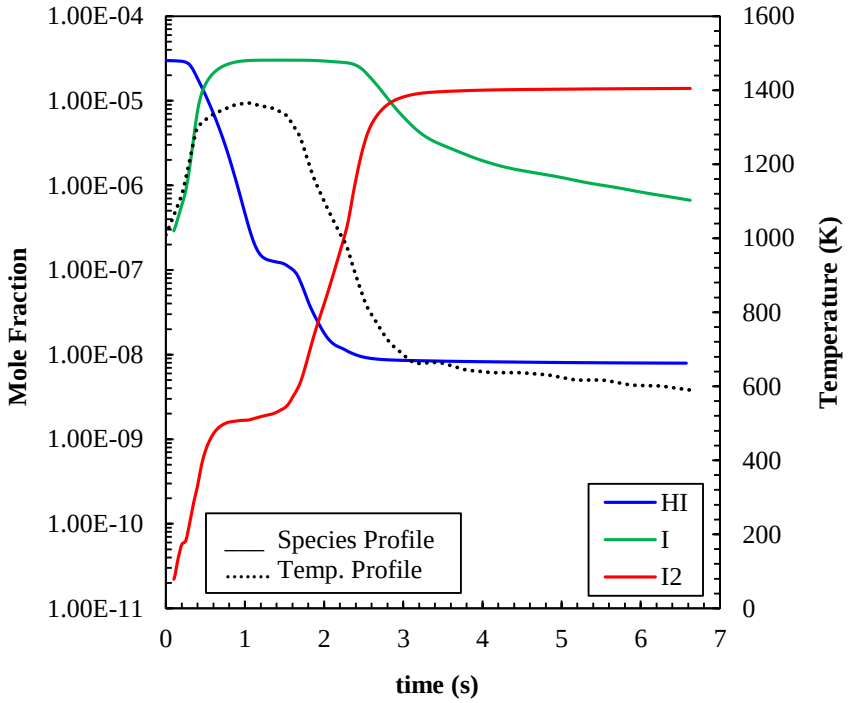

Figure 7.29 Mole fraction of HI, I and I_2 vs. time for initial NO of 30 ppm and of I 30 ppm

Figure 7.25 shows that when chlorine is added to the system, the chlorine will be mainly present as HCl, because of its strong H-Cl bond (103.1 kcal mol^{-1}), which means that not much chlorine will be available to react with mercury. However, in the case of bromine, it is observed that HBr is not dominant (bond dissociation enthalpy is 87.6 kcal mol^{-1}), which results in more bromine atoms being available to react with mercury (see Figures 7.26 and 7.27). For iodine, the decomposition of HI is significant (bond dissociation enthalpy is 71.3 kcal mol^{-1}), which explains the efficiency of iodine when oxidizing mercury (see Figures 7.28 and 7.29).

The influence of NOx on the oxidation of mercury by the addition of chlorine and bromine has been evaluated by several experimental and theoretical studies. However several of these studies present opposing results. Laudal et al.[272] studied the oxidation of mercury in the presence of different concentrations and combinations of fly ash, NO/NO_2, SOx, HCl, and Cl_2. Their results showed that when no NOx was present in the system, the conversion was 84.8%, whereas in the presence of NOx the conversion of mercury dropped to 78.7%. Niksa et al. predicted through their modeling results[273] that the lowest NO concentrations ([NO]<20 ppm) enhance the conversion of mercury, whereas higher concentrations of NO inhibit homogeneous Hg oxidation, and they state that no oxidation of mercury is observed for NO concentrations above100 ppm. Qiu and Helble[244] showed that NO inhibits mercury conversion, especially at lower concentrations of Cl_2. Byun et al. showed experimentally[274], that when the NO concentration increased from 0 to 7 ppm in the presence of $NaClO_2$(s), the Hg oxidation increased significantly to give almost 100% of Hg oxidation, but that further increase of the NO concentration resulted in monotonic decrease of the Hg oxidation to about 60% at 180 ppm NO. The

presence of the $NaClO_2$ makes the analysis more complex. Van Otten et al.[242] concluded that increasing the NO concentration in the flue gas had no effect on Hg oxidation by chlorine or bromine, but their previous experimental study did report an inhibition effect of NO on the conversion of mercury[275].

Figure 7.30 shows the modeling results obtained in this study. Results indicate that the presence of NO significantly decreases the oxidation of mercury by the addition of chlorine (Cl = 500 ppmv), decreases slightly the oxidation of mercury by the addition of bromine (Br = 40 ppmv), and does not have much effect when iodine (I= 30 ppmv) is added to the system.

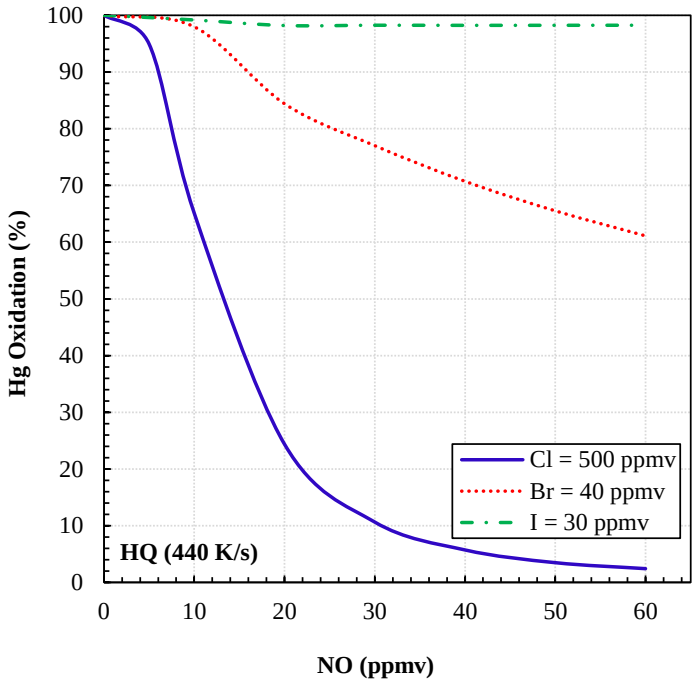

Figure 7.30 Influence of NO on the oxidation of mercury by addition of HCl, HBr or HI

Explanation for the inhibition of NO in the system includes formation of species such as X—NO where some are formed by reaction of HgX. For example, the reaction of HgX + NO → XNO + Hg is exothermic and decreases the HgX concentration. Analysis

of X—Hg bond energies includes: Cl—NO bonds are the strongest, followed by Br—NO and I—NO (see Table 7.23). In the presence of NO, several, exothermic, catalytic cycles for loss of Cl to HCl (mainly) and Cl_2 can occur, inhibiting mercury oxidation, see Table 7.24. Once ClNO is formed, it can react with OH (ClNO + OH → HOCl + NO, ΔH_{rxn}= -18.1 kcal mol^{-1}), taking away OH from the system, which will inhibit mercury conversion.

Table 7.23 Enthalpies of reaction for halogen NO reactions

Reactions	**ΔH_{rxn}**		
	Cl	**Br**	**I**
OH + XNO → HOX + NO	-18.1	-25.5	-31.3
H + X → HX	-103.1	-87.6	-71.3
X + NO → XNO	-38.4	-27.1	-20.3

Units: kcal mol^{-1}

Table 7.24 Catalytic cycle of the halogen-NOx reactions

Reactions	**ΔH_{rxn}**			**Reactions**	**ΔH_{rxn}**		
	Cl	**Br**	**I**		**Cl**	**Br**	**I**
X + NO → XNO	-38.4	-27.1	-20.3	X + NO → XNO	-38.4	-27.1	-20.3
X + XNO → X_2 + NO	-19.6	-19.0	-15.8	H + XNO → HX + NO	-64.7	-60.5	-51.0
X + X → X_2	-58.0	-46.1	-36.1	H + X → HX	-103.1	-87.6	-71.3

Units: kcal mol^{-1}

Figures 7.31, 7.32 and 7.33 show the concentrations of NO, XNO, HONO and HOX (X=Cl,Br,I), for the chlorine, bromine and iodine systems, respectively.

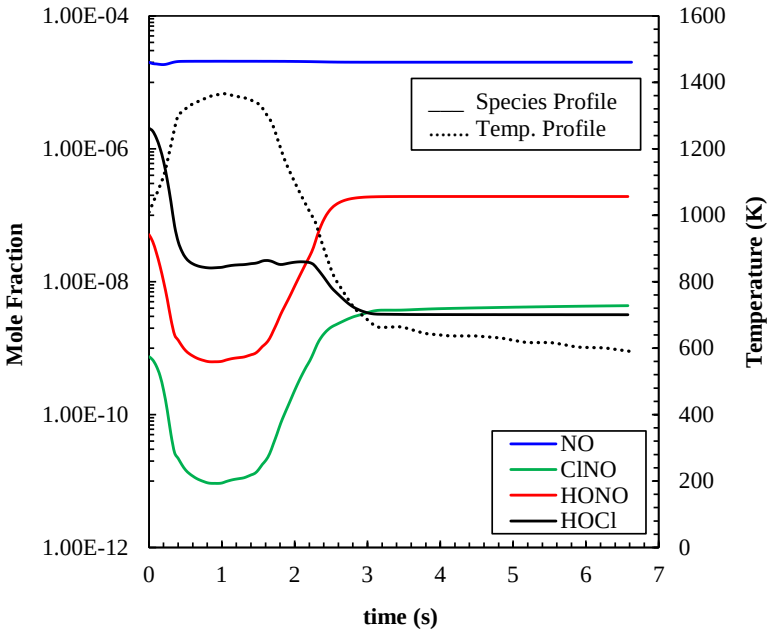

Figure 7.31 NO, ClNO, HONO and HOCl mole fractions versus time, for initial NO of 30 ppm, and Cl of 500 ppm

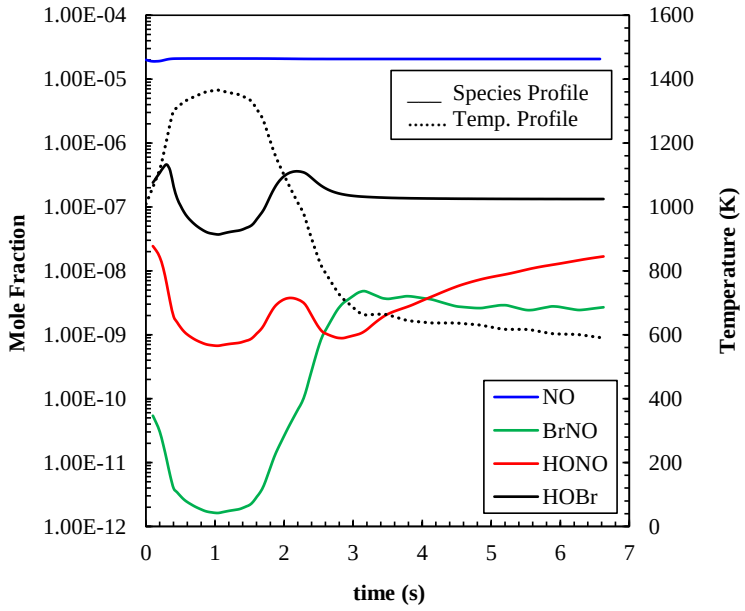

Figure 7.32 NO, BrNO, HONO and HOBr mole fractions versus time, for initial NO of 30 ppm and Br of 40 ppm

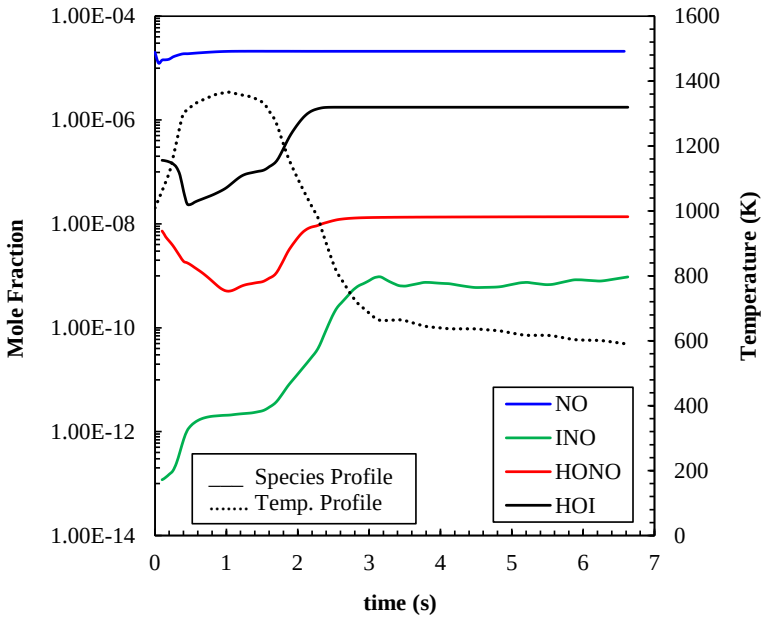

Figure 7.33 NO, INO, HONO and HOI mole fractions versus time, for initial NO of 30 ppm and I of 30 ppm

The species profiles in Figures 7.31 to 7.33 show the importance of the formation of HONO and HOX (X=Cl,Br,I) in all cases. However, because of the strong H—Cl bond, the influence of NO is stronger in the case when chlorine is added to the system. NO reacts with the OH produced by the radical pool (NO + OH → HONO, ΔH_{rxn}= 49.7 kcal mol^{-1}), taking away OH that reacts with other radicals present. If these reactions are inhibited, there will be more free H that can react with Cl (Cl + H → HCl, ΔH_{rxn}= 103.1 kcal mol^{-1}). Consequently, there will not be chlorine available to react with mercury. The sensitivity analysis of the reaction HONO + M → OH + NO + M, indicates that the increase in the formation on HONO, significantly reduces the conversion of mercury (see Figure 7.34). Figure 7.35 shows that the higher concentrations of NO leads to a higher formation of HONO, which results in a decrease in the concentration of OH in the reaction system (see Figure 7.36). The decrease of OH, implies that more H atoms are available to react with Cl atoms, and therefore, the concentration of Cl atoms also

decreases (see Figure 7.36). The decrease in the concentration of Cl atoms causes the decrease of the formation of the intermediate HgCl, and the decrease in the formation of the final product $HgCl_2$ (see Figure 7.37).

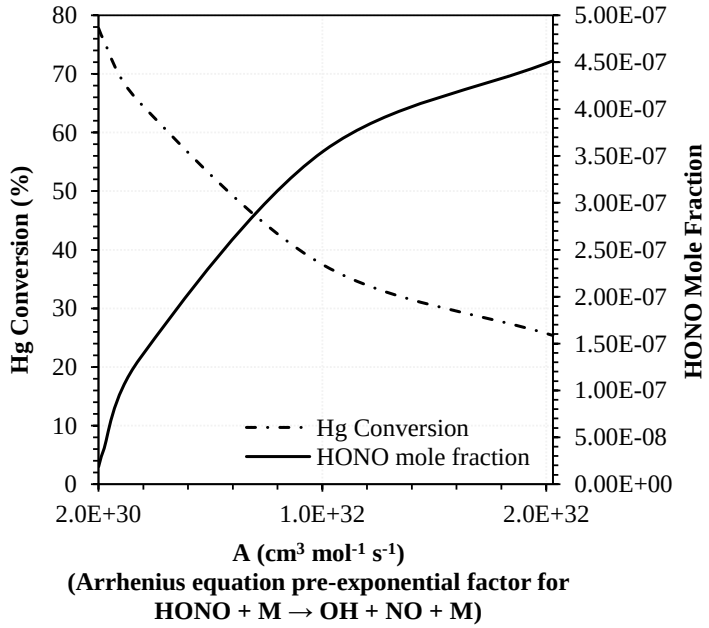

Figure 7.34 Sensitivity analysis of the HONO + M → OH + NO + M reaction

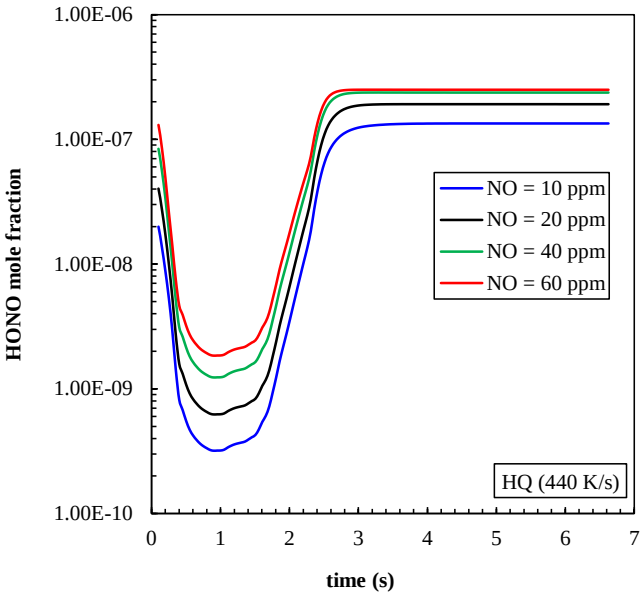

Figure 7.35 Concentration of HONO versus time, for different initial NO concentrations

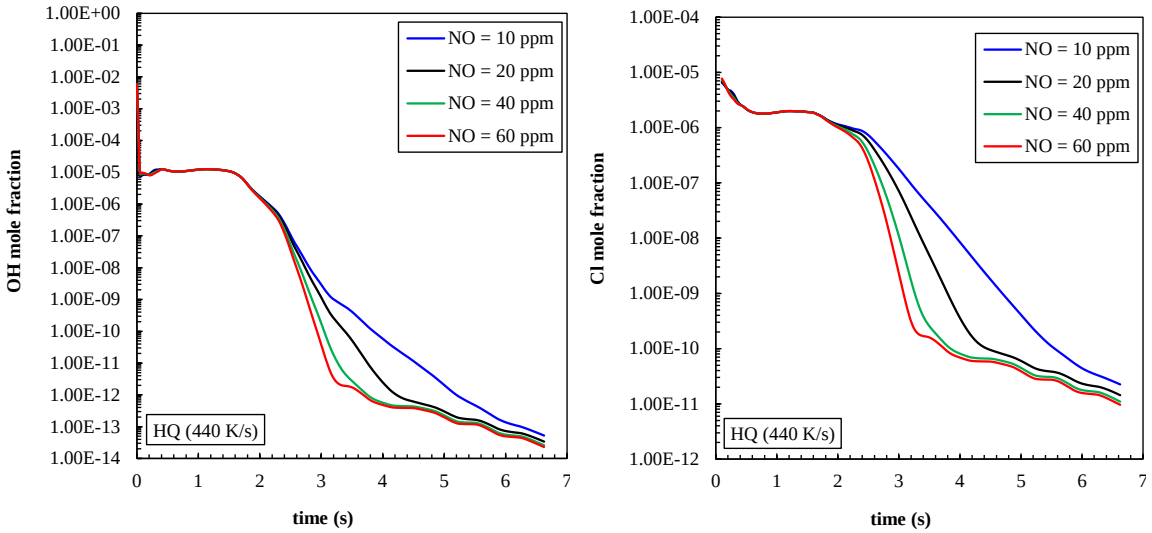

Figure 7.36 Concentration of OH and Cl versus time, for different initial NO concentrations

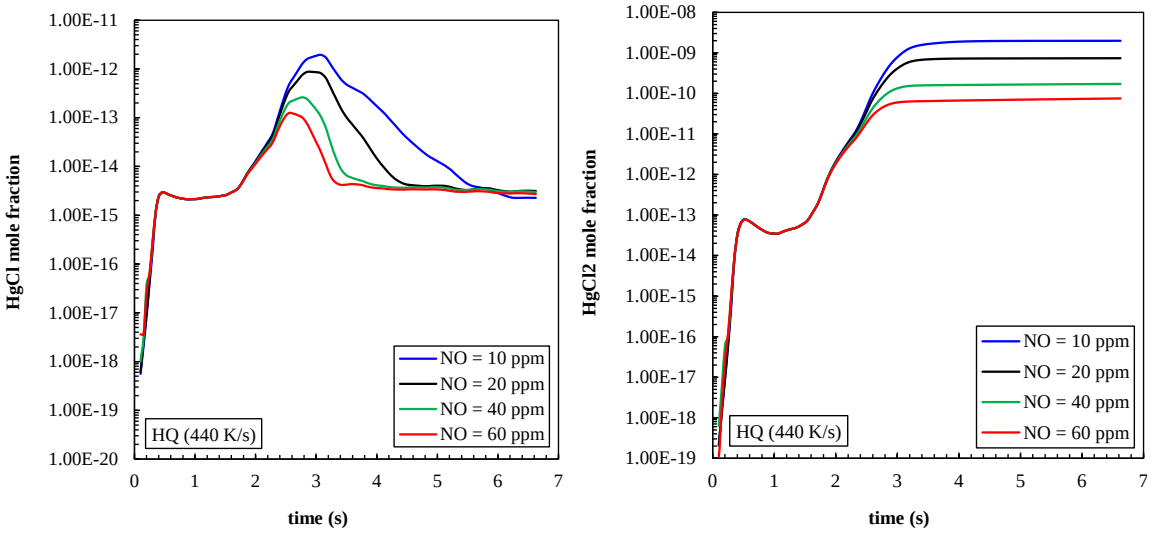

Figure 7.37 Concentration of HgCl and $HgCl_2$ versus time, for different initial NO concentrations

The effects of SO_2 on the conversion of mercury from the literature results are not well established. Ghorishi[243] showed that SO_2 can inhibit mercury oxidation with chlorine. Laudal et al.[272] showed that in the presence of SO_2, mercury conversion decreased from 84.8% to 1.9%, concluding that SO_2 has a significant inhibiting influence

on mercury conversion. Additionally, Qiu and Helble[244] illustrated the decrease on the oxidation of mercury when increasing the concentration of SOx in the system. They studied the oxidation of mercury by the addition of 250 ppm of HCl with different concentrations of SO_2 (0, 100, 400 and 500 ppm) resulting on an oxidation of 67.7, 46.4, 29.7 and 21.9%, respectively, and by the addition of 500 ppm of HCl with different concentrations of SO_2 (0, 100, and 400 ppm) resulting on an oxidation of 94.5, 77.4, and 62.4%, respectively. In 2005, Lighty et al.[275] reported that when 300 ppm SO_2 were added to the oxidation system, the mercury conversion dropped ~50%, for 500 ppm HCl. However, in their work from 2011, Van Otten et al.[242] concluded that SO_2 did not have a significant effect on mercury oxidation by chlorine, except when the HCl concentration was higher than 400 ppmv. Smith et al.[276] observed both inhibition and enhancement of mercury oxidation by chlorine when SO_2 was added to the system. They showed that when both HCl and SO_2 were present, mercury oxidation was enhanced in the presence of SO_2 when the concentration of HCl was 200 ppmv and inhibited when concentration of HCl was 555 ppmv.

Results of the modeling calculations are illustrated in Figure 7.38, for two different NO concentrations (NO=10 ppm, left, and NO=30 ppm, right).

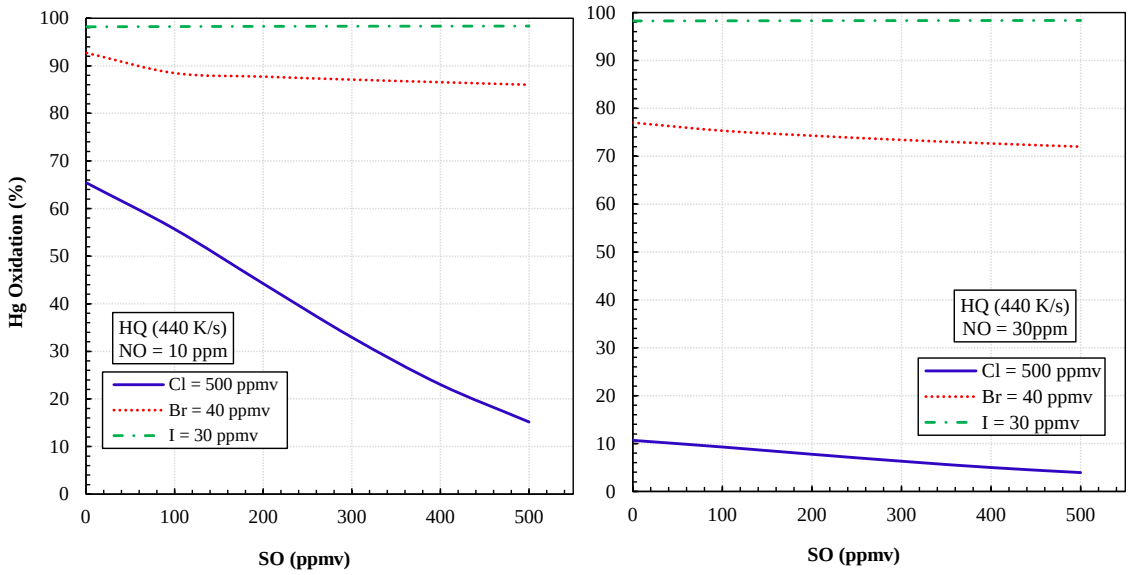

Figure 7.38 Influence of SO_2 on the oxidation of mercury, for initial NO of 10 ppm (left) and NO of 30 ppm (right) by addition of Cl, HBr, or HI

SO_2 is much more stable (ΔH_f =-70.96 kcal mol^{-1}) than SO (ΔH_f=1.20 kcal mol^{-1}), and consequently in combustion systems, sulfur is present mainly as SO_2. Therefore, in this work the influence of the addition of SO_2 in the combustion system is studied. Results indicate that the presence of SO_2 decreases the oxidation of mercury by the addition of chlorine (Cl = 500 ppmv), specially at the lower concentrations of NO, and does not have much effect when bromine (Br = 40 ppmv) or iodine (I= 30 ppmv) are added to the system

SO_2 reacts mainly to form SO_3. The reactions that affect the conversion of mercury mainly are $SO_2 + OH \rightarrow SO_3 + H$ and $SO_2 + O (+M) \rightarrow SO_3 (+M)$. This explains why chlorine gets more affected by SO_2 than bromine and iodine. Additionally, X—SO_2 bonds are weaker than the X-NO bonds (see Table 7.25), which would explain why the influence of NOx is larger than the influence of SO_2 in the conversion of mercury.

Table 7.25 Heats of reaction for halogen SO reactions

Reactions	ΔH_{rxn}		
	Cl	**Br**	**I**
$X + NO \rightarrow XNO$	-38.4	-27.1	-20.3
$X + SO_2 \rightarrow XSO_2$	15.5	4.3	---

Units: kcal mol^{-1}

Niksa et al. predicted in their simulations[273] that the addition of moisture to the system inhibited the oxidation of mercury (they observed the Hg oxidation decreased from 100% to 54% when 8% of moisture was added to the system). Figure 7.39 summarizes the results obtained in this study for the effect of varying vapor water concentration (from 5 to 45%) on the oxidation of mercury, for two different concentrations of NO (10 ppm and 30 ppm).

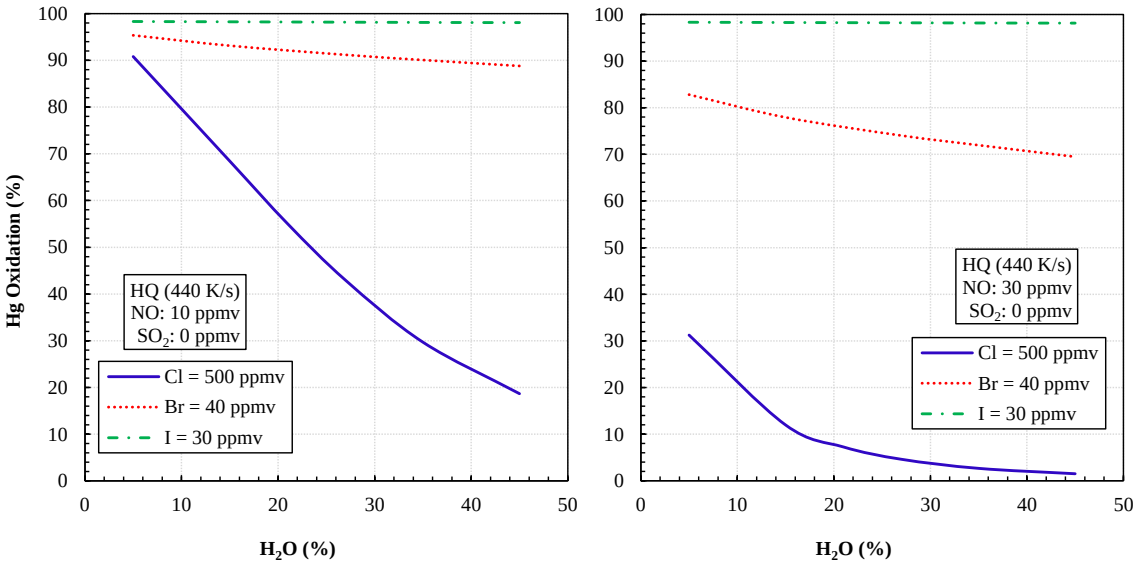

Figure 7.39 Influence of H_2O on the oxidation of mercury, for initial NO of 10 ppm (left) and NO of 30 ppm (right)

Results show that the presence of water inhibits Hg oxidation. The conversion of mercury decreases from 31.2 to 1.5% when the concentration of water is increased for a concentration of NO of 30 ppm. For a concentration of NO of 10 ppm, the conversion of mercury decreases significantly more, from 90.8 to 18.7%. As the concentration of H_2O increases, the main reason of this inhibition is the reaction $H_2O + Cl \rightarrow OH + HCl$ (ΔH_{rxn} = 15.5 kcal mol^{-1}), which inhibits the decomposition of HCl and consequently decreases the conversion of mercury by chlorine. The influence on the conversion of mercury is smaller when bromine is added. The conversion of mercury decreases from 82.8 to 69.5% for initial NO of 30 ppm, and from 95.3 to 88.8% for initial NO of 10 ppm. Calculation results show that the influence on the oxidation of mercury by addition of iodine is independent from the concentration of vapor water in the combustion system.

The impact of the modification of the fuel to air equivalence ratio on the oxidation of mercury was also studied. The fuel-air equivalence ratio is defined as indicated in Equation (7.2).

$$\phi = \frac{n_{fuel} / n_{oxidizer}}{\left(n_{fuel} / n_{oxidizer} \right)_{stoichiometric}} \tag{7.2}$$

where n_{fuel} are the moles of the fuel, and $n_{oxidizer}$ are the moles of air (21% O_2 and 79% N_2). Fuel-rich mixtures (ϕ>1) represent an excess of fuel and fuel-lean mixtures (ϕ<1), represent an excess of oxidizer. The fuel used in this study is CH_4, which has the stoichiometric ratio ($n_{fuel}/n_{oxidizer}$) of 0.105. The results in Figure 7.40 show that fuel lean mixtures (ϕ<1) lead to higher conversions of mercury for all chlorine, bromine and iodine addition.

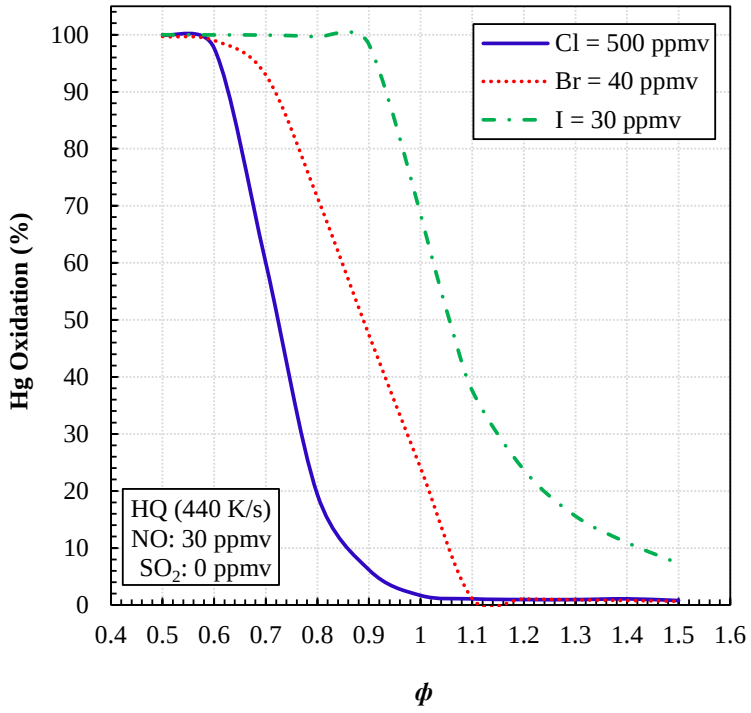

Figure 7.40 Influence of the equivalence ratio (ϕ) on the oxidation of mercury

For fuel-lean mixtures (excess of oxidizer) there is an excess of O_2 and the concentration of hydrogen is lower compared to fuel-rich mixtures. The presence of O_2 increases the oxidation of hydrocarbons and H_2 to H_2O and carbon to CO_2, and shifts the HCl concentration toward H_2O and Cl_2 allowing the halogen to oxidize Hg.

7.6 Summary

An elementary reaction mechanism (957 reactions, 203 species) developed from fundamental principles of thermodynamics and statistical mechanics is evaluated for the study of the removal of mercury by the addition of halogens (chlorine, bromine and iodine). Results illustrate, that the use of high quench temperature profiles (660 K/s) that finish at lower temperatures (370 K) lead to an increase in the conversion of mercury, that iodine and bromine are more effective than chlorine (very small concentrations of

iodine- 30 ppm - and bromine – 40 ppm – lead to >90% conversion of mercury), that NO, SO_2 and H_2O inhibit mercury conversion (significantly for the addition of chlorine, and only slightly for the addition of bromine and iodine), and that the use of fuel lean mixtures enhances the oxidation of mercury by chlorine, bromine and iodine.

CHAPTER 8

CONCLUSIONS

This work presents thermochemical, kinetic and modeling results on two reference fuels (the land vehicle fuel isooctane and the jet fuel JP-10), on smaller cyclic alkanes and ethers, and on the oxidation of mercury by the addition of halogens, in atmospheric and combustion environments.

Thermochemical parameters are presented at the B3LYP/6-31G(d,p) and CBS-QB3 level of theory for the secondary isooctane radical, the secondary isooctane hydroperoxide, the corresponding peroxy radical, and three hydroperoxy alkyl radical adducts. Thermochemical data are also presented for 14 product sets from unimolecular reactions of the adducts. Transition state structures and rate constants are presented for each of the reaction paths. The kinetic analysis shows that at low and high pressures (in the range of 1-100 atm), and temperatures above 1000 K, the main reaction channels are the formation of isooctene $(CH_3)_3CCH=C(CH_3)_2 + HO_2^{\bullet}$, and the formation of the cyclic ether $(CH_3)_3C(CHCO)(CH_3)_2$. At low temperatures (below 1000 K) the formation of the adduct - $(CH_3)_3CCH(OO^{\bullet})CH(CH_3)_2$ - is the dominant reaction channel. The study highlights the important of the formation of isooctane in the oxidation of isooctane at all temperatures. Moreover, this work notes that at low temperatures, the formation of the cyclic ethers is important, and needs to be well characterized and included in combustion mechanisms.

The enthalpies of formation, entropies and heat capacities of TCD hydroperoxides, peroxy radicals, alkyl/peroxy diradicals, TCD alkohols, alkoxy radicals,

dialkoxy diradicals and oxygenated cyclic species resultant from the oxidation of TCD were determined in this study, at the B3LYP/6-31G(d,p) Density Functional Theory level of theory in conjunction with a series of work reactions. The OO—H, O—H and R—OOH bond dissociation enthalpies are presented for the different positions of the tricyclodecane hydroperoxides and dialcohols. Results show that the bond dissociation enthalpies for most molecules are similar of that for cyclopentane, and for the linear alkanes. However, for some of the positions, the bond dissociation enthalpies are ±4 kcal mol^{-1} versus the values for cyclopentane, and the linear alkanes. The accurate bond dissociation enthalpies presented in this study is important for the construction of fundamental reaction mechanisms. Rate constants are presented for the unimolecular dissociation of the radicals and diradicals resultant from the C—H bond cleavage and C—C ring opening of the parent molecule TCD, as well as the chemical activation of the radicals/diradicals with molecular oxygen $^3O_2$, for introduction in the TCD pyrolysis and oxidation reaction mechanisms. Results show that at the low temperatures and higher pressures, the formation of oxygenated cyclic species becomes important. At high temperatures, the intramolecular hydrogen transfer reactions and beta-scission reactions are dominant. The thermochemical and kinetic properties calculated in this study were incorporated in a reaction mechanism, where further reactions of initial intermediates and products to complete oxidation are included, with the aim of determining the pyrolysis and oxidation characteristics of the jet fuel JP-10.

The study on the oxidation of isooctane and JP-10 in this work has highlighted the need of defining the thermochemical properties of small cyclic alkane and ether systems, as well as the importance of determining their oxidation and unimolecular dissociation

kinetics. This study presents thermochemical properties for the 3 to 5 member ring cyclic alkanes and ethers, their corresponding alkyl radicals, peroxy radicals, and hydroperoxyalkyl radicals. Additionally, the thermochemical properties for ring opening, unimolecular dissociation and oxidation reactions of parent and intermediate radicals for C_3 to C_5 cyclic alkane and C_2 to C_4 cyclic ether systems are presented. Kinetics for unimolecular dissociation, oxidation and intramolecular H atom transfer reactions are assembled and implemented in detailed mechanisms to evaluate importance of unimolecular dissociation versus oxidation of the diradicals. The thermochemical results of this study show the differences in the thermochemistry of cyclic alkane and ethers, and highlights the importance of determining accurate thermochemical properties for the small ring systems, in order to construct models that will predict reliable fuel characteristics. The kinetic results show that unimolecular-low energy β-scission reactions and intramolecular H abstraction reactions are important at all temperatures and dominate at high temperatures, bi-molecular oxidation reactions have some importance at lower to moderate temperatures, and cyclization reactions to smaller ring intermediates are important at low to moderate temperatures. Intermediates react mainly to lower energy products CH_2O and $CH_2{=}CH_2$ for the alkane systems and to CH_2O and unsaturated oxygenated alkenes (e.g. $CH_3CH_2OCH{=}CH_2$) from the cyclic ethers.

As for mercury, results show that a fundamentally based reaction mechanism and kinetic parameters found in the literature do not predict any significant formation of HgX_2 or loss of Hg under atmospheric conditions relative to that observed in the experimental studies. The same complete lack of conversion occurs when trying to reproduce the experimental data using the rate constants developed in this study (with

thermodynamically consistent reverse reactions with pressure dependence for the chemical activation and dissociation reactions are incorporated), when the insertion reactions ($Hg + X_2 \rightarrow HgX_2$) are included. The modeling results confirm that if the experiments had a source of X atoms, the reactions $Hg + X \rightarrow HgX$ and $HgX + X \rightarrow HgX_2$ dominate the Hg oxidation, and the experimentally observed mercury loss could be justified.

An elementary reaction mechanism developed from fundamental principles of thermodynamics and statistical mechanics has been developed in this work for the study of the removal of mercury by the addition of halogens (chlorine, bromine and iodine) from combustion effluents. Results illustrate that halogens serve to efficiently reduce the emissions of elemental mercury from coal burning plants. Results show that iodine and bromine are more effective than chlorine to convert mercury, and that the use of high quench temperature profiles that finish at lower temperatures lead to an increase in the conversion of mercury. Additionally, results illustrate that NO, SO_2 and H_2O inhibit mercury conversion (significantly for the addition of chlorine, and only slightly for the addition of bromine and iodine), and that the use of fuel lean mixtures enhances the oxidation of mercury by chlorine, bromine and iodine.

APPENDIX A

ENTHALPY OF FORMATION OF REFERENCE SPECIES

Appendix A includes the enthalpies of formation at 298 K of the reference species used in the isodesmic work reactions for the calculation of the enthalpies of formation of the target molecules.

Table A.1 Enthalpy of formation of reference species at 298 K for hydrocarbon systems

Species	$\Delta H°_{f\,298}$	Ref.	Species	$\Delta H°_{f\,298}$	Ref.
CH_3CH_3	-20.04 ± 0.07	77	CH_3OOH	-30.93 ± 0.2	277
$CH_3CH_2^{\bullet}$	28.4 ± 0.5	77	CH_3CH_2OOH	-39.5 Ave.	127,278
$CH_3CH_2CH_3$	-25.02 ± 0.12	279	$CH_3CH_2OO^{\bullet}$	-6.17 Ave.	127,278
$CH_3CH_2^{\bullet}CH_3$	22.00 ± 0.5	280	$CH_3CH_2CH_2OOH$	-43.09 ± 0.3	127
$CH_3CH_2CH_2^{\bullet}$	23.9 ± 0.5	77	$CH_3CH_2CH_2OO^{\bullet}$	-10.53	277
$CH_3CH_2CH_2CH_3$	-30.04 ± 0.14	167	$CH_3CH_2CH_2CH_2OOH$	-43.09 ± 0.2	277
$CH_3CH^{\bullet}CH_2CH_3$	16.00 ± 0.5	167	$CH_3CH_2CH_2CH_2OO^{\bullet}$	-16	277
$CH_3CH_2CH_2CH_2^{\bullet}$	18.04 ± 0.07	77	$CH_3CH(OOH)CH_3$	-49.11 ± 0.2	278
$CH_3CH_2CH_2CH_2CH_3$	-35.08 ± 0.14	281	$CH_3CH(OO^{\bullet})CH_3$	-16.48 ± 0.2	282
$CH_3CH_2CH_2CH^{\bullet}CH_3$	11.16 ± 0.5	167	$(CH_3)_2CHOOH$	-47.86 ± 0.3	127
$CH_3CH_2CH_2CH_2CH_2^{\bullet}$	13.81	(*)	$(CH_3)_2CHOO^{\bullet}$	-14.88 ± 0.3	127
$CH_3CH_2CH_2CH_2CH_2CH_3$	-39.94	283	$(CH_3)_3COOH$	-57.20 ± 0.2	127
$(CH_3)_3CCH_3$	-40.14 ± 0.15	284	$(CH_3)_3COO^{\bullet}$	-24.67 ± 0.2	127
$(CH_3)_3CCH_2CH_3$	-44.35 ± 0.23	284	$CH_3CH_2OOCH_2CH_3$	-46.12	285
$(CH_3)_3CCH_2CH_2CH_3$	-49.29 ± 0.32	284	CH_3OCH_3	-43.99 ± 0.12	77
$(CH_3)_3CH$	-32.07 ± 0.15	286	$CH_3OCH_2^{\bullet}$	0.10	287
$(CH_3)_3^{\bullet}CH$	17.00 ± 0.5	167	$HOCH_2OH$	-91.03	(*)
$CH_3C^{\bullet}(CH_3)_2$	11.00 ± 0.7	167	$HOCH_2O^{\bullet}$	-39.07	(*)
$(CH_3)_2CHCH_2CH_3$	-36.92 ± 0.20	288	$CH_3CH_2O^{\bullet}$	-4.24	(*)
$(CH_3)_2CHCH^{\bullet}CH_3$	10.01	(*)	$HOCH_2CH_2OH$	-92.00	(*)
$CH_3(CH_3)CHCH_3$	-32.07 ± 0.15	77	$HOCH_2CH_2O^{\bullet}$	-40.04	(*)
$CH_3(CH_3)CHCH_2^{\bullet}$	17.0 ± 0.5	77	$CH_3CH_2OCH_3$	-51.73 ± 0.16	77
$(CH_3)_3CCH(CH_3)_2$	-48.96 ± 0.27	284	$CH_2^{\bullet}CH_2OCH_3$	-2.50	(*)
$(CH_3)_3CC^{\bullet}(CH_3)_2$	-4.8 [(a)]	289	CH_3OCH_2OOH	-70.23	(*)
$(CH_3)_3^{\bullet}CC(CH_3)_3$	-4.92 [(a)]	289	$CH_3OCH_2OO^{\bullet}$	-36.03	(*)
$(CH_3)_3CCH_2CH(CH_3)_2$	-53.57 ± 0.32	284	$CH_3OCH_2CH_2OOH$	-71.20	(*)
$(CH_3)_3CCH_2CH_2CH(CH_3)_2$	-60.49 [(a)]	283	$CH_3OCH_2CH_2OO^{\bullet}$	-37.00	(*)
$(CH_3)_2C=C(CH_3)_2$	-16.80 ± 0.16	290	$CH_3OCH_2CH_2OH$	-87.30	(*)
$(CH_3)_2C=CHCH_3$	-9.92 ± 0.21	43	$CH_2^{\bullet}CH_2CH_2OCH_3$	-7.43	(*)
$CH_3CH=C(CH_3)CH_2CH_3$	-14.79 ± 0.21	43	$CH_3CH_2OCH_2CH_2^{\bullet}$	-10.80	(*)
$(CH_3)_2CHCH_2CH=CH_2$	-11.82 ± 0.16	43	$CH_3CH_2OCH_2CH_2OOH$	-79.50	(*)
$(CH_3)_3CC(=O)CH_3$	-69.47 [(a)]	291	$CH_3CH_2OCH_2CH_2OO^{\bullet}$	-45.30	(*)
$CH_3CH_2CH(=O)$	-45.09 [(a)]	163	$CH_3OCH_2CH_2CH_2OOH$	-76.13	(*)
$HOCH_2CH_2CH_2OH$	-96.93	(*)	$CH_3OCH_2CH_2CH_2OO^{\bullet}$	-41.93	(*)
$HOCH_2CH_2CH_2CH_2OH$	-101.86	(*)	$CH_3OCH_2CH_2OO^{\bullet}$	-35.34	(*)
$HOCH_2CH_2CH_2CH_2CH_2OH$	-106.79	(*)	$HOCH_2OCH_2O^{\bullet}$	-77.50	(*)
$HOCH_2CH_2CH_2O^{\bullet}$	-44.97	(*)	$HOCH_2CH_2CH_2O^{\bullet}$	-44.97	(*)
$HOCH_2CH_2CH_2CH_2O^{\bullet}$	-49.9	(*)	$HOCH_2OCH_2CH_2O^{\bullet}$	-78.47	(*)

Units: kcal mol^{-1}

(*) This work

Table A.1 Enthalpy of formation of reference species at 298 K for hydrocarbon systems (Continued)

Species	$\Delta H°_{f\,298}$	Ref.
$HOCH_2CH_2CH_2CH_2CH_2O^{\bullet}$	-54.83	(*)
CH_3CH_2OH	-56.04 ± 0.5	77
$CH_3CH_2O^{\bullet}$	-3.1 ± 0.2	283
$CH_3CH_2CH_2OH$	-61.2 ± 0.7	77
$CH_3CH_2CH_2O^{\bullet}$	-7.91 ± 0.2	283
$CH_3CH_2CH_2CH_2OH$	-66.0	77
$CH_3CH_2CH_2CH_2O^{\bullet}$	-14.1	(*)
$y(CH_2CH_2CH_2)$	12.74 ± 0.12	107
$y(CH_2CH_2CH_2CH_2)$	6.62 ± 0.26	107
$y(CH_2CH_2CH_2CH_2CH_2)$	-18.26 ± 0.17	107
$y(CH_2CH_2CH_2CH_2CH_2CH_2)$	-29.43	293
$y(CH_2CH_2CH_2CH_2CH_2CH_2CH_2)$	-37.4	294
$y(CH_2CHO)(CH_3)(CH_3)$	-32.6	295
$y(CH_2CHO)(CH_3)_2(CH_3)$	-42.11	295
$y(CH_2CH_2CH_2CHO)\ CH_3$	-54.58	44

Species	$\Delta H°_{f\,298}$	Ref.
$HOCH_2CH_2OCH_2CH_2O^{\bullet}$	-79.44	(*)
$HOCH_2OCH_2CH_2CH_2O^{\bullet}$	-83.40	(*)
$CH_3CH_2CH_2CH_2CH_2OH$	-71	77
$CH_3CH_2CH_2CH_2CH_2O^{\bullet}$	-19.03	(*)
$(CH_3)_2CHOH$	-65.19 [(a)]	292
$(CH_3)_2CHO^{\bullet}$	-10.48 ± 0.2	283
$(CH_3)_2CHCH_2OH$	-67.8 ± 0.2	292
$y(CH_2CH_2O)$	-12.58 ± 0.15	77
$y(CH_2CH_2CH_2O)$	-19.25 ± 0.15	77
$y(CH_2CH_2CH_2CH_2O)$	-44.03 ± 0.17	77
$y(CH_2CHO)CH_3$	-22.63 ± 0.15	77
$y(CH_2CHO)(CH_3)_2$	-33.89	44
$y(CH_2CH_2CHO)CH_3$	-30.67	44
$y(CH_2CHCH_2O)CH_3$	-27.21	44
$y(CH_2CH_2CH_2OO)$	-27.42	(*)

Units: kcal mol^{-1}
(*) This work

Table A.2 Enthalpy of formation of reference species at 298 K for mercury systems

Species	$\Delta_f H°_{298}$	Ref.
$Cl^{\bullet}$	28.992 ± 0.002	255
$Br^{\bullet}$	26.738 ± 0.029	255
$O^{\bullet}$	59.555 ± 0.024	255
$N^{\bullet}$	112.97 ± 0.096	255
$H^{\bullet}$	52.103 ± 0.001	255
Hg	14.67 ± 0.01	255
Cl_2	0	255
Br_2	7.388 ± 0.026	255
$NO^{\bullet}$	21.58	77
$NO_2^{\bullet}$	7.911	77
$NO_3^{\bullet}$	17.00	77
NH_3	-10.98 ± 0.084	255
NH_2OH	-11.95	255
ClNO	12.36	77
BrNO	19.6	257
$ClNO_2$	2.899	77
$BrNO_2$	10.8	303
HNO	23.80	77
HNO_2	-10.9	(*)
$HONO_2$	-32.101	77
$SO^{\bullet}$	1.20	77
$SO_2^{\bullet}$	-70.939 ± 0.048	255
$SO_3^{\bullet}$	-94.591	77
HSO	-5.2 ± 0.5	305
HSO_2	-42.6 ± 2.0	306
H_2O	-57.7978 ± 0.0096	255

Species	$\Delta_f H°_{298}$	Ref.
CH_3	35.1 ± 0.2	296
CH_3CH_3	-20.04 ± 0.07	297
CH_3Cl	-19.59 ± 0.16	298
CH_3Br	-8.2 ± 0.2	299
CH_3CH_2Cl	-26.83 ± 0.18	298
CH_3CH_2Br	-15.2	300
CH_3NO	16.71	107
CH_3NO_2	-19.3 ± 0.3	301
ClO	24.192	77
BrO	30	256
HgCl	18.75	77
HgBr	24.90	77
$HgCl_2$	-34.96	77
$HgBr_2$	-20.42	77
$HgCH_3$	47.6	302
HCl	-22.06 ± 0.024	255
HBr	-8.674 ± 0.038	255
HOCl	-17.80	77
HOBr	-19	304
HCl	-22.06 ± 0.024	255
HBr	-8.674 ± 0.038	255
HONO-cis	-18.40	(*)
HONO-trans	-18.90	(*)
HOOH	-32.531	77
OH	9.319	77

Units: kcal mol^{-1}

APPENDIX B

ISOOCTANE – MOLECULAR GEOMETRIES

Appendix B summarizes the molecular geometries of all the species calculated for the study of the oxidation of the secondary isooctane radical.

Table B.1 Structural parameters for the peroxy radicals, products and transition state structures optimized at the B3LYP/6-31G(d,p) level of theory

Molecule	Cartesian Coordinates		
 **c3ccqcc2**	1.24622400	-0.30235600	-0.04040900
	-0.18781500	0.13607200	-0.50754600
	2.27256800	0.72068800	-0.57618700
	3.28696500	0.36910600	-0.35762300
	2.18608000	0.84236900	-1.66123700
	2.14150900	1.70311700	-0.11987500
	1.38482600	-0.38299400	1.49433000
	0.73187700	-1.14428900	1.93228500
	2.41442100	-0.64950800	1.75854700
	1.15032800	0.57554900	1.96165100
	1.60405000	-1.67158800	-0.66447100
	2.63087800	-1.94214200	-0.39538300
	0.95557400	-2.48245700	-0.32807300
	1.55176600	-1.63184700	-1.75873700
	-0.28931100	1.56899100	-0.64914400
	-0.22289900	2.18759500	0.67375400
	-1.11867500	2.55743700	0.73195200
	-1.43331000	-0.40202600	0.24325300
	-1.54493200	-1.93491600	0.28355400
	-0.75734400	-2.40532000	0.87512200
	-2.50183900	-2.22192600	0.73239900
	-1.51589700	-2.36586100	-0.72409100
	-0.27848000	-0.14777600	-1.56789500
	-2.71812400	0.17102100	-0.38333300
	-2.71119400	1.26241300	-0.42531000
	-2.84557300	-0.19068300	-1.41086400
	-3.59641000	-0.14452100	0.18920700
	-1.36724100	-0.03974800	1.27591000

Table B.1 Structural parameters for the peroxy radicals, products and transition state structures optimized at the B3LYP/6-31G(d,p) level of theory (Continued)

Molecule	Cartesian Coordinates			Molecule	Cartesian Coordinates		
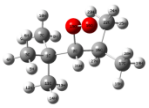 **c3ccq˙cc2**	1.38412600	-0.17865100	-0.03635000	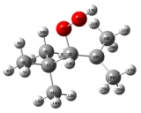 **c3ccqc˙c2**	1.33597700	-0.17491900	0.02791300
	-0.09199400	0.17338000	-0.36786500		-0.10754900	0.24753000	-0.42742800
	2.27617200	1.02290800	-0.41843700		2.35591700	0.79917200	-0.59569800
	3.33020100	0.77378000	-0.25768200		3.37571200	0.50626000	-0.32235300
	2.15294700	1.28787100	-1.47460100		2.28898800	0.79254200	-1.68955500
	2.04035500	1.90651900	0.17908300		2.18713700	1.82292700	-0.25553200
	1.58948100	-0.50905000	1.45441600		1.47601800	-0.15350300	1.56190300
	1.03818900	-1.40539800	1.75407700		0.80090900	-0.87010000	2.03969500
	2.65037900	-0.69644500	1.65185100		2.49878500	-0.42383300	1.84679300
	1.27185400	0.31956000	2.09404900		1.26519000	0.83960300	1.96780800
	1.80634300	-1.38630500	-0.89932700		1.61605200	-1.59678100	-0.49249700
	2.86851300	-1.59945500	-0.74115100		2.63913700	-1.89346100	-0.23688100
	1.25076200	-2.29524800	-0.65012100		0.93590900	-2.33229200	-0.05217400
	1.66433900	-1.18401700	-1.96687200		1.51799800	-1.65333600	-1.58258200
	-0.38126300	1.44551500	0.31640200		-0.27169900	1.58706900	0.07650600
	-1.32612600	2.14019500	-0.29646500		-1.41382600	2.17962400	-0.59897400
	-2.26498400	-0.91318500	-1.11687600		-2.09789300	2.08137800	0.08410500
	-1.83079000	-1.17465000	-2.08807300		-1.24735800	-0.64409400	-0.01462800
	-3.03350700	-1.65712800	-0.88210400		-1.90906500	-0.49386100	1.32025900
	-2.75099300	0.06192700	-1.21823600		-1.82704700	-1.40943300	1.92687800
	-0.14959000	0.41361700	-1.43441500		-1.48067800	0.32801200	1.89895200
	-1.84947800	-0.64240700	1.35809100		-2.99067500	-0.31074000	1.21240000
	-1.12066300	-0.59084500	2.17017300		-0.08788400	0.30210000	-1.52583100
	-2.42788800	0.28516000	1.36991100		-1.79754600	-1.66349100	-0.96158000
	-2.53490100	-1.46834400	1.57356800		-1.28586100	-1.65037700	-1.92850800
	-1.19274600	-0.86893300	-0.01534700		-1.72020200	-2.68629600	-0.56081800
	-0.70161800	-1.84912000	0.01121900		-2.86999400	-1.49682900	-1.15212600
Molecule	**Cartesian Coordinates**			**Molecule**	**Cartesian Coordinates**		
 **c3˙ccqcc2**	1.24486900	-0.36316700	-0.05296100	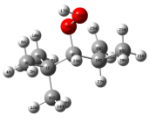 **c3ccqcc2˙**	1.35210700	-0.12741100	-0.10769300
	-0.17502300	0.13462800	-0.51717200		-0.16142500	0.19852900	-0.31168100
	1.39121300	-0.45216300	1.48189800		2.15353200	1.15419800	-0.42194400
	2.41103300	-0.76267400	1.73453000		3.22596800	0.97878600	-0.28681600
	1.20203600	0.51487500	1.95202700		1.99711700	1.47896400	-1.45739300
	0.70899100	-1.18686700	1.91837000		1.86156300	1.97228000	0.24248000
	1.50251100	-1.71585300	-0.65739000		1.67040200	-0.57065700	1.33397400
	1.32992300	-1.88894400	-1.71619000		1.15092100	-1.49734200	1.59433500
	2.05786100	-2.47113800	-0.11032700		2.74753400	-0.74236000	1.44215000
	2.31860100	0.61668600	-0.60636100		1.37580600	0.19552700	2.05657300
	3.31767200	0.22839600	-0.38507800		1.78556200	-1.23081200	-1.09295300
	2.23037500	0.72811600	-1.69141200		2.87375300	-1.35185800	-1.06035200
	2.21638900	1.60676800	-0.15556200		1.34182400	-2.19945800	-0.84612200
	-0.23539500	1.56235400	-0.66621500		1.51183800	-0.98261300	-2.12528500
	-0.13380300	2.17944400	0.65609800		-0.51190100	1.18163500	0.68790700
	-1.00708600	2.59979200	0.71138100		-1.36252700	2.19486500	0.07797600
	-1.40517400	-0.39969900	0.25539100		-0.76234500	2.95771000	0.11748100
	-1.52761100	-1.92983300	0.18487800		-1.17184300	-0.97853000	-0.27810700
	-0.65349300	-2.44395100	0.59036700		-2.54951500	-0.51758400	-0.82733500
	-2.40723100	-2.26230400	0.74702800		-2.45298900	-0.11529900	-1.84270400
	-1.65274300	-2.26500400	-0.85157800		-3.24598400	-1.36088900	-0.85931200
	-0.29458200	-0.17347400	-1.56721000		-2.97984900	0.26131000	-0.19398600
	-2.69977200	0.23749500	-0.27868600		-0.25766300	0.68878100	-1.28755200
	-2.69063100	1.32762900	-0.20426200		-1.33675300	-1.58902700	1.07688400
	-2.85441000	-0.01362700	-1.33485600		-1.44476800	-0.94843200	1.94513900
	-3.56564600	-0.13229600	0.28018400		-1.59997700	-2.63674700	1.17935500
	-1.29256000	-0.10823400	1.30594000		-0.79971700	-1.74260800	-0.97193700

APPENDIX C

ISOOCTANE – VIBRATIONAL FREQUENCIES

Appendix C includes the frequencies of the species calculated for the study of the oxidation of isooctane.

Table C.1 Vibrational frequencies **c**alculated at the B3LYP/6-31G(d,p) level

SYSTEM	Frequencies, cm^{-1}								
	61.3	64.6	87.3	186.4	189.3	194.5	223.9	236.1	257.7
	261.5	279.1	304.1	306.3	312.1	343.6	385.9	403.0	431.0
	459.6	543.9	607.0	783.0	832.8	906.5	926.1	936.9	941.8
	945.7	967.2	970.7	973.7	1010.9	1046.4	1077.5	1136.1	1139.9
c3ccqcc2	1208.0	1231.9	1252.2	1276.0	1328.1	1336.9	1357.6	1380.9	1392.4
	1411.2	1412.7	1416.3	1438.2	1445.3	1494.8	1501.4	1502.7	1505.1
	1510.5	1518.4	1520.5	1523.2	1528.0	1537.6	3014.1	3036.6	3037.4
	3040.0	3043.3	3048.1	3053.3	3100.6	3102.4	3107.7	3111.2	3121.2
	3122.1	3125.8	3127.4	3141.1	3142.4	3749.7			
	43.6	62.5	87.3	192.5	193.6	223.9	241.5	262.0	266.1
	289.0	300.7	309.2	310.4	337.2	397.3	400.1	443.7	460.4
	547.0	588.6	784.5	827.9	909.7	913.9	938.8	941.8	947.2
	968.3	969.4	1004.1	1048.0	1065.1	1129.1	1132.4	1201.3	1207.3
c3ccq˙cc2	1232.8	1253.6	1283.8	1320.2	1333.4	1372.2	1380.7	1413.7	1415.6
	1416.9	1439.0	1447.9	1495.1	1501.6	1502.8	1505.6	1510.7	1519.3
	1521.9	1524.1	1529.6	1538.3	3040.3	3040.9	3043.2	3047.6	3051.3
	3057.6	3073.7	3107.7	3108.9	3111.5	3114.7	3120.8	3124.3	3127.2
	3129.2	3138.4	3143.0						
	72.8	95.9	138.3	145.0	171.5	183.1	202.3	222.2	236.6
	258.5	285.6	300.7	312.9	325.1	357.6	370.6	398.5	425.0
	466.7	499.8	564.3	640.9	777.2	842.8	884.2	904.7	936.6
	940.7	954.5	959.5	972.1	1005.8	1013.6	1043.4	1113.2	1147.9
c3˙ccqcc2	1190.8	1195.2	1238.9	1255.8	1301.9	1346.7	1355.1	1373.2	1381.0
	1405.0	1417.8	1424.8	1437.8	1478.1	1495.5	1497.6	1502.8	1507.0
	1515.4	1518.5	1523.3	1528.0	3015.3	3038.3	3043.6	3047.1	3051.5
	3062.2	3099.5	3109.6	3114.5	3120.0	3128.1	3133.3	3139.6	3144.1
	3148.8	3248.7	3760.3						

Table C.1 Vibrational frequencies **c**alculated at the B3LYP/6-31G(d,p) level (Continued)

SYSTEM	**Frequencies, cm^{-1}**								
	34.4	63.2	78.6	111.1	136.4	185.5	192.3	215.9	220.8
	264.0	272.6	285.0	294.3	303.2	334.2	351.9	377.6	402.3
	459.5	534.6	576.7	767.6	810.8	899.8	932.3	939.6	947.3
	958.3	967.2	969.4	991.7	1014.2	1026.4	1055.0	1079.2	1199.8
c3ccqc•c2	1252.7	1255.2	1260.1	1311.5	1320.4	1366.2	1390.1	1410.2	1411.0
	1415.5	1429.7	1441.6	1479.0	1488.0	1493.2	1497.5	1503.1	1508.5
	1511.9	1517.6	1519.5	1536.3	2977.4	2984.6	3008.5	3009.7	3014.5
	3036.4	3040.8	3048.1	3101.2	3105.7	3110.4	3111.6	3118.0	3128.3
	42.6	53.5	92.9	182.5	197.8	201.6	209.2	233.3	257.6
	267.8	281.4	286.4	296.7	314.5	338.1	379.1	382.5	420.0
	454.0	534.9	576.7	611.9	784.9	851.3	914.1	921.2	939.7
	939.8	945.2	966.4	973.7	1004.0	1024.2	1051.4	1079.5	1126.0
c3ccqcc2•	1159.6	1226.5	1250.7	1277.1	1323.9	1332.7	1357.4	1366.8	1385.6
	1406.9	1413.4	1414.2	1442.1	1471.0	1492.4	1502.6	1505.3	1506.9
	1514.3	1516.8	1521.9	1536.7	3034.2	3036.8	3038.4	3042.6	3045.2
	3054.5	3100.5	3105.7	3109.4	3110.2	3120.3	3124.1	3129.2	3145.0
	3159.8	3267.3	3747.8						

APPENDIX D

ISOOCTANE – WORK REACTIONS

Appendix D summarizes the work reactions used for the determination of the heat of formation of the species calculated for the study of the oxidation of isooctane.

Table D.1 Calculated enthalpies of formation at 298 K of resulting peroxy radical from the secondary isooctane radical

Work Reactions							$\Delta_f H^o_{298}$		
							B3LYP/ 6-31G(d,p)	**CBS-QB3**	**GA[(a)]**
c3ccqcc2									
c3ccqcc2	+	cc	→	c3cq	+	c3ccc	-73.76	-75.31	
c3ccqcc2	+	cc	→	ccq	+	c3cccc2	-74.50	-75.81	
c3ccqcc2	+	ccc	→	c3cq	+	c3cccc	-74.13	-75.29	
						Ave.	**-74.13**	**-75.47**	-75.10
						σ	***0.37***	***0.29***	
c3ccq$^{\bullet}$cc2									
c3ccq$^{\bullet}$cc2	+	ccq	→	c3ccqcc2	+	ccq$^{\bullet}$	-42.77	-42.78	
c3ccq$^{\bullet}$cc2	+	c3cq	→	c3ccqcc2	+	c3cq$^{\bullet}$	-42.56	-42.63	
c3ccq$^{\bullet}$cc2	+	c2cq	→	c3ccqcc2	+	c2cq$^{\bullet}$	-43.08	-42.84	
						Ave.	**-42.80**	**-42.75**	-40.90
						σ	***0.26***	***0.10***	
						BDE	84.77	84.82	
c3$^{\bullet}$ccqcc2									
c3$^{\bullet}$ccqcc2	+	cc	→	c3ccqcc2	+	cc$^{\bullet}$	-26.97	-26.38	
c3$^{\bullet}$ccqcc2	+	ccc	→	c3ccqcc2	+	ccc$^{\bullet}$	-26.97	-26.80	
c3$^{\bullet}$ccqcc2	+	c3c	→	c3ccqcc2	+	c3$^{\bullet}$c	-26.92	-26.70	
						Ave.	**-26.96**	**-26.63**	-26.10
						σ	***-0.03***	***0.22***	
						BDE	*100.61*	*100.94*	

(a)Introduction of gauche and 1,5 interactions
Units: kcal mol^{-1}

Table D.1 Calculated enthalpies of formation at 298 K of resulting peroxy radical from the secondary isooctane radical (Continued)

Work Reactions							$\Delta_f H^o_{298}$		
							B3LYP/ 6-31G(d,p)	**CBS-QB3**	**GA**[(a)]
c3ccqc˙c2									
c3ccqc˙c2	+	ccc	→	c3ccqcc2	+	cc˙c	-32.00	-31.10	
c3ccqc˙c2	+	cccc	→	c3ccqcc2	+	cc˙cc	-31.60	-30.94	
c3ccqc˙c2	+	c3c	→	c3ccqcc2	+	cc˙c2	-32.24	-31.97	
						Ave.	**-31.94**	**-31.00**	-29.75
						σ	***0.33***	***0.55***	
						BDE	*95.63*	*96.57*	
c3ccqcc2˙									
c3ccqcc2˙	+	cc	→	c3ccqcc2	+	cc˙	-27.37	-26.43	
c3ccqcc2˙	+	ccc	→	c3ccqcc2	+	ccc˙	-27.37	-26.85	
c3ccqcc2˙	+	c3c	→	c3ccqcc2	+	c3˙c	-27.32	-26.76	
						Ave.	**-27.35**	**-26.88**	-26.10
						σ	***0.03***	***0.22***	
						BDE	*100.22*	*100.69*	

(a)Introduction of gauche and 1,5 interactions
Units: kcal mol^{-1}

Table D.2 Calculated enthalpies of formation at 298 K of resulting products from the studied reaction paths

Work Reactions							$\Delta_f H^o_{298}$		
							B3LYP/ 6-31G(d,p)	**CBS-QB3**	**GA[(a)]**
c3ccohcc2									
c3ccohcc2	+	cc	→	c2cc(oh)	+	c3ccc	-90.51	-92.25	
c3ccohcc2	+	ccc	→	c2cc(oh)	+	c3cccc	-90.88	-92.23	
c3ccohcc2	+	c3c	→	c2cc(oh)	+	c3cccc2	-91.53	-92.03	
						Ave.	**-90.97**	**-92.17**	-91.20
						σ	***0.51***	***0.12***	
c3cco˙cc2									
c3cco˙cc2	+	ccoh	→	c3ccohcc2	+	cco˙	-39.52	-38.28	
c3cco˙cc2	+	cccoh	→	c3ccohcc2	+	ccco˙	-39.14	-38.39	
c3cco˙cc2	+	c2coh	→	c3ccohcc2	+	c2co˙	-38.24	-38.49	
						Ave.	**-38.97**	**-38.39**	-39.24
						σ	***0.66***	***0.11***	
c3cc=occ2									
c3cc=occ2	+	ccc	→	c3cc=oc	+	c3cc	-81.36	-79.44	
c3cc=occ2	+	ccc	→	c3cc=oc	+	c2ccc	-80.83	-80.97	
c3cc=occ2	+	c3c	→	c3cc=oc	+	c3ccc	-81.20	-79.63	
						Ave.	**-81.28**	**-80.01**	-81.20
						σ	***0.27***	***0.13***	
c=cmcqcc2									
c=cmcqcc2	+	ccc	→	cc=cmcc	+	c3cq	-39.44	-40.69	
c=cmcqcc2	+	cc	→	cc=cmcc	+	ccqc	-38.37	-40.08	
c=cmcqcc2	+	cc	→	cc=cmcc	+	c2cq	-37.34	-40.83	
						Ave.	**-38.38**	**-40.53**	-40.60
						σ	***1.05***	***0.40***	
c3cc=cc2									
c3cc=cc2	+	cc	→	c2ccc=c	+	c3c	-24.40	-25.75	
c3cc=cc2	+	ccc	→	c2ccc=c	+	c3cc	-26.99	-25.60	
c3cc=cc2	+	c3c	→	cc=cmcc	+	c3ccc	-24.94	-25.85	
						Ave.	**-25.44**	**-25.73**	-30.39
						σ	***1.36***	***0.13***	

(a)Introduction of gauche and 1,5 interactions
Units: kcal mol^{-1}

Table D.2 Calculated enthalpies of formation at 298 K of resulting products from the studied reaction paths (Continued)

Work Reactions							$\Delta_f H^o_{298}$		
							B3LYP/ 6-31G(d,p)	**CBS-QB3**	**GA[(a)]**
c3cc=o									
c3cc=o	+	cc	→	ccc=o	+	c3c	-59.20	-60.73	
c3cc=o	+	ccc	→	ccc=o	+	c3cc	-61.15	-60.57	
c3cc=o	+	c3c	→	ccc=o	+	c3ccc	-61.03	-60.76	
						Ave.	**-60.46**	**-60.69**	-58.30
						σ	***1.10***	***0.10***	
cq=cc2									
cq=cc2	+	cc	→	cq	+	c2c=cc	-26.06	-24.31	
cq=cc2	+	ccc	→	cq	+	c2c=cc2	-28.52	-25.82	
cq=cc2	+	c3c	→	ccq	+	c2c=cc2	-27.27	-26.03	
						Ave.	**-27.28**	**-25.38**	-29.03
						σ	***1.23***	***0.94***	
c3ccqc=c									
c3ccqc=c	+	ccc	→	cc=cmcc	+	c3cq	-36.46	-39.66	
c3ccqc=c	+	cc	→	cc=cmcc	+	ccqc	-35.39	-39.05	
c3ccqc=c	+	cc	→	cc=cmcc	+	c2cq	-34.36	-39.80	
						Ave.	***-35.40***	***-39.50***	-42.95
						σ	***1.05***	***0.40***	
c2yoxtcc2									
c2yoxtcc2	+	cc	→	c-ccco	+	c3ccc	-57.06	-57.99	
c2yoxtcc2	+	ccc	→	c-ccco	+	c3cccc	-57.40	-57.99	
c2yoxtcc2	+	c3c	→	c-ccco	+	c3cccc2	-57.03	-56.89	
						Ave.	**-57.17**	**-57.62**	-55.61
						σ	***0.20***	***0.63***	
c3cycccoc									
c3cycccoc	+	cc	→	c-y(ccco)	+	c3ccc	-57.44	-58.76	
c3cycccoc	+	ccc	→	c-y(ccco)	+	c3cccc	-57.81	-58.74	
c3cycccoc	+	c3c	→	c-y(ccco)	+	c3cccc2	-57.93	-57.99	
						Ave.	**-57.73**	**-58.50**	-55.61
						σ	***0.26***	***0.44***	
c3cycocc2									
c3cycocc2	+	cc	→	c-y(coc)-c	+	c3ccc	-57.49	-59.17	
c3cycocc2	+	ccc	→	c-y(coc)-c	+	c3cccc	-57.86	-59.15	
c3cycocc2	+	c3c	→	c-y(coc)-c	+	c3cccc2	-57.99	-58.40	
						Ave.	**-57.78**	**-58.91**	-60.67
						σ	***0.26***	***0.44***	

Units: kcal mol^{-1}

Table D.3 Calculated enthalpies of formation at 298 K of the transition state structures from the studied reaction paths

Transition State Structures	$\Delta_f H^o_{298}$ / Ea	
	B3LYP/ 6-31G(d,p)	**CBS-QB3**
c3ccq˙cc2 → ts1→ c3cc=occ2 + oh		
Ea	**40.81**	**38.69**
Δ_f H (react)	-1.94	-4.06
Δ_f H (prod)	-6.68	-4.07
Δ_f H (average)	**-4.18**	**-4.07**
σ	*3.35*	*0.01*
c3ccq˙cc2 → ts2 → c3cc=cc2 + ho$_2$		
Ea	**26.20**	**30.5**
Δ_f H (react)	-16.25	-12.25
Δ_f H (prod)	-15.78	-13.97
Δ_f H (average)	**-16.19**	**-13.11**
σ	*0.33*	*1.22*
c3ccq˙cc2 → ts3 → c3˙ccqcc2		
Ea	**24.33**	**23.34**
Δ_f H (react)	-18.42	-19.41
Δ_f H (prod)	-24.81	-20.52
Δ_f H (average)	**-21.61**	**-19.96**
σ	*4.52*	*0.78*
c3˙ccqcc2 → ts4 → c=cc2+c=occ2 + oh		
Ea	**19.43**	**23.29**
Δ_f H (react)	-6.20	-3.34
Δ_f H (prod)	-0.10	-3.87
Δ_f H (average)	**-3.15**	**-3.6**
σ	*4.31*	*0.37*
c3˙ccqcc2 → ts5 → c2yoxtcc2 + oh		
Ea	**16.26**	**18.83**
Δ_f H (react)	-9.37	-4.8
Δ_f H (prod)	-8.17	-5.7
Δ_f H (average)	**-8.77**	**-5.25**
σ	*0.85*	*0.64*

Transition State Structures	$\Delta_f H^o_{298}$ / Ea	
	B3LYP/ 6-31G(d,p)	**CBS-QB3**
c3˙ccqcc2 → ts6 → c=cmcqcc2 + c˙		
Ea	**28.47**	**29.28**
Δ_f H (react)	1.84	2.65
Δ_f H (prod)	6.38	3.06
Δ_f H (average)	**4.11**	**2.86**
σ	*3.21*	*0.29*
c3ccq˙cc2 → ts7 → c3ccqc˙c2		
Ea	**29.96**	**29.46**
Δ_f H (react)	-12.79	-13.29
Δ_f H (prod)	-16.45	-13.79
Δ_f H (average)	**-14.62**	**-13.54**
σ	*2.59*	*0.35*
c3ccqc˙c2 → ts8 → cq=cc2 + c3c˙		
Ea	**26.46**	**30.45**
Δ_f H (react)	-8.45	-4.46
Δ_f H (prod)	-1.36	-1.41
Δ_f H (average)	**-4.91**	**-2.93**
σ	*5.01*	*2.16*
c3ccqc˙c2 → ts9 → c3cycocc2 + oh		
Ea	**9.86**	**11.54**
Δ_f H (react)	-25.05	-23.37
Δ_f H (prod)	-26.60	-22.4
Δ_f H (average)	**-25.82**	**-22.88**
σ	*1.10*	*0.69*
c3ccqc˙c2 → ts10 →= c3cc=cc2 + ho$_2$		
Ea	**14.64**	**18.36**
Δ_f H (react)	-20.27	-16.55
Δ_f H (prod)	-15.83	-17.77
Δ_f H (average)	**-18.05**	**-17.16**
σ	*3.14*	*0.86*

Units: kcal mol^{-1}

Table D.3 Calculated enthalpies of formation at 298 K of the transition state structures from the studied reaction paths (Continued)

Transition State Structures	$\Delta_f H^o_{298}$ / Ea	
	B3LYP/ 6-31G(d,p)	CBS-QB3
c3ccq˙cc2 → ts11 = c3ccqcc2˙		
Ea	**24.45**	**23.58**
Δ_f H (react)	-18.30	-19.17
Δ_f H (prod)	-24.54	-20.48
Δ_f H (average)	**-21.42**	**-19.83**
σ	***4.41***	***0.93***
c3ccqcc2˙ → ts12 → c3cycccoc + oh		
Ea	**12.61**	**14.32**
Δ_f H (react)	-14.27	-12.56
Δ_f H (prod)	-13.27	-11.1
Δ_f H (average)	**-13.77**	**-11.83**
σ	***0.71***	***1.03***
c3ccqcc2˙ → ts13 → c=cc + c3cc=o + oh		
Ea	**21.00**	**20.5**
Δ_f H (react)	-5.88	-6.38
Δ_f H (prod)	-1.01	-6.64
Δ_f H (average)	**-3.45**	**-6.51**
σ	***3.44***	***0.18***

Transition State Structures	$\Delta_f H^o_{298}$ / Ea	
	B3LYP/ 6-31G(d,p)	CBS-QB3
c3ccqcc2˙ → ts14 → c3ccqc=c + c˙		
Ea	**28.81**	**29.24**
Δ_f H (react)	1.93	2.37
Δ_f H (prod)	8.48	7.07
Δ_f H (average)	**5.20**	**4.72**
σ	***4.63***	***3.33***
c3˙ccqcc2 → ts15 → c3ccqc˙c2		
Ea	**14.76**	**16.83**
Δ_f H (react)	-11.87	-9.80
Δ_f H (prod)	-11.72	-9.99
Δ_f H (average)	**-11.80**	**-9.90**
σ	***0.11***	***0.14***
c3˙ccqcc2 → ts16 → c3ccqcc2˙		
Ea	**17.44**	**19.71**
Δ_f H (react)	-9.19	-6.92
Δ_f H (prod)	-6.46	-6.30
Δ_f H (average)	**-7.83**	**-6.61**
σ	***1.93***	***0.43***

Units: kcal mol^{-1}

APPENDIX E

ISOOCTANE – ENTROPY AND HEAT CAPACITY

Appendix E includes the entropy *(S)* and heat capacity *(Cp)* versus temperature for the species calculated for the study of the oxidation of isooctane.

Table E.1 Entropy *(S)* and heat capacity *(Cp) vs.* temperature for **c3ccqcc2**, contribution of SMCPS and Rotator

T (K)	SMCPS		Rotator		Total	
	Cp(T)	S(T)	Cp(T)	S(T)	Cp(T)	S(T)
5	7.95	26.48	4.09	4.19	12.04	42.39
50	8.67	44.91	3.90	15.25	12.21	71.81
100	15.33	52.69	7.87	19.14	21.23	82.72
150	22.81	60.34	10.70	22.92	30.63	93.16
200	29.28	67.78	12.37	26.25	38.35	103.04
250	35.59	74.98	13.41	29.13	45.48	112.35
298	41.88	81.74	14.02	31.55	52.25	120.91
300	42.15	82.02	14.03	31.63	52.53	121.25
400	55.45	95.95	14.45	35.75	66.11	138.22
500	67.63	109.63	14.21	38.96	77.99	154.25
600	78.10	122.88	13.65	41.50	87.86	169.34
700	86.99	135.58	12.99	43.56	96.07	183.50
800	94.60	147.69	12.34	45.25	103.01	196.77
900	101.16	159.20	11.73	46.67	108.95	209.24
1000	106.84	170.15	11.19	47.87	114.09	220.98
1100	111.78	180.55	10.72	48.92	118.55	232.05
1200	116.07	190.46	10.31	49.83	122.43	242.53
1300	119.82	199.89	9.96	50.64	125.82	252.45
1400	123.08	208.88	9.65	51.37	128.78	261.88
1500	125.94	217.47	9.39	52.03	131.37	270.85
2000	135.83	255.17	8.47	54.59	140.33	309.97
2500	141.32	286.11	7.94	56.42	145.29	341.86
3000	144.60	312.18	7.59	57.83	148.22	368.62
3500	146.70	334.64	7.34	58.98	150.06	391.61
4000	148.11	354.32	7.14	59.95	151.27	411.73
4500	149.10	371.82	6.98	60.78	152.11	429.59
5000	149.82	387.57	6.85	61.51	152.70	445.65

Units: S(cal mol^{-1}) , Cp(cal mol^{-1} K^{-1})

Table E.2 Entropy *(S)* and heat capacity *(Cp) vs.* temperature for **c3ccq˙cc2**, contribution of SMCPS and Rotator

T (K)	SMCPS		Rotator		Total	
	Cp(T)	S(T)	Cp(T)	S(T)	Cp(T)	S(T)
5	7.95	27.78	6.06	4.50	14.01	33.09
50	8.41	46.15	4.31	16.13	12.59	63.09
100	14.13	53.44	8.16	20.25	21.39	74.50
150	21.18	60.52	11.14	24.17	30.95	85.49
200	27.44	67.46	13.03	27.65	38.86	95.92
250	33.59	74.23	14.32	30.71	46.17	105.74
298	39.72	80.63	15.16	33.30	53.07	114.74
300	39.98	80.89	15.19	33.40	53.35	115.10
400	52.94	94.14	15.95	37.90	67.00	132.85
500	64.82	107.23	15.81	41.45	78.71	149.49
600	75.03	119.95	15.21	44.29	88.30	165.04
700	83.70	132.16	14.43	46.57	96.18	179.54
800	91.11	143.82	13.65	48.45	102.79	193.07
900	97.48	154.91	12.91	50.01	108.43	205.73
1000	102.99	165.46	12.26	51.34	113.27	217.60
1100	107.76	175.49	11.68	52.48	117.47	228.78
1200	111.91	185.04	11.18	53.48	121.11	239.32
1300	115.51	194.13	10.74	54.35	124.28	249.29
1400	118.65	202.80	10.37	55.14	127.03	258.74
1500	121.39	211.07	10.04	55.84	129.44	267.72
2000	130.82	247.40	8.88	58.55	137.72	306.76
2500	136.03	277.19	8.19	60.45	142.24	338.45
3000	139.13	302.28	7.71	61.90	144.86	364.99
3500	141.11	323.88	7.35	63.06	146.47	387.75
4000	142.44	342.82	7.05	64.03	147.50	407.65
4500	143.37	359.65	6.80	64.84	148.19	425.29
5000	144.05	374.79	6.59	65.55	148.66	441.14

Units: S(cal mol^{-1}) , Cp(cal mol^{-1} K^{-1})

Table E.3 Entropy *(S)* and heat capacity *(Cp) vs.* temperature for **c3˙ccqcc2**, contribution of SMCPS and Rotator

T (K)	SMCPS		Rotator		Total	
	Cp(T)	S(T)	Cp(T)	S(T)	Cp(T)	S(T)
5	7.95	32.08	2.81	3.79	10.76	34.49
50	8.57	50.48	7.51	13.92	15.88	62.99
100	14.57	58.00	12.47	20.81	26.02	76.99
150	21.80	65.28	15.07	26.42	35.41	89.37
200	28.31	72.43	16.36	30.95	43.00	100.60
250	34.66	79.41	17.03	34.68	49.91	110.93
298	40.88	86.01	17.33	37.71	56.37	120.24
300	41.14	86.29	17.33	37.82	56.64	120.61
400	53.98	99.87	17.27	42.82	69.35	138.65
500	65.50	113.15	16.68	46.61	80.25	155.30
600	75.28	125.96	15.87	49.58	89.20	170.73
700	83.54	138.18	15.01	51.97	96.59	185.03
800	90.58	149.79	14.20	53.92	102.81	198.32
900	96.65	160.80	13.47	55.55	108.15	210.73
1000	101.91	171.25	12.83	56.93	112.76	222.36
1100	106.49	181.17	12.27	58.13	116.78	233.29
1200	110.48	190.60	11.79	59.17	120.29	243.59
1300	113.96	199.57	11.38	60.10	123.36	253.33
1400	117.00	208.13	11.02	60.93	126.04	262.57
1500	119.67	216.28	10.71	61.68	128.39	271.34
2000	128.91	252.09	9.64	64.60	136.56	309.49
2500	134.06	281.44	9.00	66.68	141.07	340.48
3000	137.14	306.17	8.56	68.28	143.72	366.45
3500	139.11	327.47	8.22	69.57	145.35	388.73
4000	140.44	346.13	7.94	70.65	146.40	408.21
4500	141.37	362.73	7.71	71.57	147.10	425.49
5000	142.05	377.66	7.51	72.37	147.58	441.02

Units: S(cal mol^{-1}) , Cp(cal mol^{-1} K^{-1})

Table E.4 Entropy *(S)* and heat capacity *(Cp) vs.* temperature for **c3ccqc•c2**, contribution of SMCPS and Rotator

T (K)	SMCPS		Rotator		Total	
	Cp(T)	S(T)	Cp(T)	S(T)	Cp(T)	S(T)
5	7.95	27.82	3.09	8.99	11.04	37.62
50	8.99	46.32	9.00	18.69	17.47	65.70
100	16.33	54.57	12.07	26.06	26.17	80.41
150	23.83	62.64	13.16	31.19	33.94	92.53
200	30.12	70.36	13.75	35.06	40.45	103.18
250	36.18	77.71	14.21	38.18	46.79	112.87
298	42.19	84.56	14.56	40.72	53.04	121.61
300	42.44	84.85	14.57	40.81	53.30	121.96
400	55.07	98.76	14.93	45.06	66.17	139.05
500	66.60	112.29	14.80	48.38	77.53	155.04
600	76.50	125.31	14.37	51.05	86.96	170.01
700	84.91	137.73	13.80	53.22	94.78	184.00
800	92.09	149.53	13.19	55.02	101.35	197.08
900	98.29	160.72	12.62	56.54	106.96	209.33
1000	103.65	171.35	12.09	57.85	111.80	220.84
1100	108.31	181.44	11.63	58.98	115.98	231.69
1200	112.36	191.03	11.22	59.97	119.63	241.93
1300	115.89	200.16	10.87	60.85	122.80	251.62
1400	118.97	208.85	10.56	61.65	125.57	260.82
1500	121.66	217.15	10.30	62.37	127.99	269.56
2000	130.94	253.53	9.37	65.19	136.35	307.62
2500	136.09	283.35	8.82	67.22	140.95	338.58
3000	139.17	308.45	8.44	68.79	143.64	364.53
3500	141.14	330.05	8.15	70.07	145.32	386.80
4000	142.46	348.99	7.91	71.14	146.40	406.27
4500	143.39	365.82	7.71	72.06	147.12	423.56
5000	144.06	380.96	7.53	72.86	147.62	439.09

Units: S(cal mol^{-1}) , Cp(cal mol^{-1} K^{-1})

Table E.5 Entropy *(S)* and heat capacity *(Cp) vs.* temperature for **c3ccqcc2•**, contribution of SMCPS and Rotator

T (K)	SMCPS		Rotator		Total	
	Cp(T)	S(T)	Cp(T)	S(T)	Cp(T)	S(T)
5	7.95	29.97	4.18	1.49	12.13	30.09
50	8.50	48.36	5.98	14.64	14.31	61.59
100	14.56	55.82	11.30	20.32	24.88	74.36
150	21.86	63.12	15.49	25.78	35.91	86.62
200	28.35	70.29	17.31	30.53	44.00	98.10
250	34.66	77.28	17.83	34.47	50.73	108.63
298	40.86	83.87	17.82	37.61	56.86	118.06
300	41.12	84.15	17.82	37.72	57.11	118.43
400	53.94	97.72	17.25	42.78	69.29	136.52
500	65.46	110.99	16.44	46.54	79.97	153.13
600	75.25	123.79	15.58	49.46	88.88	168.50
700	83.51	136.01	14.76	51.80	96.31	182.75
800	90.56	147.61	14.02	53.72	102.61	196.02
900	96.63	158.62	13.36	55.34	108.02	208.41
1000	101.90	169.07	12.79	56.71	112.71	220.03
1100	106.48	178.99	12.28	57.91	116.78	230.95
1200	110.47	188.42	11.84	58.96	120.34	241.26
1300	113.96	197.39	11.45	59.89	123.43	251.01
1400	117.00	205.94	11.12	60.73	126.14	260.25
1500	119.67	214.10	10.82	61.48	128.51	269.03
2000	128.91	249.91	9.77	64.44	136.70	307.22
2500	134.06	279.26	9.13	66.54	141.20	338.24
3000	137.14	303.99	8.67	68.17	143.83	364.23
3500	139.12	325.29	8.32	69.48	145.45	386.52
4000	140.44	343.95	8.04	70.57	146.50	406.02
4500	141.38	360.55	7.80	71.50	147.19	423.31
5000	142.06	375.48	7.60	72.31	147.67	438.84

Units: S(cal mol^{-1}) , Cp(cal mol^{-1} K^{-1})

Table E.6 Entropy *(S)* and heat capacity *(Cp) vs.* temperature for products, contribution of SMCPS and Rotator

T (K)	c3ccohcc2		c3cco˙cc2		c3cc=occ2		c=cmcqcc2		c3cc=cc2	
	Cp(T)	S(T)	Cp(T)	S(T)	Cp(T)	S(T)	Cp(T)	S(T)	Cp(T)	S(T)
5	7.95	26.46	7.95	27.79	7.95	26.33	7.95	32.07	7.95	25.55
50	11.44	69.28	11.52	70.63	11.53	69.17	12.58	58.88	11.36	68.37
100	16.53	77.92	16.70	79.38	16.77	77.96	19.60	69.11	15.18	76.63
150	26.64	78.37	26.53	79.84	26.26	78.40	25.25	77.35	23.80	76.24
200	33.43	85.54	33.08	86.95	32.32	85.36	30.20	84.70	29.50	82.44
250	39.93	92.56	39.42	93.87	38.18	92.07	35.29	91.53	35.10	88.49
298	46.30	99.23	45.65	100.44	43.96	98.38	40.46	97.80	40.65	94.24
300	46.57	99.50	45.90	100.71	44.20	98.64	40.68	98.06	40.88	94.48
400	59.76	113.28	58.72	114.25	56.21	111.57	51.57	110.67	52.42	106.40
500	71.59	126.78	70.10	127.46	67.00	124.16	61.45	122.79	62.80	118.09
600	81.56	139.80	79.65	140.18	76.14	136.28	69.87	134.38	71.60	129.41
700	89.92	152.23	87.64	152.29	83.81	147.82	76.97	145.37	79.02	140.23
800	97.01	164.03	94.40	163.76	90.31	158.77	83.01	155.77	85.33	150.53
900	103.14	175.18	100.24	174.59	95.94	169.10	88.21	165.61	90.81	160.26
1000	108.43	185.82	105.26	184.91	100.78	178.96	92.70	174.92	95.53	169.58
1100	113.11	195.83	109.70	194.60	105.06	188.22	96.60	183.74	99.72	178.33
1200	117.16	205.37	113.54	203.84	108.76	197.05	99.99	192.11	103.34	186.69
1300	120.67	214.48	116.85	212.66	111.95	205.47	102.94	200.06	106.47	194.68
1400	123.71	223.19	119.71	221.07	114.71	213.52	105.51	207.64	109.17	202.32
1500	126.34	231.51	122.19	229.11	117.09	221.21	107.77	214.85	111.51	209.63
2000	135.67	267.82	130.93	264.14	125.51	254.73	115.57	246.45	119.78	241.52
2500	140.88	297.58	135.77	292.80	130.18	282.16	119.91	272.29	124.37	267.66
3000	144.00	322.65	138.67	316.92	132.97	305.24	122.51	294.03	127.12	289.69
3500	146.00	344.24	140.51	337.67	134.75	325.12	124.17	312.73	128.87	308.66
4000	147.35	363.15	141.76	355.85	135.95	342.52	125.28	329.12	130.05	325.27
4500	148.29	379.98	142.63	372.01	136.79	358.00	126.07	343.69	130.88	340.05
5000	148.98	395.11	143.26	386.55	137.40	371.92	126.64	356.79	131.48	353.35

Units: S(cal mol^{-1}) , Cp(cal mol^{-1} K^{-1})

Table E.6 Entropy *(S)* and heat capacity *(Cp) vs.* temperature for products, contribution of SMCPS and Rotator (Continued)

T (K)	c2yoxtcc2		c3cycocc2		c3cycccoc		cqdcc2		c3cc=o	
	Cp(T)	S(T)	Cp(T)	S(T)	Cp(T)	S(T)	Cp(T)	S(T)	Cp(T)	S(T)
5	7.95	27.52	7.95	26.27	7.95	28.80	7.95	28.67	7.95	27.82
50	14.82	62.31	11.40	69.09	10.00	67.15	11.77	55.31	8.11	61.62
100	20.27	72.94	15.84	77.54	14.85	75.09	15.66	64.03	10.57	67.84
150	25.03	80.46	25.10	77.55	24.01	75.09	18.77	70.18	17.80	66.13
200	29.43	87.10	31.32	84.19	29.95	81.67	21.50	75.37	21.98	70.98
250	34.35	93.28	37.40	90.69	35.92	88.07	24.30	80.01	25.87	75.62
298	39.68	99.05	43.39	96.89	41.98	94.18	27.14	84.17	29.62	79.95
300	39.91	99.28	43.63	97.14	42.23	94.43	27.26	84.33	29.77	80.13
400	51.84	111.24	55.98	109.96	55.03	107.19	33.29	92.43	37.37	88.88
500	63.09	123.12	66.98	122.53	66.51	119.82	38.82	100.00	44.06	97.27
600	72.83	134.75	76.23	134.65	76.14	132.07	43.56	107.13	49.67	105.26
700	81.12	145.98	83.95	146.20	84.16	143.79	47.57	113.84	54.35	112.80
800	88.19	156.74	90.48	157.18	90.90	154.94	51.00	120.15	58.29	119.92
900	94.28	167.00	96.11	167.53	96.68	165.46	53.96	126.09	61.71	126.59
1000	99.53	176.78	100.94	177.40	101.63	175.51	56.52	131.69	64.64	132.95
1100	104.08	186.10	105.22	186.68	105.99	184.95	58.74	136.99	67.26	138.88
1200	108.02	194.97	108.90	195.52	109.73	193.95	60.68	142.01	69.51	144.54
1300	111.43	203.42	112.08	203.96	112.96	202.53	62.37	146.77	71.45	149.94
1400	114.40	211.49	114.83	212.02	115.74	210.73	63.85	151.30	73.10	155.09
1500	116.98	219.20	117.20	219.72	118.14	218.56	65.14	155.61	74.53	160.02
2000	125.88	253.03	125.59	253.26	126.58	252.67	69.63	174.44	79.62	181.36
2500	130.77	280.79	130.23	280.70	131.23	280.56	72.13	189.82	82.44	198.79
3000	133.69	304.18	133.01	303.80	134.02	304.02	73.64	202.75	84.13	213.43
3500	135.54	324.32	134.78	323.67	135.78	324.21	74.60	213.87	85.20	226.03
4000	136.79	341.97	135.97	341.08	136.97	341.88	75.25	223.61	85.93	237.05
4500	137.66	357.66	136.81	356.56	137.81	357.59	75.70	232.26	86.43	246.85
5000	138.29	371.78	137.41	370.48	138.41	371.73	76.03	240.05	86.80	255.66

Units: S(cal mol^{-1}) , Cp(cal mol^{-1} K^{-1})

Table E.6 Entropy *(S)* and heat capacity *(Cp) vs.* temperature for products, contribution of SMCPS and Rotator (Continued)

T (K)	c=cc2		c=occ2		c3ccqcdc	
	Cp(T)	S(T)	Cp(T)	S(T)	Cp(T)	S(T)
5	7.95	24.66	7.95	26.89	7.95	31.52
50	11.16	51.17	11.29	53.42	8.59	65.40
100	12.13	58.58	13.55	61.28	14.66	72.97
150	13.25	62.89	15.60	66.37	25.30	73.59
200	14.82	66.32	17.51	70.53	32.14	80.96
250	16.85	69.39	19.67	74.22	38.42	88.12
298	19.12	72.18	22.05	77.51	44.34	94.84
300	19.22	72.30	22.15	77.65	44.58	95.11
400	24.33	77.95	27.60	84.18	56.27	108.70
500	29.18	83.45	32.86	90.46	66.30	121.67
600	33.44	88.78	37.53	96.49	74.52	133.94
700	37.12	93.90	41.56	102.27	81.27	145.47
800	40.31	98.80	45.04	107.78	86.92	156.30
900	43.10	103.47	48.07	113.02	91.76	166.42
1000	45.53	107.92	50.68	118.01	95.92	176.01
1100	47.66	112.17	52.95	122.75	99.60	184.97
1200	49.52	116.21	54.93	127.27	102.78	193.48
1300	51.14	120.08	56.64	131.57	105.53	201.57
1400	52.55	123.77	58.13	135.67	107.90	209.27
1500	53.79	127.30	59.43	139.59	109.96	216.62
2000	58.10	142.85	63.89	156.78	117.28	248.49
2500	60.49	155.64	66.35	170.87	121.37	274.46
3000	61.92	166.44	67.82	182.75	123.83	296.28
3500	62.83	175.75	68.75	192.96	125.40	315.03
4000	63.45	183.91	69.38	201.92	126.47	331.45
4500	63.88	191.18	69.81	209.88	127.21	346.03
5000	64.19	197.71	70.13	217.05	127.75	359.15

Units: S(cal mol^{-1}) , Cp(cal mol^{-1} K^{-1})

APPENDIX F

ISOOCTANE – THERMOCHEMICAL PROPERTIES IN THE NASA POLYNOMIAL FORMAT

Appendix F summarizes the thermochemical properties of the species calculated for the study of the oxidation of isooctane in the NASA polynomial format, for use in ChemKin.

Table F.1 Thermochemical properties of the isooctane system in the NASA polynomial format for use in ChemKin

```
THERMO
   300.000  1500.000  5000.000

C3CCCC2     1/8/13     C   8H  18    0    0G   300.000  5000.000 1399.000    41
 2.60960933E+01 3.86486137E-02-1.29014789E-05 1.97061528E-09-1.13043957E-13    2
-4.06393224E+04-1.17709610E+02-3.47480391E+00 1.09158113E-01-7.72868481E-05    3
 2.87418583E-08-4.38371685E-12-3.05655847E+04 4.05078516E+01                   4
C3CCJCC2    1/8/13     C   8H  17    0    0G   300.000  5000.000 1402.000    41
 2.48633722E+01 3.69236004E-02-1.22526591E-05 1.86340532E-09-1.06550935E-13    2
-1.68371541E+04-1.06034866E+02-2.59800630E+00 1.06552315E-01-8.11343829E-05    3
 3.32669702E-08-5.62080825E-12-7.85213083E+03 3.94975953E+01                   4
C3CCQCC2    1/8/13     C   8H  18O   2    0G   300.000  5000.000 1403.000    51
 2.97805759E+01 3.99792983E-02-1.33122887E-05 2.02960673E-09-1.16267703E-13    2
-5.24699329E+04-1.28497462E+02-2.61334296E+00 1.21389751E-01-9.25894264E-05    3
 3.74245079E-08-6.18765094E-12-4.18511226E+04 4.33448409E+01                   4
C3CCQCJC2   1/8/13     C   8H  17O   2    0G   300.000  5000.000 1403.000    51
 3.05165251E+01 3.74702174E-02-1.25876760E-05 1.93071785E-09-1.11071187E-13    2
-3.01419446E+04-1.31474394E+02-7.04362807E-01 1.14866662E-01-8.68022281E-05    3
 3.45482715E-08-5.62397476E-12-1.97955927E+04 3.45324653E+01                   4
C3JCCQCC2   1/8/13     C   8H  17O   2    0G   300.000  5000.000 1403.000    51
 3.17577745E+01 3.62413678E-02-1.21237142E-05 1.85400668E-09-1.06427224E-13    2
-2.79544506E+04-1.38269878E+02 1.01913640E+00 1.16373131E-01-9.37499251E-05    3
 4.01020022E-08-6.98229412E-12-1.81260680E+04 2.38364476E+01                   4
C3CCQCC2J   1/8/13     C   8H  17O   2    0G   300.000  5000.000 1387.000    51
 3.19254010E+01 3.84227083E-02-1.33879746E-05 2.10448923E-09-1.23157547E-13    2
-2.93843509E+04-1.41733853E+02-1.90171498E+00 1.17451994E-01-8.55322133E-05    3
 3.28805912E-08-5.28869653E-12-1.74881175E+04 4.01890114E+01                   4
C3CCQJCC2   1/8/13     C   8H  17O   2    0G   300.000  5000.000 1402.000    41
 3.13565503E+01 3.74319270E-02-1.26278482E-05 1.94239336E-09-1.11965029E-13    2
-3.64475609E+04-1.40031217E+02-2.67865116E+00 1.25085178E-01-1.00690095E-04    3
 4.26464871E-08-7.34109624E-12-2.54670717E+04 3.98261584E+01                   4
C3CCOHCC2   1/8/13     C   8H  18O   1    0G   300.000  5000.000 1401.000    41
 2.59586705E+01 4.15845736E-02-1.39652054E-05 2.14127335E-09-1.23146603E-13    2
-5.98386854E+04-1.18085718E+02-4.16690311E+00 1.13489601E-01-8.00818438E-05    3
 2.99933461E-08-4.64719833E-12-4.95379672E+04 4.31475954E+01                   4
C3CCOJCC2   1/8/13     C   8H  17O   1    0G   300.000  5000.000 1399.000    41
 2.60546843E+01 3.92754709E-02-1.32385761E-05 2.03505537E-09-1.17251066E-13    2
-3.26387776E+04-1.17231037E+02-3.79995995E+00 1.11039438E-01-7.98879299E-05    3
 3.04656416E-08-4.80153612E-12-2.24751144E+04 4.23838890E+01                   4
C3CC*OCC2   1/8/13     C   8H  16O   1    0G   300.000  5000.000 1399.000    41
 2.47443280E+01 3.78351007E-02-1.27405610E-05 1.95719677E-09-1.12712590E-13    2
-5.29318147E+04-1.09955657E+02-2.79149673E+00 1.02539474E-01-7.10482172E-05    3
 2.59496985E-08-3.91371537E-12-4.34137341E+04 3.77808438E+01                   4
```

Table F.1 Thermochemical properties of the isooctane system in the NASA polynomial format for use in ChemKin (Continued)

```
THERMO
   300.000  1500.000  5000.000

C*CMCQCC2   1/8/13     C   7H  14O   2    0G   300.000  5000.000 1395.000    41
 2.28471692E+01 3.49241355E-02-1.18600823E-05 1.83238688E-09-1.05948476E-13    2
-3.21958497E+04-9.81905516E+01-1.86542373E+00 9.05299285E-02-5.92597846E-05    3
 2.00904507E-08-2.79455905E-12-2.33800059E+04 3.53187978E+01                   4
C3CC*O      1/8/13     C   5H  10O   1    0G   300.000  5000.000 1401.000    21
 1.67565669E+01 2.29288040E-02-7.68316894E-06 1.17639258E-09-6.75916321E-14    2
-3.87614179E+04-6.65030060E+01-1.12965926E+00 6.68331190E-02-4.93984447E-05    3
 1.93741020E-08-3.12696758E-12-3.27776260E+04 2.87772013E+01                   4
CQ*CC2      1/8/13     C   4H   8O   2    0G   300.000  5000.000 1395.000    21
 1.47887680E+01 2.00011108E-02-6.77903770E-06 1.04595739E-09-6.04195437E-14    2
-1.99734090E+04-5.16293237E+01 1.44840219E+00 4.93207850E-02-3.09144864E-05    3
 9.89885056E-09-1.28177772E-12-1.51428490E+04 2.06920669E+01                   4
C2YOXTCC2   1/8/13     C   8H  16O   1    0G   300.000  5000.000 1393.000    31
 2.24550619E+01 4.04179796E-02-1.36802137E-05 2.10905306E-09-1.21768022E-13    2
-4.14495922E+04-9.79901374E+01-4.04512573E+00 9.53867692E-02-5.42804288E-05    3
 1.43030375E-08-1.25036968E-12-3.15801890E+04 4.67456453E+01                   4
C3CYCOCC2   1/8/13     C   8H  16O   1    0G   300.000  5000.000 1402.000    31
 2.48240125E+01 3.76166718E-02-1.25452265E-05 1.91476812E-09-1.09776068E-13    2
-4.21164008E+04-1.11146255E+02-4.19873254E+00 1.08030412E-01-7.82102066E-05    3
 2.98602956E-08-4.67482750E-12-3.23569499E+04 4.36969908E+01                   4
C3CYCCCOC   1/8/13     C   8H  16O   1    0G   300.000  5000.000 1400.000    31
 2.50015943E+01 3.81938843E-02-1.28995122E-05 1.98578828E-09-1.14534039E-13    2
-4.25272205E+04-1.14357262E+02-5.75857931E+00 1.11439516E-01-7.97279695E-05    3
 2.97657499E-08-4.54715478E-12-3.20298697E+04 5.02721219E+01                   4
C3CC*CC2    1/8/13     C   8H  16    0    0G   300.000  5000.000 1400.000    31
 2.24608848E+01 3.70429997E-02-1.23386889E-05 1.88151638E-09-1.07795420E-13    2
-5.19560832E+04-9.82806040E+01-3.53817841E+00 9.85935335E-02-6.81348376E-05    3
 2.49172336E-08-3.75772954E-12-4.30394990E+04 4.10073972E+01                   4
C*CC2       1/8/13     C   4H   8    0    0G   300.000  5000.000 1389.000    21
 9.79775383E+00 1.92218636E-02-6.52566156E-06 1.00787333E-09-5.82569471E-14    2
-7.34642224E+03-2.84485075E+01-3.64291709E-01 3.89456840E-02-1.97474091E-05    3
 4.35374738E-09-2.44113336E-13-3.36885162E+03 2.76297781E+01                   4
C*OCC2      1/8/13     C   4H   8O   1    0G   300.000  5000.000 1383.000    21
 1.17671397E+01 2.02021852E-02-6.88895304E-06 1.06734927E-09-6.18368460E-14    2
-3.20941030E+04-3.78065491E+01 5.17207345E-01 4.05821940E-02-1.82739997E-05    3
 2.39572626E-09 3.00794890E-13-2.75688716E+04 2.47525959E+01                   4
C3CCQC*C    1/8/13     C   8H  14O   2    0G   300.000  5000.000 1400.000    41
 2.72475565E+01 3.21468489E-02-1.05879727E-05 1.60392483E-09-9.15216411E-14    2
-3.09447408E+04-1.24703863E+02-1.88205352E+00 9.95633301E-02-6.83296083E-05    3
 2.31836579E-08-3.03164534E-12-2.09797265E+04 3.16068212E+01                   4
```

APPENDIX G

ISOOCTANE – RATE CONSTANTS

Appendix G summarizes the rate constants obtained from the chemical activation qRRK analysis for the oxidation of isooctane.

Table G.1 Rate constants of chemical activation from qRRK analysis 300-2100 K

Reaction	P (atm)	A (cm^3 mol^{-1} s^{-1})	n	Ea (cal mol^{-1})
c3cc•cc2+O_2 → c3ccq•cc2	0.001	4.22+167	-51.16	38352
	0.01	1.25+169	-51.14	40621
	0.1	6.01+168	-50.6	42206
	1	1.08+166	-49.36	42828
	10	2.99+160	-47.3	42337
	100	1.80+153	-44.77	41159
c3cc•cc2+O_2 → c3cc=cc2 + HO_2	0.001	6.05E+25	-3.95	7935
	0.01	3.17E+28	-4.68	10634
	0.1	2.53E+29	-4.87	12752
	1	1.09E+28	-4.38	14053
	10	7.06E+23	-3.07	14282
	100	2.25E+17	-1.08	13616
c3cc•cc2+O_2 → c3cco•cc2 + O	0.001	3.20E+33	-7.08	35632
	0.01	2.94E+35	-7.64	36818
	0.1	3.47E+39	-8.79	39540
	1	1.24E+42	-9.47	42127
	10	3.24E+41	-9.22	43687
	100	7.71E+36	-7.79	43716
c3cc•cc2+O_2 → c3cc=occ2 + OH	0.001	7.98E+22	-3.6	12496
	0.01	3.98E+26	-4.62	15461
	0.1	2.35E+28	-5.06	17857
	1	6.78E+27	-4.82	19458
	10	2.39E+24	-3.73	19963
	100	1.47E+18	-1.82	19397
c3cc•cc2+O_2 → c3•ccqcc2	0.001	9.10+108	-35.97	19797
	0.01	1.50+113	-36.81	22915
	0.1	4.18+114	-36.84	24855
	1	7.69+111	-35.66	24859
	10	3.07+104	-33.13	22635
	100	1.88E+95	-30.09	19383
c3cc•cc2+O_2 → c=cmcqcc2 + c•	0.001	7.86E+22	-3.98	18172
	0.01	2.47E+27	-5.25	21253
	0.1	1.50E+30	-6	23951
	1	2.95E+30	-6	25842
	10	5.40E+27	-5.12	26618
	100	8.60E+21	-3.34	26227

Table G.1 Rate constants of chemical activation from qRRK analysis 300-2100 K (Continued)

Reaction	P (atm)	A (cm^3 mol^{-1} s^{-1})	n	Ea (cal mol^{-1})
c3cc•cc2+O_2 → c2yoxtcc2 + OH	0.001	3.82E+22	-4.11	12502
	0.01	1.78E+26	-5.12	15459
	0.1	8.89E+27	-5.54	17832
	1	2.06E+27	-5.27	19398
	10	5.86E+23	-4.15	19871
	100	4.55E+17	-2.28	19378
c3cc•cc2+O_2 → =cc2 + c=occ2 + OH	0.001	3.57E+21	-3.95	13388
	0.01	2.80E+25	-5.03	16403
	0.1	2.40E+27	-5.52	18849
	1	8.49E+26	-5.31	20480
	10	3.46E+23	-4.23	21012
	100	3.03E+17	-2.37	20534
c3cc•cc2+O_2 → c3ccqc•c2	0.001	4.90E+29	-12.71	-2669
	0.01	2.63E+37	-14.72	-1131
	0.1	3.09E+51	-18.58	2252
	1	1.12E+72	-24.3	9073
	10	6.30E+94	-30.58	18631
	100	1.39+114	-35.79	28434
c3cc•cc2+O_2 → cq=cc2 + c3c•	0.001	4.68E+19	-2.86	15594
	0.01	1.43E+24	-4.12	18758
	0.1	6.02E+26	-4.82	21430
	1	1.87E+27	-4.88	23469
	10	2.03E+26	-4.5	25340
	100	1.86E+24	-3.78	27502
c3cc•cc2+O_2 → c3cc=cc2 + HO_2	0.001	9.68E+22	-3.69	9312
	0.01	1.32E+26	-4.54	12134
	0.1	2.38E+27	-4.83	14374
	1	4.20E+26	-4.53	15968
	10	6.70E+24	-3.9	17580
	100	5.84E+22	-3.17	19797
c3cc•cc2+O_2 → c3cycocc2 + OH	0.001	6.71E+25	-4.23	7891
	0.01	3.08E+28	-4.94	10573
	0.1	2.23E+29	-5.12	12676
	1	1.07E+28	-4.65	14017
	10	5.56E+25	-3.88	15381
	100	2.00E+24	-3.33	17780
c3cc•cc2+O_2 → c3ccqcc2•	0.001	5.15+113	-37.38	21349
	0.01	2.07+117	-38.04	24057
	0.1	4.71+117	-37.77	25210
	1	4.89+113	-36.24	24446
	10	1.01+107	-33.93	22300
	100	7.15+102	-32.36	21592
c3cc•cc2+O_2 → c3cycccoc + OH	0.001	1.37E+23	-4.26	8695
	0.01	9.71E+25	-5.02	11430
	0.1	1.02E+27	-5.24	13588
	1	6.22E+25	-4.8	14949
	10	7.60E+21	-3.57	15317
	100	4.02E+16	-1.93	15377

Table G.1 Rate constants of chemical activation from qRRK analysis 300-2100 K (Continued)

Reaction	P (atm)	A (cm^3 mol^{-1} s^{-1})	n	Ea (cal mol^{-1})
c3cc•cc2+O_2 → c=cc + c3cc=o + OH	0.001	9.64E+21	-3.78	11366
	0.01	2.73E+25	-4.73	14269
	0.1	9.44E+26	-5.11	16592
	1	1.81E+26	-4.81	18134
	10	5.73E+22	-3.7	18651
	100	2.95E+17	-2.06	18667
c3cc•cc2+O_2 → c3ccqc=c + c•	0.001	1.68E+24	-4.53	23400
	0.01	4.08E+28	-5.77	26201
	0.1	1.57E+32	-6.76	29104
	1	2.19E+33	-7.02	31282
	10	2.83E+31	-6.39	32384
	100	2.57E+26	-4.82	32361
c3ccq•cc2 → c3cc•cc2+O_2	0.001	3.96E+51	-15.08	33742
	0.01	1.80E+63	-17.82	39784
	0.1	7.59E+70	-19.41	44790
	1	2.31E+72	-19.24	47562
	10	4.95E+61	-15.44	45904
	100	8.88E+54	-12.98	45124
c3ccq•cc2 → c3cc=cc2 + HO_2	0.001	2.99E+46	-12.78	31034
	0.01	8.91E+54	-14.75	35864
	0.1	2.71E+60	-15.85	39730
	1	7.11E+60	-15.49	41669
	10	5.18E+50	-11.96	39827
	100	4.69E+44	-9.79	39002
c3ccq•cc2 → c3cco•cc2 + O	0.001	4.53E+23	-11.73	53737
	0.01	8.16E+43	-16.87	56509
	0.1	5.45E+73	-24.36	65637
	1	3.00E+96	-29.37	77377
	10	1.08E+92	-26.41	80944
	100	1.64E+84	-22.9	82386
c3ccq•cc2 → c3cc=occ2 + OH	0.001	2.70E+43	-13.75	35389
	0.01	1.00E+59	-17.5	42571
	0.1	1.17E+70	-19.93	49228
	1	1.95E+73	-20.13	53060
	10	2.53E+62	-16.15	51735
	100	1.15E+55	-13.43	51061
c3ccq•cc2 → c3•ccqcc2	0.001	7.58E+43	-10.85	26381
	0.01	7.71E+48	-12	29376
	0.1	5.01E+51	-12.51	31633
	1	1.58E+51	-12.03	32712
	10	2.30E+42	-9.02	30829
	100	3.48E+37	-7.32	30049
c3ccq•cc2 → c3ccqc•c2	0.001	2.69E+46	-12.95	31130
	0.01	2.73E+54	-14.8	35686
	0.1	3.31E+59	-15.81	39346
	1	6.96E+59	-15.43	41234
	10	5.68E+49	-11.92	39376
	100	6.14E+43	-9.78	38553

Table G.1 Rate constants of chemical activation from qRRK analysis 300-2100 K (Continued)

Reaction	P (atm)	A (cm^3 mol^{-1} s^{-1})	n	Ea (cal mol^{-1})
c3ccq•cc2 → c3ccqcc2•	0.001	2.34E+43	-10.94	26591
	0.01	2.39E+48	-12.1	29581
	0.1	1.56E+51	-12.61	31847
	1	5.04E+50	-12.12	32938
	10	6.88E+41	-9.11	31051
	100	9.99E+36	-7.4	30271
c3•ccqcc2 → c=cmcqcc2 + c•	0.001	1.44E-01	-1.98	21358
	0.01	1.44E+00	-1.98	21356
	0.1	1.37E+01	-1.97	21336
	1	8.99E+01	-1.92	21148
	10	7.92E+01	-1.64	19796
	100	5.13E+06	-2.77	18008
c3•ccqcc2 → c2yoxtcc2 + OH	0.001	7.18E+03	-2.57	13316
	0.01	7.17E+04	-2.57	13315
	0.1	7.06E+05	-2.57	13306
	1	6.14E+06	-2.55	13219
	10	5.07E+07	-2.53	12713
	100	1.00E+14	-4.05	13597
c3•ccqcc2 → c=cc2 + c=occ2 + OH	0.001	3.11E+02	-2.5	15550
	0.01	3.10E+03	-2.5	15548
	0.1	3.01E+04	-2.5	15535
	1	2.31E+05	-2.47	15405
	10	7.64E+05	-2.34	14561
	100	6.71E+11	-3.77	14640
c3•ccqcc2 → c3ccq•cc2	0.001	1.93E+22	-4.53	10174
	0.01	1.93E+23	-4.53	10174
	0.1	1.94E+24	-4.53	10176
	1	2.05E+25	-4.53	10195
	10	3.17E+26	-4.59	10359
	100	1.23E+28	-4.74	11050
c3•ccqcc2 → c3ccqc•c2	0.001	1.40E+11	-3.78	9790
	0.01	1.40E+12	-3.78	9791
	0.1	1.42E+13	-3.78	9793
	1	1.56E+14	-3.79	9815
	10	3.71E+15	-3.9	10019
	100	7.48E+18	-4.53	11298
c3•ccqcc2 → c3ccqcc2•	0.001	2.44E+04	-1.69	10478
	0.01	2.45E+05	-1.69	10478
	0.1	2.48E+06	-1.69	10478
	1	2.81E+07	-1.71	10483
	10	1.12E+09	-1.88	10595
	100	1.07E+15	-3.28	12324
c3ccqc• c2 → cq=cc2 + c3c•	0.001	1.83E+00	-1.2	21118
	0.01	6.63E-01	-0.8	19579
	0.1	2.27E+02	-1.31	16777
	1	1.00E+26	-7.68	22547
	10	2.36E+42	-11.32	30384
	100	8.46E+46	-11.59	35323

Table G.1 Rate constants of chemical activation from qRRK analysis 300-2100 K (Continued)

Reaction	P (atm)	A (cm^3 mol^{-1} s^{-1})	n	Ea (cal mol^{-1})
c3ccqc•c2 → c3cc=cc2 + HO_2	0.001	2.26E+11	-2.5	7651
	0.01	8.23E+12	-2.66	7907
	0.1	1.15E+17	-3.55	9405
	1	8.27E+26	-5.98	13943
	10	6.11E+29	-6.25	16708
	100	1.36E+30	-5.9	18365
c3ccqc•c2 → c3cycocc2 + OH	0.001	9.76E+18	-3.58	8022
	0.01	1.86E+20	-3.66	8254
	0.1	9.10E+21	-3.85	9050
	1	7.34E+25	-4.69	11134
	10	2.52E+26	-4.55	12255
	100	1.17E+26	-4.22	12941
c3ccqc•c2 → c3ccq•cc2	0.001	9.89E+07	-1.89	10066
	0.01	7.80E+08	-1.87	9600
	0.1	3.21E+14	-3.21	10552
	1	2.25E+29	-7.03	16412
	10	1.26E+34	-7.71	20094
	100	6.85E+34	-7.34	22315
c3ccqc•c2 → c3•ccqcc2	0.001	3.12E+03	-1.3	12031
	0.01	7.94E+03	-1.14	11173
	0.1	1.35E+09	-2.38	11324
	1	3.06E+26	-6.92	17660
	10	6.50E+32	-7.97	22038
	100	1.55E+34	-7.72	24698
c3ccqcc2• → c3cycccoc + OH	0.001	2.77E+12	-3.93	9825
	0.01	2.79E+13	-3.93	9826
	0.1	3.03E+14	-3.94	9845
	1	6.32E+15	-4.03	10018
	10	6.73E+18	-4.58	11132
	100	1.10E+34	-8.5	18162
c3ccqcc2• → c=cc + c3cc=o + OH	0.001	8.11E+05	-2.62	12310
	0.01	8.05E+06	-2.62	12305
	0.1	7.50E+07	-2.61	12253
	1	7.28E+08	-2.61	11944
	10	5.12E+13	-3.71	12638
	100	4.65E+37	-10.03	22524
c3ccqcc2• → c3ccqc=c + c•	0.001	2.35E-03	-2.12	28259
	0.01	2.26E-02	-2.11	28241
	0.1	1.51E-01	-2.06	28066
	1	9.69E-02	-1.74	26689
	10	1.08E+01	-2.09	23037
	100	7.87E+39	-12.67	33890
c3ccqcc2• → c3ccq•cc2	0.001	2.33E+22	-4.55	10250
	0.01	2.34E+23	-4.55	10252
	0.1	2.45E+24	-4.56	10268
	1	3.56E+25	-4.6	10411
	10	1.20E+27	-4.75	11041
	100	8.99E+33	-6.44	14353

Table G.1 Rate constants of chemical activation from qRRK analysis 300-2100 K (Continued)

Reaction	P (atm)	A (cm^3 mol^{-1} s^{-1})	n	Ea (cal mol^{-1})
c3ccqcc2• → c3ccqcc2•	0.001	7.53E+03	-1.75	10201
	0.01	7.61E+04	-1.75	10202
	0.1	8.51E+05	-1.77	10212
	1	2.64E+07	-1.91	10338
	10	2.15E+12	-3.01	11748
	100	1.52E+33	-8.47	20799

APPENDIX H

TCD – MOLECULAR GEOMETRIES

Appendix H summarizes the molecular geometries of all the species calculated for the study of the oxidation of tricyclodecane (TCD).

Table H.1 Structural parameters optimized at B3LYP/6-31G(d,p) level

Molecule	Cartesian Coordinates			Molecule	Cartesian Coordinates		
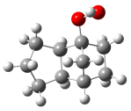	2.36030500	-1.17330500	0.48068400	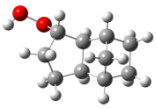	1.50450300	1.11519500	0.69908500
	2.60332300	0.32971200	0.23581300		0.64987700	1.80708900	-0.38256600
	1.29583500	0.90628300	-0.36324800		-0.46888700	0.80721400	-0.77135300
	0.49425100	-0.32989600	-0.92480900		0.01770000	-0.60548400	-0.27172900
	1.34395700	-1.58586500	-0.60398800		1.39055100	-0.38580700	0.39939800
	3.28524300	-1.75677400	0.42360800		2.55159100	1.43100600	0.70039800
	1.95045200	-1.34127700	1.48217200		1.11823800	1.31932400	1.70286400
	3.41296000	0.45394400	-0.49312200		1.26945000	2.00927100	-1.26298600
TCD-OOH-1	2.91313400	0.86168000	1.14237700	**TCD-OOH-3**	0.25156800	2.77136600	-0.04844900
	1.53598700	1.63112300	-1.14817100		-0.62447800	0.82820900	-1.85485900
	0.31366700	-0.26301400	-2.00149600		0.15347700	-1.32543700	-1.08505600
	0.72566500	-2.43750100	-0.30814500		1.54246200	-1.01346300	1.28624900
	1.87985300	-1.88359700	-1.51259400		-1.13021900	-1.06151800	0.66518100
	-0.86223100	-0.19339800	-0.17862500		-0.84708900	-1.86276100	1.35362000
	0.29995800	1.54845100	0.64125700		-1.83322100	0.97078300	-0.04955100
	0.77966900	2.21018900	1.36812200		-2.18303100	2.00637500	-0.00305300
	-1.61649300	1.02304900	-0.76749500		-2.34845100	-1.40514000	-0.22820100
	-2.65355100	1.00665300	-0.42518400		-3.12362700	-1.90998500	0.35751500
	-1.62395000	1.00114300	-1.86126200		-2.07928900	-2.07214100	-1.05326800
	-0.82608800	2.23176800	-0.17832800		-2.83729100	-0.00071500	-0.71766200
	-1.46258200	2.83800400	0.47451900		-3.85768700	0.20177800	-0.37601600
	-0.42618700	2.89594900	-0.95118800		-2.83630500	0.09080300	-1.80865200
	-0.45591700	0.33283700	1.21671900		-1.60395900	0.26275100	1.30444500
	-1.32139700	0.61384200	1.82426300		-2.52768300	0.14428900	1.88192500
	0.16469700	-0.36349500	1.78411000		-0.86363400	0.74553900	1.94592500
	-1.54210800	-1.43413600	-0.26893100		2.33017400	-0.80038400	-0.60932000
	-2.79753300	-1.33186500	0.47026300		3.66188800	-0.73751500	-0.01716200
	-2.57792800	-1.87666600	1.24345000		4.07591200	-0.08719600	-0.60658900

Molecule	Cartesian Coordinates			Molecule	Cartesian Coordinates		
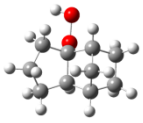	-2.26879600	-1.08033000	0.45607600	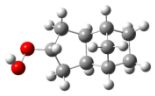	-1.68135400	0.19967800	0.19420700
	-1.55650800	-1.55444900	-0.82727400		-1.06775800	-0.99966100	-0.55068200
	-0.21037800	-0.79650900	-0.89615500		0.41881900	-0.65848300	-0.80553700
	-0.38148000	0.47941500	0.01082300		0.54696900	0.90712100	-0.62687000
	-1.78346200	0.36956500	0.66491100		-0.86816300	1.42014100	-0.27129700
	-3.35888300	-1.14066500	0.37122700		-1.63122100	0.06676800	1.28223700
	-1.99063300	-1.70896100	1.30797100		-1.60114100	-1.09136900	-1.50331600
	-2.16039800	-1.28586900	-1.70194800	**TCD-OOH-4**	-1.20523300	-1.94131300	-0.01109000
TCD-OOH-2	-1.42337500	-2.64146600	-0.85813800		0.70668500	-0.98456700	-1.81027300
	0.00935100	-0.50368300	-1.92780200		0.89972400	1.40206300	-1.53742800
	-1.78022900	0.66738700	1.71763700		-0.85933400	2.22269400	0.47291000
	-2.44826400	1.06016200	0.13430800		-1.35786300	1.81620300	-1.16855500
	0.82094400	0.38615300	0.98993500		1.61846300	1.03798700	0.48652400
	0.70415700	1.01865400	1.87250300		1.62019300	2.01483200	0.97958400
	1.02818600	-1.48837300	-0.26813900		1.43596400	-1.20447700	0.23027500
	1.10272900	-2.55164500	-0.51527000		1.27095300	-2.25384600	0.49218200
	2.12895100	0.63482600	0.20323600		2.98565100	0.64298800	-0.12338600
	2.96629300	0.74760400	0.89927300		3.80225700	0.89815800	0.55995900
	2.07222700	1.54002900	-0.40239800		3.18036300	1.16080000	-1.06836500
	2.27918800	-0.66251600	-0.65714100		2.86026500	-0.90753700	-0.29827100
	3.19423400	-1.20690400	-0.40058600		3.61239600	-1.43347400	0.29894800
	2.31519800	-0.45265900	-1.73084600		2.98947400	-1.22805000	-1.33723200
	0.90356700	-1.13750300	1.23281300		1.33400500	-0.18507500	1.38622500
	1.79027200	-1.42042900	1.81078300		2.10036100	-0.33495500	2.15513300
	0.02854700	-1.56679600	1.72551400		0.35967700	-0.16263500	1.88075900
	-0.30518900	1.60484800	-0.87148500		-3.04100300	0.46414300	-0.15540000
	-0.38836700	2.81663100	-0.05196000		-3.83859200	-0.64903600	0.34931400
	-1.23405800	3.17172800	-0.36918800		-4.34770000	-0.18824800	1.03611000

Table H.1 Structural parameters optimized at B3LYP/6-31G(d,p) level (Continued)

Molecule	Cartesian Coordinates			Molecule	Cartesian Coordinates		
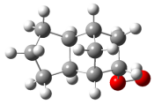 **TCD-OOH-9**	-3.01028800	-0.41884200	0.07951200	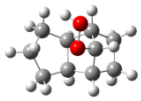 **TCD-OOH-1-10**	-2.44104900	-1.18705500	-0.27599100
	-1.94955100	-1.53189200	0.20790600		-2.30190600	0.11178400	-1.09718400
	-0.58086100	-0.89364200	-0.14237900		-1.18082400	0.95030000	-0.43271600
	-0.90329200	0.44121300	-0.91721400		-1.00173800	0.36668000	1.02625400
	-2.44840700	0.53158900	-0.99803000		-2.02529500	-0.79020400	1.15586300
	-3.99518400	-0.81456700	-0.19038200		-3.45731900	-1.59309100	-0.31357800
	-3.13941000	0.10671100	1.03139100		-1.78226300	-1.96835400	-0.66910800
	-2.16555600	-2.32619600	-0.51630100		-3.24116500	0.67526500	-1.04806500
	-1.95145200	-2.00289800	1.19737200		-2.10693800	-0.07983700	-2.15819600
	0.01161800	-1.58747500	-0.74171300		-1.46587900	2.00733000	-0.42221200
	-0.47770900	0.44422200	-1.92653900		-1.19582000	1.11895400	1.79772800
	-2.81262400	1.55911300	-0.88483200		-1.62802100	-1.63601900	1.72792000
	-2.77371600	0.19156400	-1.98843000		-2.90350800	-0.42686600	1.70258200
	-0.19503100	1.51999200	-0.05740600		0.49962000	-0.01809200	1.05976100
	-0.55912100	2.53547400	-0.23983200		0.75447200	-0.74098400	1.83918300
	0.26006500	-0.39806500	1.06547100		0.24300200	0.82437900	-1.03457200
	0.31862700	-1.11373800	1.88938500		0.27198500	0.85618300	-2.12669700
	1.33184700	1.35586900	-0.24864100		1.32888700	1.28943700	1.09968500
	1.88077800	2.21208500	0.15517200		2.38321900	1.08120000	1.30400900
	1.61785300	1.24616800	-1.29997300		0.97349900	1.96797600	1.88141700
	1.65005400	0.05698100	0.55856700		1.14906400	1.87315700	-0.34029000
	2.31305400	0.26838800	1.40587100		2.11066300	1.95740500	-0.85207600
	-0.35764900	0.98202200	1.38368100		0.68469600	2.86442300	-0.34029400
	0.22271500	1.55139200	2.11876700		0.74281900	-0.48581700	-0.39214400
	-1.38959400	0.92946600	1.73450400		0.17342000	-1.37406300	-0.67629100
	2.23289000	-0.99589800	-0.20317300		2.10458000	-0.68508200	-0.75518800
	3.59213500	-0.57567500	-0.52700000		2.54430300	-1.91180000	-0.09644700
	3.51818100	-0.49847500	-1.49187300		3.16241300	-1.54188800	0.55475000
Molecule	**Cartesian Coordinates**			**Molecule**	**Cartesian Coordinates**		
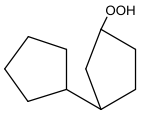 **TCD-OOH-12**	3.72792300	0.53606100	-0.62936900	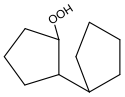 **TCD-OOH-21**	2.45035400	-1.66274900	-0.08796900
	2.38841900	1.15951000	-0.17882500		0.93820200	-1.72626400	-0.44799500
	1.39643800	-0.02028800	-0.15423300		0.25171300	-0.62024400	0.39095100
	2.26194500	-1.15623900	0.42953200		1.36332300	0.43576700	0.56412300
	3.66026500	-0.96202300	-0.20305600		2.62498900	-0.40059300	0.79760200
	3.83374000	0.61524500	-1.71674200		2.78121200	-2.56152700	0.44106600
	4.58711800	1.05547500	-0.19408800		3.05893600	-1.59448900	-0.99456600
	2.06562800	1.98143100	-0.82559500		0.50344600	-2.71093400	-0.25338500
	2.48171100	1.56654000	0.83766600		0.79152800	-1.51696100	-1.51319500
	1.14342400	-0.27846700	-1.19552200		0.07129300	-1.01328500	1.40369200
	1.84794400	-2.15214000	0.24287000		1.16046500	1.15088300	1.36950000
	4.45903800	-1.22984000	0.49531700		3.52803600	0.17439600	0.57651200
	3.77973000	-1.61209800	-1.07617500		2.67358900	-0.67285200	1.85838100
	0.08967300	0.24573800	0.59789700		-1.08384000	-0.11061700	-0.15985300
	-0.76401600	1.40699300	0.04448700		-2.19880900	-1.17263100	-0.21629000
	-0.89498800	-0.95738100	0.61407100		-1.73778000	1.01509500	0.66923300
	0.34775400	0.49148600	1.63994900		-0.91436800	0.26591900	-1.17771700
	-2.14513400	1.15605200	0.66436900		-3.48314100	-0.35252000	-0.44561400
	-0.82805200	1.32926300	-1.04890200		-2.24907200	-1.69621700	0.74936900
	-0.35337100	2.39264400	0.28278000		-2.03698900	-1.93262600	-0.98773200
	-2.32434400	-0.36615200	0.55917100		-3.23538700	1.01126700	0.26411800
	-0.75993400	-1.59715700	1.49024300		-1.25529500	1.98290100	0.50613200
	-0.75329000	-1.59172400	-0.26856200		-1.63678400	0.78015000	1.73759700
	-2.14082700	1.44546500	1.72306100		-3.63294500	-0.19560500	-1.51985300
	-2.96995600	1.69118200	0.18610800		-4.37689500	-0.86425000	-0.07540800
	-2.99883700	-0.77299700	1.32048700		-3.46336500	1.84360700	-0.40919300
	2.31930100	-1.03238500	1.51975300		-3.88096200	1.13487100	1.13928100
	-2.81929900	-0.76096200	-0.73227700		1.41597900	1.15196900	-0.67923300
	-4.21513900	-0.34364000	-0.80867200		2.39623300	2.21982700	-0.52374000
	-4.16270800	0.28125900	-1.54931900		3.04272800	1.95257700	-1.19653200

Table H.1 Structural parameters optimized at B3LYP/6-31G(d,p) level (Continued)

Molecule	Cartesian Coordinates			Molecule	Cartesian Coordinates		
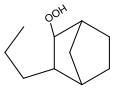	-2.02268200	-1.58466100	0.05289500	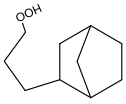	-1.51862100	1.19697300	-0.35642600
	-1.25545200	-0.94834200	-1.12955700		-0.34349500	1.74302800	0.48192200
	0.16899900	-0.36387400	-0.93282000		0.99613100	0.97593300	0.53811300
	-2.70218600	-2.33391800	-0.37306600		-2.22961700	2.01782400	-0.50873200
	-1.33009500	-2.15181800	0.68569700		-1.17941200	0.90029400	-1.35499500
	-1.88319400	-0.18916400	-1.60991700		-0.69085400	1.90765200	1.51165900
	-1.13245800	-1.74019600	-1.87929300		-0.11751300	2.74191700	0.08727200
	0.57948300	-0.30358300	-1.94854300		1.68957100	1.66802100	1.03241600
TCD-OOH-23	1.44532000	0.84188000	0.76905200	**TCD-OOH-32**	1.74398100	-1.34619100	0.36197900
	1.49889500	1.66381300	1.48607900		1.61769600	-2.40233900	0.61673300
	1.12798900	-1.23646700	-0.06548200		1.61445600	0.57283100	-0.83478400
	0.89045500	-2.30375100	-0.08947400		1.35878200	1.25299100	-1.65288900
	2.77787800	0.54324100	0.03649500		3.22373100	-0.90464600	0.24167500
	3.61645100	0.60663000	0.73661500		3.82166100	-1.67509700	-0.25620700
	2.97516500	1.25909600	-0.76798800		3.67834100	-0.72716600	1.22195300
	2.58160900	-0.91741500	-0.48538400		3.13776000	0.39385600	-0.62843600
	3.28383200	-1.60426000	-0.00105700		3.64350300	0.25524500	-1.59014200
	2.73208800	-1.00673200	-1.56596800		3.59498700	1.26212500	-0.14292900
	1.06367400	-0.54945400	1.31683200		1.17571600	-0.90045000	-1.00226100
	1.79689800	-0.94710200	2.02705500		1.65671000	-1.39304200	-1.85489400
	0.07582600	-0.56952200	1.78309500		0.09468400	-1.04096700	-1.08687800
	0.35456700	1.06663700	-0.30085100		-2.31135600	0.05410400	0.27705400
	0.66164100	1.80161500	-1.05343700		-1.75988700	-0.89452500	0.28196100
	-0.76289800	1.61766900	0.39672100		-2.58592400	0.29557800	1.31301000
	-1.68703800	2.14705700	-0.60413200		1.01004900	-0.38174700	1.32116000
	-2.49257800	1.67066900	-0.34440700		1.51356300	-0.29421500	2.28997600
	-2.85935700	-0.64309500	0.92705200		-0.00405000	-0.74089400	1.52264200
	-2.24640100	0.11371200	1.42119300		-3.49108800	-0.08494000	-0.51357900
	-3.62229000	-0.13057500	0.32421100		-4.28876800	-1.13251300	0.10740300
	-3.39731500	-1.20341600	1.69910500		-4.23350000	-1.81592100	-0.58051400

Molecule	Cartesian Coordinates			Molecule	Cartesian Coordinates		
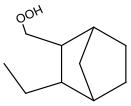	-0.52908200	2.20627800	-0.72990600	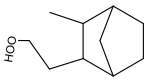	1.02260600	-0.27271100	1.57946700
	-0.86046500	0.69700300	-0.79438100		-0.45723800	-0.13437500	1.12588100
	0.29324500	-0.36524000	-0.56398800		-0.93320300	1.21567400	0.43873800
	0.30377700	2.41705300	-1.41288700		1.37762200	0.66838500	2.01360600
	-1.39286300	2.72996400	-1.16069200		1.03183500	-0.99707100	2.40437800
	-1.23599000	0.54111800	-1.81290200		-1.03380300	-0.24726100	2.05184600
	0.48516700	-0.89797600	-1.50297700		-1.71241100	1.65847700	1.07228200
	-0.33107900	-1.33230600	0.47892200		-1.59351600	0.71015600	-0.87690600
	0.41375600	-1.95891800	0.97583800	**TCD-OOH-43**	-1.68250200	1.48926700	-1.63998500
TCD-OOH-34	-1.95418700	0.21995100	0.20629700		-0.93462700	-1.21255100	0.11225600
	-2.67819300	0.99913100	0.46304700		-0.44837200	-2.18449300	0.23997500
	-1.46884600	-2.13099600	-0.19993700		-2.93477900	0.02490300	-0.52753900
	-1.79342500	-2.96028700	0.43706000		-3.51116400	-0.18644200	-1.43469700
	-1.15361900	-2.56280500	-1.15537100		-3.56277300	0.64927100	0.11647400
	-2.60339000	-1.06516900	-0.36076000		-2.47940200	-1.29812900	0.16898400
	-3.48776500	-1.34133000	0.22349800		-2.83678100	-2.17614100	-0.37957500
	-2.92664800	-0.94211900	-1.39951200		-2.84876800	-1.38677500	1.19601400
	-1.12771000	-0.36099400	1.37450400		-0.71662200	-0.50503300	-1.24441800
	-1.74418400	-0.87222600	2.12248800		-1.10603300	-1.07610000	-2.09517500
	-0.50327600	0.37480100	1.88789100		0.32528600	-0.23894000	-1.43772100
	1.65189000	0.17939800	-0.12150800		2.09567100	-0.79525400	0.61919200
	1.98302400	1.01474400	-0.74983200		2.99615900	-1.04828900	1.19225500
	1.64938200	0.51339000	0.92443900		1.76394000	-1.70091400	0.09456800
	-0.23710700	2.84283000	0.63610200		0.12116800	2.30383900	0.21316600
	0.67294300	2.45456100	1.10172600		-0.34399900	3.17489800	-0.26200200
	-0.10456900	3.92392300	0.52206200		0.55345300	2.64732200	1.15937900
	-1.06267200	2.68877500	1.33775900		0.94438500	1.96735500	-0.41987900
	2.56530500	-0.91057000	-0.26819800		2.43655300	0.21520800	-0.33153600
	3.87921900	-0.40970700	0.10751200		3.54521800	-0.31079100	-1.11368600
	4.01935400	-0.90412200	0.93178100		3.09942100	-0.46701600	-1.96288000

Table H.1 Structural parameters optimized at B3LYP/6-31G(d,p) level (Continued)

Molecule	Cartesian Coordinates			Molecule	Cartesian Coordinates		
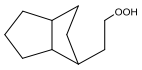	3.21135300	0.22645900	0.23084800	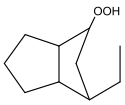	2.80621600	-0.56544400	0.35421100
	2.37335300	1.22674900	-0.58063300		2.43420100	0.91799100	0.17217700
	0.96776800	0.59317400	-0.61175900		0.95957100	0.93619100	-0.33765200
	1.22080300	-0.95181100	-0.68351400		0.66258300	-0.53943500	-0.77668900
	2.71175600	-1.14738000	-0.26334600		2.02777200	-1.25830100	-0.77418900
	4.28992100	0.36218100	0.09894700		3.88508100	-0.74571700	0.30923100
TCD-OOH-91	3.00339300	0.34729700	1.30127500		2.45962000	-0.93180600	1.32962800
	2.77078400	1.29466500	-1.60193100	**TCD-OOH-19**	3.08997500	1.36232100	-0.58610400
	2.37827300	2.24064900	-0.16441400		2.56660100	1.50525000	1.08667400
	0.40970500	0.94703000	-1.48600600		0.88467400	1.61950500	-1.18955200
	1.07836200	-1.33072500	-1.70111700		0.18827400	-0.59008200	-1.76188700
	2.82788600	-1.93061300	0.49356100		1.93828700	-2.34255700	-0.64848600
	3.30126700	-1.46124400	-1.13247100		2.53724900	-1.08469000	-1.73043900
	0.13075800	0.84382500	0.68905900		-0.10158600	1.31897400	0.73320300
	0.68963300	1.52719700	1.34097100		0.38975700	1.89279500	1.52905200
	-1.21243700	1.55928000	0.42225500		-1.22821500	2.23652900	0.20689200
	-1.70114100	1.78920800	1.37772100		-1.91407700	2.43621500	1.04140700
	-0.99786100	2.52749000	-0.04973600		-0.77724600	3.20598400	-0.04681400
	0.01496500	-0.53704300	1.39115100		-0.57998000	-0.03268600	1.32027900
	-0.92650300	-0.65697600	1.93366100		-1.62464500	-0.02677000	1.64390500
	0.82679500	-0.64106100	2.12157500		0.02054800	-0.28130600	2.20332800
	-2.23897600	0.86535400	-0.47481800		-0.34354200	-1.11531700	0.25409200
	-1.78427200	0.46765400	-1.39028800		0.01622600	-2.05011300	0.70577300
	-3.02501100	1.57591800	-0.76894900		-2.04069100	1.74126100	-0.99525300
	0.18501700	-1.57436900	0.27073900		-1.41111500	1.60625800	-1.88188700
	-0.77103400	-1.70742300	-0.24660100		-2.52874800	0.78491200	-0.79477900
	0.49068300	-2.55917600	0.64169200		-2.81267700	2.47337100	-1.25542600
	-2.82286500	-0.20320600	0.27101000		-1.51613600	-1.43191000	-0.51407900
	-3.73503500	-0.89059700	-0.63244600		-2.48756700	-2.03295100	0.39178500
	-4.58383200	-0.66707300	-0.21630000		-2.45613500	-2.95326300	0.08230400

Molecule	Cartesian Coordinates			Molecule	Cartesian Coordinates		
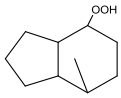	1.69453200	-1.83339700	0.65633300	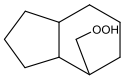	1.13880900	-2.18439100	-0.46936000
	2.45028300	-0.77920500	-0.16749300		0.27463200	-1.78009500	0.74042100
	1.35089600	0.13644400	-0.77272200		0.61133600	-0.28264400	1.02650300
	0.03402100	-0.73245400	-0.76150100		1.88071300	0.04956800	0.15634900
	0.45043100	-2.11589100	-0.19927300		2.40351400	-1.32719200	-0.31134300
	2.29020300	-2.73001800	0.85632300		1.35011500	-3.25823800	-0.50038900
	1.40080100	-1.41804800	1.62843400		0.62690700	-1.93519600	-1.40736400
TCD-OOH-1-10	2.99453700	-1.27930700	-0.97782000		0.56034600	-2.38639600	1.60782800
	3.19430700	-0.22425800	0.41255900	**TCD-OOH-10-1**	-0.79237500	-1.94625600	0.57726200
	1.59929400	0.33616800	-1.82159400		0.90781900	-0.19194600	2.07802400
	-0.34467000	-0.83663100	-1.78528100		2.63298200	0.54730300	0.78157400
	-0.36564500	-2.59387000	0.34936300		3.00305700	-1.26026800	-1.22635100
	0.71933300	-2.78515200	-1.02537000		3.04593700	-1.76466500	0.46353800
	1.20841400	1.54248000	-0.12622300		-0.55180700	0.73667100	0.84477700
	2.04825200	2.13915100	-0.50922400		-1.15488800	0.72096900	1.76207700
	-1.36257900	1.38383800	-0.28810500		0.91762200	2.31574700	-0.56303800
	-1.87745800	1.85016100	0.55709600		0.31527400	2.72352000	-1.38327900
	-2.06374400	1.40492100	-1.13120800		1.69596300	3.06154200	-0.36323300
	-0.08658700	2.18091800	-0.66190200		0.04936200	2.14968600	0.70668200
	-0.17432900	3.21499600	-0.30933600		-0.74290300	2.90714300	0.72702700
	-0.00435800	2.23771200	-1.75448600		0.66661500	2.33041800	1.59529200
	-1.10154200	-0.09597700	0.05230800		-1.55243500	0.43558900	-0.28732100
	-0.89408600	-0.20992200	1.12282800		-2.00057100	1.36404700	-0.67054700
	1.30396900	1.61776100	1.40831000		-1.10325200	-0.09845000	-1.13101700
	2.24503600	1.19863400	1.77584900		1.56576300	0.98977600	-1.01860700
	1.26833600	2.66493500	1.72888200		2.48672700	1.19625700	-1.57666100
	0.49080600	1.09604700	1.91947500		0.90226800	0.47803200	-1.72583700
	-2.25037600	-0.90805100	-0.23814800		-2.57967400	-0.37758500	0.28816500
	-3.28206500	-0.56441600	0.73426100		-3.48983700	-0.73366800	-0.79131700
	-3.91811100	-0.11289900	0.15622700		-4.26898600	-0.21408700	-0.53310100

Table H.1 Structural parameters optimized at B3LYP/6-31G(d,p) level (Continued)

Molecule	Cartesian Coordinates			Molecule	Cartesian Coordinates		
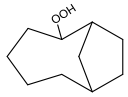	-1.77190900	0.98338900	-0.78798900	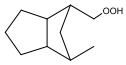	2.65143200	-1.35189100	0.21060600
	-1.16514000	2.22597600	-0.09801400		2.52230400	-0.42230500	-1.00621900
	0.37578500	2.31021200	-0.12081200		1.14352400	0.23844900	-0.81423300
	1.21624900	1.22714200	0.58780500		0.24434200	-0.88611300	-0.20209400
	1.08704000	-0.19143500	0.00872400		1.23704800	-1.95104800	0.36220500
	-2.13475200	-0.21825000	0.12586100		3.42754800	-2.11468300	0.09103800
	-2.03738900	-1.56941000	-0.62961500	**TCD-OOH-98**	2.91512700	-0.76536100	1.09965800
TCD-OOH-26	-0.59856000	-2.11553600	-0.35429100		2.52490000	-1.01786400	-1.92850100
	0.05189300	-1.13994500	0.66832700		3.33718500	0.30564500	-1.08862600
	-1.16858200	-0.44620600	1.29923500		0.74532400	0.59501400	-1.77108900
	-2.68787700	1.27465200	-1.31602900		-0.39034700	-1.35201500	-0.96139500
	-1.53077200	3.12327500	-0.61224700		1.00841200	-2.22457700	1.39780000
	-1.53758400	2.31055800	0.93088200		1.16031500	-2.87142600	-0.22719500
	0.69223400	2.33665400	-1.17327500		-0.64129700	-0.19294800	0.85819000
	0.66614600	3.28122700	0.30053700		-0.90642300	-0.88790600	1.66389200
	2.26435600	1.51591300	0.45545800		1.14668300	1.41728900	0.21474400
	1.03002900	1.22228800	1.66824000		2.16688900	1.55604700	0.59427100
	-1.08547000	0.65415800	-1.57795500		0.23627900	0.96325000	1.39006300
	0.61048500	-1.68970200	1.43472700		-0.35845300	1.78798700	1.80045800
	-0.65176900	-3.12584700	0.06273800		0.85296900	0.58817500	2.21436500
	0.00411500	-2.18999300	-1.26433400		-1.96187400	0.32008200	0.27575500
	-2.78290000	-2.27052500	-0.23916500		-2.50600000	0.92052900	1.01649500
	-2.24421600	-1.45610800	-1.69898800		-1.80365800	0.93882800	-0.61899800
	-3.15031400	-0.05527700	0.50638000		0.71657100	2.74954800	-0.41430100
	-1.63369500	-1.14634700	2.00478900		0.74817400	3.56417300	0.31759200
	-0.93257500	0.45419700	1.86860700		1.37678200	3.02320300	-1.24504300
	0.90447400	-0.11525700	-1.07029300		-0.30444700	2.69938200	-0.80974200
	2.30968700	-0.94076800	0.17002000		-2.73195000	-0.83101800	-0.06551300
	3.30807800	-0.35728200	-0.72039200		-3.99937300	-0.34683800	-0.59372100
	3.99541100	-0.13508800	-0.07248100		-3.91378000	-0.62819100	-1.51939600

Molecule	Cartesian Coordinates				Cartesian Coordinates		
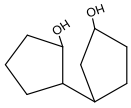	3.17849500	-1.12248600	0.28705700	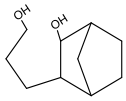	-1.99311900	-1.33684300	0.19174300
	1.68518000	-1.53643700	0.12233600		-1.10149800	-1.04892000	-1.03499800
	0.85805300	-0.22979200	0.17886200		0.34748200	-0.51702800	-0.88691200
	1.84176100	0.81149700	-0.38003800		-2.78603100	-2.00673300	-0.16377000
	3.18400500	0.42363100	0.26156800		-1.43919200	-1.90174100	0.95330900
	3.60870800	-1.50394600	1.21770200		-1.65607600	-0.39111800	-1.71358800
	3.78422000	-1.53470500	-0.52622800		-1.00530200	-2.00138700	-1.57067400
TCD-OH-OH-12	1.36321300	-2.25472100	0.88141600	**TCD-OH-OH-23**	0.82807400	-0.76614800	-1.84078000
	1.53438200	-2.02232600	-0.84994800		1.58994800	1.07853000	0.47302600
	0.68313600	0.04231100	1.23075600		1.66756800	2.07023100	0.93219500
	4.04836500	0.84348000	-0.26523700		1.20009400	-1.13704500	0.26241300
	3.18912200	0.83223000	1.27881700		0.89934200	-2.15270900	0.53225800
	-0.49752000	-0.31764900	-0.53076400		2.93801900	0.52922900	-0.05727400
	-1.41330700	-1.45026000	-0.01143100		3.75115400	0.77163600	0.63343400
	-1.38693200	0.96025200	-0.43197900		3.20290000	0.96055800	-1.02896600
	-0.29842700	-0.52021500	-1.59508200		2.69079400	-1.01296100	-0.13017200
	-2.80384900	-1.02591500	-0.49955400		3.32476700	-1.54500000	0.58700400
	-1.40441100	-1.46042500	1.08532700		2.89842400	-1.42982600	-1.12078500
	-1.11148500	-2.44249000	-0.36074500		1.10402100	-0.07245800	1.37759800
	-2.83573200	0.48168900	-0.19157800		1.77601500	-0.27095500	2.21953000
	-1.31022300	1.56832100	-1.33741700		0.09376900	0.08257500	1.76055700
	-1.08608700	1.59846400	0.40135600		0.56233100	1.02297900	-0.67900800
	-2.88794800	-1.18175600	-1.58359300		0.96232200	1.48814500	-1.59190300
	-3.63064200	-1.56879100	-0.02622400		-2.68339200	-0.13745900	0.86205900
	-3.56080300	1.01828000	-0.82150700		-1.97245600	0.42857100	1.47809100
	1.90398300	0.68188000	-1.47577500		-3.46448300	-0.51360100	1.53346300
	1.41126700	2.13102800	-0.06618400		-0.66995600	1.67161300	-0.34003800
	2.04399800	2.74913400	-0.45402400		-0.47261200	2.59521900	-0.13727400
	-3.12569500	0.71980900	1.19225400		-3.32233700	0.72132500	-0.06857300
	-4.01460400	0.38139900	1.36496900		-2.59790800	1.23063000	-0.46406100

Table H.1 Structural parameters optimized at B3LYP/6-31G(d,p) level (Continued)

Molecule	Cartesian Coordinates			Molecule	Cartesian Coordinates		
	-1.70230800	-0.44177900	-0.87340500		-3.01433200	-0.54954100	0.02568800
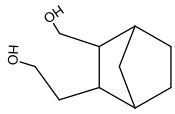	-0.15846400	-0.51270900	-0.86000100	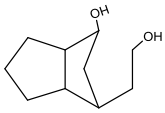	-1.94746200	-1.65844900	-0.04915500
	0.67908800	0.78579500	-0.51328300		-0.59124000	-0.94122000	-0.33920500
	-2.03336800	0.39800600	-1.49609500		-0.97975100	0.52389000	-0.74232700
	-2.07008000	-1.34400100	-1.37791400		-2.50294800	0.49201700	-0.98071000
	0.10554000	-0.80017300	-1.88447200		-4.02330800	-0.91021300	-0.19901600
	1.23065200	1.11043100	-1.40376600		-3.04717900	-0.11420200	1.03323200
	1.67468100	0.27748200	0.56514500		-2.18831600	-2.33421100	-0.87820200
	2.12839500	1.09251600	1.13323200		-1.90934200	-2.27339700	0.85611900
TCD-OH-OH-34	0.44581000	-1.56893500	0.11345900	**TCD-OH-OH-91**	-0.08493800	-1.45660700	-1.16159200
	-0.20560400	-2.43205400	0.28080400		-0.44418200	0.86926000	-1.63126600
	2.69772700	-0.66754300	-0.10696300		-2.97133300	1.47641000	-0.87437000
	3.52844400	-0.88647100	0.57216900		-2.70827200	0.14465100	-2.00123000
	3.12833200	-0.22770700	-1.01224800		0.36659800	-0.83566200	0.88148800
	1.85510200	-1.95275900	-0.39886600		0.13823500	-1.64557600	1.58485400
	2.24466500	-2.81369700	0.15495900		1.86119400	-1.01658900	0.54026400
	1.84829800	-2.22598200	-1.45910300		2.45085400	-0.90529100	1.45943800
	0.80617500	-0.72322300	1.35523800		2.01744200	-2.04930000	0.20264300
	1.37110800	-1.28535600	2.10744400		-0.01068200	0.51409100	1.54047700
	-0.05521400	-0.26350300	1.84892300		0.82015700	0.97265600	2.09066800
	-0.08936300	2.02383900	-0.05620300		-0.81264600	0.34480200	2.26924400
	-0.91492100	2.24109400	-0.75066400		-0.54417600	1.44357800	0.42844000
	-0.52915300	1.87002600	0.94090800		-1.39792600	2.03110500	0.79958400
	-2.45152700	-0.36757600	0.45487400		2.46918100	-0.09886400	-0.51484100
	-2.20176300	0.55059100	1.00689500		1.92866500	-0.20372900	-1.46921400
	-2.17382800	-1.21863800	1.09508000		2.38067500	0.95255700	-0.21604900
	0.84381900	3.10412400	-0.02724400		0.44515700	2.34728500	-0.08251000
	0.38156100	3.88695700	0.29749100		0.72614500	2.91451000	0.64795800
	-3.84244100	-0.40131500	0.13939100		3.83541400	-0.49184200	-0.66131600
	-4.33561000	-0.39006500	0.96921000		4.24240800	0.10353100	-1.30291100

Molecule	Cartesian Coordinates			Molecule	Cartesian Coordinates		
	-1.61036700	0.29867600	-0.34058200		2.82782900	-0.42454800	0.18830100
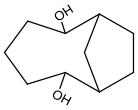	-1.33981500	1.67648100	0.30328100	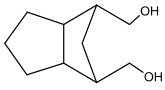	2.26760600	0.51580100	-0.89358700
	0.00043300	2.34173200	-0.07816600		0.74485900	0.44899200	-0.68154800
	1.34045700	1.67602700	0.30328300		0.46018900	-1.03521100	-0.30609400
	1.61059500	0.29816600	-0.34063000		1.81394600	-1.59168100	0.24062400
	-1.21703000	-0.93520600	0.50664900		3.84989100	-0.75610800	-0.02189400
	-0.78301400	-2.13749300	-0.37631800		2.85915400	0.09585900	1.15384300
	0.78185100	-2.13760300	-0.37678800		2.51986700	0.13002700	-1.88984500
TCD-OH-OH-26	1.21662300	-0.93569000	0.50638000	**TCD-OH-OH-98**	2.66850700	1.53466100	-0.83196000
	-0.00007300	-0.75132600	1.42502100		0.19663100	0.74642000	-1.58073300
	-2.13271400	2.35229500	-0.04413200		0.15900500	-1.61948100	-1.17975000
	-1.46184900	1.62217300	1.39138900		1.71300200	-1.99898300	1.25244800
	0.00045900	2.48113400	-1.16953900		2.15597300	-2.41760800	-0.39238000
	0.00060600	3.35323800	0.34644100		-0.70545100	-1.00286800	0.70602600
	2.13357500	2.35159900	-0.04410400		-0.64716000	-1.85782600	1.39117400
	1.46246900	1.62165100	1.39138800		0.24276200	1.30190600	0.52565300
	-1.06827700	0.26735100	-1.29980300		1.11010400	1.70265700	1.06647100
	2.11276200	-1.17208800	1.09026800		-0.53228700	0.33356200	1.46720600
	1.15754300	-3.07296200	0.05019900		-1.49572400	0.75082100	1.78106300
	1.20686800	-2.06461800	-1.38242800		0.04916900	0.16505500	2.37977600
	-1.15855900	-3.07260700	0.05134200		-2.06728100	-1.09081200	0.01530400
	-1.20867700	-2.06488500	-1.38171100		-2.86094600	-0.96841800	0.77096700
	-2.11322200	-1.17098400	1.09071400		-2.17678800	-0.27265400	-0.70853800
	-0.00016300	-1.56733000	2.15822000		-0.55642100	2.53058500	0.09727700
	0.00017600	0.17614100	2.00039500		-0.82181100	3.12390900	0.98716300
	1.06870000	0.26715300	-1.29997000		0.07387400	3.16615200	-0.54603900
	3.00905300	0.11149900	-0.60153200		-2.16475800	-2.36859900	-0.61632300
	3.27707800	0.76853600	-1.25740200		-2.94353600	-2.35679100	-1.18587700
	-3.00883600	0.11251000	-0.60175200		-1.73177600	2.11953300	-0.59951100
	-3.27646500	0.76954900	-1.25778100		-2.21143800	2.91048400	-0.87418400

Table H.1 Structural parameters optimized at B3LYP/6-31G(d,p) level (Continued)

Molecule	Cartesian Coordinates			Molecule	Cartesian Coordinates		
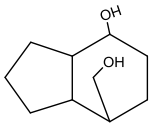	-2.13154000	-1.03626400	0.59217500	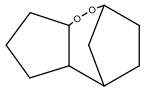	-2.57946300	-0.10973700	-0.31797000
	-1.39789800	-1.74738300	-0.55559900		-1.79751800	1.07450900	-0.95452500
	-0.36414600	-0.71182700	-1.08209200		-0.59287200	1.38005200	-0.00670500
	-0.90627900	0.69344700	-0.61829600		-1.00845000	0.70758100	1.31966100
	-2.26364100	0.40217900	0.06981900		-1.72581900	-0.56817200	0.87489000
	-3.09430200	-1.49775200	0.83680700		-3.55125100	0.22692500	0.05914700
	-1.51125600	-1.05547900	1.49564600		-2.75955900	-0.93124900	-1.01330200
	-2.11476800	-1.97790900	-1.35321500		-2.44077100	1.95586200	-1.04524500
TCD-OH-OH-1-10	-0.94807100	-2.70062300	-0.26026100	**TCD-YOO-12**	-1.45242200	0.82676000	-1.96190600
	-0.39821600	-0.71959200	-2.17759800		-0.49370300	2.46299200	0.13506800
	-1.05338300	1.33906900	-1.49259400		-0.18287000	0.49600200	2.00442600
	-2.48547000	1.14034900	0.84521100		-1.72091000	1.34963800	1.85371400
	-3.07663000	0.45074000	-0.66544800		-2.31414300	-1.03160500	1.67542200
	1.13477000	-0.99443100	-0.75219200		0.76592400	0.89850700	-0.56688800
	1.46836000	-1.73330000	-1.49653100		1.98672700	1.28195400	0.31391700
	1.48744800	1.53028700	-0.21785000		2.96693100	0.09584900	0.20797700
	2.15928100	1.70547100	0.63048500		2.04160300	-1.12559200	0.12463300
	1.54841600	2.41645200	-0.85990000		0.92054100	-0.64738000	-0.80924200
	1.95136600	0.28725700	-1.01636300		0.87685000	1.38937500	-1.54215600
	3.01633800	0.09569100	-0.83855600		1.67747500	1.40171200	1.35871500
	1.86003900	0.50460000	-2.08772300		2.43448300	2.23283700	0.00819700
	0.04289700	1.45036700	0.31320500		3.56468300	0.17820300	-0.70912300
	0.05554500	0.93917300	1.28080800		3.66861400	0.04814200	1.04633200
	1.48709800	-1.69731500	0.56568300		2.53029800	-2.03196800	-0.24396100
	0.96036400	-2.66122800	0.61419800		1.61221900	-1.35210100	1.10553200
	2.56570900	-1.92254400	0.53305100		1.23102100	-0.80343600	-1.85064800
	-0.51001200	2.76720600	0.47322600		-0.27624200	-1.42735300	-0.80043000
	-0.01527900	3.20182000	1.17995500		-0.79196400	-1.61558500	0.55109200
	1.18650000	-0.91103400	1.71757300				
	1.41096500	-1.43223500	2.49834400				

Molecule	Cartesian Coordinates			Molecule	Cartesian Coordinates		
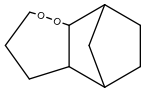	2.48636700	1.12777700	-0.02236200	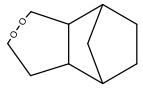	1.17179600	1.48777900	-0.70509900
	1.04919400	1.48816000	0.43117800		-0.20770800	0.79825500	-0.75894100
	-0.07738100	0.80977900	-0.36713300		-0.24408900	-0.77930300	-0.82094400
	2.85202000	1.87877500	-0.73509600		1.69457100	1.32221700	-1.65626100
	3.16288500	1.15778500	0.83828500		0.99309000	2.57054600	-0.64595800
	0.91378300	2.57468700	0.37008600		-0.66957700	1.18411800	-1.67596000
	0.94087600	1.21965500	1.48459200		-0.60922100	-1.10197900	-1.80601100
TCD-YOO-23	-0.00039000	1.09887500	-1.42357800	**TCD-YOO-34**	-1.30078600	-1.13448600	0.26257500
	-1.41238900	-1.09583000	0.40068800		-1.27319500	-2.18640400	0.56312900
	-1.43272700	-2.08453100	0.86342600		-1.16953700	1.11398800	0.42856700
	-1.49024900	1.15667400	0.18214200		-1.00527100	2.10104600	0.87219300
	-1.59706500	2.20729700	0.46771000		-2.69232500	-0.66409200	-0.22982000
	-2.47496100	-0.88169300	-0.70690700		-3.48592800	-1.08639700	0.39512900
	-3.43652800	-1.29775000	-0.39095400		-2.89331900	-0.97575300	-1.26035200
	-2.20237900	-1.37646800	-1.64476300		-2.61734700	0.89127300	-0.07204800
	-2.54642500	0.67488600	-0.83940800		-3.34033200	1.24605000	0.67008800
	-3.54115900	1.04758600	-0.57415400		-2.82308500	1.42405800	-1.00625600
	-2.32970500	1.02436300	-1.85418200		-1.00254500	-0.10024000	1.36785500
	-1.66886500	0.11986300	1.31463200		-1.74581900	-0.11205600	2.17324500
	-2.67628400	0.12609500	1.74430100		-0.00808700	-0.21350300	1.79859200
	-0.94253400	0.21265800	2.12590500		2.14993100	1.12739200	0.41384300
	2.61878200	-0.21720100	-0.73087700		3.00301600	1.81701800	0.38493400
	2.06222200	-0.19509300	-1.67945600		1.69816800	1.19498100	1.41048400
	3.66664400	-0.42491200	-0.97740000		1.09268600	-1.51062500	-0.64312900
	-0.03802100	-0.76109900	-0.21667800		0.90408700	-2.58944200	-0.56270300
	0.11376300	-1.29222100	-1.16285400		1.75881900	-1.35060500	-1.49744400
	0.96821100	-1.18096600	0.70678500		2.77718200	-0.14186600	0.24604500
	2.25307300	-1.36962200	0.02777500		1.81302200	-1.18607700	0.55220500

Table H.1 Structural parameters optimized at B3LYP/6-31G(d,p) level (Continued)

Molecule	Cartesian Coordinates			Molecule	Cartesian Coordinates		
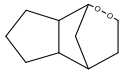 **TCD-YOO-91**	2.86180400	0.21567200	0.27640000	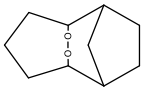 **TCD-YOO-26**	0.30735200	-1.42471900	0.25348500
	2.09697800	1.25364700	-0.55996700		1.65859900	-1.30942200	-0.49722400
	0.64628300	0.72340300	-0.62950300		2.41491600	0.00024900	-0.21909800
	0.77279200	-0.83850100	-0.54445200		1.65858300	1.30998200	-0.49676500
	2.26089600	-1.12598700	-0.18601700		0.30713000	1.42456400	0.25361600
	3.94618400	0.26461900	0.13350800		-0.97131700	-1.18847700	-0.60218100
	2.67561600	0.37639000	1.34529900		-2.18398500	-0.78138400	0.27588500
	2.52020300	1.28464800	-1.57221000		-2.18403300	0.78152300	0.27562100
	2.15999400	2.27013600	-0.15617400		-0.97133900	1.18834500	-0.60247100
	0.17287200	1.02944600	-1.56595600		-0.85596700	-0.00023100	-1.56290300
	0.50060500	-1.32966600	-1.48110000		2.30574600	-2.13342100	-0.17620400
	2.37150800	-1.92058500	0.56016800		1.49954600	-1.45176900	-1.57239300
	2.78549800	-1.46746700	-1.08551800		2.70515600	0.00011100	0.83550000
	-0.26050400	1.15888700	0.57400000		3.34390000	0.00018200	-0.80171500
	0.19704600	2.01367400	1.08574800		2.30554300	2.13401200	-0.17543100
	-1.67351800	1.59821700	0.12888600		1.49948000	1.45255300	-1.57189400
	-2.15480200	2.16918900	0.93427600		-1.15672100	2.12314100	-1.14525600
	-1.57337600	2.28700000	-0.71857900		-3.10668100	1.16347600	-0.17285900
	-0.29819100	-0.07469100	1.50358500		-2.11009400	1.19063500	1.28486600
	-1.17606300	-0.11827200	2.15616300		-3.10662700	-1.16353700	-0.17241200
	0.58605100	-0.09266000	2.15098800		-2.11004500	-1.19011900	1.28529600
	-0.23197600	-1.26741100	0.54010000		-1.15691300	-2.12341800	-1.14469100
	0.04902600	-2.20330400	1.03802300		-1.71123300	-0.00027700	-2.25019300
	-2.61719000	0.44399100	-0.25061700		0.04515500	-0.00036200	-2.17917000
	-3.39861500	0.79603800	-0.93494000		0.21650300	-2.44772800	0.64433500
	-3.11136000	0.01419600	0.62648500		0.21590600	2.44731900	0.64491200
	-1.51887100	-1.61983600	0.00404700		0.32701800	0.74684600	1.51253200
	-1.96796000	-0.61725800	-0.95788200		0.32820000	-0.74726900	1.51240700

Molecule	Cartesian Coordinates			Molecule	Cartesian Coordinates		
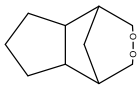 **TCD-YOO-98**	2.87161900	-0.22135000	0.31638700	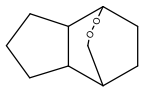 **TCD-YOO-1-10**	2.51174600	-0.04298200	0.23424300
	2.27914500	1.14827100	-0.07188100		1.92361700	1.18502900	-0.49147900
	0.80874500	0.88372200	-0.51642600		0.47320300	0.82416800	-0.90216600
	0.68434300	-0.67305000	-0.66761100		0.42796600	-0.74480600	-0.94328500
	2.13328700	-1.20354800	-0.60607900		1.77050400	-1.26477100	-0.35396600
	3.95976400	-0.26053800	0.20125500		3.59544200	-0.11407000	0.09309200
	2.65475800	-0.45276200	1.36623000		2.32709400	0.02026700	1.30770400
	2.84418200	1.56278500	-0.91472900		2.50483900	1.38926300	-1.39869800
	2.34446700	1.88116800	0.73981100		1.97197900	2.09662200	0.11576300
	0.61551900	1.39302700	-1.46641500		0.28879900	1.21250500	-1.91132000
	0.21593900	-0.94425900	-1.61788100		0.36525100	-1.05718800	-1.99286700
	2.19265400	-2.24506200	-0.27102000		1.60663200	-2.03718500	0.40178200
	2.57753000	-1.16438600	-1.60914800		2.36473100	-1.71870100	-1.15505200
	-0.22862700	-1.14647400	0.51012300		-0.67084300	1.39912500	-0.03311900
	0.22567500	-2.01238400	1.00822500		-0.63343400	2.49637000	-0.08222200
	-0.26725400	1.28063800	0.52181700		-2.08885200	-0.57789600	-0.88864100
	0.01186500	2.19717200	1.05904800		-2.98912900	-1.01192100	-0.44356700
	-0.31955400	0.06292700	1.46954900		-2.14179300	-0.78413500	-1.96477400
	-1.21873900	0.04497100	2.09278200		-2.02532800	0.95090900	-0.62889600
	0.54537800	0.07976500	2.14104300		-2.83399000	1.25703000	0.04348200
	-1.63337400	-1.58824900	0.05422600		-2.18844700	1.49199400	-1.56799900
	-1.58960300	-2.11433900	-0.90948400		-0.53615300	1.02799100	1.45435700
	-2.08441200	-2.26323900	0.79251900		0.21658100	1.65655600	1.94560200
	-1.61926500	1.55746800	-0.14643800		-1.49083400	1.15981200	1.98213700
	-2.38173700	1.83766700	0.59137500		-0.86242600	-1.30528800	-0.32345500
	-1.52431400	2.37353600	-0.87425200		-0.93319600	-2.37881300	-0.54265600
	-2.59403900	-0.53775200	-0.00052300		-0.02053800	-0.27840600	1.67607100
	-2.11137600	0.47334600	-0.93839800		-0.92585200	-1.27000400	1.12743300

APPENDIX I

TCD – WORK REACTIONS

Appendix I summarizes the work reactions used for the determination of the heat of formation of the species calculated for the study of tricyclodecane (TCD).

Table I.1 Work reactions for the TCD hydroperoxides

Work Reactions								$\Delta_f H^o_{298}$	
								a	**b**
TCD-OOH-1									
tcd-ooh-1	+	yccc	↔	tcd	+	ycccq		-40.17	
tcd-ooh-1	+	ycccc	↔	tcd	+	ycccq		-41.34	
tcd-ooh-1	+	yccccc	↔	tcd	+	ycccccq		-42.24	
							Ave.	**-41.25**	
							σ	*1.04*	
TCD-OOH-2									
tcd-ooh-2	+	yccc	↔	tcd	+	ycccq		-40.89	
tcd-ooh-2	+	ycccc	↔	tcd	+	ycccq		-42.06	
tcd-ooh-2	+	yccccc	↔	tcd	+	ycccccq		-42.97	
							Ave.	**-41.97**	
							σ	*1.04*	
TCD-OOH-3									
tcd-ooh-3	+	yccc	↔	tcd	+	ycccq		-39.57	-37.88
tcd-ooh-3	+	ycccc	↔	tcd	+	ycccq		-40.74	-39.05
tcd-ooh-3	+	yccccc	↔	tcd	+	ycccccq		-41.65	-39.96
							Ave.	**-40.66**	**-38.96**
							σ	*1.04*	*1.04*
TCD-OOH-4									
tcd-ooh-4	+	yccc	↔	tcd	+	ycccq		-39.21	-39.57
tcd-ooh-4	+	ycccc	↔	tcd	+	ycccq		-40.38	-40.74
tcd-ooh-4	+	yccccc	↔	tcd	+	ycccccq		-41.28	-41.64
							Ave.	**-40.29**	-40.65
							σ	*1.04*	*1.04*
TCD-OOH-9									
tcd-ooh-9	+	yccc	↔	tcd	+	ycccq		-38.24	-39.22
tcd-ooh-9	+	ycccc	↔	tcd	+	ycccq		-39.40	-40.39
tcd-ooh-9	+	yccccc	↔	tcd	+	ycccccq		-40.31	-41.30
							Ave.	**-39.32**	**-40.30**
							σ	*1.04*	*1.04*
TCD-OOH-10									
tcd-ooh-10	+	yccc	↔	tcd	+	ycccq		-38.13	-36.02
tcd-ooh-10	+	ycccc	↔	tcd	+	ycccq		-39.30	-37.19
tcd-ooh-10	+	yccccc	↔	tcd	+	ycccccq		-40.20	-38.09
							Ave.	**-39.21**	**-37.10**
							σ	*1.04*	*1.04*

(*) q=ooh

Units: kcal mol^{-1}

Table I.2 Work reactions for the TCD peroxy radicals

Work Reactions								$\Delta_f H^o_{298}$	
								a	**b**
TCD-OO•-1									
tcd-oo•-1	+	ycccq	↔	tcd-ooh-1	+	ycccq•		-8.42	
tcd-oo•-1	+	yccccq	↔	tcd-ooh-1	+	yccccq•		-8.52	
tcd-oo•-1	+	yccccccq	↔	tcd-ooh-1	+	yccccccq•		-7.63	
							Ave.	**-8.19**	
							σ	*0.49*	
							BDE	85.16	
TCD-OO•-2									
tcd-oo•-2	+	ycccq	↔	tcd-ooh-2	+	ycccq•		-10.27	
tcd-oo•-2	+	yccccq	↔	tcd-ooh-2	+	yccccq•		-10.36	
tcd-oo•-2	+	yccccccq	↔	tcd-ooh-2	+	yccccccq•		-9.48	
							Ave.	**-10.04**	
							σ	*0.49*	
							BDE	85.03	
TCD-OO•-3									
tcd-oo•-3	+	ycccq	↔	tcd-ooh-3	+	ycccq•		-8.42	-6.17
tcd-oo•-3	+	yccccq	↔	tcd-ooh-3	+	yccccq•		-8.51	-6.26
tcd-oo•-3	+	yccccccq	↔	tcd-ooh-3	+	yccccccq•		-7.63	-5.38
							Ave.	**-8.19**	**-5.94**
							σ	*0.49*	*0.49*
							BDE	84.57	85.13
TCD-OO•-4									
tcd-oo•-4	+	ycccq	↔	tcd-ooh-4	+	ycccq•		-7.64	-7.99
tcd-oo•-4	+	yccccq	↔	tcd-ooh-4	+	yccccq•		-7.73	-8.08
tcd-oo•-4	+	yccccccq	↔	tcd-ooh-4	+	yccccccq•		-6.85	-7.20
							Ave.	**-7.41**	**-7.75**
							σ	*0.49*	*0.49*
							BDE	84.98	85.00
TCD-OO•-9									
tcd-oo•-9	+	ycccq	↔	tcd-ooh-9	+	ycccq•		-6.44	-7.71
tcd-oo•-9	+	yccccq	↔	tcd-ooh-9	+	yccccq•		-6.38	-7.65
tcd-oo•-9	+	yccccccq	↔	tcd-ooh-9	+	yccccccq•		-5.95	-7.22
							Ave.	**-6.26**	**-7.53**
							σ	*0.49*	*0.49*
							BDE	85.16	84.88
TCD-OO•-10									
tcd-oo•-10	+	ycccq	↔	tcd-ooh-10	+	ycccq•		-6.23	-3.70
tcd-oo•-10	+	yccccq	↔	tcd-ooh-10	+	yccccq•		-6.16	-3.63
tcd-oo•-10	+	yccccccq	↔	tcd-ooh-10	+	yccccccq•		-5.74	-3.21
							Ave.	**-6.04**	**-3.51**
							σ	*0.49*	*0.49*
							BDE	85.27	85.93

(*) q=ooh

Units: kcal mol^{-1}

Table I.3 Work reactions for the TCD ring opened hydroperoxides

Work Reactions								$\Delta_f H^o_{298}$
TCD-OOH-12								
tcd-ooh-12	+	yccc	↔	tcd-h2-12	+	ycccq		-52.77
tcd-ooh-12	+	ycccc	↔	tcd-h2-12	+	ycccCq		-53.94
tcd-ooh-12	+	ycccCc	↔	tcd-h2-12	+	ycccCcq		-54.85
							Ave.	**-53.85**
							σ	*1.04*
TCD-OOH-21								
tcd-ooh-21	+	yccc	↔	tcd-h2-12	+	ycccq		-51.51
tcd-ooh-21	+	ycccc	↔	tcd-h2-12	+	ycccCq		-52.68
tcd-ooh-21	+	ycccCc	↔	tcd-h2-12	+	ycccCcq		-53.59
							Ave.	**-52.59**
							σ	*1.04*
TCD-OOH-23								
tcd-ooh-23	+	yccc	↔	tcd-h2-23	+	ycccq		-45.21
tcd-ooh-23	+	ycccc	↔	tcd-h2-23	+	ycccCq		-46.38
tcd-ooh-23	+	ycccCc	↔	tcd-h2-23	+	ycccCcq		-47.29
							Ave.	**-46.29**
							σ	*1.04*
TCD-OOH-32								
tcd-ooh-32	+	yccc	↔	tcd-h2-23	+	ycccq		-43.49
tcd-ooh-32	+	ycccc	↔	tcd-h2-23	+	ycccCq		-44.66
tcd-ooh-32	+	ycccCc	↔	tcd-h2-23	+	ycccCcq		-45.57
							Average	**-44.57**
							σ	*1.04*
TCD-OOH-34								
tcd-ooh-34	+	yccc	↔	tcd-h2-34	+	ycccq		-45.28
tcd-ooh-34	+	ycccc	↔	tcd-h2-34	+	ycccCq		-46.45
tcd-ooh-34	+	ycccCc	↔	tcd-h2-34	+	ycccCcq		-47.35
							Ave.	**-46.36**
							σ	*1.04*
TCD-OOH-43								
tcd-ooh-43	+	yccc	↔	tcd-h2-34	+	ycccq		-44.80
tcd-ooh-43	+	ycccc	↔	tcd-h2-34	+	ycccCq		-45.97
tcd-ooh-43	+	ycccCc	↔	tcd-h2-34	+	ycccCcq		-46.88
							Ave.	**-45.88**
							σ	*1.04*

(*) q=ooh

Units: kcal mol^{-1}

Table I.3 Work reactions for the TCD ring opened hydroperoxides (Continued)

Work Reactions								$\Delta_f H^o_{298}$
TCD-OOH-19								
tcd-ooh-19	+	yccc	↔	tcd-h2-19	+	ycccq		-52.71
tcd-ooh-19	+	ycccc	↔	tcd-h2-19	+	yccccq		-53.88
tcd-ooh-19	+	yccccc	↔	tcd-h2-19	+	ycccccq		-54.78
							Ave.	**-53.79**
							σ	*1.04*
TCD-OOH-91								
tcd-ooh-91	+	yccc	↔	tcd-h2-19	+	ycccq		-49.37
tcd-ooh-91	+	ycccc	↔	tcd-h2-19	+	yccccq		-50.54
tcd-ooh-91	+	yccccc	↔	tcd-h2-19	+	ycccccq		-51.45
							Ave.	**-50.46**
							σ	*1.04*
TCD-OOH-26								
tcd-ooh-26	+	yccc	↔	tcd-h2-26	+	ycccq		-46.74
tcd-ooh-26	+	ycccc	↔	tcd-h2-26	+	yccccq		-47.91
tcd-ooh-26	+	yccccc	↔	tcd-h2-26	+	ycccccq		-48.81
							Ave.	**-47.82**
							σ	*1.04*
TCD-OOH-98								
tcd-ooh-98	+	yccc	↔	tcd-h2-98	+	ycccq		-51.37
tcd-ooh-98	+	ycccc	↔	tcd-h2-98	+	yccccq		-52.54
tcd-ooh-98	+	yccccc	↔	tcd-h2-98	+	ycccccq		-53.44
							Ave.	**-52.45**
							σ	*1.04*
TCD-OOH-1-10								
tcd-ooh-1-10	+	yccc	↔	tcd-h2-1-10	+	ycccq		-51.80
tcd-ooh-1-10	+	ycccc	↔	tcd-h2-1-10	+	yccccq		-52.97
tcd-ooh-1-10	+	yccccc	↔	tcd-h2-1-10	+	ycccccq		-53.87
							Ave.	**-52.88**
							σ	*1.04*
TCD-OOH-10-1								
tcd-ooh-10-1	+	yccc	↔	tcd-h2-1-10	+	ycccq		-47.73
tcd-ooh-10-1	+	ycccc	↔	tcd-h2-1-10	+	yccccq		-48.90
tcd-ooh-10-1	+	yccccc	↔	tcd-h2-1-10	+	ycccccq		-49.81
							Ave.	**-48.81**
							σ	*1.04*

(*) q=ooh

Units: kcal mol^{-1}

Table I.4 Work reactions for the TCD ring opened peroxy radicals

Work Reactions								$\Delta_f H^o_{298}$
TCD-OO•-12								
tcd-oo•-12	+	ycccq	↔	tcd-ooh-12	+	ycccq•		-21.47
tcd-oo•-12	+	yccccq	↔	tcd-ooh-12	+	yccccq•		-21.56
tcd-oo•-12	+	yccccccq	↔	tcd-ooh-12	+	yccccccq•		-20.68
							Ave.	**-21.23**
							σ	0.49
							BDE	84.72
TCD-OO•-21								
tcd-oo•-21	+	ycccq	↔	tcd-ooh-21	+	ycccq•		-20.30
tcd-oo•-21	+	yccccq	↔	tcd-ooh-21	+	yccccq•		-20.40
tcd-oo•-21	+	yccccccq	↔	tcd-ooh-21	+	yccccccq•		-19.51
							Ave.	**-20.07**
							σ	*0.49*
							BDE	84.62
TCD-OO•-23								
tcd-oo•-23	+	ycccq	↔	tcd-ooh-23	+	ycccq•		-13.93
tcd-oo•-23	+	yccccq	↔	tcd-ooh-23	+	yccccq•		-14.02
tcd-oo•-23	+	yccccccq	↔	tcd-ooh-23	+	yccccccq•		-13.14
							Ave.	**-13.70**
							σ	*0.49*
							BDE	84.69
TCD-OO•-32								
tcd-ooj-32	+	ycccq	↔	tcd-ooh-32	+	ycccq•		-11.70
tcd-ooj-32	+	yccccq	↔	tcd-ooh-32	+	yccccq•		-11.79
tcd-ooj-32	+	yccccccq	↔	tcd-ooh-32	+	yccccccq•		-10.91
							Ave.	**-11.47**
							σ	*0.49*
							BDE	85.20
TCD-OO•-34								
tcd-oo•-34	+	ycccq	↔	tcd-ooh-34	+	ycccq•		-13.59
tcd-oo•-34	+	yccccq	↔	tcd-ooh-34	+	yccccq•		-13.68
tcd-oo•-34	+	yccccccq	↔	tcd-ooh-34	+	yccccccq•		-12.78
							Ave.	**-13.35**
							σ	*0.49*
							BDE	85.11
TCD-OO•-43								
tcd-oo•-43	+	ycccq	↔	tcd-ooh-43	+	ycccq•		-12.55
tcd-oo•-43	+	yccccq	↔	tcd-ooh-43	+	yccccq•		-12.65
tcd-oo•-43	+	yccccccq	↔	tcd-ooh-43	+	yccccccq•		-11.76
							Ave.	**-12.32**
							σ	*0.49*
							BDE	85.66

(*) q=ooh

Units: kcal mol^{-1}

Table I.4 Work reactions for the TCD ring opened peroxy radicals (Continued)

Work Reactions								$\Delta_f H^o_{298}$
TCD-OO•-19								
tcd-oo•-19	+	ycccq	↔	tcd-ooh-19	+	ycccq•		-22.26
tcd-oo•-19	+	yccccq	↔	tcd-ooh-19	+	yccccq•		-22.35
tcd-oo•-19	+	yccccccq	↔	tcd-ooh-19	+	yccccccq•		-21.46
							Ave.	**-22.02**
							σ	*0.49*
							BDE	83.87
TCD-OO•-91								
tcd-oo•-91	+	ycccq	↔	tcd-ooh-91	+	ycccq•		-17.38
tcd-oo•-91	+	yccccq	↔	tcd-ooh-91	+	yccccq•		-17.47
tcd-oo•-91	+	yccccccq	↔	tcd-ooh-91	+	yccccccq•		-16.59
							Ave.	**-17.14**
							σ	*0.49*
							BDE	85.42
TCD-OO•-26								
tcd-oo•-26	+	ycccq	↔	tcd-ooh-26	+	ycccq•		-16.70
tcd-oo•-26	+	yccccq	↔	tcd-ooh-26	+	yccccq•		-16.79
tcd-oo•-26	+	yccccccq	↔	tcd-ooh-26	+	yccccccq•		-15.91
							Ave.	**-16.47**
							σ	*0.49*
							BDE	84.45
TCD-OO•-98								
tcd-oo•-98	+	ycccq	↔	tcd-ooh-98	+	ycccq•		-19.58
tcd-oo•-98	+	yccccq	↔	tcd-ooh-98	+	yccccq•		-19.67
tcd-oo•-98	+	yccccccq	↔	tcd-ooh-98	+	yccccccq•		-18.79
							Ave.	**-19.35**
							σ	*0.49*
							BDE	85.20
TCD-OO•-1-10								
tcd-oo•-1-10	+	ycccq	↔	tcd-ooh-1-10	+	ycccq•		-20.57
tcd-oo•-1-10	+	yccccq	↔	tcd-ooh-1-10	+	yccccq•		-20.67
tcd-oo•-1-10	+	yccccccq	↔	tcd-ooh-1-10	+	yccccccq•		-19.78
							Ave.	**-20.34**
							σ	*0.49*
							BDE	84.64
TCD-OO•-10-1								
tcd-oo•-10-1	+	ycccq	↔	tcd-ooh-10-1	+	ycccq•		-15.80
tcd-oo•-10-1	+	yccccq	↔	tcd-ooh-10-1	+	yccccq•		-15.89
tcd-oo•-10-1	+	yccccccq	↔	tcd-ooh-10-1	+	yccccccq•		-15.01
							Ave.	**-15.56**
							σ	*0.49*
							BDE	85.35

(*) q=ooh

Units: kcal mol^{-1}

Table I.5 Calculations for the TCD ring opened peroxy diradicals

Species				Bond Energy		$\Delta_f H°_{298}$	
				Triplet	Singlet	Triplet	Singlet
TCD-OO•-H•-12							
tcd-oo•-12	↔ tcd-oo•-h•-12	+	H	*96.5*	*96.8*	23.17	23.47
TCD-OO•-H•-21							
tcd-oo•-21	↔ tcd-oo•-h•-21	+	H	*96.0*	*96.3*	23.87	24.17
TCD-OO•-H•-23							
tcd-oo•-23	↔ tcd-oo•-h•-23	+	H	*101.3*	*101.7*	35.50	35.90
TCD-OO•-H•-32							
tcd-oo•-32	↔ tcd-oo•-h•-32	+	H	*98.9*	*99.2*	35.33	35.65
TCD-OO•-H•-34							
tcd-oo•-34	↔ tcd-oo•-h•-34	+	H	*100.8*	*100.8*	35.35	35.35
TCD-OO•-H•-43							
tcd-oo•-43	↔ tcd-oo•-h•-43	+	H	*100.7*	*100.7*	36.28	36.28
TCD-OO•-H•-19							
tcd-oo•-19	↔ tcd-oo•-h•-19	+	H	*100.9*	*100.8*	26.78	26.68
TCD-OO•-H•-91							
tcd-oo•-91	↔ tcd-oo•-h•-91	+	H	*97.9*	*98.0*	28.66	28.66
TCD-OO•-H•-26							
tcd-oo•-26	↔ tcd-oo•-h•-26	+	H	*96.9*	*94.4*	28.33	25.83
TCD-OO•-H•-98							
tcd-oo•-98	↔ tcd-oo•-h•-98	+	H	*101.5*	*100.8*	30.05	29.35
TCD-OO•-H•-1-10							
tcd-oo•-1-10	↔ tcd-oo•-h•-1-10	+	H	*99.9*	*100.0*	27.46	27.56
TCD-OO•-H•-10-1							
tcd-oo•-10-1	↔ tcd-oo•-h•-10-1	+	H	*95.4*	*95.5*	27.74	27.84

Units: kcal mol^{-1}

Table I.6 Work reactions for the TCD alkoxides

Work Reactions							$\Delta_f H^o_{298}$			
							a	**b**	**c**	**d**
TCD-OH-OH-12										
tcd-oh-oh-12	+	ccc	↔	tcd-h2-12	+	hocccoh	-110.92	-111.52		
tcd-oh-oh-12	+	cccc	↔	tcd-h2-12	+	hoccccoh	-110.09	-110.70		
tcd-oh-oh-12	+	ccccc	↔	tcd-h2-12	+	hocccccoh	-110.14	-110.75		
						Ave.	**-110.38**	**-110.99**		
						σ	*0.46*	*0.46*		
TCD-OH-OH-23										
tcd-oh-oh-23	+	ccc	↔	tcd-h2-23	+	hocccoh	-105.78	-103.10		
tcd-oh-oh-23	+	cccc	↔	tcd-h2-23	+	hoccccoh	-104.95	-102.28		
tcd-oh-oh-23	+	ccccc	↔	tcd-h2-23	+	hocccccoh	-105.00	-102.32		
						Ave.	**-105.24**	**-102.57**		
						σ	*0.46*	*0.46*		
TCD-OH-OH-34										
tcd-oh-oh-34	+	ccc	↔	tcd-h2-34	+	hocccoh	-100.92			
tcd-oh-oh-34	+	cccc	↔	tcd-h2-34	+	hoccccoh	-100.09			
tcd-oh-oh-34	+	ccccc	↔	tcd-h2-34	+	hocccccoh	-100.14			
						Ave.	**-100.38**			
						σ	*0.46*			
TCD-OH-OH-91										
tcd-oh-oh-91	+	ccc	↔	tcd-h2-91	+	hocccoh	-107.86	-107.83		
tcd-oh-oh-91	+	cccc	↔	tcd-h2-91	+	hoccccoh	-107.03	-107.00		
tcd-oh-oh-91	+	ccccc	↔	tcd-h2-91	+	hocccccoh	-107.08	-107.05		
						Ave.	**-107.32**	**-107.29**		
						σ	*0.46*	*0.46*		
TCD-OH-OH-26										
tcd-oh-oh-26	+	ccc	↔	tcd-h2-26	+	hocccoh	-105.19	-104.94	-103.16	-103.17
tcd-oh-oh-26	+	cccc	↔	tcd-h2-26	+	hoccccoh	-104.36	-104.12	-102.34	-102.35
tcd-oh-oh-26	+	ccccc	↔	tcd-h2-26	+	hocccccoh	-104.41	-104.17	-102.39	-102.40
						Ave.	**-104.65**	**-104.41**	**-102.63**	**-102.64**
						σ	*0.46*	*0.46*	*0.46*	*0.46*
TCD-OH-OH-98										
tcd-oh-oh-98	+	ccc	↔	tcd-h2-98	+	hocccoh	-107.92			
tcd-oh-oh-98	+	cccc	↔	tcd-h2-98	+	hoccccoh	-107.10			
tcd-oh-oh-98	+	ccccc	↔	tcd-h2-98	+	hocccccoh	-107.15			
						Ave.	**-107.39**			
						σ	*0.46*			
TCD-OH-OH-1-10										
tcd-oh-oh-1-10	+	ccc	↔	tcd-h2-1-10	+	hocccoh	-106.56	-106.47		
tcd-oh-oh-1-10	+	cccc	↔	tcd-h2-1-10	+	hoccccoh	-105.73	-105.64		
tcd-oh-oh-1-10	+	ccccc	↔	tcd-h2-1-10	+	hocccccoh	-105.78	-105.69		
						Ave.	**-106.02**	**-105.93**		
						σ	*0.46*	*0.46*		

Units: kcal mol^{-1}

Table I.7 Work reactions for the TCD alkoxy radicals

Work Reactions								$\Delta_f H^o_{298}$
TCD-O•-OH-12-a								
tcd-o•-oh-12-a	+	hocccoh	↔	tcd-oh-oh-12-a	+	hoccco•		-58.27
tcd-o•-oh-12-a	+	hoccccoh	↔	tcd-oh-oh-12-a	+	hocccco•		-58.19
tcd-o•-oh-12-a	+	hocccccoh	↔	tcd-oh-oh-12-a	+	hoccccco•		-58.18
							Ave.	**-58.21**
							σ	*0.05*
							BDE	104.27
TCD-OH-O•-12-a								
tcd-oh-o•-12-a	+	hocccoh	↔	tcd-oh-oh-12-a	+	hoccco•		-58.58
tcd-oh-o•-12-a	+	hoccccoh	↔	tcd-oh-oh-12-a	+	hocccco•		-58.50
tcd-oh-o•-12-a	+	hocccccoh	↔	tcd-oh-oh-12-a	+	hoccccco•		-58.49
							Ave.	**-58.52**
							σ	*0.05*
							BDE	103.96
TCD-O•-OH-12-b								
tcd-o•-oh-12-b	+	hocccoh	↔	tcd-oh-oh-12-b	+	hoccco•		-58.36
tcd-o•-oh-12-b	+	hoccccoh	↔	tcd-oh-oh-12-b	+	hocccco•		-58.29
tcd-o•-oh-12-b	+	hocccccoh	↔	tcd-oh-oh-12-b	+	hoccccco•		-58.27
							Ave.	**-58.31**
							σ	*0.05*
							BDE	104.78
TCD-O•-OH-12-b								
tcd-o•-oh-12-b	+	hocccoh	↔	tcd-oh-oh-12-b	+	hoccco•		-58.54
tcd-o•-oh-12-b	+	hoccccoh	↔	tcd-oh-oh-12-b	+	hocccco•		-58.46
tcd-o•-oh-12-b	+	hocccccoh	↔	tcd-oh-oh-12-b	+	hoccccco•		-58.45
							Ave.	**-58.48**
							σ	*0.05*
							BDE	104.61
TCD-O•-OH-23-a								
tcd-o•-oh-23-a	+	hocccoh	↔	tcd-oh-oh-23-a	+	hoccco•		-50.13
tcd-o•-oh-23-a	+	hoccccoh	↔	tcd-oh-oh-23-a	+	hocccco•		-50.05
tcd-o•-oh-23-a	+	hocccccoh	↔	tcd-oh-oh-23-a	+	hoccccco•		-50.04
							Ave.	**-50.07**
							σ	*0.05*
							BDE	107.27
TCD-OH-O•-23-a								
tcd-oh-o•-23-a	+	hocccoh	↔	tcd-oh-oh-23-a	+	hoccco•		-53.20
tcd-oh-o•-23-a	+	hoccccoh	↔	tcd-oh-oh-23-a	+	hocccco•		-53.12
tcd-oh-o•-23-a	+	hocccccoh	↔	tcd-oh-oh-23-a	+	hoccccco•		-53.11
							Ave.	**-53.14**
							σ	*0.05*
							BDE	104.20

Units: kcal mol^{-1}

Table I.7 Work reactions for the TCD alkoxy radicals (Continued)

Work Reactions								$\Delta_f H^o_{298}$
TCD-O•-OH-23-b								
tcd-o•-oh-23-b	+	hocccoh	↔	tcd-oh-oh-23-b	+	hoccco•		-50.07
tcd-o•-oh-23-b	+	hoccccoh	↔	tcd-oh-oh-23-b	+	hocccco•		-49.99
tcd-o•-oh-23-b	+	hocccccoh	↔	tcd-oh-oh-23-b	+	hoccccco•		-49.97
							Ave.	**-50.01**
							σ	*0.05*
							BDE	104.66
TCD-O•-OH-23-b								
tcd-oh-o•-23-b	+	hocccoh	↔	tcd-oh-oh-23-b	+	hoccco•		-51.45
tcd-oh-o•-23-b	+	hoccccoh	↔	tcd-oh-oh-23-b	+	hocccco•		-51.38
tcd-oh-o•-23-b	+	hocccccoh	↔	tcd-oh-oh-23-b	+	hoccccco•		-51.36
							Ave.	**-51.40**
							σ	*0.05*
							BDE	103.31
TCD-O•-OH-34								
tcd-o•-oh-34	+	hocccoh	↔	tcd-oh-oh-34	+	hoccco•		-47.14
tcd-o•-oh-34	+	hoccccoh	↔	tcd-oh-oh-34	+	hocccco•		-47.07
tcd-o•-oh-34	+	hocccccoh	↔	tcd-oh-oh-34	+	hoccccco•		-47.05
							Ave.	**-47.09**
							σ	*0.05*
							BDE	105.39
TCD-OH-O•-34								
tcd-oh-o•-34	+	hocccoh	↔	tcd-oh-oh-34	+	hoccco•		-47.27
tcd-oh-o•-34	+	hoccccoh	↔	tcd-oh-oh-34	+	hocccco•		-47.19
tcd-oh-o•-34	+	hocccccoh	↔	tcd-oh-oh-34	+	hoccccco•		-47.18
							Ave.	**-47.21**
							σ	*0.05*
							BDE	105.27
TCD-O•-OH-91-a								
tcd-o•-oh-91-a	+	hocccoh	↔	tcd-oh-oh-91-a	+	hoccco•		-55.18
tcd-o•-oh-91-a	+	hoccccoh	↔	tcd-oh-oh-91-a	+	hocccco•		-55.11
tcd-o•-oh-91-a	+	hocccccoh	↔	tcd-oh-oh-91-a	+	hoccccco•		-55.09
							Ave.	**-55.13**
							σ	*0.05*
							BDE	104.29
TCD-OH-O•-91-a								
tcd-oh-o•-91-a	+	hocccoh	↔	tcd-oh-oh-91-a	+	hoccco•		-55.69
tcd-oh-o•-91-a	+	hoccccoh	↔	tcd-oh-oh-91-a	+	hocccco•		-55.61
tcd-oh-o•-91-a	+	hocccccoh	↔	tcd-oh-oh-91-a	+	hoccccco•		-55.59
							Ave.	**-55.63**
							σ	*0.05*
							BDE	103.79

Units: kcal mol^{-1}

Table I.7 Work reactions for the TCD alkoxy radicals (Continued)

Work Reactions								$\Delta_f H^o_{298}$
TCD-O˙-OH-91-b								
tcd-o˙-oh-91-b	+	hocccoh	↔	tcd-oh-oh-91-b	+	hoccco˙		-55.17
tcd-o˙-oh-91-b	+	hocccoh	↔	tcd-oh-oh-91-b	+	hocccco˙		-55.09
tcd-o˙-oh-91-b	+	hocccccoh	↔	tcd-oh-oh-91-b	+	hocccccco˙		-55.08
							Ave.	**-55.12**
							σ	*0.05*
							BDE	104.30
TCD-O˙-OH-91-b								
tcd-oh-o˙-91-b	+	hocccoh	↔	tcd-oh-oh-91-b	+	hoccco˙		-55.28
tcd-oh-o˙-91-b	+	hocccoh	↔	tcd-oh-oh-91-b	+	hocccco˙		-55.21
tcd-oh-o˙-91-b	+	hocccccoh	↔	tcd-oh-oh-91-b	+	hocccccco˙		-55.19
							Ave.	**-55.23**
							σ	*0.05*
							BDE	104.16
TCD-O˙-OH-26-a1								
tcd-o˙-oh-26-a1	+	hocccoh	↔	tcd-oh-oh-26-a1	+	hoccco˙		-52.07
tcd-o˙-oh-26-a1	+	hocccoh	↔	tcd-oh-oh-26-a1	+	hocccco˙		-51.99
tcd-o˙-oh-26-a1	+	hocccccoh	↔	tcd-oh-oh-26-a1	+	hocccccco˙		-51.97
							Ave.	**-52.01**
							σ	*0.05*
							BDE	104.74
TCD-OH-O˙-26-a1								
tcd-oh-o˙-26-a1	+	hocccoh	↔	tcd-oh-oh-26-a1	+	hoccco˙		-52.05
tcd-oh-o˙-26-a1	+	hocccoh	↔	tcd-oh-oh-26-a1	+	hocccco˙		-51.98
tcd-oh-o˙-26-a1	+	hocccccoh	↔	tcd-oh-oh-26-a1	+	hocccccco˙		-51.96
							Ave.	**-52.00**
							σ	*0.05*
							BDE	104.75
TCD-O˙-OH-26-a2								
tcd-o˙-oh-26-a2	+	hocccoh	↔	tcd-oh-oh-26-a2	+	hoccco˙		-48.19
tcd-o˙-oh-26-a2	+	hocccoh	↔	tcd-oh-oh-26-a2	+	hocccco˙		-48.11
tcd-o˙-oh-26-a2	+	hocccccoh	↔	tcd-oh-oh-26-a2	+	hocccccco˙		-48.09
							Ave.	**-48.13**
							σ	*0.05*
							BDE	108.38
TCD-OH-O˙-26-a2								
tcd-oh-o˙-26-a2	+	hocccoh	↔	tcd-oh-oh-26-a2	+	hoccco˙		-47.79
tcd-oh-o˙-26-a2	+	hocccoh	↔	tcd-oh-oh-26-a2	+	hocccco˙		-47.71
tcd-oh-o˙-26-a2	+	hocccccoh	↔	tcd-oh-oh-26-a2	+	hocccccco˙		-47.70
							Ave.	**-47.73**
							σ	*0.05*
							BDE	108.78

Units: kcal mol^{-1}

Table I.7 Work reactions for the TCD alkoxy radicals (Continued)

Work Reactions								$\Delta_f H^o_{298}$
TCD-O•-OH-26-b1								
tcd-o•-oh-26-b1	+	hocccoh	↔	tcd-oh-oh-26-b1	+	hoccco•		-51.52
tcd-o•-oh-26-b1	+	hocccoh	↔	tcd-oh-oh-26-b1	+	hocccco•		-51.45
tcd-o•-oh-26-b1	+	hoccccoh	↔	tcd-oh-oh-26-b1	+	hoccccco•		-51.43
							Ave.	**-51.47**
							σ	*0.05*
							BDE	103.26
TCD-O•-OH-26-b1								
tcd-oh-o•-26-b1	+	hocccoh	↔	tcd-oh-oh-26-b1	+	hoccco•		-52.43
tcd-oh-o•-26-b1	+	hocccoh	↔	tcd-oh-oh-26-b1	+	hocccco•		-52.35
tcd-oh-o•-26-b1	+	hoccccoh	↔	tcd-oh-oh-26-b1	+	hoccccco•		-52.34
							Ave.	**-52.37**
							σ	*0.05*
							BDE	102.36
TCD-O•-OH-26-b2								
tcd-o•-oh-26- b2	+	hocccoh	↔	tcd-oh-oh-26- b2	+	hoccco•		-51.93
tcd-o•-oh-26- b2	+	hocccoh	↔	tcd-oh-oh-26- b2	+	hocccco•		-51.85
tcd-o•-oh-26- b2	+	hoccccoh	↔	tcd-oh-oh-26- b2	+	hoccccco•		-51.83
							Ave.	**-51.87**
							σ	*0.05*
							BDE	102.91
TCD-O•-OH-26-b2								
tcd-oh-o•-26- b2	+	hocccoh	↔	tcd-oh-oh-26- b2	+	hoccco•		-51.52
tcd-oh-o•-26- b2	+	hocccoh	↔	tcd-oh-oh-26- b2	+	hocccco•		-51.45
tcd-oh-o•-26- b2	+	hoccccoh	↔	tcd-oh-oh-26- b2	+	hoccccco•		-51.43
							Ave.	**-51.47**
							σ	*0.05*
							BDE	103.27
TCD-O•-OH-98								
tcd-o•-oh-98	+	hocccoh	↔	tcd-oh-oh-98	+	hoccco•		-56.44
tcd-o•-oh-98	+	hocccoh	↔	tcd-oh-oh-98	+	hocccco•		-56.36
tcd-o•-oh-98	+	hoccccoh	↔	tcd-oh-oh-98	+	hoccccco•		-56.35
							Ave.	**-56.38**
							σ	*0.05*
							BDE	103.11
TCD-OH-O•-98								
tcd-oh-o•-98	+	hocccoh	↔	tcd-oh-oh-98	+	hoccco•		-55.20
tcd-oh-o•-98	+	hocccoh	↔	tcd-oh-oh-98	+	hocccco•		-55.13
tcd-oh-o•-98	+	hoccccoh	↔	tcd-oh-oh-98	+	hoccccco•		-55.11
							Ave.	**-55.15**
							σ	*0.05*
							BDE	104.34

Units: kcal mol^{-1}

Table I.7 Work reactions for the TCD alkoxy radicals (Continued)

Work Reactions								$\Delta_f H^o_{298}$
TCD-O•-OH-1-10-a								
tcd-o•-oh-1-10-a	+	hocccoh	↔	tcd-oh-oh-1-10-a	+	hoccco•		-54.87
tcd-o•-oh-1-10-a	+	hoccccoh	↔	tcd-oh-oh-1-10-a	+	hocccco•		-54.79
tcd-o•-oh-1-10-a	+	hocccccoh	↔	tcd-oh-oh-1-10-a	+	hoccccco•		-54.78
							Ave.	**-54.81**
							σ	*0.05*
							BDE	103.31
TCD-O•-OH-1-10-a								
tcd-oh-o•-1-10-a	+	hocccoh	↔	tcd-oh-oh-1-10-a	+	hoccco•		-54.47
tcd-oh-o•-1-10-a	+	hoccccoh	↔	tcd-oh-oh-1-10-a	+	hocccco•		-54.40
tcd-oh-o•-1-10-a	+	hocccccoh	↔	tcd-oh-oh-1-10-a	+	hoccccco•		-54.38
							Ave.	**-54.42**
							σ	*0.05*
							BDE	103.70
TCD-O•-OH-1-10-b								
tcd-o•-oh-1-10-b	+	hocccoh	↔	tcd-oh-oh-1-10-b	+	hoccco•		-54.99
tcd-o•-oh-1-10-b	+	hoccccoh	↔	tcd-oh-oh-1-10-b	+	hocccco•		-54.91
tcd-o•-oh-1-10-b	+	hocccccoh	↔	tcd-oh-oh-1-10-b	+	hoccccco•		-54.90
							Ave.	**-54.93**
							σ	*0.05*
							BDE	103.10
TCD-O•-OH-1-10-b								
tcd-oh-o•-1-10-b	+	hocccoh	↔	tcd-oh-oh-1-10-b	+	hoccco•		-55.00
tcd-oh-o•-1-10-b	+	hoccccoh	↔	tcd-oh-oh-1-10-b	+	hocccco•		-54.93
tcd-oh-o•-1-10-b	+	hocccccoh	↔	tcd-oh-oh-1-10-b	+	hoccccco•		-54.91
							Ave.	**-54.95**
							σ	*0.05*
							BDE	103.08

Units: kcal mol^{-1}

Table I.8 Calculations for the TCD ring opened alkoxy diradicals

Species					$\Delta_f H^o_{298}$	
					Triplet	***Singlet***
TCD-O˙-O˙-12					**-6.72**	**-5.36**
tcd-oh-o˙-12	↔	tcd-o˙-o˙-12	+	H		
TCD-O˙-O˙-23					**2.03**	**2.78**
tcd-oh-o˙-23	↔	tcd-o˙-o˙-23	+	H		
TCD-O˙-O˙-34					**5.53**	**5.76**
tcd-oh-o˙-34	↔	tcd-o˙-o˙-34	+	H		
TCD-O˙-O˙-91					**-3.44**	**-2.78**
tcd-oh-o˙-91	↔	tcd-o˙-o˙-91	+	H		
TCD-O˙-O˙-26					**8.55**	**4.72**
tcd-oh-o˙-26	↔	tcd-o˙-o˙-26	+	H		
TCD-O˙-O˙-98					**-4.13**	**-2.29**
tcd-oh-o˙-98	↔	tcd-o˙-o˙-98	+	H		
TCD-O˙-O˙-1-10					**-3.95**	**-2.10**
tcd-oh-o˙-1-10	↔	tcd-o˙-o˙-1-10	+	H		

Units: kcal mol^{-1}

Table I.9 Work reactions for the TCD oxygenated cyclic species

Work Reactions								$\Delta_f H^o_{298}$
TCD-YOO-12								
tcd-yoo-12	+	yccc	↔	tcd	+	ycccoo		-32.90
tcd-yoo-12	+	ycccc	↔	tcd	+	ycccoo		-34.51
tcd-yoo-12	+	ycccc	↔	tcd	+	ycccccoo		-36.55
							Ave.	-34.66
TCD-YOO-23								
tcd-yoo-23	+	yccc	↔	tcd	+	ycccoo		-36.28
tcd-yoo-23	+	ycccc	↔	tcd	+	ycccoo		-37.90
tcd-yoo-23	+	ycccc	↔	tcd	+	ycccccoo		-39.94
							Ave.	-38.04
TCD-YOO-34								
tcd-yoo-34	+	yccc	↔	tcd	+	ycccoo		-35.83
tcd-yoo-34	+	ycccc	↔	tcd	+	ycccoo		-37.44
tcd-yoo-34	+	ycccc	↔	tcd	+	ycccccoo		-39.49
							Ave.	-37.59
TCD-YOO-91								
tcd-yoo-91	+	yccc	↔	tcd	+	ycccoo		-43.34
tcd-yoo-91	+	ycccc	↔	tcd	+	ycccoo		-44.95
tcd-yoo-91	+	ycccc	↔	tcd	+	ycccccoo		-46.99
							Ave.	-45.09
TCD-YOO-26								
tcd-yoo-26	+	yccc	↔	tcd	+	ycccoo		-47.25
tcd-yoo-26	+	ycccc	↔	tcd	+	ycccoo		-48.86
tcd-yoo-26	+	ycccc	↔	tcd	+	ycccccoo		-50.90
							Ave.	-49.00
TCD-YOO-98								
tcd-yoo-98	+	yccc	↔	tcd	+	ycccoo		-44.18
tcd-yoo-98	+	ycccc	↔	tcd	+	ycccoo		-45.79
tcd-yoo-98	+	ycccc	↔	tcd	+	ycccccoo		-47.84
							Ave.	-45.94
TCD-YOO-1-10								
tcd-yoo-1-10	+	yccc	↔	tcd	+	ycccoo		-40.76
tcd-yoo-1-10	+	ycccc	↔	tcd	+	ycccoo		-42.37
tcd-yoo-1-10	+	ycccc	↔	tcd	+	ycccccoo		-44.41
							Ave.	-42.51

Units: kcal mol^{-1}

APPENDIX J

TCD – ENTROPY AND HEAT CAPACITY

Appendix J includes the entropy *(S)* and heat capacity *(Cp)* versus temperature for the species calculated for the study of the oxidation of tricyclodecane (TCD).

Table J.1 Entropy *(S)* and heat capacity *(Cp) vs.* temperature

T (K)	TCD-OOH-1		TCD-OOH-2		TCD-OOH-3		TCD-OOH-4		TCD-OOH-9	
	Cp(T)	S(T)	Cp(T)	S(T)	Cp(T)	S(T)	Cp(T)	S(T)	Cp(T)	S(T)
5	7.95	39.03	7.95	38.90	7.95	39.18	7.95	39.25	7.95	39.16
50	9.51	57.76	9.67	57.67	9.94	58.14	10.62	58.66	10.23	58.26
100	15.25	66.02	15.45	66.08	15.56	66.69	15.97	67.62	15.96	67.08
150	21.23	73.32	21.30	73.44	21.12	74.04	21.41	75.11	21.41	74.57
200	27.68	80.27	27.70	80.40	27.22	80.91	27.50	82.06	27.44	81.52
250	35.14	87.21	35.16	87.34	34.53	87.73	34.77	88.93	34.69	88.38
298	43.03	94.03	43.07	94.16	42.41	94.44	42.60	95.68	42.52	95.11
300	43.36	94.32	43.41	94.45	42.74	94.72	42.94	95.97	42.85	95.39
400	59.94	109.04	60.05	109.20	59.47	109.29	59.58	110.58	59.51	109.98
500	74.49	123.99	74.63	124.18	74.19	124.15	74.25	125.46	74.19	124.85
600	86.43	138.64	86.57	138.85	86.24	138.75	86.28	140.06	86.22	139.45
700	96.17	152.69	96.30	152.92	96.05	152.78	96.08	154.10	96.03	153.47
800	104.23	166.05	104.34	166.30	104.16	166.13	104.18	167.45	104.14	166.82
900	111.00	178.72	111.09	178.98	110.95	178.79	110.98	180.11	110.93	179.47
1000	116.74	190.70	116.82	190.97	116.71	190.77	116.74	192.09	116.70	191.45
1100	121.65	202.05	121.72	202.33	121.64	202.11	121.67	203.45	121.63	202.80
1200	125.88	212.81	125.93	213.09	125.87	212.87	125.90	214.21	125.86	213.56
1300	129.53	223.02	129.57	223.31	129.53	223.09	129.56	224.42	129.52	223.77
1400	132.69	232.73	132.73	233.02	132.69	232.80	132.72	234.13	132.69	233.48
1500	135.44	241.98	135.47	242.27	135.45	242.04	135.47	243.38	135.44	242.72
2000	144.85	282.35	144.87	282.65	144.86	282.41	144.88	283.76	144.86	283.10
2500	150.03	315.27	150.04	315.57	150.04	315.33	150.05	316.69	150.03	316.01
3000	153.11	342.91	153.12	343.21	153.12	342.98	153.13	344.33	153.11	343.66
3500	155.07	366.66	155.08	366.97	155.08	366.73	155.09	368.09	155.08	367.41
4000	156.39	387.46	156.39	387.76	156.39	387.53	156.40	388.88	156.39	388.21
4500	157.32	405.93	157.32	406.24	157.32	406.00	157.32	407.36	157.32	406.68
5000	157.99	422.54	157.99	422.85	157.99	422.61	158.00	423.97	157.99	423.29

Units: S(cal mol^{-1}) , Cp(cal mol^{-1} K^{-1})

Table J.1 Entropy *(S)* and heat capacity *(Cp) vs.* temperature (Continued)

T (K)	TCD-OOH-1-10		TCD-OO•-1		TCD-OO•-2		TCD-OO•-3		TCD-OO•-4	
	Cp(T)	S(T)	Cp(T)	S(T)	Cp(T)	S(T)	Cp(T)	S(T)	Cp(T)	S(T)
5	7.95	39.11	7.95	40.33	7.95	40.22	7.95	40.49	7.95	40.40
50	10.23	58.22	9.61	59.19	9.74	59.17	10.13	59.69	10.40	59.96
100	16.05	67.05	14.51	67.26	14.54	67.31	14.80	68.09	14.66	68.39
150	21.63	74.61	19.95	74.15	19.91	74.19	19.77	75.01	19.65	75.25
200	27.68	81.62	26.07	80.69	26.02	80.72	25.57	81.44	25.54	81.66
250	34.90	88.53	33.26	87.24	33.24	87.26	32.66	87.87	32.67	88.09
298	42.67	95.29	40.93	93.71	40.95	93.73	40.35	94.23	40.37	94.46
300	43.01	95.58	41.25	93.98	41.28	94.00	40.68	94.50	40.70	94.73
400	59.58	110.20	57.44	108.05	57.54	108.08	57.05	108.42	57.07	108.66
500	74.20	125.07	71.68	122.41	71.80	122.47	71.45	122.71	71.45	122.95
600	86.22	139.67	83.37	136.51	83.48	136.60	83.24	136.79	83.24	137.02
700	96.01	153.69	92.89	150.08	92.99	150.18	92.82	150.34	92.82	150.57
800	104.11	167.04	100.75	162.99	100.83	163.10	100.72	163.25	100.72	163.48
900	110.91	179.69	107.33	175.23	107.40	175.35	107.33	175.48	107.33	175.72
1000	116.68	191.67	112.91	186.82	112.96	186.95	112.91	187.08	112.92	187.31
1100	121.61	203.01	117.66	197.80	117.71	197.93	117.67	198.05	117.68	198.29
1200	125.85	213.77	121.73	208.21	121.77	208.34	121.75	208.46	121.76	208.70
1300	129.50	223.98	125.24	218.08	125.27	218.22	125.26	218.34	125.27	218.57
1400	132.67	233.69	128.27	227.47	128.30	227.61	128.29	227.73	128.30	227.96
1500	135.43	242.93	130.90	236.40	130.93	236.55	130.92	236.66	130.93	236.90
2000	144.85	283.30	139.86	275.40	139.87	275.55	139.88	275.67	139.88	275.91
2500	150.03	316.22	144.75	307.18	144.76	307.33	144.76	307.45	144.77	307.68
3000	153.11	343.86	147.65	333.84	147.65	333.99	147.66	334.11	147.66	334.35
3500	155.07	367.61	149.49	356.74	149.50	356.89	149.50	357.01	149.50	357.25
4000	156.39	388.41	150.73	376.79	150.73	376.94	150.73	377.06	150.74	377.30
4500	157.32	406.88	151.59	394.59	151.60	394.74	151.60	394.86	151.60	395.10
5000	157.99	423.49	152.22	410.59	152.23	410.75	152.23	410.87	152.23	411.11

Units: S(cal mol^{-1}) , Cp(cal mol^{-1} K^{-1})

Table J.1 Entropy *(S)* and heat capacity *(Cp) vs.* temperature (Continued)

T (K)	TCD-OO•-9		TCD-OO•-1-10		TCD-OOH-12		TCD-OOH-21		TCD-OOH-23	
	Cp(T)	S(T)	Cp(T)	S(T)	Cp(T)	S(T)	Cp(T)	S(T)	Cp(T)	S(T)
5	7.95	40.46	7.95	40.43	7.95	39.94	7.95	39.81	7.95	39.35
50	10.38	59.98	10.37	59.89	13.70	61.73	14.73	61.95	11.02	58.72
100	15.02	68.55	15.14	68.48	20.30	73.31	21.39	74.33	18.60	68.65
150	19.93	75.54	20.19	75.55	26.00	82.62	26.66	84.00	25.38	77.48
200	25.68	82.01	25.97	82.11	32.06	90.89	32.41	92.42	32.02	85.66
250	32.73	88.46	32.97	88.61	39.22	98.77	39.39	100.36	39.46	93.57
298	40.38	94.83	40.56	95.02	46.95	106.29	47.04	107.90	47.33	101.15
300	40.71	95.10	40.89	95.30	47.29	106.60	47.37	108.21	47.66	101.46
400	57.03	109.03	57.11	109.26	64.02	122.47	64.02	124.09	64.43	117.44
500	71.40	123.31	71.43	123.55	79.07	138.37	79.05	139.99	79.41	133.44
600	83.18	137.37	83.19	137.62	91.64	153.91	91.60	155.52	91.89	149.02
700	92.77	150.92	92.76	151.16	102.03	168.81	101.99	170.42	102.20	163.96
800	100.67	163.82	100.66	164.06	110.71	183.00	110.66	184.60	110.82	178.16
900	107.28	176.05	107.26	176.29	118.05	196.45	117.99	198.05	118.11	191.63
1000	112.88	187.63	112.85	187.87	124.31	209.21	124.25	210.79	124.33	204.39
1100	117.64	198.61	117.62	198.85	129.68	221.30	129.63	222.88	129.68	216.48
1200	121.72	209.02	121.70	209.25	134.31	232.77	134.26	234.35	134.29	227.95
1300	125.24	218.89	125.21	219.12	138.31	243.67	138.26	245.25	138.29	238.85
1400	128.27	228.28	128.25	228.51	141.79	254.04	141.74	255.62	141.75	249.22
1500	130.91	237.21	130.88	237.44	144.81	263.92	144.76	265.49	144.77	259.10
2000	139.87	276.21	139.85	276.44	155.16	307.13	155.13	308.69	155.12	302.29
2500	144.76	307.99	144.74	308.21	160.86	342.41	160.83	343.96	160.82	337.57
3000	147.66	334.65	147.65	334.87	164.25	372.05	164.23	373.60	164.22	367.20
3500	149.50	357.55	149.49	357.77	166.41	397.54	166.39	399.09	166.39	392.69
4000	150.73	377.60	150.73	377.82	167.86	419.86	167.85	421.40	167.84	415.00
4500	151.60	395.40	151.59	395.62	168.87	439.69	168.87	441.23	168.86	434.83
5000	152.23	411.41	152.22	411.62	169.61	457.52	169.61	459.06	169.60	452.66

Units: S(cal mol^{-1}) , Cp(cal mol^{-1} K^{-1})

Table J.1 Entropy *(S)* and heat capacity *(Cp) vs.* temperature (Continued)

T (K)	TCD-OOH-32		TCD-OOH-34		TCD-OOH-43		TCD-OOH-19		TCD-OOH-91	
	Cp(T)	S(T)	Cp(T)	S(T)	Cp(T)	S(T)	Cp(T)	S(T)	Cp(T)	S(T)
5	7.95	39.97	7.95	39.75	7.95	39.53	7.95	39.51	7.95	39.63
50	12.82	60.61	11.93	59.55	11.66	59.33	11.84	59.30	13.01	61.09
100	19.57	71.63	19.51	70.17	19.04	69.65	19.42	69.86	18.57	71.84
150	25.35	80.65	25.95	79.31	25.65	78.63	25.91	78.97	23.85	80.34
200	31.48	88.74	32.31	87.61	32.16	86.87	32.35	87.28	29.77	87.98
250	38.71	96.51	39.56	95.56	39.50	94.80	39.65	95.25	36.82	95.34
298	46.53	103.94	47.30	103.14	47.29	102.37	47.41	102.84	44.44	102.43
300	46.87	104.25	47.64	103.46	47.62	102.69	47.74	103.16	44.77	102.72
400	63.74	120.02	64.29	119.41	64.31	118.65	64.37	119.14	61.24	117.83
500	78.88	135.87	79.24	135.37	79.28	134.61	79.31	135.12	76.04	133.09
600	91.49	151.37	91.74	150.93	91.78	150.18	91.79	150.68	88.40	148.05
700	101.91	166.26	102.07	165.84	102.11	165.10	102.12	165.61	98.60	162.44
800	110.60	180.43	110.71	180.03	110.74	179.29	110.76	179.80	107.10	176.16
900	117.95	193.87	118.02	193.49	118.05	192.75	118.08	193.26	114.28	189.18
1000	124.22	206.62	124.26	206.24	124.29	205.50	124.32	206.02	120.38	201.53
1100	129.60	218.70	129.62	218.32	129.65	217.59	129.69	218.11	125.60	213.24
1200	134.24	230.17	134.25	229.79	134.27	229.06	134.31	229.59	130.09	224.35
1300	138.25	241.06	138.25	240.69	138.27	239.96	138.31	240.49	133.96	234.91
1400	141.73	251.43	141.72	251.06	141.74	250.33	141.78	250.86	137.31	244.96
1500	144.75	261.31	144.75	260.93	144.76	260.21	144.80	260.74	140.22	254.53
2000	155.13	304.50	155.11	304.12	155.13	303.40	155.16	303.94	150.14	296.35
2500	160.83	339.77	160.82	339.39	160.83	338.67	160.85	339.22	155.56	330.48
3000	164.23	369.41	164.22	369.03	164.23	368.31	164.24	368.86	158.78	359.14
3500	166.39	394.90	166.38	394.51	166.39	393.80	166.40	394.35	160.82	383.77
4000	167.85	417.21	167.84	416.83	167.84	416.11	167.85	416.67	162.19	405.34
4500	168.87	437.04	168.86	436.65	168.86	435.94	168.87	436.50	163.15	424.50
5000	169.61	454.87	169.60	454.48	169.61	453.77	169.61	454.33	163.85	441.72

Units: S(cal mol^{-1}) , Cp(cal mol^{-1} K^{-1})

Table J.1 Entropy *(S)* and heat capacity *(Cp) vs.* temperature (Continued)

T (K)	TCD-OOH-1-10		TCD-OOH-10-1		TCD-OOH-26		TCD-OOH-98		TCD-OO•-12	
	Cp(T)	S(T)	Cp(T)	S(T)	Cp(T)	S(T)	Cp(T)	S(T)	Cp(T)	S(T)
5	7.95	39.48	7.95	39.64	7.95	39.50	7.95	39.81	7.95	41.26
50	11.29	59.03	12.12	59.65	10.16	58.45	12.90	60.39	13.90	63.18
100	18.67	69.09	19.14	70.24	17.08	67.53	20.26	71.62	19.51	74.60
150	25.46	77.95	25.31	79.17	23.92	75.74	26.54	81.03	24.61	83.46
200	32.14	86.16	31.59	87.28	30.75	83.53	32.77	89.49	30.37	91.29
250	39.51	94.09	38.77	95.06	38.29	91.17	39.89	97.53	37.31	98.77
298	47.24	101.66	46.45	102.49	46.20	98.54	47.51	105.16	44.86	105.94
300	47.58	101.98	46.78	102.80	46.54	98.85	47.84	105.48	45.19	106.24
400	64.11	117.90	63.40	118.51	63.39	114.52	64.33	121.47	61.56	121.45
500	79.01	133.81	78.44	134.27	78.50	130.29	79.22	137.43	76.30	136.78
600	91.49	149.32	91.06	149.69	91.13	145.72	91.70	152.98	88.61	151.78
700	101.85	164.20	101.52	164.51	101.59	160.55	102.05	167.89	98.78	166.20
800	110.52	178.36	110.27	178.63	110.33	174.68	110.70	182.07	107.25	179.94
900	117.86	191.80	117.68	192.04	117.72	188.10	118.03	195.53	114.40	192.98
1000	124.13	204.53	124.00	204.76	124.03	200.82	124.29	208.28	120.49	205.34
1100	129.51	216.61	129.42	216.82	129.44	212.89	129.66	220.37	125.69	217.06
1200	134.15	228.07	134.09	228.28	134.10	224.34	134.29	231.84	130.17	228.18
1300	138.17	238.96	138.13	239.16	138.13	235.23	138.30	242.74	134.03	238.74
1400	141.66	249.32	141.63	249.52	141.63	245.59	141.77	253.11	137.37	248.79
1500	144.69	259.19	144.67	259.39	144.67	255.46	144.80	262.99	140.28	258.37
2000	155.09	302.37	155.09	302.57	155.08	298.63	155.16	306.20	150.17	300.20
2500	160.80	337.63	160.82	337.84	160.80	333.90	160.85	341.47	155.58	334.33
3000	164.21	367.27	164.22	367.47	164.21	363.53	164.25	371.12	158.79	363.00
3500	166.38	392.75	166.39	392.96	166.38	389.01	166.41	396.60	160.83	387.64
4000	167.83	415.06	167.84	415.27	167.84	411.33	167.86	418.92	162.20	409.20
4500	168.86	434.89	168.86	435.10	168.86	431.16	168.87	438.75	163.15	428.36
5000	169.60	452.72	169.61	452.93	169.60	448.98	169.61	456.58	163.85	445.59

Units: S(cal mol^{-1}) , Cp(cal mol^{-1} K^{-1})

Table J.1 Entropy *(S)* and heat capacity *(Cp) vs.* temperature (Continued)

T (K)	TCD-OO˙-21		TCD-OO˙-23		TCD-OO˙-32		TCD-OO˙-34		TCD-OO˙-43	
	Cp(T)	S(T)	Cp(T)	S(T)	Cp(T)	S(T)	Cp(T)	S(T)	Cp(T)	S(T)
5	7.95	41.13	7.95	40.65	7.95	41.27	7.95	41.06	7.95	40.82
50	15.15	64.05	11.25	60.16	13.00	62.20	11.94	60.98	11.94	61.06
100	20.58	76.32	18.02	70.03	18.69	73.01	18.58	71.31	18.16	71.20
150	25.26	85.53	24.16	78.49	23.90	81.56	24.47	79.96	24.19	79.70
200	30.74	93.51	30.43	86.27	29.76	89.19	30.57	87.80	30.44	87.48
250	37.53	101.05	37.62	93.79	36.81	96.55	37.64	95.35	37.60	95.00
298	45.00	108.25	45.28	101.03	44.47	103.64	45.22	102.57	45.23	102.23
300	45.32	108.55	45.61	101.33	44.80	103.94	45.55	102.88	45.56	102.53
400	61.62	123.79	62.00	116.67	61.36	119.07	61.88	118.19	61.92	117.85
500	76.33	139.12	76.66	132.09	76.20	134.36	76.54	133.58	76.59	133.25
600	88.62	154.13	88.88	147.15	88.55	149.35	88.76	148.62	88.81	148.30
700	98.77	168.55	98.96	161.60	98.73	163.76	98.86	163.06	98.91	162.75
800	107.23	182.29	107.37	175.36	107.21	177.49	107.29	176.80	107.33	176.50
900	114.37	195.32	114.46	188.41	114.35	190.52	114.40	189.84	114.44	189.54
1000	120.46	207.68	120.51	200.77	120.44	202.88	120.46	202.20	120.49	201.91
1100	125.66	219.40	125.69	212.50	125.64	214.60	125.65	213.92	125.68	213.63
1200	130.14	230.52	130.15	223.62	130.12	225.71	130.12	225.04	130.14	224.75
1300	134.00	241.08	134.00	234.18	133.98	236.27	133.97	235.60	133.99	235.31
1400	137.34	251.13	137.33	244.23	137.32	246.32	137.31	245.64	137.33	245.36
1500	140.24	260.70	140.23	253.79	140.23	255.89	140.21	255.21	140.23	254.92
2000	150.15	302.52	150.12	295.62	150.13	297.71	150.12	297.03	150.12	296.75
2500	155.56	336.65	155.54	329.74	155.55	331.84	155.54	331.15	155.54	330.87
3000	158.78	365.31	158.76	358.40	158.77	360.50	158.76	359.81	158.76	359.53
3500	160.82	389.95	160.80	383.03	160.81	385.13	160.80	384.44	160.80	384.16
4000	162.19	411.51	162.17	404.59	162.18	406.69	162.17	406.00	162.18	405.72
4500	163.15	430.67	163.14	423.75	163.14	425.85	163.14	425.16	163.14	424.88
5000	163.85	447.90	163.84	440.97	163.84	443.08	163.84	442.38	163.84	442.11

Units: S(cal mol^{-1}) , Cp(cal mol^{-1} K^{-1})

Table J.1 Entropy *(S)* and heat capacity *(Cp) vs.* temperature (Continued)

T (K)	TCD-OO•-19		TCD-OO•-91		TCD-OO•-1-10		TCD-OO•-10-1		TCD-OO•-26	
	Cp(T)	S(T)	Cp(T)	S(T)	Cp(T)	S(T)	Cp(T)	S(T)	Cp(T)	S(T)
5	7.95	40.78	7.95	40.99	7.95	40.79	7.95	40.95	7.95	40.82
50	11.91	60.70	12.78	61.74	11.91	61.07	12.43	61.52	10.21	59.88
100	18.80	71.11	19.52	72.73	18.24	71.24	18.30	71.94	16.22	68.72
150	24.70	79.85	25.35	81.74	24.35	79.79	23.90	80.41	22.51	76.47
200	30.82	87.76	31.52	89.84	30.66	87.62	29.90	88.07	29.04	83.81
250	37.88	95.36	38.73	97.61	37.75	95.19	36.89	95.45	36.38	91.04
298	45.44	102.63	46.50	105.04	45.26	102.43	44.41	102.55	44.10	98.06
300	45.77	102.93	46.84	105.36	45.58	102.74	44.73	102.84	44.43	98.36
400	62.02	118.30	63.62	121.10	61.72	118.03	61.03	117.91	60.92	113.37
500	76.63	133.71	78.73	136.92	76.28	133.37	75.76	133.12	75.72	128.56
600	88.83	148.76	91.35	152.40	88.49	148.36	88.11	148.02	88.10	143.46
700	98.92	163.21	101.79	167.26	98.61	162.76	98.33	162.37	98.33	157.81
800	107.35	176.97	110.51	181.41	107.06	176.47	106.87	176.05	106.86	171.49
900	114.46	190.01	117.88	194.85	114.21	189.49	114.07	189.05	114.07	184.48
1000	120.52	202.38	124.17	207.59	120.31	201.83	120.20	201.38	120.20	196.81
1100	125.71	214.10	129.57	219.67	125.52	213.53	125.45	213.07	125.45	208.51
1200	130.18	225.23	134.22	231.13	130.01	224.64	129.96	224.17	129.96	219.61
1300	134.03	235.79	138.24	242.03	133.89	235.19	133.85	234.72	133.85	230.16
1400	137.37	245.84	141.72	252.40	137.24	245.23	137.22	244.76	137.21	240.20
1500	140.26	255.41	144.75	262.27	140.15	254.79	140.14	254.32	140.13	249.76
2000	150.16	297.24	155.14	305.47	150.09	296.60	150.09	296.13	150.09	291.56
2500	155.57	331.37	160.84	340.74	155.52	330.72	155.53	330.25	155.53	325.68
3000	158.78	360.04	164.24	370.38	158.75	359.37	158.76	358.90	158.75	354.33
3500	160.82	384.67	166.40	395.87	160.80	384.00	160.80	383.54	160.80	378.97
4000	162.19	406.24	167.85	418.19	162.17	405.57	162.18	405.10	162.17	400.53
4500	163.15	425.39	168.87	438.02	163.13	424.72	163.14	424.26	163.14	419.69
5000	163.85	442.62	169.61	455.85	163.83	441.95	163.84	441.48	163.84	436.91

Units: S(cal mol^{-1}) , Cp(cal mol^{-1} K^{-1})

Table J.1 Entropy *(S)* and heat capacity *(Cp) vs.* temperature (Continued)

T (K)	TCD-OO•-98		TCD-OH-OH-12		TCD-OH-OH-23		TCD-OH-OH-34		TCD-OH-OH-91	
	Cp(T)	S(T)	Cp(T)	S(T)	Cp(T)	S(T)	Cp(T)	S(T)	Cp(T)	S(T)
5	7.95	41.11	7.95	39.73	7.95	39.34	7.95	41.88	7.95	39.62
50	13.02	62.19	12.92	60.71	10.58	58.68	11.25	61.34	11.80	59.47
100	19.31	73.16	19.07	71.53	17.13	67.95	18.70	71.41	18.72	69.76
150	25.04	82.06	25.21	80.41	23.60	76.11	25.31	80.25	25.22	78.57
200	31.02	90.05	31.70	88.51	30.34	83.79	31.79	88.39	31.75	86.69
250	37.96	97.68	39.13	96.35	37.98	91.34	39.09	96.23	39.11	94.53
298	45.42	104.96	47.02	103.87	46.05	98.67	46.87	103.73	46.92	102.04
300	45.75	105.26	47.36	104.18	46.40	98.98	47.20	104.05	47.25	102.35
400	61.92	120.61	64.23	120.09	63.52	114.65	63.94	119.89	64.02	118.21
500	76.51	135.99	79.31	136.05	78.75	130.47	78.98	135.78	79.06	134.12
600	88.73	151.03	91.84	151.62	91.38	145.95	91.52	151.29	91.60	149.65
700	98.84	165.46	102.16	166.55	101.78	160.81	101.87	166.17	101.95	164.54
800	107.28	179.21	110.76	180.75	110.44	174.96	110.51	180.34	110.59	178.71
900	114.41	192.25	118.03	194.21	117.76	188.38	117.81	193.77	117.89	192.15
1000	120.49	204.61	124.23	206.95	123.99	201.11	124.04	206.49	124.12	204.89
1100	125.69	216.33	129.56	219.04	129.35	213.17	129.39	218.56	129.46	216.96
1200	130.16	227.45	134.15	230.50	133.97	224.61	134.00	230.01	134.08	228.42
1300	134.02	238.01	138.13	241.39	137.97	235.49	138.00	240.88	138.07	239.30
1400	137.36	248.06	141.59	251.75	141.45	245.83	141.47	251.23	141.54	249.65
1500	140.26	257.63	144.60	261.61	144.48	255.69	144.50	261.09	144.56	259.52
2000	150.16	299.47	154.97	304.76	154.89	298.81	154.90	304.21	154.95	302.66
2500	155.57	333.60	160.70	340.00	160.65	334.04	160.65	339.44	160.69	337.89
3000	158.78	362.26	164.12	369.62	164.09	363.64	164.09	369.05	164.12	367.51
3500	160.82	386.89	166.31	395.08	166.28	389.11	166.28	394.52	166.30	392.98
4000	162.19	408.46	167.78	417.39	167.76	411.41	167.76	416.82	167.77	415.28
4500	163.15	427.62	168.81	437.21	168.79	431.23	168.79	436.64	168.81	435.10
5000	163.85	444.85	169.56	455.04	169.55	449.05	169.55	454.46	169.56	452.93

Units: S(cal mol^{-1}) , Cp(cal mol^{-1} K^{-1})

Table J.1 Entropy *(S)* and heat capacity *(Cp) vs.* temperature (Continued)

T (K)	TCD-OH-OH-26		TCD-OH-OH-98		TCD-OH-OH-1-10		TCD-OH-O•-12		TCD-OH-O•-23	
	Cp(T)	S(T)	Cp(T)	S(T)	Cp(T)	S(T)	Cp(T)	S(T)	Cp(T)	S(T)
5	7.95	39.41	7.95	41.92	7.95	39.06	7.95	39.65	7.95	39.29
50	9.79	58.34	12.09	61.80	10.14	58.12	12.68	60.66	10.79	58.64
100	15.96	66.83	19.83	72.61	16.33	66.95	18.60	71.25	16.91	67.98
150	23.23	74.66	26.13	81.86	22.86	74.79	24.52	79.89	22.98	75.96
200	30.52	82.32	32.33	90.19	29.71	82.27	30.89	87.78	29.63	83.45
250	38.34	89.94	39.43	98.13	37.37	89.69	38.21	95.42	37.29	90.84
298	46.38	97.33	47.07	105.68	45.39	96.91	45.98	102.77	45.34	98.05
300	46.72	97.64	47.40	105.99	45.74	97.21	46.31	103.08	45.68	98.35
400	63.68	113.38	63.97	121.87	62.76	112.67	62.83	118.64	62.55	113.79
500	78.80	129.22	78.94	137.76	78.00	128.32	77.48	134.24	77.38	129.35
600	91.39	144.70	91.48	153.26	90.71	143.67	89.62	149.45	89.60	144.54
700	101.78	159.57	101.84	168.14	101.20	158.44	99.60	164.01	99.62	159.11
800	110.44	173.72	110.49	182.29	109.96	172.52	107.89	177.84	107.94	172.95
900	117.76	187.14	117.81	195.72	117.36	185.89	114.89	190.95	114.95	186.06
1000	124.01	199.87	124.05	208.45	123.67	198.57	120.85	203.35	120.92	198.47
1100	129.37	211.93	129.41	220.52	129.09	210.61	125.96	215.10	126.03	210.23
1200	134.00	223.38	134.03	231.97	133.76	222.03	130.35	226.25	130.42	221.38
1300	138.00	234.25	138.03	242.85	137.80	232.89	134.15	236.82	134.22	231.96
1400	141.48	244.60	141.51	253.20	141.31	243.22	137.45	246.88	137.51	242.02
1500	144.51	254.46	144.53	263.06	144.36	253.07	140.31	256.46	140.38	251.60
2000	154.92	297.59	154.94	306.20	154.84	296.17	150.13	298.29	150.18	293.45
2500	160.67	332.82	160.68	341.43	160.63	331.39	155.52	332.41	155.56	327.58
3000	164.10	362.43	164.11	371.04	164.07	360.99	158.74	361.06	158.76	356.24
3500	166.29	387.90	166.30	396.51	166.27	386.46	160.78	385.69	160.80	380.87
4000	167.77	410.20	167.77	418.82	167.75	408.76	162.16	407.25	162.17	402.44
4500	168.80	430.02	168.80	438.64	168.79	428.58	163.12	426.41	163.14	421.59
5000	169.55	447.85	169.56	456.46	169.54	446.40	163.82	443.63	163.83	438.82

Units: S(cal mol^{-1}) , Cp(cal mol^{-1} K^{-1})

Table J.1 Entropy *(S)* and heat capacity *(Cp) vs.* temperature (Continued)

T (K)	TCD-OH-O•-34		TCD-OH-O•-91		TCD-OH-O•-26		TCD-OH-O•-98		TCD-OH-O•-1-10	
	Cp(T)	S(T)	Cp(T)	S(T)	Cp(T)	S(T)	Cp(T)	S(T)	Cp(T)	S(T)
5	7.95	39.71	7.95	39.51	7.95	38.87	7.95	39.46	7.95	39.14
50	11.50	59.38	11.49	59.25	9.52	57.64	11.71	59.12	10.24	58.17
100	18.43	69.47	17.79	69.13	15.19	65.83	18.85	69.48	16.66	67.16
150	24.66	78.13	23.88	77.49	21.87	73.23	24.75	78.25	23.21	75.14
200	31.02	86.06	30.31	85.20	28.88	80.44	30.83	86.16	29.91	82.70
250	38.26	93.72	37.67	92.72	36.62	87.69	37.91	93.77	37.37	90.14
298	45.97	101.07	45.47	99.97	44.63	94.77	45.54	101.05	45.17	97.35
300	46.30	101.38	45.81	100.28	44.97	95.07	45.87	101.35	45.50	97.65
400	62.75	116.92	62.42	115.70	61.76	110.29	62.30	116.77	62.04	112.98
500	77.41	132.51	77.18	131.23	76.61	125.67	77.02	132.26	76.78	128.41
600	89.58	147.70	89.43	146.39	88.91	140.73	89.27	147.39	89.04	143.50
700	99.59	162.26	99.49	160.93	99.03	155.20	99.35	161.91	99.15	157.98
800	107.91	176.10	107.86	174.75	107.44	168.97	107.74	175.72	107.56	171.77
900	114.94	189.21	114.91	187.86	114.53	182.02	114.81	188.81	114.65	184.84
1000	120.91	201.62	120.90	200.27	120.56	194.39	120.83	201.21	120.69	197.22
1100	126.03	213.38	126.04	212.02	125.72	206.12	125.97	212.96	125.85	208.96
1200	130.43	224.52	130.45	223.17	130.16	217.24	130.40	224.10	130.29	220.09
1300	134.23	235.11	134.26	233.76	133.99	227.81	134.22	234.69	134.12	230.67
1400	137.53	245.17	137.56	243.82	137.31	237.85	137.52	244.75	137.44	240.72
1500	140.39	254.75	140.42	253.40	140.20	247.42	140.40	254.33	140.32	250.30
2000	150.19	296.61	150.22	295.27	150.07	289.23	150.21	296.19	150.17	292.14
2500	155.57	330.74	155.60	329.41	155.49	323.34	155.59	330.32	155.56	326.27
3000	158.78	359.40	158.80	358.08	158.72	351.99	158.79	358.99	158.77	354.93
3500	160.81	384.04	160.83	382.71	160.77	376.62	160.82	383.63	160.81	379.56
4000	162.18	405.60	162.19	404.28	162.15	398.18	162.19	405.19	162.18	401.13
4500	163.14	424.76	163.15	423.44	163.11	417.33	163.15	424.35	163.14	420.28
5000	163.84	441.98	163.85	440.66	163.82	434.55	163.85	441.58	163.84	437.51

Units: S(cal mol^{-1}) , Cp(cal mol^{-1} K^{-1})

Table J.1 Entropy *(S)* and heat capacity *(Cp) vs.* temperature (Continued)

T (K)	TCD-YOO-12		TCD-YOO-23		TCD-YOO-34		TCD-YOO-91		TCD-YOO-26	
	Cp(T)	S(T)	Cp(T)	S(T)	Cp(T)	S(T)	Cp(T)	S(T)	Cp(T)	S(T)
5	7.95	38.85	7.95	39.00	7.95	38.93	7.95	38.91	7.95	38.61
50	9.10	57.46	9.03	57.58	8.92	57.49	8.86	57.43	8.40	56.99
100	13.66	65.05	13.72	65.15	13.35	64.89	13.46	64.84	12.64	63.92
150	19.17	71.60	19.31	71.74	18.87	71.32	19.07	71.33	18.47	70.11
200	25.55	77.94	25.59	78.11	25.23	77.57	25.43	77.64	25.08	76.29
250	33.06	84.41	33.00	84.58	32.71	83.97	32.90	84.08	32.70	82.66
298	41.03	90.87	40.92	91.02	40.68	90.36	40.85	90.51	40.70	89.06
300	41.37	91.14	41.26	91.30	41.02	90.63	41.19	90.78	41.04	89.33
400	58.22	105.33	58.09	105.45	57.91	104.72	58.04	104.92	57.88	103.43
500	73.08	119.93	72.96	120.02	72.83	119.26	72.92	119.48	72.75	117.95
600	85.32	134.34	85.21	134.41	85.12	133.63	85.19	133.86	85.01	132.30
700	95.33	148.25	95.24	148.30	95.18	147.51	95.23	147.75	95.06	146.16
800	103.61	161.51	103.53	161.55	103.50	160.75	103.54	161.00	103.38	159.39
900	110.56	174.11	110.50	174.14	110.48	173.34	110.51	173.59	110.36	171.96
1000	116.45	186.06	116.39	186.08	116.39	185.28	116.41	185.53	116.28	183.89
1100	121.48	197.38	121.43	197.40	121.44	196.60	121.45	196.86	121.33	195.21
1200	125.79	208.13	125.74	208.15	125.76	207.35	125.77	207.60	125.67	205.94
1300	129.50	218.34	129.46	218.35	129.48	217.56	129.49	217.81	129.39	216.14
1400	132.71	228.05	132.67	228.06	132.70	227.26	132.70	227.52	132.62	225.84
1500	135.49	237.30	135.46	237.30	135.49	236.51	135.49	236.77	135.41	235.08
2000	144.97	277.69	144.95	277.69	144.97	276.91	144.97	277.16	144.92	275.46
2500	150.13	310.64	150.12	310.63	150.14	309.85	150.14	310.11	150.11	308.40
3000	153.20	338.29	153.19	338.29	153.21	337.51	153.20	337.77	153.18	336.05
3500	155.15	362.06	155.14	362.05	155.15	361.28	155.15	361.53	155.13	359.82
4000	156.45	382.87	156.45	382.86	156.46	382.08	156.45	382.34	156.44	380.62
4500	157.37	401.35	157.36	401.34	157.37	400.57	157.37	400.82	157.36	399.10
5000	158.03	417.96	158.03	417.95	158.03	417.18	158.03	417.43	158.02	415.71

Units: S(cal mol^{-1}) , Cp(cal mol^{-1} K^{-1})

Table J.1 Entropy *(S)* and heat capacity *(Cp) vs.* temperature (Continued)

T (K)	TCD-YOO-98		TCD-YOO-1-10	
	Cp(T)	S(T)	Cp(T)	S(T)
5	7.95	38.92	7.95	38.67
50	8.80	57.43	8.99	57.21
100	13.29	64.76	13.85	64.82
150	18.86	71.17	19.40	71.46
200	25.17	77.42	25.61	77.85
250	32.60	83.79	32.92	84.31
298	40.52	90.17	40.72	90.73
300	40.86	90.44	41.05	91.00
400	57.71	104.48	57.69	105.06
500	72.64	118.97	72.50	119.54
600	84.96	133.31	84.78	133.85
700	95.05	147.16	94.87	147.67
800	103.40	160.39	103.23	160.88
900	110.40	172.97	110.25	173.44
1000	116.34	184.90	116.20	185.35
1100	121.40	196.22	121.28	196.66
1200	125.73	206.96	125.62	207.39
1300	129.46	217.16	129.37	217.59
1400	132.68	226.87	132.60	227.29
1500	135.48	236.12	135.40	236.53
2000	144.97	276.51	144.93	276.91
2500	150.15	309.46	150.12	309.85
3000	153.21	337.12	153.19	337.50
3500	155.16	360.89	155.14	361.27
4000	156.46	381.69	156.45	382.07
4500	157.37	400.17	157.36	400.55
5000	158.04	416.79	158.03	417.17

Units: S(cal mol^{-1}) , Cp(cal mol^{-1} K^{-1})

APPENDIX K

TCD – THERMOCHEMICAL PROPERTIES IN THE NASA POLYNOMIAL FORMAT

Appendix K summarizes the thermochemical properties of the species calculated for the study of the oxidation of tricyclodecane (TCD) in the NASA polynomial format, for use in ChemKin.

Table K.1 Thermochemical properties of the TCD system in the NASA polynomial format for use in ChemKin

```
THERMO
   300.000  1500.000  5000.000

TCD       TCD  level b3lC  10H  16    0    0G   300.000  5000.000 1387.000    01
 2.66446168E+01 4.06470866E-02-1.37847937E-05 2.13057139E-09-1.23308462E-13    2
-2.49729531E+04-1.31997428E+02-1.54492269E+01 1.39942716E-01-1.02889038E-04    3
 3.83374532E-08-5.74977305E-12-1.05715162E+04 9.35347207E+01                   4
TCDJ1     freqs  b3lyp/6C  10H  15    0    0G   300.000  5000.000 1388.000    01
 2.65706041E+01 3.82418286E-02-1.29706489E-05 2.00494562E-09-1.16047629E-13    2
 3.12406199E+03-1.29684759E+02-1.44381145E+01 1.36250778E-01-1.02396726E-04    3
 3.90660846E-08-6.00238146E-12 1.70207249E+04 8.95714522E+01                   4
TCDJ2     freqs  b3lyp/6C  10H  15    0    0G   300.000  5000.000 1388.000    01
 2.66969377E+01 3.81575614E-02-1.29458697E-05 2.00146504E-09-1.15858875E-13    2
-5.01775861E+02-1.29752831E+02-1.42358370E+01 1.35912201E-01-1.02033512E-04    3
 3.88612871E-08-5.95819310E-12 1.33742498E+04 8.91194723E+01                   4
TCDJ3     freqs  b3lyp/6C  10H  15    0    0G   300.000  5000.000 1388.000    01
 2.70561081E+01 3.78387190E-02-1.28335873E-05 1.98375445E-09-1.14821828E-13    2
-1.62097482E+03-1.31537305E+02-1.41836151E+01 1.37064105E-01-1.04154072E-04    3
 4.02182197E-08-6.25594669E-12 1.22869365E+04 8.87173594E+01                   4
TCDJ4     freqs  b3lyp/6C  10H  15    0    0G   300.000  5000.000 1388.000    01
 2.70939489E+01 3.78519457E-02-1.28479052E-05 1.98698452E-09-1.15049549E-13    2
-1.37510974E+03-1.30848590E+02-1.40377048E+01 1.36551602E-01-1.03410610E-04    3
 3.97857955E-08-6.16802194E-12 1.25271909E+04 8.89304128E+01                   4
TCDJ9     freqs  b3lyp/6C  10H  15    0    0G   300.000  5000.000 1389.000    01
 2.70873719E+01 3.77844387E-02-1.28088324E-05 1.97926952E-09-1.14535769E-13    2
-1.25960045E+03-1.32157975E+02-1.41803277E+01 1.37349924E-01-1.04760266E-04    3
 4.06325819E-08-6.34964873E-12 1.26301236E+04 8.81487067E+01                   4
TCDJ10    freqs  b3lyp/6C  10H  15    0    0G   300.000  5000.000 1389.000    01
 2.69135815E+01 3.78713819E-02-1.28250253E-05 1.98033231E-09-1.14537557E-13    2
 1.53206767E+03-1.30850001E+02-1.41576549E+01 1.36869706E-01-1.04069182E-04    3
 4.02152371E-08-6.25629044E-12 1.53570477E+04 8.84273868E+01                   4
TCD12JJ   freqs  b3lyp/6C  10H  16    0    0G   300.000  5000.000 1389.000    11
 2.72982178E+01 3.92185163E-02-1.31931425E-05 2.02794170E-09-1.16917117E-13    2
 1.42744415E+04-1.28802524E+02-1.21800445E+01 1.34491420E-01-1.01376028E-04    3
 3.92566895E-08-6.15870241E-12 2.75789154E+04 8.19748331E+01                   4
TCD19JJ   freqs  b3lyp/6C  10H  16    0    0G   300.000  5000.000 1395.000    21
 2.70770840E+01 3.84965590E-02-1.28399106E-05 1.96218613E-09-1.12665686E-13    2
 1.57593419E+04-1.28899419E+02-1.39644993E+01 1.40947947E-01-1.11092900E-04    3
 4.48774993E-08-7.28931689E-12 2.91876264E+04 8.89103913E+01                   4
TCD110JJ  freqs  b3lyp/6C  10H  16    0    0G   300.000  5000.000 1388.000    11
 2.70589913E+01 3.93457869E-02-1.32202611E-05 2.03042498E-09-1.16990792E-13    2
 1.54381261E+04-1.28693309E+02-1.14495017E+01 1.31864733E-01-9.84485929E-05    3
 3.78455882E-08-5.90521006E-12 2.84662326E+04 7.70683327E+01                   4
TCD23JJ   freqs  b3lyp/6C  10H  16    0    0G   300.000  5000.000 1394.000    31
 2.79458279E+01 3.78201257E-02-1.27146162E-05 1.95393636E-09-1.12644998E-13    2
 1.74812363E+04-1.36311828E+02-1.46307759E+01 1.39181392E-01-1.03487752E-04    3
 3.82193621E-08-5.55889670E-12 3.18105482E+04 9.12344890E+01                   4
```

Table K.1 Thermochemical properties of the TCD system in the NASA polynomial format for use in ChemKin (Continued)

```
THERMO
   300.000  1500.000  5000.000

TCD26JJ   freqs  b3lyp/6C  10H  16    0    0G   300.000  5000.000 1387.000    01
 2.78843600E+01 3.95849188E-02-1.34088823E-05 2.07033765E-09-1.19721119E-13    2
 1.60870957E+04-1.32732534E+02-1.09687838E+01 1.31721967E-01-9.70195452E-05    3
 3.66503926E-08-5.62172137E-12 2.93706916E+04 7.53300193E+01                   4
TCD34JJ   freqs  b3lyp/6C  10H  16    0    0G   300.000  5000.000 1397.000    31
 2.84004042E+01 3.73388136E-02-1.25274810E-05 1.92252217E-09-1.10726453E-13    2
 1.83400449E+04-1.38336924E+02-1.52253613E+01 1.44095286E-01-1.11711027E-04    3
 4.34269612E-08-6.70158217E-12 3.27432379E+04 9.38059943E+01                   4
TCD98JJ   freqs  b3lyp/6C  10H  16    0    0G   300.000  5000.000 1396.000    21
 2.71352387E+01 3.82695244E-02-1.27228747E-05 1.93992538E-09-1.11209111E-13    2
 1.73277556E+04-1.29221805E+02-1.27013100E+01 1.37546226E-01-1.07655996E-04    3
 4.32385260E-08-6.98381747E-12 3.03692553E+04 8.22362981E+01                   4
TCDOOH1   reqs   b3lyp/6C  10H  16O   2    0G   300.000  5000.000 1403.000    11
 2.94785860E+01 4.29772924E-02-1.45769231E-05 2.25102147E-09-1.30132685E-13    2
-3.66583009E+04-1.44084790E+02-1.42051748E+01 1.51748865E-01-1.18743932E-04    3
 4.77155948E-08-7.72767250E-12-2.23109799E+04 8.78855296E+01                   4
TCDOOH2   reqs   b3lyp/6C  10H  16O   2    0G   300.000  5000.000 1403.000    11
 2.95880920E+01 4.28651438E-02-1.45340792E-05 2.24390652E-09-1.29701289E-13    2
-3.70459636E+04-1.44613889E+02-1.43829866E+01 1.52852729E-01-1.20417974E-04    3
 4.87126710E-08-7.93704119E-12-2.26564655E+04 8.87009482E+01                   4
TCDOOH3   reqs   b3lyp/6C  10H  16O   2    0G   300.000  5000.000 1404.000    11
 2.94291936E+01 4.30479518E-02-1.46076493E-05 2.25648046E-09-1.30477434E-13    2
-3.64137596E+04-1.43760686E+02-1.49288275E+01 1.53608862E-01-1.20518269E-04    3
 4.84575185E-08-7.84125181E-12-2.18667003E+04 9.17329272E+01                   4
TCDOOH4   reqs   b3lyp/6C  10H  16O   2    0G   300.000  5000.000 1403.000    11
 2.94487798E+01 4.30420457E-02-1.46079498E-05 2.25676805E-09-1.30503833E-13    2
-3.64052901E+04-1.43221728E+02-1.45840939E+01 1.52362906E-01-1.18838513E-04    3
 4.74899372E-08-7.63976683E-12-2.19220946E+04 9.06978028E+01                   4
TCDOOH9   reqs   b3lyp/6C  10H  16O   2    0G   300.000  5000.000 1403.000    11
 2.94203403E+01 4.30518969E-02-1.46084516E-05 2.25656536E-09-1.30481293E-13    2
-3.62250799E+04-1.43358758E+02-1.46743999E+01 1.52571942E-01-1.19079209E-04    3
 4.76176601E-08-7.66503571E-12-2.17264298E+04 9.08727611E+01                   4
TCDOOH110 reqs   b3lyp/6C  10H  16O   2    0G   300.000  5000.000 1403.000    11
 2.93840862E+01 4.30890259E-02-1.46224524E-05 2.25885874E-09-1.30618692E-13    2
-3.56508479E+04-1.43031577E+02-1.43425067E+01 1.51307434E-01-1.17415441E-04    3
 4.66854913E-08-7.47513035E-12-2.12335615E+04 8.93832801E+01                   4
TCDOOj1   reqs   b3lyp/6C  10H  15O   2    0G   300.000  5000.000 1402.000    11
 2.87730595E+01 4.13033787E-02-1.40598093E-05 2.17654702E-09-1.26047821E-13    2
-1.97280125E+04-1.39720082E+02-1.44251338E+01 1.48073736E-01-1.15327725E-04    3
 4.58808983E-08-7.34227556E-12-5.47064137E+03 8.99370683E+01                   4
TCDOOj2   reqs   b3lyp/6C  10H  15O   2    0G   300.000  5000.000 1402.000    11
 2.88276629E+01 4.12587655E-02-1.40444743E-05 2.17413287E-09-1.25905617E-13    2
-2.06652117E+04-1.39996228E+02-1.46152444E+01 1.49226313E-01-1.17165570E-04    3
 4.70371488E-08-7.59691776E-12-6.38216769E+03 9.07586408E+01                   4
TCDOOj3   reqs   b3lyp/6C  10H  15O   2    0G   300.000  5000.000 1403.000    11
 2.87670917E+01 4.13282001E-02-1.40729006E-05 2.17907546E-09-1.26215102E-13    2
-1.97877046E+04-1.39568926E+02-1.51990653E+01 1.50367966E-01-1.17850316E-04    3
 4.71100400E-08-7.56554950E-12-5.32190172E+03 9.40259977E+01                   4
TCDOOj4   reqs   b3lyp/6C  10H  15O   2    0G   300.000  5000.000 1402.000    11
 2.87749525E+01 4.13273447E-02-1.40740575E-05 2.17941999E-09-1.26242189E-13    2
-1.95723606E+04-1.39503402E+02-1.51609728E+01 1.50216196E-01-1.17642056E-04    3
 4.69974126E-08-7.54450533E-12-5.10670130E+03 9.39616612E+01                   4
TCDOOj9   reqs   b3lyp/6C  10H  15O   2    0G   300.000  5000.000 1402.000    11
 2.87196366E+01 4.13803564E-02-1.40935233E-05 2.18256937E-09-1.26429687E-13    2
-1.94428467E+04-1.39004053E+02-1.50231895E+01 1.49516831E-01-1.16626582E-04    3
 4.63971764E-08-7.41780020E-12-5.01382240E+03 9.35312714E+01                   4
TCDOOj110 reqs   b3lyp/6C  10H  15O   2    0G   300.000  5000.000 1402.000    11
 2.87096245E+01 4.13654204E-02-1.40832803E-05 2.18044731E-09-1.26285164E-13    2
-1.86692529E+04-1.38802301E+02-1.46870914E+01 1.48279282E-01-1.14996999E-04    3
 4.54598979E-08-7.22043989E-12-4.32178886E+03 9.20163779E+01                   4
TCDOOH12  reqs   b3lyp/6C  10H  15O   2    0G   300.000  5000.000 1477.000    11
 4.09068200E+01 3.43866051E-02-1.24440772E-05 2.00620075E-09-1.19493469E-13    2
-4.86456131E+04-2.05883689E+02-9.35882587E+00 1.30002201E-01-6.75899096E-05    3
 7.77012890E-09 2.14390053E-12-2.95082293E+04 7.09866313E+01                   4
```

Table K.1 Thermochemical properties of the TCD system in the NASA polynomial format for use in ChemKin (Continued)

```
THERMO
   300.000  1500.000  5000.000

TCDOOH21  reqs   b3lyp/6C  10H  15O   2    0G   300.000  5000.000 1476.000    11
 4.08478931E+01 3.44359355E-02-1.24608859E-05 2.00879884E-09-1.19643582E-13    2
-4.79834726E+04-2.04720193E+02-9.13263148E+00 1.29055804E-01-6.63440173E-05    3
 7.08137133E-09 2.28206453E-12-2.89091945E+04 7.07407377E+01                   4
TCDOOH23  reqs   b3lyp/6C  10H  15O   2    0G   300.000  5000.000 1493.000    11
 4.09623831E+01 3.43199575E-02-1.24163741E-05 2.00135276E-09-1.19188947E-13    2
-4.48316399E+04-2.08647062E+02-9.31185650E+00 1.31067178E-01-7.01052175E-05    3
 9.64620468E-09 1.68812378E-12-2.57813361E+04 6.79108046E+01                   4
TCDOOH32  reqs   b3lyp/6C  10H  18O   2    0G   300.000  5000.000 1401.000    11
 3.02802900E+01 4.72992150E-02-1.60463308E-05 2.47809041E-09-1.43259409E-13    2
-3.96214402E+04-1.45271281E+02-1.24064166E+01 1.49170943E-01-1.08742153E-04    3
 4.06894133E-08-6.15698713E-12-2.51380662E+04 8.30073804E+01                   4
TCDOOH34  reqs   b3lyp/6C  10H  18O   2    0G   300.000  5000.000 1400.000    11
 3.03492744E+01 4.72088024E-02-1.60078072E-05 2.47128905E-09-1.42830726E-13    2
-3.98264065E+04-1.45867086E+02-1.14500203E+01 1.46534490E-01-1.05931084E-04    3
 3.93326272E-08-5.90989881E-12-2.55950384E+04 7.78282169E+01                   4
TCDOOH43  reqs   b3lyp/6C  10H  18O   2    0G   300.000  5000.000 1400.000    11
 3.03816225E+01 4.71781991E-02-1.59965595E-05 2.46946146E-09-1.42721404E-13    2
-3.95999113E+04-1.46436878E+02-1.15791992E+01 1.47166957E-01-1.06858555E-04    3
 3.98873565E-08-6.02801911E-12-2.53409438E+04 7.80246926E+01                   4
TCDOOH19  reqs   b3lyp/6C  10H  18O   2    0G   300.000  5000.000 1352.000    11
 2.22838793E+01 5.62975371E-02-1.97491122E-05 3.12696019E-09-1.84098324E-13    2
-3.90794959E+04-9.78728670E+01-1.19624381E+01 1.54553679E-01-1.26591458E-04    3
 5.48775590E-08-9.51940603E-12-2.93593134E+04 7.89939487E+01                   4
TCDOOH91  reqs   b3lyp/6C  10H  18O   2    0G   300.000  5000.000 1384.000    11
 3.05568139E+01 4.59833147E-02-1.53948328E-05 2.35896691E-09-1.35713471E-13    2
-4.24590838E+04-1.48294054E+02-1.18919723E+01 1.37332370E-01-8.51027849E-05    3
 2.38074175E-08-2.12959603E-12-2.72476343E+04 8.19365112E+01                   4
TCDOOH110 reqs   b3lyp/6C  10H  18O   2    0G   300.000  5000.000 1399.000    11
 3.01762167E+01 4.73782848E-02-1.60714199E-05 2.48176835E-09-1.43463568E-13    2
-4.30441104E+04-1.45672533E+02-1.10941810E+01 1.44430671E-01-1.02749506E-04    3
 3.74290492E-08-5.50802359E-12-2.88883257E+04 7.55578133E+01                   4
TCDOOH101 reqs   b3lyp/6C  10H  18O   2    0G   300.000  5000.000 1399.000    11
 2.99712223E+01 4.76218783E-02-1.61709515E-05 2.49893106E-09-1.44529117E-13    2
-4.10326471E+04-1.44336774E+02-1.16611141E+01 1.44854718E-01-1.02128573E-04    3
 3.66793918E-08-5.30046495E-12-2.66939306E+04 7.90578688E+01                   4
TCDOOH26  reqs   b3lyp/6C  10H  18O   2    0G   300.000  5000.000 1399.000    11
 3.00365286E+01 4.75387797E-02-1.61364449E-05 2.49295715E-09-1.44158130E-13    2
-4.05598539E+04-1.46706576E+02-1.23961568E+01 1.48099141E-01-1.06874877E-04    3
 3.95473877E-08-5.91808987E-12-2.60841864E+04 8.04774399E+01                   4
TCDOOH98  reqs   b3lyp/6C  10H  18O   2    0G   300.000  5000.000 1585.000    11
-2.37344375E+02 4.16506658E-01-1.73643150E-04 2.75315978E-08-1.43130811E-12    2
 9.13311811E+04 1.41042818E+03-8.69310525E+01 5.61561305E-01-8.46341741E-04    3
 5.58118092E-07-1.28677423E-10-1.90025460E+04 4.13733185E+02                   4
TCDOOj12  reqs   b3lyp/6C  10H  17O   2    0G   300.000  5000.000 1399.000    11
 2.96838341E+01 4.55465645E-02-1.55050927E-05 2.40016306E-09-1.38986032E-13    2
-2.69310592E+04-1.40285498E+02-1.21162728E+01 1.44078109E-01-1.03657331E-04    3
 3.79720911E-08-5.59876027E-12-1.26323931E+04 8.36761288E+01                   4
TCDOOj21  reqs   b3lyp/6C  10H  17O   2    0G   300.000  5000.000 1399.000    11
 2.96654686E+01 4.55357605E-02-1.54955208E-05 2.39805955E-09-1.38838864E-13    2
-2.63201544E+04-1.38970315E+02-1.18942879E+01 1.43315931E-01-1.02724837E-04    3
 3.74582508E-08-5.49276659E-12-1.20881799E+04 8.37640322E+01                   4
TCDOOj23  reqs   b3lyp/6C  10H  17O   2    0G   300.000  5000.000 1400.000    11
 2.97706012E+01 4.53908637E-02-1.54330784E-05 2.38700153E-09-1.38141492E-13    2
-2.30865584E+04-1.43059864E+02-1.20184199E+01 1.45032528E-01-1.06022648E-04    3
 3.97055144E-08-6.00949507E-12-8.89669050E+03 8.04536084E+01                   4
TCDOOj32  reqs   b3lyp/6C  10H  17O   2    0G   300.000  5000.000 1400.000    11
 2.96562255E+01 4.55377052E-02-1.54950310E-05 2.39787382E-09-1.38823993E-13    2
-2.20253225E+04-1.41327639E+02-1.28389474E+01 1.46783087E-01-1.07370890E-04    3
 4.01307294E-08-6.05054590E-12-7.59647148E+03 8.59765017E+01                   4
TCDOOj34  reqs   b3lyp/6C  10H  17O   2    0G   300.000  5000.000 1399.000    11
 2.96981513E+01 4.54667220E-02-1.54624363E-05 2.39191831E-09-1.38441367E-13    2
-2.29006168E+04-1.41906194E+02-1.18749330E+01 1.44051492E-01-1.04427370E-04    3
 3.87021908E-08-5.78951189E-12-8.73193746E+03 8.06411361E+01                   4
```

Table K.1 Thermochemical properties of the TCD system in the NASA polynomial format for use in ChemKin (Continued)

```
THERMO
   300.000  1500.000  5000.000

TCDOOj43  reqs   b3lyp/6C  10H  17O   2    0G   300.000  5000.000 1400.000    11
 2.97295060E+01 4.54438732E-02-1.54552780E-05 2.39086752E-09-1.38382606E-13    2
-2.23902208E+04-1.42250611E+02-1.19561275E+01 1.44524212E-01-1.05152092E-04    3
 3.91474143E-08-5.88614153E-12-8.20480218E+03 8.08201651E+01                   4
TCDOOj19  reqs   b3lyp/6C  10H  17O   2    0G   300.000  5000.000 1399.000    11
 2.97523210E+01 4.54415227E-02-1.54583531E-05 2.39176152E-09-1.38451702E-13    2
-2.72759343E+04-1.42164647E+02-1.15361775E+01 1.42881981E-01-1.02835219E-04    3
 3.77773121E-08-5.59619729E-12-1.31566482E+04 7.90269529E+01                   4
TCDOOj91  reqs   b3lyp/6C  10H  17O   2    0G   300.000  5000.000 1383.000    11
 3.26860361E+01 4.52643558E-02-1.59101291E-05 2.51576978E-09-1.47839120E-13    2
-2.66872782E+04-1.59512354E+02-1.10098148E+01 1.41093863E-01-9.47301906E-05    3
 3.15342495E-08-4.20399888E-12-1.08380704E+04 7.74661238E+01                   4
TCDOOj110 reqs   b3lyp/6C  10H  17O   2    0G   300.000  5000.000 1398.000    11
 2.94797315E+01 4.56929649E-02-1.55494186E-05 2.40642132E-09-1.39323126E-13    2
-2.63614280E+04-1.40772890E+02-1.12590548E+01 1.40843718E-01-9.97113959E-05    3
 3.59145197E-08-5.20473623E-12-1.23272845E+04 7.78319132E+01                   4
TCDOOj101 reqs   b3lyp/6C  10H  17O   2    0G   300.000  5000.000 1398.000    11
 2.93298080E+01 4.58723082E-02-1.56231115E-05 2.41918267E-09-1.40117951E-13    2
-2.40099120E+04-1.40103671E+02-1.20547610E+01 1.42337487E-01-1.00633339E-04    3
 3.60729653E-08-5.18775742E-12-9.74297729E+03 8.20200955E+01                   4
TCDOOj26  reqs   b3lyp/6C  10H  17O   2    0G   300.000  5000.000 1398.000    11
 2.93298137E+01 4.58652972E-02-1.56191985E-05 2.41842053E-09-1.40067582E-13    2
-2.44831353E+04-1.42403340E+02-1.26982550E+01 1.44897492E-01-1.04247506E-04    3
 3.82268481E-08-5.64879941E-12-1.00949885E+04 8.28060315E+01                   4
TCDOOj98  reqs   b3lyp/6C  10H  17O   2    0G   300.000  5000.000 1399.000    11
 2.96936186E+01 4.55167830E-02-1.54899412E-05 2.39727917E-09-1.38796764E-13    2
-2.59297731E+04-1.40696452E+02-1.13041223E+01 1.41530749E-01-1.00672899E-04    3
 3.64213733E-08-5.29916674E-12-1.18386077E+04 7.91955723E+01                   4
TCDOOjHj12reqs   b3lyp/6C  10H  16O   2    0G   300.000  5000.000 1396.000    11
 2.91010160E+01 4.31208306E-02-1.45966496E-05 2.25172004E-09-1.30099153E-13    2
-3.88148324E+03-1.33867442E+02-1.08468969E+01 1.34144761E-01-9.16333535E-05    3
 3.08712573E-08-4.04060871E-12 1.00251833E+04 8.11651171E+01                   4
TCDOOjHj21reqs   b3lyp/6C  10H  16O   2    0G   300.000  5000.000 1396.000    11
 2.90742215E+01 4.31194566E-02-1.45908102E-05 2.25024724E-09-1.29990595E-13    2
-3.39828048E+03-1.32504105E+02-1.06189387E+01 1.33360401E-01-9.06890422E-05    3
 3.03622435E-08-3.93779649E-12 1.04376385E+04 8.12250389E+01                   4
TCDOOjHj23reqs   b3lyp/6C  10H  16O   2    0G   300.000  5000.000 1400.000    11
 2.93514928E+01 4.32491295E-02-1.47053668E-05 2.27455929E-09-1.31640603E-13    2
 2.45169020E+03-1.38359758E+02-1.12707379E+01 1.40569092E-01-1.03675365E-04    3
 3.91501643E-08-5.97060622E-12 1.61924818E+04 7.87384298E+01                   4
TCDOOjHj32reqs   b3lyp/6C  10H  16O   2    0G   300.000  5000.000 1397.000    11
 2.90600484E+01 4.31298419E-02-1.45940385E-05 2.25071551E-09-1.30016468E-13    2
 1.38716362E+03-1.34833032E+02-1.15685432E+01 1.36857606E-01-9.53855865E-05    3
 3.30685004E-08-4.50330545E-12 1.54180417E+04 8.34586847E+01                   4
TCDOOjHj34reqs   b3lyp/6C  10H  16O   2    0G   300.000  5000.000 1400.000    11
 2.92781153E+01 4.33261690E-02-1.47351906E-05 2.27955263E-09-1.31945026E-13    2
 2.39196310E+03-1.37199433E+02-1.10987721E+01 1.39465371E-01-1.01896773E-04    3
 3.80326466E-08-5.72529748E-12 1.61061881E+04 7.87930855E+01                   4
TCDOOjHj43reqs   b3lyp/6C  10H  16O   2    0G   300.000  5000.000 1400.000    11
 2.93093778E+01 4.33034346E-02-1.47280768E-05 2.27850911E-09-1.31886695E-13    2
 3.16410955E+03-1.37543303E+02-1.11799332E+01 1.39938041E-01-1.02621539E-04    3
 3.84779445E-08-5.82194867E-12 1.68950169E+04 7.89719405E+01                   4
TCDOOjHj19reqs   b3lyp/6C  10H  16O   2    0G   300.000  5000.000 1399.000    11
 2.93183515E+01 4.33197180E-02-1.47389331E-05 2.28074564E-09-1.32038737E-13    2
-1.38368239E+03-1.37378100E+02-1.07593416E+01 1.38305779E-01-1.00347304E-04    3
 3.71494246E-08-5.54366321E-12 1.22749956E+04 7.71736515E+01                   4
TCDOOjHj91reqs   b3lyp/6C  10H  16O   2    0G   300.000  5000.000 1382.000    11
 3.15667017E+01 4.36125663E-02-1.53280149E-05 2.42359968E-09-1.42418808E-13    2
-3.36984577E+03-1.50006658E+02-9.63050155E+00 1.31137260E-01-8.33656756E-05    3
 2.52071772E-08-2.87069188E-12 1.18173287E+04 7.43585863E+01                   4
TCDOOjHj11reqs   b3lyp/6C  10H  16O   2    0G   300.000  5000.000 1399.000    11
 2.90540579E+01 4.35597852E-02-1.48251418E-05 2.29455212E-09-1.32856683E-13    2
-1.31264225E+03-1.36033420E+02-1.04695345E+01 1.36187836E-01-9.70628859E-05    3
 3.51647065E-08-5.12142018E-12 1.22624635E+04 7.59239764E+01                   4
```

Table K.1 Thermochemical properties of the TCD system in the NASA polynomial format for use in ChemKin (Continued)

```
THERMO
   300.000  1500.000  5000.000

TCDOOjHj10reqs   b3lyp/6C  10H  16O   2    0G   300.000  5000.000 1395.000    11
 2.87395624E+01 4.34561716E-02-1.47184840E-05 2.27137093E-09-1.31268762E-13    2
 4.87866983E+04-1.33642403E+02-1.07695453E+01 1.32323699E-01-8.84763455E-05    3
 2.88828888E-08-3.60855592E-12 6.26557749E+04 7.94376531E+01                   4
TCDOOjHj26reqs   b3lyp/6C  10H  16O   2    0G   300.000  5000.000 1395.000    11
 2.87539099E+01 4.34314569E-02-1.47077330E-05 2.26950246E-09-1.31153526E-13    2
-2.76166359E+03-1.36027563E+02-1.14242808E+01 1.34934807E-01-9.21754636E-05    3
 3.10969064E-08-4.08477430E-12 1.12385474E+04 8.02756765E+01                   4
TCDOOjHj98reqs   b3lyp/6C  10H  16O   2    0G   300.000  5000.000 1399.000    11
 2.92735167E+01 4.33763352E-02-1.47627391E-05 2.28492082E-09-1.32300863E-13    2
-2.34532988E+02-1.35989283E+02-1.05275940E+01 1.36943258E-01-9.81404464E-05    3
 3.57507608E-08-5.23472878E-12 1.34020718E+04 7.73457638E+01                   4
TCDOHOH12 reqs   b3lyp/6C  10H  18O   2    0G   300.000  5000.000 1402.000    11
 3.04785574E+01 4.69183257E-02-1.58691314E-05 2.44574979E-09-1.41189625E-13    2
-7.23418187E+04-1.46161937E+02-1.23375254E+01 1.50460358E-01-1.11599570E-04    3
 4.26213399E-08-6.58512720E-12-5.79622794E+04 8.23059791E+01                   4
TCDOHOH23 reqs   b3lyp/6C  10H  18O   2    0G   300.000  5000.000 1402.000    11
 3.01901865E+01 4.71791545E-02-1.59627375E-05 2.46074896E-09-1.42078985E-13    2
-6.94316732E+04-1.47338587E+02-1.34026869E+01 1.53228312E-01-1.14798580E-04    3
 4.43476865E-08-6.93545823E-12-5.48489018E+04 8.50601897E+01                   4
TCDOHOH34 reqs   b3lyp/6C  10H  18O   2    0G   300.000  5000.000 1402.000    11
 3.02528410E+01 4.71176640E-02-1.59397899E-05 2.45699290E-09-1.41853432E-13    2
-6.66734888E+04-1.45005237E+02-1.20130262E+01 1.48217388E-01-1.08085796E-04    3
 4.04674844E-08-6.12109886E-12-5.23698351E+04 8.09173329E+01                   4
TCDOHOH91 reqs   b3lyp/6C  10H  18O   2    0G   300.000  5000.000 1401.000    11
 3.03327763E+01 4.70690903E-02-1.59273967E-05 2.45551977E-09-1.41786547E-13    2
-7.04757104E+04-1.46320124E+02-1.20528816E+01 1.48549840E-01-1.08556050E-04    3
 4.07427796E-08-6.18007598E-12-5.61385920E+04 8.02133494E+01                   4
TCDOHOH26 reqs   b3lyp/6C  10H  18O   2    0G   300.000  5000.000 1401.000    11
 3.01924430E+01 4.72031932E-02-1.59769222E-05 2.46358837E-09-1.42269971E-13    2
-6.91262847E+04-1.47997237E+02-1.27658651E+01 1.50771371E-01-1.11438190E-04    3
 4.24156985E-08-6.53612574E-12-5.46586962E+04 8.13569105E+01                   4
TCDOHOH98 reqs   b3lyp/6C  10H  18O   2    0G   300.000  5000.000 1401.000    11
 3.02417555E+01 4.71577814E-02-1.59605238E-05 2.46095579E-09-1.42113839E-13    2
-7.04814058E+04-1.43969762E+02-1.14280475E+01 1.45624206E-01-1.04230499E-04    3
 3.81190629E-08-5.61401583E-12-5.62633781E+04 7.91872868E+01                   4
TCOHOH110 reqs   b3lyp/6C  10H  18O   2    0G   300.000  5000.000 1401.000    11
 2.97476762E+01 4.76364389E-02-1.61384718E-05 2.49005331E-09-1.43861101E-13    2
-6.97696579E+04-1.45932359E+02-1.33087987E+01 1.50624803E-01-1.10082218E-04    3
 4.13136326E-08-6.26893758E-12-5.51897158E+04 8.42315924E+01                   4
TCDOHOj12 reqs   b3lyp/6C  10H  17O   2    0G   300.000  5000.000 1401.000    11
 3.02986818E+01 4.47933192E-02-1.51948581E-05 2.34653996E-09-1.35654933E-13    2
-4.56913947E+04-1.44920003E+02-1.22119558E+01 1.48274503E-01-1.11731101E-04    3
 4.33149106E-08-6.79182929E-12-3.14759005E+04 8.16887756E+01                   4
TCDOHOj21 reqs   b3lyp/6C  10H  17O   2    0G   300.000  5000.000 1401.000    11
 3.02892634E+01 4.48130041E-02-1.52040865E-05 2.34822309E-09-1.35762407E-13    2
-4.55978849E+04-1.43843008E+02-1.19368619E+01 1.47160908E-01-1.10153769E-04    3
 4.23788784E-08-6.59265077E-12-3.14350477E+04 8.14027633E+01                   4
TCDOHOj23 reqs   b3lyp/6C  10H  17O   2    0G   300.000  5000.000 1401.000    11
 3.03503869E+01 4.47889660E-02-1.52020181E-05 2.34855353E-09-1.35808261E-13    2
-4.30808525E+04-1.47733544E+02-1.34368820E+01 1.52859651E-01-1.17812434E-04    3
 4.67950072E-08-7.51756449E-12-2.85798222E+04 8.51663924E+01                   4
TCDOHOj32 reqs   b3lyp/6C  10H  17O   2    0G   300.000  5000.000 1401.000    11
 3.01388239E+01 4.49351957E-02-1.52450580E-05 2.35450024E-09-1.36123266E-13    2
-4.14437340E+04-1.46314564E+02-1.28969659E+01 1.50321277E-01-1.14338084E-04    3
 4.48076610E-08-7.10589363E-12-2.71098952E+04 8.28804174E+01                   4
TCDOHOj34 reqs   b3lyp/6C  10H  17O   2    0G   300.000  5000.000 1401.000    11
 3.03203287E+01 4.48358581E-02-1.52229160E-05 2.35230718E-09-1.36046711E-13    2
-4.00603361E+04-1.45971338E+02-1.20023891E+01 1.47006789E-01-1.09500267E-04    3
 4.18405676E-08-6.45883583E-12-2.58271226E+04 7.99303707E+01                   4
TCDOHOj43 reqs   b3lyp/6C  10H  17O   2    0G   300.000  5000.000 1401.000    11
 3.03203287E+01 4.48358581E-02-1.52229160E-05 2.35230718E-09-1.36046711E-13    2
-3.99999435E+04-1.45971338E+02-1.20023891E+01 1.47006789E-01-1.09500267E-04    3
 4.18405676E-08-6.45883583E-12-2.57667300E+04 7.99303707E+01                   4
```

Table K.1 Thermochemical properties of the TCD system in the NASA polynomial format for use in ChemKin (Continued)

```
THERMO
   300.000  1500.000  5000.000

TCDOHOj19 reqs   b3lyp/6C  10H  17O   2    0G   300.000  5000.000 1400.000    11
 3.00292423E+01 4.50728692E-02-1.53025181E-05 2.36451619E-09-1.36749097E-13    2
-4.42245947E+04-1.44531075E+02-1.20105287E+01 1.46022734E-01-1.07832424E-04    3
 4.08198017E-08-6.24180953E-12-3.00313222E+04 8.00536203E+01                   4
TCDOHOj91 reqs   b3lyp/6C  10H  17O   2    0G   300.000  5000.000 1401.000    11
 3.02939368E+01 4.48943158E-02-1.52513557E-05 2.35763240E-09-1.36393400E-13    2
-4.40994457E+04-1.46517817E+02-1.26227005E+01 1.48732027E-01-1.11340552E-04    3
 4.27410224E-08-6.62692290E-12-2.96902079E+04 8.24708482E+01                   4
TCDOHOj26 reqs   b3lyp/6C  10H  17O   2    0G   300.000  5000.000 1400.000    11
 2.99197636E+01 4.51795871E-02-1.53429260E-05 2.37124196E-09-1.37159019E-13    2
-4.03004724E+04-1.47139053E+02-1.34497477E+01 1.50671853E-01-1.13689635E-04    3
 4.40893805E-08-6.91429267E-12-2.57874106E+04 8.40807245E+01                   4
TCDOHOj98 reqs   b3lyp/6C  10H  17O   2    0G   300.000  5000.000 1400.000    11
 3.01762275E+01 4.50275015E-02-1.53044268E-05 2.36664233E-09-1.36946891E-13    2
-4.47018028E+04-1.45334224E+02-1.20937718E+01 1.46039510E-01-1.07249588E-04    3
 4.02367497E-08-6.08505974E-12-3.03887734E+04 8.06427567E+01                   4
TCDOHOj110reqs   b3lyp/6C  10H  17O   2    0G   300.000  5000.000 1400.000    11
 3.00167439E+01 4.51609658E-02-1.53503160E-05 2.37381219E-09-1.37365338E-13    2
-4.39456035E+04-1.46356867E+02-1.24991484E+01 1.47118050E-01-1.08672623E-04    3
 4.11077924E-08-6.28012453E-12-2.95751616E+04 8.08246978E+01                   4
TCDOHOj101reqs   b3lyp/6C  10H  17O   2    0G   300.000  5000.000 1400.000    11
 3.01005950E+01 4.50791396E-02-1.53192895E-05 2.36864193E-09-1.37049940E-13    2
-4.39376962E+04-1.45338793E+02-1.21047445E+01 1.46291576E-01-1.07960654E-04    3
 4.08192355E-08-6.23436558E-12-2.96718259E+04 8.01837996E+01                   4
TCDOjOj21 reqs   b3lyp/6C  10H  16O   2    0G   300.000  5000.000 1399.000    11
 3.04001650E+01 4.29067134E-02-1.47051846E-05 2.28655705E-09-1.32817998E-13    2
-1.91752466E+04-1.45793106E+02-1.19786248E+01 1.45372136E-01-1.09750640E-04    3
 4.24674090E-08-6.65066289E-12-4.90492771E+03 8.04090976E+01                   4
TCDOjOj23 reqs   b3lyp/6C  10H  16O   2    0G   300.000  5000.000 1399.000    11
 3.04557122E+01 4.28981746E-02-1.47107948E-05 2.28832501E-09-1.32957095E-13    2
-1.55244004E+04-1.48628286E+02-1.32015333E+01 1.49955993E-01-1.15832931E-04    3
 4.59489374E-08-7.37687678E-12-9.67616315E+02 8.38756342E+01                   4
TCDOjOj34 reqs   b3lyp/6C  10H  16O   2    0G   300.000  5000.000 1399.000    11
 3.04250249E+01 4.29449793E-02-1.47315764E-05 2.29205542E-09-1.33194107E-13    2
-1.33457334E+04-1.46866006E+02-1.17877808E+01 1.44164456E-01-1.07591853E-04    3
 4.10312587E-08-6.32523851E-12 9.48637167E+02 7.87423480E+01                   4
TCDOjOj91 reqs   b3lyp/6C  10H  16O   2    0G   300.000  5000.000 1399.000    11
 3.03997502E+01 4.30020803E-02-1.47594614E-05 2.29728530E-09-1.33534897E-13    2
-1.79382860E+04-1.47417487E+02-1.24000274E+01 1.45865000E-01-1.09402224E-04    3
 4.19154429E-08-6.49004611E-12-3.46958721E+03 8.12430458E+01                   4
TCDOjOj26 reqs   b3lyp/6C  10H  16O   2    0G   300.000  5000.000 1398.000    11
 3.00200350E+01 4.32949889E-02-1.48541179E-05 2.31140869E-09-1.34331281E-13    2
-1.22376004E+04-1.48002678E+02-1.32015748E+01 1.47725492E-01-1.11660119E-04    3
 4.32177988E-08-6.76871359E-12 2.32574736E+03 8.27276243E+01                   4
TCDOjOj98 reqs   b3lyp/6C  10H  16O   2    0G   300.000  5000.000 1398.000    11
 3.02835998E+01 4.31328763E-02-1.48116043E-05 2.30614946E-09-1.34080166E-13    2
-1.82164096E+04-1.46247668E+02-1.19017340E+01 1.43271255E-01-1.05432315E-04    3
 3.94767284E-08-5.96135449E-12-3.83533641E+03 7.95648797E+01                   4
TCDOjOj110reqs   b3lyp/6C  10H  16O   2    0G   300.000  5000.000 1398.000    11
 3.01211285E+01 4.32709331E-02-1.48593847E-05 2.31363525E-09-1.34517503E-13    2
-1.80044659E+04-1.47251488E+02-1.22595918E+01 1.44192872E-01-1.06661334E-04    3
 4.02426724E-08-6.13538298E-12-3.57899959E+03 7.95100960E+01                   4
TCDYOO12 reqs   b3lyp/6C  10H  16O   2    0G   300.000  5000.000 1401.000    11
 2.89165857E+01 4.37340894E-02-1.48994402E-05 2.30774124E-09-1.33692715E-13    2
-3.34394602E+04-1.43154845E+02-1.55987526E+01 1.52756436E-01-1.17265622E-04    3
 4.60336012E-08-7.28250948E-12-1.86336574E+04 9.38831035E+01                   4
TCDYOO23 reqs   b3lyp/6C  10H  16O   2    0G   300.000  5000.000 1401.000    11
 2.88414199E+01 4.38034906E-02-1.49245851E-05 2.31178986E-09-1.33933404E-13    2
-3.51273527E+04-1.42681685E+02-1.55905135E+01 1.52368471E-01-1.16555051E-04    3
 4.55697354E-08-7.17891498E-12-2.03253370E+04 9.39996338E+01                   4
TCDYOO34 reqs   b3lyp/6C  10H  16O   2    0G   300.000  5000.000 1401.000    11
 2.88163386E+01 4.38608976E-02-1.49523712E-05 2.31695885E-09-1.34268059E-13    2
-3.49287222E+04-1.42955495E+02-1.58355771E+01 1.52889937E-01-1.16935052E-04    3
 4.56866623E-08-7.19118455E-12-2.00458447E+04 9.49241542E+01                   4
```

Table K.1 Thermochemical properties of the TCD system in the NASA polynomial format for use in ChemKin (Continued)

```
THERMO
   300.000  1500.000  5000.000

TCDYOO19 reqs   b3lyp/6C  10H  16O   2    0G   300.000  5000.000 1401.000    11
 2.88577732E+01 4.38078809E-02-1.49302939E-05 2.31312974E-09-1.34029957E-13    2
-3.86988518E+04-1.43070071E+02-1.56528832E+01 1.52442562E-01-1.16483062E-04    3
 4.54690485E-08-7.15062342E-12-2.38585474E+04 9.40738668E+01                   4
TCDYOO26 reqs   b3lyp/6C  10H  16O   2    0G   300.000  5000.000 1400.000    11
 2.87015715E+01 4.39372313E-02-1.49741106E-05 2.31988011E-09-1.34419228E-13    2
-4.06199664E+04-1.42930687E+02-1.56678399E+01 1.52117366E-01-1.16015634E-04    3
 4.52331338E-08-7.10955504E-12-2.58111076E+04 9.35075248E+01                   4
TCDYOO98 reqs   b3lyp/6C  10H  16O   2    0G   300.000  5000.000 1400.000    11
 2.87369315E+01 4.39543364E-02-1.49905055E-05 2.32353831E-09-1.34676918E-13    2
-3.91359022E+04-1.42670745E+02-1.57733884E+01 1.52002772E-01-1.15290930E-04    3
 4.45955827E-08-6.94525293E-12-2.42397553E+04 9.46747922E+01                   4
TCDYOO110 reqs   b3lyp/6C  10H  16O   2    0G   300.000  5000.000 1399.000    11
 2.85773083E+01 4.40868503E-02-1.50357159E-05 2.33055658E-09-1.35084405E-13    2
-3.73453158E+04-1.41454034E+02-1.50679082E+01 1.48826735E-01-1.10856984E-04    3
 4.20275540E-08-6.41085144E-12-2.26170598E+04 9.17085754E+01                   4
```

APPENDIX L

TCD – RATE CONSTANTS

Appendix L summarizes the rate constants obtained from the chemical activation qRRK analysis for the oxidation of isooctane.

Table L.1 Dissociation high pressure rate constants

Reaction	A (cm^3 mol^{-1} s^{-1})	n	Ea (cal mol^{-1})
TCD <=> TCD-Hj-3 +H	3.2500E16	0.00	95400.00
TCD <=> TCD-Hj-4 +H	6.500E+15	0.00	95900.00
TCD = TCD-Hj-9 + H	3.25E+16	0.00	95400.
TCD = TCD-Hj-Hj-1-9	8.55E14	1.0	47550.
TCD = TCD-Hj-Hj-1-10	2.5E16	0.00	55950.
TCD-Hj-3 = YC5EYC5jS	5.5E13	0.00	29.6E3
YC5EYC5jS = YC5ECMjCV	3.2E13	0.00	30.0E3
YC5ECMjCV = YC5Ej1 + VCV	7.1E12	0.00	22.4E3
YC5Ej1 = YC5DE + H	5.0E12	0.00	45.2E3
YC5Ej1 = VVCj	1.6E13	0.00	23.6E3
TCD-Hj-3 = VBIY221Cj	3.2E13	0.00	31.7E3
VBIY221Cj = YC5jCV2	3.2E13	0.00	28.1E3
YC5jCV2 = VCCMjCV2	3.2E13	0.00	27.0E3
VCCMjCV2 = VCjV + VCV	7.6E12	0.00	27.5E3
TCD-Hj-4 = VCBIY221j	5.5E13	0.00	32.2E3
VCBIY221j = VCVYC5j	5.5E13	0.00	26.2E3
VCVYC5j = VCCMjCV2	3.2E13	0.00	23.0E3
VCCMjCV2 = VCVV + CjC=C	1.6E13	0.00	17.9E3
TCD-Hj-9 = YC5jYC5E3	5.5E13	0.00	19.7E3
YC5jYC5E3 = YC5E + YC5Ej2	5.5E13	0.00	13.6E3
YC5Ej2 = YC5DE + H	1.0E13	0.00	45.2E3
YC5Ej2 = VVCj	3.2E13	0.00	76.9E3
YC5Ej1 = YC5Ej2	5.0E12	0.00	18.4E3
TCDj9 = YC5YC5jV	5.5E13	0.00	21.3E3
YC5YC5jV = VYC5CjV	7.1E12	0.00	15.9E3
VYC5CjV = VCjCCCVV	7.1E12	0.00	24.4E3
VCjCCCVV = CjCVV + C=CC=C	3.2E13	0.00	37.7E3
CjCVV = C=CC=Cj + C2H4	3.2E13	0.00	63.3E3
CjCVV = VVV + H	8.0E12	0.00	32.0E3
CjCVV = YC6Ej	1.0E12	0.00	13.0E3
YC6Ej = YC6DE13 + H	1.0E13	0.00	47.4E3
TCD-Hj-Hj-1-9 = YC5YC5V	1.9E10	1.0	8.8E3
TCD-Hj-Hj-1-9 = YC5YE1CC	1.9E10	1.0	15.9E3
TCD-Hj-Hj-1-9 = YC5YE2CC	1.9E10	1.0	33.0E3
TCD-Hj-Hj-1-9 = YC5YC5jj + C2H4	3.2E13	0.00	40.4E3
YC5YC5jj = YC8DE	1.9E10	1.0	1.8E3

Table L.1 Dissociation high pressure rate constants (Continued)

Reaction	**A** (cm^3 mol^{-1} s^{-1})	**n**	**Ea** (cal mol^{-1})
TCD-Hj-Hj-1-10= BI340V	1.9E10	1.0	8.8E3
TCD-Hj-Hj-1-10 = BI340E1M	1.9E10	1.0	15.6E3
TCD-Hj-Hj-1-10 = BI340E2M	1.9E10	1.0	33.0E3
TCD-Hj-Hj-1-10 = YC5VCMjCj	3.2E13	0.00	25.1E3
YC5VCMjCj => YC5jV + C=CCj	7.1E12	0.00	21.2E3
YC5jV => VVCCCj	1.6E13	0.00	24.8E3
VVCCCj => VVCj + C2H4	1.6E13	0.00	23.4E3
VVCCCj => YC6ECj	5.4E7	0.00	6.6E3
YC6ECj => YC6EV + H	5.0E13	0.00	32.7E3
YC5jV => YC5EV + H	5.0E13	0.00	30.0E3

Table L.2 Chemical activation rate constants

Reaction	A (cm^3 mol^{-1} s^{-1})	n	Ea (cal mol^{-1})
TCD-Qj-3 = TCD-Hj-3 + O2	1.00E15	0.00	28.6E3
TCD-Qj-3 = TCD- Oj-3	2.17E12	0.53	60.1E3
TCD-Qj-3 = TCD-Q-3-Hj-4	5.43E12	0.3	18.0E3
TCD-Qj-3 = TCD-D-34	1.59E13	0.3	26.9E3
TCD-Qj-3 = TCD-DO-3	5.43E12	0.19	40.0E3
TCD-Qj-4 = TCD-Hj-4 + O2	1.00E15	0.00	32.8E3
TCD-Qj-4 = TCD- Oj-4	2.17E12	0.53	59.7E3
TCD-Qj-4 = TCD-Q-4-Hj-5	5.43E12	0.3	17.6E3
TCD-Qj-4 = TCD-D-45	1.59E13	0.3	26.1E3
TCD-Qj-4 = TCD-DO-4	5.43E12	0.19	40.0E3
TCD-Qj-9 = TCD-Hj-9 + O2	1.00E15	0.00	32.6E3
TCD-Qj-9 = TCD- Oj-9	2.17E12	0.53	59.4E3
TCD-Qj-9 = TCD-Q-9-Hj-8	5.43E12	0.3	17.3E3
TCD-Qj-9 = TCD-D-89	1.59E13	0.3	27.7E3
TCD-Qj-9 = TCD-DO-9	5.43E12	0.19	40.0E3
TCD-Qj-Hj-1-9 (t) = TCD-Hj-Hj-1-9 + O2	1.00E15	0.00	30.5E3
TCD-Qj-Hj-1-9 (t) = TCD-Qj-Hj-1-9 (s)	9.0E13		1.5E3
TCD-Qj-Hj-1-9 (s) = TCD-YOO-19	3.50E12	0.00	0.0
TCD-YOO-19 = TCD-Oj-Oj-1-9	5.0E15		26.01E3
TCD-Oj-Oj-1-9 = YC5jC(CC=O)CCOj	1.0E13		6.5E3
TCD-Oj-Oj-1-9 = BIY330=OCO	3.0E13		6.5E3
YC5jCCOCOj = YC5jCCCOCj + CH2=O	3.0E13		16.5E3
TCD-Qj-Hj-1-10 (t) = TCD-Hj-Hj-1-10 + O2	1.00E15	0.00	30.11E3
TCD-Qj-Hj-1-10 (t) = TCD-Qj-Hj-1-10 (s)	9.0E13		1.5E3
TCD-Qj-Hj-1-10 (s) = TCD-YOO-1-10	3.50E12	0.00	0.0
TCD-YOO-1-10 = TCD-Oj-Oj-1-10	5.0E15		22.91E3
TCD-Oj-Oj-1-10 = YC5jC(COj)C3=O	1.0E13		6.5E3
TCD-Oj-Oj-1-10 = YC5YC6(=O)COH	3.0E13		6.5E3
YC5jC(COj)C3=O = YC5jCjC3=O + CH2=O	3.0E+13		16.1E3

APPENDIX M

CYCLIC ALKANES – MOLECULAR GEOMETRIES

Appendix M summarizes the molecular geometries of all the species calculated for the study of the oxidation of cyclic alkanes.

Table M.1 Structural parameters optimized at the B3LYP/6-31G(d,p) level

Molecule	**Cartesian Coordinates**		
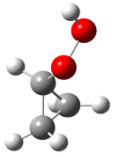 **y(ccc)q**	-1.12411500	0.91523700	-0.12489800
	-1.58923100	-0.52259700	-0.13850200
	-0.27414500	-0.15858000	0.49362600
	-0.76661400	1.33388300	-1.05934400
	-1.61652300	1.61947500	0.53845800
	-1.54085600	-1.05564900	-1.08202600
	-2.39679000	-0.82781300	0.51914900
	-0.17051800	-0.19655800	1.57781300
	0.82811700	-0.62768300	-0.21942100
	1.90182900	0.36789300	-0.05857500
	2.57668500	-0.19937600	0.34856400
Molecule	**Cartesian Coordinates**		
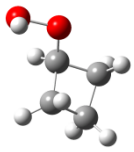 **y(cccc)q**	1.99449500	0.29395800	-0.00795900
	1.16155000	-1.01838800	-0.03645500
	-0.06805900	-0.17809600	0.36742400
	0.66824600	1.09763000	-0.11184100
	2.48709700	0.44209500	0.95732500
	2.73332700	0.43521400	-0.80023500
	1.45078700	-1.84362600	0.61832800
	1.04008900	-1.39469500	-1.05662900
	-0.24441100	-0.17505000	1.44939200
	0.56410900	2.00837400	0.48316100
	0.41088500	1.31200100	-1.15436600
	-1.23661200	-0.59663900	-0.30812400
	-2.32619300	0.25315900	0.16601800
	-2.47683100	0.79291000	-0.62714000
Molecule	**Cartesian Coordinates**		
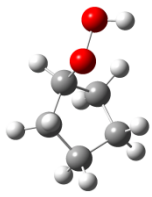 **y(ccccc)q**	-1.29987200	1.07274600	-0.44622100
	-1.99160300	-0.29009900	-0.25163500
	-0.85014600	-1.26037700	0.15171600
	-0.20728400	1.06014600	0.63310500
	-0.83554800	1.11968800	-1.43837000
	-1.98695200	1.92008400	-0.36140500
	-2.53322800	-0.62623800	-1.14063600
	-2.72396500	-0.21614200	0.56108800
	-1.14428100	-1.93378000	0.96146100
	-0.53316000	-1.88907500	-0.68642600
	-0.65097300	1.23374800	1.62201100
	0.58409400	1.80211600	0.49649500
	0.34549600	-0.37141200	0.57623400
	0.81865800	-0.68871100	1.51196900
	1.30007200	-0.53583600	-0.48665700
	2.50956000	0.18240700	-0.09991400
	2.54874900	0.83972000	-0.81281100

APPENDIX N

CYCLIC ALKANES – VIBRATIONAL FREQUENCIES

Appendix N includes the frequencies of the species calculated for the study of cyclic alkanes.

Table N.1 Vibrational frequencies **c**alculated at the B3LYP/6-31G(d,p) level

SYSTEM	Frequencies, cm^{-1}								
y(ccc)q	127.0	166.5	260.6	402.8	497.4	760.1	825.6	841.9	891.2
	957.4	996.2	1056.8	1073.1	1122.8	1196.5	1206.6	1231.1	1358.4
	1396.1	1468.2	1510.4	3128.4	3151.0	3155.1	3236.7	3248.5	3764.2
y(c˙cc)	568.0	770.5	778.9	851.8	938.3	1034.5	1063.6	1097.3	1105.5
	1165.3	1270.6	1469.5	1498.8	3098.3	3098.6	3163.0	3175.1	3230.7
y(ccc)q˙	56.8	286.0	377.4	499.5	751.9	812.6	838.7	929.5	974.5
	1058.6	1078.7	1108.2	1164.7	1190.7	1201.1	1230.2	1367.3	1468.1
	1509.9	3151.3	3152.7	3206.5	3234.6	3246.6			
y(c˙cc)q	108.2	177.0	255.0	385.5	463.2	618.1	811.6	877.4	896.5
	926.0	951.1	1045.4	1077.0	1106.1	1150.9	1258.2	1355.5	1373.8
	1466.5	3101.0	3107.4	3178.4	3250.5	3759.0			
y(cccc)q	99.2	149.3	193.1	259.3	432.0	458.1	637.0	770.2	795.8
	903.8	918.5	928.9	956.5	975.3	1066.3	1097.7	1176.1	1200.9
	1254.0	1255.3	1263.0	1277.9	1308.2	1359.2	1389.9	1486.5	1500.0
	1523.6	3059.5	3066.5	3075.6	3078.3	3121.3	3130.8	3141.2	3757.4
y(c˙ccc)	87.1	257.8	746.1	752.6	793.7	908.7	913.1	976.9	1003.6
	1011.9	1043.3	1191.0	1219.2	1223.1	1253.7	1295.9	1327.3	1471.1
	1479.0	1510.1	2991.3	2996.0	3014.7	3018.3	3076.9	3129.7	3202.9
y(cccc)q˙	49.9	138.2	275.5	418.5	455.4	646.2	770.0	791.7	908.2
	925.7	941.9	958.0	1059.6	1066.9	1158.7	1194.0	1206.0	1252.4
	1254.1	1259.6	1279.5	1302.4	1361.8	1487.5	1500.8	1523.5	3078.1
	3080.2	3083.2	3111.7	3129.5	3139.0	3148.5			

Table N.1 Vibrational frequencies **c**alculated at the B3LYP/6-31G(d,p) level (Continued)

SYSTEM	Frequencies, cm^{-1}								
	76.0	119.0	193.3	252.4	329.1	434.4	460.5	737.3	762.4
	863.1	902.9	928.7	951.2	985.1	1038.4	1067.9	1117.2	1203.0
	1214.4	1243.9	1287.2	1313.5	1339.0	1366.9	1471.6	1492.2	3001.7
	3009.3	3036.6	3080.5	3139.8	3219.8	3761.1			
y(cc˙cc)q	92.7	132.7	179.3	233.2	257.8	423.2	468.8	710.9	789.6
	859.8	919.3	965.0	969.3	976.8	1031.1	1054.6	1086.5	1197.9
	1213.6	1251.0	1285.0	1317.1	1359.4	1380.2	1459.4	1478.1	2984.3
	2999.7	3047.0	3054.1	3078.6	3223.1	3758.3			
y(ccccc)q	57.4	142.7	205.2	232.3	281.0	381.9	476.6	588.1	694.9
	795.5	838.6	869.9	901.4	910.3	934.6	940.6	991.7	1016.6
	1045.5	1097.7	1192.4	1204.4	1238.2	1256.1	1307.4	1312.3	1338.3
	1350.9	1356.3	1373.1	1390.3	1494.2	1496.9	1505.3	1525.2	3043.4
y(c˙cccc)	173.0	238.9	345.2	569.8	661.5	824.1	853.6	897.4	899.8
	915.5	934.5	1014.4	1035.2	1051.1	1097.6	1191.8	1229.2	1242.8
	1296.3	1308.6	1338.9	1359.5	1378.0	1484.3	1485.8	1505.8	1521.9
y(ccccc)q˙	55.6	106.1	220.5	294.9	383.4	496.8	590.2	687.2	773.9
	825.1	869.5	904.8	907.8	926.7	962.2	1018.1	1043.2	1100.1
	1183.8	1193.6	1207.5	1237.2	1254.9	1301.0	1314.1	1339.0	1348.7
	1364.6	1369.7	1492.3	1494.2	1507.6	1525.7	3050.1	3051.9	3058.9
y(c˙ccccq)	89.7	149.6	189.4	214.9	277.5	363.8	465.1	473.1	606.1
	748.1	822.9	846.8	884.4	896.8	923.1	927.8	947.1	1027.8
	1044.3	1062.2	1142.7	1204.1	1237.8	1289.0	1302.5	1322.7	1335.6
	1356.2	1371.2	1382.2	1477.3	1496.1	1512.6	2964.2	3038.7	3043.2
y(cc˙ccc)q	98.2	148.2	178.2	218.6	276.8	343.8	370.0	480.2	671.7
	740.7	820.4	837.9	895.0	918.1	923.0	946.6	972.5	1015.8
	1045.0	1062.3	1131.1	1193.7	1227.0	1274.7	1302.8	1309.9	1346.1
	1360.3	1384.2	1388.7	1468.3	1483.9	1503.8	2966.7	2977.5	3039.5
	3044.4	3058.0	3072.9	3122.5	3217.5	3768.1			

APPENDIX O

CYCLIC ALKANES – ROTATIONAL ANALYSIS

Appendix O includes the results of the rotational analysis for the cyclic alkanes.

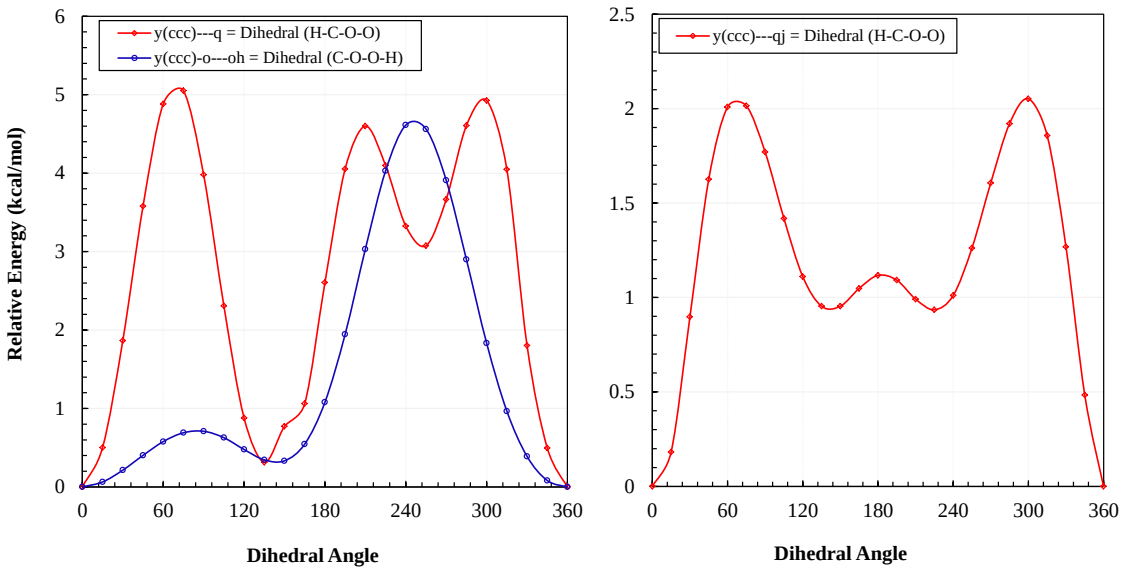

Figure O.1 Potential energy profiles for internal rotations in y(ccc)q (left) and y(ccc)q• (right)

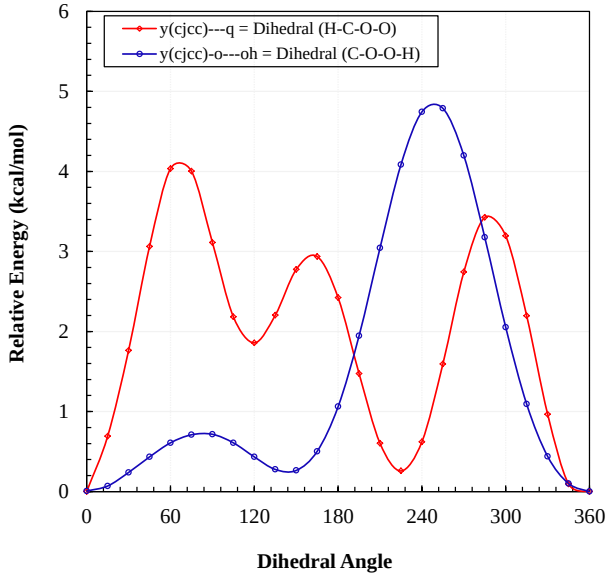

Figure O.2 Potential energy profiles for internal rotations in y(c•cc)q

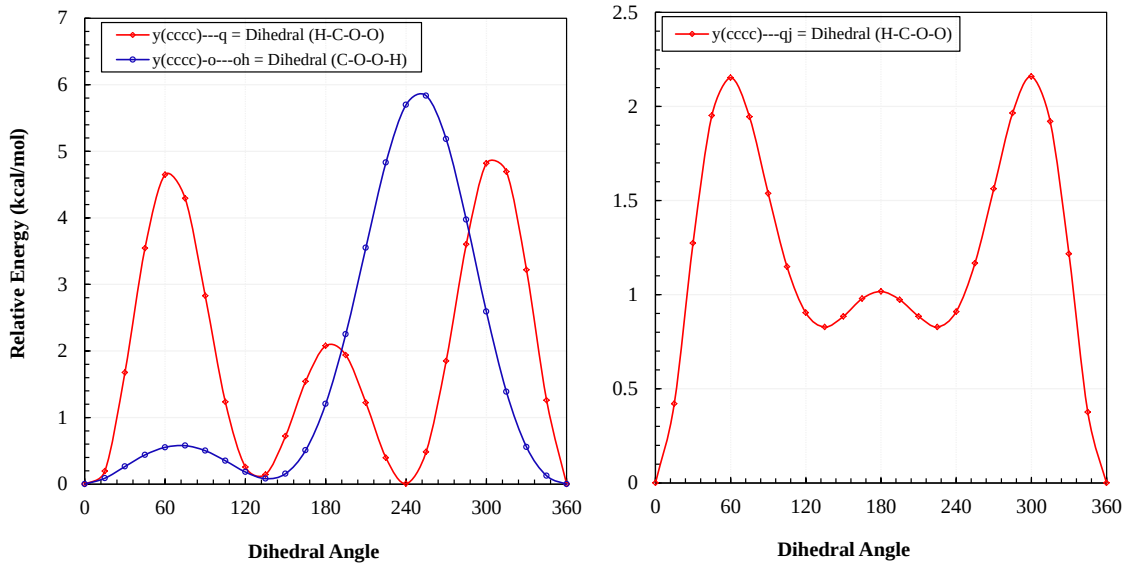

Figure O.3 Potential energy profiles for internal rotations in y(cccc)q (left) and y(cccc)q• (right)

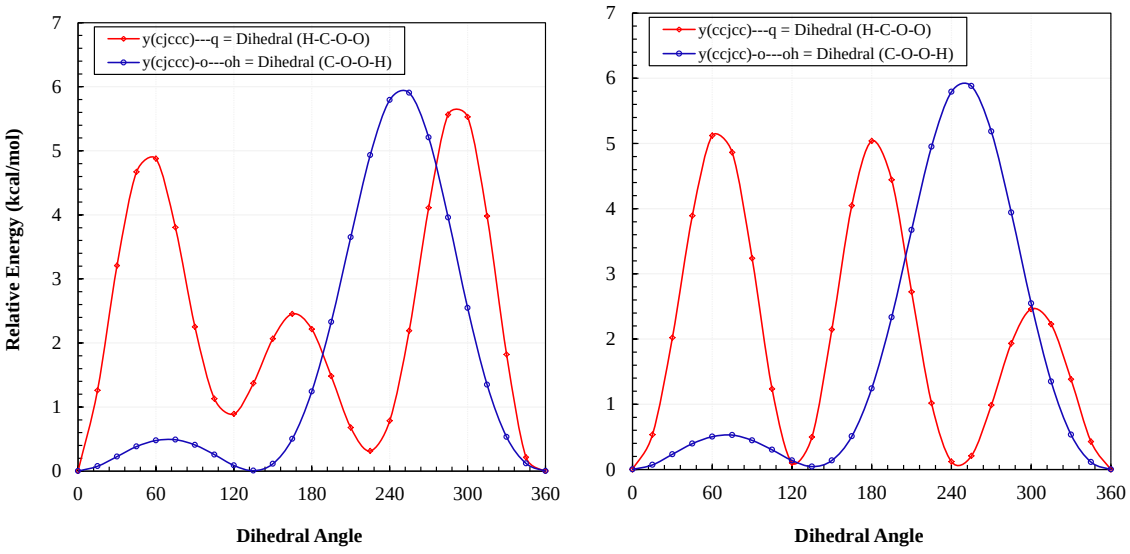

Figure O.4 Potential energy profiles for internal rotations in y(c•ccc)q (left) and y(cc•cc)q (right)

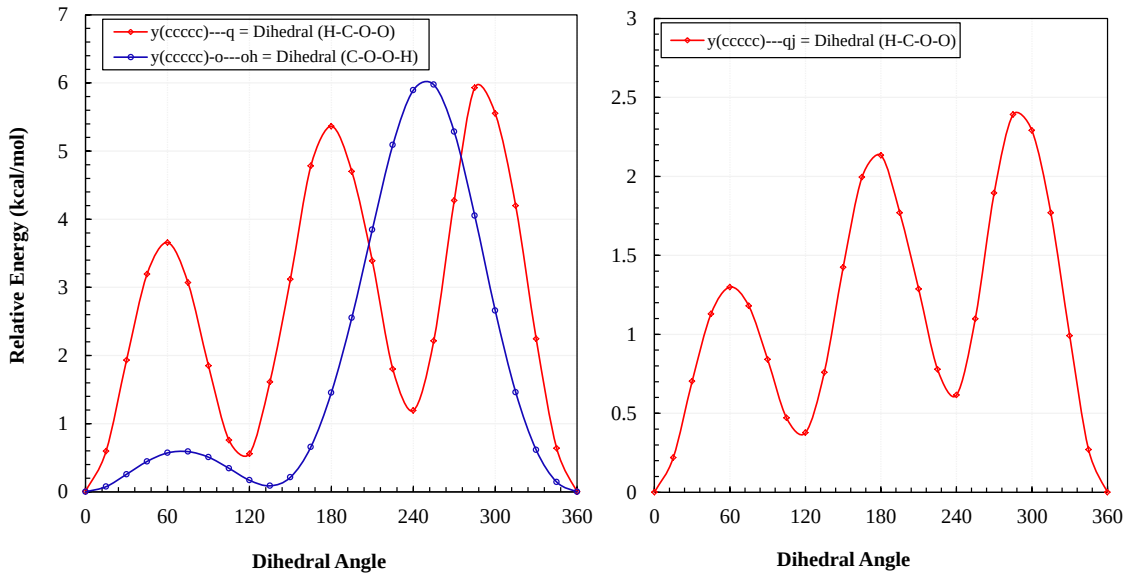

Figure O.5 Potential energy profiles for internal rotations in y(ccccc)q (left) and y(ccccc)q• (right)

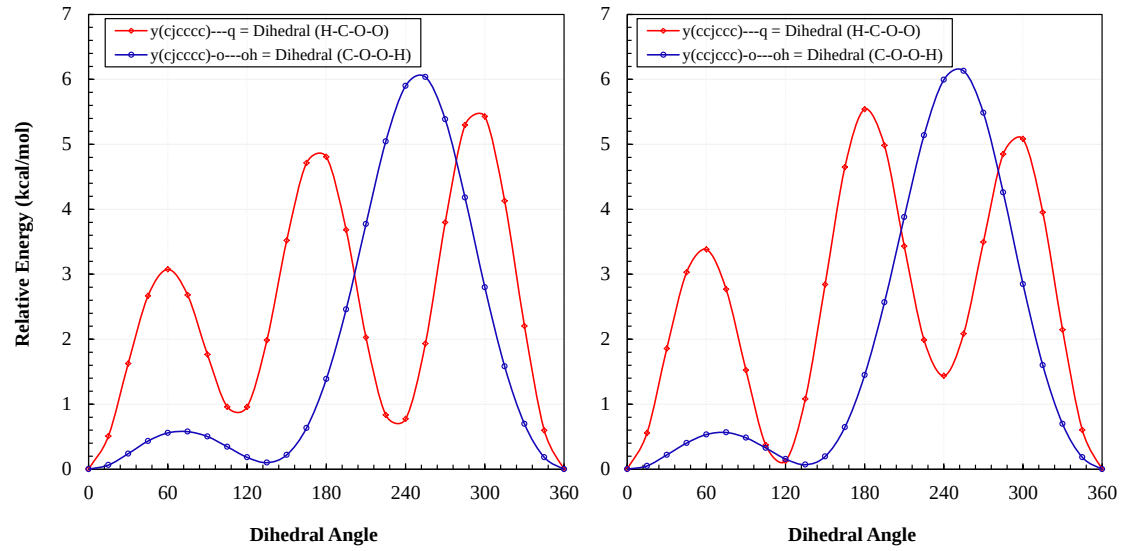

Figure O.6 Potential energy profiles for internal rotations in y(c•cccc)q (left) and y(cc•ccc)q (right)

APPENDIX P

CYCLIC ALKANES – WORK REACTIONS

Appendix P summarizes the work reactions used for the determination of the heat of formation of the species calculated for the study of cyclic alkanes.

Table P.1 Calculated enthalpies of formation at 298 K of cyclopropane radical and cyclopropane peroxide and peroxy radicals

Work Reactions						$\Delta_f H°_{298}$					
						B3LYP		CBS-QB3	G3MP2B3	Average methods	Therm
						6-31G(d,p)	6-31G(2d,2p)				
y(ccc)q											
y(ccc)q	+ cc	= y(ccc)	+ ccq			-9.10	-8.94	-8.29	-8.13		
y(ccc)q	+ ccc	= y(ccc)	+ c2cq			-8.73	-8.74	-7.38	-7.30		
y(ccc)q	+ ccc	= y(ccc)	+ cccq			-8.01	-7.85	-7.14	-7.00		
				Ave.		-9.08	-9.03	-7.57	-7.50	***-8.30***	-11.33
				σ						*0.88*	
y(c˙cc)											
y(c˙cc)	+ ccc	= y(ccc)	+ cc˙c			69.93	69.97	70.10	69.89		
y(c˙cc)	+ cccc	= y(ccc)	+ ccc˙c			68.72	68.77	68.88	68.65		
y(c˙cc)	+ c2ccc	= y(ccc)	+ c2cc˙c			70.77	70.85	70.63	70.29		
				Ave.		69.81	69.86	69.87	69.61	***69.79***	59.09
				σ						*0.12*	
				BDE		109.1	109.2	109.2	110.0	*109.1*	98.5
y(ccc)q˙											
y(ccc)q˙	+ ccq	= y(ccc)q	+ ccq˙			26.77	26.59	27.24	27.32		
y(ccc)q˙	+ ccqc	= y(ccc)q	+ ccq˙c			26.82	26.71	27.32	27.37		
y(ccc)q˙	+ c3cq	= y(ccc)q	+ c3cq˙			27.30	27.19	27.57	27.59		
				Ave.		26.96	26.83	27.38	27.43	***27.15***	22.87
				σ						*0.30*	
				BDE		86.6	86.5	87.0	87.1	*86.8*	86.3

Units: kcal mol^{-1}

Table P.1 Calculated enthalpies of formation at 298 K of cyclopropane radical and cyclopropane peroxide and peroxy radicals (Continued)

Work Reactions	$\Delta_f H^o_{298}$					
	B3LYP		CBS-QB3	G3MP2B3	Average methods	Therm
	6-31G(d,p)	6-31G(2d,2p)				
y(c˙cc)q						
y(c˙cc)q + cc = y(ccc)q + cc˙	50.00	49.95	50.44	50.28		
y(c˙cc)q + ccc = y(ccc)q + cc˙c	48.78	48.75	49.23	49.04		
y(c˙cc)q + c3c = y(ccc)q + cc˙c2	50.84	50.83	50.98	50.68		
Ave.	49.87	49.84	50.22	50.00	***49.98***	35.02
σ					*0.17*	
BDE	109.5	109.5	109.9	109.6	*109.6*	98.5

Units: kcal mol^{-1}

Table P.2 Calculated enthalpies of formation at 298 K of cyclobutane radical and cyclobutane peroxide and peroxy radicals

Work Reactions					$\Delta_f H^o_{298}$					
					B3LYP		CBS-QB3	G3MP2B3	Average methods	Therm
					6-31G(d,p)	6-31G(2d,2p)				
y(cccc)q										
y(cccc)q	+ cc	= y(cccc)	+	ccq	-17.75	-17.69	-18.07	-18.00		
y(cccc)q	+ ccc	= y(cccc)	+	c2cq	-17.38	-17.48	-17.16	-17.17		
y(cccc)q	+ c3c	= y(cccc)	+	c3cq	-18.04	-18.15	-16.81	-16.93		
				Ave.	-17.73	-17.77	-17.35	-17.36	***-17.55***	-17.28
				σ					*0.23*	
y(c˙ccc)										
y(c˙ccc)	+ ccc	= y(cccc)	+	cc˙c	54.60	54.57	55.14	55.14		
y(c˙ccc)	+ cccc	= y(cccc)	+	ccc˙c	53.38	53.37	53.93	53.89		
y(c˙ccc)	+ c2ccc	= y(cccc)	+	c2cc˙c	55.44	55.45	55.67	55.53		
				Ave.	54.47	54.46	54.91	54.85	***54.68***	53.14
				σ					*0.24*	
				BDE	99.9	99.9	100.4	100.3	*100.2*	98.5
y(cccc)q˙										
y(cccc)q˙	+ ccq	= y(cccc)q	+	ccq˙	15.41	15.34	15.86	15.91		
y(cccc)q˙	+ ccqc	= y(cccc)q	+	ccq˙c	15.46	15.46	15.93	15.96		
y(cccc)q˙	+ c3cq	= y(cccc)q	+	c3cq˙	15.94	15.94	16.19	16.18		
				Ave.	15.60	15.58	16.00	16.02	***15.80***	16.92
				σ					*0.24*	
				BDE	85.3	85.3	85.7	85.7	*85.5*	86.3
y(c˙ccc)q										
y(c˙ccc)q	+ cc	= y(cccc)q	+	cc˙	31.49	31.38	32.08	32.00		
y(c˙ccc)q	+ ccc	= y(cccc)q	+	cc˙c	31.27	30.19	30.87	30.76		
y(c˙ccc)q	+ c3c	= y(cccc)q	+	cc˙c2	32.32	32.26	32.62	32.40		
				Ave.	31.36	31.28	31.86	31.72	***31.55***	29.07
				σ					*0.28*	
				BDE	101.0	100.9	101.5	101.4	*101.2*	98.5

Units: kcal mol^{-1}

Table P.2 Calculated enthalpies of formation at 298 K of cyclobutane radical and cyclobutane peroxide and peroxy radicals (Continued)

Work Reactions						$\Delta_f H^o_{298}$					
						B3LYP					
						6-31G(d,p)	6-31G(2d,2p)	CBS-QB3	G3MP2B3	Average methods	Therm
y(cc˙cc)q											
y(cc˙cc)q	+	cc	=	y(cccc)q	+ cc˙	31.21	31.21	31.57	31.58		
y(cc˙cc)q	+	ccc	=	y(cccc)q	+ cc˙c	30.00	30.00	30.35	30.34		
y(cc˙cc)q	+	c3c	=	y(cccc)q	+ cc˙c2	32.06	32.08	32.11	31.98		
					Ave.	31.09	31.10	31.34	31.30	***31.21***	29.07
					σ					*0.14*	
					BDE	100.7	100.7	101.0	101.0	*100.9*	98.5

Units: kcal mol^{-1}

Table P.3 Calculated enthalpies of formation at 298 K of cyclopentane radical and cyclopentane peroxide and peroxy radicals

Work Reactions						$\Delta_f H^o_{298}$					
						B3LYP					
						6-31G(d,p)	6-31G(2d,2p)	CBS-QB3	G3MP2B3	Average methods	Therm
y(ccccc)q											
y(ccccc)q	+ cc	= y(ccccc)	+ ccq			-41.70	-41.60	-42.95	-42.83		
y(ccccc)q	+ ccc	= y(ccccc)	+ c2cq			-41.33	-41.40	-42.05	-41.99		
y(ccccc)q	+ c3c	= y(ccccc)	+ c3cq			-41.98	-42.07	-41.70	-41.76		
				Ave.		-41.67	-41.69	-42.23	-42.20	***-41.95***	-42.81
				σ						*0.31*	
y(c˙ccc)											
y(c˙cccc)	+ ccc	= y(ccccc)	+ cc˙c			26.92	26.95	26.33	26.35		
y(c˙cccc)	+ cccc	= y(ccccc)	+ ccc˙c			25.70	25.75	25.12	25.11		
y(c˙cccc)	+ c2ccc	= y(ccccc)	+ c2cc˙c			27.76	27.82	26.86	26.75		
				Ave.		26.79	26.84	26.10	26.07	***26.45***	27.61
				σ						*0.42*	
				BDE		97.15	97.20	96.46	96.43	*96.81*	98.45
y(ccccc)q˙											
y(ccccc)q˙	+ ccq	= y(ccccc)q	+ ccq˙			-9.22	-9.27	-9.13	-9.08		
y(ccccc)q˙	+ ccqc	= y(ccccc)q	+ ccq˙c			-9.17	-9.15	-9.06	-9.03		
y(ccccc)q˙	+ c3cq	= y(ccccc)q	+ c3cq˙			-8.69	-8.67	-8.81	-8.81		
				Ave.		-9.03	-9.03	-9.00	-8.97	***-9.01***	-8.61
				σ						*0.03*	
				BDE		85.02	85.01	85.05	85.07	*85.04*	86.3
y(c˙cccc)q											
y(c˙cccc)q	+ cc	= y(ccccc)q	+ cc˙			3.67	3.83	3.98	4.01		
y(c˙cccc)q	+ ccc	= y(ccccc)q	+ cc˙c			2.45	2.64	2.76	2.76		
y(c˙cccc)q	+ c3c	= y(ccccc)q	+ cc˙c2			4.51	4.71	4.51	4.40		
				Ave.		3.54	3.73	3.75	3.72	***3.69***	3.54
				σ						*0.10*	
				BDE		97.59	97.78	97.80	97.77	*97.73*	98.45

Units: kcal mol^{-1}

Table P.3 Calculated enthalpies of formation at 298 K of cyclopentane radical and cyclopentane peroxide and peroxy radicals (Continued)

Work Reactions						$\Delta_f H^o_{298}$					
						B3LYP					
						6-31G(d,p)	6-31G(2d,2p)	CBS-QB3	G3MP2B3	Average methods	Therm
y(cc˙ccc)q											
y(cc˙ccc)q	+ cc	= y(ccccc)q	+	cc˙		3.52	3.56	3.55	3.53		
y(cc˙ccc)q	+ ccc	= y(ccccc)q	+	cc˙c		2.30	2.36	2.34	2.30		
y(cc˙ccc)q	+ c3c	= y(ccccc)q	+	cc˙c2		4.36	4.44	4.09	3.94		
					Ave.	3.39	3.45	3.33	3.26	***3.36***	3.54
					σ					*0.08*	
					BDE	97.4	97.5	97.4	97.3	*97.4*	98.5

Units: kcal mol^{-1}

APPENDIX Q

CYCLIC ALKANES – ENTROPY AND HEAT CAPACITIES

Appendix Q includes the entropy *(S)* and heat capacity *(Cp)* versus temperature for the species calculated for the study of cyclic alkanes.

Table Q.1 Entropy *(S)* and heat capacity *(Cp) vs.* temperature

T (K)	y(ccc)q		y(c˙cc)		y(ccc)q˙		y(c˙cc)q		y(cccc)q	
	Cp(T)	S(T)	Cp(T)	S(T)	Cp(T)	S(T)	Cp(T)	S(T)	Cp(T)	S(T)
5	8.13	31.56	7.95	27.38	7.95	32.73	7.95	32.73	8.23	33.36
50	10.76	52.25	7.95	45.69	9.87	52.09	11.19	52.50	10.88	55.24
100	12.64	60.38	7.96	51.20	12.82	59.89	13.58	61.13	13.53	63.65
150	14.13	65.78	8.17	54.45	14.19	65.37	15.16	66.92	15.75	69.54
200	16.08	70.09	8.97	56.89	15.43	69.61	17.22	71.54	18.32	74.41
250	18.63	73.94	10.39	59.03	17.24	73.23	19.72	75.64	21.45	78.81
298	21.43	77.44	12.12	60.99	19.41	76.43	22.29	79.32	24.84	82.86
300	21.55	77.58	12.20	61.08	19.51	76.56	22.39	79.47	24.99	83.02
400	27.43	84.58	16.06	65.11	24.36	82.83	27.34	86.60	32.27	91.20
500	32.36	91.23	19.47	69.06	28.68	88.73	31.28	93.13	38.69	99.09
600	36.19	97.46	22.27	72.86	32.21	94.27	34.30	99.10	43.96	106.62
700	39.17	103.24	24.58	76.46	35.08	99.45	36.68	104.57	48.25	113.71
800	41.57	108.59	26.52	79.87	37.44	104.29	38.63	109.59	51.80	120.39
900	43.58	113.57	28.20	83.09	39.44	108.81	40.27	114.23	54.80	126.66
1000	45.28	118.21	29.64	86.13	41.13	113.05	41.68	118.55	57.35	132.56
1100	46.76	122.55	30.91	89.02	42.60	117.04	42.91	122.58	59.54	138.12
1200	48.04	126.64	32.01	91.75	43.86	120.80	43.98	126.35	61.43	143.38
1300	49.17	130.48	32.98	94.35	44.96	124.35	44.92	129.91	63.08	148.36
1400	50.15	134.12	33.83	96.82	45.91	127.72	45.75	133.27	64.51	153.09
1500	51.02	137.57	34.57	99.18	46.75	130.91	46.48	136.45	65.75	157.58
2000	54.08	152.50	37.16	109.51	49.63	144.79	49.04	150.20	70.06	177.14
2500	55.82	164.59	38.61	117.97	51.23	156.05	50.49	161.31	72.44	193.04
3000	56.87	174.71	39.49	125.09	52.19	165.48	51.37	170.59	73.86	206.38
3500	57.55	183.39	40.04	131.22	52.80	173.57	51.93	178.55	74.77	217.84
4000	58.00	190.99	40.42	136.60	53.21	180.65	52.31	185.51	75.38	227.86
4500	58.33	197.73	40.68	141.37	53.50	186.93	52.58	191.69	75.81	236.77
5000	58.56	203.79	40.88	145.67	53.71	192.58	52.78	197.24	76.11	244.77

Units: S(cal mol^{-1}) and Cp(kcal mol^{-1} K^{-1})

Table Q.1 Entropy *(S)* and heat capacity *(Cp) vs.* temperature (Continued)

T (K)	y(c•ccc)		y(cccc)q•		y(c•ccc)q		y(cc•cc)q		y(ccccc)q	
	Cp(T)	S(T)	Cp(T)	S(T)	Cp(T)	S(T)	Cp(T)	S(T)	Cp(T)	S(T)
5	7.95	30.30	7.95	34.54	8.76	34.93	8.96	34.94	7.97	36.06
50	8.02	48.62	11.61	54.55	11.26	55.89	10.61	56.48	11.28	56.65
100	8.67	54.35	13.98	63.56	14.58	64.80	14.40	65.06	16.18	66.07
150	9.50	58.01	15.20	69.43	16.90	71.15	17.10	71.42	19.65	73.30
200	10.89	60.91	17.12	74.04	19.37	76.33	19.70	76.68	23.09	79.41
250	13.03	63.55	19.78	78.13	22.33	80.96	22.68	81.38	27.07	84.97
298	15.58	66.05	22.81	81.85	25.51	85.14	25.85	85.63	31.33	90.07
300	15.69	66.15	22.94	82.00	25.65	85.31	25.98	85.80	31.51	90.28
400	21.39	71.43	29.63	89.50	32.32	93.60	32.61	94.18	40.55	100.57
500	26.53	76.76	35.66	96.76	38.08	101.43	38.33	102.07	48.56	110.48
600	30.82	81.98	40.66	103.71	42.73	108.79	42.95	109.47	55.15	119.92
700	34.38	86.99	44.77	110.29	46.48	115.66	46.67	116.38	60.54	128.83
800	37.38	91.78	48.19	116.49	49.56	122.07	49.72	122.80	65.02	137.20
900	39.94	96.33	51.07	122.32	52.14	128.05	52.28	128.80	68.80	145.07
1000	42.15	100.65	53.53	127.83	54.33	133.65	54.46	134.42	72.02	152.48
1100	44.05	104.75	55.64	133.03	56.21	138.92	56.32	139.70	74.79	159.47
1200	45.70	108.65	57.45	137.94	57.83	143.87	57.93	144.66	77.19	166.08
1300	47.13	112.36	59.02	142.60	59.23	148.56	59.33	149.36	79.26	172.34
1400	48.38	115.90	60.38	147.02	60.46	152.99	60.54	153.79	81.06	178.27
1500	49.46	119.27	61.56	151.23	61.52	157.19	61.60	158.00	82.63	183.92
2000	53.20	134.06	65.61	169.54	65.19	175.44	65.24	176.27	88.05	208.50
2500	55.26	146.17	67.84	184.44	67.23	190.22	67.26	191.06	91.04	228.49
3000	56.49	156.36	69.16	196.93	68.44	202.59	68.47	203.43	92.82	245.25
3500	57.27	165.12	70.00	207.66	69.22	213.20	69.23	214.05	93.96	259.65
4000	57.80	172.81	70.57	217.04	69.74	222.48	69.75	223.33	94.72	272.24
4500	58.16	179.64	70.97	225.38	70.10	230.71	70.11	231.56	95.24	283.43
5000	58.43	185.78	71.26	232.87	70.36	238.11	70.36	238.96	95.62	293.49

Units: S(cal mol^{-1}) and Cp(kcal mol^{-1} K^{-1})

Table Q.1 Entropy *(S)* and heat capacity *(Cp) vs.* temperature (Continued)

T (K)	y(c˙cccc)		y(ccccc)q˙		y(c˙cccc)q		y(cc˙ccc)q	
	Cp(T)	S(T)	Cp(T)	S(T)	Cp(T)	S(T)	Cp(T)	S(T)
5	7.95	32.51	7.95	35.94	7.97	35.98	8.14	35.97
50	8.06	50.83	11.46	56.04	10.59	56.89	10.75	57.71
100	9.16	56.71	14.87	65.13	14.97	65.51	14.52	66.30
150	10.74	60.70	17.27	71.62	18.84	72.34	18.04	72.85
200	12.94	64.07	19.96	76.93	22.30	78.22	21.63	78.52
250	15.91	67.25	23.35	81.73	26.08	83.58	25.66	83.76
298	19.29	70.32	27.14	86.14	30.05	88.49	29.83	88.61
300	19.44	70.45	27.30	86.32	30.21	88.69	30.01	88.81
400	26.91	77.05	35.64	95.29	38.53	98.51	38.59	98.61
500	33.69	83.78	43.21	104.06	45.79	107.90	45.98	108.02
600	39.39	90.43	49.54	112.50	51.73	116.77	51.96	116.94
700	44.14	96.86	54.78	120.53	56.56	125.11	56.80	125.31
800	48.15	103.01	59.16	128.12	60.57	132.92	60.80	133.16
900	51.56	108.87	62.86	135.30	63.94	140.24	64.16	140.51
1000	54.50	114.45	66.02	142.09	66.81	147.13	67.02	147.41
1100	57.03	119.76	68.73	148.50	69.28	153.61	69.48	153.91
1200	59.21	124.82	71.07	154.58	71.41	159.72	71.59	160.04
1300	61.11	129.63	73.09	160.34	73.26	165.51	73.43	165.84
1400	62.76	134.21	74.84	165.82	74.87	170.99	75.02	171.34
1500	64.19	138.59	76.36	171.03	76.27	176.20	76.41	176.56
2000	69.11	157.79	81.56	193.78	81.10	198.87	81.19	199.26
2500	71.81	173.52	84.41	212.31	83.77	217.27	83.83	217.68
3000	73.42	186.76	86.11	227.85	85.36	232.69	85.41	233.11
3500	74.44	198.16	87.19	241.21	86.37	245.93	86.41	246.35
4000	75.12	208.15	87.91	252.90	87.05	257.51	87.08	257.94
4500	75.61	217.02	88.42	263.29	87.52	267.79	87.55	268.22
5000	75.96	225.01	88.78	272.62	87.86	277.03	87.88	277.46

Units: S(cal mol^{-1}) and Cp(kcal mol^{-1} K^{-1})

APPENDIX R

CYCLIC ALKANES – GROUPS DEVELOPED

Appendix R includes a summary of the groups used for the determination of the thermochemical properties of cyclic alkanes by the use of the group additivity method.

Table R.1 Groups included for the determination of the heat of formation

y(ccc)q		**y(cccc)q**		**y(ccccc)q**	
c/c2/h2	2	c/c2/h2	3	c/c2/h2	5
c/c2/h/o	1	c/c2/h/o	1	c/c2/h/o	1
o/c/h	1	o/c/h	1	o/c/h	1
o/h/o	1	o/h/o	1	o/h/o	1
cy/c3	1	cy/c4	1	cy/c5	1

y(c•cc)		**y(c•ccc)**		**y(c•cccc)**	
c/c2/h2	3	c/c2/h2	4	c/c2/h2	5
cy/c3	1	cy/c4	1	cy/c5	1
sec radical	1	sec radical	1	sec radical	1

y(ccc)q•		**y(cccc)q•**		**y(ccccc)q•**	
c/c2/h2	2	c/c2/h2	3	c/c2/h2	4
c/c2/h/o	1	c/c2/h/o	1	c/c2/h/o	1
o/c/h	1	o/c/h	1	o/c/h	1
o/h/o	1	o/h/o	1	o/h/o	1
cy/c3	1	cy/c4	1	cy/c5	1
peroxy radical		peroxy radical	1	peroxy radical	1

y(c•cc)q		**y(c•ccc)q**		**y(c•cccc)q**	
c/c2/h2	2	c/c2/h2	3	c/c2/h2	4
c/c2/h/o	1	c/c2/h/o	1	c/c2/h/o	1
o/c/h	1	o/c/h	1	o/c/h	1
o/h/o	1	o/h/o	1	o/h/o	1
cy/c3	1	cy/c4	1	cy/c5	1
sec radical		sec radical	1	sec radical	1

y(cc•cc)q		**y(cc•ccc)q**	
c/c2/h2	3	c/c2/h2	4
c/c2/h/o	1	c/c2/h/o	1
o/c/h	1	o/c/h	1
o/h/o	1	o/h/o	1
cy/c4	1	cy/c5	1
sec radical	1	sec radical	1

Table R.2 Groups included for the determination of cyclopropane peroxy radicals

Three membered ring								
 **y(ccc)**	c/c2/h2 cy/c3	3 1	 **y(c•cc)**	c/c2/h2 cy/c3 **cy/c3j**	3 1 1			
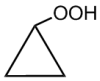 **y(cccq)**	c/c2/h2 c/c2/h/o o/c/h o/h/o **cy/c3/q**	2 1 1 1 1	 **y(ccc)q•**	c/c2/h2 c/c2/h/o o/c/h o/h/o **cy/c3/q** **cy/c3/qj**	2 1 1 1 1 1	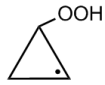 **y(c•cc)q**	c/c2/h2 c/c2/h/o o/c/h o/h/o **cy/c3/q** **cy/cj3/q**	2 1 1 1 1 1

Table R.3 Groups included for the determination of cyclobutane peroxy radicals

Four membered ring								
 **y(cccc)**	c/c2/h2 cy/c4	4 1	 **y(c•ccc)**	c/c2/h2 cy/c4 **cy/c4j**	4 1 1			
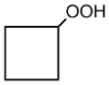 **y(cccc)q**	c/c2/h2 c/c2/h/o o/c/h o/h/o **cy/c4/q**	3 1 1 1 1						
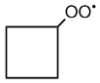 **y(cccc)q•**	c/c2/h2 c/c2/h/o o/c/h o/h/o **cy/c4/q** **cy/c4/qj**	3 1 1 1 1 1	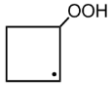 **y(c•ccc)q**	c/c2/h2 c/c2/h/o o/c/h o/h/o **cy/c4/q** **cy/cj4/q**	3 1 1 1 1 1	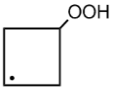 **y(cc•cc)q**	c/c2/h2 c/c2/h/o o/c/h o/h/o **cy/c4/q** **cy/cjs4/q**	

Table R.4 Groups included for the determination of cyclopentane peroxy radicals

Five membered ring								
 **y(ccccc)**	c/c2/h2 cy/c5	5 1	 **y(c˙cccc)**	c/c2/h2 cy/c5 **cy/c5j**	5 1 1			
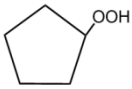 **y(ccccc)q**	c/c2/h2 c/c2/h/o o/c/h o/h/o **cy/c5/q**	5 1 1 1 1						
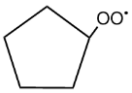 **y(ccccc)q˙**	c/c2/h2 c/c2/h/o o/c/h o/h/o **cy/c5/q** **cy/c5/qj**	4 1 1 1 1 1	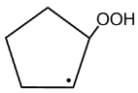 **y(c˙cccc)q**	c/c2/h2 c/c2/h/o o/c/h o/h/o **cy/c5/q** **cy/cj5/q**	4 1 1 1 1 1	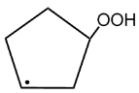 **y(cc˙ccc)q**	c/c2/h2 c/c2/h/o o/c/h o/h/o **cy/c5/q** **y/cjs5/q**	4 1 1 1 1 1

APPENDIX S

CYCLIC ETHERS – MOLECULAR GEOMETRIES

Appendix S summarizes the molecular geometries of all the species calculated for the study of the oxidation of cyclic ethers.

Table S.1 Structural parameters optimized at the B3LYP/6-31G(d,p) level

Species	Cartesian Coordinates			Species	Cartesian Coordinates		
 **y(cco)**	-0.66311200	-0.48797300	0.00000000	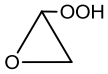 **y(cco)q**	-0.28620900	-0.12883800	0.47836300
	0.00000000	0.82323200	0.00000000		-1.60010800	-0.39323500	-0.10626500
	-1.10664200	-0.86773700	0.92028300		-0.99660000	0.91614800	-0.16648200
	-1.10664200	-0.86773700	-0.92028300		-0.11878900	0.00486800	1.54578300
	0.04293500	1.40562400	0.92025400		-2.47149700	-0.48416500	0.54047800
	0.04293500	1.40562400	-0.92025400		-1.65095100	-0.92372200	-1.05530700
	0.76326100	-0.38591600	0.00000000		0.78698900	-0.66512900	-0.20799800
					1.92785400	0.20903600	0.05017200
					1.81319500	0.85502100	-0.66907900

Species	Cartesian Coordinates			Species	Cartesian Coordinates		
 **y(ccco)**	0.00003900	1.07717800	-0.00009600	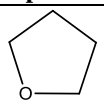 **y(cccco)**	0.73330200	0.99632700	0.22731500
	1.03691000	-0.06495400	-0.00011200		-0.73335800	0.99624200	-0.22736300
	-1.03691100	-0.06488300	0.00020300		-1.16560000	-0.43032900	0.13205300
	0.00019500	1.71030200	0.88979100		1.16563400	-0.43029300	-0.13192900
	-0.00006900	1.71001300	-0.89018900		1.34352500	1.76065200	-0.26192000
	1.67319600	-0.13074700	0.89189600		0.79568500	1.15396500	1.31001000
	1.67310600	-0.13083500	-0.89217700		-0.79571300	1.15368800	-1.31008900
	-1.67292900	-0.13062700	0.89240600		-1.34365400	1.76063200	0.26168000
	-1.67338500	-0.13071800	-0.89166600		-1.53551000	-0.48094600	1.16771200
	-0.00004300	-1.07268000	-0.00000300		-1.95041600	-0.82150300	-0.52543900
					1.95013900	-0.82147500	0.52593000
					1.53593000	-0.48100300	-1.16743600
					0.00001800	-1.25196100	-0.00011300

Species	Cartesian Coordinates			Species	Cartesian Coordinates		
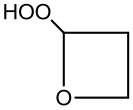 **y(ccco)q_{eth}**	1.55608600	-0.50681800	0.27110600	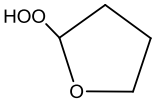 **y(cccco)q_{eth}**	-2.00376500	0.20970000	-0.14851300
	0.87306900	0.80013800	0.70853900		-0.87475300	1.23894700	0.07118600
	-0.00925300	0.58989900	-0.53560100		0.32745300	0.37845800	0.50852600
	2.59473700	-0.41147100	-0.06201800		-1.22475100	-1.09395300	-0.34037600
	1.46978100	-1.35351500	0.96061000		-2.63578000	0.13664800	0.74182000
	1.49414000	1.69743300	0.68954000		-2.64309100	0.45230900	-1.00134400
	0.31508800	0.74255600	1.64225200		-1.12210400	1.98991200	0.82420700
	0.05707100	1.33581500	-1.33877800		-0.61489800	1.76232500	-0.85350300
	0.64931200	-0.64325700	-0.86027300		0.76250600	0.61005300	1.48464300
	-1.39113700	0.44246800	-0.38532800		-0.87204700	-1.19926600	-1.37580600
	-1.63585900	-0.54328000	0.65573100		-1.77454300	-1.99531000	-0.06023700
	-1.42876200	-1.35758400	0.16309900		-0.11036100	-0.96829500	0.55842900
					1.31225200	0.55013200	-0.49535700
					2.47667100	-0.21151600	-0.08140900
					2.12636200	-1.11815700	-0.15801900

Species	Cartesian Coordinates			Species	Cartesian Coordinates		
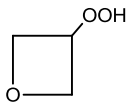 **y(ccco)q_{sec}**	0.86070800	-1.03409100	-0.06189400	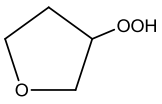 **y(cccco)q_{sec}**	-0.33402200	-0.31828000	0.56376200
	0.00186900	-0.04868000	0.75556900		0.27494600	1.08905200	0.56827600
	0.83651500	1.04559300	0.06015300		1.39665400	0.94031700	-0.46049900
	1.41539600	-1.79421100	0.50004400		0.85706800	-1.21773800	0.16324300
	0.31580000	-1.50356300	-0.88773600		-0.79366400	-0.59900700	1.51849900
	0.14926800	-0.11069700	1.83826200		0.69400500	1.30601100	1.55675300
	1.37127000	1.75174500	0.70617700		-0.46854100	1.85029100	0.32478700
	0.28022700	1.59734900	-0.70760900		0.99716400	1.01164600	-1.48349000
	1.71417300	0.04820900	-0.50754000		2.20940900	1.66249600	-0.34825300
	-1.40366000	-0.06494100	0.64080100		0.55603500	-1.86998700	-0.66899500
	-1.74634200	-0.04656000	-0.77793100		1.19096400	-1.84723700	0.99457200
	-2.23988000	0.78877900	-0.81474400		1.93291000	-0.36129600	-0.21309800
					-1.29238700	-0.49104800	-0.48732600
					-2.44621600	0.33758900	-0.16170900
					-3.10771000	-0.35627700	-0.00550600

APPENDIX T

CYCLIC ETHERS – VIBRATIONAL FREQUENCIES

Appendix T includes the frequencies of the species calculated for the study of cyclic ethers.

Table T.1 Vibrational frequencies calculated at the B3LYP/6-31G(d,p) level

System	Frequencies, cm^{-1}							
y(cco)	817.22	859.30	900.49	1041.71	1145.27	1158.52	1170.06	1180.81
	1309.77	1520.04	1559.60	3091.03	3099.03	3173.03	3188.27	
y(ccco)	62.33	770.14	815.57	843.85	933.19	948.33	1047.65	1053.52
	1152.19	1167.35	1199.93	1239.69	1269.61	1317.70	1392.43	1506.25
	1531.32	1562.25	3017.84	3029.27	3062.60			
y(cccco)	61.86	265.47	581.62	675.28	846.79	889.21	911.64	921.93
	930.90	970.88	1034.91	1109.44	1177.75	1189.12	1200.29	1260.65
	1266.08	1322.89	1351.47	1373.99	1412.18	1501.82	1512.16	1537.92
	1552.75	2985.23	3010.14	3052.65	3058.25	3067.49	3081.92	3112.87
	3121.49							
y(c˙co)	792.95	813.20	948.25	1046.50	1080.70	1128.88	1191.15	1364.77
	1540.16	3102.65	3137.38	3195.13				
y(c˙cco)	211.48	583.93	799.21	846.04	932.69	940.46	1020.04	1059.16
	1145.86	1157.38	1193.40	1252.36	1269.52	1375.48	1495.69	1532.33
	3029.36	3063.04	3075.36	3120.67	3180.65			
y(cc˙co)	199.51	232.65	851.44	870.51	917.17	943.18	1003.73	1015.23
	1089.75	1110.08	1116.83	1270.60	1298.90	1371.01	1496.84	1525.01
	2962.52	2976.46	2994.74	2994.86	3247.21			
y(c˙ccco)	171.43	243.84	492.72	606.30	731.81	864.44	882.70	923.24
	943.38	967.54	1029.00	1082.00	1192.33	1198.31	1215.96	1253.36
	1303.99	1315.31	1359.60	1409.67	1496.04	1510.25	1531.99	2990.83
	3020.50	3053.45	3071.76	3115.85	3126.43	3218.00		
y(cc˙cco)	165.20	224.50	276.71	641.95	727.81	867.01	924.75	929.29
	942.36	968.53	1025.53	1047.61	1110.60	1185.26	1197.23	1254.84
	1294.01	1323.90	1359.38	1408.93	1482.83	1507.97	1532.89	2910.12
	2971.61	2985.60	3013.28	3056.33	3107.94	3239.40		

Table T.1 Vibrational frequencies calculated at the B3LYP/6-31G(d,p) level (Continued)

System	Frequencies, cm^{-1}							
y(cco)q	118.58	265.97	325.08	469.01	577.93	815.46	860.57	913.01
	963.75	1101.05	1145.91	1158.73	1183.71	1301.95	1378.65	1411.70
	1533.08	3108.75	3160.79	3202.76	3729.94			
y(ccco)q_{eth}	101.97	174.11	273.65	362.80	450.62	639.31	741.29	819.43
	885.32	913.25	960.98	1000.41	1013.59	1110.89	1130.16	1170.30
	1226.99	1264.60	1269.67	1364.82	1391.03	1405.64	1488.88	1545.03
	3049.77	3057.54	3099.37	3109.37	3178.45	3722.57		
y(ccco)q_{sec}	92.23	163.49	231.06	293.72	392.53	582.19	688.01	868.98
	880.24	906.97	997.16	1029.51	1038.08	1126.26	1141.54	1157.76
	1185.15	1254.68	1305.97	1341.47	1368.05	1418.88	1510.05	1540.53
	3033.11	3049.76	3080.78	3095.18	3107.29	3765.52		
y(cccco)q_{eth}	75.44	147.43	226.22	278.22	388.51	426.78	586.12	615.58
	731.84	837.89	874.19	926.77	935.70	946.93	960.52	1001.33
	1049.11	1089.70	1150.22	1222.27	1233.05	1263.10	1310.79	1330.74
	1361.90	1375.60	1401.53	1417.39	1492.98	1510.85	1532.46	3025.43
	3072.71	3084.11	3099.55	3120.04	3125.97	3140.42	3701.85	
y(cccco)q_{sec}	68.70	142.82	187.58	230.91	273.55	387.88	483.02	654.52
	740.13	844.79	876.71	924.73	928.06	937.88	975.98	1009.69
	1085.76	1117.93	1153.10	1199.88	1238.72	1260.27	1303.06	1326.33
	1355.15	1372.74	1374.84	1416.51	1492.06	1517.86	1534.82	3007.99
	3022.87	3055.50	3072.87	3088.65	3113.90	3146.09	3755.07	

Table T.1 Vibrational frequencies calculated at the B3LYP/6-31G(d,p) level (Continued)

System	Frequencies, cm^{-1}							
y(cco)q$^{\cdot}$	57.84	319.64	450.66	498.37	807.60	851.03	947.96	1097.18
	1107.88	1146.96	1169.84	1197.79	1288.44	1404.67	1534.30	3115.38
	3185.57	3212.91						
y(ccco)$q_{eth}^{\cdot}$	113.89	144.28	306.76	406.70	634.78	716.62	809.05	884.98
	946.99	957.87	1036.33	1073.20	1125.20	1159.31	1172.00	1222.00
	1268.46	1286.95	1374.51	1387.33	1480.75	1536.40	3067.51	3091.70
	3110.29	3124.71	3176.86					
y(ccco)$q_{sec}^{\cdot}$	94.62	132.36	306.15	373.92	608.70	685.22	869.65	870.34
	952.14	1022.77	1038.82	1071.10	1132.70	1161.94	1170.25	1192.31
	1260.22	1310.00	1355.87	1403.50	1503.43	1530.62	3043.21	3053.29
	3102.23	3103.22	3139.49					
y(cccco)$q_{eth}^{\cdot}$	72.70	121.40	186.16	306.85	418.33	482.71	632.14	737.40
	825.98	870.89	907.23	931.06	951.89	959.69	1039.07	1114.66
	1165.03	1199.23	1209.60	1217.21	1251.49	1312.06	1334.66	1346.94
	1354.42	1414.99	1495.59	1510.36	1543.61	3052.37	3071.89	3081.90
	3109.02	3126.69	3136.35	3150.80				
y(cccco)$q_{sec}^{\cdot}$	62.59	105.94	218.08	288.92	387.36	504.42	648.70	742.49
	805.23	878.26	920.04	933.06	944.48	1006.62	1080.24	1117.51
	1132.77	1195.41	1202.19	1231.80	1255.06	1295.26	1325.85	1340.98
	1373.46	1412.70	1490.22	1518.44	1536.54	3004.58	3026.30	3077.35
	3091.21	3117.88	3128.09	3144.15				

Table T.1 Vibrational frequencies calculated at the B3LYP/6-31G(d,p) level (Continued)

System	Frequencies, cm^{-1}							
y(c˙co)q	127.51	269.63	308.22	470.01	542.46	696.71	845.62	889.51
	996.52	1071.27	1133.72	1182.38	1314.24	1369.26	1448.80	3166.43
	3187.19	3737.68						
y(c˙co)q_{eth}	140.15	185.26	281.12	346.63	448.39	579.78	646.68	758.91
	882.58	902.14	936.14	1011.41	1018.19	1088.89	1151.93	1155.25
	1236.42	1254.06	1336.85	1395.60	1401.28	1484.87	3064.01	3090.44
	3113.38	3194.78	3725.55					
y(cc˙co)q_{eth}	141.63	157.66	234.67	277.97	364.36	453.48	671.80	821.01
	892.79	936.69	941.85	966.46	969.79	1031.44	1111.36	1122.15
	1234.32	1276.58	1349.24	1372.89	1397.53	1513.43	2997.48	3025.74
	3037.90	3261.05	3728.19					
y(c˙co)q_{sec}	147.60	188.40	249.21	330.86	416.09	516.81	643.42	762.88
	872.13	905.46	936.03	996.01	1068.40	1092.80	1162.32	1166.06
	1219.63	1271.26	1338.95	1385.52	1390.94	1505.73	3049.04	3091.98
	3169.12	3195.98	3703.03					
y(c˙cco)q_{eth}	47.67	139.21	218.01	271.73	360.19	431.19	541.01	574.22
	670.61	768.68	846.37	899.97	930.24	948.99	984.15	1002.25
	1067.98	1086.56	1162.93	1207.93	1242.02	1290.56	1319.16	1349.51
	1378.88	1399.55	1410.31	1490.97	1508.00	2968.48	3082.89	3091.63
	3095.03	3143.50	3210.21	3720.95				
y(cc˙cco)q_{eth}	101.86	131.14	170.70	261.81	289.02	378.99	417.54	576.72
	749.14	781.56	835.83	926.01	943.11	945.91	962.80	978.73
	1021.49	1056.28	1095.25	1186.36	1193.24	1294.18	1311.36	1355.71
	1371.59	1399.12	1416.91	1471.12	1510.18	2958.05	2998.15	3023.79
	3065.94	3105.28	3247.06	3700.76				
y(ccc˙co)q_{eth}	100.73	138.04	196.70	269.39	346.09	388.83	447.49	583.42
	660.01	799.96	855.16	902.96	925.34	943.61	958.56	981.80
	1033.66	1044.16	1092.41	1196.02	1247.39	1294.44	1303.69	1358.79
	1367.68	1388.46	1407.30	1478.81	1530.20	2988.09	3037.77	3064.76
	3070.76	3126.01	3256.10	3715.36				

Table T.1 Vibrational frequencies calculated at the B3LYP/6-31G(d,p) level (Continued)

System	Frequencies, cm^{-1}							
	99.49	162.41	177.56	211.06	296.76	350.34	440.01	472.74
	682.63	773.03	825.24	853.90	892.97	944.13	959.12	974.56
y(c˙ccco)q$_{sec}$	1037.14	1103.05	1194.53	1219.20	1240.89	1300.45	1312.63	1328.40
	1346.03	1370.56	1432.58	1494.85	1525.48	3051.05	3063.30	3076.21
	3129.20	3150.84	3264.28	3760.67				
	92.27	135.59	155.45	208.32	257.29	341.96	405.67	521.20
	727.85	793.86	840.98	924.93	928.82	939.13	950.01	967.10
y(ccc˙co)q$_{sec}$	1038.07	1104.57	1127.34	1186.86	1249.40	1285.27	1326.84	1337.16
	1355.31	1371.43	1409.01	1501.16	1518.33	2924.81	2991.97	3013.05
	3041.00	3109.00	3254.08	3752.56				
	92.55	142.26	172.61	205.63	268.98	369.91	473.41	508.73
	757.08	801.69	854.74	881.41	926.00	962.40	969.84	975.94
y(cccc˙o)q$_{sec}$	1047.15	1110.40	1175.54	1204.38	1254.83	1263.27	1312.80	1344.95
	1365.15	1376.54	1418.76	1483.47	1514.12	2950.85	3044.33	3061.21
	3107.46	3108.88	3219.28	3756.59				

APPENDIX U

CYCLIC ETHERS – ROTATIONAL ANALYSIS

Appendix U includes the results of the rotational analysis for the cyclic ethers.

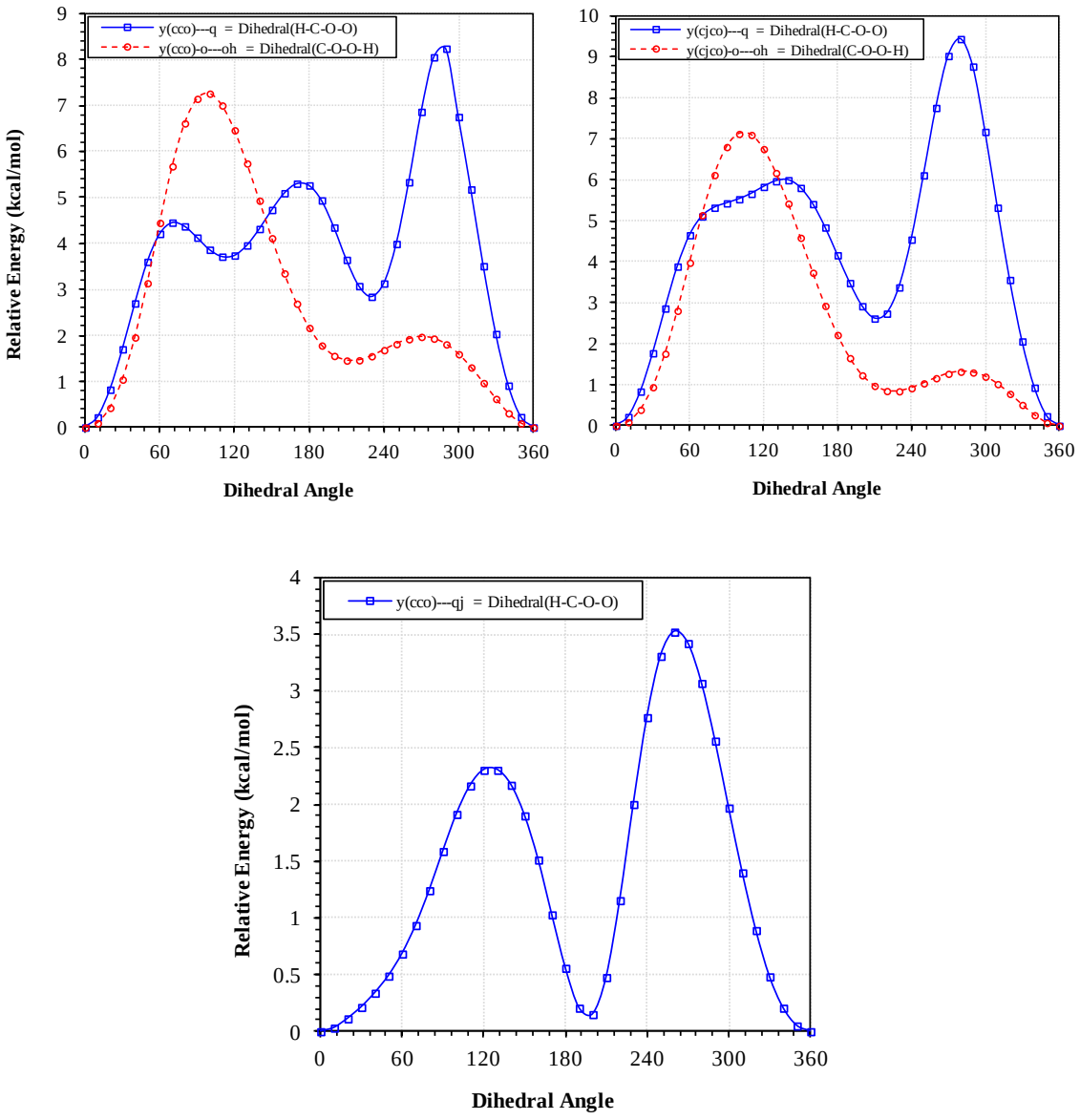

Figure U.1 Potential energy profiles for internal rotations in oxirane hydroperoxide and its derivative radicals (j=radical site)

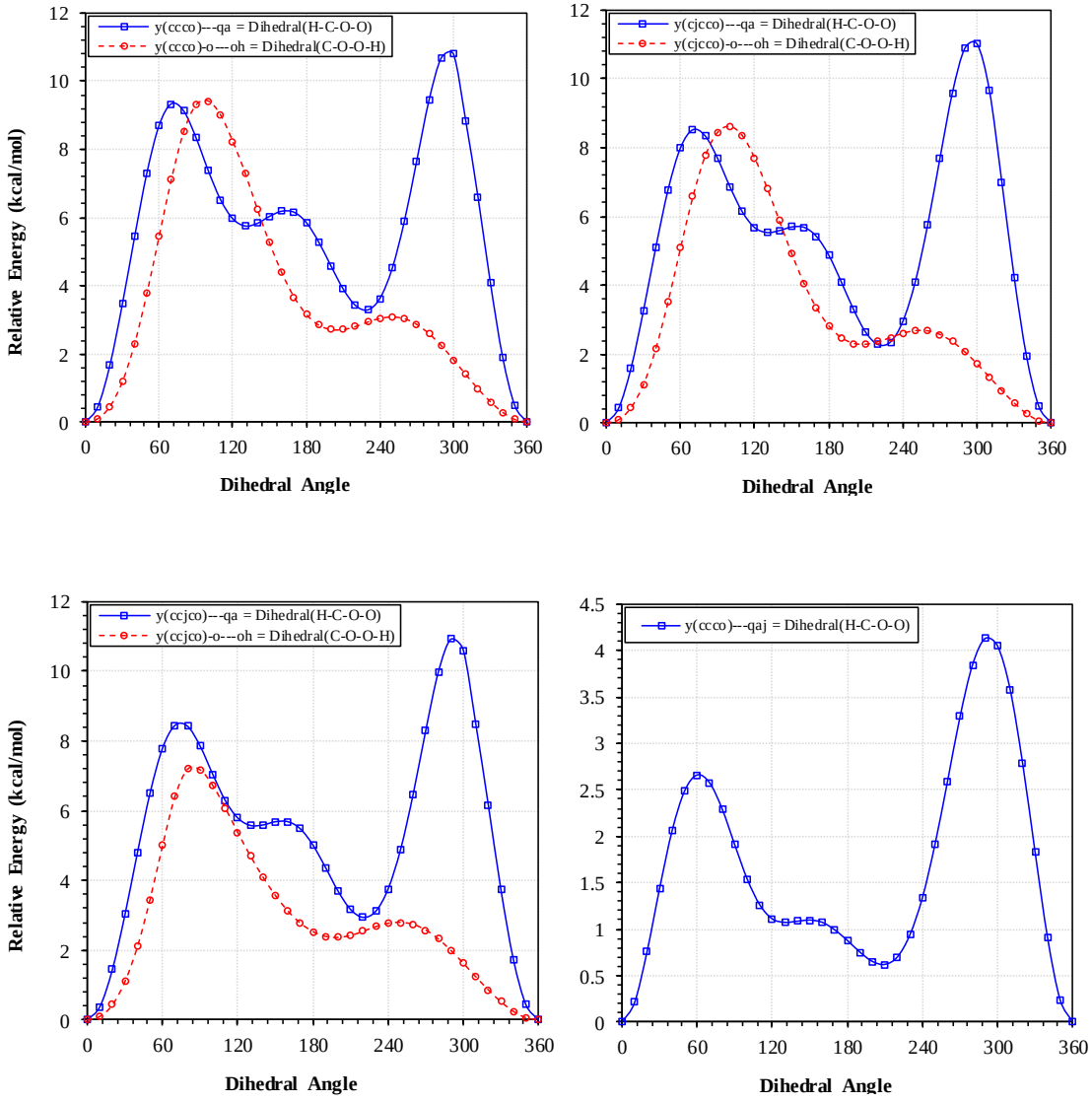

Figure U.2 Potential energy profiles for internal rotations in oxetane (a=eth) hydroperoxide and its derivative radicals (j=radical site)

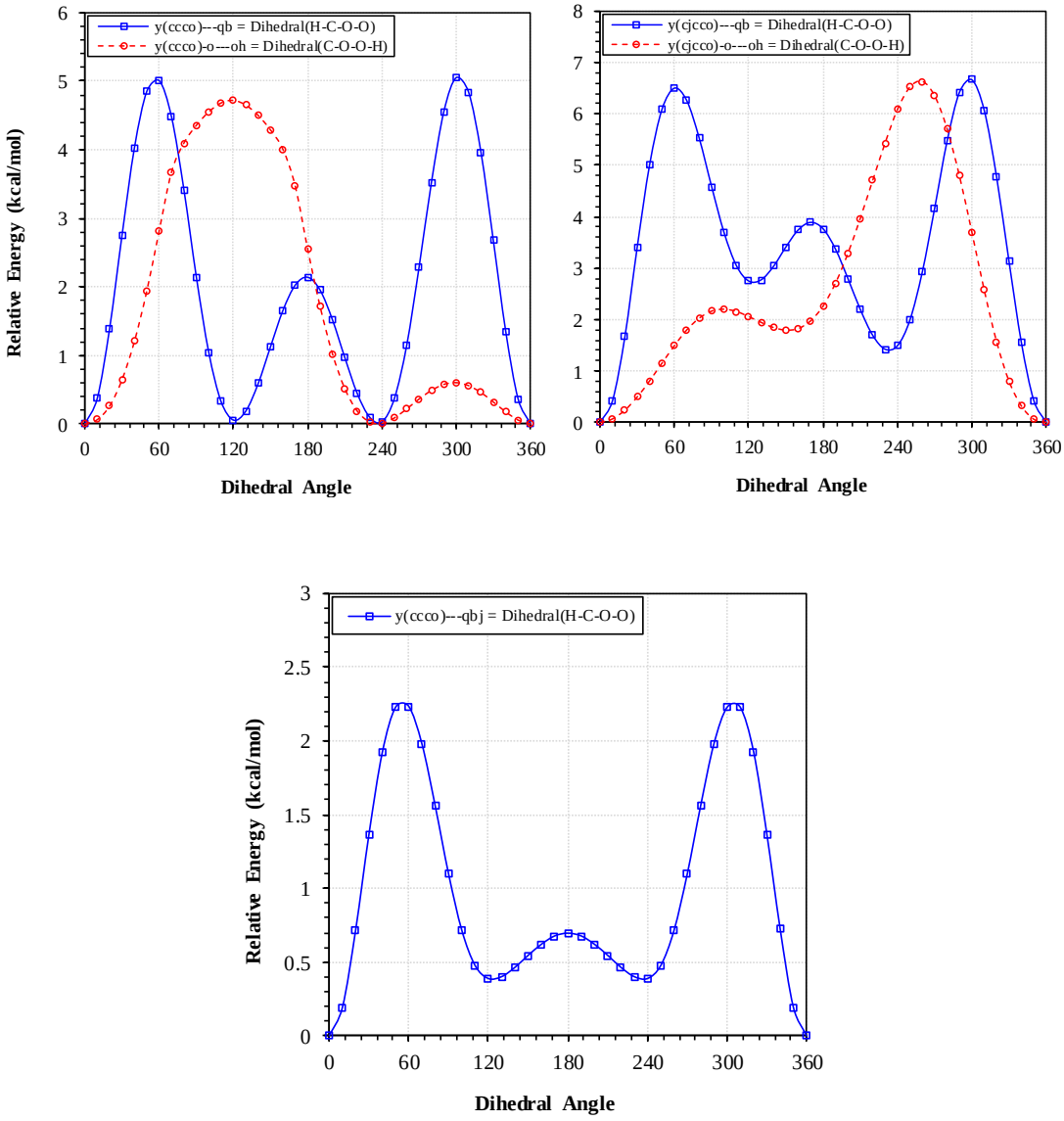

Figure U.3 Potential energy profiles for internal rotations in oxetane (b=sec) hydroperoxide and its derivative radicals (j=radical site)

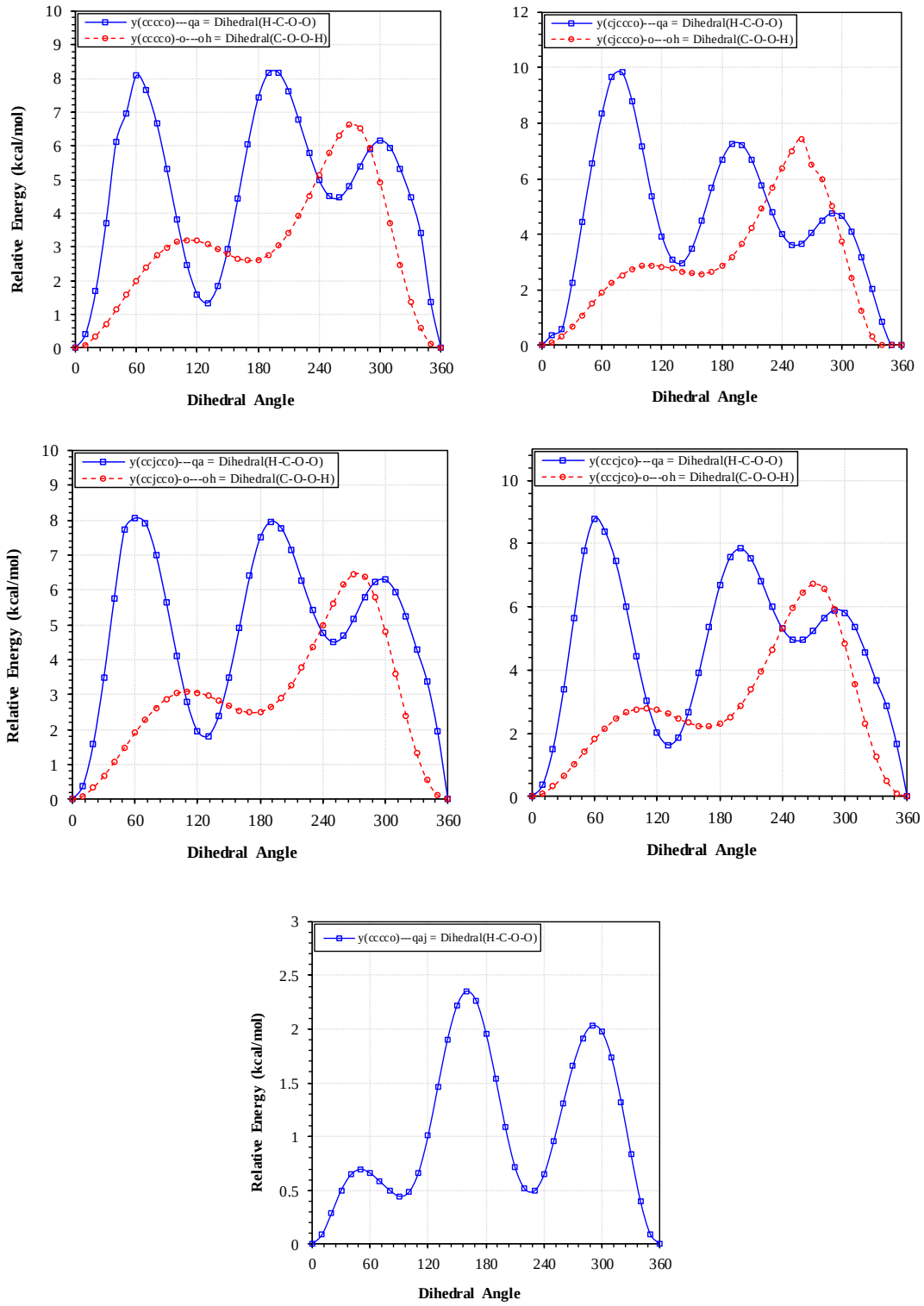

Figure U.4 Potential energy profiles for internal rotations in oxolane (a=eth) hydroperoxide and its derivative radicals (j=radical site)

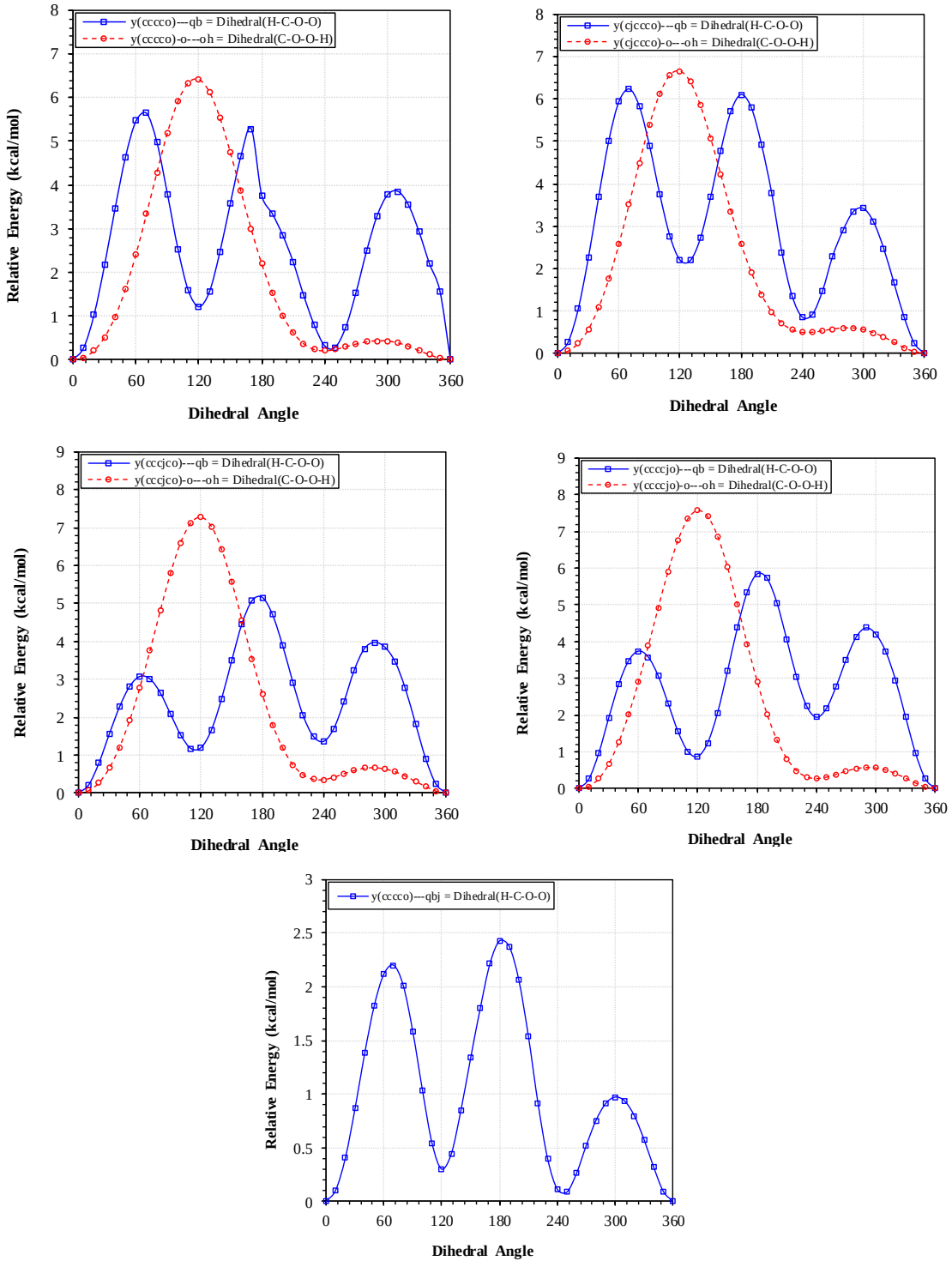

Figure U.5 Potential energy profiles for internal rotations in oxolane (b=sec) hydroperoxide and its derivative radicals (j=radical site)

APPENDIX V

CYCLIC ETHERS – WORK REACTIONS

Appendix V summarizes the work reactions used for the determination of the heat of formation of the species calculated for the study of cyclic ethers.

Table V.1 Calculated enthalpies of formation at 298 K of three member ring cyclic ethers

Work Reactions	$\Delta_f H°_{298}$					
	B3LYP					
	6-31G(d,p)	6-31G(2d,2p)	CBS-QB3	G3MP2B3	Average DFT	Average Ab initio
y(cco)						
y(cco) + ccc → y(ccc) + coc	-12.76	-12.32	-12.86	-13.01		
y(cco) + cccc → y(ccc) + cocc	-13.66	-11.71	-12.40	-12.60		
Ave.	**-13.21**	**-12.02**	***-12.63***	***-12.80***	***-12.61***	***-12.72***
y(cco)q						
y(cco)q + y(ccc) → y(cco) + y(ccc)q	-39.39	-39.28	-39.02	-39.14		
y(cco)q + y(cccc) → y(cco) + y(cccc)q	-40.56	-40.36	-39.07	-39.10		
y(cco)q + y(ccccc) → y(cco) + y(ccccc)q	-41.47	-41.29	-39.03	-39.12		
Ave.	**-40.47**	**-40.31**	***-39.04***	***-39.12***	***-40.39***	***-39.08***
y(c˙co)						
y(c˙co) + y(ccc) → y(cco) + y(c˙cc)	39.45	39.43	39.82	39.57		
y(c˙co) + y(cccc) → y(cco) + y(c˙ccc)	39.93	39.96	39.92	39.46		
y(c˙co) + y(ccccc) → y(cco) + y(c˙cccc)	38.82	38.80	39.94	39.45		
Ave.	**39.40**	**39.40**	**39.89**	**39.49**	***39.40***	***39.69***
BDE	*104.22*	*104.22*	*104.71*	*104.31*	*104.22*	*104.51*
y(cco)q˙						
y(cco)q˙ + y(ccc) → y(cco) + y(ccc)q˙	-1.39	-0.60	-0.72	-0.85		
y(cco)q˙ + y(cccc) → y(cco) + y(cccc)q˙	-0.68	-0.95	-0.94	-1.03		
y(cco)q˙ + y(ccccc) → y(cco) + y(ccccc)q˙	-0.60	-0.88	-0.48	-0.59		
Ave.	**-0.89**	**-0.81**	**-0.71**	**-0.82**	***-0.85***	***-0.77***
BDE	*90.29*	*90.37*	*90.47*	*90.36*	*90.33*	*90.41*

Units: kcal mol^{-1}

Table V.1 Calculated enthalpies of formation at 298 K of three member ring cyclic ethers (Continued)

Work Reactions	$\Delta_f H^o_{298}$					
	B3LYP					
	6-31G(d,p)	6-31G(2d,2p)	CBS-QB3	G3MP2B3	Average DFT	Average Ab initio
y(c˙co)q						
y(c˙co)q + y(ccc) → y(cco) + y(c˙cc)q	12.59	12.47	13.24	13.01		
y(c˙co)q + y(cccc) → y(cco) + y(c˙ccc)q	12.58	12.52	13.09	12.77		
y(c˙co)q + y(ccccc) → y(cco) + y(c˙cccc)q	12.81	12.47	13.60	13.18		
Ave.	**12.66**	**12.49**	**13.31**	**12.99**	***12.57***	***13.15***
BDE	*103.84*	*103.67*	*104.49*	*104.17*	*103.75*	*104.33*
y(cc˙o)q						
y(cc˙o)q + y(ccc) → y(cco) + y(c˙cc)q	14.99	14.95	15.90	15.89		
y(cc˙o)q + y(cccc) → y(cco) + y(c˙ccc)q	14.99	15.00	15.75	15.66		
y(cc˙o)q + y(ccccc) → y(cco) + y(c˙cccc)q	15.21	14.96	16.26	16.06		
Ave.	**15.06**	**14.97**	**15.97**	**15.87**	***15.02***	***15.92***
BDE	*106.24*	*106.15*	*107.15*	*107.05*	*106.20*	*107.10*

Units: kcal mol^{-1}

Table V.2 Calculated enthalpies of formation at 298 K of four member ring cyclic ethers

Work Reactions	$\Delta_f H^o_{298}$					
	B3LYP					
	6-31G(d,p)	6-31G(2d,2p)	CBS-QB3	G3MP2B3	Average DFT	Average Ab initio
y(ccco)						
y(ccco) + ccc → y(cccc) + coc	-19.32	-19.13	-19.68	-19.07		
y(ccco) + cccc → y(cccc) + cocc	-20.22	-18.52	-19.23	-18.66		
Ave.	**-19.77**	**-18.83**	**-19.46**	**-18.86**	**-19.30**	**-19.16**
y(ccco)q_{eth}						
y(ccco)q_{eth} + y(ccc) → y(ccco) + y(ccc)q	-50.95	-50.94	-50.66	-51.57		
y(ccco)q_{eth} + y(cccc) → y(ccco) + y(cccc)q	-52.11	-52.02	-50.70	-51.52		
y(ccco)q_{eth} + y(ccccc) → y(ccco) + y(ccccc)q	-53.02	-52.96	-50.67	-51.54		
Ave.	**-52.03**	**-51.98**	**-50.68**	**-51.54**	***-52.00***	***-51.11***
y(ccco)q_{sec}						
y(ccco)q_{sec} + y(ccc) → y(ccco) + y(ccc)q	-39.82	-39.88	-39.47	-40.42		
y(ccco)q_{sec} + y(cccc) → y(ccco) + y(cccc)q	-40.98	-40.96	-39.51	-40.37		
y(ccco)q_{sec} + y(ccccc) → y(ccco) + y(ccccc)q	-41.89	-41.89	-39.47	-40.39		
Ave.	**-40.90**	**-40.91**	**-39.48**	**-40.39**	***-40.90***	***-39.94***
y(c$^{\bullet}$cco)						
y(c$^{\bullet}$cco) + y(ccc) → y(ccco) + y(c$^{\bullet}$cc)	24.29	24.21	24.91	24.27		
y(c$^{\bullet}$cco) + y(cccc) → y(ccco) + y(c$^{\bullet}$ccc)	24.76	24.75	25.01	24.16		
y(c$^{\bullet}$cco) + y(ccccc) → y(ccco) + y(c$^{\bullet}$cccc)	23.65	23.59	25.03	24.15		
Ave.	**24.23**	**24.18**	**24.98**	**24.20**	***24.21***	***24.59***
BDE	*95.49*	*95.44*	*96.24*	*95.46*	*95.47*	*95.85*
y(cc$^{\bullet}$co)						
y(cc$^{\bullet}$co) + y(ccc) → y(ccco) + y(c$^{\bullet}$cc)	30.64	30.71	31.15	30.58		
y(cc$^{\bullet}$co) + y(cccc) → y(ccco) + y(c$^{\bullet}$ccc)	31.11	31.25	31.25	30.48		
y(cc$^{\bullet}$co) + y(ccccc) → y(ccco) + y(c$^{\bullet}$cccc)	30.01	30.08	31.27	30.47		
Ave.	**30.59**	**30.68**	**31.22**	**30.51**	***30.63***	***30.87***
BDE	*101.85*	*101.94*	*102.48*	*101.77*	*101.89*	*102.13*

Units: kcal mol^{-1}

Table V.2 Calculated enthalpies of formation at 298 K of four member ring cyclic ethers (Continued)

Work Reactions	$\Delta_f H^o_{298}$ B3LYP 6-31G(d,p)	B3LYP 6-31G(2d,2p)	CBS-QB3	G3MP2B3	Average DFT	Average ab-initio
y(ccco)$q_{eth}^{\bullet}$						
y(ccco)$q_{eth}^{\bullet}$ + y(ccc) → y(ccco)q_{eth} + y(ccc)$q^{\bullet}$	-13.40	-12.44	-13.21	-13.21		
y(ccco)$q_{eth}^{\bullet}$ + y(cccc) → y(ccco)q_{eth} + y(cccc)$q^{\bullet}$	-12.70	-12.79	-13.43	-13.43		
y(ccco)$q_{eth}^{\bullet}$ + y(ccccc) → y(ccco)q_{eth} + y(ccccc)$q^{\bullet}$	-12.61	-12.71	-12.97	-12.97		
Ave.	**-12.90**	**-12.65**	**-13.20**	**-13.44**	***-12.78***	***-13.32***
BDE	*90.31*	*90.56*	*90.01*	*89.77*	*90.43*	*89.89*
y(c$^{\bullet}$cco)q_{eth}						
y(c$^{\bullet}$cco)q_{eth} + y(ccc) → y(ccco)q_{eth} + y(c$^{\bullet}$cc)q	-4.57	-4.67	-4.95	-4.90		
y(c$^{\bullet}$cco)q_{eth} + y(cccc) → y(ccco)q_{eth} + y(cc$^{\bullet}$cc)q	-4.77	-4.91	-5.07	-5.19		
y(c$^{\bullet}$cco)q_{eth} + y(ccccc) → y(ccco)q_{eth} + y(cc$^{\bullet}$ccc)q	-4.65	-4.84	-4.63	-4.72		
Ave.	**-4.66**	**-4.81**	**-4.88**	**-4.93**	***-4.73***	***-4.91***
BDE	*98.55*	*98.40*	*98.33*	*98.28*	*98.48*	*98.30*
y(cc$^{\bullet}$co)q_{eth}						
y(cc$^{\bullet}$co)q_{eth} + y(ccc) → y(ccco)q_{eth} + y(c$^{\bullet}$cc)q	1.04	1.20	0.53	0.57		
y(cc$^{\bullet}$co)q_{eth} + y(cccc) → y(ccco)q_{eth} + y(c$^{\bullet}$ccc)q	1.04	1.25	0.38	0.33		
y(cc$^{\bullet}$co)q_{eth} + y(ccccc) → y(ccco)q_{eth} + y(c$^{\bullet}$cccc)q	1.26	1.20	0.89	0.74		
Ave.	**1.11**	**1.21**	**0.60**	**0.55**	***1.16***	***0.57***
BDE	*104.32*	*104.42*	*103.81*	*103.76*	*104.37*	*103.78*
y(ccco)$q_{sec}^{\bullet}$						
y(ccco)$q_{sec}^{\bullet}$ + y(ccc) → y(ccco)q_{sec} + y(ccc)$q^{\bullet}$	-5.88	-4.96	-5.44	-5.56		
y(ccco)$q_{sec}^{\bullet}$ + y(cccc) → y(ccco)q_{sec} + y(cccc)$q^{\bullet}$	-5.17	-5.31	-5.65	-5.74		
y(ccco)$q_{sec}^{\bullet}$ + y(ccccc) → y(ccco)q_{sec} + y(ccccc)$q^{\bullet}$	-5.09	-5.23	-5.20	-5.29		
Ave.	**-5.38**	**-5.17**	**-5.43**	**-5.53**	***-5.27***	***-5.48***
BDE	*86.66*	*86.87*	*86.61*	*86.51*	*86.77*	*86.56*
y(c$^{\bullet}$cco)q_{sec}						
y(c$^{\bullet}$cco)q_{sec} + y(ccc) → y(ccco)q_{sec} + y(c$^{\bullet}$cc)q	2.33	2.34	2.31	2.41		
y(c$^{\bullet}$cco)q_{sec} + y(cccc) → y(ccco)q_{sec} + y(c$^{\bullet}$ccc)q	2.32	2.39	2.15	2.18		
y(c$^{\bullet}$cco)q_{sec} + y(ccccc) → y(ccco)q_{sec} + y(c$^{\bullet}$cccc)q	2.55	2.34	2.66	2.58		
Ave.	**2.40**	**2.36**	**2.37**	**2.39**	***2.38***	***2.38***
BDE	*94.44*	*94.40*	*94.41*	*94.43*	*94.42*	*94.42*

Units: kcal mol^{-1}

Table V.3 Calculated enthalpies of formation at 298 K of five member ring cyclic ethers

Work Reactions	$\Delta_f H^o_{298}$					
	B3LYP					
	6-31G(d,p)	6-31G(2d,2p)	CBS-QB3	G3MP2B3	Average DFT	Average Ab initio
y(cccco)						
y(cccco) + ccc → y(ccccc) + coc	-44.06	-44.24	-44.53	-43.83		
y(cccco) + cccc → y(ccccc) + cocc	-44.96	-43.63	-44.08	-43.43		
Ave.	**-44.51**	**-43.93**	**-44.30**	**-43.63**	***-44.22***	***-43.97***
y(cccco)q_{eth}						
y(cccco)q_{eth} + y(ccc) → y(cccco) + y(ccc)q	-74.85	-74.33	-75.31	-75.95		
y(cccco)q_{eth} + y(cccc) → y(cccco) + y(cccc)q	-76.02	-75.41	-75.36	-75.90		
y(cccco)q_{eth} + y(ccccc) → y(cccco) + y(ccccc)q	-76.92	-76.35	-75.32	-75.92		
Ave.	**-75.93**	**-75.36**	**-75.33**	**-75.93**	***-75.65***	***-75.63***
y(cccco)q_{sec}						
y(cccco)q_{sec} + y(ccc) → y(cccco) + y(ccc)q	-65.32	-64.95	-66.15	-66.85		
y(cccco)q_{sec} + y(cccc) → y(cccco) + y(cccc)q	-66.49	-66.03	-66.20	-66.81		
y(cccco)q_{sec} + y(ccccc) → y(cccco) + y(ccccc)q	-67.39	-66.96	-66.16	-66.82		
Ave.	**-66.40**	**-65.98**	**-66.17**	**-66.83**	***-66.19***	***-66.50***
y(c˙cco)						
y(c˙cco) + y(ccc) → y(cccco) + y(c˙cc)	-2.47	-2.12	-1.76	-2.14		
y(c˙cco) + y(cccc) → y(cccco) + y(c˙ccc)	-2.00	-1.58	-1.67	-2.25		
y(c˙cco) + y(ccccc) → y(cccco) + y(c˙cccc)	-3.10	-2.75	-1.65	-2.25		
Ave.	**-2.52**	**-2.15**	**-1.69**	**-2.21**	***-2.34***	***-1.95***
BDE	*93.55*	*93.92*	*94.38*	*93.86*	*93.73*	*94.12*
y(cc˙cco)						
y(cc˙cco) + y(ccc) → y(cccco) + y(c˙cc)	2.23	2.59	2.72	2.32		
y(cc˙cco) + y(cccc) → y(cccco) + y(c˙ccc)	2.70	3.13	2.81	2.21		
y(cc˙cco) + y(ccccc) → y(cccco) + y(c˙cccc)	1.59	1.97	2.83	2.20		
Ave.	**2.17**	**2.56**	**2.79**	**2.24**	***2.37***	***2.52***
BDE	*98.24*	*98.63*	*98.86*	*98.31*	*98.44*	*98.59*

Units: kcal mol^{-1}

Table V.3 Calculated enthalpies of formation at 298 K of five member ring cyclic ethers (Continued)

Work Reactions	$\Delta_f H^o_{298}$ B3LYP 6-31G(d,p)	B3LYP 6-31G(2d,2p)	CBS-QB3	G3MP2B3	Average DFT	Average ab-initio
y(cccco)$q_{eth}^{\bullet}$						
y(cccco)$q_{eth}^{\bullet}$ + y(ccc) → y(ccccо)q_{eth} + y(ccc)$q^{\bullet}$	-39.47	-38.64	-39.06	-39.19		
y(cccco)$q_{eth}^{\bullet}$ + y(cccc) → y(ccccо)q_{eth} + y(cccc)$q^{\bullet}$	-38.76	-38.99	-39.27	-39.37		
y(cccco)$q_{eth}^{\bullet}$ + y(ccccc) → y(ccccо)q_{eth} + y(ccccc)$q^{\bullet}$	-38.68	-38.91	-38.81	-38.92		
Ave.	**-38.97**	**-38.85**	**-39.05**	**-39.16**	***-38.91***	***-39.10***
BDE	*88.76*	*88.88*	*88.68*	*88.57*	*88.82*	*88.63*
y(c$^{\bullet}$ccco)q_{eth}						
y(c$^{\bullet}$ccco)q_{eth} + y(ccc) → y(ccccо)q_{eth} + y(c$^{\bullet}$cc)q	-31.00	-31.14	-30.76	-30.75		
y(c$^{\bullet}$ccco)q_{eth} + y(cccc) → y(ccccо)q_{eth} + y(cc$^{\bullet}$cc)q	-31.20	-31.39	-30.88	-31.04		
y(c$^{\bullet}$ccco)q_{eth} + y(ccccc) → y(ccccо)q_{eth} + y(cc$^{\bullet}$ccc)q	-31.08	-31.32	-30.44	-30.57		
Ave.	**-31.09**	**-31.28**	**-30.69**	**-30.79**	***-31.19***	***-30.74***
BDE	*96.64*	*96.45*	*97.04*	*96.94*	*96.54*	*96.99*
y(cc$^{\bullet}$cco)q_{eth}						
y(cc$^{\bullet}$cco)q_{eth} + y(ccc) → y(ccccо)q_{eth} + y(c$^{\bullet}$cc)q	-28.57	-28.53	-28.69	-28.61		
y(cc$^{\bullet}$cco)q_{eth} + y(cccc) → y(ccccо)q_{eth} + y(cc$^{\bullet}$cc)q	-28.58	-28.48	-28.84	-28.85		
y(cc$^{\bullet}$cco)q_{eth} + y(ccccc) → y(ccccо)q_{eth} + y(cc$^{\bullet}$ccc)q	-28.35	-28.52	-28.33	-28.45		
Ave.	**-28.50**	**-28.51**	**-28.62**	**-28.63**	***-28.50***	***-28.63***
BDE	*99.23*	*99.22*	*99.11*	*99.10*	*99.23*	*99.10*
y(ccc$^{\bullet}$co)q_{eth}						
y(ccc$^{\bullet}$co)q_{eth} + y(ccc) → y(ccccо)q_{eth} + y(c$^{\bullet}$cc)q	-27.95	-27.76	-27.95	-27.85		
y(ccc$^{\bullet}$co)q_{eth} + y(cccc) → y(ccccо)q_{eth} + y(c$^{\bullet}$ccc)q	-28.15	-28.01	-28.06	-28.14		
y(ccc$^{\bullet}$co)q_{eth} + y(ccccc) → y(ccccо)q_{eth} + y(c$^{\bullet}$cccc)q	-28.03	-27.94	-27.62	-27.67		
Ave.	**-28.05**	**-27.90**	**-27.88**	**-27.89**	***-27.97***	***-27.88***
BDE	*99.68*	*99.83*	*99.85*	*99.84*	*99.76*	*99.85*

Units: kcal mol^{-1}

Table V.3 Calculated enthalpies of formation at 298 K of five member ring cyclic ethers (Continued)

Work Reactions	$\Delta_f H^o_{298}$					
	B3LYP					
	6-31G(d,p)	6-31G(2d,2p)	CBS-QB3	G3MP2B3	Average DFT	Average Ab initio
y(cccco)$q_{sec}^{\bullet}$						
y(cccco)$q_{sec}^{\bullet}$ + y(ccc) → y(ccccо)q_{sec} + y(ccc)$q^{\bullet}$	-33.05	-32.03	-32.33	-32.39		
y(cccco)$q_{sec}^{\bullet}$ + y(cccc) → y(ccccо)q_{sec} + y(cccc)$q^{\bullet}$	-32.35	-32.38	-32.54	-32.57		
y(cccco)$q_{sec}^{\bullet}$ + y(ccccc) → y(ccccо)q_{sec} + y(ccccc)$q^{\bullet}$	-32.26	-32.31	-32.09	-32.13		
Ave.	**-32.56**	**-32.24**	**-32.32**	**-32.36**	***-32.40***	***-32.34***
BDE	*86.04*	*86.36*	*86.28*	*86.24*	*86.20*	*86.26*
y(c$^{\bullet}$ccco)q_{sec}						
y(c$^{\bullet}$ccco)q_{sec} + y(ccc) → y(ccccо)q_b + y(c$^{\bullet}$cc)q	-26.74	-26.57	-26.26	-26.00		
y(c$^{\bullet}$ccco)q_{sec} + y(cccc) → y(ccccо)q_b + y(c$^{\bullet}$ccc)q	-26.74	-26.52	-26.42	-26.23		
y(c$^{\bullet}$ccco)q_{sec} + y(ccccc) → y(ccccо)q_b + y(c$^{\bullet}$cccc)q	-26.52	-26.56	-25.91	-25.83		
Ave.	**-26.66**	**-26.55**	**-26.20**	**-26.02**	***-26.61***	***-26.11***
BDE	*91.94*	*92.05*	*92.40*	*92.58*	*91.99*	*92.49*
y(ccc$^{\bullet}$co)q_{sec}						
y(ccc$^{\bullet}$co)q_{sec} + y(ccc) → y(ccccо)q_{sec} + y(c$^{\bullet}$cc)q	-17.79	-17.91	-17.72	-17.67		
y(ccc$^{\bullet}$co)q_{sec} + y(cccc) → y(ccccо)q_{sec} + y(c$^{\bullet}$ccc)q	-17.79	-17.86	-17.87	-17.91		
y(ccc$^{\bullet}$co)q_{sec} + y(ccccc) → y(ccccо)q_{sec} + y(c$^{\bullet}$cccc)q	-17.57	-17.90	-17.36	-17.51		
Ave.	**-17.72**	**-17.89**	**-17.65**	**-17.70**	***-17.80***	***-17.67***
BDE	*100.88*	*100.71*	*100.95*	*100.90*	*100.80*	*100.93*
y(cccc$^{\bullet}$o)q_{sec}						
y(cccc$^{\bullet}$o)q_{sec} + y(ccc) → y(ccccо)q_{sec} + y(c$^{\bullet}$cc)q	-23.27	-23.47	-23.19	-23.15		
y(cccc$^{\bullet}$o)q_{sec} + y(cccc) → y(ccccо)q_{sec} + y(cc$^{\bullet}$cc)q	-23.48	-23.71	-23.31	-23.44		
y(cccc$^{\bullet}$o)q_{sec} + y(ccccc) → y(ccccо)q_{sec} + y(cc$^{\bullet}$ccc)q	-23.36	-23.64	-22.86	-22.97		
Ave.	**-23.37**	**-23.61**	**-23.12**	**-23.18**	***-23.49***	***-23.15***
BDE	*95.23*	*94.99*	*95.48*	*95.42*	*95.11*	*95.45*

Units: kcal mol^{-1}

APPENDIX W

CYCLIC ETHERS – ENTROPY AND HEAT CAPACITY

Appendix W includes the entropy *(S)* and heat capacity *(Cp)* versus temperature for the species calculated for the study of cyclic ethers.

Table W.1 Entropy *(S)* and heat capacity *(Cp) vs.* temperature

T(K)	y(cco)		y(ccco)		y(cccco)		y(c•co)		y(c•cco)	
	$S^O(T)$	Cp(T)	$S^O(T)$	Cp(T)	$S^O(T)$	Cp(T)	$S^O(T)$	Cp(T)	$S^O(T)$	Cp(T)
5	26.01	7.95	28.94	7.95	31.15	7.95	27.04	7.95	30.08	7.95
50	44.31	7.95	47.25	7.95	49.46	8.01	45.34	7.95	48.38	7.95
100	49.82	7.95	52.76	7.96	55.18	8.66	50.85	7.95	53.89	7.99
150	53.05	8.04	56.01	8.18	58.87	9.69	54.09	8.04	57.18	8.35
200	55.41	8.45	58.46	9.06	61.87	11.38	56.45	8.44	59.70	9.37
250	57.38	9.33	60.64	10.72	64.65	13.90	58.41	9.25	61.96	11.06
298	59.11	10.54	62.70	12.87	67.34	16.90	60.11	10.30	64.07	13.11
400	59.19	10.60	62.78	12.97	67.45	17.03	60.18	10.35	64.16	13.20
500	62.63	13.57	67.19	18.06	73.27	23.90	63.49	12.83	68.58	17.83
600	65.96	16.42	71.73	22.78	79.29	30.29	66.60	15.12	73.01	22.02
700	69.17	18.86	76.24	26.71	85.29	35.71	69.53	17.04	77.33	25.48
800	72.23	20.91	80.59	29.88	91.14	40.25	72.27	18.62	81.47	28.33
900	75.13	22.64	84.75	32.43	96.76	44.07	74.85	19.94	85.41	30.70
1000	77.88	24.13	88.69	34.52	102.13	47.32	77.26	21.07	89.14	32.71
1100	80.49	25.41	92.41	36.23	107.26	50.10	79.53	22.04	92.67	34.42
1200	82.96	26.52	95.93	37.65	112.14	52.48	81.67	22.87	96.02	35.88
1300	85.31	27.49	99.25	38.84	116.79	54.54	83.69	23.60	99.19	37.15
1400	87.54	28.33	102.40	39.84	121.23	56.32	85.60	24.23	102.21	38.24
1500	89.67	29.06	105.38	40.70	125.45	57.86	87.41	24.78	105.07	39.19
2000	91.69	29.71	108.21	41.42	129.49	59.20	89.14	25.26	107.80	40.02
2500	100.57	31.92	120.49	43.84	147.20	63.77	96.65	26.92	119.74	42.85
3000	107.84	33.15	130.42	45.11	161.72	66.28	102.77	27.85	129.48	44.41
3500	113.95	33.89	138.72	45.85	173.94	67.77	107.90	28.40	137.66	45.34
4000	119.21	34.36	145.82	46.32	184.46	68.71	112.30	28.75	144.70	45.93
4500	123.82	34.67	152.03	46.63	193.68	69.35	116.15	28.99	150.86	46.32
5000	127.91	34.89	157.53	46.85	201.87	69.79	119.58	29.15	156.33	46.60

Units: S(cal mol^{-1}) , Cp(cal mol^{-1} K^{-1})

Table W.1 Entropy *(S)* and heat capacity *(Cp) vs.* temperature (Continued)

T(K)	y(cc•co)		y(c•ccco)		y(cc•cco)		y(cco)q		y(ccco)q_{eth}	
	S^O(T)	Cp(T)	S^O(T)	Cp(T)	S^O(T)	Cp(T)	S^O(T)	Cp(T)	S^O(T)	Cp(T)
5	30.08	7.95	32.37	7.95	32.37	7.95	31.38	7.95	33.01	7.95
50	48.40	8.06	50.69	8.04	50.70	8.12	50.22	9.39	51.59	8.82
100	54.20	8.80	56.47	8.85	56.71	9.48	57.37	11.42	58.44	11.32
150	57.89	9.44	60.27	10.08	60.81	10.86	62.41	13.61	63.52	13.95
200	60.72	10.40	63.41	11.93	64.16	12.61	66.64	15.96	67.91	16.83
250	63.20	11.97	66.32	14.46	67.21	15.02	70.45	18.41	72.01	20.18
298	65.45	13.91	69.10	17.34	70.07	17.81	73.89	20.84	75.85	23.71
400	65.55	14.00	69.21	17.47	70.19	17.93	74.03	20.94	76.01	23.86
500	70.17	18.46	75.09	23.82	76.19	24.18	80.72	25.76	83.86	31.08
600	74.73	22.53	81.03	29.56	82.20	29.87	86.89	29.61	91.46	37.15
700	79.14	25.92	86.84	34.36	88.07	34.65	92.55	32.44	98.66	41.85
800	83.35	28.72	92.44	38.34	93.71	38.61	97.71	34.54	105.38	45.44
900	87.33	31.05	97.77	41.66	99.08	41.93	102.42	36.15	111.63	48.22
1000	91.10	33.03	102.84	44.48	104.18	44.74	106.75	37.46	117.43	50.44
1100	94.67	34.72	107.65	46.89	109.01	47.14	110.76	38.57	122.84	52.25
1200	98.04	36.17	112.21	48.96	113.60	49.20	114.47	39.51	127.89	53.77
1300	101.24	37.41	116.54	50.74	117.95	50.97	117.95	40.33	132.62	55.05
1400	104.28	38.49	120.66	52.29	122.09	52.50	121.20	41.05	137.06	56.14
1500	107.16	39.42	124.58	53.62	126.03	53.83	124.26	41.68	141.26	57.09
2000	109.91	40.23	128.32	54.79	129.78	54.98	127.16	42.24	145.22	57.91
2500	121.89	43.00	144.68	58.78	146.18	58.91	139.60	44.19	162.30	60.72
3000	131.66	44.51	158.05	60.96	159.58	61.06	149.58	45.29	176.03	62.28
3500	139.86	45.41	169.28	62.27	170.83	62.34	157.90	45.96	187.47	63.21
4000	146.91	45.98	178.94	63.10	180.50	63.15	165.02	46.39	197.26	63.80
4500	153.07	46.37	187.41	63.65	188.97	63.70	171.24	46.68	205.80	64.20
5000	158.55	46.64	194.93	64.04	196.50	64.08	176.75	46.89	213.38	64.48

Units: S(cal mol^{-1}) , Cp(cal mol^{-1} K^{-1})

Table W.1 Entropy *(S)* and heat capacity *(Cp) vs.* temperature (Continued)

T(K)	y(ccco)q_{sec}		y(cccco)q_{eth}		y(cccco)q_{sec}		y(cco)$q^{\cdot}$		y(ccco)$q_{eth}^{\cdot}$	
	S^{O}(T)	Cp(T)	S^{O}(T)	Cp(T)	S^{O}(T)	Cp(T)	S^{O}(T)	Cp(T)	S^{O}(T)	Cp(T)
5	34.34	10.06	34.55	7.95	34.64	7.95	32.59	7.95	34.25	7.95
50	55.83	9.86	53.30	9.47	55.53	12.13	50.90	7.97	53.36	10.12
100	63.49	12.54	61.13	13.57	65.19	16.04	56.55	8.59	61.66	13.94
150	69.02	14.86	67.33	17.25	72.30	19.19	60.28	9.94	67.66	15.59
200	73.60	17.21	72.79	21.01	78.23	22.31	63.35	11.57	72.32	17.01
250	77.72	19.91	77.91	25.24	83.57	25.84	66.12	13.45	76.32	19.05
298	81.46	22.81	82.71	29.62	88.41	29.58	68.65	15.41	79.86	21.50
400	81.61	22.94	82.90	29.81	88.61	29.73	68.75	15.49	80.01	21.61
500	89.05	29.13	92.71	38.83	98.23	37.62	73.76	19.54	86.96	27.13
600	96.14	34.59	102.21	46.51	107.38	44.55	78.49	23.01	93.55	32.09
700	102.84	39.03	111.24	52.59	116.00	50.22	82.94	25.80	99.76	36.16
800	109.12	42.60	119.71	57.33	124.09	54.84	87.08	28.02	105.59	39.46
900	115.00	45.52	127.60	61.09	131.66	58.65	90.94	29.82	111.03	42.17
1000	120.50	47.94	134.97	64.13	138.75	61.85	94.54	31.30	116.13	44.43
1100	125.66	49.98	141.86	66.65	145.40	64.56	97.90	32.55	120.90	46.34
1200	130.50	51.72	148.31	68.78	151.66	66.88	101.05	33.60	125.39	47.96
1300	135.06	53.21	154.36	70.58	157.56	68.87	104.01	34.49	129.62	49.34
1400	139.37	54.49	160.07	72.13	163.14	70.60	106.80	35.26	133.62	50.53
1500	143.45	55.61	165.46	73.47	168.42	72.09	109.43	35.92	137.40	51.56
2000	147.31	56.57	170.57	74.63	173.44	73.39	111.93	36.49	140.99	52.45
2500	164.08	59.89	192.63	78.61	195.22	77.84	122.72	38.44	156.53	55.49
3000	177.66	61.71	210.43	80.81	212.87	80.29	131.42	39.50	169.10	57.14
3500	189.01	62.80	225.28	82.12	227.65	81.75	138.68	40.13	179.61	58.12
4000	198.74	63.49	238.00	82.95	240.32	82.68	144.90	40.53	188.62	58.75
4500	207.25	63.96	249.12	83.51	251.40	83.29	150.33	40.80	196.49	59.16
5000	214.80	64.28	258.98	83.90	261.24	83.72	155.14	40.99	203.48	59.46

Units: S(cal mol^{-1}) , Cp(cal mol^{-1} K^{-1})

Table W.1 Entropy *(S)* and heat capacity *(Cp) vs.* temperature (Continued)

T(K)	y(ccco)$q_{sec}^{\bullet}$		y(cccco)$q_{eth}^{\bullet}$		y(cccco)$q_{sec}^{\bullet}$		y(c$^{\bullet}$co)q		y(c$^{\bullet}$cco)q_{eth}	
	S^{O}(T)	Cp(T)	S^{O}(T)	Cp(T)	S^{O}(T)	Cp(T)	S^{O}(T)	Cp(T)	S^{O}(T)	Cp(T)
5	34.37	7.95	35.84	7.95	35.91	8.02	32.63	7.95	34.28	7.95
50	54.60	12.51	55.12	10.62	57.26	11.38	51.54	9.36	52.95	9.16
100	63.82	13.53	64.04	15.28	65.97	13.95	58.85	12.09	60.31	12.53
150	69.41	14.28	70.72	17.62	72.04	16.17	64.19	14.31	66.02	15.88
200	73.72	15.92	76.06	19.73	77.02	18.69	68.56	16.19	71.06	19.37
250	77.50	18.21	80.74	22.52	81.50	21.78	72.38	18.19	75.76	23.03
298	80.91	20.80	84.96	25.75	85.60	25.17	75.74	20.22	80.10	26.52
400	81.05	20.92	85.13	25.89	85.77	25.31	75.87	20.31	80.28	26.66
500	87.83	26.58	93.55	33.10	94.04	32.66	82.28	24.41	88.85	33.11
600	94.31	31.63	101.63	39.61	102.04	39.26	88.09	27.75	96.79	38.14
700	100.44	35.78	109.34	45.02	109.69	44.73	93.38	30.23	104.08	41.93
800	106.21	39.14	116.61	49.45	116.92	49.21	98.18	32.06	110.77	44.82
900	111.61	41.91	123.45	53.11	123.73	52.92	102.55	33.43	116.90	47.09
1000	116.68	44.22	129.88	56.19	130.14	56.03	106.54	34.49	122.55	48.92
1100	121.44	46.16	135.93	58.79	136.18	58.66	110.22	35.35	127.78	50.43
1200	125.91	47.81	141.63	61.01	141.87	60.91	113.62	36.07	132.64	51.70
1300	130.13	49.22	147.02	62.91	147.25	62.83	116.79	36.67	137.19	52.79
1400	134.12	50.43	152.12	64.56	152.34	64.49	119.74	37.19	141.45	53.71
1500	137.89	51.48	156.95	65.97	157.17	65.92	122.51	37.63	145.45	54.51
2000	141.47	52.38	161.54	67.20	161.76	67.16	125.12	38.02	149.24	55.21
2500	157.00	55.45	181.50	71.40	181.71	71.38	136.26	39.37	165.47	57.58
3000	169.57	57.12	197.70	73.69	197.90	73.68	145.13	40.12	178.47	58.88
3500	180.07	58.11	211.26	75.05	211.46	75.04	152.49	40.57	189.28	59.66
4000	189.08	58.74	222.90	75.91	223.10	75.91	158.76	40.86	198.51	60.15
4500	196.95	59.16	233.07	76.49	233.27	76.49	164.23	41.06	206.56	60.47
5000	203.93	59.45	242.11	76.90	242.31	76.89	169.08	41.19	213.70	60.70

Units: S(cal mol^{-1}) , Cp(cal mol^{-1} K^{-1})

Table W.1 Entropy *(S)* and heat capacity *(Cp) vs.* temperature (Continued)

T(K)	y(cc•co)q_{eth}		y(c•cco)q_{sec}		y(c•ccco)q_{eth}		y(cc•cco)q_{eth}		y(ccc•co)q_{eth}	
	S^O(T)	Cp(T)	S^O(T)	Cp(T)	S^O(T)	Cp(T)	S^O(T)	Cp(T)	S^O(T)	Cp(T)
5	34.27	7.95	34.39	7.95	35.87	7.95	35.82	7.95	35.84	7.95
50	53.02	9.43	53.06	9.17	55.39	10.30	55.54	10.24	54.57	9.48
100	60.78	13.41	60.50	12.79	63.66	14.04	63.88	14.51	62.52	14.11
150	66.87	16.85	66.35	16.27	70.03	17.62	70.60	18.93	69.12	18.74
200	72.16	20.13	71.50	19.75	75.59	21.39	76.62	23.18	75.12	23.30
250	77.02	23.61	76.28	23.35	80.80	25.60	82.24	27.47	80.80	27.81
298	81.45	27.01	80.67	26.77	85.65	29.88	87.42	31.58	86.04	32.00
400	81.63	27.15	80.85	26.91	85.85	30.06	87.62	31.75	86.25	32.17
500	90.34	33.62	89.47	33.25	95.67	38.57	97.85	39.61	96.59	39.98
600	98.40	38.72	97.44	38.22	105.04	45.51	107.38	45.97	106.20	46.28
700	105.80	42.52	104.74	41.97	113.82	50.81	116.20	50.91	115.08	51.18
800	112.57	45.37	111.43	44.84	121.95	54.85	124.34	54.78	123.26	55.02
900	118.78	47.57	117.56	47.10	129.48	58.04	131.86	57.89	130.80	58.11
1000	124.48	49.32	123.21	48.92	136.47	60.63	138.82	60.46	137.79	60.65
1100	129.75	50.76	128.44	50.43	142.96	62.80	145.30	62.61	144.29	62.78
1200	134.64	51.97	133.31	51.70	149.03	64.63	151.35	64.45	150.35	64.60
1300	139.20	52.99	137.85	52.78	154.72	66.20	157.02	66.04	156.04	66.16
1400	143.48	53.87	142.11	53.70	160.07	67.56	162.36	67.40	161.38	67.52
1500	147.50	54.63	146.12	54.51	165.12	68.73	167.40	68.59	166.43	68.69
2000	151.29	55.30	149.90	55.20	169.89	69.76	172.16	69.63	171.20	69.72
2500	167.53	57.58	166.13	57.57	190.49	73.31	192.73	73.21	191.78	73.26
3000	180.53	58.86	179.13	58.88	207.07	75.28	209.29	75.21	208.36	75.24
3500	191.33	59.63	189.94	59.65	220.91	76.46	223.11	76.41	222.18	76.42
4000	200.56	60.12	199.17	60.14	232.75	77.21	234.95	77.17	234.02	77.18
4500	208.61	60.45	207.22	60.47	243.09	77.72	245.29	77.68	244.36	77.69
5000	215.74	60.68	214.36	60.70	252.27	78.07	254.46	78.03	253.53	78.04

Units: S(cal mol^{-1}) , Cp(cal mol^{-1} K^{-1})

Table W.1 Entropy *(S)* and heat capacity *(Cp) vs.* temperature (Continued)

T(K)	y(c•ccco)q_{sec}		y(ccc•co)q_{sec}		y(cccc•o)q_{sec}	
	S^O(T)	Cp(T)	S^O(T)	Cp(T)	S^O(T)	Cp(T)
5	35.92	7.95	35.95	7.95	35.91	7.95
50	55.46	10.44	54.80	9.93	54.66	9.67
100	64.10	15.02	63.35	15.31	62.95	14.80
150	70.95	18.94	70.44	19.90	69.79	19.19
200	76.90	22.70	76.75	24.20	75.88	23.43
250	82.39	26.79	82.60	28.47	81.57	27.79
298	87.44	30.94	87.93	32.47	86.80	31.98
400	87.64	31.11	88.15	32.64	87.01	32.15
500	97.73	39.36	98.59	40.23	97.37	40.15
600	107.25	46.10	108.24	46.43	107.03	46.59
700	116.12	51.25	117.14	51.29	115.97	51.53
800	124.32	55.18	125.33	55.12	124.20	55.34
900	131.89	58.29	132.89	58.20	131.79	58.38
1000	138.90	60.82	139.89	60.74	138.80	60.86
1100	145.41	62.93	146.40	62.88	145.32	62.94
1200	151.49	64.73	152.47	64.70	151.40	64.71
1300	157.19	66.27	158.17	66.26	157.09	66.24
1400	162.54	67.61	163.52	67.61	162.44	67.57
1500	167.59	68.77	168.57	68.78	167.49	68.72
2000	172.37	69.78	173.35	69.80	172.26	69.73
2500	192.97	73.30	193.95	73.32	192.84	73.24
3000	209.55	75.27	210.54	75.28	209.41	75.21
3500	223.38	76.45	224.38	76.46	223.23	76.40
4000	235.22	77.20	236.22	77.21	235.07	77.16
4500	245.56	77.71	246.56	77.71	245.41	77.67
5000	254.74	78.06	255.74	78.06	254.58	78.03

Units: S(cal mol^{-1}) , Cp(cal mol^{-1} K^{-1})

APPENDIX X

CYCLIC ETHERS – GROUPS DEVELOPED

Appendix X includes a summary of the groups used for the determination of the thermochemical properties of cyclic ethers by the use of the group additivity method.

Table X.1 Groups included for the determination of oxirane and its derivatives

Three membered ring								
 **y(cco)**	c/c/h2/o	2	 **y(c˙co)**	c/c/h2/o	2			
	o/c2	1		o/c2	1			
	cy/c2o	1		***cy/c2o***	1			
				cy/cj2o	1			
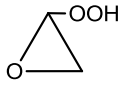 **y(cco)q**	c/c/h2/o	1	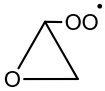 **y(cco)q˙**	c/c/h2/o	1	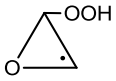 **y(c˙co)q**	c/c/h2/o	1
	c/c/h/o2	1		c/c/h/o2	1		c/c/h/o2	1
	o/c2	1		o/c2	1		o/c2	1
	o/c/o	1		o/c/o	1		o/c/o	1
	o/h/o	1		o/h/o	1		o/h/o	1
	cy/c2o/q	1		***cy/c2o/q***	1		***cy/c2o/q***	1
				cy/c2o/qj	1		***cy/cj2o/q***	1

(j=radical site)

Table X.2 Groups included for the determination of oxetane and its derivatives

Four membered ring								
 **y(ccco)**	c/c2/h2/o	2	 **y(c˙cco)**	c/c2/h2/o	2	 **y(cc˙co)**	c/c2/h2/o	2
	c/c2/h2	1		c/c2/h2	1		c/c2/h2	1
	o/c2	1		o/c2	1		o/c2	1
	cy/c3o	1		***cy/cj3o-e***	1		***cy/cj3o-s***	1
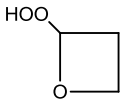 **y(ccco)q_{eth}**	c/c2/h2	1	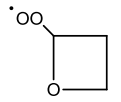 **y(ccco)q_{eth}˙**	c/c2/h2	1			
	c/c/h2/o	1		c/c/h2/o	1			
	c/c/h/o2	1		c/c/h/o2	1			
	o/c2	1		o/c2	1			
	o/c/o	1		o/c/o	1			
	o/h/o	1		o/h/o	1			
	cy/c3o/qe	1		***cy/c3o/qe***	1			
				cy/c3o/qej	1			
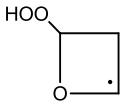 **y(c˙ccc)q_{eth}**	c/c2/h2	1	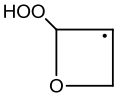 **y(cc˙cc)q_{eth}**	c/c2/h2	1			
	c/c/h2/o	1		c/c/h2/o	1			
	c/c/h/o2	1		c/c/h/o2	1			
	o/c2	1		o/c2	1			
	o/c/o	1		o/c/o	1			
	o/h/o	1		o/h/o	1			
	cy/c3o/qe	1		***cy/c3o/qe***	1			
	cy/cj3o-s/qe	1		***cy/cj3o-s/qe***	1			
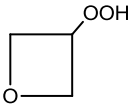 **y(ccco)q_{sec}**	c/c/h2/o	2	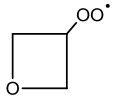 **y(ccco)q_{sec}˙**	c/c/h2/o	2			
	c/c2/h/o	1		c/c2/h/o	1			
	o/c2	1		o/c2	1			
	o/c/o	1		o/c/o	1			
	o/h/o	1		o/h/o	1			
	cy/c3o/qs	1		***cy/c3o/qs***	1			
				cy/c3o/qsj	1			
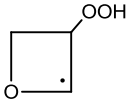 **y(c˙ccc)q_{sec}**	c/c/h2/o	2						
	c/c2/h/o	1						
	o/c2	1						
	o/c/o	1						
	o/h/o	1						
	cy/c3o/qs	1						
	cy/cj3o/qs	1						

(j=radical site)

Table X.3 Groups included for the determination of oxolane and its derivatives

Five membered ring								
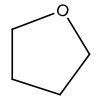 **y(cccco)**	c/c/o/h2	2	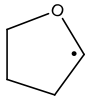 **y(c•ccco)**	c/c/o/h2	2	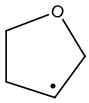 **y(cc•cco)**	c/c/o/h2	2
	c/c2/h2	2		c/c2/h2	2		c/c2/h2	2
	o/c2	1		o/c2	1		o/c2	1
	cy/c4o	1		***cy/c4o***	1		***cy/c4o***	1
				cy/cj4o-e	1		***cy/cj4o-s***	1
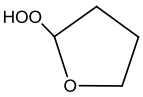 **y(cccco)q_{eth}**	c/c/o/h2	1	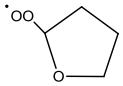 **y(cccco)$q_{et\dot{h}}$**	c/c/o/h2	1			
	c/c2/h2	2		c/c2/h2	2			
	c/c/h/o2	1		c/c/h/o2	1			
	o/c2	1		o/c2	1			
	o/c/o	1		o/c/o	1			
	o/h/o	1		o/h/o	1			
	cy/c4o/qe	1		***cy/c4o/qe***	1			
				cy/c4o/qej	1			
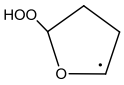 **y(c•ccco)q_{eth}**	c/c/o/h2	1	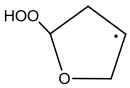 **y(cc•cco)q_{eth}**	c/c/o/h2	1	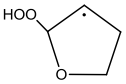 **y(ccc•co)q_{eth}**	c/c/o/h2	1
	c/c2/h2	2		c/c2/h2	2		c/c2/h2	2
	c/c/h/o2	1		c/c/h/o2	1		c/c/h/o2	1
	o/c2	1		o/c2	1		o/c2	1
	o/c/o	1		o/c/o	1		o/c/o	1
	o/h/o	1		o/h/o	1		o/h/o	1
	cy/c4o/qe	1		***cy/c4o/qe***	1		***cy/c4o/qe***	1
	cy/cj4o-e/qe	1		***cy/cj4o-s/qe***	1		***cy/cj4o-s2/qe***	1
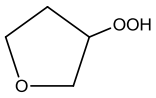 **y(cccco)q_{sec}**	c/c/o/h2	2	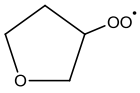 **y(cccco)q_{sec}•**	c/c/o/h2	2			
	c/c2/h2	1		c/c2/h2	1			
	c/c2/h/o	1		c/c2/h/o	1			
	o/c2	1		o/c2	1			
	o/c/o	1		o/c/o	1			
	o/h/o	1		o/h/o	1			
	cy/c4o/qs	1		***cy/c4o/qs***	1			
				cy/c4o/qsj	1			
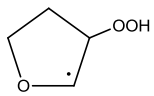 **y(c•ccco)q_{sec}**	c/c/o/h2	2	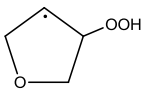 **y(ccc•co)q_{sec}**	c/c/o/h2	2	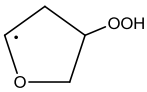 **y(cccc•o)q_{sec}**	c/c/o/h2	2
	c/c2/h2	1		c/c2/h2	1		c/c2/h2	1
	c/c2/h/o	1		c/c2/h/o	1		c/c2/h/o	1
	o/c2	1		o/c2	1		o/c2	1
	o/c/o	1		o/c/o	1		o/c/o	1
	o/h/o	1		o/h/o	1		o/h/o	1
	cy/c4o/qs	1		***cy/c4o/qs***	1		***cy/c4o/qs***	1
	cy/cj4o-e2/qs	1		***cy/cj4o-s/qs***	1		***cy/cj4o-e/qs***	1

(j=radical site)

APPENDIX Y

CYCLIC ALKANE AND ETHERS – THERMOCHEMICAL PROPERTIES IN THE NASA POLYNOMIAL FORMAT

Appendix Y summarizes the thermochemical properties of the species calculated for the study of the 3-5 member ring cyclic alkane and ethers in the NASA polynomial format, for use in ChemKin.

Table Y.1 Thermochemical properties of the cyclic alkane system in the NASA polynomial format for use in ChemKin

```
THERMO
   300.000  1500.000  5000.000

YCCC        1/9/13     C   3H   6    0    0G   300.000  5000.000 1402.000    01
 8.16869450E+00 1.39622417E-02-4.74502846E-06 7.33448618E-10-4.24208798E-14    2
 1.91796428E+03-2.32488714E+01-3.32640604E+00 4.20072762E-02-3.12660111E-05    3
 1.22704154E-08-1.98036369E-12 5.78927182E+03 3.80604885E+01                   4
YCCCC       1/9/13     C   4H   8    0    0G   300.000  5000.000 1397.000    01
 1.05915375E+01 1.93185071E-02-6.54670353E-06 1.01027587E-09-5.83735930E-14    2
-2.76663327E+03-3.69806588E+01-4.63351215E+00 5.34909414E-02-3.51421310E-05    3
 1.15781529E-08-1.50735587E-12 2.62394258E+03 4.52206944E+01                   4
YCCCCC      1/9/13     C   5H  10    0    0G   300.000  5000.000 1395.000    01
 1.30254911E+01 2.48383373E-02-8.44096370E-06 1.30515909E-09-7.55185013E-14    2
-1.69682730E+04-5.26990015E+01-7.18452311E+00 6.97305020E-02-4.53463755E-05    3
 1.45624513E-08-1.81443636E-12-9.77425882E+03 5.65692700E+01                   4
YCJCC       1/9/13     C   3H   5    0    0G   300.000  5000.000 1392.000    01
 7.35238947E+00 1.11094066E-02-3.78829712E-06 6.13048329E-10-3.72127556E-14    2
 3.12365922E+04-1.68715607E+01-2.05396994E+00 3.42363861E-02-2.59897664E-05    3
 1.04870359E-08-1.74177948E-12 3.43985452E+04 3.32555811E+01                   4
YCJCCC      1/9/13     C   4H   7    0    0G   300.000  5000.000 1406.000    01
 9.71333495E+00 1.66500895E-02-5.44937991E-06 8.21676186E-10-4.67244747E-14    2
 2.22564135E+04-3.05872401E+01-4.19027484E+00 4.96171611E-02-3.47715978E-05    3
 1.24062597E-08-1.75647052E-12 2.69470474E+04 4.37615566E+01                   4
YCJCCCC     1/9/13     C   5H   9    0    0G   300.000  5000.000 1403.000    01
 1.20630652E+01 2.21836203E-02-7.33188253E-06 1.11273159E-09-6.35575891E-14    2
 6.26200238E+03-4.45922024E+01-5.97223475E+00 6.46022243E-02-4.48561312E-05    3
 1.59137807E-08-2.25486622E-12 1.24055200E+04 5.20138389E+01                   4
YCCCQ       1/9/13     C   3H   6O   2    0G   300.000  5000.000 1414.000    21
 1.37132522E+01 1.31895425E-02-4.41281582E-06 6.74982388E-10-3.87561965E-14    2
-1.00364418E+04-4.63722669E+01-2.64077974E+00 5.92455692E-02-5.45243612E-05    3
 2.53620336E-08-4.63406435E-12-5.20681008E+03 3.85638803E+01                   4
YCCCCQ      1/9/13     C   4H   8O   2    0G   300.000  5000.000 1403.000    21
 1.57039235E+01 1.93458102E-02-6.58185454E-06 1.01833560E-09-5.89437674E-14    2
-1.65429628E+04-5.81578845E+01-3.24032324E+00 6.65739780E-02-5.20152317E-05    3
 2.09968329E-08-3.42952361E-12-1.03100147E+04 4.24472649E+01                   4
YCCCCCQ     1/9/13     C   5H  10O   2    0G   300.000  5000.000 1391.000    21
 2.04604804E+01 2.37470937E-02-8.27781444E-06 1.30168764E-09-7.61997431E-14    2
-3.15366754E+04-8.46588884E+01-3.23230622E+00 7.94645294E-02-5.87361528E-05    3
 2.22897979E-08-3.45969426E-12-2.33348025E+04 4.24742148E+01                   4
YCCCQJ      1/9/13     C   3H   5O   2    0G   300.000  5000.000 1406.000    11
 1.18861787E+01 1.29454232E-02-4.39937852E-06 6.80128208E-10-3.93450139E-14    2
 8.17590966E+03-3.61764331E+01-6.67746333E-01 4.41628407E-02-3.42760324E-05    3
 1.37176883E-08-2.21791172E-12 1.23076191E+04 3.05090706E+01                   4
YCCCCQJ     1/9/13     C   4H   7O   2    0G   300.000  5000.000 1401.000    11
 1.44140654E+01 1.84849678E-02-6.32128553E-06 9.81407673E-10-5.69437606E-14    2
 7.44067603E+02-5.08939839E+01-2.84018800E+00 5.96307429E-02-4.37908323E-05    3
 1.64683540E-08-2.50538229E-12 6.60930300E+03 4.14019110E+01                   4
```

Table Y.1 Thermochemical properties of the cyclic alkane system in the NASA polynomial format for use in ChemKin (Continued)

```
THERMO
   300.000  1500.000  5000.000

YCCCCCQJ  1/9/13     C   5H   9O   2    0G   300.000  5000.000 1398.000    11
 1.71033780E+01 2.38094229E-02-8.15126807E-06 1.26645319E-09-7.35197367E-14    2
-1.34568914E+04-6.67972155E+01-3.96386074E+00 7.27905922E-02-5.13528673E-05    3
 1.84607035E-08-2.67956102E-12-6.15941448E+03 4.63584200E+01                   4
YCJCCQ    1/9/13     C   3H   5O   2    0G   300.000  5000.000 1407.000    21
 1.33699311E+01 1.10815719E-02-3.71609034E-06 5.69205907E-10-3.27116958E-14    2
 1.95170007E+04-4.21095026E+01 1.35329122E-02 5.00344610E-02-4.78320916E-05    3
 2.31826920E-08-4.39685808E-12 2.33698691E+04 2.68544546E+01                   4
YCJCCCQ   1/9/13     C   4H   7O   2    0G   300.000  5000.000 1405.000    21
 1.61115729E+01 1.65273165E-02-5.62585591E-06 8.70760354E-10-5.04163354E-14    2
 8.43492461E+03-5.80367549E+01-1.79888094E+00 6.28149414E-02-5.19913559E-05    3
 2.21166877E-08-3.77722824E-12 1.41608194E+04 3.64924555E+01                   4
YCCJCCQ   1/9/13     C   4H   7O   2    0G   300.000  5000.000 1405.000    21
 1.62493003E+01 1.64220541E-02-5.59193224E-06 8.65697594E-10-5.01304537E-14    2
 8.17777343E+03-5.85107607E+01-1.55364561E+00 6.25052743E-02-5.18480352E-05    3
 2.21103386E-08-3.78533871E-12 1.38636789E+04 3.54278357E+01                   4
YCJCCCCQ  1/9/13     C   5H   9O   2    0G   300.000  5000.000 1403.000    21
 1.88311084E+01 2.17694349E-02-7.41480520E-06 1.14807748E-09-6.64885064E-14    2
-7.26513879E+03-7.44808842E+01-2.86266379E+00 7.63696423E-02-6.06102195E-05    3
 2.48893052E-08-4.13534970E-12-1.70399630E+02 4.05573788E+01                   4
YCCJCCCQ  1/9/13          5    9    2    0    300.000  5000.000 1403.000    21
 1.90509214E+01 2.16142473E-02-7.36814933E-06 1.14150407E-09-6.61342550E-14    2
-7.58920602E+03-7.57253044E+01-3.69947655E+00 8.01640403E-02-6.58904538E-05    3
 2.79585249E-08-4.77861676E-12-2.75136296E+02 4.44631379E+01                   4
YCCO      1/9/13     C   2H   4O   1    0G   300.000  5000.000 1432.000    01
 4.44690554E+01 3.91714636E-04 1.17004618E-07-5.73608466E-11 5.39080845E-15    2
-3.90299362E+04-2.87687280E+02 9.94387110E+01-5.95239642E-01 1.15069046E-03    3
-7.98121930E-07 1.85993619E-10-1.82695628E+04-4.28247305E+02                   4
YCCCO     1/9/13     C   3H   6O   1    0G   300.000  5000.000 1407.000    01
 5.22606301E+01 4.59609501E-04 1.37781870E-07-6.74554017E-11 6.33790937E-15    2
-4.48221981E+04-3.33611671E+02 8.82645689E+01-5.77337441E-01 1.20987310E-03    3
-8.78449115E-07 2.11466487E-10-1.93509194E+04-3.70717613E+02                   4
YCCCCO    1/9/13     C   4H   8O   1    0G   300.000  5000.000 1710.000    01
 2.31578774E+06-4.25494979E+03 2.68738633E+00-6.76045819E-04 5.64257218E-08    2
-9.38039331E+08-1.28861352E+07 4.93843179E+01 5.15646821E-02-6.94071261E-05    3
 4.06801564E-08-8.69024804E-12-3.86077424E+04-2.85497955E+02                   4
YCJCO     1/9/13     C   2H   3O   1    0G   300.000  5000.000 1432.000    01
 4.33599299E+01 3.65901192E-04 1.21346353E-07-5.72800063E-11 5.34495106E-15    2
-1.17885727E+04-2.80393098E+02 9.68022950E+01-5.78796198E-01 1.11890190E-03    3
-7.76072637E-07 1.80854860E-10 8.40177419E+03-4.17021215E+02                   4
YCJCCO    1/9/13     C   3H   5O   1    0G   300.000  5000.000 1432.000    01
 5.21048886E+01 4.60830884E-04 1.36246618E-07-6.70513429E-11 6.30598313E-15    2
-2.61841004E+04-3.37373429E+02 1.17423743E+02-7.07410187E-01 1.36753377E-03    3
-9.48525365E-07 2.21043595E-10-1.50423711E+03-5.04360183E+02                   4
YCCJCO    1/9/13     C   3H   5O   1    0G   300.000  5000.000 1478.000    01
 5.31383456E+01 4.73983564E-04 1.37162563E-07-6.80528998E-11 6.40968757E-15    2
-2.73662138E+04-3.48325649E+02 1.30361407E+02-7.46015742E-01 1.36437462E-03    3
-9.06287161E-07 2.03656540E-10-5.32507647E+02-5.66359302E+02                   4
YCJCCCO   1/9/13     C   4H   7O   1    0G   300.000  5000.000 1478.000    01
 6.17730366E+01 5.55874877E-04 1.57237517E-07-7.86985928E-11 7.42410318E-15    2
-5.12481228E+04-4.05031932E+02 1.52547748E+02-8.76999982E-01 1.60392924E-03    3
-1.06541160E-06 2.39414311E-10-1.96969867E+04-6.61301220E+02                   4
YCCJCCO   1/9/13     C   4H   7O   1    0G   300.000  5000.000 1580.000    01
 6.38047453E+01-1.25610034E-03 9.78531776E-07-2.29724720E-10 1.71901294E-14    2
-5.42609161E+04-4.21867343E+02 1.44499644E+02-7.92518566E-01 1.37284743E-03    3
-8.60421047E-07 1.82563843E-10-1.71092219E+04-6.31825825E+02                   4
YCCOQ     1/9/13     C   2H   4O   3    0G   300.000  5000.000 1655.000    21
 6.16178027E+01 5.49171382E-04 1.59405292E-07-7.89977999E-11 7.43903639E-15    2
-7.73304089E+04-4.10475722E+02 1.14051665E+02-5.87802957E-01 9.40820527E-04    3
-5.25208429E-07 9.66797877E-11-3.48661396E+04-5.01446171E+02                   4
YCCCOQe   1/9/13     C   3H   6O   3    0G   300.000  5000.000 1657.000    21
 7.15024239E+01-1.39092013E-03 1.08922736E-06-2.56104664E-10 1.91782127E-14    2
-9.23792228E+04-4.75740940E+02 1.30133947E+02-6.73701066E-01 1.07830719E-03    3
-6.01960801E-07 1.10808977E-10-4.29671987E+04-5.71482289E+02                   4
YCCCOQs   1/9/13     C   3H   6O   3    0G   300.000  5000.000 1657.000    21
 7.26333612E+01-1.44299119E-03 1.11993031E-06-2.62635619E-10 1.96428477E-14    2
-8.78444406E+04-4.83959669E+02 1.32209023E+02-6.84784350E-01 1.09604659E-03    3
-6.11863139E-07 1.12631263E-10-3.76097428E+04-5.81158275E+02                   4
```

Table Y.2 Thermochemical properties of the cyclic ether system in the NASA polynomial format for use in ChemKin

```
THERMO
   300.000  1500.000  5000.000

YCCCCOQe  1/9/13    C  4H  8O  3   0G   300.000  5000.000 1313.000    21
-8.58716473E+01 2.29193822E-01-1.05571170E-04 2.00024660E-08-1.33473203E-12    2
-3.40264621E+04 4.28738163E+02 1.29313919E+02-6.19619668E-01 9.04488918E-04    3
-4.48971833E-07 7.25389925E-11-5.62152559E+04-5.73510469E+02                   4
YCCCCOQs  1/9/13    C  4H  8O  3   0G   300.000  5000.000 1312.000    21
-8.71952925E+01 2.32440204E-01-1.06708819E-04 2.01581937E-08-1.34189689E-12    2
-2.93833209E+04 4.35119926E+02 1.31730346E+02-6.31584751E-01 9.21999055E-04    3
-4.57699634E-07 7.39499500E-11-5.19471550E+04-5.84434986E+02                   4
YCCOQJ    1/9/13    C  2H  3O  3   0G   300.000  5000.000 1478.000    11
 5.42757604E+01 4.67807671E-04 1.47515727E-07-7.08925614E-11 6.63784646E-15    2
-4.42506003E+04-3.55255893E+02 1.33256707E+02-7.63109506E-01 1.39563824E-03    3
-9.27055012E-07 2.08323326E-10-1.67968538E+04-5.78219453E+02                   4
YCCCOQeJ  1/9/13    C  3H  5O  3   0G   300.000  5000.000 1657.000    11
 6.95659396E+01-1.37651497E-03 1.07014844E-06-2.51086186E-10 1.87835034E-14    2
-7.14738534E+04-4.63496854E+02 1.26484259E+02-6.54207617E-01 1.04710671E-03    3
-5.84543141E-07 1.07602418E-10-2.34840993E+04-5.56372825E+02                   4
YCCCOQsJ  1/9/13    C  3H  5O  3   0G   300.000  5000.000 1712.000    11
 6.99056676E+01-1.43278330E-03 1.08805251E-06-2.54107527E-10 1.89697748E-14    2
-6.55954079E+04-4.63723636E+02 1.43860275E+02-7.52683489E-01 1.23644682E-03    3
-7.24462767E-07 1.42657339E-10-2.17550181E+04-6.33614738E+02                   4
YCCCCOQeJ 1/9/13    C  4H  7O  3   0G   300.000  5000.000 1657.000    11
 7.94522900E+01-1.55611171E-03 1.21503187E-06-2.85442840E-10 2.13666540E-14    2
-9.40437483E+04-5.29462125E+02 1.44981867E+02-7.53006951E-01 1.20524437E-03    3
-6.72825388E-07 1.23854213E-10-3.88125152E+04-6.36449683E+02                   4
YCCCCOQsJ 1/9/13    C  4H  7O  3   0G   300.000  5000.000 1657.000    11
 7.95641193E+01-1.55887956E-03 1.21699096E-06-2.85889256E-10 2.13995798E-14    2
-9.07499171E+04-5.30523796E+02 1.45190145E+02-7.54119414E-01 1.20702500E-03    3
-6.73819460E-07 1.24037206E-10-3.54369076E+04-6.37667305E+02                   4
YCJCOQ    1/9/13    C  2H  3O  3   0G   300.000  5000.000 1711.000    21
 6.15694245E+01-4.61876772E-04 5.90670698E-07-1.56274227E-10 1.23727364E-14    2
-4.86967064E+04-4.07535779E+02 1.27346328E+02-6.63886888E-01 1.09078667E-03    3
-6.39340004E-07 1.25961640E-10-1.02756137E+04-5.60536454E+02                   4
YCJCCOQe  1/9/13    C  3H  5O  3   0G   300.000  5000.000 1312.000    21
-7.41265217E+01 1.99140802E-01-9.14181612E-05 1.72692996E-08-1.14957448E-12    2
 8.52151466E+02 3.70082262E+02 1.13447150E+02-5.41180034E-01 7.90023687E-04    3
-3.92183208E-07 6.33641307E-11-1.84762359E+04-5.03450909E+02                   4
YCCJCOQe  1/9/13    C  3H  5O  3   0G   300.000  5000.000 1312.000    21
-7.52889287E+01 2.02107046E-01-9.27802400E-05 1.75266524E-08-1.16670820E-12    2
 3.67612542E+03 3.75973100E+02 1.15079601E+02-5.49252119E-01 8.01807849E-04    3
-3.98033411E-07 6.43093328E-11-1.59392426E+04-5.10572609E+02                   4
YCJCCOQs  1/9/13    C  3H  5O  3   0G   300.000  5000.000 1312.000    21
-7.45061806E+01 2.00109903E-01-9.18631669E-05 1.73533803E-08-1.15517235E-12    2
 4.54246589E+03 3.72051338E+02 1.13980743E+02-5.43818546E-01 7.93875613E-04    3
-3.94095530E-07 6.36731061E-11-1.48796037E+04-5.05733537E+02                   4
 YCJCCCOQe  1/9/13    C  4H  7O  3   0G   300.000  5000.000 1474.000    21
 7.91044023E+01 5.88895747E-03-2.49988595E-06 4.43893928E-10-2.81276331E-14    2
-3.85009181E+04-4.35651808E+02 8.20481677E+01 5.94027655E-03-1.13017682E-05    3
 8.34881997E-09-1.97952236E-12-4.01129598E+04-4.53778238E+02                   4
YCCJCCOQe  1/9/13    C  4H  7O  3   0G   300.000  5000.000 1312.000    21
-8.66103800E+01 2.30954834E-01-1.06026731E-04 2.00293339E-08-1.33331914E-12    2
-1.03603643E+04 4.33280457E+02 1.30919273E+02-6.27574497E-01 9.16145410E-04    3
-4.54794240E-07 7.34805424E-11-3.27784976E+04-5.79767499E+02                   4
YCCCJCOQe  1/9/13    C  4H  7O  3   0G   300.000  5000.000 1312.000    21
-8.60691736E+01 2.29563869E-01-1.05387953E-04 1.99086103E-08-1.32527934E-12    2
-1.00099843E+04 4.30871973E+02 1.30145441E+02-6.23748091E-01 9.10559473E-04    3
-4.52021477E-07 7.30328717E-11-3.22963150E+04-5.76063322E+02                   4
YCJCCCOQs  1/9/13    C  4H  7O  3   0G   300.000  5000.000 1312.000    21
-8.67190560E+01 2.31231117E-01-1.06153602E-04 2.00533032E-08-1.33491477E-12    2
-9.08555884E+03 4.33486902E+02 1.31070377E+02-6.28321601E-01 9.17235897E-04    3
-4.55335442E-07 7.35679615E-11-3.15307054E+04-5.80771634E+02                   4
YCCCJCOQs  1/9/13    C  4H  7O  3   0G   300.000  5000.000 1312.000    21
-8.72902572E+01 2.32671332E-01-1.06814848E-04 2.01781836E-08-1.34322464E-12    2
-5.25198200E+03 4.37044582E+02 1.31848467E+02-6.32169222E-01 9.22853450E-04    3
-4.58125248E-07 7.40193594E-11-2.78413432E+04-5.83513629E+02                   4
```

Table Y.2 Thermochemical properties of the cyclic ether system in the NASA polynomial format for use in ChemKin (Continued)

```
THERMO
   300.000  1500.000  5000.000

YCCCCJOQs  1/9/13     C   4H   7O   3    0G   300.000  5000.000 1312.000    21
-8.66702075E+01 2.31097626E-01-1.06092247E-04 2.00416811E-08-1.33413879E-12    2
-7.93256296E+03 4.33780291E+02 1.30989546E+02-6.27921986E-01 9.16652784E-04    3
-4.55046460E-07 7.35216045E-11-3.03672736E+04-5.79883379E+02                   4
YCCOm          1/9/13          3    6    1    0    300.000  5000.000 1395.000    11
 9.69409520E+00 1.47910101E-02-5.03166771E-06 7.78311444E-10-4.50392710E-14    2
-1.64197512E+04-3.04144922E+01-1.14654114E+00 3.96800682E-02-2.69218315E-05    3
 9.58532299E-09-1.41527071E-12-1.25962961E+04 2.79857172E+01                   4
YCCOm2     1/9/13     C   4H   8O   1    0G   300.000  5000.000 1394.000    21
 1.27772484E+01 1.92419584E-02-6.53393922E-06 1.00936575E-09-5.83538533E-14    2
-2.34563758E+04-4.87050050E+01-6.91577229E-01 5.08393038E-02-3.53841666E-05    3
 1.32458038E-08-2.08740372E-12-1.87463999E+04 2.36596152E+01                   4
YCCOmm     1/9/13     C   4H   8O   1    0G   300.000  5000.000 1390.000    21
 1.22412772E+01 1.97389896E-02-6.71542338E-06 1.03880121E-09-6.01145334E-14    2
-2.28934313E+04-4.64929984E+01-9.84003011E-02 4.53502398E-02-2.60245731E-05    3
 7.22670431E-09-7.48822213E-13-1.82575064E+04 2.09672304E+01                   4
YCCOm2m    1/9/13     C   5H  10O   1    0G   300.000  5000.000 1389.000    31
 1.50917680E+01 2.43951087E-02-8.29032672E-06 1.28140102E-09-7.41102565E-14    2
-2.89132849E+04-6.36349335E+01 8.23501141E-01 5.35060515E-02-2.97249390E-05    3
 7.91526537E-09-7.69954009E-13-2.34835599E+04 1.45787733E+01                   4
YCCOm2m2   1/9/13     C   6H  12O   1    0G   300.000  5000.000 1394.000    41
 8.69222937E+00 3.95713734E-02-1.35098544E-05 2.04737651E-09-1.15081335E-13    2
-3.16045138E+04-2.10816829E+01-5.18743256E-01 5.52091439E-02-2.21156675E-05    3
 3.50946478E-09-6.89582362E-14-2.76165083E+04 3.08039040E+01                   4
YCCCOme    1/9/13     C   4H   8O   1    0G   300.000  5000.000 1395.000    11
 1.25833744E+01 1.99831009E-02-6.82472614E-06 1.05853898E-09-6.13741190E-14    2
-2.16601120E+04-4.75509194E+01-3.72465572E+00 5.81826886E-02-4.11929513E-05    3
 1.52154266E-08-2.31405745E-12-1.60021712E+04 4.00042467E+01                   4
YCCCOms    1/9/13     C   4H   8O   1    0G   300.000  5000.000 1394.000    11
 1.24857715E+01 2.00964656E-02-6.87074398E-06 1.06645572E-09-6.18652053E-14    2
-1.99244391E+04-4.76478843E+01-3.52534194E+00 5.67556128E-02-3.88413475E-05    3
 1.37358057E-08-1.99104172E-12-1.42849191E+04 3.86132050E+01                   4
YCCCCOme   1/9/13     C   5H  10O   1    0G   300.000  5000.000 1394.000    11
 1.51599845E+01 2.53710763E-02-8.66999995E-06 1.34532130E-09-7.80261445E-14    2
-3.53695137E+04-6.26990471E+01-5.21859983E+00 7.22365186E-02-4.97805208E-05    3
 1.77534456E-08-2.59694687E-12-2.82140857E+04 4.70159602E+01                   4
YCCCCOms   1/9/13     C   5H  10O   1    0G   300.000  5000.000 1396.000    11
 1.38613467E+01 2.59744660E-02-8.77258132E-06 1.35072211E-09-7.79229750E-14    2
-3.34866356E+04-5.47753891E+01-5.47683492E+00 6.77878546E-02-4.16109211E-05    3
 1.22648100E-08-1.32325491E-12-2.64965152E+04 5.01708937E+01                   4
YCjCOm         1/9/13     C   3H   5O   1    0G   300.000  5000.000 1401.000    11
 8.73201722E+00 1.25379444E-02-4.14777806E-06 6.29897445E-10-3.59951492E-14    2
 1.05305980E+04-2.43595631E+01-1.76176761E+00 3.79391529E-02-2.76030538E-05    3
 1.04377505E-08-1.60004839E-12 1.40453800E+04 3.16154805E+01                   4
YCCjOm         1/9/13     C   3H   5O   1    0G   300.000  5000.000 1400.000    11
 8.59831292E+00 1.26897753E-02-4.20757806E-06 6.39927814E-10-3.66050351E-14    2
 9.77202141E+03-2.31104245E+01-1.35293322E+00 3.58119781E-02-2.43889363E-05    3
 8.48622575E-09-1.18055480E-12 1.31981257E+04 3.03072161E+01                   4
YCCOmj         1/9/13     C   3H   5O   1    0G   300.000  5000.000 1409.000    11
 9.18534365E+00 1.20818871E-02-3.97177134E-06 6.00251032E-10-3.41741057E-14    2
 7.63068027E+03-2.55817271E+01-1.65235009E+00 4.08023358E-02-3.34398082E-05    3
 1.43843940E-08-2.49146647E-12 1.10157458E+04 3.13511362E+01                   4
YCjCOmm    1/9/13     C   4H   7O   1    0G   300.000  5000.000 1392.000    21
 1.16818947E+01 1.77800965E-02-6.06516014E-06 9.39969571E-10-5.44685065E-14    2
 2.83240088E+03-4.05291402E+01-1.21295875E+00 4.62697653E-02-2.97226154E-05    3
 9.73919627E-09-1.29457313E-12 7.48715780E+03 2.93255285E+01                   4
YCCOmmj    1/9/13     C   4H   7O   1    0G   300.000  5000.000 1395.000    21
 1.19112079E+01 1.75548688E-02-5.98031074E-06 9.25946707E-10-5.36194623E-14    2
 7.07548416E+02-4.22933255E+01-1.61907043E+00 4.92785015E-02-3.46913369E-05    3
 1.28888837E-08-1.98852112E-12 5.41387143E+03 3.03629934E+01                   4
YCjCOm2    1/9/13     C   4H   7O   1    0G   300.000  5000.000 1396.000    21
 6.13341513E+00 2.32250680E-02-7.74954244E-06 1.15503143E-09-6.41351984E-14    2
 5.25547774E+03-7.45891491E+00-4.68102118E-01 3.57722309E-02-1.64159437E-05    3
 3.75381117E-09-3.52479043E-13 7.94254272E+03 2.91909340E+01                   4
```

Table Y.3 Thermochemical properties of the cyclic alkane and ring opened diradical system in the NASA polynomial format for use in ChemKin

```
THERMO
   300.000  1500.000  5000.000

JCCJ      freqs  b3lyp/6C   2H   4    0    0G   300.000  5000.000 1400.000    01
 6.22158753E+00 7.88637264E-03-2.62729795E-06 4.00371780E-10-2.29175763E-14    2
 3.61591386E+04-1.02284200E+01 2.01235324E+00 1.92941490E-02-1.51410337E-05    3
 6.82079093E-09-1.28605160E-12 3.75108598E+04 1.18973755E+01                   4
TJCCJ     freqs  b3lyp/6C   2H   4    0    0G   300.000  5000.000 1400.000    01
 6.22158753E+00 7.88637264E-03-2.62729795E-06 4.00371780E-10-2.29175763E-14    2
 3.61591386E+04-9.43325145E+00 2.01235324E+00 1.92941490E-02-1.51410337E-05    3
 6.82079093E-09-1.28605160E-12 3.75108598E+04 1.26925441E+01                   4
JCCCJ     freqs  b3lyp/6C   3H   6    0    0G   300.000  5000.000 1398.000    01
 9.41325188E+00 1.26963308E-02-4.26090944E-06 6.52838187E-10-3.75198537E-14    2
 3.19906717E+04-2.54077387E+01 1.76986686E+00 3.11900122E-02-2.19117482E-05    3
 8.54005813E-09-1.41563047E-12 3.46197130E+04 1.54787099E+01                   4
TJCCCJ    freqs  b3lyp/6C   3H   6    0    0G   300.000  5000.000 1398.000    01
 9.41325188E+00 1.26963308E-02-4.26090944E-06 6.52838187E-10-3.75198537E-14    2
 3.19906717E+04-2.47132243E+01 1.76986686E+00 3.11900122E-02-2.19117482E-05    3
 8.54005813E-09-1.41563047E-12 3.46197130E+04 1.61732242E+01                   4
JCCCCJ    freqs  b3lyp/6C   4H   8    0    0G   300.000  5000.000 1396.000    01
 1.22759585E+01 1.78811944E-02-6.04376890E-06 9.30582635E-10-5.36712737E-14    2
 2.79113208E+04-4.00682485E+01 1.23189965E+00 4.33827681E-02-2.89316247E-05    3
 1.04775190E-08-1.61371320E-12 3.18254013E+04 1.94313238E+01                   4
TJCCCCJ   freqs  b3lyp/6C   4H   8    0    0G   300.000  5000.000 1396.000    01
 1.22759585E+01 1.78811944E-02-6.04376890E-06 9.30582635E-10-5.36712737E-14    2
 2.79113208E+04-3.93737342E+01 1.23189965E+00 4.33827681E-02-2.89316247E-05    3
 1.04775190E-08-1.61371320E-12 3.18254013E+04 2.01258381E+01                   4
JCCCCCJ   freqs  b3lyp/6C   5H  10    0    0G   300.000  5000.000 1395.000    01
 1.51743534E+01 2.30207957E-02-7.80838554E-06 1.20525877E-09-6.96367583E-14    2
 2.38258995E+04-5.55398599E+01 5.31810716E-01 5.57673697E-02-3.57781822E-05    3
 1.21272332E-08-1.72233634E-12 2.91051233E+04 2.36965393E+01                   4
TJCCCCCJ  freqs  b3lyp/6C   5H  10    0    0G   300.000  5000.000 1395.000    01
 1.51743534E+01 2.30207957E-02-7.80838554E-06 1.20525877E-09-6.96367583E-14    2
 2.38258995E+04-5.48453456E+01 5.31810716E-01 5.57673697E-02-3.57781822E-05    3
 1.21272332E-08-1.72233634E-12 2.91051233E+04 2.43910537E+01                   4
JCCCQJ    freqs  b3lyp/6C   3H   6O   2    0G   300.000  5000.000 1397.000    01
 1.31582826E+01 1.48225126E-02-5.04309760E-06 7.80180370E-10-4.51523590E-14    2
 1.32027872E+04-4.20818956E+01 1.27925253E+00 4.28968009E-02-3.05681786E-05    3
 1.14119051E-08-1.75493918E-12 1.72959892E+04 2.16006726E+01                   4
TJCCCQJ   freqs  b3lyp/6C   3H   6O   2    0G   300.000  5000.000 1397.000    01
 1.31582826E+01 1.48225126E-02-5.04309760E-06 7.80180370E-10-4.51523590E-14    2
 1.32027872E+04-4.13873813E+01 1.27925253E+00 4.28968009E-02-3.05681786E-05    3
 1.14119051E-08-1.75493918E-12 1.72959892E+04 2.22951870E+01                   4
JCCCCQJ   freqs  b3lyp/6C   4H   8O   2    0G   300.000  5000.000 1395.000    01
 1.60445255E+01 1.99807632E-02-6.81587774E-06 1.05630224E-09-6.12086908E-14    2
 8.84449780E+03-5.75818207E+01 5.89003904E-01 5.52439154E-02-3.73815086E-05    3
 1.30563162E-08-1.86520793E-12 1.42973620E+04 2.57239505E+01                   4
TJCCCCQJ  freqs  b3lyp/6C   4H   8O   2    0G   300.000  5000.000 1395.000    01
 1.60445255E+01 1.99807632E-02-6.81587774E-06 1.05630224E-09-6.12086908E-14    2
 8.84449780E+03-5.68873063E+01 5.89003904E-01 5.52439154E-02-3.73815086E-05    3
 1.30563162E-08-1.86520793E-12 1.42973620E+04 2.64184648E+01                   4
JCCCCCQJ  freqs  b3lyp/6C   5H  10    0    0G   300.000  5000.000 1395.000    01
 1.51743534E+01 2.30207957E-02-7.80838554E-06 1.20525877E-09-6.96367583E-14    2
 5.65277408E+03-5.48453456E+01 5.31810716E-01 5.57673697E-02-3.57781822E-05    3
 1.21272332E-08-1.72233634E-12 1.09319979E+04 2.43910537E+01                   4
TJCCCCCQJ freqs  b3lyp/6C   5H  10    0    0G   300.000  5000.000 1395.000    01
 1.51743534E+01 2.30207957E-02-7.80838554E-06 1.20525877E-09-6.96367583E-14    2
 5.65277408E+03-5.41508312E+01 5.31810716E-01 5.57673697E-02-3.57781822E-05    3
 1.21272332E-08-1.72233634E-12 1.09319979E+04 2.50855680E+01                   4
JOCCOJ    b3lyp/6-31g(d,C   2H   4O   2    0G   300.000  5000.000 1396.000    01
 1.02698034E+01 9.94047553E-03-3.42695926E-06 5.34955797E-10-3.11577453E-14    2
-7.77450592E+02-3.03142597E+01 2.48465742E-01 3.43468410E-02-2.64015832E-05    3
 1.04644906E-08-1.68743898E-12 2.59355943E+03 2.31372896E+01                   4
JOCCCOJ   freqs  b3lyp/6C   3H   6O   2    0G   300.000  5000.000 1395.000    01
 1.30499050E+01 1.51735994E-02-5.22241876E-06 8.14308160E-10-4.73902238E-14    2
-3.51330985E+03-4.53007673E+01-1.14563668E+00 4.88245551E-02-3.58489218E-05    3
 1.35558293E-08-2.09044010E-12 1.35620404E+03 3.07455055E+01                   4
```

Table Y.3 Thermochemical properties of the cyclic alkane and ring opened diradical system in the NASA polynomial format for use in ChemKin (Continued)

```
THERMO
   300.000  1500.000  5000.000

TJOCCCOJ  freqs  b3lyp/6C   3H   6O   2    0G   300.000  5000.000 1395.000    01
 1.30499050E+01 1.51735994E-02-5.22241876E-06 8.14308160E-10-4.73902238E-14    2
-3.51330985E+03-4.46062529E+01-1.14563668E+00 4.88245551E-02-3.58489218E-05    3
 1.35558293E-08-2.09044010E-12 1.35620404E+03 3.14400199E+01                   4
JOCCCCOJ  freqs  b3lyp/6C   4H   8O   2    0G   300.000  5000.000 1389.000    01
 1.63267825E+01 1.99090026E-02-6.82895092E-06 1.06233591E-09-6.17232781E-14    2
-6.63087103E+03-5.77194981E+01 1.57282941E+00 5.09329393E-02-3.04268321E-05    3
 8.61673791E-09-8.82458686E-13-1.16700269E+03 2.27323973E+01                   4
TJOCCCCOJ freqs  b3lyp/6C   4H   8O   2    0G   300.000  5000.000 1389.000    01
 1.63267825E+01 1.99090026E-02-6.82895092E-06 1.06233591E-09-6.17232781E-14    2
-6.63087103E+03-5.70249837E+01 1.57282941E+00 5.09329393E-02-3.04268321E-05    3
 8.61673791E-09-8.82458686E-13-1.16700269E+03 2.34269117E+01                   4
JOC5OJ   freqs  b3lyp/6C   5H  10O   2    0G   300.000  5000.000 1390.000    01
 1.91299894E+01 2.51702663E-02-8.64439551E-06 1.34585572E-09-7.82401172E-14    2
-1.05068336E+04-7.55832293E+01-1.66348275E-02 6.62441426E-02-4.10291855E-05    3
 1.24068468E-08-1.43937152E-12-3.49152292E+03 2.85430692E+01                   4
TJOC5OJ  freqs  b3lyp/6C   5H  10O   2    0G   300.000  5000.000 1390.000    01
 1.91299894E+01 2.51702663E-02-8.64439551E-06 1.34585572E-09-7.82401172E-14    2
-1.05068336E+04-7.48887150E+01-1.66348275E-02 6.62441426E-02-4.10291855E-05    3
 1.24068468E-08-1.43937152E-12-3.49152292E+03 2.92375835E+01                   4
JCCOJ    freqs  b3lyp/6C   2H   4O   1    0G   300.000  5000.000 1398.000    01
 8.24561706E+00 8.90457399E-03-3.02223604E-06 4.66719038E-10-2.69756565E-14    2
 1.95422746E+04-1.88981369E+01 1.24896669E+00 2.62434887E-02-1.98729995E-05    3
 8.07056028E-09-1.35838501E-12 2.18876796E+04 1.83501637E+01                   4
TJCCOJ   freqs  b3lyp/6C   2H   4O   1    0G   300.000  5000.000 1398.000    01
 8.24561706E+00 8.90457399E-03-3.02223604E-06 4.66719038E-10-2.69756565E-14    2
 1.95422746E+04-1.82036225E+01 1.24896669E+00 2.62434887E-02-1.98729995E-05    3
 8.07056028E-09-1.35838501E-12 2.18876796E+04 1.90446780E+01                   4
JCCCOJ   freqs  b3lyp/6C   3H   6O   1    0G   300.000  5000.000 1396.000    01
 1.13067339E+01 1.38774380E-02-4.72258690E-06 7.30625702E-10-4.22830954E-14    2
 1.47025674E+04-3.36066335E+01 1.16212962E+00 3.76893095E-02-2.63831094E-05    3
 9.83911478E-09-1.53371863E-12 1.82380074E+04 2.08750258E+01                   4
TJCCCOJ  freqs  b3lyp/6C   3H   6O   1    0G   300.000  5000.000 1396.000    01
 1.13067339E+01 1.38774380E-02-4.72258690E-06 7.30625702E-10-4.22830954E-14    2
 1.47025674E+04-3.29121192E+01 1.16212962E+00 3.76893095E-02-2.63831094E-05    3
 9.83911478E-09-1.53371863E-12 1.82380074E+04 2.15695402E+01                   4
JCCCCOJ  freqs  b3lyp/6C   4H   8O   1    0G   300.000  5000.000 1394.000    01
 1.42025481E+01 1.90173944E-02-6.48695108E-06 1.00522576E-09-5.82427389E-14    2
 1.05726864E+04-4.95571162E+01 4.14208501E-01 5.02844242E-02-3.35553190E-05    3
 1.16957939E-08-1.68873557E-12 1.54798296E+04 2.48695369E+01                   4
TJCCCCOJ freqs  b3lyp/6C   4H   8O   1    0G   300.000  5000.000 1394.000    01
 1.42025481E+01 1.90173944E-02-6.48695108E-06 1.00522576E-09-5.82427389E-14    2
 1.05726864E+04-4.88626018E+01 4.14208501E-01 5.02844242E-02-3.35553190E-05    3
 1.16957939E-08-1.68873557E-12 1.54798296E+04 2.55640513E+01                   4
JCOCJ    b3lyp/6-31G(d,C   2H   4O   1    0G   300.000  5000.000 1402.000    01
 8.16398931E+00 8.76843307E-03-2.92982487E-06 4.47558704E-10-2.56682597E-14    2
 2.04992595E+04-1.93168382E+01 2.28698074E+00 2.36422792E-02-1.77534915E-05    3
 7.30821240E-09-1.25383068E-12 2.24415152E+04 1.18656740E+01                   4
TJCOCJ   b3lyp/6-31G(d,C   2H   4O   1    0G   300.000  5000.000 1402.000    01
 8.16398931E+00 8.76843307E-03-2.92982487E-06 4.47558704E-10-2.56682597E-14    2
 2.04992595E+04-1.86223238E+01 2.28698074E+00 2.36422792E-02-1.77534915E-05    3
 7.30821240E-09-1.25383068E-12 2.24415152E+04 1.25601883E+01                   4
JCOCCJ   b3lyp/6-31g(d,C   3H   6O   1    0G   300.000  5000.000 1399.000    01
 1.12734671E+01 1.37420091E-02-4.63934426E-06 7.13801576E-10-4.11476191E-14    2
 1.53783882E+04-3.49132616E+01 1.68038218E+00 3.71187603E-02-2.69672124E-05    3
 1.06315712E-08-1.75542732E-12 1.86409835E+04 1.63100283E+01                   4
TJCOCCJ  b3lyp/6-31g(d,C   3H   6O   1    0G   300.000  5000.000 1399.000    01
 1.12734671E+01 1.37420091E-02-4.63934426E-06 7.13801576E-10-4.11476191E-14    2
 1.53783882E+04-3.42187472E+01 1.68038218E+00 3.71187603E-02-2.69672124E-05    3
 1.06315712E-08-1.75542732E-12 1.86409835E+04 1.70045427E+01                   4
JCOCCCJ  b3lyp/6-31g(d,C   4H   8O   1    0G   300.000  5000.000 1395.000    01
 1.41105340E+01 1.89418934E-02-6.42651403E-06 9.92176955E-10-5.73356023E-14    2
 1.12632954E+04-4.93091312E+01 1.33504906E+00 4.79594942E-02-3.16535408E-05    3
 1.10255521E-08-1.60195885E-12 1.58114677E+04 1.96434986E+01                   4
```

Table Y.3 Thermochemical properties of the cyclic alkane and ring opened diradical system in the NASA polynomial format for use in ChemKin (Continued)

```
THERMO
   300.000  1500.000  5000.000

TJCOCCCJ  b3lyp/6-31g(d,C   4H   8O   1    0G   300.000  5000.000 1395.000    01
 1.41105340E+01 1.89418934E-02-6.42651403E-06 9.92176955E-10-5.73356023E-14    2
 1.12632954E+04-4.86146168E+01 1.33504906E+00 4.79594942E-02-3.16535408E-05    3
 1.10255521E-08-1.60195885E-12 1.58114677E+04 2.03380130E+01                   4
JCCOCCJ   b3lyp/6-31g(d,C   4H   8O   1    0G   300.000  5000.000 1397.000    01
 1.44710755E+01 1.86338257E-02-6.31966500E-06 9.75424499E-10-5.63567406E-14    2
 1.29097186E+04-5.27027673E+01 8.38643410E-01 5.13982087E-02-3.70332309E-05    3
 1.43293542E-08-2.31607671E-12 1.75842542E+04 2.02386729E+01                   4
TJCCOCCJ  b3lyp/6-31g(d,C   4H   8O   1    0G   300.000  5000.000 1397.000    01
 1.44710755E+01 1.86338257E-02-6.31966500E-06 9.75424499E-10-5.63567406E-14    2
 1.29097186E+04-5.20082530E+01 8.38643410E-01 5.13982087E-02-3.70332309E-05    3
 1.43293542E-08-2.31607671E-12 1.75842542E+04 2.09331872E+01                   4
JOCOJ     b3lyp/6-31G(d,C   1H   2O   2    0G   300.000  5000.000 1390.000    01
 7.20667095E+00 5.05044739E-03-1.77337470E-06 2.80262903E-10-1.64648363E-14    2
 6.93567830E+03-1.53822434E+01 1.05741389E+00 1.96426156E-02-1.49960894E-05    3
 5.72631815E-09-8.76983758E-13 9.03392089E+03 1.75387210E+01                   4
TJOCOJ    b3lyp/6-31G(d,C   1H   2O   2    0G   300.000  5000.000 1390.000    01
 7.20667095E+00 5.05044739E-03-1.77337470E-06 2.80262903E-10-1.64648363E-14    2
 6.93567830E+03-1.46877291E+01 1.05741389E+00 1.96426156E-02-1.49960894E-05    3
 5.72631815E-09-8.76983758E-13 9.03392089E+03 1.82332353E+01                   4
TJOCCOJ   b3lyp/6-31g(d,C   2H   4O   2    0G   300.000  5000.000 1396.000    01
 1.02698034E+01 9.94047553E-03-3.42695926E-06 5.34955797E-10-3.11577453E-14    2
-7.77450592E+02-3.10087741E+01 2.48465742E-01 3.43468410E-02-2.64015832E-05    3
 1.04644906E-08-1.68743898E-12 2.59355943E+03 2.24427753E+01                   4
TJOCCOJ   b3lyp/6-31g(d,C   2H   4O   2    0G   300.000  5000.000 1396.000    01
 1.02698034E+01 9.94047553E-03-3.42695926E-06 5.34955797E-10-3.11577453E-14    2
-7.77450592E+02-3.03142597E+01 2.48465742E-01 3.43468410E-02-2.64015832E-05    3
 1.04644906E-08-1.68743898E-12 2.59355943E+03 2.31372896E+01                   4
JCOCQJ    b3lyp/6-31G(d,C   2H   4O   3    0G   300.000  5000.000 1400.000    01
 1.21998757E+01 1.06577947E-02-3.63236991E-06 5.62665961E-10-3.25958170E-14    2
-4.77958275E+02-3.85420990E+01 1.92691502E+00 3.61692533E-02-2.81519815E-05    3
 1.13717497E-08-1.86639622E-12 2.92170838E+03 1.60652159E+01                   4
TJCOCQJ   b3lyp/6-31G(d,C   2H   4O   3    0G   300.000  5000.000 1400.000    01
 1.21998757E+01 1.06577947E-02-3.63236991E-06 5.62665961E-10-3.25958170E-14    2
-4.77958275E+02-3.70373179E+01 1.92691502E+00 3.61692533E-02-2.81519815E-05    3
 1.13717497E-08-1.86639622E-12 2.92170838E+03 1.75699970E+01                   4
JCOCCQJ   b3lyp/6-31g(d,C   3H   6O   3    0G   300.000  5000.000 1397.000    01
 1.50677696E+01 1.58447288E-02-5.41799042E-06 8.41102963E-10-4.87996607E-14    2
-4.25990111E+03-5.36135207E+01 1.09038632E+00 4.88439072E-02-3.52407223E-05    3
 1.31217119E-08-1.99217824E-12 5.43195848E+02 2.13030101E+01                   4
TJCOCCQJ  b3lyp/6-31g(d,C   3H   6O   3    0G   300.000  5000.000 1397.000    01
 1.50677696E+01 1.58447288E-02-5.41799042E-06 8.41102963E-10-4.87996607E-14    2
-4.25990111E+03-5.21540341E+01 1.09038632E+00 4.88439072E-02-3.52407223E-05    3
 1.31217119E-08-1.99217824E-12 5.43195848E+02 2.27624968E+01                   4
JCOCCCQJ  b3lyp/6-31g(d,C   4H   8O   3    0G   300.000  5000.000 1395.000    01
 1.79153651E+01 2.09976239E-02-7.18056772E-06 1.11476884E-09-6.46782547E-14    2
-8.83686631E+03-6.87073342E+01 5.07826585E-01 6.08520373E-02-4.17469377E-05    3
 1.46395312E-08-2.08162713E-12-2.72658060E+03 2.50421314E+01                   4
TJCOCCCQJ b3lyp/6-31g(d,C   4H   8O   3    0G   300.000  5000.000 1395.000    01
 1.79153651E+01 2.09976239E-02-7.18056772E-06 1.11476884E-09-6.46782547E-14    2
-8.83686631E+03-6.72025531E+01 5.07826585E-01 6.08520373E-02-4.17469377E-05    3
 1.46395312E-08-2.08162713E-12-2.72658060E+03 2.65469124E+01                   4
JCCOCCQJ  b3lyp/6-31g(d,C   4H   8O   3    0G   300.000  5000.000 1396.000    01
 1.82694632E+01 2.07197682E-02-7.08968603E-06 1.10109210E-09-6.39022666E-14    2
-6.96397362E+03-7.03529944E+01 4.74145982E-01 6.23178533E-02-4.42554310E-05    3
 1.62195643E-08-2.42753100E-12-7.99728524E+02 2.51871129E+01                   4
TJCCOCCQJ b3lyp/6-31g(d,C   4H   8O   3    0G   300.000  5000.000 1396.000    01
 1.82694632E+01 2.07197682E-02-7.08968603E-06 1.10109210E-09-6.39022666E-14    2
-6.96397362E+03-6.88935077E+01 4.74145982E-01 6.23178533E-02-4.42554310E-05    3
 1.62195643E-08-2.42753100E-12-7.99728524E+02 2.66465996E+01                   4
JOCOCOJ   b3lyp/6-31G(d,C   2H   4O   3    0G   300.000  5000.000 1396.000    01
 1.23845577E+01 1.07713285E-02-3.73225560E-06 5.84655390E-10-3.41374536E-14    2
-2.14376768E+04-4.15663773E+01 4.46155577E-02 4.10836710E-02-3.24185361E-05    3
 1.29984300E-08-2.09953628E-12-1.73300136E+04 2.41313916E+01                   4
```

Table Y.3 Thermochemical properties of the cyclic alkane and ring opened diradical system in the NASA polynomial format for use in ChemKin (Continued)

```
THERMO
   300.000  1500.000  5000.000

TJOCOCOJ  b3lyp/6-31G(d,C   2H   4O   3    0G   300.000  5000.000 1396.000    01
 1.23845577E+01 1.07713285E-02-3.73225560E-06 5.84655390E-10-3.41374536E-14    2
-2.14376768E+04-4.01068907E+01 4.46155577E-02 4.10836710E-02-3.24185361E-05    3
 1.29984300E-08-2.09953628E-12-1.73300136E+04 2.55908782E+01                   4
JOCOCCOJ  b3lyp/6-31g(d,C   3H   6O   3    0G   300.000  5000.000 1395.000    01
 1.51315167E+01 1.59967911E-02-5.51681397E-06 8.61419089E-10-5.01824519E-14    2
-2.51768164E+04-5.63232141E+01-7.38015261E-01 5.38056329E-02-4.00599697E-05    3
 1.52621305E-08-2.35955526E-12-1.97630291E+04 2.86052749E+01                   4
TJOCOCCOJ b3lyp/6-31g(d,C   3H   6O   3    0G   300.000  5000.000 1395.000    01
 1.51315167E+01 1.59967911E-02-5.51681397E-06 8.61419089E-10-5.01824519E-14    2
-2.51768164E+04-5.48637274E+01-7.38015261E-01 5.38056329E-02-4.00599697E-05    3
 1.52621305E-08-2.35955526E-12-1.97630291E+04 3.00647616E+01                   4
JOCOCCCOJ b3lyp/6-31g(d,C   4H   8O   3    0G   300.000  5000.000 1393.000    01
 1.81593482E+01 2.10486834E-02-7.25625940E-06 1.13270887E-09-6.59731349E-14    2
-2.78132433E+04-7.14787323E+01-1.37980270E+00 6.61446278E-02-4.67456430E-05    3
 1.67573491E-08-2.42611172E-12-2.10000501E+04 3.36079430E+01                   4
TJOCOCCCOJb3lyp/6-31g(d,C   4H   8O   3    0G   300.000  5000.000 1393.000    01
 1.81593482E+01 2.10486834E-02-7.25625940E-06 1.13270887E-09-6.59731349E-14    2
-2.78132433E+04-7.00192457E+01-1.37980270E+00 6.61446278E-02-4.67456430E-05    3
 1.67573491E-08-2.42611172E-12-2.10000501E+04 3.50674297E+01                   4
JOCCOCCOJ b3lyp/6-31g(d,C   4H   8O   3    0G   300.000  5000.000 1390.000    01
 1.83231497E+01 2.08708922E-02-7.18606405E-06 1.12080281E-09-6.52406517E-14    2
-2.50304016E+04-7.13493410E+01 1.19371684E+00 5.78238272E-02-3.64147704E-05    3
 1.10882845E-08-1.27902894E-12-1.87956865E+04 2.16990063E+01                   4
TJOCCOCCOJb3lyp/6-31g(d,C   4H   8O   3    0G   300.000  5000.000 1390.000    01
 1.83231497E+01 2.08708922E-02-7.18606405E-06 1.12080281E-09-6.52406517E-14    2
-2.50304016E+04-6.98898544E+01 1.19371684E+00 5.78238272E-02-3.64147704E-05    3
 1.10882845E-08-1.27902894E-12-1.87956865E+04 2.31584930E+01                   4
JCOCCOJ  b3lyp/6-31g(d,C   3H   6O   2    0G   300.000  5000.000 1395.000    01
 1.31451073E+01 1.49288208E-02-5.10086637E-06 7.91400132E-10-4.58949523E-14    2
-2.25303674E+03-4.52443195E+01 8.71943881E-01 4.37243032E-02-3.10602793E-05    3
 1.15086921E-08-1.75524289E-12 1.99980230E+03 2.06307290E+01                   4
TJCOCCOJ  b3lyp/6-31g(d,C   3H   6O   2    0G   300.000  5000.000 1395.000    01
 1.31451073E+01 1.49288208E-02-5.10086637E-06 7.91400132E-10-4.58949523E-14    2
-2.25303674E+03-4.37848329E+01 8.71943881E-01 4.37243032E-02-3.10602793E-05    3
 1.15086921E-08-1.75524289E-12 1.99980230E+03 2.20902156E+01                   4
JOCCJ    b3lyp/6-31g(d,C   2H   4O   1    0G   300.000  5000.000 1398.000    01
 8.24561706E+00 8.90457399E-03-3.02223604E-06 4.66719038E-10-2.69756565E-14    2
 1.84099142E+04-2.07602405E+01 1.24896669E+00 2.62434887E-02-1.98729995E-05    3
 8.07056028E-09-1.35838501E-12 2.07553192E+04 1.64880600E+01                   4
TJOCCJ   b3lyp/6-31g(d,C   2H   4O   1    0G   300.000  5000.000 1398.000    01
 8.24561706E+00 8.90457399E-03-3.02223604E-06 4.66719038E-10-2.69756565E-14    2
 1.84099142E+04-1.93007539E+01 1.24896669E+00 2.62434887E-02-1.98729995E-05    3
 8.07056028E-09-1.35838501E-12 2.07553192E+04 1.79475467E+01                   4
YCCCOO   freqs  b3lyp/6C   3H   6O   2    0G   300.000  5000.000 1403.000    11
 1.06398664E+01 1.60994339E-02-5.39577563E-06 8.26776893E-10-4.75446171E-14    2
-1.82453735E+04-3.57845822E+01-4.66694516E+00 5.28544092E-02-3.88134550E-05    3
 1.44746134E-08-2.15659142E-12-1.31084643E+04 4.59361122E+01                   4
YCCCCOO  freqs  b3lyp/6C   4H   8O   2    0G   300.000  5000.000 1401.000    11
 1.33753248E+01 2.13950917E-02-7.21614832E-06 1.11020819E-09-6.40175374E-14    2
-2.58134704E+04-5.16214224E+01-5.67651360E+00 6.61613938E-02-4.69301194E-05    3
 1.68992463E-08-2.43464146E-12-1.93006624E+04 5.04763385E+01                   4
YCCCCCOO freqs  b3lyp/6C   5H  10O   2    0G   300.000  5000.000 1397.000    11
 1.62084922E+01 2.66253359E-02-9.01940884E-06 1.39165393E-09-8.04061347E-14    2
-3.29252097E+04-6.79348471E+01-6.43536205E+00 7.85370769E-02-5.36959155E-05    3
 1.85218998E-08-2.54563376E-12-2.50333767E+04 5.39080660E+01                   4
YCOO     b3lyp/6-31G(d.C   1H   2O   2    0G   300.000  5000.000 1399.000    01
 6.13826605E+00 5.79655553E-03-1.99467713E-06 3.11020486E-10-1.81016122E-14    2
-5.08499407E+03-9.29601367E+00 6.00418502E-01 1.82643892E-02-1.23824089E-05    3
 4.08906248E-09-5.18947524E-13-3.13887010E+03 2.05717873E+01                   4
YCCOO    b3lyp/6-31g(d,C   2H   4O   2    0G   300.000  5000.000 1398.000    01
 8.91533203E+00 1.10212883E-02-3.78525277E-06 5.89438077E-10-3.42737782E-14    2
-6.95234404E+03-2.45776926E+01-1.49938577E+00 3.48966236E-02-2.42996389E-05    3
 8.42480888E-09-1.15422722E-12-3.32615670E+03 3.14563726E+01                   4
```

Table Y.3 Thermochemical properties of the cyclic alkane and ring opened diradical system in the NASA polynomial format for use in ChemKin (Continued)

```
THERMO
   300.000  1500.000  5000.000

YCOCOO    b3lyp/6-31G(d,C   2H   4O   3    0G   300.000  5000.000 1397.000    01
 1.09872854E+01 1.18759355E-02-4.09646823E-06 6.39861576E-10-3.72887367E-14    2
-3.47443069E+04-3.59013149E+01-2.21672279E+00 4.32964498E-02-3.24607456E-05    3
 1.21787820E-08-1.82111283E-12-3.02701516E+04 3.47187157E+01                   4
YCOCCOO   b3lyp/6-31g(d,C   3H   6O   3    0G   300.000  5000.000 1396.000    01
 1.37881264E+01 1.70996041E-02-5.88995288E-06 9.18998920E-10-5.35111946E-14    2
-3.94021779E+04-5.20608729E+01-3.65367726E+00 5.85543085E-02-4.34852811E-05    3
 1.63910371E-08-2.49039004E-12-3.34601878E+04 4.12869801E+01                   4
YCOCCCOO  b3lyp/6-31g(d,C   4H   8O   3    0G   300.000  5000.000 1395.000    01
 1.66529800E+01 2.22520209E-02-7.65545453E-06 1.19343935E-09-6.94476466E-14    2
-4.77204504E+04-6.77207516E+01-4.34933170E+00 7.10530145E-02-5.06836412E-05    3
 1.83264616E-08-2.67097688E-12-4.04419569E+04 4.50985143E+01                   4
YCCOCCOO  b3lyp/6-31g(d,C   4H   8O   3    0G   300.000  5000.000 1394.000    01
 1.67615279E+01 2.21778431E-02-7.63379454E-06 1.19046283E-09-6.92905552E-14    2
-4.45243398E+04-6.86215165E+01-4.03216456E+00 7.02558646E-02-4.97513082E-05    3
 1.78280381E-08-2.57232012E-12-3.72924847E+04 4.31647370E+01                   4
YCOCCO    b3lyp/6-31g(d,C   3H   6O   2    0G   300.000  5000.000 1390.000    01
 1.12988721E+01 1.65920625E-02-5.69891905E-06 8.87543943E-10-5.16142369E-14    2
-4.29923232E+04-3.78355870E+01-3.13285891E+00 4.77064161E-02-3.00220941E-05    3
 8.91503914E-09-9.57402835E-13-3.77676523E+04 4.05152191E+01                   4
CH2       CBS-APNO,Chad C   1H   2    0    0G   300.000  5000.000 1387.000    01
 3.24709565E+00 2.31058554E-03-4.66682011E-07 3.95404861E-11-1.06799498E-15    2
 5.02342877E+04 3.00716610E+00 3.65300791E+00 1.48759807E-03 1.54875301E-07    3
-1.71129442E-10 2.64849132E-14 5.00767091E+04 7.75931410E-01                   4
TCH2      CBS-APNO,Chad C   1H   2    0    0G   300.000  5000.000 1387.000    01
 3.24709565E+00 2.31058554E-03-4.66682011E-07 3.95404861E-11-1.06799498E-15    2
 4.65100804E+04 4.46665277E+00 3.65300791E+00 1.48759807E-03 1.54875301E-07    3
-1.71129442E-10 2.64849132E-14 4.63525017E+04 2.23541808E+00                   4
CH2O              C   1H   2O   1    0G   300.000  5000.000 1492.000    01
 3.91527967E+00 5.13066169E-03-1.76213301E-06 2.74302764E-10-1.59427842E-14    2
-1.53684091E+04 1.70259206E+00 2.97646460E+00 3.31251523E-03 4.55181503E-06    3
-4.59001475E-09 1.14482312E-12-1.46244762E+04 8.19564357E+00                   4
HCO2H     b3lyp/6-31g(d,C   1H   2O   2    0G   300.000  5000.000 1401.000    01
 5.95472291E+00 5.76232715E-03-1.94119263E-06 2.98357999E-10-1.71905102E-14    2
 4.29009922E+04-7.02389927E+00 1.30515188E+00 1.65417788E-02-1.13637713E-05    3
 3.98533245E-09-5.61388771E-13 4.45094432E+04 1.79518412E+01                   4
HCO2J     b3lyp/6-31g(d,C   1H   1O   2    0G   300.000  5000.000 1398.000    01
 5.95193002E+00 3.47168738E-03-1.20695032E-06 1.89534101E-10-1.10870685E-14    2
-2.17234282E+04-6.56987849E+00 1.70153319E+00 1.33197225E-02-9.70261032E-06    3
 3.41657367E-09-4.64081611E-13-2.02652360E+04 1.62428514E+01                   4
CH2CH2            C   2H   4    0    0G   300.000  5000.000 1394.000    01
 5.21495849E+00 8.96066623E-03-3.04712995E-06 4.71094610E-10-2.72474916E-14    2
 3.61069874E+03-7.42632336E+00 3.89634275E-01 1.90115733E-02-1.08369348E-05    3
 3.15370853E-09-3.75480468E-13 5.43953625E+03 1.89729102E+01                   4
CCCDC     3/ 8/11 THERMC   4H   8    0    0G   300.000  5000.000 1396.000    11
 1.11983764E+01 1.80420642E-02-6.03241734E-06 9.22319339E-10-5.29419341E-14    2
-5.84084835E+03-3.43125593E+01-1.03518355E+00 4.61694226E-02-3.06577426E-05    3
 1.07068621E-08-1.54358485E-12-1.54837640E+03 3.15466696E+01                   4
CCCCDC    3/ 8/11 THERMC   5H  10    0    0G   300.000  5000.000 1395.000    21
 1.44642525E+01 2.23531566E-02-7.49188779E-06 1.14742046E-09-6.59443529E-14    2
-9.96570233E+03-5.04275776E+01-1.34906635E+00 5.87137130E-02-3.92840366E-05    3
 1.37429277E-08-1.97627696E-12-4.42305670E+03 3.46932255E+01                   4
O*CCOH    b3lyp/6-31g(d,C   2H   4O   2    0G   300.000  5000.000 1393.000    01
 9.13739870E+00 1.07040224E-02-3.64650508E-06 5.64659207E-10-3.27024605E-14    2
-4.05544374E+04-2.35547023E+01 1.10423887E+00 2.84124947E-02-1.81921130E-05    3
 5.84600035E-09-7.45896730E-13-3.76629824E+04 1.99564586E+01                   4
COC*C     b3lyp/6-31g(d,C   3H   6O   1    0G   300.000  5000.000 1393.000    01
 9.77523327E+00 1.50889705E-02-5.12159272E-06 7.91002996E-10-4.57236243E-14    2
-1.75210220E+04-2.87460300E+01-1.66515366E-01 3.67780229E-02-2.28291977E-05    3
 7.23137718E-09-9.27220504E-13-1.38984374E+04 2.52188374E+01                   4
CCOC*C    b3lyp/6-31g(d,C   4H   8O   1    0G   300.000  5000.000 1393.000    01
 1.27527315E+01 2.01383980E-02-6.84976843E-06 1.05941546E-09-6.13004858E-14    2
-2.33399821E+04-4.44195997E+01-9.27021181E-01 5.01074769E-02-3.14564138E-05    3
 1.00765527E-08-1.30769142E-12-1.83705186E+04 2.97868086E+01                   4
```

APPENDIX Z

CYCLIC ALKANE AND ETHERS – REACTION MECHANISMS

Appendix Z includes the mechanism used for the kinetic study of the unimolecular dissociation and oxidation of the ring opened 3 to 5 member ring cyclic alkanes and ethers.

Table Z.1 Three member cyclic alkane system

```
ELEMENTS
H  C  O  N
END

SPECIES
N2       O2        CH2O          CH2CH2
CH2    HCO2J    HCO2H        HCO
H        CO         HO2
YCCC           YCCCOO      JCCCJ       JOCCCOJ
JCCCQJ         TJCCCQJ     JCCOJ       YCCO
END

REACTIONS

! Ring-opening
YCCC = JCCCJ                          1.0E18      0.0     63.50E3

! Dissociation
JCCCJ => CH2CH2 + CH2                  1.0E9       0.0     35.77E3

! Triplet-Singlet conversion
JCCCQJ = TJCCCQJ                      9.0E+13     0.0     1.5E3

! Chemical activation
JCCCJ + O2 = TJCCCQJ                  4.77E+09    -4.91    -5904.
JCCCJ + O2 = JCCCQJ                   9.71E+09    -4.91    -5902.
JCCCJ + O2 = YCCCOO                   1.64E+09    -5.54     3666.
JCCCJ + O2 = JOCCCOJ                  2.90E+13    -6.01     4863.
JCCCJ + O2 = CH2O + JCCOJ             1.88E+26    -4.21     3818.

! For important paths from chemical activation
JCCCQJ = YCCCOO                       1.1E+11     0.0     2.5E3
YCCCOO = JOCCCOJ                      2.5E+16     0.0     28.53E3
JOCCCOJ = CH2O + JCCOJ                3.0E13      0.0     20.04E3
JCCOJ => CH2O + CH2                   1.0E9       0.0     34.38E3
JCCOJ => YCCO                         1.1E+11     0.0     2.5E3

END
```

Table Z.2 Four member cyclic alkane system

```
ELEMENTS
H  C  O  N
END

SPECIES
N2       O2        CH2O          CH2CH2
CH2    HCO2J    HCO2H        HCO
H        CO         HO2
YCCCC          YCCCCOO      JCCCCJ     JOCCCCOJ
JCCCCQJ        TJCCCCQJ     JCCCOJ     JCCJ
CCCDC          YCCCO
END

REACTIONS

! Ring-opening

YCCCC = JCCCCJ                    3.4E18    -0.797   64.85E3

! Dissociation + Intramolecular H transfer

JCCCCJ => CCCDC                   3.72E+5    2.17    16.44E3
JCCCCJ => CH2CH2 + CH2CH2         2.09E+7    1.44     3.03E3

! Triplet-Singlet conversion

JCCCCQJ = TJCCCCQJ                9.0E+13    0.0      1.5E3

! Chemical activation

JCCCCJ + O2 = TJCCCCQJ            9.21E-03   -1.52   -11290.
JCCCCJ + O2 = JCCCCQJ             1.86E-02   -1.52   -11289.
JCCCCJ + O2 = YCCCCOO             2.04E+10   -5.61     4371.
JCCCCJ + O2 = JOCCCCOJ            8.89E+06   -4.13     2545.
JCCCCJ + O2 = CH2O+JCCCOJ         5.13E+22   -3.13     3318.

! For important paths from chemical activation

JCCCCQJ = YCCCCOO                 1.1E+11    0.0      2.5E3
YCCCCOO = JOCCCCOJ                2.5E+16    0.0     37.25E3
JOCCCCOJ => CH2O + JCCCOJ         3.0E+13    0.0     16.78E3
JCCCOJ => CH2CH2 + CH2O           3.0E13     0.0     6.3E3
JCCCOJ => YCCCO                   1.1E+11    0.0     2.5E3

!Stabilization Reactions

JCCCCQJ => CDCCCQ                 1.5E9      0.77     11.1E3
JCCCCQJ => CJCCDC + HO2           9.2E9      0.95     27.1E3

JOCCCCOJ => ODCCCCOH              1.28E10    0.10     2.E3

END
```

Table Z.3 Five member cyclic alkane system

```
ELEMENTS
H  C  O  N
END

SPECIES
N2       O2        CH2O          CH2CH2
CH2    HCO2J    HCO2H        HCO
H        CO         HO2
YCCCCC         YCCCCCOO      JCCCCCJ      JOC5OJ
JCCCCCQJ       TJCCCCCQJ     JOC5OJ       JCCCCOJ
JCCCJ            JCCOJ         CCCCDC       YCCCCO
YCCO            YCCC
END

REACTIONS

! Ring-opening

!YCCCCC = JCCCCCJ                    1.3E18     -0.466   85.18E3

! Dissociation + Intramolecular H transfer

JCCCCCJ => CCCCDC                   5.9E+6      1.48     7.76E3
JCCCCCJ => CH2CH2 + JCCCJ           2.09E+7     1.44    25.29E3
JCCCJ => CH2CH2 + CH2               1.0E9       0.0     35.77E3
JCCCJ => YCCC                       1.1E+11     0.0      2.5E3

! Triplet-Singlet conversion

JCCCCCQJ = TJCCCCCQJ                9.0E+13     0.0      1.5E3

! Chemical activation

JCCCCCJ + O2 = TJCCCCCQJ            1.24E-16    2.64   -17133.
JCCCCCJ + O2 = JCCCCCQJ             2.48E-16    2.64   -17134.
JCCCCCJ + O2 = YCCCCCOO             8.87E-10    0.03   -16696.
JCCCCCJ + O2 = JOC5OJ               3.80E+01   -2.42     -432.
JCCCCCJ + O2 = CH2O + JCCCCOJ 9.51E+17   -1.61     2022.

! For important paths from chemical activation

JCCCCCQJ = YCCCCCOO                 1.1E+11     0.0      2.5E3
YCCCCCOO = JOC5OJ                   2.5E+16     0.0     43.7E3
JOC5OJ = CH2O + JCCCCOJ             3.0E+13     0.0     16.2E3
JCCCCOJ => CH2CH2 + JCCOJ           2.0E13      0.0     30.4E3
JCCCCOJ => CH2O + JCCCJ             2.0E13      0.0     16.9E3
JCCCCOJ => YCCCCO                   1.1E+11     0.0      2.5E3
JCCOJ => CH2O + CH2                 1.0E9       0.0     32.13E3
JCCOJ => YCCO                       1.1E+11     0.0      2.5E3

END
```

Table Z.4 Three member cyclic ether system

```
ELEMENTS
H  C  O  N
END

SPECIES
N2       O2        CH2O          CH2CH2
CH2    HCO2J    HCO2H        HCO
H        CO         HO2
YCCO           YCOCOO       JCOCJ       JOCOCOJ
JCOCQJ         TJCOCQJ      JOCOJ       YCOO
END

REACTIONS

! Ring-opening

!YCCO = JCOCJ                      1.0E18      0.0     64.72E3

! Dissociation

JCOCJ => CH2O + CH2                1.0E9       0.0     30.61E3

! Triplet-Singlet conversion

JCOCQJ = TJCOCQJ                   9.0E+13     0.0     1.5E3

! Chemical activation

JCOCJ + O2 = TJCOCQJ               2.08E-04   -0.94    -9494.
JCOCJ + O2 = JCOCQJ                4.18E-04   -0.95    -9494.
JCOCJ + O2 = YCOCOO                3.21E+05   -4.47     3202.
JCOCJ + O2 = JOCOCOJ               1.99E+14   -6.18     6540.
JCOCJ + O2 = CH2O + JOCOJ          2.80E+22   -3.17     3089.

! For important paths from chemical activation

!JCOCQJ = YCOCOO                  1.1E+11     0.0      2.5E3
!YCOCOO = JOCOCOJ                 2.5E+16     0.0    24.87E3
!JOCOCOJ => CH2O + JOCOJ          2.0E13      0.0    30.93E3
JOCOJ => HCO2J + H                4.0E13      0.0     4.0E3
JOCOJ => YCOO                     1.1E+11     0.0     2.5E3
JOCOJ => HCO2H                    4.0E13      0.0    10.0E3

END
```

Table Z.5 Four member cyclic ether system

```
ELEMENTS
H  C  O  N
END

SPECIES
N2       O2        CH2O          CH2CH2
CH2    HCO2J    HCO2H        HCO
H        CO         HO2
YCCCO          YCOCCOO       JCOCCJ     JOCOCCOJ
JCOCCQJ        TJCOCCQJ      JOCCOJ     O*CCOH
YCCOO          COC*C
END

REACTIONS

! Ring-opening

YCCCO = JCOCCJ                      1.3E18     -0.466   64.13E3

! Dissociation + Intramolecular H transfer

JCOCCJ => COC*C                   3.72E+5     2.17    16.44E3
JCOCCJ => CH2O + CH2CH2         2.09E+7     1.44     3.70E3

! Triplet-Singlet conversion

JCOCCQJ = TJCOCCQJ                9.0E+13     0.0     1.5E3

! Chemical activation

JCOCCJ + O2 = TJCOCCQJ           8.67E-05   -0.91   -12412.
JCOCCJ + O2 = JCOCCQJ            1.75E-04   -0.91   -12412.
JCOCCJ + O2 = YCOCCOO            3.49E+10   -5.79     4762.
JCOCCJ + O2 = JOCOCCOJ           2.86E+11   -5.37     4333.
JCOCCJ + O2 = CH2O + JOCCOJ   4.23E+22   -3.13     3292.

! For important paths from chemical activation

JCOCCQJ = YCOCCOO                1.1E+11     0.0     2.5E3
YCOCCOO = JOCOCCOJ               2.5E+16     0.0    26.6E3
JOCOCCOJ => CH2O + JOCCOJ    3.0E+13     0.0   23.07E3
JOCCOJ => CH2O + CH2O          3.0E+13     0.0      6.5E3
JOCCOJ => O*CCOH                3.72E+5     2.17  16.44E3
JOCCOJ => YCCOO                 1.1E+11     0.0     2.5E3

END
```

Table Z.6 Five member cyclic ether system 1

```
ELEMENTS
H  C  O  N
END

SPECIES
N2      O2       CH2O          CH2CH2
CH2    HCO2J    HCO2H         HCO
H       CO       HO2
YCCCCO       YCOCCCOO    JCOCCCJ       JOCOCCCOJ
JCOCCCQJ     TJCOCCCQJ    JOCCCOJ       JCCOJ
JCCOJ          COCCDC         YCCCOO       YCCOCCOO
JCCOCCJ       JCCOCCQJ      JOCCOCCOJ     JCOCCOJ
JCOCJ          CCOCDC        YCOCCO       JCCCJ
YCCC           YCCO
END

REACTIONS

! Ring-opening 1

YCCCCO = JCOCCCJ                1.3E18     -0.466   80.83E3

! Dissociation + Intramolecular H transfer

JCOCCCJ => COCCDC                5.9E+6       1.48     7.76E3
JCOCCCJ => CH2O + JCCCJ          2.09E+7     1.44    13.37E3
JCCCJ => CH2CH2 + CH2            1.0E9        0.0      45.60E3
JCCCJ => YCCC                    1.1E+11     0.0        2.5E3

! Triplet-Singlet conversion

JCOCCCQJ = TJCOCCCQJ             9.0E+13      0.0      1.5E3

! Chemical activation

JCOCCCJ + O2 = TJCOCCCQJ         2.03E-18    3.17   -17538.
JCOCCCJ + O2 = JCOCCQJ           4.05E-18    3.17   -17539.
JCOCCCJ + O2 = YCOCCCOO          4.19E+07   -4.58     2120.
JCOCCCJ + O2 = JOCOCCCOJ         3.54E+09   -4.74     3450.
JCOCCCJ + O2 = CH2O + JOCCCOJ  4.13E+18   -1.84     2252.

! For important paths from chemical activation

JCOCCCQJ = YCOCCCOO              1.1E+11     0.0     2.5E3
YCOCCCOO = JOCOCCCOJ             2.5E+16     0.0    38.0E3
JOCOCCCOJ => CH2O + JOCCCOJ   3.0E+13     0.0   19.54E3
JOCCCOJ => CH2O + JCCOJ          2.0E13      0.0    22.9E3
JOCCCOJ => YCCCOO                1.1E+11     0.0     2.5E3

JCCOJ => CH2O + CH2              1.0E9        0.0   34.38E3
JCCOJ => YCCO                    1.1E+11     0.0       2.5E3

END
```

Table Z.7 Five member cyclic ether system 2

```
ELEMENTS
H  C  O  N
END

SPECIES
N2       O2        CH2O          CH2CH2
CH2    HCO2J    HCO2H        HCO
H        CO         HO2
YCCCCO         YCOCCCOO     JCOCCCJ       JOCCCOJ
JCOCCCQJ      TJCOCCCQJ    JOCOCCCOJ     JCCOJ
JCCOJ           COCCDC       YCCCOO        YCCOCCOO
JCCOCCJ       JCCOCCQJ     TJCCOCCQJ     JOCCOCCOJ
JCOCCOJ       JCOCJ        CCOCDC        YCOCCO
YCCO

END

REACTIONS

YCCCCO = JCCOCCJ                    1.3E18     -0.466   87.28E3

! Dissociation + Intramolecular H transfer

JCCOCCJ => CCOCDC                   5.9E+6      1.48     7.76E3
JCCOCCJ => CH2CH2 + JCCOJ           2.09E+7     1.44    20.14E3
JCCOJ => CH2O + CH2                 1.0E9       0.0     34.38E3
JCCOJ => YCCO                       1.1E+11     0.0      2.5E3

! Triplet-Singlet conversion

JCCOCCQJ = TJCCOCCQJ                9.0E+13     0.0     1.5E3

! Chemical activation

JCCOCCJ + O2 = TJCCOCCQJ            3.53E-18    3.06   -17951.
JCCOCCJ + O2 = JCCOCCQJ             7.07E-18    3.06   -17952.
JCCOCCJ + O2 = YCCOCCOO             1.28E+06   -4.16     1260.
JCCOCCJ + O2 = JOCCOCCOJ            1.12E+10   -4.84     4420.
JCCOCCJ + O2 = CH2O + JCOCCOJ       5.55E+18   -1.89     2330.

! For important paths from chemical activation

JCCOCCQJ = YCCOCCOO                 1.1E+11     0.0      2.5E3
YCCOCCOO = JOCCOCCOJ                2.5E+16     0.0     36.97E3
JOCCOCCOJ => CH2O + JCOCCOJ         3.0E+13     0.0     19.54E3
JCOCCOJ => CH2O + JCOCJ             2.0E13      0.0     19.46E3
JCOCCOJ => YCOCCO                   1.1E+11     0.0      2.5E3

JCOCJ => CH2O + CH2                 1.0E9       0.0     30.61E3
JCOCJ => YCCO                       1.1E+11     0.0      2.5E3

END
```

APPENDIX AA

UNCERTAINTY ANALYSIS

Appendix AA summarizes the calculation method followed for the determination of the uncertainties. Two types of error are considered in the analysis of enthalpy of formation:

- uncertainty in values of the reference species.
- uncertainty in calculation from the work computational chemistry.

For small samples, assuming the population follows approximately a normal distribution, the Student's t distribution can be applied:

$$\bar{X} \pm \left(t_{n-1}, \alpha/2\right) \frac{s}{\sqrt{n}}$$

where $\bar{X}$ is the mean of the sample, *s* is the standard deviation of the sample, and *n* is the population in the sample. To obtain 95% confidence limit, $100(1-\alpha)\% \rightarrow \alpha = 0.05$.

This study uses three sets of reactions for the determination of the heat of formation, the population has 3 items (n=3) $\rightarrow (t_2, 0.025) = 4.303$

Different reaction sets have been used for the determination of the uncertainties for enthalpy of formation data on the stable molecules and for the radicals.

Table AA.1 lists the work reactions used for evaluation of the uncertainty for stable molecule enthalpy, and Table AA.2 summarizes the work reactions used for the uncertainty of the radical enthalpy.

Table AA.1 Reactions used for stable molecules

Reactions for Stable Molecules							
1)	y(CH_3OCH_3)	+	$CH_3CH_2CH_3$	→	y($CH_3CH_2CH_3$)	+	CH_3OCH_3
2)	y(CH_3OCH_3)	+	$CH_3CH_2CH_2CH_3$	→	y($CH_3CH_2CH_3$)	+	$CH_3CH_2OCH_3$
3)	y($CH_3OCH_2CH_3$)	+	$CH_3CH_2CH_3$	→	y($CH_3CH_2CH_2CH_3$)	+	CH_3OCH_3
4)	y($CH_3OCH_2CH_3$)	+	$CH_3CH_2CH_2CH_3$	→	y($CH_3CH_2CH_2CH_3$)	+	$CH_3CH_2OCH_3$
5)	y($CH_3OCH_2CH_2CH_3$)	+	$CH_3CH_2CH_3$	→	y($CH_3CH_2CH_2CH_2CH_3$)	+	CH_3OCH_3
6)	y($CH_3OCH_2CH_2CH_3$)	+	$CH_3CH_2CH_2CH_3$	→	y($CH_3CH_2CH_2CH_2CH_3$)	+	$CH_3CH_2OCH_3$

Table AA.2 Reactions used for radicals

Reactions for Radicals							
1)	y($CH_2^{\bullet}CH_2CH_3$)	→	$CH_3CH_2CH_3$	+	y($CH_3CH_2CH_3$)	+	$CH_3CH^{\bullet}CH_3$
2)	y($CH_2^{\bullet}CH_2CH_3$)	→	$CH_3CH_2CH_2CH_3$	+	y($CH_3CH_2CH_3$)	+	$CH_3CH_2CH^{\bullet}CH_3$
3)	y($CH_2^{\bullet}CH_2CH_3$)	→	$CH_3CH_2CH_2CH_2CH_3$	+	y($CH_3CH_2CH_3$)	+	$CH_3CH_2CH_2CH^{\bullet}CH_3$
4)	y($CH_2^{\bullet}CH_2CH_2CH_3$)	→	$CH_3CH_2CH_3$	+	y($CH_3CH_2CH_2CH_3$)	+	$CH_3CH^{\bullet}CH_3$
5)	y($CH_2^{\bullet}CH_2CH_2CH_3$)	→	$CH_3CH_2CH_2CH_3$	+	y($CH_3CH_2CH_2CH_3$)	+	$CH_3CH_2CH^{\bullet}CH_3$
6)	y($CH_2^{\bullet}CH_2CH_2CH_3$)	→	$CH_3CH_2CH_2CH_2CH_3$	+	y($CH_3CH_2CH_2CH_3$)	+	$CH_3CH_2CH_2CH^{\bullet}CH_3$
7)	y($CH_2^{\bullet}CH_2CH_2CH_2CH_3$)	→	$CH_3CH_2CH_3$	+	y($CH_3CH_2CH_2CH_2CH_3$)	+	$CH_3CH^{\bullet}CH_3$
8)	y($CH_2^{\bullet}CH_2CH_2CH_2CH_3$)	→	$CH_3CH_2CH_2CH_3$	+	y($CH_3CH_2CH_2CH_2CH_3$)	+	$CH_3CH_2CH^{\bullet}CH_3$
9)	y($CH_2^{\bullet}CH_2CH_2CH_2CH_3$)	→	$CH_3CH_2CH_2CH_2CH_3$	+	y($CH_3CH_2CH_2CH_2CH_3$)	+	$CH_3CH_2CH_2CH^{\bullet}CH_3$

Table AA.3 and AA.4 summarize the enthalpy of reaction from the work reactions used to calculate the uncertainties for stable molecules and radicals, respectively.

Table AA.3 Calculated enthalpy of reactions for the parent ether molecules

Reactions	$\Delta_{rxn}H^{o}_{298}$				Δ(calc - ref)		
	B3LYP				B3LYP		
	6-31G(d,p)	6-31G(2d,2p)	CBS-QB3	Literature	6-31G(d,p)	6-31G(2d,2p)	CBS-QB3
1)	6.53	6.09	6.62	6.35	0.18	-0.26	0.28
2)	4.70	2.75	3.44	3.62	1.08	-0.87	-0.18
3)	6.97	6.78	7.33	6.90	0.07	-0.12	0.43
4)	5.14	3.44	4.15	4.17	0.97	-0.73	-0.02
5)	6.82	7.01	7.30	6.80	0.03	0.21	0.50
6)	4.99	3.67	4.12	4.07	0.93	-0.40	0.05

Units: kcal mol^{-1}

Table AA.4 Calculated enthalpy of reactions for radical species

Reactions	$\Delta_{rxn}H^{o}_{298}$				Δ(calc – ref)		
	B3LYP				B3LYP		
	6-31G(d,p)	6-31G(2d,2p)	CBS-QB3	Literature	6-31G(d,p)	6-31G(2d,2p)	CBS-QB3
1)	-10.17	-10.21	-10.34	-9.74	-0.43	-0.47	-0.60
2)	-9.95	-10.00	-10.11	-10.73	0.78	0.73	0.62
3)	-10.01	-10.06	-10.15	-10.52	0.51	0.46	0.37
4)	-0.96	-0.93	-1.50	-0.36	-0.60	-0.57	-0.14
5)	-0.73	-0.72	-1.28	-1.35	0.62	0.63	0.07
6)	0.80	-0.78	-1.31	-1.14	0.34	0.36	-0.17
7)	1.84	1.81	2.43	3.06	-1.22	-1.25	-0.63
8)	2.07	2.02	2.65	2.07	0.00	-0.05	0.08
9)	2.00	1.97	2.62	2.28	-0.28	-0.31	0.34

Units: kcal mol^{-1}

Table AA.5 summarizes the root mean squared (RMS) of the uncertainties reported in the literature for the reference species used in each of the reactions from

Table AA.3, stable molecules. The same procedure has been followed for data on radicals, Table AA.4.

Table AA.5 RMS of the uncertainties in each reaction

Parameters	Uncertainties In Ref Species	RMS
1)	± 0.12 ± 0.12 ± 0.12	0.12
2)	±0.14 ±0.12 ±0.16	0.14
3)	± 0.12 ± 0.26 ± 0.12	0.18
4)	±0.14 ±0.26 ±0.16	0.19
5)	± 0.12 ± 0.17 ± 0.12	0.14
6)	±0.14 ±0.17 ±0.16	0.16

Example for reaction 2:

$$RMS = \sqrt{\frac{\sum a_i^2}{n}} = \sqrt{\frac{(0.14)^2 + (0.12)^2 + (0.16)^2}{3}} = 0.14$$

Three sets of reactions are defined from Table AF.4:

SET 1: reactions 1 and 2, SET 2: reactions 3 and 4, SET 3: reactions 5 and 6.

Table AA.6 contains the results of the 95% confidence limits calculated for the three different sets of reactions, for the different studied methods.

Table AA.6 95% confidence limit for each of the work reaction sets and for the uncertainty in reference species in the work reactions of that set

Parameters	B3LYP/ 6-31G(d,p)	B3LYP/ 6-31G(2d,2p)	CBS-QB3	Reference species
SET 1				
s	0.64	0.43	0.32	0.01
$\left(t_{n-1}, \alpha/2\right)\frac{s}{\sqrt{n}} = 95\%cl$	1.58	1.07	0.79	0.04
SET 2				
s	0.64	0.43	0.32	0.01
$\left(t_{n-1}, \alpha/2\right)\frac{s}{\sqrt{n}} = 95\%cl$	1.58	1.07	0.79	0.03
SET 3				
s	0.64	0.43	0.32	0.01
$\left(t_{n-1}, \alpha/2\right)\frac{s}{\sqrt{n}} = 95\%cl$	1.58	1.07	0.79	0.03
RMS sets	1.58	1.07	0.79	0.03

$$95\%cl = \left(t_{n-1}, \alpha/2\right)\frac{s}{\sqrt{n}} = \left(t_2, 0.025\right)\frac{0.64}{\sqrt{3}} = 4.303\frac{0.64}{\sqrt{3}} = 1.58$$

The Root Mean Square is then calculated for the 3 sets.

Example for B3LYP/6-31G(d,p) (RMS of set 1, set 2 and set 3):

$$RMS = \sqrt{\frac{\sum a_i^2}{n}} = \sqrt{\frac{(1.58)^2 + (1.58)^2 + (1.58)^2}{3}} = 1.58$$

The Root Mean Square is taken for each of the two uncertainty types to account for the combined uncertainty from the work reactions, and from the reference species. Table AA.7 summarizes the results obtained for the uncertainty from the work reactions, and the uncertainty from the reference species.

Table AA.7 Calculated uncertainties for each method, for stable molecules

Parameters	**B3LYP/ 6-31G(d,p)**	**B3LYP/ 6-31G(2d,2p)**	**CBS-QB3**
Uncertainty from method	1.58	1.07	0.79
Uncertainty from reference species	0.03	0.03	0.03
RMS	±1.12	±0.76	±0.56

In order to account for the uncertainty from the work reactions, and uncertainty from the reference species, the Root Mean Square of the two values is calculated.

Example for B3LYP/6-31G(d,p):

$$RMS = \sqrt{\frac{\sum a_i^2}{n}} = \sqrt{\frac{(1.58)^2 + (0.03)^2}{2}} = 1.12$$

The same procedure has been followed for the determination of the uncertainties for the radicals, using the data from Table AA.4. The uncertainties calculated for the radicals are summarized in Table AA.8.

Table AA.8 Calculated uncertainties for each method, for radicals

Parameters	**B3LYP/ 6-31G(d,p)**	**B3LYP/ 6-31G(2d,2p)**	**CBS-QB3**
Uncertainty from Calculation method	1.90	1.89	1.59
Uncertainty from reference species	0.19	0.19	0.19
RMS	**±1.35**	**±1.34**	**±1.13**

APPENDIX AB

MERCURY NOX/SOX SPECIES – MOLECULAR GEOMETRIES

Appendix AB summarizes the molecular geometries of all the species calculated for the study of the mercury-halogen-NOx-SOx systems.

Table AB.1 Structural parameters for the optimized geometries at the CBS-QB3 level of theory

Molecule	Bond Distance (Å)		Angle (°)	
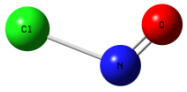	R(1,2)	1.1237	A(2,1,3)	113.1726
	R(1,3)	1.942		
ClNO				

Molecule	Bond Distance (Å)		Angle (°)	
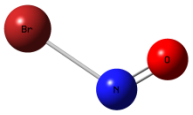	R(1,2)	1.1234	A(2,1,3)	114.1493
	R(1,3)	2.1043		
BrNO				

Molecule	Bond Distance (Å)		Angle (°)		Dihedral (°)	
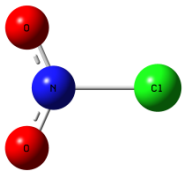	R(1,2)	1.8186	A(1,2,3)	114.3125	D(1,2,4,3)	-180.0
	R(2,3)	1.1825	A(1,2,4)	114.3125		
	R(2,4)	1.1825	A(3,2,4)	131.375		
$ClNO_2$						

Table AB.1 Structural parameters for the optimized geometries at the CBS-QB3 level of theory (Continued)

Molecule	Bond Distance (Å)		Angle (°)		Dihedral (°)	
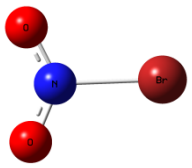	R(1,2)	1.1843	A(2,1,3)	130.7992	D(2,1,4,3)	180.0
	R(1,3)	1.1843	A(2,1,4)	114.6004		
	R(1,4)	1.9783	A(3,1,4)	114.6004		
$BrNO_2$						

Molecule	Bond Distance (Å)		Angle (°)		Dihedral (°)	
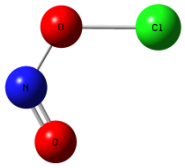	R(1,2)	1.6864	A(1,2,3)	115.8627	D(1,2,3,4)	0.0
	R(2,3)	1.4046	A(2,3,4)	115.9906		
	R(3,4)	1.1526				
ClONO-cis						

Molecule	Bond Distance (Å)		Angle (°)		Dihedral (°)	
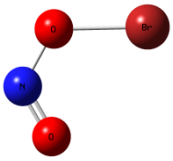	R(1,2)	1.8444	A(1,2,3)	117.2851	D(1,2,3,4)	0.0
	R(2,3)	1.3647	A(2,3,4)	116.9909		
	R(3,4)	1.16				
BrONO-cis						

Molecule	Bond Distance (Å)		Angle (°)		Dihedral (°)	
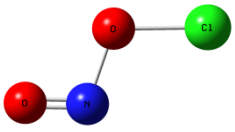	R(1,2)	1.4599	A(2,1,4)	109.5096	D(4,1,2,3)	180.0
	R(1,4)	1.6709	A(1,2,3)	108.506		
	R(2,3)	1.1456				
ClONO-trans						

Table AB.1 Structural parameters for the optimized geometries at the CBS-QB3 level of theory (Continued)

Molecule	Bond Distance (Å)		Angle (°)		Dihedral (°)	
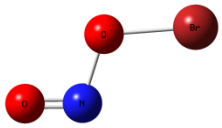	R(1,2)	1.8151	A(1,2,3)	110.4524	D(1,2,3,4)	180.0
	R(2,3)	1.4416	A(2,3,4)	108.7213		
	R(3,4)	1.1496				
BrONO-trans						

Molecule	Bond Distance (Å)		Angle (°)		Dihedral (°)	
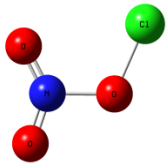	R(1,2)	1.4503	A(2,1,3)	109.6422	D(3,1,2,5)	180.0001
	R(1,3)	1.1824	A(2,1,4)	117.6656	D(4,1,2,5)	0.0001
	R(1,4)	1.1808	A(3,1,4)	132.6922	D(2,1,3,4)	-180.0
	R(2,5)	1.6665	A(1,2,5)	113.5317		
$ClONO_2$						

Molecule	Bond Distance (Å)		Angle (°)		Dihedral (°)	
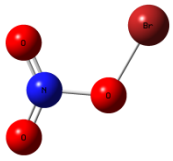	R(1,3)	1.8156	A(3,2,4)	110.3089	D(4,2,3,1)	-179.9996
	R(2,3)	1.4271	A(3,2,5)	118.1	D(5,2,3,1)	0.0005
	R(2,4)	1.1855	A(4,2,5)	131.591	D(3,2,4,5)	-180.0
	R(2,5)	1.1856	A(1,3,2)	115.0619		
$BrONO_2$						

Table AB.2 Structural parameters for the optimized geometries at the M06-2X/aug-cc-pVTZ-PP level of theory

Molecule	Bond Distance (Å)		Angle (°)	
	R(1,2)	1.1375	A(2,1,3)	115.929
	R(1,3)	3.4769		
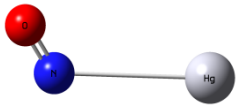				
HgNO				

Molecule	Bond Distance (Å)		Angle (°)		Dihedral (°)	
	R(1,2)	1.1802	A(2,1,3)	134.9286	D(2,1,3,4)	180.0
	R(1,3)	1.1802	A(2,4,3)	31.5451		
	R(1,4)	3.4069				
	R(2,4)	4.0102				
	R(3,4)	4.0102				
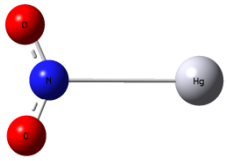						
$HgNO_2$						

Molecule	Bond Distance (Å)		Angle (°)		Dihedral (°)	
	R(1,2)	1.3422	A(2,1,4)	107.5075	D(4,1,2,3)	180.0
	R(1,4)	2.1744	A(1,2,3)	111.6678		
	R(2,3)	1.1795				
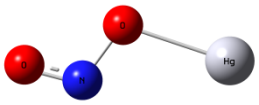						
HgONO						

Molecule	Bond Distance (Å)		Angle (°)		Dihedral (°)	
	R(1,2)	1.3035	A(2,1,3)	118.9752	D(3,1,2,5)	180.0
	R(1,3)	1.1964	A(2,1,4)	116.7675	D(4,1,2,5)	0.0
	R(1,4)	1.245	A(3,1,4)	124.2573	D(2,1,3,4)	-180.0
	R(2,5)	2.2423	A(1,2,5)	101.3483		
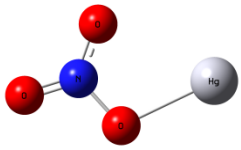						
$HgONO_2$						

Table AB.2 Structural parameters for the optimized geometries at the M06-2X/aug-cc-pVTZ-PP level of theory (Continued)

Molecule	Bond Distance (Å)		Angle (°)		Dihedral (°)	
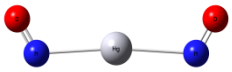	R(1,2)	1.1694	A(1,2,3)	113.346	D(2,3,4,5,1)	181.913
	R(2,3)	2.2713	A(3,4,5)	113.3461	D(2,3,4,5,2)	184.1139
	R(3,4)	2.2713			D(1,2,4,5)	-70.7012
	R(4,5)	1.1694				
NOHgNO						

Molecule	Bond Distance (Å)		Angle (°)		Dihedral (°)	
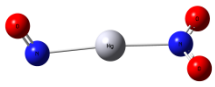	R(1,2)	1.2125	A(2,1,3)	124.5712	D(1,4,5,2,1)	178.951
	R(1,3)	1.2121	A(2,1,4)	117.5748	D(1,4,5,2,2)	185.5098
	R(1,4)	2.1823	A(3,1,4)	117.854	D(2,1,3,4)	179.943
	R(4,5)	2.2178	A(4,5,6)	114.2572	D(2,1,5,6)	115.4325
	R(5,6)	1.1579			D(3,1,5,6)	-65.7331
$NOHgNO_2$						

Molecule	Bond Distance (Å)		Angle (°)		Dihedral (°)	
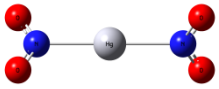	R(1,2)	1.2071	A(2,1,3)	125.9171	D(1,4,5,2,1)	180.0
	R(1,3)	1.2071	A(2,1,4)	117.0415	D(1,4,5,2,2)	179.9999
	R(1,4)	2.1037	A(3,1,4)	117.0414	D(2,1,5,6)	-85.32
	R(4,5)	2.1037	A(4,5,6)	117.0415	D(2,1,5,7)	94.68
	R(5,6)	1.2071	A(4,5,7)	117.0414	D(3,1,5,6)	94.68
	R(5,7)	1.2071	A(6,5,7)	125.9171	D(3,1,5,7)	-85.3199
NO_2HgNO_2						

Table AB.2 Structural parameters for the optimized geometries at the M06-2X/aug-cc-pVTZ-PP level of theory (Continued)

Molecule	Bond Distance (Å)		Angle (°)		Dihedral (°)	
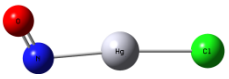	R(1,2)	1.1626	A(1,2,3)	114.5913	L(2,3,4,1,-1)	182.4704
	R(2,3)	2.193			L(2,3,4,1,-2)	179.9997
	R(3,4)	2.3422				
ClHgNO						

Molecule	Bond Distance (Å)		Angle (°)		Dihedral (°)	
	R(1,2)	1.1617	A(1,2,3)	114.6148	L(2,3,4,1,-1)	182.3864
	R(2,3)	2.2111			L(2,3,4,1,-2)	180.0012
	R(3,4)	2.4721				
BrHgNO						

Molecule	Bond Distance (Å)		Angle (°)		Dihedral (°)	
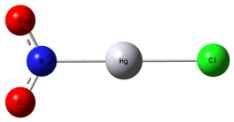	R(1,2)	1.2083	A(2,1,3)	125.4699	L(1,4,5,2,-1)	179.9999
	R(1,3)	1.2083	A(2,1,4)	117.2652	L(1,4,5,2,-2)	179.9998
	R(1,4)	2.098	A(3,1,4)	117.265	D(2,1,4,3)	-180.0
	R(4,5)	2.2728				
$ClHgNO_2$						

Molecule	Bond Distance (Å)		Angle (°)		Dihedral (°)	
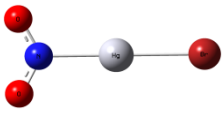	R(1,2)	1.2086	A(2,1,3)	125.3755	L(1,4,5,2,-1)	179.9998
	R(1,3)	1.2086	A(2,1,4)	117.312	L(1,4,5,2,-2)	180.0
	R(1,4)	2.1125	A(3,1,4)	117.3125	D(2,1,4,3)	180.0
	R(4,5)	2.3979				
$BrHgNO_2$						

Table AB.2 Structural parameters for the optimized geometries at the M06-2X/aug-cc-pVTZ-PP level of theory (Continued)

Molecule	Bond Distance (Å)		Angle (°)		Dihedral (°)	
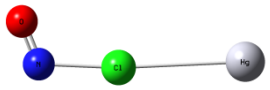	R(1,2)	1.1227	A(1,2,3)	113.0789	L(2,3,4,1,-1)	176.4862
	R(2,3)	1.9543			L(2,3,4,1,-2)	180.0068
	R(3,4)	3.4608				
HgClNO						

Molecule	Bond Distance (Å)		Angle (°)		Dihedral (°)	
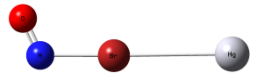	R(1,2)	1.1234	A(1,2,4)	114.0481	L(2,4,3,1,-1)	179.8033
	R(2,4)	2.1149			L(2,4,3,1,-2)	179.9894
	R(3,4)	3.4928				
HgBrNO						

Molecule	Bond Distance (Å)		Angle (°)		Dihedral (°)	
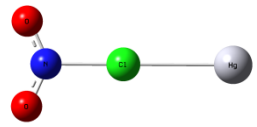	R(1,2)	1.1827	A(2,1,3)	131.3581	L(1,4,5,2,-1)	179.9998
	R(1,3)	1.1827	A(2,1,4)	114.321	L(1,4,5,2,-2)	180.0004
	R(1,4)	1.8309	A(3,1,4)	114.321	D(2,1,4,3)	-180.0
	R(4,5)	3.3335				
$HgClNO_2$						

Molecule	Bond Distance (Å)		Angle (°)		Dihedral (°)	
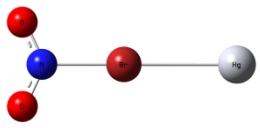	R(1,2)	1.1856	A(2,1,3)	130.5428	L(1,5,4,2,-1)	179.9999
	R(1,3)	1.1856	A(2,1,5)	114.7286	L(1,5,4,2,-2)	180.0059
	R(1,5)	1.9962	A(3,1,5)	114.7286	D(2,1,5,3)	-179.9999
	R(4,5)	3.2712				
$HgBrNO_2$						

Table AB.3 Structural parameters for the optimized geometries at the CBS-QB3 level of theory

Molecule	Bond Distance (Å)		Angle (°)	
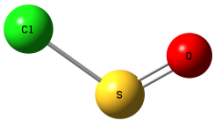	R(1,2)	1.4718	A(1,2,3)	110.5888
	R(2,3)	2.1205		
ClSO				

Molecule	Bond Distance (Å)		Angle (°)	
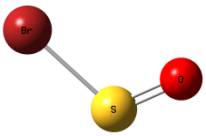	R(1,3)	1.4754	A(1,3,2)	111.149
	R(2,3)	2.2896		
BrSO				

Molecule	Bond Distance (Å)		Angle (°)		Dihedral (°)	
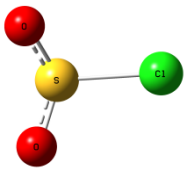	R(1,4)	2.1766	A(1,4,2)	108.2007	D(1,4,3,2)	126.785
	R(2,4)	1.4461	A(1,4,3)	108.2007		
	R(3,4)	1.4461	A(2,4,3)	122.4593		
$ClSO_2$						

Molecule	Bond Distance (Å)		Angle (°)		Dihedral (°)	
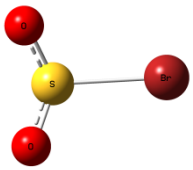	R(1,4)	1.4452	A(1,4,2)	121.7685	D(1,4,3,2)	135.2531
	R(2,4)	1.4452	A(1,4,3)	109.1335		
	R(3,4)	2.4067	A(2,4,3)	109.1335		
$BrSO_2$						

Table AB.4 Structural parameters for the optimized geometries at the M06-2X/aug-cc-pVTZ-PP level of theory

Molecule	Bond Distance (Å)		Angle (°)	
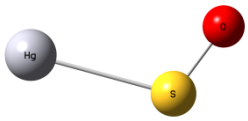	R(1,3)	1.4935	A(1,3,2)	109.8985
	R(2,3)	2.7135		
HgSO				

Table AB.4 Structural parameters for the optimized geometries at the M06-2X/aug-cc-pVTZ-PP level of theory (Continued)

Molecule	Bond Distance (Å)		Angle (°)		Dihedral (°)	
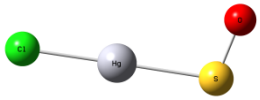	R(1,4)	1.5106	A(1,4,2)	104.727	L(3,2,4,1,-1)	178.7407
	R(2,3)	2.3129				180.0001
	R(2,4)	2.3751			L(3,2,4,1,-2)	
ClHgSO						

Molecule	Bond Distance (Å)		Angle (°)		Dihedral (°)	
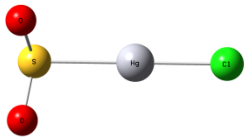	R(1,5)	1.453	A(1,5,2)	118.3845	L(4,3,5,2,-1)	179.946
	R(2,5)	1.453	A(1,5,3)	102.9182	L(4,3,5,2,-2)	179.7741
	R(3,4)	2.3323	A(2,5,3)	102.917	D(1,5,3,2)	123.5729
	R(3,5)	2.592				
$ClHgSO_2$						

Molecule	Bond Distance (Å)		Angle (°)		Dihedral (°)	
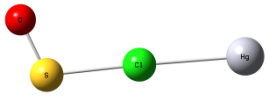	R(1,4)	1.4683	A(1,4,2)	108.8301	L(3,2,4,1,-1)	180.6413
	R(2,3)	3.5637			L(3,2,4,1,-2)	180.0013
	R(2,4)	2.0625				
HgClSO						

Table AB.4 Structural parameters for the optimized geometries at the M06-2X/aug-cc-pVTZ-PP level of theory (Continued)

Molecule	Bond Distance (Å)		Angle (°)		Dihedral (°)	
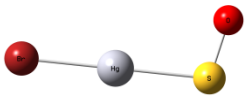	R(1,4)	1.511	A(1,4,2)	104.6959	L(3,2,4,1,-1)	178.6865
	R(2,3)	2.4392				180.0
	R(2,4)	2.3889			L(3,2,4,1,-2)	
BrHgSO						

Molecule	Bond Distance (Å)		Angle (°)		Dihedral (°)	
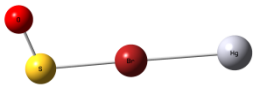	R(1,4)	1.4717	A(1,4,3)	109.3043	L(2,3,4,1,-1)	180.1172
	R(2,3)	3.5369			L(2,3,4,1,-2)	179.9912
	R(3,4)	2.2309				
HgBrSO						

APPENDIX AC

MERCURY NOX/SOX SPECIES – VIBRATIONAL FRQUENCIES

Appendix AH includes the frequencies of the species calculated for the study of the mercury-halogen-NOx-SOx systems.

Table AC.1 Vibrational frequencies calculated at the CBS-QB3 (B3LYP/6-31G(2d,d,p)) level

SYSTEM	Frequencies, cm^{-1}		
ClNO	344.1379	631.0684	1953.8594
BrNO	290.6012	589.8841	1955.2698
$ClNO_2$	436.7604 839.5914	438.9947 1389.8384	709.8594 1784.9082
$BrNO_2$	340.4053 836.5363	377.4931 1391.7899	667.2356 1765.3293
ClONO-cis	279.1858 711.8157	366.6925 913.7609	584.7105 1835.2520
BrONO-cis	231.4115 715.8055	375.6610 898.6193	565.2178 1794.4902
ClONO-trans	173.7339 742.7973	299.4196 941.6075	490.4209 1889.9874
BrONO-trans	163.6765 710.4244	261.1095 917.7294	463.1605 1870.2286
$ClONO_2$	119.6447 665.0754 883.7281	281.5960 785.0578 1392.4763	495.0539 856.7942 1829.7459
$BrONO_2$	111.1870 673.0082 873.1734	233.8938 794.1590 1385.6984	434.5396 828.4134 1800.3343

Table AC.2 Vibrational frequencies calculated at M06-2X/aug-cc-pVTZ-PP level

SYSTEM	Frequencies, cm^{-1}		
HgNO	40.0182	80.6432	2061.1633
$HgNO_2$	23.6275	25.9270	47.4659
	778.7504	1460.2693	1776.2609
HgONO	140.1928	156.9954	298.5436
	774.7463	982.3651	1727.8356
$HgONO_2$	90.0787	103.2219	249.0568
	729.0777	762.8912	856.0296
	1065.0692	1280.9644	1647.1384
NOHgNO	47.7978	86.3720	102.5690
	180.1315	235.3654	461.6967
	464.9814	1688.7995	1782.2319
$NOHgNO_2$	34.8430	60.7121	85.1735
	184.9655	202.4672	276.1673
	412.5632	542.0375	851.1346
	1448.8621	1613.0382	1770.9586
NO_2HgNO_2	26.7506	66.5823	68.1415
	224.5793	231.9550	248.1297
	316.2819	505.8974	512.0974
	856.9269	866.7654	1443.2390
	1454.5262	1652.4715	1653.2163

Table AC.2 Vibrational frequencies calculated at M06-2X/aug-cc-pVTZ-PP level (Continued)

SYSTEM	Frequencies, cm^{-1}		
ClHgNO	68.6335	92.5185	230.7417
	331.2737	536.3394	1753.7363
BrHgNO	58.6127	81.2120	192.1389
	261.6538	524.2100	1756.5895
$ClHgNO_2$	74.6097	84.4120	240.1364
	276.9310	377.6449	506.0458
	858.3483	1446.4912	1631.5732
$BrHgNO_2$	60.0896	68.5618	228.4119
	229.1491	299.4950	494.1586
	856.0003	1444.3781	1627.9933
HgClNO	33.4119	39.4585	72.3801
	350.5140	626.7613	1966.4360
HgBrNO	16.8448	28.9226	37.3887
	285.4924	583.2661	1949.3594
$HgClNO_2$	26.6425	37.2691	43.2581
	414.8723	433.9114	703.3778
	835.6835	1389.0691	1783.9427
$HgBrNO_2$	32.9334	32.9720	45.6744
	320.9700	369.0074	654.6317
	834.4423	1391.7386	1758.4123

Table AC.3 Vibrational frequencies calculated at the CBS-QB3 (B3LYP/6-31G(2d,d,p)) level

SYSTEM	**Frequencies, cm^{-1}**		
ClSO	283.7656	460.2215	1151.1414
BrSO	235.5088	388.6186	1140.0409
$ClSO_2$	242.5866 488.4661	251.7799 1086.5491	430.0513 1288.4493
$BrSO_2$	155.8874 490.4434	191.3924 1098.4656	358.9790 1303.8973

Table AC.4 Vibrational frequencies calculated at M06-2X/aug-cc-pVTZ-PP level

SYSTEM	Frequencies, cm^{-1}		
HgSO	89.5658	179.6974	1171.0538
ClHgSO	71.1327 329.9410	90.4178 367.2308	198.5188 1055.3292
$ClHgSO_2$	48.4907 129.6133 507.8116	48.6301 231.1786 1129.2452	78.5506 329.6655 1334.7963
HgClSO	24.0552 309.9322	25.9683 498.3895	35.8517 1211.5664
BrHgSO	57.5834 239.8448	75.8905 346.9986	185.1020 1060.1027
HgBrSO	22.9650 256.4556	25.7002 415.8727	36.1216 1199.2790

APPENDIX AD

MERCURY NOX/SOX SPECIES – WORK REACTIONS

Appendix AD summarizes the work reactions used for the determination of the heat of formation of the species calculated for the study of the mercury-halogen-NOx-SOx systems.

Table AD.1 Calculated enthalpies of formation at 298 K

Work Reactions		$\Delta_f H^o_{298}$ CBS-QB3	B3LYP/ LANL2DZ	B3LYP/ SDD	B2PLYP/ AVTZ	M06-2X/ AVTZ	Ref.
ClO							
$ClO + H_2O \rightarrow HCl + HO_2$		24.24	33.95	32.66	24.67	23.94	
$ClO + HOOH \rightarrow HOCl + HO_2$		23.97	26.54	26.31	24.60	25.14	
	Ave.	**24.10**	**30.25**	**29.49**	**24.64**	**24.54**	24.19
	σ	*0.19*	*5.24*	*4.49*	*0.05*	*0.85*	
HCl							
$HCl + HOOH \rightarrow HOCl + H_2O$		-22.33	-29.47	-28.41	-22.13	-20.86	
$HCl + NH_2OH \rightarrow HOCl + NH_3$		-21.29	-19.72	-18.67	-20.48	-20.66	
	Ave.	**-21.81**	**-24.59**	**-23.54**	**-21.31**	**-20.76**	-22.06
	σ	*0.74*	*6.89*	*6.89*	*1.17*	*0.14*	
HOCl							
$HOCl + H_2O \rightarrow HOOH + HCl$		-17.54	-10.40	-11.46	-17.74	-19.01	
$HOCl + NH_3 \rightarrow NH_2OH + HCl$		-18.58	-20.15	-21.20	-19.39	-19.21	
	Ave.	**-18.06**	**-15.28**	**-16.33**	**-18.56**	**-19.11**	-17.81
	σ	*0.74*	*6.89*	*6.89*	*1.17*	*0.14*	
ClNO							
$ClNO + CH_4 \rightarrow HNO + CH_3Cl$		12.21	7.11	6.39	7.38	13.52	
$ClNO + CH_3CH_3 \rightarrow HNO + CH_3CH_2Cl$		12.10	7.38	6.65	6.83	12.76	
	Ave.	**12.15**	**7.24**	**6.52**	**7.10**	**13.14**	12.36
	σ	*0.08*	*0.19*	*0.19*	*0.38*	*0.53*	
$ClNO_2$							
$ClNO_2 + HNO \rightarrow HNO_2 + ClNO$		2.55	5.05	4.76	4.71	1.46	
$ClNO_2 + CH_4 \rightarrow HNO_2 + CH_3Cl$		2.40	-0.20	-1.21	-0.27	2.62	
$ClNO_2 + CH_3CH_3 \rightarrow HNO_2 + CH_3CH_2Cl$		2.29	0.07	-0.95	-0.81	1.87	
	Ave.	**2.34**	**-0.07**	**-1.08**	**-0.54**	**2.24**	2.99
	σ	*0.08*	*0.19*	*0.19*	*0.38*	*0.53*	
ClONO-cis							
ClONO-cis + HNO → HONO-cis + ClNO		15.72	67.75	67.34	17.00	80.51	
$ClONO\text{-cis} + CH_4 \rightarrow HONO\text{-cis} + CH_3Cl$		15.57	6.27	5.08	12.01	15.88	
$ClONO\text{-cis} + CH_3CH_3 \rightarrow HONO\text{-cis} + CH_3CH_2Cl$		15.46	6.53	5.35	11.47	15.13	
	Ave.	**15.52**	**6.40**	**5.21**	**11.74**	**15.50**	---
	σ	*0.08*	*0.19*	*0.19*	*0.38*	*0.53*	

Units: kcal mol^{-1}

Table AD.1 Calculated enthalpies of formation at 298 K (Continued)

Work Reactions	$\Delta_f H^o_{298}$ CBS-QB3	B3LYP/ LANL2DZ	B3LYP/ SDD	B2PLYP/ AVTZ	M06-2X/ AVTZ	Ref.
ClONO-trans						
ClONO-trans + HNO → HONO-trans + ClNO	17.54	19.14	18.67	20.97	18.10	
ClONO-trans + CH_4 → HONO-trans + CH_3Cl	17.39	13.89	12.70	15.99	19.25	
ClONO-trans + CH_3CH_3 → HONO-trans + CH_3CH_2Cl	17.27	14.16	12.96	15.44	18.50	
Ave.	**17.33**	**14.03**	**12.83**	**15.71**	**18.88**	---
σ	*0.08*	*0.19*	*0.19*	*0.38*	*0.53*	
$ClONO_2$						
$ClONO_2$ → Cl + NO_3	4.91	19.35	17.80	3.15	7.24	
$ClONO_2$ + H_2O → HOCl + $HONO_2$	6.21	8.26	7.87	5.39	8.93	
$ClONO_2$ + Cl → Cl_2 + NO_3	6.63	-6.52	-5.26	-0.62	7.76	
Ave.	**6.42**	**0.87**	**1.30**	**2.38**	**8.35**	---
σ	*0.30*	*10.45*	*9.28*	*4.25*	*0.82*	

Units: kcal mol^{-1}

Table AD.1 Calculated enthalpies of formation at 298 K (Continued)

Work Reactions		$\Delta_f H^o_{298}$ CBS-QB3	B3LYP/ LANL2DZ	B3LYP/ SDD	B2PLYP/ AVTZ	M06-2X/ AVTZ	Ref.
BrO							
$BrO + H_2O \rightarrow HBr + HO_2$		30.56	36.93	37.89	29.45	30.17	
$BrO + HOOH \rightarrow HOBr + HO_2$		30.04	28.16	27.51	28.55	29.29	
	Ave.	**30.30**	**32.55**	**32.70**	**29.00**	**29.73**	30.0
	σ	*0.37*	*6.21*	*7.34*	*0.64*	*0.62*	
HBr							
$HBr + HOOH \rightarrow HOBr + H_2O$		-9.19	-17.45	-19.06	-9.58	-9.56	
$HBr + NH_2OH \rightarrow HOBr + NH_3$		-8.15	-7.70	-9.31	-7.93	-9.35	
	Ave.	**-8.67**	**-12.58**	**-14.18**	**-8.76**	**-9.46**	-8.67
	σ	*0.74*	*6.89*	*6.89*	*1.17*	*0.14*	
HOBr							
$HOBr + HCl \rightarrow HBr + HOCl$		-16.14	-15.02	-12.36	-15.56	-14.31	
$HOBr + H_2O \rightarrow HBr + HOOH$		-15.88	-7.62	-6.02	-15.49	-15.52	
$HOBr + NH_3 \rightarrow HBr + NH_2OH$		-16.93	-17.37	-15.76	-17.15	-15.72	
	Ave.	**-16.32**	**-13.34**	**-11.38**	**-16.06**	**-15.18**	-19.0
	σ	*0.54*	*5.09*	*4.95*	*0.94*	*0.76*	
BrNO							
$BrNO + CH_4 \rightarrow HNO + CH_3Br$		21.52	15.81	15.42	15.23	21.27	
$BrNO + CH_3CH_3 \rightarrow HNO + CH_3CH_2Br$		21.02	15.34	15.07	14.70	20.35	
	Ave.	**21.27**	**15.57**	**15.25**	**14.97**	**20.81**	19.60
	σ	*0.35*	*0.33*	*0.25*	*0.37*	*0.65*	
$BrNO_2$							
$BrNO_2 + HNO \rightarrow HNO_2 + BrNO$		9.16	10.28	10.32	10.49	7.78	
$BrNO_2 + CH_4 \rightarrow HNO_2 + CH_3Br$		11.07	6.49	6.15	6.12	9.45	
$BrNO_2 + CH_3CH_3 \rightarrow HNO_2 + CH_3CH_2Br$		10.58	6.02	5.79	5.60	8.53	
	Ave.	**10.83**	**6.26**	**5.97**	**5.86**	**8.99**	---
	σ	*0.35*	*0.33*	*0.25*	*0.37*	*0.65*	
BrONO-cis							
BrONO-cis + HNO → HONO-cis + BrNO		18.11	11.53	12.21	18.48	16.95	
BrONO-cis + CH_4 → HONO-cis + CH_3Br		20.02	7.74	8.04	14.11	18.62	
BrONO-cis + CH_3CH_3 → HONO-cis + CH_3CH_2Br		19.52	7.27	7.68	13.58	17.70	
	Ave.	**19.77**	**7.50**	**7.86**	**13.84**	**18.16**	---
	σ	*0.35*	*0.33*	*0.25*	*0.37*	*0.65*	
BrONO-trans							
BrONO-trans + HNO → HONO-trans + BrNO		20.32	19.61	20.13	23.22	21.37	
BrONO-trans + CH_4 → HONO-trans + CH_3Br		22.24	15.81	15.95	18.85	23.04	
BrONO-trans + CH_3CH_3 → HONO-trans + CH_3CH_2Br		21.74	15.34	15.59	18.33	22.12	
	Ave.	**21.99**	**15.58**	**15.77**	**18.59**	**22.58**	---
	σ	*0.35*	*0.33*	*0.25*	*0.37*	*0.65*	

Units: kcal mol^{-1}

Table AD.1 Calculated enthalpies of formation at 298 K (Continued)

Work Reactions	$\Delta_f H^o_{298}$ CBS-QB3	B3LYP/ LANL2DZ	B3LYP/ SDD	B2PLYP/ AVTZ	M06-2X/ AVTZ	Ref.
$BrONO_2$						
$BrONO_2 \rightarrow BrO + NO_2$	5.66	13.09	13.54	10.05	5.84	
$BrONO_2 + H_2O \rightarrow HOBr + HONO_2$	10.99	0.13	0.76	5.53	11.01	
$BrONO_2 \rightarrow Br + NO_3$	9.23	8.78	8.55	6.88	9.97	
Ave.	**8.63**	**7.33**	**7.62**	**7.48**	**8.94**	---
σ	*2.72*	*6.60*	*6.44*	*2.32*	*2.73*	

Units: kcal mol^{-1}

Table AD.1 Calculated enthalpies of formation at 298 K (Continued)

Work Reactions	$\Delta_f H^o_{298}$ B3LYP/ LANL2DZ	B3LYP/ SDD	B2PLYP/ AVTZ	M06-2X/ AVTZ	Ref.
HgNO					
$HgNO + CH_3Cl \rightarrow HgCH_3 + ClNO$	37.63	37.68	36.36	30.95	
$HgNO + Cl_2 \rightarrow HgCl + ClNO$	51.20	44.13	35.90	35.47	
$HgNO + Br_2 \rightarrow HgBr + BrNO$	48.85	44.27	37.62	36.73	
$HgNO + CH_3Br \rightarrow HgCH_3 + BrNO$	38.05	37.76	37.63	32.31	
Ave.	**43.93**	**40.96**	**36.88**	**33.87**	---
σ	*7.10*	*3.75*	*0.88*	*2.69*	
$HgNO_2$					
$HgNO_2 + CH_3Cl \rightarrow HgCH_3 + ClNO_2$	22.71	24.29	21.58	21.76	
$HgNO_2 + Cl_2 \rightarrow HgCl + ClNO_2$	36.29	30.75	21.11	26.28	
$HgNO_2 + Br_2 \rightarrow HgBr + BrNO_2$	35.28	31.91	23.64	27.81	
$HgNO_2 + CH_3Br \rightarrow HgCH_3 + BrNO_2$	24.48	25.40	23.65	23.38	
Ave.	**29.69**	**28.09**	**22.49**	**24.81**	---
σ	*7.08*	*3.80*	*1.34*	*2.74*	
HgONO					
$HgONO + CH_3Cl \rightarrow HgCH_3 + ClONO$	30.24	35.80	43.22	36.73	
$HgONO + Cl_2 \rightarrow HgCl + ClONO$	43.82	42.26	42.76	41.25	
$HgONO + Br_2 \rightarrow HgBr + BrONO$	43.78	43.72	45.01	42.03	
$HgONO + CH_3Br \rightarrow HgCH_3 + BrONO$	32.98	37.21	45.02	37.60	
Ave.	**37.70**	**39.75**	**44.00**	**39.40**	---
σ	*7.12*	*3.84*	*1.18*	*2.63*	
NOHgNO					
$NOHgNO + Cl \rightarrow HgNO + ClNO$	74.80	72.69	---	96.80	
$NOHgNO + Br \rightarrow HgNO + BrNO$	80.23	78.96	---	97.28	
$NOHgNO + Hg \rightarrow HgNO + HgNO$	83.54	80.95	---	98.66	
$NOHgNO + CH_3 \rightarrow HgNO + CH_3NO$	82.32	79.16	---	99.69	
Ave.	**80.22**	**77.94**	**---**	**98.11**	---
σ	*3.87*	*3.61*	---	*1.32*	
$NOHgNO_2$					
$NOHgNO_2 + Cl \rightarrow HgNO + ClNO_2$	36.64	35.92	52.50	54.29	
$NOHgNO_2 + Br \rightarrow HgNO + BrNO_2$	43.45	43.24	58.02	55.06	
$NOHgNO_2 + Hg \rightarrow HgNO + HgNO_2$	51.23	48.50	56.76	56.28	
$NOHgNO_2 + Cl \rightarrow HgNO_2 + ClNO$	42.49	40.24	58.23	54.42	
$NOHgNO_2 + Br \rightarrow HgNO_2 + BrNO$	47.93	46.52	62.92	54.90	
$NOHgNO_2 + CH_3 \rightarrow HgNO_2 + CH_3NO$	50.01	46.71	55.35	57.31	
Ave.	**45.29**	**43.52**	**57.30**	**55.38**	---
σ	*5.49*	*4.75*	*3.47*	*1.18*	
NO_2HgNO_2					
$NOHgNO_2 + Cl \rightarrow HgNO_2 + ClNO_2$	8.82	7.60	24.02	19.32	
$NOHgNO_2 + Br \rightarrow HgNO_2 + BrNO_2$	15.63	14.92	29.54	20.10	
$NOHgNO_2 + Hg \rightarrow HgNO_2 + HgNO_2$	23.42	20.18	28.27	21.31	
Ave.	**15.95**	**14.23**	**27.28**	**20.24**	---
σ	*7.30*	*6.32*	*2.89*	*1.00*	

Units: kcal mol^{-1}

Table AD.1 Calculated enthalpies of formation at 298 K (Continued)

Work Reactions	$\Delta_f H^o_{298}$ B3LYP/ LANL2DZ	B3LYP/ SDD	B2PLYP/ AVTZ	M06-2X/ AVTZ	Ref.
ClHgNO					
$ClHgNO + CH_3 \rightarrow HgNO + CH_3Cl$	19.08	16.90	27.10	30.63	
$ClHgNO + Cl_2 \rightarrow HgCl_2 + ClNO$	30.41	25.18	28.74	27.43	
$ClHgNO + Br_2 \rightarrow HgBr_2 + ClNO$	25.47	22.03	28.38	27.99	
$ClHgNO + OH \rightarrow HgNO + HOCl$	14.07	12.82	27.06	29.86	
Ave.	**22.26**	**19.23**	**27.82**	**28.98**	---
σ	*7.16*	*5.47*	*0.87*	*1.52*	
$ClHgNO_2$					
$ClHgNO_2 + CH_3 \rightarrow HgNO_2 + CH_3Cl$	-10.26	-12.04	-3.34	-6.09	
$ClHgNO_2 + Cl_2 \rightarrow HgCl_2 + ClNO_2$	-4.79	-8.08	-7.43	-9.42	
$ClHgNO_2 + Br_2 \rightarrow HgBr_2 + ClNO_2$	-9.72	-11.23	-7.78	-8.86	
$ClHgNO_2 + OH \rightarrow HgNO_2 + HOCl$	-15.27	-16.12	-3.39	-6.86	
Ave.	**-10.01**	**-11.87**	**-5.48**	**-7.81**	---
σ	*4.28*	*3.31*	*2.45*	*1.59*	
HgClNO					
$HgClNO + CH_3 \rightarrow HgCH_3 + ClNO$	23.15	23.19	24.42	24.64	
$HgClNO + Cl_2 \rightarrow HgCl_2 + ClNO$	30.72	27.66	23.56	24.36	
$HgClNO + Br_2 \rightarrow HgBr_2 + ClNO$	25.79	24.51	23.21	24.92	
$HgClNO + OH \rightarrow HgNO + HOCl$	14.39	15.30	21.88	26.79	
Ave.	**23.51**	**22.67**	**23.27**	**25.18**	---
σ	*6.84*	*5.26*	*1.06*	*1.10*	
$HgClNO_2$					
$HgClNO_2 + CH_3 \rightarrow HgCH_3 + ClNO_2$	7.42	9.25	11.68	13.17	
$HgClNO_2 + Cl_2 \rightarrow HgCl_2 + ClNO_2$	17.33	16.07	13.17	15.23	
$HgClNO_2 + Br_2 \rightarrow HgBr_2 + ClNO_2$	12.40	12.91	12.81	15.79	
$HgClNO_2 + OH \rightarrow HgNO_2 + HOCl$	6.85	8.03	17.21	17.79	
Ave.	**11.00**	**11.57**	**13.72**	**15.49**	---
σ	*4.90*	*3.65*	*2.41*	*1.90*	

Units: kcal mol^{-1}

Table AD.1 Calculated enthalpies of formation at 298 K (Continued)

Work Reactions		$\Delta_f H^\circ_{298}$ B3LYP/ LANL2DZ	B3LYP/ SDD	B2PLYP/ AVTZ	M06-2X/ AVTZ	Ref.
BrHgNO						
$BrHgNO + CH_3 \rightarrow HgNO + CH_3Br$		29.01	28.07	34.65	37.45	
$BrHgNO + Cl_2 \rightarrow HgCl_2 + BrNO$		40.77	36.44	37.55	35.61	
$BrHgNO + Br_2 \rightarrow HgBr_2 + BrNO$		35.83	33.28	37.19	36.17	
$BrHgNO + OH \rightarrow HgNO + HOBr$		23.01	21.22	33.29	34.47	
	Ave.	**32.16**	**29.75**	**35.67**	**35.93**	---
	σ	*7.77*	*6.65*	*2.05*	*1.24*	
$BrHgNO_2$						
$BrHgNO_2 + CH_3 \rightarrow HgNO_2 + CH_3Br$		-0.81	-1.25	4.08	0.45	
$BrHgNO_2 + Cl_2 \rightarrow HgCl_2 + BrNO_2$		6.46	3.84	2.09	-1.23	
$BrHgNO_2 + Br_2 \rightarrow HgBr_2 + BrNO_2$		1.53	0.69	1.73	-0.67	
$BrHgNO_2 + OH \rightarrow HgNO_2 + HOBr$		-6.81	-8.10	2.72	-2.54	
	Ave.	**0.09**	**-1.20**	**2.65**	**-1.00**	---
	σ	*5.51*	*5.05*	*1.03*	*1.24*	
HgBrNO						
$HgBrNO + CH_3 \rightarrow HgCH_3 + BrNO$		32.36	31.90	33.18	34.39	
$HgBrNO + Cl_2 \rightarrow HgCl_2 + BrNO$		39.93	36.38	32.32	34.11	
$HgBrNO + Br_2 \rightarrow HgBr_2 + BrNO$		35.00	33.22	31.96	34.67	
$HgBrNO + OH \rightarrow HgNO + HOBr$		22.17	21.16	28.06	32.96	
	Ave.	**32.36**	**30.67**	**31.38**	**34.03**	---
	σ	*7.48*	*6.61*	*2.27*	*0.75*	
$HgBrNO_2$						
$HgBrNO_2 + CH_3 \rightarrow HgCH_3 + BrNO_2$		18.23	19.57	21.10	22.79	
$HgBrNO_2 + Cl_2 \rightarrow HgCl_2 + BrNO_2$		25.80	24.05	20.24	22.51	
$HgBrNO_2 + Br_2 \rightarrow HgBr_2 + BrNO_2$		20.87	20.89	19.88	23.07	
$HgBrNO_2 + OH \rightarrow HgNO_2 + HOBr$		12.53	12.11	20.88	21.20	
	Ave.	**19.36**	**19.16**	**20.52**	**22.39**	---
	σ	*5.53*	*5.06*	*0.56*	*0.83*	

Units: kcal mol^{-1}

Table AD.1 Calculated enthalpies of formation at 298 K (Continued)

Work Reactions	$\Delta_f H^o_{298}$ CBS-QB3	B3LYP/ LANL2DZ	B3LYP/ SDD	B2PLYP/ AVTZ	M06-2X/ AVTZ	Ref.
ClSO						
$ClSO + CH_4 \rightarrow HSO + CH_3Cl$	-24.29	-17.38	-19.31	-24.34	-22.16	
$ClSO + CH_3CH_3 \rightarrow HSO + CH_3CH_2Cl$	-24.41	-17.11	-19.05	-24.89	-22.91	
$ClSO + HCl \rightarrow HSO + Cl_2$	-25.04	-14.27	-13.81	-25.12	-22.51	
Ave.	**-24.58**	**-16.25**	**-17.39**	**-24.78**	**-22.53**	*-24.50*[259]
σ	*0.40*	*0.19*	*0.19*	*0.38*	*0.53*	
$ClSO_2$						
$ClSO_2 + CH_4 \rightarrow HSO_2 + CH_3Cl$	-57.19	-57.40	-60.62	-57.53	-55.92	
$ClSO_2 + CH_3CH_3 \rightarrow HSO_2 + CH_3CH_2Cl$	-57.30	-57.14	-60.35	-58.07	-56.67	
$ClSO_2 + HCl \rightarrow HSO_2 + Cl_2$	-57.93	-54.30	-55.11	-58.30	-56.28	
						-53.95[260]
Ave.	**-57.47**	**-56.28**	**-58.69**	**-57.96**	**-56.29**	*-63.13*[261]
						-49.65[262]
σ	*0.40*	*0.19*	*0.19*	*0.38*	*0.53*	
BrSO						
$BrSO + CH_4 \rightarrow HSO + CH_3Br$	-12.35	-8.97	-10.15	-14.64	-12.85	
$BrSO + CH_3CH_3 \rightarrow HSO + CH_3CH_2Br$	-12.85	-9.44	-10.51	-15.16	-13.77	
$BrSO + HBr \rightarrow HSO + Br_2$	-17.25	-6.03	-9.47	-14.93	-12.13	
Ave.	**-14.15**	**-8.15**	**-10.04**	**-14.91**	**-12.91**	
σ	*2.70*	*0.33*	*0.25*	*0.37*	*0.65*	
$BrSO_2$						
$BrSO_2 + CH_4 \rightarrow HSO_2 + CH_3Br$	-46.70	-42.47	-47.62	-50.20	-48.86	
$BrSO_2 + CH_3CH_3 \rightarrow HSO_2 + CH_3CH_2Br$	-47.20	-42.94	-47.97	-50.72	-49.78	
$BrSO_2 + HBr \rightarrow HSO_2 + Br_2$	-51.60	-39.54	-46.93	-50.49	-48.14	
Ave.	**-48.50**	**-41.65**	**-47.51**	**-50.47**	**-48.93**	*-49.80*[260]
σ	*2.70*	*0.33*	*0.25*	*0.37*	*0.65*	

Units: kcal mol^{-1}

Table AD.1 Calculated enthalpies of formation at 298 K (Continued)

Work Reactions	$\Delta_f H^o_{298}$ B3LYP/ LANL2DZ	B3LYP/ SDD	B2PLYP/ AVTZ	M06-2X/ AVTZ	Ref.
HgSO					
$HgSO + CH_3Cl \rightarrow HgCH_3 + ClSO$	19.97	23.00	33.44	33.95	
$HgSO + Cl_2 \rightarrow HgCl + ClSO$	33.55	29.46	32.97	38.47	
$HgSO + Br_2 \rightarrow HgBr + BrSO$	32.79	30.78	34.15	39.48	
$HgSO + CH_3Br \rightarrow HgCH_3 + BrSO$	21.99	24.27	34.16	35.06	
Ave.	**27.07**	**26.87**	**33.68**	**36.74**	---
σ	*7.09*	*3.82*	*0.58*	*2.66*	

Units: kcal mol^{-1}

Table AD.1 Calculated enthalpies of formation at 298 K (Continued)

Work Reactions		$\Delta_f H^o_{298}$ B3LYP/ LANL2DZ	B3LYP/ SDD	B2PLYP/ AVTZ	M06-2X/ AVTZ	Ref.
ClHgSO						
$ClHgSO + CH_3 \rightarrow HgSO + CH_3Cl$		-13.41	-16.54	-10.43	-12.36	
$ClHgSO + Cl_2 \rightarrow HgCl_2 + ClSO$		-23.46	-26.66	-15.44	-16.29	
$ClHgSO + Br_2 \rightarrow HgBr_2 + ClSO$		-28.39	-29.81	-15.79	-15.73	
$ClHgSO + OH \rightarrow HgSO + HOCl$		-18.42	-20.62	-10.47	-13.13	
	Ave.	**-20.92**	**-23.41**	**-13.03**	**-14.38**	---
	σ	*6.45*	*5.96*	*2.98*	*1.92*	
$ClHgSO_2$						
$ClHgSO_2 + CH_3 \rightarrow HgSO_2 + CH_3Cl$		-72.14	-67.66	-54.17	-57.68	
$ClHgSO_2 + Cl_2 \rightarrow HgCl_2 + ClSO_2$		-66.12	-64.03	-59.44	-61.84	
$ClHgSO_2 + Br_2 \rightarrow HgBr_2 + ClSO_2$		-71.05	-67.18	-59.79	-61.28	
$ClHgSO_2 + OH \rightarrow HgSO_2 + HOCl$		-77.14	-71.74	-54.22	-58.45	
	Ave.	**-71.61**	**-67.65**	**-56.91**	**-59.81**	---
	σ	*4.52*	*3.17*	*3.13*	*2.06*	
HgClSO						
$HgClSO + CH_3 \rightarrow HgCH_3 + ClSO$		-17.19	-14.88	-12.12	-10.66	
$HgClSO + Cl_2 \rightarrow HgCl_2 + ClSO$		-9.62	-10.41	-12.97	-10.94	
$HgClSO + Br_2 \rightarrow HgBr_2 + ClSO$		-14.55	-13.56	-13.33	-10.38	
$HgClSO + OH \rightarrow HgSO + HOCl$		-4.58	-4.37	-8.01	-7.79	
	Ave.	**-11.48**	**-10.81**	**-11.61**	**-9.94**	---
	σ	*5.57*	*4.68*	*2.45*	*1.46*	
BrHgSO						
$BrHgSO + CH_3 \rightarrow HgSO + CH_3Br$		-3.56	-5.56	-2.64	-5.44	
$BrHgSO + Cl_2 \rightarrow HgCl_2 + BrSO$		-9.88	-12.71	-5.22	-6.55	
$BrHgSO + Br_2 \rightarrow HgBr_2 + BrSO$		-14.82	-15.87	-5.58	-5.99	
$BrHgSO + OH \rightarrow HgSO + HOBr$		-9.56	-12.41	-3.99	-8.43	
	Ave.	**-9.46**	**-11.64**	**-4.36**	**-6.60**	---
	σ	*4.61*	*4.34*	*1.33*	*1.30*	
HgBrSO						
$HgBrSO + CH_3 \rightarrow HgCH_3 + BrSO$		-4.73	-2.64	-0.43	0.91	
$HgBrSO + Cl_2 \rightarrow HgCl_2 + BrSO$		2.84	1.84	-1.28	0.63	
$HgBrSO + Br_2 \rightarrow HgBr_2 + BrSO$		-2.09	-1.32	-1.64	1.19	
$HgBrSO + OH \rightarrow HgSO + HOBr$		3.17	2.14	-0.05	-1.25	
	Ave.	**-0.20**	**0.01**	**-0.85**	**0.37**	---
	σ	*3.86*	*2.35*	*0.74*	*1.10*	

Units: kcal mol^{-1}

APPENDIX AE

MERCURY NOX/SOX SPECIES – ENTROPY AND HEAT CAPACITY

Appendix AE includes the entropy *(S)* and heat capacity *(Cp)* versus temperature for the species calculated for the study of the mercury-halogen-NOx-SOx systems.

Table AE.1 Entropy *(S)* and heat capacity *(Cp) vs.* temperature

T	ClNO		BrNO		$ClNO_2$		$BrNO_2$	
(K)	S	Cp	S	Cp	S	Cp	S	Cp
5	28.161	7.949	30.540	7.949	31.156	7.949	33.354	7.949
50	46.464	7.949	48.843	7.949	49.459	7.950	51.658	7.953
100	51.976	7.968	54.356	7.978	54.996	8.102	57.225	8.222
150	55.229	8.121	57.622	8.172	58.370	8.631	60.672	8.863
200	57.602	8.396	60.014	8.478	60.951	9.369	63.326	9.630
250	59.507	8.684	61.938	8.775	63.126	10.150	65.558	10.397
298.15	61.058	8.930	63.505	9.016	64.976	10.869	67.449	11.090
300	61.113	8.938	63.561	9.025	65.043	10.895	67.518	11.116
400	63.743	9.352	66.214	9.419	68.363	12.206	70.893	12.374
500	65.868	9.698	68.352	9.749	71.206	13.276	73.769	13.405
600	67.664	10.007	70.156	10.045	73.705	14.130	76.289	14.232
700	69.228	10.279	71.724	10.308	75.936	14.803	78.534	14.885
800	70.616	10.512	73.116	10.535	77.948	15.331	80.557	15.398
900	71.866	10.709	74.368	10.728	79.779	15.746	82.395	15.802
1000	73.003	10.874	75.507	10.889	81.456	16.075	84.077	16.123
1500	77.521	11.372	80.029	11.378	88.176	16.985	90.811	17.009
2000	80.826	11.592	83.336	11.596	93.120	17.357	95.761	17.371
2500	83.426	11.705	85.937	11.707	97.015	17.540	99.658	17.550
3000	85.566	11.769	88.077	11.771	100.223	17.643	102.867	17.649
3500	87.384	11.809	89.895	11.810	102.948	17.706	105.593	17.711
4000	88.962	11.835	91.474	11.836	105.315	17.747	107.961	17.751
4500	90.358	11.853	92.869	11.854	107.407	17.776	110.053	17.779
5000	91.607	11.866	94.119	11.867	109.281	17.796	111.928	17.799

Units: S(cal mol^{-1}) and Cp(kcal mol^{-1} K^{-1})

Table AE.1 Entropy *(S)* and heat capacity *(Cp) vs.* temperature (Continued)

T (K)	ClONO-cis		BrONO-cis		ClONO-trans		BrONO-trans	
	S	Cp	S	Cp	S	Cp	S	Cp
5	30.980	7.949	33.133	7.949	30.527	7.949	32.631	7.949
50	49.283	7.955	51.437	7.954	48.833	7.976	50.943	8.011
100	54.861	8.274	57.009	8.259	54.497	8.550	56.689	8.757
150	58.357	9.079	60.501	9.077	58.139	9.497	60.427	9.754
200	61.103	10.072	63.249	10.090	61.006	10.467	63.368	10.725
250	63.457	11.040	65.608	11.072	63.439	11.359	65.857	11.601
298.15	65.473	11.865	67.631	11.904	65.505	12.108	67.965	12.330
300	65.547	11.894	67.705	11.934	65.580	12.135	68.041	12.356
400	69.162	13.230	71.333	13.278	69.248	13.358	71.766	13.534
500	72.223	14.192	74.405	14.244	72.330	14.254	74.884	14.394
600	74.877	14.908	77.069	14.960	74.992	14.932	77.568	15.045
700	77.218	15.451	79.417	15.501	77.334	15.454	79.927	15.548
800	79.310	15.871	81.516	15.917	79.426	15.863	82.029	15.940
900	81.199	16.198	83.410	16.240	81.313	16.184	83.926	16.250
1000	82.919	16.457	85.135	16.495	83.032	16.440	85.651	16.496
1500	89.751	17.173	91.979	17.195	89.857	17.158	92.493	17.187
2000	94.737	17.466	96.970	17.480	94.840	17.456	97.481	17.473
2500	98.652	17.611	100.887	17.621	98.753	17.604	101.397	17.615
3000	101.871	17.693	104.107	17.699	101.970	17.687	104.617	17.695
3500	104.602	17.743	106.839	17.748	104.701	17.739	107.348	17.745
4000	106.974	17.776	109.211	17.779	107.072	17.772	109.720	17.777
4500	109.069	17.798	111.307	17.801	109.167	17.796	111.815	17.799
5000	110.945	17.815	113.183	17.817	111.043	17.812	113.691	17.815

Units: S(cal mol^{-1}) and Cp(kcal mol^{-1} K^{-1})

Table AE.1 Entropy *(S)* and heat capacity *(Cp) vs.* temperature (Continued)

T (K)	$ClONO_2$		$BrONO_2$		HgNO		$HgNO_2$	
	S	Cp	S	Cp	S	Cp	S	Cp
5	32.903	7.949	34.853	7.949	35.000	7.949	37.652	8.013
50	51.212	7.989	53.174	8.058	54.010	9.241	60.076	11.552
100	56.908	8.636	59.004	8.951	60.612	9.727	68.197	11.828
150	60.606	9.727	62.844	10.093	64.582	9.840	73.014	11.943
200	63.582	11.055	65.922	11.389	67.419	9.881	76.474	12.137
250	66.199	12.443	68.608	12.731	69.626	9.903	79.210	12.408
298.15	68.500	13.706	70.957	13.954	71.372	9.921	81.421	12.712
300	68.585	13.753	71.043	13.999	71.434	9.921	81.500	12.724
400	72.857	15.952	75.377	16.138	74.296	9.988	85.254	13.417
500	76.604	17.618	79.161	17.766	76.537	10.114	88.323	14.106
600	79.932	18.869	82.514	18.990	78.395	10.281	90.951	14.724
700	82.915	19.814	85.514	19.915	79.994	10.462	93.261	15.244
800	85.610	20.535	88.221	20.620	81.402	10.637	95.325	15.670
900	88.062	21.091	90.683	21.164	82.665	10.796	97.191	16.014
1000	90.308	21.526	92.935	21.588	83.809	10.935	98.894	16.292
1500	99.299	22.706	101.945	22.739	88.340	11.384	105.674	17.081
2000	105.905	23.180	108.559	23.200	91.647	11.595	110.639	17.411
2500	111.105	23.412	113.763	23.425	94.248	11.705	114.544	17.575
3000	115.386	23.542	118.046	23.551	96.388	11.769	117.757	17.667
3500	119.022	23.621	121.682	23.628	98.205	11.808	120.485	17.723
4000	122.180	23.674	124.841	23.679	99.784	11.835	122.854	17.761
4500	124.970	23.709	127.632	23.714	101.179	11.853	124.947	17.786
5000	127.470	23.735	130.132	23.739	102.429	11.866	126.822	17.805

Units: S(cal mol^{-1}) and Cp(kcal mol^{-1} K^{-1})

Table AE.1 Entropy *(S)* and heat capacity *(Cp) vs.* temperature (Continued)

T (K)	HgONO		NOHgNO		$NOHgNO_2$		NO_2HgNO_2	
	S	Cp	S	Cp	S	Cp	S	Cp
5	35.538	7.949	36.775	7.949	38.107	7.949	39.059	7.949
50	53.966	8.429	56.217	10.581	58.271	11.256	59.332	11.223
100	60.240	9.787	64.566	13.581	67.159	14.581	68.185	14.703
150	64.398	10.725	70.457	15.485	73.531	16.863	74.709	17.530
200	67.583	11.432	75.101	16.774	78.615	18.476	80.057	19.654
250	70.203	12.071	78.943	17.641	82.874	19.688	84.630	21.345
298.15	72.379	12.643	82.103	18.236	86.425	20.634	88.511	22.727
300	72.457	12.665	82.216	18.256	86.553	20.667	88.651	22.777
400	76.247	13.694	87.597	19.150	92.726	22.269	95.546	25.189
500	79.394	14.514	91.950	19.873	97.842	23.591	101.386	27.167
600	82.100	15.155	95.630	20.496	102.242	24.683	106.486	28.764
700	84.475	15.653	98.830	21.025	106.116	25.567	111.019	30.028
800	86.591	16.040	101.667	21.463	109.578	26.274	115.096	31.020
900	88.499	16.343	104.217	21.822	112.707	26.837	118.797	31.799
1000	90.233	16.582	106.532	22.115	115.558	27.286	122.180	32.415
1500	97.103	17.239	115.685	22.962	126.901	28.547	135.701	34.112
2000	102.104	17.507	122.347	23.322	135.195	29.066	145.622	34.799
2500	106.026	17.638	127.572	23.503	141.711	29.323	153.427	35.137
3000	109.249	17.712	131.867	23.604	147.071	29.468	159.851	35.326
3500	111.983	17.757	135.511	23.667	151.621	29.556	165.306	35.442
4000	114.356	17.786	138.674	23.708	155.572	29.614	170.044	35.517
4500	116.453	17.807	141.468	23.737	159.062	29.655	174.231	35.570
5000	118.329	17.822	143.970	23.758	162.188	29.683	177.980	35.608

Units: S(cal mol^{-1}) and Cp(kcal mol^{-1} K^{-1})

Table AE.1 Entropy *(S)* and heat capacity *(Cp) vs.* temperature (Continued)

T (K)	ClHgNO		BrHgNO		$ClHgNO_2$		$BrHgNO_2$	
	S	Cp	S	Cp	S	Cp	S	Cp
5	35.825	7.949	37.363	7.949	37.779	7.949	39.078	7.949
50	54.690	9.213	56.426	9.538	56.754	9.335	58.357	9.666
100	61.624	10.963	63.695	11.559	63.853	11.450	65.797	12.104
150	66.350	12.374	68.653	12.886	68.883	13.413	71.096	14.043
200	70.055	13.368	72.487	13.754	72.954	14.885	75.330	15.382
250	73.116	14.047	75.623	14.335	76.400	15.996	78.874	16.376
298.15	75.632	14.510	78.183	14.731	79.293	16.855	81.827	17.151
300	75.722	14.525	78.274	14.744	79.397	16.885	81.933	17.179
400	79.996	15.178	82.599	15.312	84.456	18.289	87.060	18.476
500	83.436	15.649	86.063	15.738	88.659	19.380	91.298	19.508
600	86.324	16.026	88.965	16.089	92.271	20.235	94.930	20.329
700	88.818	16.332	91.467	16.379	95.443	20.900	98.114	20.972
800	91.015	16.581	93.670	16.616	98.269	21.417	100.949	21.474
900	92.980	16.781	95.639	16.809	100.816	21.821	103.502	21.866
1000	94.757	16.943	97.418	16.965	103.132	22.138	105.822	22.176
1500	101.729	17.407	104.397	17.416	112.302	23.006	115.002	23.023
2000	106.767	17.602	109.437	17.607	118.974	23.355	121.679	23.365
2500	110.707	17.699	113.377	17.703	124.206	23.526	126.913	23.533
3000	113.939	17.754	116.610	17.757	128.505	23.622	131.212	23.627
3500	116.678	17.788	119.350	17.790	132.151	23.681	134.859	23.684
4000	119.055	17.811	121.727	17.812	135.316	23.719	138.024	23.722
4500	121.154	17.826	123.826	17.827	138.111	23.746	140.820	23.748
5000	123.033	17.837	125.704	17.838	140.614	23.765	143.323	23.766

Units: S(cal mol^{-1}) and Cp(kcal mol^{-1} K^{-1})

Table AE.1 Entropy *(S)* and heat capacity *(Cp) vs.* temperature (Continued)

T (K)	HgClNO		HgBrNO		$HgClNO_2$		$HgBrNO_2$	
	S	Cp	S	Cp	S	Cp	S	Cp
5	38.067	7.952	38.976	7.987	39.791	7.955	40.474	7.963
50	59.062	11.146	61.623	11.668	61.710	11.508	62.524	11.540
100	67.093	12.051	69.944	12.449	69.878	12.156	70.805	12.539
150	72.128	12.834	75.142	13.224	74.992	13.188	76.125	13.785
200	75.918	13.521	79.038	13.862	78.943	14.336	80.251	14.926
250	78.996	14.062	82.186	14.347	82.259	15.398	83.690	15.912
298.15	81.508	14.461	84.744	14.697	85.050	16.298	86.564	16.733
300	81.598	14.474	84.835	14.709	85.151	16.331	86.668	16.762
400	85.847	15.060	89.141	15.223	90.067	17.855	91.690	18.160
500	89.256	15.490	92.581	15.610	94.184	19.033	95.865	19.257
600	92.112	15.846	95.457	15.938	97.738	19.949	99.455	20.120
700	94.578	16.147	97.936	16.220	100.869	20.659	102.610	20.795
800	96.751	16.400	100.118	16.460	103.665	21.211	105.422	21.322
900	98.696	16.610	102.068	16.661	106.189	21.643	107.958	21.735
1000	100.455	16.785	103.833	16.829	108.488	21.984	110.266	22.061
1500	107.375	17.309	110.766	17.331	117.611	22.924	119.411	22.962
2000	112.391	17.540	115.786	17.553	124.265	23.306	126.074	23.328
2500	116.318	17.657	119.716	17.666	129.488	23.494	131.301	23.508
3000	119.544	17.724	122.943	17.730	133.782	23.599	135.597	23.609
3500	122.280	17.766	125.680	17.770	137.425	23.663	139.241	23.671
4000	124.654	17.793	128.054	17.796	140.588	23.706	142.405	23.711
4500	126.751	17.812	130.152	17.815	143.382	23.735	145.199	23.740
5000	128.628	17.826	132.029	17.828	145.883	23.756	147.702	23.760

Units: S(cal mol^{-1}) and Cp(kcal mol^{-1} K^{-1})

Table AE.1 Entropy *(S)* and heat capacity *(Cp) vs.* temperature (Continued)

T (K)	ClSO		BrSO		$ClSO_2$		$BrSO_2$	
	S	Cp	S	Cp	S	Cp	S	Cp
5	30.597	7.949	32.854	7.949	32.879	7.949	35.053	7.949
50	48.900	7.949	51.157	7.952	51.193	8.025	53.410	8.203
100	54.430	8.065	56.716	8.182	56.986	8.929	59.453	9.436
150	57.764	8.433	60.121	8.650	60.844	10.180	63.521	10.677
200	60.247	8.840	62.668	9.062	63.927	11.259	66.733	11.654
250	62.260	9.207	64.727	9.401	66.535	12.129	69.419	12.425
298.15	63.909	9.526	66.409	9.691	68.734	12.835	71.663	13.056
300	63.968	9.538	66.469	9.701	68.813	12.860	71.743	13.079
400	66.792	10.098	69.332	10.214	72.683	14.043	75.661	14.165
500	69.093	10.525	71.656	10.610	75.916	14.930	78.916	15.000
600	71.041	10.838	73.618	10.902	78.699	15.581	81.709	15.625
700	72.730	11.066	75.315	11.116	81.139	16.058	84.154	16.087
800	74.219	11.233	76.810	11.273	83.307	16.411	86.325	16.431
900	75.550	11.359	78.145	11.391	85.256	16.676	88.276	16.690
1000	76.752	11.454	79.350	11.481	87.024	16.878	90.045	16.889
1500	81.452	11.701	84.058	11.714	93.987	17.406	97.011	17.410
2000	84.833	11.795	87.442	11.803	99.026	17.609	102.050	17.611
2500	87.470	11.841	90.080	11.845	102.967	17.706	105.992	17.707
3000	89.632	11.866	92.242	11.869	106.200	17.760	109.225	17.761
3500	91.462	11.881	94.073	11.883	108.941	17.793	111.966	17.793
4000	93.049	11.891	95.661	11.892	111.318	17.814	114.343	17.815
4500	94.450	11.897	97.062	11.899	113.417	17.829	116.442	17.829
5000	95.704	11.902	98.316	11.903	115.296	17.840	118.321	17.840

Units: S(cal mol^{-1}) and Cp(kcal $mol^{-1} K^{-1}$)

Table AE.1 Entropy *(S)* and heat capacity *(Cp) vs.* temperature (Continued)

T (K)	HgSO		ClHgSO		$ClHgSO_2$		HgClSO	
	S	Cp	S	Cp	S	Cp	S	Cp
5	36.028	7.949	37.500	7.949	39.099	7.949	39.522	7.956
50	54.401	8.254	55.849	8.184	58.395	10.093	59.838	9.790
100	60.415	9.120	61.940	9.678	66.202	12.554	66.798	10.439
150	64.198	9.513	66.155	11.128	71.630	14.224	71.196	11.305
200	66.964	9.712	69.499	12.101	75.888	15.364	74.552	12.033
250	69.149	9.875	72.275	12.774	79.411	16.204	77.300	12.598
298.15	70.902	10.041	74.569	13.267	82.323	16.866	79.558	13.037
300	70.965	10.047	74.651	13.283	82.427	16.890	79.639	13.052
400	73.904	10.406	78.581	14.018	87.446	18.004	83.495	13.754
500	76.262	10.725	81.765	14.510	91.559	18.859	86.622	14.261
600	78.240	10.976	84.442	14.845	95.057	19.501	89.256	14.627
700	79.947	11.166	86.749	15.079	98.101	19.978	91.532	14.893
800	81.448	11.310	88.774	15.246	100.793	20.335	93.534	15.089
900	82.787	11.418	90.577	15.368	103.205	20.605	95.320	15.235
1000	83.994	11.502	92.201	15.460	105.387	20.813	96.931	15.347
1500	88.708	11.722	98.523	15.693	113.948	21.358	103.219	15.636
2000	92.093	11.807	103.051	15.781	120.126	21.570	107.735	15.747
2500	94.733	11.848	106.578	15.822	124.951	21.672	111.255	15.800
3000	96.895	11.871	109.465	15.845	128.908	21.728	114.138	15.830
3500	98.726	11.884	111.908	15.859	132.260	21.763	116.580	15.847
4000	100.314	11.893	114.027	15.868	135.168	21.785	118.697	15.859
4500	101.715	11.900	115.896	15.874	137.735	21.801	120.565	15.867
5000	102.969	11.904	117.569	15.879	140.032	21.812	122.237	15.873

Units: S(cal mol^{-1}) and Cp(kcal mol^{-1} K^{-1})

Table AE.1 Entropy *(S)* and heat capacity *(Cp) vs.* temperature (Continued)

T (K)	BrHgSO		HgBrSO	
	S	Cp	S	Cp
5	38.875	7.949	40.309	7.955
50	57.256	8.330	60.620	9.836
100	63.598	10.226	67.705	10.783
150	68.037	11.646	72.269	11.755
200	71.514	12.495	75.752	12.449
250	74.366	13.065	78.586	12.946
298.15	76.705	13.486	80.900	13.324
300	76.788	13.500	80.982	13.337
400	80.767	14.148	84.907	13.949
500	83.975	14.594	88.071	14.400
600	86.665	14.904	90.727	14.731
700	88.979	15.122	93.017	14.974
800	91.010	15.279	95.029	15.152
900	92.816	15.395	96.822	15.287
1000	94.443	15.481	98.438	15.389
1500	100.770	15.703	104.738	15.656
2000	105.301	15.786	109.258	15.758
2500	108.828	15.826	112.780	15.808
3000	111.715	15.847	115.665	15.835
3500	114.159	15.861	118.107	15.851
4000	116.278	15.869	120.224	15.862
4500	118.147	15.875	122.093	15.869
5000	119.820	15.879	123.765	15.875

Units: S(cal mol^{-1}) and Cp(kcal mol^{-1} K^{-1})

APPENDIX AF

MERCURY OXIDATION – THERMOCHEMICAL PROPERTIES IN THE NASA POLYNOMIAL FORMAT

Appendix AF summarizes the thermochemical properties of the species calculated for the study of the oxidation of mercury in the NASA polynomial format, for use in ChemKin.

Table AF.1 Thermochemical properties of reactants, products and intermediate species in the mercury system in the NASA polynomial format for use in ChemKin

```
THERMO
   300.000  1500.000  5000.000
AR                AR 1    0    0    0G   300.000  5000.000 1000.000    01
 2.46581825E+00 0.00000000E+00 0.00000000E+00 0.00000000E+00 0.00000000E+00    2
-7.35183695E+02 4.52147182E+00 2.46581825E+00 0.00000000E+00 0.00000000E+00    3
 0.00000000E+00 0.00000000E+00-7.35183695E+02 4.52147182E+00                   4
HE                HE 1    0    0    0G   300.000  5000.000 1000.000    01
 2.46581825E+00 0.00000000E+00 0.00000000E+00 0.00000000E+00 0.00000000E+00    2
-7.35183695E+02 1.09922721E+00 2.46581825E+00 0.00000000E+00 0.00000000E+00    3
 0.00000000E+00 0.00000000E+00-7.35183695E+02 1.09922721E+00                   4
O                 O  1    0    0    0G   300.000  5000.000 1000.000    01
 2.55136704E+00 0.00000000E+00 0.00000000E+00 0.00000000E+00 0.00000000E+00    2
 2.92091138E+04 4.82418517E+00 2.55136704E+00 0.00000000E+00 0.00000000E+00    3
 0.00000000E+00 0.00000000E+00 2.92091138E+04 4.82418517E+00                   4
N                 N  1    0    0    0G   300.000  5000.000 1000.000    01
 2.50104422E+00 0.00000000E+00 0.00000000E+00 0.00000000E+00 0.00000000E+00    2
 5.61038359E+04 4.17481976E+00 2.50104422E+00 0.00000000E+00 0.00000000E+00    3
 0.00000000E+00 0.00000000E+00 5.61038359E+04 4.17481976E+00                   4
S                 S  1    0    0    0G   300.000  5000.000 1000.000    01
 2.68723866E+00 0.00000000E+00 0.00000000E+00 0.00000000E+00 0.00000000E+00    2
 3.25254231E+04 4.86534294E+00 2.68723866E+00 0.00000000E+00 0.00000000E+00    3
 0.00000000E+00 0.00000000E+00 3.25254231E+04 4.86534294E+00                   4
H                 H  1    0    0    0G   300.000  5000.000 1000.000    01
 2.50104422E+00 0.00000000E+00 0.00000000E+00 0.00000000E+00 0.00000000E+00    2
 2.54747466E+04-4.65341317E-01 2.50104422E+00 0.00000000E+00 0.00000000E+00    3
 0.00000000E+00 0.00000000E+00 2.54747466E+04-4.65341317E-01                   4
HG                HG 1    0    0    0G   300.000  5000.000 1000.000    01
 2.50104422E+00 0.00000000E+00 0.00000000E+00 0.00000000E+00 0.00000000E+00    2
 6.63730315E+03 6.79686305E+00 2.50104422E+00 0.00000000E+00 0.00000000E+00    3
 0.00000000E+00 0.00000000E+00 6.63730315E+03 6.79686305E+00                   4
C                 C  1    0    0    0G   300.000  5000.000 1000.000    01
 2.50248202E+00 0.00000000E+00 0.00000000E+00 0.00000000E+00 0.00000000E+00    2
 8.54692856E+04 4.74538974E+00 2.50248202E+00 0.00000000E+00 0.00000000E+00    3
 0.00000000E+00 0.00000000E+00 8.54692856E+04 4.74538974E+00                   4
O2                O  2    0    0    0G   300.000  5000.000 1390.000    01
 3.49867171E+00 9.83498169E-04-3.24499882E-07 4.89727401E-11-2.78161186E-15    2
-1.16416229E+03 4.28650737E+00 2.93391267E+00 2.28611775E-03-1.48998393E-06    3
 5.33085312E-10-8.15901258E-14-9.64207826E+02 7.32914415E+00                   4
O3           Bsn         0O  3    0    0G   300.000  5000.000 1412.000    01
 5.90674067E+00 1.01943605E-03-3.73382754E-07 6.06757421E-11-3.63393743E-15    2
 1.49958380E+04-5.99211167E+00 2.20547809E+00 1.12389887E-02-1.11556146E-05    3
 5.18370890E-09-9.22860421E-13 1.60931998E+04 1.32768508E+01                   4
```

Table AF.1 Thermochemical properties of reactants, products and intermediate species in the mercury system in the NASA polynomial format for use in ChemKin (Continued)

```
THERMO
   300.000  1500.000  5000.000
H2                H   2    0    0    0G   300.000  5000.000 1376.000    01
 2.81195744E+00 1.04575931E-03-2.67740432E-07 2.91628067E-11-1.09392425E-15    2
-7.57505577E+02-3.59411904E-01 3.58486499E+00-5.64107562E-04 9.96597011E-07    3
-4.24622923E-10 6.32407753E-14-1.05175016E+03-4.59049908E+00                   4
H2O               H   2O   1    0    0G   300.000  5000.000 1423.000    01
 2.41475714E+00 3.33625226E-03-1.02625633E-06 1.47123915E-10-8.03476673E-15    2
-2.97677739E+04 8.39211813E+00 4.03199655E+00-4.22695962E-04 1.96270639E-06    3
-7.57197744E-10  6.14909745E-14-3.02883042E+04-2.29797138E-01                                  4
OH                O   1H   1    0    0G   300.000  5000.000 1351.000    01
 2.65468640E+00 1.29298552E-03-3.52129761E-07 4.17820354E-11-1.79886781E-15    2
 4.10509895E+03 6.93704320E+00 3.40656145E+00 4.11051767E-04-5.12365624E-07    3
 5.36603136E-10-1.48306635E-13 3.74564446E+03 2.57010011E+00                   4
HO2               H   1O   2    0    0G   300.000  5000.000 1376.000    01
 3.97050185E+00 2.52314144E-03-8.59136347E-07 1.32923269E-10-7.69147310E-15    2
 3.06175710E+02 3.86759013E+00 3.45660464E+00 2.62271677E-03 2.11691376E-07    3
-8.18856175E-10 2.23580026E-13 6.13933765E+02 7.05001965E+00                   4
H2O2              H   2O   2    0    0G   300.000  5000.000 1418.000    01
 4.93048351E+00 3.76020387E-03-1.18073923E-06 1.72515156E-10-9.57780274E-15    2
-1.81717693E+04-1.56873802E+00 3.07087589E+00 8.97828869E-03-6.87481545E-06    3
 2.99554537E-09-5.38753268E-13-1.76158813E+04 8.10365449E+00                   4
N2                N   2    0    0    0G   300.000  5000.000 1537.000    01
 3.02594893E+00 1.18659801E-03-3.41459160E-07 4.36765971E-11-2.05955265E-15    2
-9.26733744E+02 5.51049904E+00 3.26021756E+00 5.91317650E-04 2.24046940E-07    3
-1.95572834E-10 3.61873213E-14-9.99926012E+02 4.27471788E+00                   4
NO                N   1O   1    0    0G   300.000  5000.000 1400.000    01
 3.33598753E+00 1.00903780E-03-3.06239904E-07 4.15856658E-11-2.08817847E-15    2
 9.79150056E+03 5.97646717E+00 3.18302769E+00 1.26159592E-03-4.40480299E-07    3
 6.32411731E-11-1.29137935E-15 9.85926756E+03 6.84194443E+00                   4
NO2               N   1O   2    0    0G   300.000  5000.000 1502.000    01
 5.25702696E+00 1.59120482E-03-5.75149250E-07 9.26518503E-11-5.51558889E-15    2
 1.98171365E+03-2.31252609E+00 2.83832551E+00 6.42094161E-03-3.71675514E-06    3
 7.13464780E-10 2.36187146E-14 2.88065443E+03 1.09303844E+01                   4
NO3               N   1O   3    0    0G   300.000  5000.000 1409.000    01
 8.05234885E+00 1.81617641E-03-6.65230967E-07 1.08106795E-10-6.47488733E-15    2
 5.40561277E+03-1.74924570E+01 5.28803619E-01 2.36342842E-02-2.48882237E-05    3
 1.21937821E-08-2.27359379E-12 7.54434055E+03 2.13259798E+01                   4
S2                S   2    0    0    0G   300.000  5000.000 1391.000    01
 3.89656541E+00 8.50722875E-04-2.69829625E-07 3.94225831E-11-2.18874469E-15    2
 1.42156695E+04 4.90350019E+00 3.62666242E+00 1.42953249E-03-7.44861473E-07    3
 2.19536612E-10-2.91294481E-14 1.43167937E+04 6.37506647E+00                   4
SO                O   1S   1    0    0G   300.000  5000.000 1390.000    01
 3.75878573E+00 8.50694004E-04-2.89265332E-07 4.48229083E-11-2.58804080E-15    2
-6.47076349E+02 4.82778708E+00 3.02820510E+00 2.63044758E-03-1.97919206E-06    3
 7.88054392E-10-1.29619928E-13-3.99859065E+02 8.72694578E+00                   4
SO2               O   2S   1    0    0G   300.000  5000.000 1401.000    01
 5.86421731E+00 1.04258812E-03-3.78185254E-07 6.10682966E-11-3.64153312E-15    2
-3.78031051E+04-4.50481781E+00 2.95891547E+00 8.94704098E-03-8.65823042E-06    3
 3.99420119E-09-7.12875654E-13-3.69230595E+04 1.06737029E+01                   4
CO2               C   1O   2    0    0G   300.000  5000.000 1672.000    01
 4.82545967E+00 2.52456043E-03-9.38613007E-07 1.54548505E-10-9.35205682E-15    2
-4.91052860E+04-3.06225684E+00 3.25098291E+00 5.34950736E-03-2.32155526E-06    3
 1.62010075E-10 7.79617497E-14-4.85094926E+04 5.65068968E+00                   4
CO                C   1    0    0O   1G   300.000  5000.000 1424.000    01
 3.16769526E+00 1.08083087E-03-3.04694579E-07 3.83919701E-11-1.78824732E-15    2
-1.42968136E+04 5.38395365E+00 3.16744731E+00 9.92161721E-04-1.51874397E-07    3
-4.89619632E-11 1.49600003E-14-1.42834682E+04 5.42393948E+00                   4
CL                0    0CL  1    0G   300.000  5000.000 1000.000    01
 2.71958905E+00 0.00000000E+00 0.00000000E+00 0.00000000E+00 0.00000000E+00    2
 1.37789885E+04 4.37402802E+00 2.71958905E+00 0.00000000E+00 0.00000000E+00    3
 0.00000000E+00 0.00000000E+00 1.37789885E+04 4.37402802E+00                   4
```

Table AF.1 Thermochemical properties of reactants, products and intermediate species in the mercury system in the NASA polynomial format for use in ChemKin (Continued)

```
THERMO
   300.000  1500.000  5000.000
CL2                     0    0CL  2    0G   300.000  5000.000 1393.000    01
 4.68722369E+00-2.88785951E-04 2.05481238E-07-4.90451057E-11 3.77253004E-15    2
-1.53958856E+03-1.18221739E-01 3.59183238E+00 2.35122034E-03-2.34527045E-06    3
 1.12156277E-09-2.07823110E-13-1.15680719E+03 5.75327148E+00                   4
HCL                     0H   1CL  1    0G   300.000  5000.000 1372.000    01
 2.77866043E+00 1.28715601E-03-3.58920205E-07 4.44565918E-11-2.03145865E-15    2
-1.18661877E+04 6.42843533E+00 3.35788046E+00 5.35082941E-05 6.14342418E-07    3
-2.94539482E-10 4.22173554E-14-1.20803636E+04 3.27330958E+00                   4
HOCL       JANAF,LZ     H   1O   1CL  1    0G   300.000  5000.000 1417.000    01
 4.46665835E+00 1.93289058E-03-6.19187445E-07 9.17606913E-11-5.14698586E-15    2
-1.05812079E+04 2.22763733E+00 3.19365799E+00 5.80335445E-03-5.16500957E-06    3
 2.48777519E-09-4.76679303E-13-1.02280715E+04 8.74710857E+00                   4
CLO        TRC DISK          0    0CL  1O   1G   300.000  5000.000 1394.000    01
 4.04012668E+00 5.28121299E-04-1.99225802E-07 3.20373629E-11-1.82222077E-15    2
 1.09101899E+04 3.87010082E+00 2.91064370E+00 3.67667618E-03-3.59787934E-06    3
 1.69950289E-09-3.12229758E-13 1.12469733E+04 9.74797683E+00                   4
CLO2                    0    0CL  1O   2G   300.000  5000.000 1410.000    01
 6.19909535E+00 7.51514158E-04-2.76319871E-07 4.50169848E-11-2.70085529E-15    2
 1.03881056E+04-5.27927192E+00 2.36631120E+00 1.23060599E-02-1.35605284E-05    3
 6.87099031E-09-1.31413081E-12 1.14361484E+04 1.43444593E+01                   4
CLOO          TRC(disk) O   2CL  1    0    0G   300.000  5000.000 1408.000    01
 6.14785968E+00 7.95941001E-04-2.91827932E-07 4.74551789E-11-2.84347950E-15    2
 1.01732910E+04-4.97193068E+00 2.89960320E+00 1.01365008E-02-1.05772216E-05    3
 5.14158207E-09-9.52459824E-13 1.11038642E+04 1.18146656E+01                   4
CLNO       DFT          CL  1O   1N   1    0G   300.000  5000.000 1395.000    11
 4.45889813E+00 1.54099670E-03-6.23199426E-07 1.16687497E-10-7.72839808E-15    2
 4.61840633E+03 4.66687699E+00 3.56315015E+00 3.86191309E-03-2.96055937E-06    3
 1.19668170E-09-1.99235085E-13 4.90462832E+03 9.39329753E+00                   4
CLNO2      DFT          CL  1O   2N   1    0G   300.000  5000.000 1378.000    11
 6.17130953E+00 2.95272417E-03-1.04791174E-06 1.66758170E-10-9.84277242E-15    2
-1.23274212E+03-4.22346720E+00 3.01804279E+00 1.02914155E-02-7.76053667E-06    3
 3.05999370E-09-5.04484867E-13-1.16840916E+02 1.27524514E+01                   4
CLONOcis  DFT          CL  1O   2N   1    0G   300.000  5000.000 1384.000    11
 7.00541288E+00 2.25866056E-03-8.12182200E-07 1.30387444E-10-7.74352096E-15    2
 5.14499993E+03-8.62446837E+00 3.04207676E+00 1.22013380E-02-1.04909307E-05    3
 4.46505041E-09-7.57063180E-13 6.44568391E+03 1.24071508E+01                   4
CLONOtran DFT          CL  1O   2N   1    0G   300.000  5000.000 1469.000    11
 5.57468933E+00 3.14524615E-03-7.89196235E-07 3.50922251E-11 4.71533312E-15    2
 7.16693193E+03 5.71735223E-01 3.44043817E+00 1.19639690E-02-1.15161305E-05    3
 5.37892123E-09-9.85772717E-13 7.25574328E+03 1.02612628E+01                   4
CLONO2     DFT          CL  1O   3N   1    0G   300.000  5000.000 1409.000    11
 9.66493811E+00 2.60167704E-03-9.44224120E-07 1.52571821E-10-9.10350609E-15    2
-5.76736161E+02-2.31069089E+01 1.92089030E+00 2.31062915E-02-2.16396048E-05    3
 9.56307319E-09-1.62896291E-12 1.80434070E+03 1.75159922E+01                   4
CLSO       DFT          CL  1S   1O   1    0G   300.000  5000.000 1402.000    11
 5.06655188E+00 1.09428906E-03-3.51682833E-07 5.23198915E-11-2.94557888E-15    2
-1.40310176E+04 2.75246955E+00 3.77306241E+00 5.13775238E-03-5.21623929E-06    3
 2.66890877E-09-5.26915221E-13-1.36826436E+04 9.33913220E+00                   4
CLSO2      DFT          CL  1S   1O   2    0G   300.000  5000.000 1412.000    11
 7.71952704E+00 1.46664382E-03-4.98212007E-07 7.71502863E-11-4.47300680E-15    2
-9.81924236E+03-1.05471035E+01 3.96828763E+00 1.23441507E-02-1.25640099E-05    3
 6.08783060E-09-1.12969646E-12-8.75358744E+03 8.80660069E+00                   4
BR                      BR 1    0    0    0    300.000  5000.000 1000.000    01
 2.54202138E+00 0.00000000E+00 0.00000000E+00 0.00000000E+00 0.00000000E+00    2
 1.26995700E+04 6.56842446E+00 2.54202138E+00 0.00000000E+00 0.00000000E+00    3
 0.00000000E+00 0.00000000E+00 1.26995700E+04 6.56842446E+00                   4
BR2             J12/61BR 2    0    0    0G   300.000  5000.000 1422.000    01
 4.55024476E+00-9.12671312E-06 2.46775944E-08-6.35743880E-12 4.54786790E-16    2
 2.30297333E+03 3.47346750E+00 4.18018746E+00 8.17264690E-04-7.21994207E-07    3
 3.19446289E-10-5.63019482E-14 2.44230100E+03 5.48554939E+00                   4
```

Table AF.1 Thermochemical properties of reactants, products and intermediate species in the mercury system in the NASA polynomial format for use in ChemKin (Continued)

```
THERMO
   300.000  1500.000  5000.000
HBR                 H   1BR  1    0    0G   300.000  5000.000 1345.000    01
 2.93035581E+00 1.22945720E-03-3.36156616E-07 4.04145601E-11-1.76364104E-15    2
-5.25484475E+03 6.95097476E+00 3.32683251E+00 3.27297195E-04 4.32189089E-07    3
-2.51924604E-10 4.04880882E-14-5.39327469E+03 4.81565697E+00                   4
HOBR                H   1BR  1O   1    0G   300.000  5000.000 1436.000    11
 3.87748840E+00 1.83476950E-03-5.48066531E-07 7.68623671E-11-4.12833508E-15    2
-9.39926937E+03 7.27168976E+00 4.02196738E+00 1.85385241E-03-1.06053707E-06    3
 5.55764171E-10-1.29528504E-13-9.47653637E+03 6.38296629E+00                   4
BRO                 BR  1O   1    0    0G   300.000  5000.000 1312.000    01
 3.72103562E+00 5.70307208E-04-1.69252602E-07 2.25819115E-11-1.11267519E-15    2
 1.41196323E+04 7.24601188E+00 3.76799381E+00 4.35792812E-04-2.59489578E-08    3
-4.47695025E-11 1.06849090E-14 1.41066351E+04 7.00399312E+00                   4
BRCL                CL  1BR  1    0    0G   300.000  5000.000 1393.000    01
 4.66389438E+00-2.33554879E-04 1.61798194E-07-3.82527712E-11 2.92313207E-15    2
 2.69566446E+02-1.16373055E+01 3.90371972E+00 1.55664134E-03-1.52935593E-06    3
 7.24317065E-10-1.33386412E-13 5.40510924E+02-7.54595584E+00                   4
BRNO     DFT        BR  1O   1N   1    0G   300.000  5000.000 1395.000    11
 4.49761732E+00 1.48947819E-03-5.96448948E-07 1.11310481E-10-7.36650959E-15    2
 9.20197023E+03 5.70082588E+00 3.64340321E+00 3.68610424E-03-2.79395639E-06    3
 1.12139515E-09-1.85808965E-13 9.47701948E+03 1.02147136E+01                   4
BRNO2    DFT        BR  1O   2N   1    0G   300.000  5000.000 1394.000    11
 6.21095426E+00 2.82921456E-03-9.84389321E-07 1.54581638E-10-9.03968506E-15    2
 3.11622559E+03-3.01956371E+00 2.49387779E+00 1.38442906E-02-1.39042381E-05    3
 7.06827220E-09-1.40194007E-12 4.20107948E+03 1.61621515E+01                   4
BRONOcis DFT        BR  1O   2N   1    0G   300.000  5000.000 1381.000    11
 7.25477479E+00 2.05260654E-03-7.42576464E-07 1.19692228E-10-7.12816354E-15    2
 7.20687380E+03-8.92635902E+00 3.35550137E+00 1.13766273E-02-9.17464041E-06    3
 3.54701400E-09-5.35757211E-13 8.51787544E+03 1.19035056E+01                   4
BRONOtran DFT       BR  1O   2N   1    0G   300.000  5000.000 1468.000    11
 5.63804642E+00 3.09702914E-03-7.75926172E-07 3.32808370E-11 4.82416786E-15    2
 9.51080749E+03 1.49624285E+00 3.65852718E+00 1.14879365E-02-1.10457126E-05    3
 5.15464323E-09-9.44391108E-13 9.55338987E+03 1.03796471E+01                   4
BRONO2   DFT        BR  1O   3N   1    0G   300.000  5000.000 1409.000    11
 9.72958726E+00 2.56776714E-03-9.37043829E-07 1.51911908E-10-9.08344564E-15    2
 5.25532791E+02-2.22038324E+01 2.40880665E+00 2.13686738E-02-1.92332458E-05    3
 8.13981854E-09-1.32611126E-12 2.82973924E+03 1.63971803E+01                   4
BRSO     DFT        BR  1S   1O   1    0G   300.000  5000.000 1363.000    11
-7.92268780E-01 8.67238991E-03-3.41261453E-06 5.17399814E-10-2.58017041E-14    2
-2.74877603E+04 3.83839971E+01 3.78238954E+00 4.57737298E-03-3.05330386E-06    3
 9.52861326E-12 4.45199656E-13-3.02274224E+04 1.06366838E+01                   4
BRSO2    DFT        BR  1S   1O   2    0G   300.000  5000.000 1414.000    11
 7.72258929E+00 1.46771577E-03-4.99378770E-07 7.74142495E-11-4.49165299E-15    2
-2.71029236E+04-9.07720846E+00 4.19037216E+00 1.14632201E-02-1.13168990E-05    3
 5.34343207E-09-9.70260646E-13-2.60776377E+04 9.22931834E+00                   4
I       09/29/10 NIST I   1    0    0    0G   300.000  5000.000 1000.000    01
 2.50320091E+00 0.00000000E+00 0.00000000E+00 0.00000000E+00 0.00000000E+00    2
 1.20971534E+04 7.48412215E+00 2.50320091E+00 0.00000000E+00 0.00000000E+00    3
 0.00000000E+00 0.00000000E+00 1.20971534E+04 7.48412215E+00                   4
I2      09/29/10 NIST I   2    0    0    0G   300.000  5000.000 1414.000    01
 4.00166376E+00 7.43481283E-04-1.96750777E-07 2.26961825E-11-9.42508116E-16    2
 6.29191733E+03 8.29469569E+00 4.10581209E-01 1.63880367E-02-2.31382750E-05    3
 1.39401370E-08-3.00467508E-12 6.83629077E+03 2.50446149E+01                   4
HI      09/29/10 NIST I   1H   1    0    0G   300.000  5000.000 1537.000    01
 3.00373329E+00 1.27990632E-03-3.66624170E-07 4.67428761E-11-2.19879026E-15    2
 2.26208449E+03 7.42809865E+00 3.24260509E+00 6.71960480E-04 2.11956562E-07    3
-1.98533528E-10 3.70982132E-14 2.18756018E+03 6.16839393E+00                   4
HGI     09/29/10 NIST I   1HG  1    0    0G   300.000  5000.000 1380.000    01
 4.31042621E+00 6.58032982E-04-1.88284785E-07 2.40549290E-11-1.12863233E-15    2
 1.47630362E+04 9.06747619E+00 4.47167724E+00 2.80854859E-04 1.46643868E-07    3
-1.10560617E-10 1.96047216E-14 1.47075534E+04 8.20237179E+00                   4
```

Table AF.1 Thermochemical properties of reactants, products and intermediate species in the mercury system in the NASA polynomial format for use in ChemKin (Continued)

```
THERMO
   300.000  1500.000  5000.000
HGI2      09/29/10 NIST I   2HG  1    0    0G   300.000  5000.000 3000.000    01
 7.49306810E+00 0.00000000E+00 0.00000000E+00 0.00000000E+00 0.00000000E+00    2
-4.17668530E+03-2.24960112E+00 7.49306810E+00 0.00000000E+00 0.00000000E+00    3
 0.00000000E+00 0.00000000E+00-4.17668530E+03-2.24960112E+00                   4
IO        DFT          I  1O  1    0    0G   300.000  5000.000 1394.000    01
 4.66663836E+00-3.64432690E-04 2.30427821E-07-5.38362456E-11 4.12985284E-15    2
 1.95483869E+04 1.57909115E+00 3.52124571E+00 2.72864673E-03-3.09356885E-06    3
 1.60436649E-09-3.13361173E-13 1.99100394E+04 7.59199795E+00                   4
HOI       DFT          O  1H  1I  1    0G   300.000  5000.000 1415.000    01
 4.66526589E+00 1.73387590E-03-5.43587866E-07 7.92169581E-11-4.38591404E-15    2
-9.89161887E+03 3.57764993E+00 3.34803709E+00 6.50675460E-03-6.90512527E-06    3
 3.73847591E-09-7.69289606E-13-9.59780893E+03 1.00598497E+01                   4
ICL       09/17/12 NIST I   1CL  1    0    0G   300.000  5000.000 1413.000    01
 4.60265153E+00-1.03530845E-04 8.19398883E-08-1.95664136E-11 1.47394986E-15    2
 6.55635079E+02 3.41167676E+00 4.07046442E+00 1.08985479E-03-9.97778643E-07    3
 4.51755122E-10-8.08113504E-14 8.54617733E+02 6.30227254E+00                   4
INO       09/17/12 NIST I   1N   1O   1    0G   300.000  5000.000 1372.000    01
 5.94491924E+00 9.36796999E-04-3.32856534E-07 5.30245965E-11-3.13247291E-15    2
 1.15084018E+04-4.50384521E-01 4.79496522E+00 3.42722072E-03-2.30840419E-06    3
 7.29070169E-10-8.61426636E-14 1.19247164E+04 5.79096208E+00                   4
INO2      DFT          I  1N   1O   2    0G   300.000  5000.000 1401.000    01
 8.28395648E+00 1.57678528E-03-5.72309024E-07 9.24522275E-11-5.51451631E-15    2
 4.24737308E+03-1.25973667E+01 3.61224085E+00 1.45471339E-02-1.44485750E-05    3
 6.81738100E-09-1.24006101E-12 5.63830720E+03 1.17204471E+01                   4
HGCL              HG  1CL  1    0    0G   300.000  5000.000 1358.000    01
 4.40173570E+00 2.63571867E-04-8.44186556E-08 1.18832742E-11-5.88776088E-16    2
 8.09491844E+03 6.08121556E+00 4.26650201E+00 5.82463951E-04-3.73501017E-07    3
 1.32445461E-10-2.01831235E-14 8.14143765E+03 6.80627776E+00                   4
HGCL2             HG  1CL  2    0    0G   300.000  5000.000 1401.000    01
 6.92841571E+00 6.81979183E-05-2.53098533E-08 4.14855462E-12-2.49944441E-16    2
-1.92776030E+04-2.48489601E+00 5.93022067E+00 3.67949657E-03-4.83161241E-06    3
 2.76917879E-09-5.79317995E-13-1.90556995E+04 2.42767036E+00                   4
HGBR              HG  1BR  1    0    0G   300.000  5000.000 1496.000    01
 4.44494224E+00 7.65569434E-05-3.68727790E-08 7.84988337E-12-6.04539157E-16    2
 1.11922824E+04 7.15578555E+00 4.38814244E+00 2.78624477E-04-2.86123057E-07    3
 1.39275707E-10-2.60982714E-14 1.12029454E+04 7.43289166E+00                   4
HGBR2             HG  1BR  2    0    0G   300.000  5000.000 1427.000    01
 7.45878811E+00 2.10129452E-05-3.10114268E-10-4.76264096E-13 3.55195705E-17    2
-1.28026790E+04-5.17301268E+00 7.42544070E+00 6.36139712E-05-1.32087185E-08    3
-2.11142353E-12 8.97792105E-16-1.27852987E+04-4.97776829E+00                   4
HGBRCL            HG  1BR  1CL  1    0G   300.000  5000.000 1450.000    01
 7.42244038E+00 6.43412694E-05-2.00792485E-08 3.17809828E-12-2.01197614E-16    2
-1.75672474E+04-5.62261889E+00 7.42724750E+00 3.56096295E-05 1.75669051E-08    3
-1.53131659E-11 2.98285086E-15-1.75659165E+04-5.64025394E+00                   4
HGOHCL            HG  1CL  1O   1H   1G   300.000  5000.000 1422.000    01
 8.03158535E+00 1.44286949E-03-4.49639718E-07 6.53740165E-11-3.61776719E-15    2
-1.85015699E+04-8.70999026E+00 5.54423743E+00 9.43415482E-03-1.00943953E-05    3
 5.19717569E-09-1.01363171E-12-1.78711502E+04 3.84912765E+00                   4
HGCLO             HG  1CL  1O   1    0G   300.000  5000.000 1958.000    01
 4.61998819E+02-8.49273566E-01 5.28076382E-04-1.29256146E-07 1.05037598E-11    2
-1.56011534E+05-2.51662985E+03 7.65622123E+00 6.84140172E-05 1.20750237E-07    3
-1.28034155E-10 3.16093245E-14 1.23384912E+04-8.46306247E+00                   4
HGBROH            HG  1BR  1O   1H   1G   300.000  5000.000 1395.000    11
 8.59255865E+00 8.17058696E-04-2.92806359E-07 4.69038185E-11-2.78137976E-15    2
-1.34421353E+04-1.08447030E+01 5.88245421E+00 9.61040665E-03-1.12293248E-05    3
 6.09256187E-09-1.24018604E-12-1.27374377E+04 2.85365377E+00                   4
HGBRO             HG  1BR  1O   1    0G   300.000  5000.000 1430.000    01
 7.93366321E+00 3.94793650E-05-6.54952169E-09 3.82396389E-13-5.57929358E-18    2
 9.80638544E+03-6.62859603E+00 7.92220771E+00 3.53511864E-05 1.91583789E-08    3
-1.61134552E-11 3.10974652E-15 9.81544833E+03-6.55292634E+00                   4
```

Table AF.1 Thermochemical properties of reactants, products and intermediate species in the mercury system in the NASA polynomial format for use in ChemKin (Continued)

```
THERMO
   300.000  1500.000  5000.000
HGOH                HG  1O  1H  1    0G   300.000  5000.000 1421.000    01
 4.72142363E+00 1.57771910E-03-4.67355871E-07 6.51098970E-11-3.47881432E-15    2
 1.64419041E+02 3.71925647E+00 3.05079384E+00 7.98752400E-03-9.21268586E-06    3
 5.13402707E-09-1.06377808E-12 4.93094043E+02 1.18003310E+01                   4
HGO                 HG  1O  1   0    0G   300.000  5000.000 1386.000    01
 4.51178867E+00-7.51776369E-05 1.07116280E-07-3.08449739E-11 2.62892585E-15    2
 2.99088996E+04 2.79442234E+00 3.48190125E+00 2.45474763E-03-2.36515801E-06    3
 1.10675643E-09-2.02292888E-13 3.02605985E+04 8.29237896E+00                   4
HGOHO               HG  1O  2H  1    0G   300.000  5000.000 1316.000    11
 3.50231657E+04-6.39875657E+01 4.02133571E-02-1.00763042E-05 8.38695887E-10    2
-1.43141579E+07-1.95084643E+05 5.50263431E+00 1.79963346E-02-2.46670877E-05    3
 1.45906224E-08-3.12864317E-12 1.20933151E+04 1.55368576E+00                   4
HGOH2               HG  1O  2H  2    0G   300.000  5000.000 1386.000    21
 9.35147156E+00 2.35466358E-03-8.36904587E-07 1.33315472E-10-7.87453981E-15    2
-1.63743136E+04-1.67679810E+01 5.64506398E+00 1.28008939E-02-1.25659717E-05    3
 6.21336757E-09-1.20800321E-12-1.52428100E+04 2.54323748E+00                   4
HGOHOH              HG  1O  2H  2    0G   300.000  5000.000 1386.000    21
 9.35147156E+00 2.35466358E-03-8.36904587E-07 1.33315472E-10-7.87453981E-15    2
-1.63743136E+04-1.67679810E+01 5.64506398E+00 1.28008939E-02-1.25659717E-05    3
 6.21336757E-09-1.20800321E-12-1.52428100E+04 2.54323748E+00                   4
HGNO    DFT         HG  1O  1N  1    0G   300.000  5000.000 1394.000    11
 4.72588194E+00 9.41862899E-04-2.13839359E-07 2.44531140E-11-1.15312310E-15    2
 2.06467462E+04 8.69463148E+00 4.64865340E+00 1.10057144E-03-3.37438251E-07    3
 6.86679788E-11-7.40351383E-15 2.06766429E+04 9.11858866E+00                   4
HGNO2   DFT         HG  1O  2N  1    0G   300.000  5000.000 1390.000    11
 6.61956863E+00 2.39814659E-03-9.47194838E-07 1.67879398E-10-1.05932136E-14    2
 1.26267503E+04 2.06112556E+00 4.40276007E+00 8.29038855E-03-7.02105636E-06    3
 3.02999898E-09-5.26173860E-13 1.33172503E+04 1.37007170E+01                   4
HGONO   DFT         HG  1O  2N  1    0G   300.000  5000.000 1469.000    11
 5.82972797E+00 2.90126146E-03-7.08369785E-07 2.58377524E-11 4.93205396E-15    2
 1.73417785E+04 2.63815958E+00 3.91351286E+00 1.08732024E-02-1.03877952E-05    3
 4.82827568E-09-8.82150270E-13 1.74058834E+04 1.13030688E+01                   4
HGONO2  DFT         HG  1O  3N  1    0G   300.000  5000.000 1424.000    11
 9.25170388E+00 2.99624119E-03-1.09001242E-06 1.76340635E-10-1.05285807E-14    2
 2.86658664E+03-1.71655862E+01 3.49288573E+00 1.51709044E-02-9.84837640E-06    3
 2.45603452E-09-1.07964981E-13 4.92412863E+03 1.40996844E+01                   4
NOHGNO  DFT         HG  1O  2N  2    0G   300.000  5000.000 1404.000    11
 1.02187834E+01 1.91064646E-03-6.56005920E-07 1.02302909E-10-5.95992368E-15    2
 3.68270766E+04-1.83630532E+01 5.87826295E+00 1.41178015E-02-1.38628587E-05    3
 6.55960364E-09-1.19904044E-12 3.81024053E+04 4.17292044E+00                   4
NOHGNO2 DFT         HG  1O  3N  2    0G   300.000  5000.000 1406.000    11
 1.22939769E+01 2.68396660E-03-9.21408985E-07 1.43694167E-10-8.37179906E-15    2
 1.83825976E+04-2.87096799E+01 5.19659774E+00 2.34156121E-02-2.41642913E-05    3
 1.18650170E-08-2.23018049E-12 2.03941346E+04 7.87179461E+00                   4
NO2HGNO2 DFT        HG  1O  4N  2    0G   300.000  5000.000 1401.000    11
 1.31642305E+01 4.39620513E-03-1.49269087E-06 2.31006743E-10-1.33852035E-14    2
 3.10430624E+03-3.34759724E+01 4.95484918E+00 2.73104817E-02-2.62007848E-05    3
 1.23139168E-08-2.25160947E-12 5.54423355E+03 9.22635395E+00                   4
CLHGNO  DFT         HG  1O  1N  1CL  1G   300.000  5000.000 1415.000    11
 7.76675344E+00 1.39265063E-03-4.65041207E-07 7.11630437E-11-4.09119431E-15    2
 8.56738090E+03-7.16293002E+00 4.99887939E+00 9.19232662E-03-8.87461739E-06    3
 4.15185728E-09-7.50432039E-13 9.37438844E+03 7.19433269E+00                   4
BRHGNO  DFT         HG  1O  1N  1BR  1G   300.000  5000.000 1417.000    11
 7.81639773E+00 1.18680996E-03-3.57793360E-07 5.06401988E-11-2.74281910E-15    2
 1.37042143E+04-5.76886131E+00 5.71587845E+00 8.61175457E-03-9.98698854E-06    3
 5.45537379E-09-1.10990878E-12 1.41762268E+04 4.60926864E+00                   4
CLHGNO2 DFT         HG  1O  2N  1CL  1G   300.000  5000.000 1399.000    11
 9.52919572E+00 2.41880662E-03-8.14586426E-07 1.25347986E-10-7.23357616E-15    2
-8.39346681E+03-1.59812695E+01 4.88828871E+00 1.62127592E-02-1.66705913E-05    3
 8.34523789E-09-1.60761711E-12-7.08424428E+03 7.88441688E+00                   4
```

Table AF.1 Thermochemical properties of reactants, products and intermediate species in the mercury system in the NASA polynomial format for use in ChemKin (Continued)

```
THERMO
   300.000  1500.000  5000.000
BRHGNO2   DFT         HG 1O  2N  1BR 1G   300.000  5000.000 1408.000    11
 9.83482536E+00 2.21195394E-03-7.54989398E-07 1.17278992E-10-6.81400145E-15    2
-3.45167989E+03-1.65138560E+01 5.01722349E+00 1.55866521E-02-1.49994211E-05    3
 6.96614731E-09-1.25160693E-12-2.02402533E+03 8.55198367E+00                   4
HGCLNO    DFT         HG 1O  1N  1CL 1G   300.000  5000.000 1419.000    11
 7.62262198E+00 1.47336672E-03-4.83810268E-07 7.31582336E-11-4.16984836E-15    2
 9.26303843E+03-3.34656095E+00 5.15410075E+00 8.40025698E-03-7.91384387E-06    3
 3.65800737E-09-6.55970052E-13 9.98484628E+03 9.46680765E+00                   4
HGBRNO    DFT         HG 1O  1N  1BR 1G   300.000  5000.000 1409.000    11
 7.63404150E+00 1.31810045E-03-3.98106988E-07 5.64332245E-11-3.06047168E-15    2
 1.38240657E+04-1.54022127E+00 4.56041731E+00 1.25656216E-02-1.53935686E-05    3
 8.65870492E-09-1.79602866E-12 1.44874050E+04 1.35285945E+01                   4
HGCLNO2   DFT         HG 1O  2N  1CL 1G   300.000  5000.000 1412.000    11
 9.75138724E+00 2.26067097E-03-7.67070837E-07 1.18686209E-10-6.87697595E-15    2
 2.05197089E+03-1.44579252E+01 4.67026217E+00 1.65725093E-02-1.62082052E-05    3
 7.62323827E-09-1.38248009E-12 3.53573520E+03 1.19036094E+01                   4
HGBRNO2   DFT         HG 1O  2N  1BR 1G   300.000  5000.000 1408.000    11
 9.73603315E+00 2.28695147E-03-7.79005937E-07 1.20843654E-10-7.01438046E-15    2
 6.26408710E+03-1.36058848E+01 4.80114489E+00 1.60386928E-02-1.54852758E-05    3
 7.22074943E-09-1.30236796E-12 7.72215733E+03 1.20532879E+01                   4
HGSO      DFT         HG 1S  1O  1   0G   300.000  5000.000 1404.000    11
 4.93058817E+00 1.13557279E-03-3.49570190E-07 5.02892761E-11-2.75853508E-15    2
 1.69378052E+04 7.18694589E+00 4.21000293E+00 3.80772153E-03-4.00051990E-06    3
 2.19790325E-09-4.60341343E-13 1.70969509E+04 1.07190638E+01                   4
HGSO2     DFT         HG 1S  1O  2   0G   300.000  5000.000 1399.000    11
 7.53676305E+00 1.66688432E-03-5.77156184E-07 9.04951125E-11-5.29123382E-15    2
-3.24675467E+04-1.98017832E+00 4.78246361E+00 8.30407821E-03-6.55716584E-06    3
 2.47511350E-09-3.59392573E-13-3.15555611E+04 1.26998795E+01                   4
CLHGSO    DFT         HG 1CL 1S  1O  1G   300.000  5000.000 1653.000    21
-3.34815000E+00 1.56035789E-02-6.43553969E-06 1.01817010E-09-5.33364112E-14    2
-4.43252023E+03 5.69471393E+01 3.00659383E+00 2.00804436E-02-3.25320834E-05    3
 2.24226514E-08-5.29374796E-12-8.78036267E+03 1.56648709E+01                   4
BRHGSO    DFT         HG 1BR 1S  1O  1G   300.000  5000.000 1577.000    21
-6.86248755E+00 2.11748506E-02-9.41428771E-06 1.64694423E-09-9.86198993E-14    2
-2.56484411E+04 7.81197682E+01 3.26254720E+00 1.93505942E-02-3.17287733E-05    3
 2.20250470E-08-5.21993354E-12-3.16941956E+04 1.54688192E+01                   4
CLHGSO2   DFT         HG 1CL 1S  1O  2G   300.000  5000.000 1767.000    21
 3.88154768E+00 8.88434349E-03-3.14849442E-06 3.84653603E-10-1.11922836E-14    2
-5.56906582E+03 1.87506555E+01 4.71994959E+00 1.80733519E-02-2.24090089E-05    3
 1.23762078E-08-2.38038734E-12-7.03842510E+03 1.00346903E+01                   4
HGCLSO    DFT         HG 1CL 1S  1O  1G   300.000  5000.000 1435.000    21
-8.42950317E+00 2.28542846E-02-1.00627637E-05 1.75928991E-09-1.05939713E-13    2
 2.00988461E+03 8.88566838E+01 3.34447436E+00 1.67518580E-02-2.49065572E-05    3
 1.58359193E-08-3.41841907E-12-4.87294601E+03 1.69590616E+01                   4
HGBRSO    DFT         HG 1BR 1S  1O  1G   300.000  5000.000 1435.000    21
-7.61801504E+00 2.17361339E-02-9.56674117E-06 1.67766915E-09-1.01605212E-13    2
 5.14197515E+03 8.48899890E+01 3.67948846E+00 1.58441144E-02-2.39073423E-05    3
 1.53326070E-08-3.32353207E-12-1.43256152E+03 1.59551609E+01                   4
CH4               C  1H  4   0   0G   300.000  5000.000 1706.000    01
 1.78092211E+00 9.74452639E-03-3.42930517E-06 5.43903042E-10-3.20521160E-14    2
-1.00945292E+04 9.16546733E+00 3.19715119E+00 2.00818162E-03 8.06603744E-06    3
-6.00052219E-09 1.24529966E-12-1.01110356E+04 3.22246966E+00                   4
CH3               C  1H  3   0   0G   300.000  5000.000 1396.000    01
 3.48038476E+00 5.04251727E-03-1.63067195E-06 2.43262855E-10-1.37097321E-14    2
 1.61476903E+04 1.82459735E+00 3.32587630E+00 4.54419935E-03-4.68848257E-07    3
-4.68342127E-10 1.23727601E-13 1.63252643E+04 3.02183670E+00                   4
CH3O      Hf/tsang webC  1H  3O  1   0G   300.000  5000.000 1532.000    01
 4.69610864E+00 6.99420519E-03-2.40123979E-06 3.73754382E-10-2.17235659E-14    2
-3.37327396E+02-2.56214971E+00 1.53542602E+00 1.04245018E-02-6.87255907E-07    3
-2.72666753E-09 8.91536914E-13 1.15332818E+03 1.58110648E+01                   4
```

Table AF.1 Thermochemical properties of reactants, products and intermediate species in the mercury system in the NASA polynomial format for use in ChemKin (Continued)

```
THERMO
   300.000  1500.000  5000.000
CH3OO               C   1H   3O   2    0G   300.000  5000.000 1388.000    11
 8.40358655E+00 6.10859279E-03-2.12817408E-06 3.34625531E-10-1.95903631E-14    2
-1.21631166E+03-2.03365730E+01 1.71899630E+00 2.12174825E-02-1.48476829E-05    3
 5.06002386E-09-6.71016242E-13 1.13195546E+03 1.57042647E+01                   4
C2H5                C   2H   5    0    0G   300.000  5000.000 1379.000    11
 5.55201098E+00 1.08474115E-02-3.70872121E-06 5.75466261E-10-3.33687128E-14    2
 1.12963170E+04-7.21892358E+00 1.78913597E+00 1.60871012E-02-4.81868556E-06    3
-4.81374851E-10 3.59196140E-13 1.30374797E+04 1.43820780E+01                   4
C2H6                C   2H   6    0    0G   300.000  5000.000 1384.000    11
 5.80495823E+00 1.30538057E-02-4.44197297E-06 6.87039005E-10-3.97491525E-14    2
-1.34622353E+04-1.12318777E+01 5.26536600E-01 2.21339177E-02-9.32566455E-06    3
 1.32811088E-09 6.01508284E-14-1.12271105E+04 1.83977859E+01                   4
CH2OH       Hf/tsang webC   1H   3O   1    0G   300.000  5000.000 1413.000    11
 5.83378502E+00 5.10482972E-03-1.64182989E-06 2.44192495E-10-1.37391566E-14    2
-3.31600408E+03-5.73809265E+00 2.53721091E+00 1.40077136E-02-1.09991479E-05    3
 4.73482855E-09-8.33897171E-13-2.29739726E+03 1.15294246E+01                   4
CH3OH               C   1H   4O   1    0G   300.000  5000.000 1383.000    11
 4.62903122E+00 8.77948682E-03-2.93065370E-06 4.47462309E-10-2.56560590E-14    2
-2.65242698E+04-1.27346652E+00 1.61416329E+00 1.32488373E-02-4.08270395E-06    3
-4.07510151E-10 3.29375551E-13-2.51904322E+04 1.58798963E+01                   4
CH2O                C   1H   2O   1    0G   300.000  5000.000 1492.000    01
 3.91527967E+00 5.13066169E-03-1.76213301E-06 2.74302764E-10-1.59427842E-14    2
-1.48953342E+04 1.70259206E+00 2.97646460E+00 3.31251523E-03 4.55181503E-06    3
-4.59001475E-09 1.14482312E-12-1.41514012E+04 8.19564357E+00                   4
HCO                 C   1H   1O   1    0G   300.000  5000.000 1369.000    01
 3.68595737E+00 3.17769699E-03-1.08209015E-06 1.67411390E-10-9.68635143E-15    2
 3.82993636E+03 4.75119660E+00 3.50805155E+00 1.96602789E-03 1.65981499E-06    3
-1.66101511E-09 3.85812256E-13 4.08914803E+03 6.34184451E+00                   4
C2H3                C   2H   3    0    0G   300.000  5000.000 1392.000    01
 5.67024497E+00 5.73958776E-03-1.87941798E-06 2.83437286E-10-1.61182759E-14    2
 3.32849788E+04-6.75088410E+00 1.90424398E+00 1.41044653E-02-8.74924065E-06    3
 2.74533585E-09-3.37551174E-13 3.46247416E+04 1.36093709E+01                   4
C2H4                C   2H   4    0    0G   300.000  5000.000 1394.000    01
 5.21495849E+00 8.96066623E-03-3.04712995E-06 4.71094610E-10-2.72474916E-14    2
 3.60063331E+03-7.42632336E+00 3.89634275E-01 1.90115733E-02-1.08369348E-05    3
 3.15370853E-09-3.75480468E-13 5.42947082E+03 1.89729102E+01                   4
CH2       CBS-APNO,Chad C   1H   2    0    0G   300.000  5000.000 1387.000    01
 3.24709565E+00 2.31058554E-03-4.66682011E-07 3.95404861E-11-1.06799498E-15    2
 4.63892953E+04 4.46665277E+00 3.65300791E+00 1.48759807E-03 1.54875301E-07    3
-1.71129442E-10 2.64849132E-14 4.62317166E+04 2.23541808E+00                   4
CH2(S)    CBS-APNO,Chad C   1H   2    0    0G   300.000  5000.000 1377.000    01
 2.50665012E+00 3.24692404E-03-8.02146283E-07 8.75440537E-11-3.51235354E-15    2
 5.08791239E+04 7.92415787E+00 3.68685529E+00 7.97916901E-04 1.08010909E-06    3
-5.53420255E-10 7.89911433E-14 5.04320525E+04 1.46550640E+00                   4
CH                  C   1H   1    0    0G   300.000  5000.000 1368.000    01
 2.42767102E+00 1.93572344E-03-5.52507872E-07 7.01488880E-11-3.30451276E-15    2
 7.08103978E+04 7.89921915E+00 3.35518292E+00-3.85582754E-05 9.98320987E-07    3
-4.64610698E-10 6.52448478E-14 7.04680186E+04 2.84757503E+00                   4
HCOH      2/26/ 2     C   1H   2O   1    0G   300.000  5000.000 1370.000    11
 5.72229867E+00 3.27182785E-03-1.14345339E-06 1.80097741E-10-1.05539185E-14    2
-3.93941507E+04-4.97180437E+00 3.83608482E+00 6.31256398E-03-2.38146595E-06    3
 1.24300309E-11 1.24330822E-13-3.85850265E+04 5.67242361E+00                   4
C2H2          lz/JANAFC   2H   2    0    0G   300.000  5000.000 1679.000    01
 5.04909187E+00 4.64011757E-03-1.62038922E-06 2.56386353E-10-1.51065350E-14    2
 2.52663557E+04-6.59733080E+00 3.00595262E+00 8.35126056E-03-3.50931601E-06    3
 3.29512345E-10 8.44226885E-14 2.60351715E+04 4.69328648E+00                   4
C2H       H/web/tsang C   2H   1    0    0G   300.000  5000.000 1361.000    01
 4.83278721E+00 1.91273694E-03-6.76669099E-07 1.07455090E-10-6.33325450E-15    2
 6.51515097E+04-3.68549808E+00 3.41768684E+00 4.21683818E-03-1.58037276E-06    3
-7.97201949E-11 1.17545220E-13 6.57477672E+04 4.27795416E+00                   4
```

Table AF.1 Thermochemical properties of reactants, products and intermediate species in the mercury system in the NASA polynomial format for use in ChemKin (Continued)

```
THERMO
   300.000  1500.000  5000.000
KETENE     trc disk     C   2H   2O   1    0G   300.000  5000.000 1400.000    01
 6.57630093E+00 5.26966691E-03-1.77737272E-06 2.73293285E-10-1.57474816E-14    2
-8.41426534E+03-1.08995844E+01 2.53967643E+00 1.55693264E-02-1.21353905E-05    3
 5.11063402E-09-8.89022620E-13-7.08896907E+03 1.04881151E+01                   4
C4H2       trc disk     C   4H   2    0    0G   300.000  5000.000 1391.000    11
 9.48527471E+00 6.28959737E-03-2.68266540E-06 4.99497517E-10-3.25203877E-14    2
 5.04951216E+04-2.69108191E+01 3.78357574E+00 2.21967376E-02-1.97525405E-05    3
 8.79027989E-09-1.55795595E-12 5.21801182E+04 2.73379659E+00                   4
C#COH      8/25/99 THERMC   2H   2O   1    0G   300.000  5000.000 1680.000    11
 7.18273874E+00 4.80904184E-03-1.74625698E-06 2.83537892E-10-1.70061481E-14    2
 7.61595240E+03-1.38049035E+01 3.41192337E+00 1.28581354E-02-7.62742513E-06    3
 1.96346265E-09-1.57392254E-13 8.91769203E+03 6.60065107E+00                   4
C.H*C*O    8/25/99 THERMC   2H   1O   1    0G   300.000  5000.000 1455.000    01
 3.38632564E+00 6.98784179E-03-2.54645576E-06 3.66227749E-10-1.70062586E-14    2
 2.03231743E+04 1.05031981E+01 3.18155346E+00 1.33750718E-02-1.24127506E-05    3
 5.65827080E-09-1.02162411E-12 1.93712057E+04 8.83666156E+00                   4
C.C#C      hf/tsang webC   3H   3    0    0G   300.000  5000.000 1383.000    11
 7.92217083E+00 6.57459108E-03-2.30058859E-06 3.62675558E-10-2.12671687E-14    2
 3.72874394E+04-1.87602961E+01 2.21047060E+00 1.92587864E-02-1.30997017E-05    3
 4.60216827E-09-6.74452468E-13 3.93619196E+04 1.21914381E+01                   4
NC4H3      8/25/99 THERMC   4H   3    0    0G   300.000  5000.000 1400.000    11
 1.11413772E+01 6.34118482E-03-2.21100109E-06 3.47857814E-10-2.03741951E-14    2
 5.95354393E+04-3.33123329E+01 1.02851566E+00 3.34671298E-02-3.04602387E-05    3
 1.37846550E-08-2.45828206E-12 6.26662862E+04 1.97066431E+01                   4
C.H2CHO    9/ 1/99 THERMC   2H   3O   1    0G   300.000  5000.000 1380.000    11
 7.59875757E+00 6.87910492E-03-2.41255261E-06 3.80898993E-10-2.23592833E-14    2
-1.88799544E+03-1.67058233E+01 1.66232715E+00 1.96734472E-02-1.28060914E-05    3
 4.20203493E-09-5.65162473E-13 3.05264394E+02 1.55988915E+01                   4
CH2CLO.    8/25/99 THERMC   1H   2O   1CL  1G   300.000  5000.000 1354.000    01
-1.57054355E+01 3.52603829E-02-1.48562099E-05 2.50575880E-09-1.45740271E-13    2
-2.87614185E+03 1.25346246E+02 5.81935006E+00 9.41693998E-04 1.77655571E-05    3
-2.09294878E-08 6.78989156E-12-1.41755165E+04 2.62859912E-01                   4
C2H4OCL    8/25/99 THERMC   2H   4O   1CL  1G   300.000  5000.000 1358.000    21
 9.25880383E+00 1.04000185E-02-3.68739778E-06 5.86404163E-10-3.45958758E-14    2
 1.04842978E+04-1.99349546E+01 2.25625245E+00 2.08874236E-02-6.52164847E-06    3
-1.29996775E-09 7.62744867E-13 1.35568834E+04 1.98481443E+01                   4
CHCLC.H    8/25/99 THERMC   2H   2CL  1    0G   300.000  5000.000 1407.000    01
 7.49330037E+00 4.41108055E-03-1.46650946E-06 2.23466218E-10-1.28004362E-14    2
 2.93086497E+04-1.27576941E+01 1.82045304E+00 2.02122742E-02-1.84866588E-05    3
 8.54083261E-09-1.55208166E-12 3.10009597E+04 1.67664887E+01                   4
CH3CL      trc/jongwoo  C   1H   3CL  1    0G   300.000  5000.000 1387.000    01
 4.87939240E+00 6.75800016E-03-2.30086184E-06 3.56031819E-10-2.06058080E-14    2
-1.21832780E+04-2.71233961E+00 1.64066513E+00 1.26347728E-02-5.72941810E-06    3
 9.21337259E-10 2.66691086E-14-1.08660712E+04 1.53197795E+01                   4
COCL       Gurvich/119, C   1O   1CL  1    0G   300.000  5000.000 1393.000    01
 5.23928123E+00 1.79279915E-03-7.44331920E-07 1.39810168E-10-9.21739789E-15    2
-3.67997323E+03 1.37819919E+00 4.16427064E+00 4.65354754E-03-3.68977335E-06    3
 1.52327682E-09-2.57294545E-13-3.34623171E+03 7.02014828E+00                   4
CH2CL          jongwoo  C   1H   2CL  1    0G   300.000  5000.000 1421.000    01
 5.71482502E+00 3.31632237E-03-1.07732089E-06 1.61593503E-10-9.15465420E-15    2
 1.24026565E+04-4.91796614E+00 1.92490517E+00 1.33892352E-02-1.12999805E-05    3
 4.83763733E-09-8.18227430E-13 1.35668346E+04 1.49532259E+01                   4
CH2CLO.            THERMC   1H   2O   1CL  1G   300.000  5000.000 1394.000    01
 6.52283566E+00 5.51007046E-03-1.90436640E-06 2.97780751E-10-1.73644605E-14    2
-3.29892729E+03-7.90882888E+00 1.05028286E+00 1.85201814E-02-1.37751218E-05    3
 5.24608612E-09-8.11884066E-13-1.42720445E+03 2.13917821E+01                   4
C2H5CL         j/ JANAFC   2H   5CL  1    0G   300.000  5000.000 1392.000    11
 8.42602350E+00 1.08670043E-02-3.69875171E-06 5.72375356E-10-3.31331698E-14    2
-1.75817705E+04-2.02070663E+01 3.66148399E-01 2.94578293E-02-2.02144179E-05    3
 7.32637257E-09-1.10750593E-12-1.47415074E+04 2.31928787E+01                   4
```

Table AF.1 Thermochemical properties of reactants, products and intermediate species in the mercury system in the NASA polynomial format for use in ChemKin (Continued)

```
THERMO
   300.000  1500.000  5000.000
COCL2     Hfnistweb,Ped5C   1O   1CL  2    0G   300.000  5000.000 1394.000    01
 7.32540686E+00 2.34739068E-03-8.27745046E-07 1.31182235E-10-7.72153612E-15    2
-2.78867496E+04-9.12586984E+00 3.82635318E+00 1.14292586E-02-1.00157366E-05    3
 4.40508265E-09-7.71485061E-13-2.67674669E+04 9.33601318E+00                   4
C2H3CL    jongwoo       C   2H   3CL  1    0G   300.000  5000.000 1399.000    01
 7.52713624E+00 7.00950060E-03-2.37896598E-06 3.67472427E-10-2.12462804E-14    2
-8.27030170E+02-1.48260615E+01 7.55730147E-01 2.43921790E-02-1.98105125E-05    3
 8.42413956E-09-1.45442692E-12 1.36594310E+03 2.09819726E+01                   4
CH3C.HCL  jongwoo       C   2H   4CL  1    0G   300.000  5000.000 1387.000    11
 8.13376273E+00 8.59414378E-03-2.92116291E-06 4.51704038E-10-2.61364030E-14    2
 5.96743166E+03-1.59874394E+01 1.84670929E+00 2.28508421E-02-1.53326847E-05    3
 5.42129196E-09-8.01718637E-13 8.21162671E+03 1.79606856E+01                   4
CH2CLC.H2 jongwoo       C   2H   4CL  1    0G   300.000  5000.000 1393.000    11
 8.15254462E+00 8.48693313E-03-2.86291146E-06 4.40311143E-10-2.53772911E-14    2
 8.10278518E+03-1.57270117E+01 2.38722763E+00 2.21747220E-02-1.55751517E-05    3
 5.94436191E-09-9.58100659E-13 1.01048554E+04 1.51947669E+01                   4
CH3BR               C   1H   3BR  1    0G   300.000  5000.000 1391.000    01
 5.08920420E+00 6.53524214E-03-2.21413349E-06 3.41461500E-10-1.97155431E-14    2
-6.60971507E+03-2.37349517E+00 1.78091211E+00 1.32936953E-02-7.30962875E-06    3
 2.03086887E-09-2.28184004E-13-5.33897310E+03 1.57792489E+01                   4
CH2BR               C   1H   2BR  1    0G   300.000  5000.000 1428.000    01
 5.32638547E+00 3.40193818E-03-1.05346725E-06 1.52353867E-10-8.39463339E-15    2
 1.89275303E+04-1.46122739E+00 2.51357397E+00 1.19037927E-02-1.08241183E-05    3
 5.15565732E-09-9.63865396E-13 1.96931461E+04 1.29293618E+01                   4
C2H5BR              C   2H   5BR  1    0G   300.000  5000.000 1385.000    01
 9.15740830E+00 1.03559502E-02-3.46234308E-06 5.29928343E-10-3.04589472E-14    2
-1.20769613E+04-2.30607874E+01 4.72048131E-01 2.98405677E-02-1.97365771E-05    3
 6.52911770E-09-8.51583199E-13-9.00524037E+03 2.38295885E+01                   4
C2H3BR              C   2H   3BR  1    0G   300.000  5000.000 1399.000    01
 8.38311863E+00 6.17441662E-03-2.07279699E-06 3.18236568E-10-1.83343717E-14    2
 5.75843559E+03-1.83148471E+01 5.50281729E-01 2.60577136E-02-2.14144048E-05    3
 8.85549335E-09-1.45531337E-12 8.27640240E+03 2.31174958E+01                   4
CH3I      DFT       C   1H   3I   1    0G   300.000  5000.000 1397.000    01
 4.95834648E+00 6.50519132E-03-2.17271499E-06 3.31775199E-10-1.90215650E-14    2
-4.91153854E+02 6.27605213E-01 2.00450715E+00 1.28308045E-02-7.32284263E-06    3
 2.24864553E-09-2.96844551E-13 6.13648376E+02 1.67306801E+01                   4
CH2I      DFT       C   1H   2I   1    0G   300.000  5000.000 1405.000    01
 5.37570704E+00 3.63933068E-03-1.19106657E-06 1.79174780E-10-1.01585832E-14    2
 2.54828623E+04-3.26671163E-01 3.31667421E+00 1.04393322E-02-9.92452001E-06    3
 5.16590798E-09-1.05862703E-12 2.60282320E+04 1.00739653E+01                   4
CH2I2     DFT       C   1H   2I   2    0G   300.000  5000.000 1636.000    01
-3.31114223E+01 6.11337844E-02-2.73200989E-05 4.88427385E-09-3.02506325E-13    2
 3.12099415E+04 2.28374189E+02-2.57153502E+00 5.10283711E-02-8.24953516E-05    3
 5.59806733E-08-1.28756671E-11 1.32648663E+04 4.06873217E+01                   4
C2H5I     DFT       C   2H   5I   1    0G   300.000  5000.000 1397.000    11
 6.68707159E+00 1.16476380E-02-3.82043791E-06 5.76482597E-10-3.27845157E-14    2
-4.27692569E+03-8.70202774E+00 5.95871307E-01 2.40853134E-02-1.26537655E-05    3
 2.97818977E-09-1.88484322E-13-1.99773774E+03 2.46207014E+01                   4
NH3                 N   1H   3    0    0G   300.000  5000.000 1389.000    01
 2.97970283E+00 5.36649584E-03-1.72269063E-06 2.55767509E-10-1.43684723E-14    2
-6.74869190E+03 4.46279294E+00 3.24695602E+00 3.11219418E-03 1.94311268E-06    3
-1.94660238E-09 4.40577526E-13-6.64082104E+03 3.66779176E+00                   4
N2O                 N   2O   1    0    0G   300.000  5000.000 1417.000    01
 5.86045875E+00 1.06423530E-03-3.90161927E-07 6.34418784E-11-3.80123510E-15    2
 7.68593755E+03-8.11498378E+00 1.94164096E+00 1.18007331E-02-1.16025408E-05    3
 5.32866198E-09-9.36946295E-13 8.85313041E+03 1.23111353E+01                   4
HNO2                H   1N   1O   2    0G   300.000  5000.000 1407.000    01
 6.26685332E+00 3.01027317E-03-1.00567220E-06 1.53786762E-10-8.83208193E-15    2
-1.16241246E+04-7.51882774E+00 2.10974724E+00 1.45013513E-02-1.32717782E-05    3
 6.09272207E-09-1.09849490E-12-1.03776914E+04 1.41438370E+01                   4
```

Table AF.1 Thermochemical properties of reactants, products and intermediate species in the mercury system in the NASA polynomial format for use in ChemKin (Continued)

```
THERMO
   300.000  1500.000  5000.000
NH                N   1H   1    0    0G   300.000  5000.000 1370.000    01
 2.71550981E+00 1.32711303E-03-3.63447918E-07 4.36644920E-11-1.91055130E-15    2
 4.24160851E+04 6.19345229E+00 3.49617414E+00-2.58512175E-04 8.00229743E-07    3
-3.18729017E-10 3.76580302E-14 4.21181590E+04 1.91107216E+00                   4
NH2               N   1H   2    0    0G   300.000  5000.000 1379.000    01
 2.81084091E+00 3.24676776E-03-1.05043680E-06 1.56667098E-10-8.82503594E-15    2
 2.19519094E+04 6.57719876E+00 4.10811906E+00-1.25157469E-03 4.38306008E-06    3
-2.62867768E-09 5.10376766E-13 2.16908328E+04 2.01300266E-01                   4
N2H4              N   2H   4    0    0G   300.000  5000.000 1399.000    11
 6.51535345E+00 7.45035239E-03-2.52984541E-06 3.90697761E-10-2.25791187E-14    2
 8.55432595E+03-1.19149927E+01 8.18811920E-01 2.28521914E-02-1.91832572E-05    3
 8.76414838E-09-1.63696475E-12 1.03626513E+04 1.80013589E+01                   4
NNH               N   2H   1    0    0G   300.000  5000.000 1571.000    01
 4.16742324E+00 2.46673016E-03-8.65307304E-07 1.36642744E-10-8.02228288E-15    2
 2.83839161E+04 2.06115982E+00 3.73530531E+00 1.00340366E-03 3.26619818E-06    3
-2.89569630E-09 6.96522347E-13 2.87981270E+04 5.28804436E+00                   4
N2H3              N   2H   3    0    0G   300.000  5000.000 1408.000    01
 5.17455623E+00 6.20839948E-03-2.04623022E-06 3.09591871E-10-1.76333269E-14    2
 2.43234664E+04-4.69414987E+00 1.55383766E+00 1.53873329E-02-1.11813102E-05    3
 4.51731655E-09-7.65249770E-13 2.55157480E+04 1.45063789E+01                   4
N2H2              N   2H   2    0    0G   300.000  5000.000 1588.000   -11
 4.26060055E+00 5.08713262E-03-1.71197198E-06 2.63079947E-10-1.51600955E-14    2
 2.10976752E+04-2.65500543E-01 3.10781739E+00 4.30293567E-03 3.03231620E-06    3
-3.63463889E-09 9.35075869E-13 2.18616004E+04 7.18630176E+00                   4
H2NN              N   2H   2    0    0G   300.000  5000.000 1672.000    01
 3.83297667E+00 5.48981925E-03-1.96634414E-06 3.15852765E-10-1.87874159E-14    2
 3.20409335E+04 2.23143930E+00 2.50864040E+00 6.50923475E-03-4.12190469E-07    3
-1.43534326E-09 4.24019703E-13 3.26730888E+04 1.00468431E+01                   4
HNOH              N   1H   2O   1    0G   300.000  5000.000 1375.000    11
 5.24159967E+00 3.64132381E-03-1.26199881E-06 1.97647401E-10-1.15363358E-14    2
 8.79675205E+03-2.52971860E+00 3.42226375E+00 6.62639037E-03-2.62136519E-06    3
 1.83974140E-10 7.81187768E-14 9.57854845E+03 7.72947370E+00                   4
HNO               H   1N   1O   1    0G   300.000  5000.000 1671.000    01
 3.78577435E+00 2.86062727E-03-1.02423923E-06 1.64463141E-10-9.77943632E-15    2
 1.14004150E+04 3.87180706E+00 3.33656432E+00 2.67682948E-03 5.61801224E-07    3
-1.11362277E-09 2.84076438E-13 1.16664201E+04 6.71330622E+00                   4
HON               H   1N   1O   1    0G   300.000  5000.000 1671.000    01
 3.78577435E+00 2.86062727E-03-1.02423923E-06 1.64463141E-10-9.77943632E-15    2
 2.93319702E+04 3.12193287E+00 3.33656432E+00 2.67682948E-03 5.61801224E-07    3
-1.11362277E-09 2.84076438E-13 2.95979753E+04 5.96343204E+00                   4
HNOO              N   1H   1O   2    0G   300.000  5000.000 2022.000    11
 6.27806117E+00 3.90405601E-03-1.66047770E-06 2.96410587E-10-1.89019449E-14    2
 2.57031279E+04-8.10087489E+00 2.82368537E+00 9.26021904E-03-3.10310401E-06    3
-6.57972735E-10 3.64685899E-13 2.71092467E+04 1.13391551E+01                   4
HONO              N   1H   1O   2    0G   300.000  5000.000 1377.000    11
 6.11754443E+00 3.00786121E-03-1.06923897E-06 1.70344656E-10-1.00625642E-14    2
-1.17949476E+04-6.16262748E+00 2.75201622E+00 1.05958044E-02-7.62288666E-06    3
 2.77356132E-09-4.14321178E-13-1.05902472E+04 1.20246760E+01                   4
HNNO              N   2H   1O   1    0G   300.000  5000.000 1389.000    01
 6.24923397E+00 3.26982591E-03-1.14794125E-06 1.81382848E-10-1.06538432E-14    2
 2.53822146E+04-7.09498045E+00 2.40143952E+00 1.26718684E-02-1.00828327E-05    3
 4.10522704E-09-6.79228428E-13 2.66782706E+04 1.34257466E+01                   4
NH2O              N   1H   2O   1    0G   300.000  5000.000 1398.000    01
 4.26222946E+00 4.60071183E-03-1.52686780E-06 2.32081626E-10-1.32607909E-14    2
 6.26937944E+03 1.89523866E+00 2.62132820E+00 8.05594277E-03-4.34199726E-06    3
 1.31067675E-09-1.79413143E-13 6.89825876E+03 1.08768221E+01                   4
NH2NO             N   2H   2O   1    0G   300.000  5000.000 1377.000    11
 8.35645419E+00 4.59104236E-03-1.83368539E-06 3.12986502E-10-1.93224729E-14    2
 5.24021483E+03-2.07973793E+01 1.30310021E+00 1.94969060E-02-1.34642267E-05    3
 4.29560482E-09-5.24866849E-13 7.86417437E+03 1.76712433E+01                   4
```

Table AF.1 Thermochemical properties of reactants, products and intermediate species in the mercury system in the NASA polynomial format for use in ChemKin (Continued)

```
THERMO
   300.000  1500.000  5000.000
NH2OH               N   1H   3O   1    0G   300.000  5000.000 1412.000    11
 5.12276976E+00 5.73428235E-03-1.86277360E-06 2.78938294E-10-1.57685162E-14    2
-7.42648115E+03-3.34064378E+00 1.59842447E+00 1.54722272E-02-1.24132632E-05    3
 5.50996691E-09-1.00114327E-12-6.34935611E+03 1.50585858E+01                   4
HNNNH2              N   3H   3    0    0G   300.000  5000.000 1387.000    11
 6.69002977E+00 7.47314743E-03-2.57645357E-06 4.02077694E-10-2.34100066E-14    2
 2.41665872E+04-1.12237243E+01 1.77934214E+00 1.84512488E-02-1.22068379E-05    3
 4.40169331E-09-6.88479410E-13 2.59657724E+04 1.53992811E+01                   4
H2NNHO              N   2H   3O   1    0G   300.000  5000.000 1405.000    11
 6.76839973E+00 6.93278545E-03-2.28605864E-06 3.45978136E-10-1.97094460E-14    2
 1.42869506E+04-9.16405730E+00 2.56091925E+00 1.79916567E-02-1.37740394E-05    3
 5.87277137E-09-1.04140755E-12 1.56384603E+04 1.30177571E+01                   4
HONHO               N   1H   2O   2    0G   300.000  5000.000 1416.000    11
 8.93497753E+00 3.30770129E-03-1.20772778E-06 1.95857004E-10-1.17134360E-14    2
-1.46490671E+03-2.26038531E+01 8.79575635E-02 2.51912561E-02-2.14675867E-05    3
 8.50478683E-09-1.28236512E-12 1.39294083E+03 2.43240957E+01                   4
HNNHO               N   2H   2O   1    0G   300.000  5000.000 1382.000    11
 6.90419698E+00 5.93493210E-03-2.30332640E-06 3.85553342E-10-2.34769344E-14    2
 9.94153064E+03-1.35078795E+01 5.11596286E-01 1.95396804E-02-1.31481290E-05    3
 4.26547682E-09-5.54657472E-13 1.23230197E+04 2.13441690E+01                   4
HCN                 H   1C   1N   1    0G   300.000  5000.000 1394.000   -11
 4.14927792E+00 2.75915258E-03-9.32137167E-07 1.43421224E-10-8.26578626E-15    2
 1.47264308E+04-5.23696279E-01 2.85596122E+00 6.10771314E-03-4.55238135E-06    3
 2.02415423E-09-3.88077850E-13 1.51690916E+04 6.34976775E+00                   4
CN                  C   1N   1    0    0G   300.000  5000.000 1415.000    01
 3.14887755E+00 1.16843961E-03-3.44267037E-07 4.54058479E-11-2.21768247E-15    2
 5.13428610E+04 6.07261290E+00 3.15725687E+00 1.05392235E-03-1.60373509E-07    3
-5.86680755E-11 1.78191434E-14 5.13535565E+04 6.06796993E+00                   4
HCNO                H   1N   1C   1O   1G   300.000  5000.000 1382.000    01
 6.59860963E+00 3.02778176E-03-1.07704170E-06 1.71666204E-10-1.01439167E-14    2
 1.85981362E+04-1.03306840E+01 2.64728954E+00 1.27504947E-02-1.04793593E-05    3
 4.41428601E-09-7.57511793E-13 1.99310282E+04 1.07332568E+01                   4
NCO                 N   1C   1O   1    0G   300.000  5000.000 1383.000   -11
 5.61055963E+00 1.70150289E-03-6.09806403E-07 9.76869117E-11-5.79292075E-15    2
 1.38072715E+04-5.26992558E+00 2.91689747E+00 8.02844550E-03-6.22000591E-06    3
 2.33065249E-09-3.42747536E-13 1.47273691E+04 9.16504917E+00                   4
HNCO                H   1N   1C   1O   1G   300.000  5000.000 1369.000    11
 6.44993880E+00 2.72947182E-03-9.74239492E-07 1.55636356E-10-9.21143714E-15    2
-1.63583014E+04-9.56790707E+00 3.32075040E+00 9.16891675E-03-5.65090853E-06    3
 1.51468689E-09-1.25530318E-13-1.51905797E+04 7.53721773E+00                   4
HOCN                H   1N   1C   1O   1G   300.000  5000.000 1368.000    11
 5.89785505E+00 3.16788876E-03-1.11800872E-06 1.77242802E-10-1.04338945E-14    2
-3.43453705E+03-6.18170948E+00 3.78605347E+00 6.88666302E-03-3.21484585E-06    3
 5.17171771E-10 1.19418528E-14-2.55498549E+03 5.63290792E+00                   4
CH3NO               H   3N   1C   1O   1G   300.000  5000.000 1388.000    11
 6.13898635E+00 7.80970812E-03-2.66333307E-06 4.12585740E-10-2.38979919E-14    2
 6.45852873E+03-7.09474823E+00 2.13850410E+00 1.53552284E-02-7.47157269E-06    3
 1.49265672E-09-5.01847223E-14 8.05351674E+03 1.50713506E+01                   4
H2CN                H   2C   1N   1    0G   300.000  5000.000 1447.000    01
 5.10020034E+00 4.02780457E-03-1.36439687E-06 2.10725390E-10-1.21898913E-14    2
 2.75503212E+04-4.27685973E+00 2.45567298E+00 7.78048129E-03-1.59463948E-06    3
-1.33785619E-09 5.32582058E-13 2.86868687E+04 1.07457988E+01                   4
HCNH                H   2C   1N   1    0G   300.000  5000.000 2006.000    01
 4.36369836E+00 4.90387832E-03-1.73220628E-06 2.75795925E-10-1.63084707E-14    2
 3.14619807E+04 1.22358113E+00 2.29069023E+00 8.81553459E-03-3.94922755E-06    3
 5.50527293E-10 4.11232910E-14 3.22302552E+04 1.26287011E+01                   4
CH2NN               H   2N   2C   1O   0G   300.000  5000.000 1394.000    01
 6.93551165E+00 5.19106951E-03-1.80090527E-06 2.82284903E-10-1.64876419E-14    2
 3.14873720E+04-1.32390672E+01 1.35048340E+00 1.95270191E-02-1.62924218E-05    3
 7.08039927E-09-1.24896691E-12 3.33088967E+04 1.63171721E+01                   4
```

Table AF.1 Thermochemical properties of reactants, products and intermediate species in the mercury system in the NASA polynomial format for use in ChemKin (Continued)

```
THERMO
   300.000  1500.000  5000.000
HCNN                C   1H   1N   2    0G   300.000  5000.000 1550.000    01
 6.69235162E+00 2.94630683E-03-1.05005007E-06 1.67688883E-10-9.92562522E-15    2
 5.21131302E+04-1.04086173E+01 2.51215416E+00 1.14099220E-02-6.74320099E-06    3
 1.43556888E-09-6.76770857E-15 5.36571759E+04 1.24410841E+01                   4
HNC                 H   1C   1N   1    0G   300.000  5000.000 1394.000   -11
 4.14927792E+00 2.75915258E-03-9.32137167E-07 1.43421224E-10-8.26578626E-15    2
 2.12186301E+04-2.04250130E-02 2.85596122E+00 6.10771314E-03-4.55238135E-06    3
 2.02415423E-09-3.88077850E-13 2.16612909E+04 6.85303902E+00                   4
CH2NO               H   2N   1C   1O   1G   300.000  5000.000 1394.000    01
 6.93551165E+00 5.19106951E-03-1.80090527E-06 2.82284903E-10-1.64876419E-14    2
 1.78889823E+04-1.16990571E+01 1.35048340E+00 1.95270191E-02-1.62924218E-05    3
 7.08039927E-09-1.24896691E-12 1.97105071E+04 1.78571822E+01                   4
N*CHOH              H   2N   1C   1O   1G   300.000  5000.000 1413.000    01
 6.93897452E+00 4.71821384E-03-1.53385743E-06 2.29772554E-10-1.29916458E-14    2
 4.28624059E+03-1.01541211E+01 9.77462017E-01 2.41423841E-02-2.55329376E-05    3
 1.33329489E-08-2.65581629E-12 5.80631061E+03 1.99108380E+01                   4
CH3NH2              H   5C   1N   1    0G   300.000  5000.000 1387.000    11
 5.23365635E+00 1.08525478E-02-3.65205276E-06 5.60552544E-10-3.22553445E-14    2
-5.52829585E+03-5.21507439E+00 1.69170299E+00 1.60389158E-02-4.99028408E-06    3
-3.83481486E-10 3.57345771E-13-3.94057425E+03 1.49835076E+01                   4
CH3N.H              H   4C   1N   1    0G   300.000  5000.000 1404.000    11
 4.90528427E+00 8.50385563E-03-2.82356460E-06 4.29267835E-10-2.45297886E-14    2
 1.94541504E+04-1.35290193E+00 1.53882580E+00 1.62436536E-02-9.89573367E-06    3
 3.49954465E-09-5.53823533E-13 2.06715088E+04 1.68295525E+01                   4
C.H2NH2             H   4C   1N   1    0G   300.000  5000.000 1397.000    11
 6.11432304E+00 7.69126261E-03-2.59025727E-06 3.97713573E-10-2.28883271E-14    2
 1.55835139E+04-8.93053847E+00 2.56157776E+00 1.60730711E-02-1.05960330E-05    3
 4.07638792E-09-6.95570459E-13 1.68563723E+04 1.01987687E+01                   4
H2C*NH              H   3C   1N   1    0G   300.000  5000.000 1577.000    01
 4.54737803E+00 7.17720940E-03-2.47935296E-06 3.87692345E-10-2.26113071E-14    2
 8.64056520E+03-1.16687451E+00 2.81849503E+00 5.11983263E-03 6.38887100E-06    3
-6.61374634E-09 1.65531930E-12 9.88442608E+03 1.03390635E+01                   4
CH2*NNH2            H   4N   2C   1O   0G   300.000  5000.000 2024.000    11
 7.02918655E+00 1.07349675E-02-3.96902197E-06 6.51073701E-10-3.92938358E-14    2
 1.94717934E+04-1.31884644E+01 1.72189952E+00 1.97412946E-02-7.76110660E-06    3
 2.13931609E-10 3.32392443E-13 2.15558783E+04 1.64022700E+01                   4
CH3N*NH             H   4N   2C   1O   0G   300.000  5000.000 1374.000    11
 7.15922588E+00 9.68053382E-03-3.35166216E-06 5.24593968E-10-3.06073574E-14    2
 1.79983421E+04-1.46381737E+01 2.15378337E+00 1.76553455E-02-6.42988202E-06    3
-7.32179130E-11 3.65051122E-13 2.01548171E+04 1.36411729E+01                   4
NH2NO2              N   2H   2O   2    0G   300.000  5000.000 1387.000    11
 8.81477821E+00 5.43771668E-03-1.82922027E-06 2.81195692E-10-1.62135680E-14    2
-2.65682894E+03-1.89708069E+01 3.23962569E+00 1.87039154E-02-1.38471402E-05    3
 5.21220151E-09-7.89699939E-13-7.63827212E+02 1.08543873E+01                   4
C.*C*O    10/ 2/ 8 THERMC   2H   1O   1    0G   300.000  5000.000 1420.000    01
 7.08844349E+00 2.47836871E-03-7.66266424E-07 1.10686351E-10-6.09327677E-15    2
 1.83359290E+04-1.12572855E+01 2.76123658E+00 1.68803861E-02-1.86395238E-05    3
 9.82647374E-09-1.94988258E-12 1.93879371E+04 1.04230847E+01                   4
NCN                 C   1N   2    0    0G   300.000  5000.000 1444.000    11
 5.60966825E+00 1.71713033E-03-6.18685433E-07 9.94518305E-11-5.91151073E-15    2
 4.61122617E+04-5.22381790E+00 4.00561368E+00 3.56023430E-03 1.72553361E-07    3
-1.49802718E-09 4.77710926E-13 4.68419519E+04 4.03722322E+00                   4
NCCN      nogen     C   2N   2    0    0G   300.000  5000.000 1379.000    11
 7.51071286E+00 2.65053479E-03-9.40406818E-07 1.49622572E-10-8.83019382E-15    2
 3.44534099E+04-1.52329663E+01 4.49552737E+00 1.01619977E-02-8.45555610E-06    3
 3.71536417E-09-6.73262323E-13 3.54774815E+04 8.35200361E-01                   4
SN                  N   1S   1    0    0G   300.000  5000.000 1390.000    01
 3.89798242E+00 6.31279451E-04-2.16999939E-07 3.37708997E-11-1.94972616E-15    2
 3.04461123E+04 4.15001810E+00 3.29541748E+00 2.11848642E-03-1.64837344E-06    3
 6.71128268E-10-1.11995649E-13 3.06477236E+04 7.35851114E+00                   4
```

Table AF.1 Thermochemical properties of reactants, products and intermediate species in the mercury system in the NASA polynomial format for use in ChemKin (Continued)

```
THERMO
   300.000  1500.000  5000.000
CS                C   1S   1    0    0G   300.000  5000.000 1391.000    01
 3.75694271E+00 7.70142906E-04-2.71372366E-07 4.30800166E-11-2.51582074E-15    2
 3.24710335E+04 3.46727587E+00 2.87970663E+00 2.99673217E-03-2.47540271E-06    3
 1.04930129E-09-1.79763240E-13 3.27573417E+04 8.11477057E+00                   4
COS               O   1C   1S   1    0G   300.000  5000.000 1385.000    01
 5.60404412E+00 1.69949255E-03-6.07299045E-07 9.70949945E-11-5.74997228E-15    2
-1.87228699E+04-5.25594309E+00 3.01607100E+00 7.91127266E-03-6.31352241E-06    3
 2.48477066E-09-3.89744465E-13-1.78480331E+04 8.57239597E+00                   4
HS2               H   1S   2    0    0G   300.000  5000.000 1399.000    01
 5.19307706E+00 1.52902438E-03-5.26847320E-07 8.22293768E-11-4.78934616E-15    2
 1.07496122E+04-1.00747077E-02 3.34347050E+00 6.21704197E-03-5.12060138E-06    3
 2.14142273E-09-3.58870885E-13 1.13497757E+04 9.78413475E+00                   4
H2S2              H   2S   2    0    0G   300.000  5000.000 1405.000    01
 6.40378918E+00 2.95490097E-03-9.98421682E-07 1.53764229E-10-8.87182659E-15    2
-4.73538486E+02-7.87544431E+00 3.27747999E+00 1.11568010E-02-9.35423150E-06    3
 4.04846789E-09-7.02965186E-13 5.14340712E+02 8.58253662E+00                   4
SO3               O   3S   1    0    0G   300.000  5000.000 1405.000    01
 7.95068457E+00 1.89875954E-03-6.92700907E-07 1.12273628E-10-6.71212482E-15    2
-5.06582593E+04-1.62412490E+01 2.40564312E+00 1.64934130E-02-1.53516672E-05    3
 6.75464382E-09-1.14763548E-12-4.89419933E+04 1.28817538E+01                   4
H2SO4             O   4H   2S   1    0G   300.000  5000.000 1414.000    01
 1.31458375E+01 4.90783184E-03-1.68626552E-06 2.63107564E-10-1.53339666E-14    2
-9.33403333E+04-4.26248987E+01 2.96617927E+00 3.17953506E-02-2.87311719E-05    3
 1.25068196E-08-2.11174931E-12-9.02053479E+04 1.07948356E+01                   4
HOSO              O   2H   1S   1    0G   300.000  2000.000 1000.000    01
 4.28317645E+00 9.67387302E-03-9.99330458E-06 5.39574689E-09-1.15219973E-12    2
-3.06675833E+04 7.07647740E+00 4.28317645E+00 9.67387302E-03-9.99330458E-06    3
 5.39574689E-09-1.15219973E-12-3.06675833E+04 7.07647740E+00                   4
HOSO2             O   3H   1S   1    0G   300.000  2000.000 1000.000    01
 2.50369806E+00 2.95642136E-02-3.97059532E-05 2.51999115E-08-6.01921745E-12    2
-4.63918014E+04 1.40808710E+01 2.50369806E+00 2.95642136E-02-3.97059532E-05    3
 2.51999115E-08-6.01921745E-12-4.63918014E+04 1.40808710E+01                   4
HSO               O   1H   1S   1    0G   300.000  2000.000 1000.000    01
 1.31019613E+00 1.63456955E-02-2.36430659E-05 1.71199432E-08-4.68300083E-12    2
-3.65755094E+03 1.76695677E+01 1.31019613E+00 1.63456955E-02-2.36430659E-05    3
 1.71199432E-08-4.68300083E-12-3.65755094E+03 1.76695677E+01                   4
HSOH              O   1H   2S   1    0G   300.000  2000.000 1000.000    01
 1.84565871E+00 1.61386139E-02-1.64218888E-05 8.76780691E-09-1.94435992E-12    2
-1.54922131E+04 1.48606919E+01 1.84565871E+00 1.61386139E-02-1.64218888E-05    3
 8.76780691E-09-1.94435992E-12-1.54922131E+04 1.48606919E+01                   4
SH                H   1S   1    0    0G   300.000  5000.000 1401.000    01
 3.25746777E+00 9.49222158E-04-2.84408333E-07 3.94121834E-11-2.09336961E-15    2
 1.57343324E+04 4.66089227E+00 3.20037150E+00 1.02848004E-03-3.07528792E-07    3
 3.13617007E-11 1.42965728E-15 1.57616841E+04 4.99018760E+00                   4
H2SO              O   1H   2S   1    0G   300.000  2000.000 1000.000    01
 4.04891973E-01 2.00225704E-02-2.22477950E-05 1.41711290E-08-3.74090131E-12    2
-6.50717418E+03 2.14217740E+01 4.04891973E-01 2.00225704E-02-2.22477950E-05    3
 1.41711290E-08-3.74090131E-12-6.50717418E+03 2.14217740E+01                   4
H2S               H   2S   1    0    0G   300.000  5000.000 1682.000    01
 3.35560838E+00 3.26113205E-03-1.17070412E-06 1.88226014E-10-1.11998367E-14    2
-3.67804257E+03 4.55164496E+00 3.91615504E+00-6.65450486E-05 3.93189574E-06    3
-2.77355901E-09 5.75347173E-13-3.66020143E+03 2.29155778E+00                   4
```

Table AF.1 Thermochemical properties of reactants, products and intermediate species in the mercury system in the NASA polynomial format for use in ChemKin (Continued)

```
THERMO
   300.000  1500.000  5000.000

HSO2                O   2H   1S   1    0G   300.000  2000.000 1000.000    01
 5.41519318E-01 2.73988761E-02-3.79389716E-05 2.57863013E-08-6.66841425E-12    2
-1.81024388E+04 2.19334480E+01 5.41519318E-01 2.73988761E-02-3.79389716E-05    3
 2.57863013E-08-6.66841425E-12-1.81024388E+04 2.19334480E+01                   4
HOS                 O   1H   1S   1    0G   300.000  2000.000 1000.000    01
 2.13958640E+00 1.11982848E-02-1.54840024E-05 1.08037701E-08-2.83656318E-12    2
-1.01885716E+03 1.38411198E+01 2.13958640E+00 1.11982848E-02-1.54840024E-05    3
 1.08037701E-08-2.83656318E-12-1.01885716E+03 1.38411198E+01                   4
HOSHO               O   2H   2S   1    0G   300.000  2000.000 1000.000    01
 9.09515802E-01 2.74983512E-02-3.07393817E-05 1.71387299E-08-3.75101251E-12    2
-3.37199352E+04 2.03025712E+01 9.09515802E-01 2.74983512E-02-3.07393817E-05    3
 1.71387299E-08-3.75101251E-12-3.37199352E+04 2.03025712E+01                   4
SCL                 CL  1S   1    0    0G   300.000  5000.000 1494.000    01
 8.13033888E+00-7.04377360E-03 4.56149892E-06-1.13619569E-09 9.27711270E-14    2
 1.62488698E+04-1.69016569E+01 4.47211024E+00 8.87235641E-04-2.10346178E-06    3
 2.11343471E-09-7.40305768E-13 1.74643078E+04 2.85185607E+00                   4
```

APPENDIX AG

REACTION MECHANISM – MERCURY OXIDATION

Appendix AG includes the mechanism used for the kinetic study of the oxidation of mercury.

Table AG.1 Mercury oxidation mechanism

```
ELEMENTS
H  CL  O  BR  HG  N  C  AR  HE   S I
END

SPECIES
HE      AR      H       O       C
N       N2      O3      O2      H2
OH      HO2     H2O     H2O2
!Mercury Species
HG
HGO             HGOH            HGOH2       HGOHOH      HGOHO
HGCL            HGCL2           HGCLO       HGBRCL      HGOHCL
HGBR            HGBR2           HGBRO       HGBROH
HGNO            HGNO2           HGONO       NOHGNO
NOHGNO2     NO2HGNO2    CLHGNO      BRHGNO      CLHGNO2
BRHGNO2     HGCLNO      HGBRNO      HGCLNO2     HGBRNO2
HGSO            HGSO2           CLHGSO      BRHGSO      CLHGSO2
HGCLSO      HGBRSO
!Chlorine Species
CL              CL2             HCL
CLO             CLO2            HOCL            CLOO
CLNO            CLNO2           CLONOcis        CLONOtran
CLONO2
CLSO            CLSO2
!Bromine Species
BR              BR2             HBR
BRO             HOBR
BRNO            BRNO2           BRONOcis        BRONOtran
BRONO2
BRSO            BRSO2
BRCL
!Iodine Species
I               I2              HI
HGI             HGI2            IO
HOI             ICL             INO
INO2            CH3I            CH2I
CH2I2           C2H5I
! Hydrocarbons
CO2             CO              CH4             CH3             C2H5
CH3O            CH3OO           C2H6            CH2OH           CH3OH
CH3BR           CH2BR           C2H5BR          C2H3BR
C2H3            C2H4            CH2             CH2(S)          C2H
CH3CL           C2H2            C#COH           C.H*C*O
CH2CL           CH2CLO.
KETENE          C2H5CL          COCL2           C2H4OCL         CHCLC.H
CH2O            HCO             COCL            C2H3CL          CH3C.HCL
CH2CLC.H2       C.*C*O          CH              C.H2CHO
```

Table AG.1 Mercury oxidation mechanism (Continued)

```
!Nitrogenated
NO              NO2          NO3
NH3             N2O          HNO          NH2O          N2H4
HNO2            NH           NH2          NNH           NH2NO2
N2H3            N2H2         H2NN         HNOH          NH2NO
HON             HNOO         HONO         HNNO          CH2NO
NH2OH           HNNNH2       H2NNHO       HCOH          H2CN
HONHO           HNNHO        HCN          CN            HCNO
NCO             HNCO         HOCN         CH3NO         HCNH
CH2NN           HCNN         HNC          NCN           NCCN
N*CHOH          CH3NH2       CH3N.H       CH3N*NH       CH2*NNH2
C.H2NH2         H2C*NH
!Sulfur species
S               S2           H2S          SO            SO2
SN              HS2          H2S2         SO3           H2SO4
HOSO            HOSO2        HSO          HSOH          SH
H2SO            HSO2         HOS          HOSHO         SCL
CS              COS
END

REACTIONS
!*****************************************************
!************************ Hg ***************************
!*****************************************************

!*****************************************
!*************** Hg-Br ********************
!*****************************************
!Wilcox et al., Auzmendi&Bozzelli
HG + BR = HGBR                  2.75E11    0.0    -1620.     !Wilcox,2009
HGBR + BR2 = HGBR2 + BR         1.11E14    0.0    60.        ! Niksa 2009
HG + BR2 = HGBR + BR            1.15E15    0.0    30100      ! Wilcox 2011
HGBR + BR =  HGBR2              3.87E15   -0.57   0.00       ! Goodsite 2004
HG + BR2 = HGBR2                2.83E10    1.06   33.63E3    ! NJ IT Ea= m06-2x/aug-cc-pVTZ-PP
HG + HBR = HGBR + H             1.86E13    0.0    8602.9     ! Wilcox 2011
HGBR + HBR = HGBR2 + H          9.41E12    0.0    2235.4     ! Wilcox 2011
!***** Hg-Br-HOx *****
!K.A. Peterson
HGBR + OH <=> HG + HOBR         3.27E12    0.0    1000.      ! dH -35.
HGBR + O = BRO + HG             3.35E13    0.0    1300.      ! dH -39.
HGBR + HOBR <=> HGBR2 + OH      2.27E12    0.0    1700.      ! dH -10. jwb
HGBR + BRO = HGBR2 + O          2.25E12    0.0    1150.      ! dH -7. Petsn 0 barrier
HGOH + BR <=> HGBROH            1.57E30   -7.28   1903.      !  1.00E+00 atm,  200-1400 K
HGOH + BR <=> HGBR + OH         6.67E13   -0.36   218.       !  1.00E+00 atm,  200-1400 K
HGBR + OH <=> HGBROH            2.19E29   -5.77   2976.      !  1.00E+00 atm,  200-1400 K
HGO + BR <=> HGBRO              8.29E24   -4.75   1735.      !  1.00E+00 atm,  200-1400 K
HGBROH + OH = HGBRO + H2O       2.45E12    0.0    850.       ! jwb abstn
HGBRO + HO2 = HGBROH + O2       5.5E11     0.0    0.0        ! disprop jwb

!*****************************************
!*************** Hg-Cl ********************
!*****************************************
!Wilcox et al.
HG + CL = HGCL                  2.4E8          1.4    -14400        !Widmer, 2000
HGCL + CL2 = HGCL2 + CL         1.39E14        0.0    1000.         !Widmer, 2000
HG + CL2 = HGCL + CL            6.15E13        0.0    43300.        !Wilcox, 2009
HGCL + CL = HGCL2               2.19E14        0.0    3100          !Widmer, 2000
HG + CL2 = HGCL2                1.35E10        1.24   39.51E3    ! NJIT Ea= m06-2x/aug-cc-pvtz-PP
HG + HCL = HGCL + H             1.93E13        0.0    11213.        ! Wilcox 2009
HGCL + HCL <=> HGCL2 + H        3.11E11        0.0    3642.         ! Wilcox 2003
!***** Hg-Cl-HOx *****
!Ariya et al.
 HG + CLO = HGO + CL            1.38E12        0.0    8320.         !  Widmer
HGCL + OH <=> HGOHCL            6.77E25       -9.17   593.          !  1.00E+00 atm,  300-2000 K
```

Table AG.1 Mercury oxidation mechanism (Continued)

```
HGCL + OH <=> HGOH + CL          1.07E23   -4.17     2017.     !  1.00E+00 atm,  300-2000 K
HGOHCL <=> HGOH + CL             3.81E30   -5.62    66104.     !  1.00E+00 atm,  300-2000 K
HGOH + OH <=> HGOHOH             2.93E39   -9.13     5052.     !  1.00E+00 atm,  300-2000 K
HGOH + CL <=> HGO + HCL          1.00E13    0.0     10000.     ! endo 10 kcal W?
HGOHCL + CL <=> HGCLO + HCL      1.00E13    0.0     12000.     ! endo 10 kcal
HGOHOH + CL <=> HGOHO + HCL      1.00E13    0.0     12000.     ! endo 11
HGOHOH + OH = HGOHO + H2O        2.45E12    0.0      4500.     ! exo 7.
HGOHCL + OH = HGCLO + H2O        2.45E12    0.0      4100.     ! exo 8.
HGCL + HOCL <=> HGCL2 + OH       3.48E10    0.0        60.     ! Wilcox 2009
HG + HO2 <=> HGO   + OH          5.50E11    0.0     62500.     ! Endo goes in reverse
HGO = HG + O                     1.00E11    0.0      5000.     ! Exo rxn wow ?
HG + HOCL = HGCL + OH            2.50E12    0.0     32000.     ! endo 30.
HGO + HCL = HGCL + OH            9.63E04    0.0      8920.     ! Widmer
HGO + HOCL = HGCL + HO2          4.11E13    0.0     60470.     ! Widmer
!HG + CLO2 = HGO + CLO           1.87E07    0.0     51270.     !  Widmer

!*********************************************
!*************** Hg-I ************************
!*********************************************
!Auzmendi&Bozzelli
HG + I <=> HGI                   1.86E17   -2.38      0.0      !  Goodsite, 2004
HG + I2 = HGI + I                2.79E13    2.22     27796     !  jwb-auzmendi 2012
HGI + I2 <=> HGI2 + I            2.76E09    2.72      0.0      !  jwb-auzmendi 2012
HGI + I = HGI2                   1.05E05    2.24      0.0      !  jwb-auzmendi 2012
HG + I2 = HGI2                   2.37E10    1.06     38020     !  NJIT Ea= m06-2x/aug-cc-pvtz-PP

!*********************************************
!*************** Hg-Cl-Br ********************
!*********************************************
!Bozzelli
HGCL + BR2 = HGBRCL + BR         8.2E11    0.0      1050.
HGBR + CL2 = HGBRCL + CL         6.7E12    0.0      1250

!*********************************************
!***************** Hg-HOx ********************
!*********************************************
!Bozzelli
HG + OH <=> HGOH                 1.98E21   -3.68     2249.     !  1.00E+00 atm,  300-2000 K
HGOHO + HO2 = HGOH2 + O2          5.5E11     0.0      0.0      ! disprop jwb          HGOH2= Hg(OH)2

!*********************************************
!*************** Hg-NOx **********************
!*********************************************
!Auzmendi &Bozzelli
!HG + NO = HGNO                  1.0E11    0.0      6000.0     ! dHrxn = -2.
!HG + NO2 = HGNO2                 1.0E11    0.0     6000.0     ! dHrxn = 2.2
!HG + NO2 = HGONO                 1.0E11    0.0      6000.0    ! dHrxn = 16.8
!HGNO + NO = NOHGNO               1.0E11    0.0      48.7E3    ! dHrxn = 42.7
!HGNO + NO2 = NOHGNO2             1.0E11    0.0      19.6E3    ! dHrxn = 13.6
!HGNO2 + NO = NOHGNO2             1.0E11    0.0      15.0E3    ! dHrxn = 9.0
HGNO2 + NO2 = NO2HGNO2           2.0E14    0.0        3E3     ! dHrxn = -12.5    auz&jwb

!*********************************************
!*************** Hg-Halo-NOx *****************
!*********************************************
!Auzmendi &Bozzelli
!********** Hg-Cl-NOx **************
HGCL + NO = CLHGNO               2.0E14    0.0        3E3     ! dHrxn = -11.4   auz&jwb
HGCL + NO2 = CLHGNO2             2.0E15    0.0        3E3     ! dHrxn = -34.5   auz&jwb
HGCL + NO = HGCLNO               2.0E14    0.0        3E3     ! dHrxn = -15.2   auz&jwb
HGCL + NO2 = HGCLNO2             2.0E14    0.0        3E3     ! dHrxn = -11.2   auz&jwb
CL + HGNO = CLHGNO               2.0E15    0.0        3E3     ! dHrxn = -33.9
CL + HGNO2 = CLHGNO2             2.0E15    0.0        3E3     ! dHrxn = -61.6
```

Table AG.1 Mercury oxidation mechanism (Continued)

```
HG + CLNO = HGCLNO              2.0E15     0.0          3E3       ! dHrxn = -2.6
HG + CLNO2 = HGCLNO2            2.0E15     0.0          3E3       ! dHrxn = -1.4
HG + CLNO = CLHGNO              7.5E12     0.0     40000.0    ! dHrxn = 1.2       auz&jwb
HG + CLNO2 = CLHGNO2            7.5E12     0.0     40000.0    ! dHrxn = -24.7     auz&jwb
CL + HGNO = HGCLNO              2.5E11     0.0     40000.0    ! dHrxn = -37.7     auz&jwb
CL + HGNO2 = HGCLNO2            2.5E11     0.0     40000.0    ! dHrxn = -38.3     auz&jwb
HGCL + CLNO = HGCL2 + NO        6.15E13     0.0      43300.      ! dHrxn = -43.42   auz&jwb
HGCL + CLNO2 = HGCL2 + NO2      6.15E13     0.0      43300.      ! dHrxn = -47.28   auz&jwb
!************ Hg-Br-NOx ********************
HGBR + NO = BRHGNO                2.0E14     0.0     3E3          ! dHrxn = -10.6   auz&jwb
HGBR + NO2 = BRHGNO2              2.0E15     0.0     3E3          ! dHrxn = -33.8   auz&jwb
HGBR + NO = HGBRNO                2.0E14     0.0     3E3          ! dHrxn = -12.5   auz&jwb
HGBR + NO2 = HGBRNO2              2.0E14     0.0     3E3          ! dHrxn = -10.4   auz&jwb
BR + HGNO = BRHGNO                2.0E15     0.0     3E3          ! dHrxn = -24.7
BR + HGNO2 = BRHGNO2              2.0E15     0.0     3E3          ! dHrxn = -52.5
HG + BRNO = HGBRNO                2.0E15     0.0     3E3          ! dHrxn = -1.5
HG + BRNO2 = HGBRNO2              2.0E15     0.0     3E3          ! dHrxn = -1.3
HG + BRNO = BRHGNO              7.5E12    0.0    40000.0    ! dHrxn = 0.5      auz&jwb
HG + BRNO2 = BRHGNO2            7.5E12    0.0    40000.0    ! dHrxn = -24.8    auz&jwb
BR + HGNO = HGBRNO              2.5E11    0.0    40000.0    ! dHrxn = -26.6    auz&jwb
BR + HGNO2 = HGBRNO2            2.5E11    0.0    40000.0    ! dHrxn = -29.2    auz&jwb
HGBR + BRNO = HGBR2 + NO        6.15E13  0.0     43300.      ! dHrxn = -45.57   auz&jwb
HGBR + BRNO2 = HGBR2 + NO2      6.15E13  0.0     43300.      ! dHrxn = -48.8    auz&jwb

!*********************************************
!*************** Hg-SOx *********************
!*********************************************
!Auzmendi &Bozzelli
HG + SO = HGSO                    1.0E11     0.0        6000.0     ! dHrxn = 20.9    auz&jwb
HG + SO2 = HGSO2                1.0E11     0.0          6000.0     ! dHrxn = -3.0    auz&jwb

!*************************************************
!*************** Hg-Halo-SOx **********************
!*************************************************
!Auzmendi &Bozzelli
!********** Hg-Cl-SOx ***************
HGCL + SO = CLHGSO              2.0E14     0.0          3E3              ! dHrxn = -34.3   auz&jwb
HGCL + SO2 = CLHGSO2            2.0E15     0.0          3E3              ! dHrxn = -7.6    auz&jwb
HGCL + SO = HGCLSO              2.0E14     0.0        3E3              ! dHrxn = -29.9   auz&jwb
CL + HGSO = CLHGSO              2.0E15     0.0          3E3              ! dHrxn = -80.1   auz&jwb
CL + HGSO2 = CLHGSO2            2.0E15     0.0          3E3              ! dHrxn = -29.6   auz&jwb
HG + CLSO = HGCLSO              2.0E15     0.0          3E3              ! dHrxn = 0       auz&jwb
HG + CLSO = CLHGSO              7.5E12     0.0     40000.0           ! dHrxn = -4.5    auz&jwb
HG + CLSO2 = CLHGSO2            7.5E12     0.0     40000.0           ! dHrxn = -17.0   auz&jwb
CL + HGSO = HGCLSO              2.5E11     0.0     40000.0           ! dHrxn = -75.7   auz&jwb
!********** Hg-Br-SOx ***************
HGBR + SO = BRHGSO              2.0E14     0.0          3E3              ! dHrxn = -32.7    auz&jwb
HGBR + SO = HGBRSO              2.0E14     0.0        3E3              ! dHrxn = -25.7    auz&jwb
BR + HGSO = BRHGSO              2.0E14     0.0          3E3              ! dHrxn = -70.1    auz&jwb
HG + BRSO = HGBRSO              2.0E14     0.0          3E3              ! dHrxn = -0.2     auz&jwb
HG + BRSO = BRHGSO              7.5E12     0.0     40000.0           ! dHrxn = -7.1     auz&jwb
BR + HGSO = HGBRSO              7.5E12     0.0     40000.0           ! dHrxn = -63.1    auz&jwb

!*********************************************
!***************** Hg-Others ***************
!*********************************************
!Bozzelli
HG + O3 = HGO + O2              7.02E14     0.0     42190.          ! Widmer
HG + N2O = HGO + N2             5.08E10     0.0     59810.          ! Widmer
```

Table AG.1 Mercury oxidation mechanism (Continued)

```
!*******************************************************
!************************ Br ***************************
!*******************************************************

!************ Br-Hx-HOx-O *************
!Bozzelli
BR + BR + M = BR2 + M                    1.48E14      0.0     -1700       ! Baulch, 1981
BR2 + H= HBR + BR                        2.28E11      1.       440.       !81BAU/DUX
HBR + H = H2 + BR                        1.26E10     1.05      160.       !91SEA/PIL2
BR + H + M = HBR + M                     4.78E21     -1.963    510.5      !fit 81BAU/DUX(M=Ar)
HBR + OH = BR + H2O                      6.62E12      0.         0.       !92ATK/BAU
HBR + O = BR + OH                        3.97E12      0.      3060.       !89ATK/BAU
BR + H2O2 = HBR + HO2                    6.03E12      0.      5960.       !87DEM/GOL
BRO +H = BR + OH                         4.00E13      0.         0.       ! jwb97
BRO + H = HBR + O                        5.00E12      0.         0.       ! jwb97
HOBR + H = HBR + OH                      9.5E13       0.      7620.
BR + HOBR = HBR + BRO                    4.00E12      0.     21100.       ! jwb Hrxn = +12.39
HOBR + O = BRO + OH                      6.00E12      0.      4400.       ! Hrxn = -4, A, Ea both lo
HOBR + OH = BRO + H2O                    2.00E12      0.      1000.
BR + OH <=> HOBR                         7.7E21      -3.98    1114.       ! 1 atm - Need to improve Chmdis
BR + HO2 = BRO + OH                      4.00E12      0.0    10000.       ! jwb Hrxn = 8.09
BR + HO2 = HBR + O2                      4.64E12      0.0      900.       ! iupac06
BRO + HO2 = HOBR + O2                    2.7E12       0.0     1000.       ! iupac06
BR2 + OH = HOBR + BR                     2.00E12      0.0     3500.       ! iupac06 Hrxn=-9.18 jwb
BRO + O = BR + O2                        1.02E13      0.0     -520.       !94DEM/SAN
BR2 + O = BR + BRO                       1.00E13      0.0        0.       !89ATK/BAU
BRO + BRO = BR + BR + O2                 2.40E12      0.0      380.       !94DEM/SAN
BRO + BRO = BR2 + O2                     2.52E10      0.0    -1320.       !94DEM/SAN
BRO + H2 = HOBR + H                      6.00E11      0.0    14100.       !96BAB/NOT (CL)
BRO + H2O2 = HOBR + HO2                  5.00E12      0.0     2000.       !96BAB/NOT (CL)
HOBR (+M) = BR + OH (+M)                 3.00E15      0.0    50000.       !96BAB/NOT (CL)
    LOW/2.00E20  -3.  51000./
!************ Br-NOx ***************
!NIST
!BR + NO + M = BRNO + M                  9.5E14      -0.175      0.0       ! jwb mod cloo
BR + NO <=> BRNO                         5.87E20      -3.95      1084.          ! dHrxn= -27.1     1.00E+00 atm,  200-1400 K
!BR + NO2 + M = BRNO2 + M                1.5E17       0.0        0.0       ! dHrxn= -23.8    iupac06
BR + NO2 <=> BRNO2                       1.09E29     -6.20     2304.        !  1.00E+00 atm,  200-1400 K
BRNO + BR = BR2 + NO                     5.0E12       0.0        0.0       ! jwb
BRNO2 + BR = BR2 + NO2                   5.5E12       0.0     1200.        ! jwb
BR + NO2 = BRONOcis                      5.5E12       0.0     2200.          ! dHrxn= -14.9    auz&jwb
BR + NO2 = BRONOtran                     5.5E12       0.0     2200.          ! dHrxn= -12.7    auz&jwb
BR + NO3 = BRONO2                        5.5E12       0.0     2200.          ! dHrxn= -35.1    auz&jwb
BRNO + H = HBR + NO                      3.8E13       0.0     1000.         ! jwb dh-50
BRNO2 + H = HBR + NO2                    1.0E12       0.0     2500.         ! dHrxn = -63
BRNO + O = BRO + NO                      1.5E13       0.0      750.         ! jwb dh-27
BRNO + OH = HOBR + NO                    5.5E12       0.0      740.         ! jwb
BRNO + OH = HONO + BR                    2.0E12       0.0     7500.         ! dHrxn =-18.39
BRNO2 + OH = HOBR + NO2                  1.0E11       0.0     1000.         ! dHrxn = -31
BRO + NO = NO2 + BR                      1.0E11       0.0     1500.         ! dHrxn = -15.77
HNO + BR = HBR + NO                      2.0E12       0.0     1500.         ! dHrxn = -52.9
HONO + BR = HBR + NO2                    2.0E12       0.0     1500.         ! dHrxn = -8.9
!****** SOx-Br reaction***********
!auzmendi&bozzelli
BR + SO = BRSO                           9.87E21     -3.95     1084.         ! dHrxn = -42.09     auz&jwb
BR + SO2 = BRSO2                         1.09E29     -6.20     2304.         ! dHrxn = -4.30      auz&jwb
!************ Br-CH ***************
!Bozzelli
CH3 + HBR = CH4 + BR                     9.46E11      0.00      -380.       !92SEA/PIL
C2H5 + HBR = C2H6 + BR                   1.02E12      0.00     -1000.       !92SEA/PIL
CH2OH + HBR = CH3OH + BR                 5.24E11      0.00      -880.       !92SEE/GUT
CH2O + BR = HCO + HBR                    1.02E13      0.00      1600.       !92ATK/BAU
CH3BR = CH3 + BR                         1.58E13      0.00     71700.       !91SUZ/INO
CH3BR + H = CH3 + HBR                    5.11E13      0.00      5840.       !81BAU/DUX
```

Table AG.1 Mercury oxidation mechanism (Continued)

```
CH3BR + O = CH3 + BRO                1.00E13    0.00     13500.      !83WES
CH3BR + O = CH2BR + OH               2.00E13    0.00      7750.      !88HER
CH3BR + OH = CH3 + HOBR              1.00E13    0.00     13500.      !83WES
CH3BR + OH = CH2BR + H2O             7.60E07    1.30       500.      !91COH/WES
CH3BR + HO2 = CH2BR + H2O2           1.00E13    0.00     16700.      !96BAB/NOT (upper-limit)
CH3BR + CH3 = CH4 + CH2BR            1.26E12    0.00     10100.      !72KON
CH3 + BR2 = CH3BR + BR               1.21E13    0.00      -390.      !90TIM/SEE
CH3BR + BR = CH2BR + HBR             1.00E14    0.00     16310.      !72KON
CH3BR + BRO = CH2BR + HOBR           3.00E11    0.00     10700.      !96BAB/NOT (CL)
CH3 + BR = CH2 + HBR                 1.10E14    0.00     22968.      !90GOL/TAM
CH2BR + BR = CH2 + BR2               5.00E09    0.00     10200.      !72KON
C2H5 + BR2 = C2H5BR + BR             1.57E13    0.00      -820.      !90TIM/SEE
C2H5BR + H = C2H5 + HBR              1.00E14    0.00      5000.      !96BAB/NOT (upper-limit)
C2H3BR + H = C2H3 + HBR              1.00E14    0.00      6000.      !96BAB/NOT (upper-limit)
C2H3 + BR2 = C2H3BR + BR             3.02E13    0.00      -477.      !88TIM
BR + CH3OO = BRO + CH3O              3.4E12     0.00       450.      ! jwb
! Additional reactions from Richard Larson (Sandia)
CH2BR + CH3 = C2H5BR                 3.10E11    0.00     -4300.      !96BAB/NOT (CL)
CH2BR + CH3 = HBR + C2H4             5.40E12    0.00      1400.      !96BAB/NOT (CL)
CH2BR + CH3 = BR + C2H5              1.00E13    0.00      7000.      !96BAB/NOT (CL)
CH2BR + H2 = CH3BR + H               2.00E12    0.00     13100.      !96BAB/NOT (CL)

!*****************************************************
!********************** Cl ***************************
!*****************************************************
!********* Cl-hydroxide **********
!J.W.Bozzelli and R. Asatryan
CL + CL + M = CL2 + M                  1.25E15     0.0       -1630.
H + HOCL = HCL + OH                    9.55E13     0.0        7620.
O + HOCL = OH + CLO                    6.03E12     0.0        4370.
OH + HOCL = H2O + CLO                  1.81E12     0.0         990.
HOCL = H + CLO                         8.13E14    -2.09      93690.
COCL + O = CO + CLO                    1.00E14     0.0           0.
COCL + OH = CO + HOCL                  3.30E12     0.0           0.
HCO + CLO = CO + HOCL                  3.16E13     0.0           0.
H + CL + M = HCL + M                   7.20E21     -2.0          0.      !PITZ, WESTBROOK
! old # H + CL + M = HCL + M           1.00E17     0.0           0.
H + CL2   = HCL + CL                   7.94E13     0.0        1200.
O + HCL = OH + CL                      5.25E12     0.0        6400.
O + CL2 = CLO + CL                     1.26E13     0.0        2800.
O + CLO = CL + O2                      5.75E13     0.0         400.
OH + HCL = H2O + CL                    2.20E12     0.0        1000.
HOCL = CL + OH                         1.76E20    -3.01      56720.      !HO DISSOC
CL + H2 = HCL + H                      4.80E13     0.0        5000.
CL + CO = COCL                         1.95E19    -3.01       8070.
CL + HCO = HCL + CO                    1.41E14    -0.35        510.
duplicate
HCO + CL = CO + HCL                    1.50E13     0.00          0.      !WON '91    DUPLICATE / LIZHU ADD
duplicate
CL + HO2 = HCL + O2                    1.08E13     0.00        100.      ! won
CL + HO2 = CLO + OH                    5.47E13     0.00        894.      ! jwb 99
CL + HOCL = CL2 + OH                   1.81E13     0.00       3360.      !jongwoo 99
CL + HOCL = HCL + CLO                  1.81E13     0.00        258.      !jwb 99
CLO + H2 = HOCL + H                   1.00E13      0.00      13500.
!****** NOx-Cl reaction**********
!NIST
CL + NO <=> CLNO                       1.3E19      -3.21       1371.      ! dHrxn = -38.4   1.00E+00 atm,  300-1900 K
CL + NO2 <=> CLNO2                     1.59E29     -6.63       2944.      ! dHrxn = -34.6  1.00E+00 atm,  300-1900 K
CL + NO2 = CLONOcis                    5.5E12       0.0        2200.      ! dHrxn = -21.4          auz&jwb
CL + NO2 = CLONOtran                   5.5E12       0.0        2200.      ! dHrxn = -19.6          auz&jwb
CL + NO3 = CLONO2                      5.5E12       0.0        2200.      ! dHrxn = -39.6          auz&jwb
CLNO + H = HCL + NO                    4.60E13      0.0        1910.      !  Nist-wag 76
```

Table AG.1 Mercury oxidation mechanism (Continued)

```
CLNO2 + H = HCL + NO2                2.0E13      0.0       910.        !  h-clno-nist
CLNO + OH = HONO + CL                5.55E10     0.0         0.        ! nist
CLNO  OH = HOCL + NO                 5.42E12     0.0       2.25E3      ! jwb  oh + cl2 dh =-17.5
CL +CLNO =  CL2 + NO                 2.4E13      0.0         0.        ! jwb abstn dh=-20
CL + CLNO2 = CL2 + NO2               2.1E13      0.0         0.        ! dh=-20 - k from cl + ccl4 - seetula 98
CLNO2+ OH = HOCL + NO2               1.07E12     0.0         1.38      ! jwb-eval from atk-bau oh + cl2 dh= -18
CLNO + O = CLO + NO                  5.00E12     0.0      3000.        ! AH = -25.42
CLO + NO = NO2 + CL                  5.00E11     0.0      7300.        ! AH = -9.11
!****** SOx-Cl reaction***********
!auzmendi&bozzelli
CL + SO = CLSO                       9.9E18     -3.21      1371.       ! dHrxn = -54.77    auz&jwb
CL + SO2 = CLSO2                    1.59E30     -6.63      2944.       ! dHrxn = -15.52    auz&jwb
!********* Chlorocarbon mech *************
!Bozzelli
CLO + CO = CO2 + CL                 6.02E11      0.0       7400.
CLO + CH3 = CH3CL + O               6.00E12      0.00      4000.        !WON '91
H2O2 + CL = HCL + HO2               1.02E12      0.0        800.
H2O2 + CLO = HOCL + HO2             5.00E12      0.0       2000.
CH2O + CL = HCO + HCL               4.40E13      0.00         0.        !ATKINSON '89
CH2O + CLO = HCO + HOCL             6.03E11      0.00      4200.        !DEMORE '87
COCL + CL = COCL2                   3.40E28     -5.61      3390.
COCL + CL = CO + CL2                1.49E19     -2.17      1470.
COCL + H = CO + HCL                 3.54E16     -0.79      1060.
COCL + H = HCO + CL                 3.42E09      1.15       -180.
COCL + O2 = CO2 + CLO               7.94E10      0.0       3300.
COCL + O = CO2 + CL                 1.00E13      0.0          0.0
CLOO <=> CL+O2                      1.80E12     -1.15      3298.        !  disso rev=(7ATK/BAU)1.69e14,3.617
CLOO + CL <=> 2CLO                  7.23E12      0.           0.        !  nist 97DEM/SAN
CLOO + CL <=> CL2 + O2              3.00E13      0.           0.        !  add 8/31/99
CH3 + CLO = CH3O + CL               2.28E07      1.54      -820.
CH3 + CLO = HCL + CH2O              5.50E14     -0.51       710.
CH3 + CL = CH2 + HCL                7.00E13      0.00      7500.        !jwb abstn
CH4 + CLO = CH3 + HOCL              6.03E11      0.0      15000.
CH4 + CL = CH3 + HCL                5.00E13      0.00      3900.       ! BENSON,WEISS
CH3 + H = CH4                       7.09E31     -5.77      5890.
CH4 + O2 = CH3 + HO2                7.90E13      0.       56000.
CH4 + H = CH3 + H2                  2.20E04      3.000     8750.
CH4 + OH = CH3 + H2O                1.60E06      2.100     2460.
CH4 + HO2 = CH3 + H2O2              1.80E11      0.       18700.
CH3 + H = CH2 + H2                  9.00E13      0.       15100.
CH3 + CH3 = C2H6                    2.68E29     -4.95      6130.
CH3 + O2 = CH3O + O                 2.05E19     -1.570     29229.
CH3 + O = CH2O + H                  8.00E13      0.           0.
CH3 + OH = CH2 + H2O                7.50E06      2.000     5000.
CH3 + HO2 = CH3O + OH               2.00E13      0.           0.
CH2 + H = CH + H2                   1.00E18     -1.560        0.
CH2 + O = CO + 2H                   5.00E13      0.           0.
CH2 + O = CO + H2                   3.00E13      0.           0.
CH2 + OH = CH + H2O                 1.13E07      2.000     3000.
CH2 + OH = CH2O + H                 2.50E13      0.           0.
CH2 + O2 = CO2 + 2H                 1.60E12      0.        1000.
CH2 + O2 = CH2O + O                 5.00E13      0.        9000.
CH2 + O2 = CO2 + H2                 6.90E11      0.         500.
CH2 + O2 = CO + H2O                 1.90E10      0.       -1000.
CH2 + O2 = CO + OH + H              8.60E10      0.        -500.
CH2 + O2 = HCO + OH                 4.30E10      0.        -500.
CH2 + CO2 = CH2O + CO               1.10E11      0.        1000.
CH2 + C.H*C*O = C2H3 + CO           3.00E13      0.           0.
2CH2 = C2H2 + H2                    4.00E13      0.           0.
CH2(S) + M = CH2 + M                1.00E13      0.           0.
  H/0.0/
CH2(S) + CH4 = 2CH3                 4.00E13      0.           0.
CH2(S) + C2H6 = CH3 + C2H5          1.20E14      0.           0.
CH2(S) + O2 = CO + OH + H           3.00E13      0.           0.
```

Table AG.1 Mercury oxidation mechanism (Continued)

CH2(S) + H2 = CH3 + H	7.00E13	0.	0.	
CH2(S) + H = CH2 + H	2.00E14	0.	0.	
CH + H = C + H2	1.50E14	0.	0.	
CH + O2 = HCO + O	3.30E13	0.	0.	
CH + O = CO + H	5.70E13	0.	0.	
CH + OH = HCO + H	3.00E13	0.	0.	
CH + CH2 = C2H2 + H	4.00E13	0.	0.	
CH + CH3 = C2H3 + H	3.00E13	0.	0.	
CH + CH4 = C2H4 + H	6.00E13	0.	0.	
!CH + C2H2 = C3H2 + H	1.00E14	0.	0.	
CH + CO2 = HCO + CO	3.40E12	0.	690.	
CH + H2O = CH2O + H	1.17E15	-0.750	0.	
CH + CH2O = KETENE + H	9.46E13	0.	-515.	
C + O2 = CO + O	2.00E13	0.	0.	
C + OH = CO + H	5.00E13	0.	0.	
C + CH3 = C2H2 + H	5.00E13	0.	0.	
C + CH2 = C2H + H	5.00E13	0.	0.	
CH2OH + M = CH2O + H + M	1.00E14	0.	25000.	
CH2OH + H = CH3 + OH	1.00E14	0.	0.	
CH2OH + H = CH2O + H2	2.00E13	0.	0.	
CH2OH + O = CH2O + OH	1.00E13	0.	0.	
CH2OH + O2= CH2O + HO2	1.48E13	0.	1500.	
CH2OH + OH= CH2O + H2O	1.00E13	0.	0.	
CH2O + H = HCO + H2	2.19E08	1.770	3000.	
CH2O + M = HCO + H + M	3.31E16	0.	81000.	
CH2O + O = HCO + OH	1.80E13	0.	3080.	
CH2O + OH = HCO + H2O	3.43E09	1.180	-447.	
CH3O + H = CH3 + OH	1.00E14	0.	0.	
CH3O + M = CH2O + H + M	1.00E14	0.	25000.	
CH3O + H = CH2O + H2	2.00E13	0.	0.	
CH3O + O = CH2O + OH	1.00E13	0.	0.	
CH3O + O2 = CH2O + HO2	6.30E10	0.	2600.	
CH3O + OH = CH2O + H2O	1.00E13	0.	0.	
HCO + M = H + CO + M	2.50E14	0.	16802.	
CO/1.9/ H2/1.9/ CH4/2.8/ CO2/3.0/ H2O/5.0/				
HCO + H = CO + H2	1.19E13	.250	0.	
HCO + O = CO + OH	3.00E13	0.	0.	
HCO + O = CO2 + H	3.00E13	0.	0.	
HCO + O2 = HO2 + CO	3.30E13	-0.400	0.	
HCO + OH = H2O + CO	1.00E14	0.	0.	
CO + O + M = CO2 + M	6.17E14	0.	3000.	
CO + O2 = CO2 + O	1.60E13	0.	41000.	
CO + OH = CO2 + H	1.51E07	1.300	-758.	
CO + HO2 = CO2 + OH	5.80E13	0.	22934.	
C2H6 + H = C2H5 + H2	5.40E02	3.500	5210.	
C2H6 + CH3= C2H5 + CH4	5.50E01	4.000	8300.	
C2H6 + O = C2H5 + OH	3.00E07	2.000	5115.	
C2H6 + OH = C2H5 + H2O	8.70E09	1.050	1810.	
C2H3 = C2H2 + H	5.62E31	-6.06	51720.	
C2H3 + H = C2H2 + H2	4.00E13	0.	0.	
C2H3 + O = KETENE + H	3.00E13	0.	0.	
C2H3 + O2 = C2H2 + HO2	1.21E11	0.	0.	! 86TSA/HAM
C2H3 + O2 = CH2O + HCO	4.57E16	-1.39	1013.	! nist 96MEB/DIA2
C2H3 + O2 = C.H2CHO + O	3.03E11	-0.29	10.	! add 8/24/99 nist 96MEB/DIA2
C2H3 + OH = C2H2 + H2O	5.00E12	0.	0.	
C2H3 + CH2= C2H2 + CH3	3.00E13	0.	0.	
C2H3 + C2H= 2C2H2	3.00E13	0.	0.	
C2H3 + CH = CH2 + C2H2	5.00E13	0.	0.	
C2H4 + M = C2H2 + H2 + M	1.50E15	0.	55800.	
C2H4 + M = C2H3 + H + M	1.40E15	0.	82360.	
C2H4 + H = C2H3 + H2	1.10E14	0.	8500.	
C2H4 + H = C2H5	5.41E35	-6.78	11700.	

Table AG.1 Mercury oxidation mechanism (Continued)

C2H4 + O = CH3 + HCO	1.60E09	1.2	746.	
C2H4 + OH = C2H3 + H2O	2.02E13	0.	5955.	
CH2 + CH3 = C2H4 + H	3.00E13	0.	0.	
C2H5 + H = 2CH3	8.73E14	-0.08	3080.	
C2H5 + H = C2H6	5.18E35	-6.83	6810.	
C2H5 + O2 = C2H4 + HO2	8.43E11	0.	3875.	
H2 + C2H = C2H2 + H	4.09E05	2.390	864.	
C2H2 + O = CH2 + CO	1.02E07	2.000	1900.	
C2H2 + O = C.H*C*O + H	1.03E07	2.000	1900.	
C2H2 + O = C2H + OH	3.16E15	-0.600	15000.	
C2H2 + O2 = C.H*C*O + OH	2.00E08	1.500	30100.	
C2H2 + M = C2H + H + M	4.20E16	0.	107000.	
OH + C2H2 = C2H + H2O	3.37E07	2.000	14000.	
OH + C2H2 = C#COH + H	5.04E05	2.300	13500.	
OH + C2H2 = KETENE + H	2.18E04	4.500	-1000.	
OH + C2H2 = CH3 + CO	4.83E04	4.000	-2000.	
C2H + O2 = 2CO + H	5.00E13	0.	1500.	
C2H + O = CH + CO	5.00E13	0.	0.	
C2H + OH = C.H*C*O + H	2.00E13	0.	0.	
C#COH + H = KETENE + H	1.00E13	0.	0.	
KETENE = CH2 + CO	2.01E35	-6.68	82990.	
KETENE + O = CO2 + CH2	1.75E12	0.	1350.	
KETENE + H = CH3 + CO	1.13E13	0.	3428.	
KETENE + H = C.H*C*O + H2	5.00E13	0.	8000.	
KETENE + O = C.H*C*O + OH	1.00E13	0.	8000.	
KETENE + OH= C.H*C*O + H2O	7.50E12	0.	2000.	
2C.H*C*O = C2H2 + 2CO	1.00E13	0.	0.	
C.H*C*O + H = CH2(S) + CO	1.00E14	0.	0.	
C.H*C*O + O = H + 2CO	1.00E14	0.	0.	
C.H*C*O + O2 = 2CO + OH	1.60E12	0.	854.	
C.H*C*O + CH = C2H2 + CO	5.00E13	0.	0.	
!C3H2 + O2 = HCO + C.H*C*O	1.00E13	0.	0.	
CH3CL + OH = CH2CL + H2O	1.32E12	0.0	2300.	
CH3CL + O = OH + CH2CL	1.70E13	0.0	7300.	
CH3CL + H = H2 + CH2CL	6.66E13	0.0	10600.	
CH3CL + O2 = HO2 + CH2CL	4.00E13	0.0	52200.	
CH3CL + HO2= H2O2 + CH2CL	1.00E13	0.0	16700.	
CH3CL + CLO= HOCL + CH2CL	5.00E12	0.0	8700.	
CH3CL + CL = CH3 + CL2	1.00E14	0.00	25000.	!K-M (KERR&MOS)
CH3CL + CL = HCL + CH2CL	3.16E13	0.0	2300.	
CH3CL + CH3= CH4 + CH2CL	3.31E11	0.0	9400.	
CH3CL + H = HCL + CH3	5.40E13	0.0	6500.	
CH3CL = CH3 + CL	5.53E31	-5.63	88810.	
CH3CL = CH2 + HCL	1.82E25	-4.69	132460.	
CH3CL = CH2CL + H	1.31E30	-5.23	106100.	
CH2CL + O2 = CLO + CH2O	8.46E13	-1.03	8180.	
CH2CL + H = CH3 + CL	1.68E16	-0.68	1020.	
CH2CL + HO2= CH2CLO. + OH	5.19E14	-0.51	840.	
CH2CL + OH = CH2O + HCL	4.10E21	-2.57	3740.	
CH2CL + OH = CH2OH + CL	9.24E11	0.38	2970.	
CH2CL + CH3= C2H5CL	1.62E43	-9.89	7545.	
CH2CL + CH3= C2H5 + CL	2.68E14	-0.57	2395.	
!C2H5 + CL = CH3 + CH2CL	1.50E21	-1.94	17720.	! DUPLICATE LIzhu
CH2CL + CH3= C2H4 + HCL	4.26E19	-2.02	3623.	
CH2CL + O = CH2CLO.	2.55E15	-2.02	1230.	
CH2CLO. = CH2O + CL	2.51E24	-4.78	10070.	
CH2CL + O = CH2O + CL	8.31E13	-0.18	800.	
C2H2 + CL = HCL + C2H	1.00E13	0.0	32800.	
C2H3 + CL = C2H3CL	6.50E34	-6.63	8610.	
C2H3 + CL = C2H2 + HCL	2.40E24	-3.22	9070.	
C2H4 + CLO = CH2CL + CH2O	9.26E18	-1.98	8430.	
C2H4 + CLO = C2H4OCL	1.75E32	-6.32	7900.	
C2H4 + CL = HCL + C2H3	3.00E13	0.0	8100.	
C2H5 + CL = C2H5CL	8.39E36	-7.38	9550.	

Table AG.1 Mercury oxidation mechanism (Continued)

```
C2H5 + CL = C2H4 + HCL                  6.12E24     -3.38      9040.
C2H5 + CLO = CH3 + CH2O + CL             1.54E13      0.00     1500.0    !JWB 99 mod prod & Ea
C2H5 + CLO = C2H5CL + O                  9.54E11      0.00      270.     !JWB 99
C2H5 + CL2 = C2H5CL + CL                 7.54E11      0.00      100.     ! JONGWOO 99
C2H6 + CL = C2H5 + HCL                   4.64E13      0.00      170.     !DEMORE '87
C2H6 + CLO = C2H5 + HOCL                 7.64E11      0.00     9170.     !JWB 99
H + C2H3CL = HCL + C2H3                  1.00E13      0.0      9800.
H + C2H3CL = H2 + CHCLC.H                1.55E13      0.0      4730.
H + C2H3CL = C2H4 + CL                   3.01E13      0.0      4223.
H + C2H3CL = CH3C.HCL                    5.50E34     -6.56    11950.
CL + C2H3CL= HCL + CHCLC.H               5.00E12      0.0      5870.
CHCLC.H = CL + C2H2                      8.23E29     -5.99     25760.
H + CH3C.HCL = C2H5CL                    8.01E11      0.0      -5090.
H + CH3C.HCL = C2H5 + CL                 3.39E21     -2.42      8880.
H + CH3C.HCL = CH3 + CH2CL               6.67E19     -1.55      9430.
H + CH3C.HCL = C2H4 + HCL                3.72E30     -5.10      9330.
H + C2H5CL = HCL + C2H5                  1.00E13      0.0      7100.
H + C2H5CL = H2 + CH3C.HCL               1.00E13      0.0      8100.
O + C2H5CL = OH + CH3C.HCL               2.00E13      0.0      8100.
OH + C2H5CL= H2O + CH3C.HCL              8.00E12      0.0      1100.
OH + C2H5CL= HOCL + C2H5                 4.00E12      0.0      9100.
CL + C2H5CL= HCL + CH2CLC.H2             1.12E13      0.0      1500.
CH2CLC.H2 = CL + C2H4                    6.24E36     -8.05     26340.

!*********************************************************
!*********************** I ***************************
!*********************************************************
!***** Hx-HOx-O *****
! Nist
I + I + M = I2 + M                       2.00E14      0.       -1143.     !   Baulch, 1981 (NIST)
H + I = HI                               2.00E21     -1.87       0.      !   Lifshitz, 2008
HI + I = I2 + H                          8.02E14      0.      37161.     !   Garrett, 1979 (NIST)
HI + O = OH + I                          1.06E13      0.       1417.     !   Persky, 1987
HI + HI = H2 + I2                        2.50E13      0.      43719.     !   Baulch, 1981
HI + O2 = HO2 + I                        1.00E13      0.      23648.     !   Shum, 1983
H2 + I = HI + H                          2.36E15      0.      42522.     !   Michael, 2000
HI + OH = I + H2O                        9.64E12      0.       -874.     !   Atkinson, 2007
HOI + OH = IO + H2O                      3.01E12      0.         0.      !   Riffault, 2005
IO + HO2 = HOI + O2                      9.03E12      0.       2166.     !   Atkinson, 2007
I2 + OH = HOI + I                        1.26E14      0.         0.      !   Atkinson, 2007
IO + O = I + O2                          8.43E13      0.         0.      !   Atkinson, 2007
I2 + O = I + IO                          7.53E13      0.         0.      !   Atkinson, 2007
IO + IO = I + I + O2                     3.13E13      0.         0.      !   Vipond, 2002
IO + IO = I2 + O2                        3.01E12      0.         0.      !   Harwood, 1997
I + O3 = O2 + IO                         1.26E13      0.       1649.     ! Atkinson, 2007
!***** NOx *****
! Nist
I + NO + M = INO + M                     1.96E18     -1.0        0.0      !  Atkinson, 2007
I + NO2 + M = INO2 + M                   2.98E19     -1.0        0.0      !  Atkinson, 2007
I + N2O = N2 + IO                        2.8E14       0.0     37956.      !  Kaufman, 1956
HNO + HI = H2 + INO                      3.66E8       0.0     38505.      !  Holmes, 1966
!***** CH + I *****
! Nist
CH3 + HI = CH4 + I                       2.69E12      0.0      -27.82     !   Seetula, 1991
!CH4 + I = CH3 + HI                      1.48E14      0.0     32988.      !   Pardini, 1983
C2H5 + HI = C2H6 + I                     2.75E12      0.0      -763.      !   Seetula, 1990
CH2OH + HI = CH3OH + I                   1.62E13      0.0      -1147.     !   Seetula, 1992
CH2O + I = HCO + HI                      8.32E13      0.0     1.74E+4     !   Benson, 1966
CH3I = CH3 + I                           2.62E15      0.0     3.95E+4     !   Kumaran, 1997
CH3I + H = CH3 + HI                      2.50E12      0.0      5000.      !   Hynes, 2000
CH3I + O = CH3 + IO                      3.73E12      0.0      -678.      !   Holscher, 1998
CH3I + O = CH2I + OH                     1.81E12      0.0       139.      !   Gilles, 1996
CH3I + OH = CH3 + HOI                    5.53E2      -3.97      6399.     !   Marshall, 1997
CH3I + OH = CH2I + H2O                   1.87E12      0.0       2226.     !   Atkinson, 2001
```

Table AG.1 Mercury oxidation mechanism (Continued)

```
CH3I + CH3 = CH4 + CH2I          6.31E11    0.0      1.21E+4    !  Saito, 1980
CH3 + I2 = CH3I + I              1.00E13    0.0      1498.      !  Flowers, 1963
!CH3I + I = CH3 + I2             2.00E14    0.0      20468.     !  Benson, 1961 (NIST)
CH3I + IO = CH2I + HOI           2.41E10    0.0      0.         !  Enami, 2006
CH3 + I = CH2 + HI               7.05E12    0.0      0.         !  Mulenko, 1987
CH2I + I = CH2I2                 8.00E13    0.0      0.         !  Hunter, 1982
CH2I + HI = CH3I + I             1.02E12    0.0      -382.      !  Seetula, 1991
C2H5 + I2 = C2H5I + I            3.01E13    0.0      0.         !  Hayes, 1986
C2H5I + H = C2H5 + HI            4.22E10    0.0      0.         !  Rebbert, 1973
I + CH3OO = IO + CH3O            1.20E13    0.0      0.         !  Dillo, 2006
CH2BR + HI = CH3BR + I           9.04E11    0.0      -191.      !  Seetula, 1991
CH2CL + HI = CH3CL + I           7.83E11    0.0      262.       !  Seetula, 1991
!HCO + HI = CH2O + I             1.86E12    0.0      197.       !  Becerra, 1997
!CH2O + I = HCO + HI             8.32E13    0.0      17428.     !  Benson, 1966
!CH3OH + I = CH2OH + HI          3.16E14    0.0      26032.     !  Croickshank, 1969

!*****************************************************
!********************** Br-Cl-I ************************
!*****************************************************
! Nist, bozzelli
CL + BR + M = BRCL + M           3.9E14     0.0      0.0        ! HYNE Br-Br JPC06
BRCL + CL = CL2 + BR             5.5E12     0.0      1000.      ! jwb
BRCL + BR = BR2 + CL             3.35E12    0.0      8900.      ! jwb dh=+6.5
BRCL + OH = HOBR + CL            6.2E12     0.0      5200.      ! jwb
BRCL + OH = HOCL + BR            1.6E12     0.0      2400.      ! jwb
BRCL + H = HCL + BR              2.4E13     0.0      0.83
BRCL + H = HBR + CL              2.7E12     2.05     -1.80
ICL + CL = CL2 + I               7.23E12    0.       0.         ! Chesnokov, 1991
ICL + H = HCL + I                1.00E12    0.       3219.      ! Mayer, 1967
HI + CL = ICL + H                3.62E14    0.0      23250.     ! Garrett, 1979
HI + CL = HCL + I                1.39E16    -4.45    2981.      ! Mei, 1977
I + CLO2 = IO + CLO              5.85E12    0.0      2365.      ! Bedjanian, 1996
HI + BR = HBR + I                7.46E12    0.0      63.59      ! Mei, 1979

!*****************************************************
!****************** H2 / O2 Mech **********************
!*****************************************************
!J.W.Bozzelli and R. Asatryan
2H + M    = H2 + M               1.00E18    -1.0     0.
  H2/0.0/   H2O/0.0/   CO2/0.0/
2H + H2   = 2H2                  9.20E16    -0.6     0.
H + O2 + M= HO2 + M              3.61E17    -0.72    0.
  H2O/18.6/   CO2/4.2/   H2/2.9/   CO/2.1/   N2/1.3/
H + OH + M= H2O + M              1.60E22    -2.0     0.
H + O + M = OH + M               6.20E16    -0.6     0.
  H2O/5.0/
H + HO2 = H2 + O2                1.25E13    0.       0.
H + HO2 = 2OH                    1.40E14    0.       1073.
2H + H2O = H2 + H2O              6.00E19    -1.25    0.
2H + CO2 = H2 + CO2              5.49E20    -2.0     0.
H2 + O2 = 2OH                    1.70E13    0.       47780.
2OH = O + H2O                    6.00E08    1.3      0.
OH + H2 = H2O + H                1.17E09    1.3      3626.
OH + HO2 = H2O + O2              7.50E12    0.0      0.
2O + M = O2 + M                  1.89E13    0.       -1788.
O + OH = O2 + H                  4.00E14    -0.5     0.
O + H2 = OH + H                  5.06E04    2.67     6290.
O + HO2 = O2 + OH                1.40E13    0.       1073.
2HO2 = H2O2 + O2                 2.00E12    0.       0.
H2O2 + M = 2OH + M               1.30E17    0.       45500.
H2O2 + H = HO2 + H2              1.60E12    0.       3800.
H2O2 + OH = H2O + HO2            1.00E13    0.       1800.
```

Table AG.1 Mercury oxidation mechanism (Continued)

```
!*****************************************************
!************************ NOx ************************
!*****************************************************

! A. M. Dean and J. W. Bozzelli
! Reaction below taken from chapter.mec  8/25/98 version

O + N2 = N + NO                          1.95E14     0.00     76817
NO + M = N + O + M                       9.60E14     0.00     148429    ! M=AR
            N2/1.5/  O2/1.5/  H2/1.5/  H2O/10./   CO2/3.0/  CH4/3.0/
N2O + M = N2 + O + M                     4.00E14     0.00     56093     ! M=AR
            N2/1.5/  O2/1.5/  H2/1.5/  H2O/10./   CO2/3.0/  CH4/3.0/
N2O + O = N2 + O2                        1.40E12     0.00     10809
N2O + O = 2NO                            2.90E13     0.00     23149
NH3 + M = NH2 + H + M                    2.50E16     0.00     93786     ! M=AR
     N2/1.5/  O2/1.5/  H2/1.5/  H2O/10./   CO2/3.0/  CH4/3.0/
NH3 + H = NH2 + H2                       5.40E05     2.40     9915
NH3 + OH = NH2 + H2O                     5.00E07     1.60     954
NH3 + O = NH2 + OH                       9.40E06     1.94     6458
NH2 + H = NH + H2                        4.80E08     1.50     7938      ! 1/15/96 UPDATE
HO2 + NO = NO2 + OH                      2.20E12     0.00     -477
N2O + H + M = HNNO + M                   1.10E27     -3.48    10770     ! M= N2, OK IF P=10, T=1000 OR P=1, T=300
    AR/0.7/  H2O/7.0/  CO2/2.0/  CH4/2.0/
N2O + H = N2 + OH                        2.20E14     0.00     16750     !  T=1000-2000K
H + N2O = NH + NO                        8.50E20     -1.62    35369
H + N2O = NNH + O                        2.40E19     -1.26    47092
NH + NO = N2 + OH                        1.40E17     -1.49    1311
NH + NO = NNH + O                        1.70E14     -0.20    12200
NH + O2 + M = HNOO + M                   3.03E26     -4.00    2295      ! M=N2, SLIGHT FALLOFF T=300, P=10
   AR/0.7/  H2O/7.0/  CO2/2.0/  CH4/2.0/
NH + O2 = NO + OH                        7.60E10     0.00     1530
NH + O2 = H + NO2                        2.30E10     0.00     2484
NH + O2 = HNO + O                        4.60E05     2.00     6497
NH2 + O2 = NH2O + O                      2.50E11     0.48     29586     !1/24/96 UPDATE
NH2 + O2 = HNO + OH                      6.20E07     1.23     35100     !1/24/96 UPDATE
NH2 + HO2 = NH2O + OH                    2.50E13     0.00     0
NH2 + HO2 = NH3 + O2                     9.20E05     1.94     -1152     !1/15/96 UPDATE
NH2 + O = HNO + H                        4.60E13     0.00     0
NH2 + O = NH + OH                        7.00E12     0.00     0         ! ADDITION
DUPLICATE
NH2 + O = NH + OH                        3.33E08     1.50     5077      !1/15/96 UPDATE (ABSTRACTION)
DUPLICATE
NH2 + OH = NH2OH                         3.90E33     -7.00    4441      !1.0 ATM  1/15/96
NH2 + OH = NH + H2O                      2.40E06     2.00     50        !  1/15/96 UPDATE
NH2 + NH2 = N2H4                         5.60E48     -11.30   11882     ! 1/26/96 1 ATM N2 M(600-2500K)
NH2 + NH2 = H2NN + H2                    1.20E21     -3.08    3368      ! 1/26/96 1 ATM N2
NH2 + NH2 = N2H3 + H                     1.20E12     -0.03    10084     ! 1/26/96 1 ATM N2
NH2 + NH2 = NH3 + NH                     5.00E13     0.00     9935
NH2 + NO = N2 + H2O                      4.70E12     -0.25    -1204     !  UPDATED 9/25/96
NH2 + NO = NNH + OH                      3.50E10     0.34     -765      !  UPDATED 9/25/96
NH2 + NO = NH2NO                         3.53E31     -6.75    3725      ! 1.0 ATM N2 ADDED 10/31/97
CH3 + NO = CH3NO                         1.02E37     -8.38    5228.     !8/22/98 update 1.0 atm,  300-2500 K
CH3 + NO = H2CN+OH                       2.15E09     0.75     11724.    ! 8/22/98 update
CH3 + NO = HCN+H2O                       4.87E08     0.46     12392.    !8/22/98 update
CH3 + N = H2CN + H                       6.10E14     -0.31    288
CH3 + N = HCN + H2                       3.70E12     0.15     -89
CH3 + N = HCNH + H                       1.20E11     0.52     -368
CH3 + NH2 = CH3NH2                       5.10E52     -11.99   16790     !1.0 ATM N2(600-2500K)
CH3 + NH2 = C.H2NH2+H                    1.40E14     -0.43    11107     ! 1.0ATM N2
CH3 + NH2 = CH3N.H + H                   4.40E13     -0.31    16641     ! 1.0ATM N2
CH3 + NH2 = H2C*NH + H2                  4.80E11     -0.20    19403     ! 1.0 ATM N2
CH3 + NH2 = CH4 + NH                     2.80E06     1.94     9210      ! 1/15/96 UPDATE
CH3 + NH2 = CH2 + NH3                    1.60E06     1.87     7570      ! 1/15/96 UPDATE
CH2 + N2 = CH2NN                         1.60E32     -7.07    19969     ! 1 ATM N2
```

Table AG.1 Mercury oxidation mechanism (Continued)

CH2 + N2 = HCN + NH	1.00E13	0.00	73996	
CH2 + NO = HCNO + H	3.80E13	-0.36	576	
CH2 + NO = HCN + OH	2.90E14	-0.69	755	
CH2 + NO = HNCO + H	3.10E17	-1.38	1272	
CH2 + NO = NH2 + CO	2.30E16	-1.43	1331	
CH2 + NO = H2CN + O	8.10E07	1.42	4113	
CH + N2 = HCNN	3.60E28	-5.84	2623	! 1 ATM N2
CH + N2 = HCN + N	4.40E12	0.00	21976	
CH + NO = HCN + O	5.30E13	0.00	0	
CH + NO = H + NCO	2.00E13	0.00	0	
CH + NO = N + HCO	2.90E13	0.00	0	!12/16/95 UPDATE
CH + NO = NH + CO	5.50E12	0.00	0	!12/16/95 UPDATE
CH + NO = OH + CN	3.30E12	0.00	0	!12/16/95 UPDATE
N + O2 = NO + O	9.00E09	1.00	6497	
N + OH = NO + H	1.10E14	0.00	1123	! UPDATE 8/13/94
CH + N = CN + H	1.67E14	-0.09	0	!BROWNSWORD ET AL (1966)
CH2 + N = HCN + H	5.00E13	0.00	0	
NH + N = N2 + H	1.50E13	0.00	0	! UPDATE 8/13/94
NH2 + N = N2 + 2H	7.10E13	0.00	0	
CN + N = C + N2	2.40E13	0.00	-556	!UPDATE 8/5/97
2NH = N2 + 2H	5.10E13	0.00	0	
NH2 + NH = N2H2 + H	1.50E15	-0.50	0	
NH2 + NH = NH3 + N	9.20E05	1.94	2444	! ABSTRACTION 1/15/96
NH + OH = HNO + H	2.00E13	0.00	0	
NH + OH = N + H2O	1.20E06	2.00	-487	!ABSTRACTION 1/15/96
NH + H = N + H2	3.50E13	0.00	1728	! 8/5/97 UPDATE
NH + O = NO + H	6.00E13	0.00	0	! UPDATE 1/29/96
NH + O = N + OH	1.70E08	1.50	3368	!ABSTRACTION 1/15/96
NH + CH3 = H2C*NH + H	4.00E13	0.00	0	
NH + CH3 = N + CH4	8.20E05	1.87	5852	! ABSTRACTION 1/29/96
NNH = N2 + H	3.00E08	0.00	0	!PRESSURE INDEPENDENT
NNH + M = N2 + H + M	1.00E13	0.50	3060	!PRESSURE DEPENDENT
AR/0.7/ H2O/7.0/ CO2/2.0/ CH4/2.0/				
NNH + O2 = N2 + HO2	1.20E12	-0.34	149	
NNH + O2 = N2O + OH	2.90E11	-0.34	149	
NNH + H = N2 + H2	2.40E08	1.50	-894	!ABSTRACTION 1/15/96
NNH + OH = N2 + H2O	2.40E22	-2.88	2454	!ADDITION
DUPLICATE				
NNH + OH = N2 + H2O	1.20E06	2.00	-1192	!ABSTRACTION 1/15/96
DUPLICATE				
NNH + O = N2 + OH	1.70E16	-1.23	497	!RECOMBINATION
DUPLICATE				
NNH + O = N2 + OH	1.70E08	1.50	-894	!ABSTRACTION 1/15/96
DUPLICATE				
NNH + NH2 = N2 + NH3	9.20E05	1.94	-1152	!ABSTRACTION 1/15/96
NNH + HO2 = N2 + H2O2	1.40E04	2.69	-1600	!ABSTRACTION 2/3/96
NNH + HO2 = HNNO + OH	2.40E13	0.00	1699	!RECOMB 2/3/96
NNH + NO = HNO + N2	1.20E06	2.00	-1192	!ABSTRACTION EST 2/12/96
N2H2 = NNH + H	1.79E40	-8.41	73391	!1.00E+00 ATM, 600-2500 K
DUPLICATE				
N2H2 = NNH + H	2.60E40	-8.53	72925	!1.00E+00 ATM, 600-2500 K
DUPLICATE				
N2H2 = H2NN	1.98E41	-9.38	68453	!1.00E+00 ATM, 600-2500 K
N2H2 + H = NNH + H2	4.80E08	1.50	1580	! HTRAN EST. 12/22/95
N2H2 + O = NNH + OH	3.30E08	1.50	497	! HTRAN EST. 12/22/95
N2H2 + OH = NNH + H2O	2.40E06	2.00	-1192	! HTRAN EST. 12/22/95
N2H2 + NH2 = NH3 + NNH	1.80E06	1.94	-1152	! HTRAN EST. 12/22/95
N2H2 + CH3 = NNH + CH4	1.60E06	1.87	2971	! HTRAN EST. 12/22/95
N2H2 + NH = NNH + NH2	2.40E06	2.00	-1192	!SAME AS OH
N2H2 + NO = N2O + NH2	4.00E12	0.00	11922	
H2NN = H + NNH	9.60E35	-7.57	54838	!1.00E+00 ATM, 600-2500 K
DUPLICATE				
H2NN = H + NNH	3.19E31	-6.22	52321	!1.00E+00 ATM, 600-2500 K
DUPLICATE				

Table AG.1 Mercury oxidation mechanism (Continued)

H2NN + O2 = NH2 + NO2	1.50E12	0.00	5961	!ADDUCT FORMATION
H2NN + H = NNH + H2	4.80E08	1.50	-894	!ABSTRACTION
H2NN + H = N2H2 + H	1.83E10	0.97	4471	! 2/2/98 TST CALC.
H2NN + O = NNH + OH	3.30E08	1.50	-894	!ABSTRACTION
H2NN + O = NH2 + NO	3.18E09	1.03	2695	! 2/2/98 TST CALC.
H2NN + OH = NNH + H2O	2.40E06	2.00	-1192	!ABSTRACTION
H2NN + OH = NH2NO + H	2.00E12	0.00	0	!9/16/96 UPDATE RECOMBINATION
H2NN + CH3 = CH2*NNH2 + H	8.30E05	1.93	6506	! 2/7/98 TST/2
H2NN + CH3 = CH3N*NH + H	8.30E05	1.93	6506	! 2/7/98 TST/2
H2NN + CH3 = CH4 + NNH	1.60E06	1.87	129	!ABSTRACTION
H2NN + NH2 = HNNNH2 + H	7.88E06	1.90	-1333	! 2/7/98 TST CALC.
H2NN + NH2 = NNH + NH3	1.80E06	1.94	-1152	!ABSTRACTION
H2NN + HO2 = NH2NO + OH	6.56E05	1.94	7053	! 2/7/98 TST CALC.
H2NN + HO2 = NNH + H2O2	2.90E04	2.69	-1600	!ABSTRACTION
N2H3 = N2H2 + H	3.60E47	-10.38	69009	! 1 ATM N2 600-2500K)
N2H3 + H = N2H2 + H2	2.40E08	1.50	-10	!ABSTRACTION 1/15/96
N2H3 + O = NH2 + HNO	3.00E13	0.00	0	
N2H3 + O = NH2NO + H	3.00E13	0.00	0	
N2H3 + O = N2H2 + OH	1.70E08	1.50	-646	!ABSTRACTION 1/15/96
N2H3 + OH = N2H2 + H2O	1.20E06	2.00	-1192	!ABSTRACTION 1/15/96
N2H3 + OH = H2NN + H2O	3.00E13	0.00	0	! 2/15/96 SAME AS ADDUCT FORMATION
N2H3 + CH3 = N2H2 + CH4	8.20E05	1.87	1818	!ABSTRACTION 1/15/96
N2H3 + CH3 = H2NN + CH4	3.00E13	0.00	0	!RECOMB.SAME AS NH2
N2H3 + NH2 = N2H2 + NH3	9.20E05	1.94	-1152	!ABSTRACTION 1/15/96
N2H3 + NH2 = H2NN + NH3	3.00E13	0.00	0	!SAME AS ADDUCT FORM. (2/20/96)
N2H3 + HO2 = H2NNHO + OH	3.00E13	0.00	0	!RECOMBINATION(-5KCAL)
N2H3 + HO2 = N2H2 + H2O2	2.90E04	2.69	-1600	! UPDATE 10/18/97
N2H3 + HO2 = N2H4 + O2	9.20E05	1.94	2126	!NH2 WITH ADJUSTED THERMO
N2H4 = H2NN + H2	5.27E39	-8.35	69303	!1.00E+00 ATM, 600-2500 K, ADDED 12/3/97
N2H4 + H = N2H3 + H2	9.60E08	1.50	4838	! HTRAN EST. 12/22/95
N2H4 + O = N2H3 + OH	6.70E08	1.50	2851	! HTRAN EST. 12/22/95
N2H4 + OH = N2H3 + H2O	4.80E06	2.00	-646	! HTRAN EST. 12/22/95
N2H4 + CH3 = N2H3 + CH4	3.30E06	1.87	5325	! HTRAN EST. 12/22/95
N2H4 + NH2 = N2H3 + NH3	3.70E06	1.94	1629	! HTRAN EST. 12/22/95
NO + C = CO + N	1.70E13	0.00	0	
NO + C = CN + O	1.10E13	0.00	0	
NO + C.*C*O = HCNO + CO	4.60E13	0.00	695	! ADDED 10/2/96
NO + C.*C*O = HCN + CO2	1.40E13	0.00	695	! ADDED 10/2/96
NO2 + H = NO + OH	1.30E14	0.00	358	
NO2 + O = NO + O2	3.90E12	0.00	-238	
NO2 + M = NO + O + M	4.00E15	0.00	59988	! RORHIG ET AL 1997 M=AR
N2/1.5/ O2/1.5/ H2/1.5/ H2O/10./ CO2/3.0/ CH4/3.0/				
NO2 + NH2 = N2O + H2O	1.54E16	-1.44	268	! PARK-LIN (ADDED 7/2/97
NO2 + NH2 = NH2O + NO	6.56E16	-1.44	268	! PARK-LIN (ADDED 7/2/97
NO2 + CH3 = CH3O + NO	1.40E13	0.00	0	! ADDED 9/27/96
N2O + OH = N2 + HO2	1.29E02	4.72	36561	! MEBEL ET AL (1996) 1000-5000
HNO + M = H + NO + M	1.80E16	0.00	48682	! M=AR
N2/1.5/ O2/1.5/ H2/1.5/ H2O/10./ CO2/3.0/ CH4/3.0/				
2HNO = N2O + H2O	8.50E08	0.00	3080	! 1 ATM
HNO + OH = NO + H2O	1.30E07	1.88	-954	!SOTO/PAGE
HNO + H = H2 + NO	4.50E11	0.72	656	
HNO + O = OH + NO	4.50E11	0.72	656	! SAME AS H
HNO + NH2 = NH3 + NO	9.20E05	1.94	-1152	! HTRAN EST. 12/22/95
HNO + NO = N2O + OH	8.50E12	0.00	29586	!DIAU ET AL 1995
HNO + O2 = NO + HO2	2.00E13	0.00	15896	
HNO + CH3 = NO + CH4	8.20E05	1.87	954	! HTRAN EST. 12/22/95
NH2O + M = HNO + H + M	2.79E24	-2.83	64915	! M=N2
AR/0.7/ H2O/7.0/ CO2/2.0/ CH4/2.0/				
NH2O + M = HNOH + M	1.07E29	-3.99	43982	! M=N2, OK T>1000
AR/0.7/ H2O/7.0/ CO2/2.0/ CH4/2.0/				
NH2O + H = NH2 + OH	4.00E13	0.00	0	!RECOMBINATION
NH2O + H = HNO + H2	4.80E08	1.50	1560	!ABSTRACTION
NH2O + O = HNO + OH	3.30E08	1.50	487	!ABSTRACTION
NH2O + OH = HNO + H2O	2.40E06	2.00	-1192	!ABSTRACTION

Table AG.1 Mercury oxidation mechanism (Continued)

NH2O + CH3 = CH3O + NH2	2.00E13	0.00	0	!RECOMBINATION
NH2O + CH3 = HNO + CH4	1.60E06	1.87	2961	!ABSTRACTION
NH2O + NH2 = HNO + NH3	1.80E06	1.94	-1152	!ABSTRACTION
NH2O + HO2 = HNO + H2O2	2.90E04	2.69	-1600	!ABSTRACTION
NH2O + HO2 = NH2OH + O2	2.90E04	2.69	-1600	!SAME AS 37H1
HNOH + M = H + HNO + M	1.97E24	-2.84	58934	! M=N2
AR/0.7/ H2O/7.0/ CO2/2.0/ CH4/2.0/				
HNOH + H = NH2 + OH	4.00E13	0.00	0	!RECOMBINATION
HNOH + H = HNO + H2	4.80E08	1.50	378	!ABSTRACTION
HNOH + O = HNO + OH	7.00E13	0.00	0	!RECOMBINATION
DUPLICATE				
HNOH + O = HNO + OH	3.30E08	1.50	-358	!ABSTRACTION
DUPLICATE				
HNOH + OH = HNO + H2O	2.40E06	2.00	-1192	!ABSTRACTION
HNOH + CH3 = CH3N.H + OH	2.00E13	0.00	0	!RECOMBINATION
HNOH + CH3 = HNO + CH4	1.60E06	1.87	2096	!ABSTRACTION
HNOH + NH2 = HNO + NH3	1.80E06	1.94	-1152	!ABSTRACTION
HNOH + NH2 = N2H3 + OH	6.72E06	1.82	715	!(+15) 1.00E+00 ATM, 300-2400 K, 17% ERR,
1.00 X N2				
HNOH + NH2 = H2NN + H2O	4.57E19	-1.94	1927	! (+15) 1.00E+00 ATM, 300-2400 K, 13%
ERR, 1.00 X N2				
HNOH + HO2 = HONHO + OH	4.00E13	0.00	0	!RECOMBINATION (-11 KCAL)
HNOH + HO2 = HNO + H2O2	2.90E04	2.69	-1600	!ABSTRACTION
HNOH + HO2 = NH2OH + O2	2.90E04	2.69	-1600	!SAME AS 38G2
HNOO + M = OH + NO + M	1.52E36	-6.18	31131	! m=n2
AR/0.7/ H2O/7.0/ CO2/2.0/ CH4/2.0/				
HONO + M = OH + NO + M	2.05E31	-4.56	51175	! M=N2
AR/0.7/ H2O/7.0/ CO2/2.0/ CH4/2.0/				
HONO + H = H2 + NO2	2.00E08	1.55	6614	!HSU ET AL ('97) ADDED 7/2/97
HONO + H = HNO + OH	5.63E10	0.86	4969	!HSU ET AL ('97) ADDED 7/2/97
HONO + H = H2O + NO	8.13E06	1.89	3846	!HSU ET AL ('97) ADDED 7/2/97
HONO + O = OH + NO2	1.70E08	1.50	3030	! HTRAN EST. 12/22/95
HONO + OH = H2O + NO2	1.20E06	2.00	-596	! HTRAN EST. 12/22/95
HONO + CH3 = NO2 + CH4	8.10E05	1.87	5504	! HTRAN EST. 12/22/95
HONO + NH2 = NO2 + NH3	9.20E05	1.94	1917	! HTRAN EST. 12/22/95
HNO2 = HONO	1.30E29	-5.47	52814	! 1 ATM N2
HNO2 + H = H2 + NO2	2.40E08	1.50	4163	! HTRAN EST. 12/22/95
HNO2 + O = OH + NO2	1.70E08	1.50	2365	! HTRAN EST. 12/22/95
HNO2 + OH = H2O + NO2	1.20E06	2.00	-795	! HTRAN EST. 12/22/95
HNO2 + CH3 = NO2 + CH4	8.10E05	1.87	4838	! HTRAN EST. 12/22/95
HNO2 + NH2 = NO2 + NH3	9.20E05	1.94	874	! HTRAN EST. 12/22/95
HCN + M = HNC + M	1.56E26	-3.23	49576	! M=N2 (T>1000K)
AR/0.7/ H2O/7.0/ CO2/2.0/ CH4/2.0/				
HCN + OH = CN + H2O	3.90E06	1.83	10293	! 11/95 UPDATE
OH + HCN = HNCO + H	4.40E03	2.26	6398	!MILLER/MELIUS
OH + HCN = HOCN + H	1.10E06	2.03	13373	!MILLER/MELIUS
OH + HCN = NH2 + CO	1.60E02	2.56	9001	!MILLER/MELIUS
OH + HCN = N*CHOH	2.80E30	-6.37	5345	! 1 ATM N2
HCN + O = NH + CO	5.40E08	1.21	7491	! PERRY-MELIUS
HCN + O = NCO + H	2.00E08	1.47	7590	! PERRY-MELIUS
HCN + O = CN + OH	4.20E10	0.40	20675	!CHEMACT
O + HNC = NH + CO	4.60E12	0.00	2186	
OH + HNC = HNCO + H	2.80E13	0.00	3696	
HNC + O2 = HNCO + O	1.50E12	0.01	4113	
HNC + O2 = NH + CO2	1.60E19	-2.25	1778	
CN + H2 = HCN + H	3.60E08	1.55	3000	
CN + O = CO + N	7.70E13	0.00	0	
CN + O2 = NCO + O	1.00E13	0.00	0	! 8/5/97 UPDATE
CN + OH = NCO + H	4.00E13	0.00	0	
CN + HCN = NCCN + H	1.50E07	1.71	1530	
CN + N2O = NCN + NO	4.20E11	0.00	7173	! UPDATE WILLIAMS 1995
CN + NO2 = NCO + NO	6.20E15	-0.75	348	! UPDATE 8/13/94
CN + CH4 = HCN + CH3	1.20E05	2.64	-159	
CN + NH3 = HCN + NH2	9.20E12	0.00	-358	

Table AG.1 Mercury oxidation mechanism (Continued)

H2CN = HCN + H	6.00E31	-6.46	32110	! 1 ATM N2
H2CN + HO2 = CH2NO + OH	3.00E13	0.00	0	
H2CN + HO2 = HCN + H2O2	1.45E04	2.69	-1604	! EST SP2
H2CN + HO2 = H2C*NH + O2	1.45E04	2.69	-1604	!SAME AS OTHER CHANNEL
H2CN + O2 = CH2O + NO	3.00E12	0.00	5961	
H2CN + CH3 = HCN + CH4	8.10E05	1.87	-1113	!ABSTRACTION
H2CN + OH = HCN + H2O	1.50E19	-2.18	2166	! 1 ATM N2
DUPLICATE				
H2CN + OH = HCN + H2O	1.20E06	2.00	-1192	!ABSTRACTION
DUPLICATE				
H2CN + N = N2 + CH2	6.00E13	0.00	397	
H2CN + H = HCN + H2	2.40E08	1.50	-894	!ABSTRACTION
H2CN + NH2 = HCN + NH3	9.20E05	1.94	-1152	!ABSTRACTION
H2CN + O = HCN + OH	1.70E08	1.50	-894	!ABSTRACTION
H2CN + O = HNCO + H	6.00E13	0.00	0	!EST. 12/30/97
H2CN + O = HCNO + H	2.00E13	0.00	0	!EST. 12/30/97
HCNH = HCN + H	6.10E28	-5.69	24271	! 1 ATM N2
HCNH + H = H2CN + H	2.00E13	0.00	0	!RECOMBINATION
HCNH + H = HCN + H2	2.40E08	1.50	-894	!ABSTRACTION
HCNH + O = HNCO + H	7.00E13	0.00	0	!RECOMBINATION
HCNH + O = HCN + OH	1.70E08	1.50	-894	!ABSTRACTION
HCNH + OH = HCN + H2O	1.20E06	2.00	-1192	!ABSTRACTION
HCNH + CH3 = HCN + CH4	8.20E05	1.87	-1113	!ABSTRACTION
HCNN + O2 = H + CO2 + N2	4.00E12	0.00	0	! assuming rapid dissociation of hco2.
HCNN + O2 = HCO + N2O	4.00E12	0.00	0	
H2C*NH + H = H2CN + H2	2.40E08	1.50	7322	! HTRAN EST. 12/22/95
H2C*NH + O = H2CN + OH	1.70E08	1.50	4630	! HTRAN EST. 12/22/95
H2C*NH + OH = H2CN + H2O	1.20E06	2.00	-89	! HTRAN EST. 12/22/95
H2C*NH + CH3 = H2CN + CH4	8.20E05	1.87	7123	! HTRAN EST. 12/22/95
H2C*NH + NH2 = H2CN + NH3	9.20E05	1.94	4441	! HTRAN EST. 12/22/95
H2C*NH + H = HCNH + H2	3.00E08	1.50	6130	! EST (RESON.) 12/22/95
H2C*NH + O = HCNH + OH	2.20E08	1.50	5404	! EST (RESON.) 12/22/95
H2C*NH + OH = HCNH + H2O	2.40E06	2.00	457	! EST (RESON.) 12/22/95
H2C*NH + CH3 = HCNH + CH4	5.30E05	1.87	9687	! EST RESON. 12/22/95
H2C*NH + NH2 = HCNH + NH3	1.80E06	1.94	6090	! EST SP3 12/22/95
H2C*NH + O = CH2O + NH	1.70E06	2.08	0	
CH3N.H = H2C*NH + H	1.30E42	-9.24	41340	! 1 ATM N2 (600-2500K)
CH3N.H + H = H2C*NH + H2	7.20E08	1.50	-894	!ABSTRACTION
CH3N.H + O = H2C*NH + OH	5.00E08	1.50	-894	!ABSTRACTION
CH3N.H + OH = H2C*NH + H2O	3.60E06	2.00	-1192	!ABSTRACTION
CH3N.H + CH3 = H2C*NH + CH4	2.40E06	1.87	-1113	!ABSTRACTION
C.H2NH2 = H2C*NH + H	2.40E48	-10.82	52040	! 1 ATM N2 (600-2500K)
C.H2NH2 + O2 = NH2 + CH2O + O	6.00E18	-1.59	30192	! assume fast dissoc of nh2ch2o to nh2+ch2o
C.H2NH2 + O2 = H2C*NH + HO2	1.00E22	-3.09	6756	
C.H2NH2 + H = H2C*NH + H2	4.80E08	1.50	-894	!ABSTRACTION
C.H2NH2 + O = CH2O + NH2	7.00E13	0.00	0	
C.H2NH2 + O = H2C*NH + OH	3.33E08	1.50	-894	!ABSTRACTION
C.H2NH2 + OH = CH2OH + NH2	4.00E13	0.00	0	
C.H2NH2 + OH = H2C*NH + H2O	2.40E06	2.00	-1192	!ABSTRACTION
C.H2NH2 + CH3 = C2H5 + NH2	2.00E13	0.00	2702	
C.H2NH2 + CH3 = H2C*NH + CH4	1.60E06	1.87	-626	!ABSTRACTION
CH3NH2 + H = C.H2NH2 + H2	5.60E08	1.50	5464	! EST PARTIAL RESON. 9/16/96
CH3NH2 + O = C.H2NH2 + OH	4.00E08	1.50	5196	! EST PARTIAL RESON. 9/16/96
CH3NH2 + OH = C.H2NH2 + H2O	3.60E06	2.00	238	! EST PARTIAL RESON. 9/16/96
CH3NH2 + CH3 = C.H2NH2 + CH4	1.50E06	1.87	9170	! EST PARTIAL RESON. 9/16/96
CH3NH2 + NH2 = C.H2NH2 + NH3	2.80E06	1.94	5494	! EST SP3 12/22/95
CH3NH2 + H = CH3N.H + H2	4.80E08	1.50	9706	! N EST. 12/22/95
CH3NH2 + O = CH3N.H + OH	3.30E08	1.50	6348	! N EST. 12/22/95
CH3NH2 + OH = CH3N.H + H2O	2.40E06	2.00	447	! N EST. 12/22/95
CH3NH2 + CH3 = CH3N.H + CH4	1.60E06	1.87	8842	! N EST. 12/22/95
CH3NH2 + NH2 = CH3N.H + NH3	1.80E06	1.94	7143	! EST SP3 12/22/95

Table AG.1 Mercury oxidation mechanism (Continued)

NCCN + M = CN + CN + M	1.10E34	-4.32	130079	! M=AR
N2/1.5/ O2/1.5/ H2/1.5/ H2O/10./ CO2/3.0/ CH4/3.0/				
NCCN + O = NCO + CN	4.60E12	0.00	8882	
NCCN + OH = HOCN + CN	2.00E12	0.00	19000	! ADDED 12/30/97
NCO + NO = CO2 + N2	7.84E17	-1.73	763	! UPDATE 8/13/94
NCO + NO = N2O + CO	6.16E17	-1.73	763	! UPDATE 8/13/94
NCO + M = N + CO + M	2.20E14	0.00	54046	!MERTENS 26 SYMP (2370-3050K) ADDED 8/12/97
N2/1.5/ O2/1.5/ H2/1.5/ H2O/10./ CO2/3.0/ CH4/3.0/				
NCO + H2 = HNCO + H	7.60E02	3.00	3974	
NCO + O = NO + CO	4.20E13	0.00	0	
NCO + O = N + CO2	8.00E12	0.00	2500	!ADDED 12/30/97
NCO + H = NH + CO	5.20E13	0.00	0	
NCO + N = N2 + CO	3.31E13	0.00	0	! BROWNSWORD ET AL 1997
NCO + OH = HNCO + O	7.80E04	2.27	-984	!TSANG
NCO + OH = HON + CO	5.30E12	-0.07	5126	
NCO + OH = H + CO + NO	8.30E12	-0.05	18042	
NCO + NO2 = CO2 + N2O	2.30E12	0.00	-874	
NCO + NO2 = CO + 2NO	2.10E11	0.00	-874	
NCO + CH4 = HNCO + CH3	9.80E12	0.00	8127	! UPDATE 8/13/94
NCO + NH3 = HNCO + NH2	2.77E04	2.48	981	! BECKER ET AL (997) ADDED 7/2/97
HCNO = HCN + O	4.20E31	-6.12	61210	! P=1.0 ATM N2
HCNO + H = HNCO + H	2.10E15	-0.69	2851	
HCNO + H = HCN + OH	2.70E11	0.18	2116	
HCNO + H = NH2 + CO	1.70E14	-0.75	2891	
HCNO + H = HOCN + H	1.40E11	-0.19	2484	
HCNO + O = HCO + NO	7.00E13	0.00	0	
HCNO + OH = HCOH + NO	4.00E13	0.00	0	
HOCN + H = HNCO + H	3.10E08	0.84	1917	
H + HOCN = NH2 + CO	1.20E08	0.61	2076	
HOCN + H = H2 + NCO	2.40E08	1.50	6617	! HTRAN EST. 12/22/95
HOCN + O = OH + NCO	1.70E08	1.50	4133	! HTRAN EST. 12/22/95
HOCN + OH = H2O + NCO	1.20E06	2.00	-248	! HTRAN EST. 12/22/95
HOCN + CH3 = CH4 + NCO	8.20E05	1.87	6617	! HTRAN EST. 12/22/95
HOCN + NH2 = NCO + NH3	9.20E05	1.94	3646	! HTRAN EST. 12/22/95
HNCO + M = NH + CO + M	8.40E15	0.00	84368	! ADDED 9/27/96
N2/1.5/ O2/1.5/ H2/1.5/ H2O/10./ CO2/3.0/ CH4/3.0/				
HNCO + H = NH2 + CO	3.60E04	2.49	2345	! UPDATE 9/27/96
HNCO + O = HNO + CO	1.70E06	2.08	0	
HNCO + O = NH + CO2	1.70E06	2.08	0	
HNCO + OH = NH2 + CO2	6.30E10	-0.06	11644	
HNCO + OH = NCO + H2O	5.20E10	-0.03	17565	
DUPLICATE				
HNCO + OH = NCO + H2O	3.60E07	1.50	3594	! 8/5/97 UPDATE
DUPLICATE				
CH2NO = HNCO + H	2.30E42	-9.11	53838	! 1 ATM N2 (600-2500K)
CH2NO + O2 = CH2O + NO2	1.20E15	-1.01	20128	! 12/3/97 UPDATE 1000-2500K (ALLYL+O2)
CH2NO + H = CH3 + NO	4.00E13	0.00	0	
CH2NO + H = HCNO + H2	4.80E08	1.50	-894	!ABSTRACTION
CH2NO + O = CH2O + NO	7.00E13	0.00	0	
CH2NO + O = HCNO + OH	3.30E08	1.50	-894	!ABSTRACTION
CH2NO + OH = CH2OH + NO	4.00E13	0.00	0	
CH2NO + OH = HCNO + H2O	2.40E06	2.00	-1192	!ABSTRACTION
CH2NO + CH3 = C2H5 + NO	3.00E13	0.00	0	
CH2NO + CH3 = HCNO + CH4	1.60E06	1.87	-1113	!ABSTRACTION
CH2NO + NH2 = C.H2NH2 + NO	3.00E13	0.00	0	
CH2NO + NH2 = HCNO + NH3	1.80E06	1.94	-1152	!ABSTRACTION
CH3NO + H = CH2NO + H2	4.40E08	1.50	378	! EST (RESON.) 12/22/95
CH3NO + O = CH2NO + OH	3.30E08	1.50	3616	! EST (RESON.) 12/22/95
CH3NO + OH = CH2NO + H2O	3.60E06	2.00	-1192	! EST (RESON.) 12/22/95
CH3NO + CH3 = CH2NO + CH4	7.90E05	1.87	5415	! EST RESON. 12/22/95
CH3NO + NH2 = CH2NO + NH3	2.80E06	1.94	1073	! EST SP3 12/22/95
CH3NO + H = CH3 + HNO	1.80E13	0.00	2782	
CH3NO + O = CH3 + NO2	1.70E06	2.08	0	

Table AG.1 Mercury oxidation mechanism (Continued)

```
CH3NO + OH = CH3 + HONO              2.50E12      0.00     994
 HON + M = NO + H + M                5.09E19     -1.73     16045     !M=N2
      AR/0.7/  H2O/7.0/  CO2/2.0/  CH4/2.0/
 HON + H = HNO + H                   2.00E13      0.00     0
 HON + H = OH + NH                   2.00E13      0.00     0
 HON + O = OH + NO                   7.00E13      0.00     0
 HON + OH = HONO + H                 4.00E13      0.00     0
 HON + O2 = HONO + O                 1.00E12      0.00     4968      ! 2/4/98
 HCOH = CH2O                        2.10E19      -3.07     9538      !10 KCAL BARRIER, 1.0 ATM
 NH2OH + H = HNOH + H2               4.80E08      1.50     6249      !HTRANS 2/6/96
 NH2OH + H = NH2O + H2               2.40E08      1.50     5067      !HTRANS 2/6/96
 NH2OH + O = HNOH + OH               3.30E08      1.50     3865      !HTRANS 2/6/96
 NH2OH + O = NH2O + OH               1.70E08      1.50     3010      !HTRANS 2/6/96
 NH2OH + OH = HNOH + H2O             2.40E06      2.00     -328      !HTRANS 2/6/96
 NH2OH + OH = NH2O + H2O             1.20E06      2.00     -596      !HTRANS 2/6/96
 NH2OH + CH3 = HNOH + CH4            1.60E06      1.87     6348      !HTRANS 2/6/96
 NH2OH + CH3 = NH2O + CH4            8.20E05      1.87     5494      !HTRANS 2/6/96
 NH2OH + NH2 = HNOH + NH3           1.80E06      1.94     3229      !HTRANS 2/6/96
 NH2OH + NH2 = NH2O + NH3            9.20E05      1.94     1888      !HTRANS 2/6/96
 NH2OH + HO2 = HNOH + H2O2          2.90E04      2.69     9557      !HTRANS 2/6/96
 NH2OH + HO2 = NH2O + H2O2          1.40E04      2.69     6418      !HTRANS 2/6/96
 NH2NO = N2 + H2O                    3.10E34     -7.11     36283     !DISSOC (TOT.) 1.0 ATM
 NH2NO + H = HNNO + H2               4.80E08    1.50      7412      !HTRANS 2/6/96
 NH2NO + O = HNNO + OH               3.30E08      1.50     4699      !HTRANS 2/6/96
 NH2NO + OH = HNNO + H2O             2.40E06      2.00     -70       !HTRANS 2/6/96
 NH2NO + CH3 = HNNO + CH4            1.60E06      1.87     7183      !HTRANS 2/6/96
 NH2NO + NH2 = HNNO + NH3           1.80E06      1.94     4540      !HTRANS 2/6/96
 NH2NO + HO2 = HNNO + H2O2          2.90E04      2.69     12627     !HTRANS 2/6/96
 H2NNHO = NH2 + HNO                  2.40E40     -8.73     41608     !1.00E+00 ATM
 H2NNHO + H = HNNHO + H2             4.80E08      1.50     -894      !HTRANS 2/6/96
 H2NNHO + O = HNNHO + OH             3.30E08      1.50     -894      !HTRANS 2/6/96
 H2NNHO + OH = HNNHO + H2O          2.40E06      2.00     -1192     !HTRANS 2/6/96
 H2NNHO + CH3 = HNNHO + CH4         1.60E06      1.87     378       !HTRANS 2/6/96
 H2NNHO + NH2 = HNNHO + NH3         1.80E06      1.94     -1152     !HTRANS 2/6/96
 H2NNHO + HO2 = HNNHO + H2O2        2.90E04      2.69     -1600     !HTRANS 2/6/96

!*****************************************************
!********************** SOx **************************
!*****************************************************
! Leeds University
H2S+M =  S+H2+M                    1.600E+24    -2.61        44841.47      !   [00GLA/ALZ]
 N2/1.5/ SO2/10/ H2O/10/
H2S+H =  SH+H2                      1.2E07       2.10         352.29       !  293 - 2237K [92YOS/KOS]
H2S+O =  SH+OH                      7.5E07       1.75         1459.49      !   [00GLA/ALZ]
H2S+OH =  SH+H2O                    2.7E12       0.00         0.00         !   [91TYN/RAV]
H2S+S =  2SH                        8.3E13       0.00         3724.21      !  [00GLA/ALZ]
H2S+S =  HS2+H                      2.0E13       0.00         3724.21      !   [00GLA/ALZ]
S+H2 =  SH+H                        1.4E14       0.00         9713.14      !  [00GLA/ALZ]
SH+O =  H+SO                        1.0E14       0.00         0.00         !   [00GLA/ALZ]
SH+OH =  S+H2O                      1.0E13       0.00         0.00         !   [00GLA/ALZ] (estimate)
SH+HO2 =  HSO+OH                    1.0E12       0.00         0.00         !   [00GLA/ALZ]
SH+O2 =  HSO+O                      1.9E13       0.00         9021.14      !   [00GLA/ALZ]
S+OH =  H+SO                        4.0E13       0.00         0.00         !   [00GLA/ALZ]
S+O2 =  SO+O                        5.2E06       1.81         -603.93      !   [00GLA/ALZ]
2SH =  S2+H2                        1.0E12       0.00         0.00         !   [00GLA/ALZ]
SH+S =  S2+H                        3.0E13       0.00         0.00         !   [00GLA/ALZ]
S2+M =  2S+M                        4.8E13       0.00         38751.89     !   [80HIG/SAI]
S2+H+M =  HS2+M                     1.0E16       0.00         0.00         !   [00GLA/ALZ]
S2+O =  SO+S                        1.0E13       0.00         0.00         !   [00GLA/ALZ]
HS2+H =  S2+H2                      1.2E07       2.10         352.29       !   [00GLA/ALZ]
HS2+O =  S2+OH                      7.5E07       1.75         1459.49      !   [00GLA/ALZ]
HS2+OH =  S2+H2O                    2.7E12       0.00         0.00         !   [00GLA/ALZ]
HS2+S =  S2+SH                      2.0E13       0.00         3724.21      !   [00GLA/ALZ]
HS2+H+M =  H2S2+M                   1.0E16       0.00         0.00         !   [00GLA/ALZ]
```

Table AG.1 Mercury oxidation mechanism (Continued)

H2S2+H = HS2+H2	1.2E07	2.10	352.29	! [00GLA/ALZ]
H2S2+O = HS2+OH	7.5E07	1.75	1459.49	! [00GLA/ALZ]
H2S2+OH = HS2+H2O	2.7E12	0.00	0.00	! [00GLA/ALZ]
H2S2+S = HS2+SH	2.0E13	0.00	3724.21	! [00GLA/ALZ]
SO3+H = HOSO+O	2.5E05	2.92	25314.55	! [00GLA/ALZ]
SO3+O = SO2+O2	2.0E12	0.00	10065.43	! [00GLA/ALZ]
SO3+SO = 2SO2	1.0E12	0.00	5032.71	! [00GLA/ALZ]
SO+O(+M) = SO2(+M)	3.2E13	0.00	0.00	! [00GLA/ALZ]
N2/1.5/ SO2/10/ H2O/10/				
LOW / 1.200E+21 -1.54 0.00 /				
TROE / 0.5500 1.0e-30 1e+30 /				
SO2+O(+M) = SO3(+M)	9.2E10	0.00	1199.80	! [00GLA/ALZ]
N2/1.3/ SO2/10/ H2O/10/				
LOW / 4.000E+28 -4.00 2642.17 /				
SO2+OH(+M) = HOSO2(+M)	7.2E12	0.00	359.84	! [00GLA/ALZ]
N2/1.5/ SO2/10/ H2O/10/				
LOW / 4.500E+25 -3.30 359.84 /				
TROE / 0.7000 1.0e-30 1e+30 /				
SO2+OH = HOSO+O	3.9E08	1.89	38248.62	! [96GLA/KUB]
SO2+OH = SO3+H	4.9E02	2.69	12003.02	! [96GLA/KUB]
SO2+CO = SO+CO2	2.7E12	0.00	24308.00	! [00GLA/ALZ]
SO+M = S+O+M	4.0E14	0.00	53850.03	! [96GLA/KUB]
SO+H+M = HSO+M	5.0E15	0.00	0.00	! [96GLA/KUB]
N2/1.5/ SO2/10/ H2O/10/				
SO+OH(+M) = HOSO(+M)	1.6E12	0.50	-201.31	! [00GLA/ALZ]
N2/1.5/ SO2/10/ H2O/10/				
LOW / 9.500E+27 -3.48 488.17 /				
!SO+OH = SO2+H	5.2E13	0.00	0.00	! [96GLA/KUB]
SO+OH = SO2+H	1.1E17	-1.35	0	
SO+O2 = SO2+O	7.6E03	2.37	1494.72	! [00GLA/ALZ]
2SO = SO2+S	2.0E12	0.00	2013.09	! [96GLA/KUB]
HSO+H = HSOH	2.5E20	-3.14	463.01	! [96GLA/KUB]
HSO+H = SH+OH	4.9E19	-1.86	785.10	! [96GLA/KUB]
HSO+H = S+H2O	1.6E09	1.37	-171.11	! [96GLA/KUB]
HSO+H = H2SO	1.8E17	-2.47	25.16	! [96GLA/KUB]
HSO+H = H2S+O	1.1E06	1.03	5234.02	! [96GLA/KUB]
HSO+H = SO+H2	1.0013	0.00	0.00	! [00GLA/ALZ]
HSO+O+M = HSO2+M	1.10E19	-1.73	-25.16	! [96GLA/KUB]
HSO+O = SO2+H	4.5E14	-0.40	0.00	! [96GLA/KUB]
HSO+O+M = HOSO+M	6.9E19	-1.61	800.20	! [96GLA/KUB]
HSO+O = O+HOS	4.8E08	1.02	2687.47	! [96GLA/KUB]
HSO+O = OH+SO	1.4E13	0.15	150.98	! [96GLA/KUB]
HSO+OH = HOSHO	5.2E28	-5.44	1595.37	! [96GLA/KUB]
HSO+OH = HOSO+H	5.3E07	1.57	1887.27	! [00GLA/ALZ]
HSO+OH = SO+H2O	1.7E09	1.03	236.54	! [96GLA/KUB]
HSO+O2 = SO2+OH	1.0E12	0.00	5032.71	! [96GLA/KUB]
HSOH = SH+OH	2.8E39	-8.75	37846.00	! [96GLA/KUB]
HSOH = S+H2O	5.8E29	-5.60	27428.28	! [96GLA/KUB]
HSOH = H2S+O	9.8E16	-3.40	43532.97	! [96GLA/KUB]
H2SO = H2S+O	4.9E28	-6.66	36084.55	! [96GLA/KUB]
HOSO(+M) = H+SO2(+M)	1.7E10	0.80	23620.03	! [00GLA/ALZ]
N2/1/ SO2/10/ H2O/10/				
LOW / 1.500E+31 -4.53 24749.88 /				
TROE / 0.3000 1.0e-30 1e+30 /				
HOSO(+M) = HSO2(+M)	1.0E09	1.03	25163.56	! [00GLA/ALZ]
N2/1/ SO2/10/ H2O/10/				
LOW / 1.700E+35 -5.64 27881.23 /				
TROE / 0.4000 1.0e-30 1e+30 /				
HOSO+M = O+HOS+M	2.5E30	-4.80	59889.28	! [96GLA/KUB]
HOSO+H = SO2+H2	3.0E13	0.00	0.00	! [00GLA/ALZ]
HOSO+H = SO+H2O	6.3E10	6.29	-956.22	! [00GLA/ALZ]
HOSO+OH = SO2+H2O	1.0E12	0.00	0.00	! [00GLA/ALZ]
HOSO+O2 = HO2+SO2	1.0E12	0.00	503.27	! [00GLA/ALZ]1

Table AG.1 Mercury oxidation mechanism (Continued)

HSO2+H = SO2+H2	3.0E13	0.00	0.00	! [00GLA/ALZ]
HSO2+OH = SO2+H2O	1.0E13	0.00	0.00	! [00GLA/ALZ]
HSO2+O2 = HO2+SO2	1.0E13	0.00	0.00	! [00GLA/ALZ]
HSO2(+M) = H+SO2(+M)	2.0E11	0.90	9240.06	! [00GLA/ALZ]
N2/1/ SO2/10/ H2O/10/				
LOW / 3.500E+25 -3.29 9612.48 /				
HOSO2 = HOSO+O	5.4E18	-2.34	53497.74	! [96GLA/KUB]
HOSO2 = SO3+H	1.4E18	-2.91	27629.59	! [96GLA/KUB]
HOSO2+H = SO2+H2O	1.0E12	0.00	0.00	! [00GLA/ALZ]
HOSO2+O = SO3+OH	5.0E12	0.00	0.00	! [00GLA/ALZ]
HOSO2+OH = SO3+H2O	1.0E12	0.00	0.00	! [96GLA/KUB] (estimate)
HOSO2+O2 = HO2+SO3	7.8E11	0.00	330.15	! [96GLA/KUB]
HOSHO = HOSO+H	6.4E30	-5.89	37141.42	! [96GLA/KUB]
HOSHO = SO+H2O	1.2E24	-3.59	29944.64	! [96GLA/KUB]
HOSHO+H = HOSO+H2	1.0E12	0.00	0.00	! [96GLA/KUB]
HOSHO+O = HOSO+OH	5.0E12	0.00	0.00	! [96GLA/KUB]
HOSHO+OH = HOSO+H2O	1.0E12	0.00	0.00	! [96GLA/KUB]
! extra reactions from leeds mechanism				
C+SO2 = CO+SO	4.16E13	0.00	0.00	! [91DOR/CAU]
HOSO2+H = SO3+H2	1.0E12	0.00	0.00	! [91CHA/GOD]
S+CH4 = SH+CH3	6.0E14	0.00	12078	! [96GLA/KUB]
H2S+CH3 = CH4+SH	1.8E11	0.00	1177	! linear fit to NIST values
S+OH = SH+O	6.3E11	0.5	4030	! [83WEN/WOO]
C+H2S = CH+SH	1.2 E14	0.00	4450	! estimate by KJH
O+COS = CO+SO	1.93E13	0.00	2329	! fit to NIST data
O+CS = CO+S	1.626E14	0.00	759.94	! [92ATK/BAU]
COS+M = CO+S+M	1.43E14	0.00	30700	! fit to NIST Data
O+COS = CO2+S	5.0E13	0.00	5530.45	! [88SIN/CVE]
SH+O2 = SO+OH	1.0E12	0.00	5032	! [96GLA/KUB] estimate
CH+SO = CO+SH	1.0E13	0.00	0.00	! [89PFE/CHU] estimate
SO3+S = SO+SO2	5.12E11	0.00	0.00	! [78MUL/SCH]
SH+NO = SN+OH	1.0E13	0.00	8901	! [91CHA/GOD]
S+NO = SN+O	1.0E12	0.5	17500	! [83WEN/WOO]
SH+NH = SN+H2	1.0E14	0.00	0.00	! [91CHA/GOD] estimate
N+SO = NO+S	6.31E11	0.50	1010	! [83WEN/WOO] estimate
N+SH = SN+H	6.31E11	0.50	4030	! [83WEN/WOO] estimate
!SN+NO = N2+SO	1.0E14	0.00	0.00	! [91CHA/GOD] estimate
SN+NO = N2+SO	1.81E10	0.00	0.00	! exp. meas. Chem. Dep. in Leeds
SN+O2 = SO+NO	3.0E8	0.00	0.00	! exp. meas. Chem. Dep. in Leeds
SN+NO2=S+NO+NO	4.07E15	-0.9805	0.00	! exp. meas. Chem. Dep. in Leeds
N+SN = N2+S	6.3E11	0.5	0.00	! [83WEN/WOO]
SO2+NO2 = NO+SO3	4.25E19	8.9	3797	! fit to all NIST data
SO+NO2 = SO2+NO	8.43E12	0.00	0.00	! [92ATK/BAU]
SN+O = SO+N	6.31E11	0.50	4030	! [83WEN/WOO]
S+NH = SH+N	1.0E13	0.00	0.00	! [89PFE/CHU] estimate
!NH+SO = NO+SH	1.0E13	0.00	0.00	! [89PFE/CHU] estimate
NH+SO = NO+SH	3.01E13	0.00	0.00	! exp. meas. Chem. Dep. in Leeds
HSO+NO2 = HOSO+NO	5.8E12	0.00	0.00	! [96GLA/KUB]

REFERENCES

1. Kong, S.-C.; Marriott, C.; Reitz, R. D. *Society of Automotive Engineers (SAE)* **2002**, *01-0419*.
2. Wilhelmsson, C.; Tunestål, P.; Johansson, B. *Society of Automotive Engineering (SAE)* **2007**, *01-1855*.
3. Bruno, T. J.; Huber, M. L.; Laesecke, A.; Lemmon, E. W.; Perkins, R. A. Thermochemical and Thermophysical Properties of JP-10, 2006, Physical and Chemical Properties Division, National Institute of Standards and Technology, Boulder, CO.
4. Auzmendi-Murua, I.; Bozzelli, J. W. *J. Phys. Chem. A* **2012**, *Submitted*.
5. Chen, C.-C.; Liaw, H.-J.; Shu, C.-M.; Hsieh, Y.-C. *J. Chem. Eng. Data* **2010**, *55*, 5059-5064.
6. Fournet, R.; Glaude, P. A.; Bounaceur, R.; Molière, M. "Theoretical kinetic study of the low temperature oxidation of ethanol"; Proceeding of the European Combustion Meeting, 2009, Vienna, Austria.
7. Lee, C.; Vranckx, S.; Heufer, K. A.; Khomik, S.; Uygun, Y.; Olivier, H.; Fernandes, R. X. *Z. Phys. Chem.* **2012**, *226*, 1-28.
8. Silverwood, R.; Thomas, J. H. *J. Chem. Soc. Faraday Trans. 1* **1967**, *63*, 2476-2479.
9. Sun, H.; Bozzelli, J. W. *J. Phys. Chem. A* **2001**, *105*, 4504-4516.
10. Galmiche, B.; Togbé, C.; Dagaut, P.; Halter, F.; Foucher, F. *Energy Fuels* **2011**, *25*, 2013-2021.
11. Johnson, M. V.; Goldsborough, S. S.; Serinyel, Z.; O'Toole, P.; Larkin, E.; O'Malley, G.; Curran, H. J. *Energy Fuels* **2009**, *23*, 5886-5898.
12. Serinyel, Z.; Dooley, S.; Farouk, T. I.; Jahangirian, S.; Curran, H. J.; Dryer, F. L. "A Pyrolytic Flow Reactor Study of iso-Propanol"; 7th US National Combustion Meeting of the Combustion Institute, 2011, Atlanta, Georgia.
13. Sun, H.; Bozzelli, J. W. *J. Phys. Chem. A* **2002**, *106*, 3947-3956.
14. Togbé, C.; Dagaut, P.; Halter, F.; Foucher, F. *Energy Fuels* **2011**, *25*, 676-683.
15. Veloo, P. S.; Egolfopoulos, F. N. *Combust. Flame* **2011**, *158*, 501-510.
16. Xingcai, L.; Yuchun, H.; Libin, J.; Linlin, Z.; Zhen, H. *Energy Fuels* **2006**, *20*, 1870-1878.
17. Zador, J.; Miller, J. A. "Hydrogen abstraction from n-,i-propanol and n-butanol: a systematic theoretical approach"; 7th US National Technical Meeting of the Combustion Institute, 2011, Atlanta, GA.
18. Alecu, I. M.; Zheng, J.; Papajak, E.; Yu, T.; Truhlar, D. G. *J. Phys. Chem. A* **2012**, *116*, 12206-12213.
19. Cai, J.; Zhang, L.; Zhang, F.; Wang, Z.; Cheng, Z.; Yuan, W.; Qi, F. *Energy Fuels* **2012**, *26*, 5550-5568.
20. El-Nahas, A. M.; Mangood, A. H.; El-Meleigy, A. B. *Comp. Theor. Chem.* **2012**, *997*, 94-102.
21. Karwat, D. M.; Wagnon, S. W.; Teini, P. D.; Wooldridge, M. S. *J. Phys. Chem. A* **2011**, *115*, 4909-4921.

22. Karwat, D. M. A.; Wagnon, S. W.; Wooldridge, M. S.; Westbrook, C. K. *J. Phys. Chem. A* **2012**, *116*, 12406-12421.
23. Rosado-Reyes, C. M.; Tsang, W. *J. Phys. Chem. A* **2012**, *116*, 9825-9831.
24. Sarathy, S. M.; Vranckx, S.; Yasunaga, K.; Mehl, M.; Oßwald, P.; Metcalfe, W. K.; Westbrook, C. K.; Pitz, W. J.; Kohse-Höinghaus, K.; Fernandes, R. X.et al. *Combust. Flame* **2012**, *159*, 2028-2055.
25. Togbé, C.; Mzé-Ahmed, A.; Dagaut, P. *Energy Fuels* **2010**, *24*, 5244-5256.
26. Welz, O.; Savee, J. D.; Eskola, A. J.; Sheps, L.; Osborn, D. L.; Taatjes, C. A. *Proc. Combust. Inst.* **2013**, *34*, 493-500.
27. Yasunaga, K.; Mikajiri, T.; Sarathy, S. M.; Koike, T.; Gillespie, F.; Nagy, T.; Simmie, J. M.; Curran, H. J. *Combust. Flame* **2012**, *159*, 2009-2027.
28. Zhang, J.; Wei, L.; Man, X.; Jiang, X.; Zhang, Y.; Hu, E.; Huang, Z. *Energy Fuels* **2012**, *26*, 3368-3380.
29. Zhou, C.-W.; Simmie, J. M.; Curran , H. J. *Int. J. Chem. Kinet.* **2012**, *44*, 155-164.
30. Tsujimura, T.; Pitz, W. J.; Yang, Y.; Dec, J. E. *SAE International Journal of Fuels and Lubricants* **2011**, *4*, 257-270.
31. Welz, O.; Zádor, J.; Savee, J. D.; Ng, M. Y.; Meloni, G.; Fernandes, R. X.; Sheps, L.; Simmons, B. A.; Lee, T. S.; Osborn, D. L.et al. *Phys. Chem. Chem. Phys.* **2012**, *14*, 3112-3127.
32. Dayma, G.; Togbé, C.; Dagaut, P. *Energy Fuels* **2011**, *25*, 4986-4998.
33. Heufer, K. A.; Sarathy, S. M.; Curran, H. J.; Davis, A. C.; Westbrook, C. K.; Pitz, W. J. *Energy Fuels* **2012**, *26*, 6678-6685.
34. Tsujimura, T.; Pitz, W. J.; Gillespie, F.; Curran, H. J.; Weber, B. W.; Zhang, Y.; Sung, C.-J. *Energy Fuels* **2012**, *26*, 4871-4886.
35. Zhao, L.; Ye, L.; Zhang, F.; Zhang, L. *J. Phys. Chem. A* **2012**, *116*, 9238-9244.
36. Cole-Filipiak, N. C.; O'Connor, A.; Elrod, M. J. *Environ. Sci. Technol.* **2010**, *44*, 6718-6723.
37. Minerath, E. C.; Schultz, M. P.; Elrod, M. J. *Environ. Sci. Technol.* **2009**, *43*, 8133-8139.
38. Auzmendi-Murua, I.; Charaya, S.; Bozzelli, J. W. *J. Phys. Chem. A* **2013**, *117*, 378-392.
39. Auzmendi-Murua, I.; Hudzik, J. M.; Bozzelli, J. W. *Int. J. Chem. Kinet.* **2012**, *44*, 232-256.
40. Dagaut, P.; Reuillon, M.; Cathonnet, M.; Presvots, D. *Chromatographia* **1995**, *40*, 147-154.
41. Lay, T. H.; Tsai, P. L.; Yamada, T.; Bozzelli, J. W. *J. Phys. Chem. A* **1997**, *101*, 2471-2477.
42. Sirjean, B.; Glaude, P. A.; Ruiz-Lopez, M. F.; Fournet, R. *J. Phys. Chem. A* **2008**, *112*, 11598-11610.
43. Wiberg, K. B.; Hao, S. *J. Org. Chem.* **1991**, *56*, 5108-5110.
44. Wijaya, C. D.; Sumathi, R.; Green, W. H. *J. Phys. Chem. A* **2003**, *107*, 4908-4920.
45. Yang, Y.; Boehman, A. L. *Combust. Flame* **2010**, *157*, 495-505.
46. Senior, C. L. "Behavior of Mercury in Air Pollution Control Devices on Coal-Fired Utility Burners"; Power Production in the 21st Century: Impacts of Fuel Quality and Operations, Engineering Foundation Conference, 2001, Snowbird, UT.
47. Streets, D. G.; Zhang, Q.; Wu, Y. *Environ. Sci. Technol.* **2009**, *43*, 2983-2988.

48. Lindqvist, O.; Rodhe, H. *Tellus B* **1985**, *37*, 136-159.
49. Lodenius, M.; Laaksovirte, K. *Ann. Bot. Fennici* **1979**, *16*, 208-212.
50. *Changing Metal Cycles and Human Health (Life Sciences Research Reports)*; Nriagu, J. O., Ed. Berlin, Germany, 1984.
51. Peterson, K. A.; Balabanov, N. B. *J. Phys. Chem. A* **2003**, *107*, 7465-7470.
52. Peterson, K. A.; Balanov, N. B.; Shepler, B. C. *J. Phys. Chem. A* **2005**, *109*, 8765-8773.
53. Srivastava, R. K. "Controlling SO_2 emissions: A review of technologies", 2000, U.S. Environmental Protection Agency, Technical Report, Washington, DC.
54. Becke, A. D. *J. Chem. Phys.* **1993**, *98*, 1372-1377.
55. Hamprecht, F. A.; Cohen, A. J.; Tozer, D. J.; Handy, N. C. *J. Phys. Chem. A* **1998**, *109*, 6264-6272.
56. Boese, A. D.; Martin, J. M. L. *J Chem Phys* **2004**, *121*, 3405-3416.
57. Becke, A. D. *J. Chem. Phys.* **1996**, *104*, 1040-1047.
58. Curtiss, L. A.; Raghavachari, K.; Trucks, G. W.; Pople, J. A. *J. Chem. Phys.* **1991**, *94*, 7221-7230.
59. Chai, J. D.; Head-Gordon, M. *J. Chem. Phys.* **2008**, *128*, 40-55.
60. Grimme, S. *J. Chem. Phys.* **2006**, *124*, 67-83.
61. Zhao, Y.; Truhlar, D. G. *Theor. Chem. Account.* **2008**, *120*, 215-241.
62. *Advances in Chemical Physics*; Cizek, J., Ed.; Wiley Interscience: New York, 1696; Vol. 14.
63. Purvis III, G. D.; Bartlett, R. J. *J. Chem. Phys.* **1982**, *76*, 1910-1918.
64. Scuseria, G. E.; Janssen, C. L.; Schaefer III, H. F. *J. Chem. Phys.* **1988**, *89*, 7382-7387.
65. Scuseria, G. E.; Schaefer III, H. F. *J. Chem. Phys.* **1989**, *90*, 3700-3703.
66. Pople, J. A.; Head-Gordon, M.; Raghavachari, K. *J. Chem. Phys.* **1987**, *87*, 5968-5975.
67. Hay, P. J.; Wadt, W. R. *J. Chem. Phys.* **1985**, *82*, 270-284.
68. Häussermann, U.; Dolg, M.; Stoll, H.; Preuss, H.; Schwerdtfeger, P.; R.M., P. *Mol. Phys.* **1993**, *78*, 1211-1224.
69. Schwerdtfeger, P.; Dolg, M.; Schwarz, W. H. E.; Bowmaker, G. A.; Boyd, P. D. W. *J. Chem. Phys.* **1989**, *91*, 1762-1774.
70. Wedig, U.; Dolg, M.; Stoll, H.; Preuss, H. *Quantum Chemistry: The Challenge of Transition Metals and Coordination Chemistry*; Springer: Dordrecht, Holland, 1986.
71. Figgen, D.; Rauhut, G.; Dolg, M.; Stoll, H. *Chem. Phys.* **2005**, *311*, 227-244.
72. Frisch, M. J.; Trucks, G. W.; Schlegel, H. B.; Scuseria, G. E.; Robb, M. A.; Cheeseman, J. R.; Montgomery, J. A., Jr.; Vreven, T.; Kudin, K. N.; Burant, J. C.et al. Gaussian03; Gaussian, Inc.: Wallingford, CT, 2003.
73. Frisch, M. J.; Trucks, G. W.; Schlegel, H. B.; Scuseria, G. E.; Robb, M. A.; Cheeseman, J. R.; Scalmani, G.; Barone, V.; Mennucci, B.; Petersson, G. A.et al. Gaussian 09, Revision A.1. In *Gaussian, Inc.* Wallingford CT, 2009.
74. Petersson, G. A.; Malick, D. K.; Wilson, W. G.; Ochterski, J. W.; Montgomery, J. A.; Frisch, M. J. *J. Chem. Phys.* **1998**, *109*, 10570-10579.
75. Hehre, W. J.; Ditchfield, R.; Radom, L.; Pople, J. A. *J. Am. Chem. Soc.* **1970**, *92*, 4796-4801.

76. Yamaguchi, K.; Jensen, F.; Dorigo, A.; Houk, K. N. *Chem. Phys. Lett.* **1988**, *149*, 537-542.
77. NIST-JANAF Themochemical Tables, Fourth Edition. In *J. Phys. Chem. Ref. Data, Monograph 9* Gaithersburg, MA, 1998; pp 1-1951.
78. Sheng, C. *"Elementary, pressure dependent model for combustion of C1, C2 and nitrogen containing hydrocarbons : operation of a pilot scale incinerator and model comparison", Ph.D. Thesis* **2002**, *New Jersey Institute of Technology, NJ*.
79. Pitzer, K. S. *J. Chem. Phys.* **1937**, *59*, 276–279.
80. Pitzer, K. S.; Gwinn, W. D. *J. Chem. Phys.* **1942**, *10*, 428-442.
81. Benson, S. W. *Thermochemical Kinetics: methods for the estimation of thermochemical data and rate parameters*John Wiley & Sons, Inc., New York, NY, 1976.
82. Benson, S. W.; Buss, J. H. *J .Chem. Phys.* **1958**, *29*, 546-573.
83. Truhlar, D. G.; Garrett, B. C. *Annual Review of Physical Chemistry* **1984**, *35*, 159-189.
84. Carstensen, H.-H.; Dean, A. M. *Comprehensive Chemical Kinetics: Modeling of Chemical Reactions - Volume 42*; Elsevier: Bloomington, MN, USA, 2007; Vol. The Kinetics of Pressure-Dependent Reactions.
85. Rice, O. K.; Ramsperger, H. C. *J. Am. Chem. Soc.* **1927**, *49*, 1617-1629.
86. Kassel, L. S. *J. Phys. Chem.* **1928**, *32*, 225-242.
87. Troe, J.; Wagner, H. G. *Ber. Bunsenges. Phys. Chem.* **1967**, *71*, 937-979.
88. Golden, D. M.; Solly, R. K.; Benson, S. W. *J. Phys. Chem.* **1971**, 1333-1338.
89. Chang, A. Y.; Bozzelli, J. W.; Dean, A. M. *Zeitschrift fuer Physikalische Chemie* **2000**, *214*, 1533–1568.
90. Dean, A. M.; Bozzelli, J. W.; Ritter, E. R. *Combust. Sci. Technol.* **1991**, *80*, 63-85.
91. Mokrushin, V.; Bedanov, V.; Tsang, W.; Zachariah, M. R.; Knyazev, V. D.; McGivern, W. S. ChemRate National Institute of Standards and Technology, Gaithersburg, MD, 2011.
92. Buda, F.; Bounaceur, R.; Warth, V.; Glaude, P. A.; Fournet, R.; Battin-Leclerc, F. *Combust. Flame* **2005** *142*, 170-186.
93. Buda, F.; Heyberger, B.; Fournet, R.; Glaude, P. A.; Warth, V.; Battin-Leclerc, F. *Energy & Fuels* **2006**, *20*, 1450-1459.
94. Buda, F.; Heyberger, B.; Fournet, R.; Glaude, P.-A.; Warth, V.; Battin-Leclerc, F. *Energy Fuels* **2006**, *20*, 1450-1459.
95. Chen, J. S.; Litzinger, T. A.; Curran, H. J. *Combust. Sci. Technol.* **2001**, *172*, 71-80.
96. Ciajolo, A.; D'Anna, A. *Combust. Flame* **1998**, *112*, 617-622.
97. Curran, H. J.; Gaffuri, P.; Pitz, W. J.; Westbrook, C. K. *Combust. Flame* **2002**, *129*, 253-280.
98. He, X.; Walton, S. M.; Zigler, B. T.; Wooldridge, M. S.; Atreya, A. *Int. J. Chem. Kinet.* **2007**, *39*, 498-517.
99. Minetti, R.; Carlier, M.; Ribaucour, M.; Therssen, E.; Sochet, J. R. *P. Combust. Inst.* **1996**, *26*, 747-753.
100. Shen, H. P. S.; Vanderover, J.; Oehlschlaeger, M. A. *Combust. Flame* **2008**, *155*, 739-755.
101. Vanhove, G.; Minetti, R.; Touchard, S.; Fournet, R.; Glaude, P. A.; Battin-Leclerc, F. *Combust. Flame* **2006**, *145*, 272–281.

102. Hudzik, J. M.; Bozzelli, J. W. *J. Phys. Chem. A* **2012**, *116*, 5707-5722.
103. Chang, A. Y.; Dean, A. M.; Bozzelli, J. W. *Z. Phys. Chem.* **2000**, *214*, 1533-1568.
104. Asatryan, R.; Bozzelli, J. W.; Simmie, J. *J. Phys. Chem. A* **2008**, *112*, 3172-3185.
105. Hehre, W.; Radom, L.; Schleyer, P. R.; Pople, J. A. *Ab Initio Molecular Orbital Theory* John Wiley & Sons: New York, NY, 1986.
106. Snitsiriwat, S.; Bozzelli, J. W. *J. Phys. Chem. A* **2012**, *Accepted*.
107. Pedley, J. B. *Thermochemical Data and Structures of Organic Compounds*; CRC Press: Leeds, UK, 1994.
108. Miyoshi, A. *J. Phys. Chem. A* **2011**, *115*, 3301-3325.
109. Villano, S. M.; Cartensen, H. H.; Dean, A. M.; Huynh, L. K. *J. Phys. Chem. A* **2011**, *115*, 13425-13442.
110. Sharma, S.; Raman, S.; Green, W. H. *J. Phys. Chem. A* **2010**, *114*, 5689-5701.
111. Chen , C. C.; Bozzelli, J. W. *J. Phys. Chem. A* **2003**, *107*, 4531-4546.
112. Chenoweth, K.; van Duin, A. C. T.; Dasgupta, S.; Goddard III, W. A. *J. Phys. Chem. A* **2009**, *113*, 1740-1746.
113. Davidson, D. F.; Horning, D. C.; Oehlschlaeger, M. A.; Hanson, R. K. "The Decomposition Products of JP-10"; Proceedings of the 37th AIAA/ASME/SAE/ASEE Joint Propulsion Conference and Exhibit, 2001, Salt Lake City, UT.
114. Li, S. C.; Varatharajan, B.; Williams, F. A. *AIAA* **2001**, *39*, 2351-2356.
115. Nageswara Rao, P.; Kunzru, D. *J. Anal. Applied Pyrolysis* **2006**, *76*, 154-160.
116. Nakra, S.; Green, R. J.; Anderson, S. L. *Combustion and Flame* **2006**, *144*, 662-674.
117. Park, S. H.; Kwon, C. H.; Kim, J.; Chun, B. H.; Kang, J. W.; Han, J. S.; Jeong, B. H.; Kim, S. H. *Ind. Eng. Chem. Res.* **2010**, *49*, 8319-8324.
118. Striebich, R. C.; Lawrence, J. J. *Anal. Appl. Pyrolysis* **2003**, *70*, 339-352.
119. Xing, Y.; Fang, W.; Xie, W.; Guo, Y.; Lin, R. *Ind. Eng. Chem. Res.* **2008**, *47*, 10034-10040.
120. Xing, Y.; Li, D.; Xie, W.; Fang, W.; Guo, Y.; Lin, R. *Fuel* **2010**, *89*, 1422-1428.
121. Davidson, D. F.; Horning, D. C.; Herbon, J. T.; Hanson, R. K. *Proceedings of the Combustion Institute* **2000**, *28*, 1687-1692.
122. He, K. Y.; Androulakis, I. P.; Ierapetritou, M. G. *Energy Fuels* **2010**, *24*, 309-317.
123. Herbinet, O.; Sirjean, B.; Bounaceur, R.; Fournet, R.; Battin-Leclerc, F.; Scacchi, G.; Marquaire, P. M. *J Phys Chem A* **2006**, *110*, 11298–11314.
124. Hudzik, J. M.; Asatryan, R.; Bozzelli, J. W. **2010**, *114*, 9545-9553.
125. Hudzik, J. M.; Bozzelli, J. W. *J. Phys. Chem. A* **2012**, *Submitted*.
126. Auzmendi-Murua, I.; Bozzelli, J. W. *J. Phys. Chem. A* **2012**, *116*, 7550-7563.
127. Simmie, J. M.; Black, G.; Curran, H. J.; Hinde, J. P. *J Phys Chem A* **2008**, *112*, 5010-5016.
128. Sirjean, B.; Glaude, P. A.; Ruiz-Lopez, M. F.; Fournet, R. *J. Phys. Chem. A* **2006**, *110*, 12693-12704.
129. Reyniers, M. F.; Sabbe, M. K.; Van Speybroeck, V.; Waroquier, M.; Marin, G. B. *Chem.Phys.Chem.* **2008**, *9*, 124-140.
130. Dean, A. M. *J. Phys. Chem. A* **1985**, *89*, 4600-4608.
131. Jones, J. H.; Fenske, M. R. *Ind. Eng. Chem.* **1959**, *51*, 262-266.
132. Ciajolo, A.; D'Anna, A. *Combust. Flame* **1998**, *112*, 617-622.

133. Dagaut, P.; Reuillon, M.; Cathonnet, M. *Combust. Flame* **1995**, *101*, 132-140.
134. Lee, C.; Vranckx, S.; Heufer, K. A.; Khomik, S.; Uygun, Y.; Olivier, H.; Fernandes, R. X. *Zeitschrift für Physikalische Chemie* **2012**, *226*, 1-28.
135. Zhou, C. "Rate Constants for Hydrogen-Abstraction by HO2 from n-Butanol"; 7th Intern. Conference on Chemical Kinetics, 2011, MIT, Camebridge, MA, USA.
136. Welz, O.; Zádor, J.; Savee, J. D.; Ng, M. Y.; Meloni, G.; Fernandes, R. X.; Sheps, L.; Simmons, B. A.; Lee, T. S.; Osborn, D. L.et al. *Phys. Chem. Chem. Phys.* **2012**, *14*, 3112-3127.
137. Lemaire, O.; Ribaucour, M.; Carlier, M. R.; Minetti, R. *Combust. Flame* **2001**, *127*, 1971-1980.
138. Buda, F.; Heyberger, B.; Fournet, R.; Glaude, P. A.; Warth, V.; Battin-Leclerc, F. *Energy & Fuels* **2006**, *20*, 1450-1459.
139. Law, M. E.; Westmoreland, P. R.; Cool, T. A.; Wang, J.; Hansen, N.; Taatjes, C. A.; Kasper, T. *Proc. Combust. Inst.* **2007**, *31*, 565-573.
140. Pitz, W. J.; Naik, C. V.; Mhaolduin, T. N.; Westbrook, C. K.; Curran, H. J.; Orme, J. P.; Simmie, J. M. *Proc. Combust. Inst.* **2007**, *31*, 267-275.
141. Zhang, H. R.; Huynh, L. K.; Kungwan, N.; Yang, Z.; Zhang, S. *J. Phys. Chem. A* **2007**, *111*, 4102-4115.
142. Mittal, G.; Sung, C. J. *Combust. Flame* **2009**, *156*, 1852-1855.
143. Vasu, S. S.; Davidson, D. F.; Hong, Z.; Hanson, R. K. *Energy Fuels* **2009**, *23*, 175-185.
144. Ristori, A.; Dagaut, P.; Bakali, A. E.; Cathonnet, M. *Combust. Sci. Technol.* **2001**, *165*, 197-228.
145. Chae, K.; Violi, A. *J. Org. Chem.* **2007**, *72*, 3179-3185.
146. Vanderover, J.; Oehlschlaeger, M. A. *Int. J. Chem. Kinet.* **2009**, *41*, 82-91.
147. Sirjean, B.; Glaude, P. A.; Ruiz-Lopez, M. F.; Fournet, R. *J. Phys. Chem. A* **2009**, *113*, 6924-6935.
148. Simmie, J. M. *J. Phys. Chem. A* **2012**, *116*, 4528-4538.
149. Battin-Leclerc, F. *Progress in Energy and Combustion Science* **2008**, *34*, 440-498.
150. Ruzsinszky, A.; C.V., A.; Csonka, G. I. *J. Phys. Chem. A* **2003**, *107*, 736-744.
151. Bozzelli, J. W.; Rajasekaran, I.; Hur, J. *Phys. Org. Chem.* **2006**, *19*, 93-103.
152. Agapito, F.; Costa Cabral, B. J.; Martinho Simoes, J. A. *Journal of Molecular Structure: THEOCHEM* **2005**, *719*, 109-114.
153. Bach, R. D.; Dmitrenko, O. *J. Am. Chem. Soc.* **2006**, *128*, 4598-4611.
154. Muller, C.; Michel, V.; Scacchi, G.; Come, G. M. *J. Chim. Phys. Phys.- Chim. Biol.* **1995**, *92*, 1154-1178.
155. Raman, S.; Green, W. H. *Phys. Chem. Chem. Phys.* **2003**, *5*, 3402-3417
156. Ritter, E. R. *J. Chem. of. Comput. Sci.* **1991**, *31*, 400-408.
157. Asatryan, R.; Bozzelli, J. W.; Simmie, J. M. *International Journal of Chemical Kinetics* **2007**, *39*, 378-398.
158. Hehre, W. J.; Radom, L.; Schleyer, P. V.; Pople, J. *Ab Initio Molecular Orbital Theory*NY, 1986.
159. Curtiss, L. A.; Raghavachari, K.; P.C., R.; Pople, J. A. *J. Chem. Phys.* **1997**, *106*, 1063-1079.
160. Luo, Y. R. *Handbook of Bond Dissociation Energies in Organic Compounds*Boca Raton, FL, 2003.

161. Douslin, D. R.; Scott, D. W.; Good, W. D.; Osborn, A. G. *Ft. Belvoir Defense Technical Information Center, VA* **1976**, *76*, 97-116.
162. Pell, A. S.; Pilcher, G. *Trans. Faraday Soc.* **1965**, *61*, 71-77.
163. Zhu, L.; Bozzelli, J. W.; Kardos, L. M. *J. Phys. Chem. A* **2007**, *111*, 6361-6377.
164. Wiberg, K. B.; Waldron, R. F. *J. Am. Chem. Soc.* **1991**, *113*, 7697-7705.
165. Dmitriev, Y. G.; Kotovich, K. Z.; Kochubei, V. V.; Mineravina, L. O. *Vestn. L'vov. Politekhn. Inst.* **1988**, *221*, 34-35.
166. Schröder, D.; Goldbergb, N.; Zummacka, W.; Schwarza, H.; Poutsmac, J.; Squiresc, R. R. *Int. J. Mass Spectrom. Ion Processes* **1997**, *165–166*, 71–82.
167. Tsang, W. *Heats of Formation of Organic Free Radicals by Kinetic Methods in Energetics of Organic Free Radicals*; Blackie Academic and Professional: London, UK, 1996.
168. Chen, C. C.; Bozzelli, J. W. *J. Phys. Chem A* **2003**, *107*, 4531–4546.
169. Baulch, D. L.; Bowman, C. T.; Cobos, C. J.; Cox, R. A.; Just, T.; Kerr, J. A.; Pilling, M. J.; Stocker, D.; Troe, J.; Tsang, W.et al. *J. Phys. Chem. Ref. Data* **2005**, *24*, 757-1397.
170. Herbinet, O.; Sirjean, B.; Bounaceur, R.; Fournet, R.; Battin-Leclerc, F.; Scacchi, G.; Marquaire, P. M. *J. Phys. Chem. A* **2006**, *110*, 11298-11314.
171. Reyniers, M. F., Sabbe, M.K., Van Speybroeck, V., Waroquier, M., Marin, G.B., . *Chem.Phys.Chem.* **2008**, *9*, 124-140.
172. Kee, R. J.; Rupley, F. M.; Miller, J. A.; Coltrin, M. E.; Grcar, J. F.; Meeks, E.; Moffat, H. K.; Lutz, A. E.; Dixon-Lewis, G.; Smooke, M. D.et al. CHEMKIN; Sandia National Laboratories: Livermore, CA, 2001.
173. Sheng, C.; Bozzelli, J. W.; Chang, A. Y.; Dean, A. M. *J. Phys. Chem. A.* **2002**, *106*, 7276-7293.
174. Environmental Protection Agency, E.; http://www.epa.gov/air/mercuryrule/, April, 2010.
175. Ogg, R. A.; Martin, H. C.; Leighton, P. A. *J. Am. Chem. Soc.* **1936**, *58*, 1922-1924.
176. P'yankov, V. A. *Zhur. Obschev. Khim. (J. Gen. Chem.)* **1949**, *19*, 224-229.
177. Menke, R.; Wallis, G. *Amer. Ind. Hyg. Assoc. J.* **1980**, *41*, 120-124
178. Hall, B.; Lindqvist, O.; Ljungstrom, E. *Environ. Sci. Technol.* **1990**, *24*, 108-111.
179. Fontijn, A.; Hranisavljevic, R. J. *J. Phys. Chem. A* **1997**, *101*, 2323-2326.
180. Schroeder, W. H.; Niki, H.; Yarwood, G. *Water, Air, and Soil Pollution* **1991**, *56*, 653-666.
181. Kramlich, J. C.; Sliger, N.; Marinov, N. M. *Fuel Process. Technol.* **2000**, *65-66*, 423-438.
182. Edwards, J. R.; Srivastava, R. K.; Kilgroe, J. D. *J. Air Waste Manage. Assoc.* **2001**, *51*, 869-877.
183. Ariya, P. A.; Khalizov, A.; Gidas, A. *J. Phys. Chem. A* **2002**, *106*, 7310-7320.
184. Raofie, F.; Snider, G.; Ariya, P. A. *Can. J. Chem.* **2008**, *86*, 811-820.
185. Chang, S. G.; Miller, C.; Liu, S. H.; Yan, N. Q.; Liu, Z. R.; Qu, Z.; Wang, P. H. *Environ. Sci. Technol.* **2007**, *41*, 1405-1412.
186. Chang, S. G.; Miller, C.; Yan, N. Q.; Liu, S. H. *Ind. Eng. Chem. Res.* **2005**, *44*, 5567-5574.
187. Yan, N.; Qu, Z.; Liu, P.; Chi, Y.; Jia, J. *Environ. Sci. Technol.* **2009**, *43*, 8610-8615.
188. Qu, Z.; Yan, N.; Liu, P.; Jia, J.; Yang, S. *J. Hazard. Mater.* **2010**, *183*, 132-137.

189. Ariya, P. A.; Khalizov, A. F.; Virwanathan, B.; Larregaray, P. *J. Phys. Chem. A* **2003**, *33*, 6360-6365.
190. Goodsite, M. E.; Plane, J. M. C.; Skov, H. *Environ. Sci. Technol.* **2004**, *38*, 1772-1776.
191. Peterson, K. A.; Shepler, B. C.; Balabanov, N. B. *J. Phys. Chem. A* **2005**, *109*, 10363-10372.
192. Wilcox, J. *J. Phys. Chem. A* **2009**, *113*, 6633-6639.
193. Stevens, W. J.; Krauss, M.; Basch, H.; Jasien, P. G. *Can. J. Chem.* **1992**, *70*, 612-630
194. Wilcox, J.; Okano, T. *Energy Fuels* **2011**, *25*, 1348-1356.
195. Liu, J.; Yuan, J.; Qu, W.; Wang, S.; Qiu, J.; Zheng, C. *Energy Fuels* **2010**, *24*, 117-122.
196. Fry, A. R.; Cauch, B.; Lighty, J. S.; Senior, C. L.; Silcox, G. D. *P. Combust. Inst.* **2007**, *31*, 2855-2861.
197. Hutson, N. D. *Water, Air, Soil Pollut.* **2008**, *8*, 323-331.
198. Niksa, S.; Fujiwara, N.; Helble, J. J. *Environ. Sci. Technol.* **2001**, *35*, 3701-3706
199. Qiu, J.; Helble, J. J.; Sterling, R. O. "Development of an Improved Model for Determining the Effects of SO_2 on Homogeneous Mercury Oxidation"; Proceedings of the 28th International Technical Conference on Coal Utilization & Fuel Systems, 2003, Clearwater, FL.
200. Schofield, K. *Environ. Sci. Technol.* **2008**, *42*, 9014-9030.
201. Senior, C. L.; Helble, J. J.; Mamani-Paco, R.; Sarofim, A. F.; Zeng, T. *Fuel Process. Technol.* **2000**, *63*, 197-213
202. Widmer, N. C. *Combust. Sci. Technol.* **1998**, *134*, 315-326.
203. Widmer, N. C.; West, J.; Cole, J. A. Thermochemical Study of Mercury Oxidation in Utility Boiler Flue Gases. In *Proceedings of the Air & Waste Management Association 93rd Annual Conference and Exhibition* Salt Lake City, UT, 2000.
204. Xu, M.; Qiao, Y.; Zheng, C.; Li, L.; Liu, J. *Combust. Flame* **2003**, *132*, 208–218.
205. Peterson, K. A.; Shepler, B. C. *J. Phys. Chem. A* **2003**, *107*, 1783-1787.
206. Widman, R. P.; DeGraff, B. A. *J. Phys. Chem. A* **1973**, *77*, 1325-1328.
207. Baulch, D. L.; Duxbury, J.; Grant, S. J.; Montague, D. C. *J. Phys. Chem. Ref. Data* **1982**, *10*, 1-721.
208. Aylett, B. J. *Comprehensive Inorganic Chemistry*Pergamon Press, Elmsford, NY, 1973.
209. Bell, S.; McKenzie, R. D.; Coon, J. B. *J. Mol. Spectrosc.* **1966**, *20*, 217-225.
210. Adams, D. M.; Hills, D. J. J. *Journal of the Chemical Society, Dalton Transactions* **1978**, 776-782.
211. Bermejo, D.; Jimenez, J. J.; Martinez, R. Z. J. *Mol. Spectrosc.* **2002**, *212*, 186-193
212. Stroemberg, D.; Gropen, O.; Wahlgren, U. *Chem. Phys.* **1989**, *133*, 207-219.
213. Kaupp, M.; Vonschnering, H. G. *Inorg. Chem.* **1994**, *33*, 2555-2564.
214. Givan, A.; Loewenschuss, A. *J. Chem. Phys.* **1976**, *64*, 1967-1972.
215. Clark, R. J. H.; Rippon, D. M. *J. Chem. Soc., Faraday Trans. 2: Molecular and Chemical Physics* **1973**, *69*, 1496-1501.
216. Spiridonov, V. P.; Gershikov, A. G.; Butayev, B. S. *J. Mol. Struct.* **1979**, *52*, 53-62.
217. Martin, F.; Bacis, R.; Churassy, S.; Verges, J. *J. Mol. Spectrosc.* **1986**, *116*, 71-100.

218. Deyanov, R. Z.; Petrov, K. P.; Ugarov, V. V.; Shchedrin, B. M.; Rambidi, N. G. *Zh. Strukt. Khim. (J. Struct. Chem.)* **1985**, *26*, 698-703.
219. Huber, K. P.; Herzberg, G. *In Molecular Spectra and Molecular Structure IV. Constants of Diatomic Molecules*Van Nostrand Reinhold Company, New York, NY, 1979.
220. Tellinghuisen, J.; Ashmore, J. G. *Appl. Phys. Lett.* **1982**, *40*, 867-869.
221. Sponer, H.; Teller, E. *Electronic spectra of polyatomic molecules*American Physical Society, Ridge, NY, 1941.
222. Malt'sev, A. A.; Selivanov, G. K.; Yampolsky, V. I.; Zavalishin, N. I. *Nature Physical Science* **1971**, *231*, 157-158.
223. Braune, H.; Engelbrecht, G. *Z. Phys. Chem. Abt. B* **1932**, *19*, 303-315.
224. Focsa, C.; Li, H.; Bernath, P. F. *Journal of Molecular Spectroscopy* **2000**, *200*, 104–119.
225. Beattie, I. R.; Horder, J. R. *J. Chem. Soc. A* **1970**, *14*, 2433-2435.
226. *Key World Energy STATISTICS* International Energy Agency, Paris, France, 2012.
227. Streets, D. G.; Zhang, Q.; Wu, Y. *Envrion. Sci. Technol.* **2009**, *43*, 2983-2988.
228. Streets, D. G.; Devane, M. K.; Bond, T. C.; Sunderland, E. M.; Jacob, D. J. *Environ. Sci. Technol.* **2011**, *45*, 10485-10491.
229. Environmental Protection Agency, E.; http://www.epa.gov/hg/, February, 2013.
230. *Large-Scale Mercury Control Testing for Lignite-Fired Utilities-Oxidation Systems for Wet FGD* Benson, S. A.; Holmes, M. J.; McCollar, D. P.; Mackenzie, J. M.; Crocker, C. R.; Kong, L.; Galbreath, K.; Dombrowski, K.; Richardson, C., Eds. Grand Forks, ND, 2007.
231. Environmental Solutions, A.; http://www.adaes.com/, January, 2013.
232. Helfritch, D. J.; Feldman, P. L. "Coal Combustion Mercury Control by Means of Corona Discharge "; IEEE International Conference on Plasma Science, 1999, Baltimore, MD.
233. Helfritch, D.; Feldman, P. L.; Pass, D. J. "A Circulating Fluid Bed Fine Particulate and Mercury Control Concept"; EPRI-DOE-EPA Combined Utility Air Pollutant Control Symposium, 1997, Washington DC.
234. Clean Energy Technology, P.; http://powerspan.com/, January, 2013.
235. Hall, B.; Lindqvist, O.; Schager, P. *Water, Air, Soil Pollut.* **1991**, *56*, 3-14.
236. Widmer, N. C.; J.A., C.; J., W. "Thermochemical Study of Mercury Oxidation in Utility Boiler Flue Gases"; Proceedings of the Air & Waste Management Association 93rd Annual Conference and Exhibition, 2000, Salt Lake City, UT.
237. Sliger, R. N.; Kramlich, J. C.; Marinov, N. M. *Fuel Process. Technol.* **2000**, *65-66*, 423-438.
238. Sliger, R. N.; Kramlich, J. C.; Marinov, N. M. "Development of an Elementary Homogeneous Mercury Oxidation Mechanism"; Proceedings of the Air & Waste Management Association 93rd Annual Conference and Exhibition, 2000, Salt Lake City, UT.
239. Edwards, J. R.; Kilgroe, J. D.; Srivastava, R. K. *J. Air Waste Manage. Assoc.* **2001**, *51*, 869-877.
240. Krishnakumar, B.; Helble, J. J. *Environ. Sci. Technol.* **2007**, *41*, 7870-7875.

241. Fry, A.; Lighty, J.; Senior, C.; Silcox, G. *Experimental and Kinetic Modeling Investigation of Gas-Phase Mercury Oxidation reactions with Chlorine* **2008**, *Ph.D. Dissertation*, University of Utah, UT.
242. Van Otten, B.; Buitrago, P. A.; Senior, C. L.; Silcox, G. D. *Energy Fuels* **2011**, *25*, 3530-3536.
243. Ghorishi, S. B. "Fundamentals of Mercury Speciation and Control in Coal-Fired Boilers," 1998.
244. Qiu, J.; Helble, J. J.; Sterling, R. O. "Development of an Improved Model for Determining the Effects of SO2 on Homogeneous Mercury Oxidation"; Proceedings of the 28th International Technical Conference on Coal Utilization & Fuel Systems, March 10-13, 2003, Clearwater, FL.
245. Liu, J.; Qu, W.; Yuan, J.; Wang, S.; Qiu, J.; Zheng, C. *Energy Fuels* **2010**, *24*, 117-122.
246. Donohoue, D. L.; Bauer, D.; Hynes, A. J. *J. Phys. Chem. A* **2005**, *109*, 7732-7741.
247. Donohoue, D. L.; Bauer, D.; Cossairt, B.; Hynes, A. J. *J. Phys. Chem. A* **2006**, *110*, 6623-6632.
248. Peterson, K. A.; Figgen, D.; Goll, E.; Stoll, H.; Dolg, M. *J. Chem. Phys.* **2003**, *119*, 11113-11127.
249. Peterson, K. A.; Puzzarini, C. *Theor. Chem. Acc.* **2005**, *114*, 283-296.
250. Curtiss, L. A.; Raghavachari, K.; Redfern, P. C.; Rassolov, V.; Pople, J. A. *J. Chem. Phys.* **1998**, *109*, 7764-7777.
251. Montgomery, J. A., Jr.; Frisch, M. J.; Ochterski, J. W.; Petersson, G. A. *J. Chem. Phys.* **1999**, *110*, 2822-2827.
252. Ochterski, J. W.; Petersson, G. A.; Montgomery Jr., J. A. *J. Chem. Phys.* **1996**, *104*, 2598-25619.
253. Kaupp, M.; Vonschnering, H. G. *Inorg. Chem.* **1994**, *33*, 4179-4185.
254. Ruscic, B.; Feller, D.; Dixon, D. A.; Peterson, K. A.; Harding, L. B.; Asher, R. L.; Wagner, A. F. *J. Phys. Chem A* **2001**, *105*, 1-4.
255. Cox, J. D.; Wagman, D. D.; Medvedev, V. A. *CODATA Key Values for Thermodynamics*; Hemisphere Publishing Corp.: New York, NY, 1984; Vol. 1.
256. Wilmouth, D. M.; Hanisco, T. F.; Donahue, N. M.; Anderson, J. G. *J. Phys. Chem. A* **1999**, *103*, 8935-8945.
257. Wagman, D. D.; Evans, W. H.; Parker, V. B.; Schumm, R. H.; Halow, I.; Bailey, S. M.; Churney, K. L.; Nutall, R. L. *J. Phys. Chem. Ref. Data* **1982**, *11*, 1-392.
258. Dibble, T. S.; Zelie, M. J.; Mao, H. *Atmos. Chem. Phys.* **2012**, *12*, 10271-10279.
259. Szori, M.; Csizmadia, I. G.; Fittschen, C.; Viskolcz, B. *J. Phys. Chem. A* **2009**, *113*, 9981-9987.
260. Khalizov, A. F.; Ariya, P. A. *Chem. Phys. Lett.* **2001**, *350*, 173-180.
261. Boyd, R. J.; Gupta, A.; Langrer, R. F.; Lownie, S. P.; Pincock, J. A. *Can. J. Chem.* **1980**, *58*, 331-338.
262. Li, Z. *Chem. Phys. Lett.* **1997**, *269*, 128-137.
263. Chang, A. Y.; Dean, A. M.; Bozzelli, J. W. *Int. J. Chem. Kint.* **1997**, *29*, 161-170.
264. IUPAC - http://goldbook.iupac.org (2006-) created by M. Nic, J. J., and B. Kosata; updates compiled by A.D. Jenkins.
265. Tsang, W.; Babushok, V. *Bromocarbon Mechanism NIST (National Institute of Standards and Technology)* **2001**.

266. Ho, W.; Barat, R. B.; Bozzelli, J. W. *Combust. Flame* **1992**, *88*, 265-295.
267. Ho, W.; Bozzelli, J. W. *Twenty-Fourth Symposium on Combustion, Combustion Inst.* **1992**, *24*, 743-748
268. Ho, W.; Yu, C.; Bozzelli, J. W. *Combust. Sci. Technol.* **1992**, *85*, 23-63.
269. Asatryan, R.; Bozzelli, J. W.; Simmie, J. M. *Int. J. Chem. Kinet.* **2007**, *39*, 378-398.
270. Bozzelli, J. W.; Dean, A. M. Gas-Phase combustion Chemistry, . In *Combustion Chemistry of Nitrogen*; Springer, N., Ed. W.C. Gardiner, 1999; Vol. Chapter 2.
271. Hughes, K. J.; Tomlin, A. S.; Dupont, V. A.; Pourkashanian, M. *Faraday Discuss.* **2001**, *119*, 337-352.
272. Laudal, D. L.; Brown, T. D.; Nott, B. R. *Fuel Process. Technol.* **2000**, *65-66*, 157-165.
273. Niksa, S.; Helble, J. J.; Fujiwara, N. *Environ. Sci. Technol.* **2001**, *35*, 3701-3706.
274. Byun, Y.; Cho, M.; Namkung, W.; Lee, K.; Koh, D. J.; Shin, D. N. *Environ. Sci. Technol.* **2010** *44*, 1624-1629.
275. Lighty, J. S.; Silcox, G.; Fry, A. "Fundamentals of Mercury Oxidation in Flue Gas," 2005.
276. Smith, C.; Krishnakumar, B.; Helble, J. J. *Energy Fuels* **2011**, *25*, 4367-4376.
277. Simmie, J. M.; Black, G.; Curran, H. J.; Hinde, J. P. *J. Phys. Chem. A* **2008**, *112*, 5010-5016.
278. Sheng, C.; Bozzelli, J. W. *J. Phys. Chem. A* **2002**, *106*, 1113-1121.
279. Holmes, J. L.; Lossing, F. P. *J. Am. Chem. Soc.* **1982**, *104*, 2648-2649.
280. Pittam, D. A.; Pilcher, G. *J. Chem. Soc. Faraday Trans. 1* **1972**, *68*, 2224-2229.
281. Good, W. D. *J. Chem. Thermodyn.* **1970**, *2*, 237-244.
282. Chen, C. J.; Bozzelli, J. W. *J. Phys. Chem. A* **2000**, *104*, 9715-9732.
283. Good, W. D. *J. Chem. Eng. Data* **1969**, *14*, 231-235.
284. Prosen, E. J.; Rossini, F. D. *J. Res. Nat. Bur. Stand.* **1945**, 263-267.
285. Liu, C. X.; Li, Z. R.; Zhou, C. W.; Li, X. Y. *J. Comput. Chem.* **2009**, *30*, 1007-1015.
286. Pittam, D. A.; Pilcher, G. *J. Chem. Soc. Faraday Trans. 1* **1972**, *68*, 2224-2229.
287. Yamada, T.; Bozzelli, J. W. *Int. J. Chem. Kinet.* **2000**, *32*, 435-452.
288. Prosen, E. J.; Rossini, F. D. *J. Res. NBS* **1945**, 263-267.
289. Lee, J.; Chen, C. J.; Bozzelli, J. W. *J. Phys. Chem. A* **2002**, *106*, 7155-7170.
290. Steele, W. V.; Chirico, R. D.; Cowell, A. B.; Knipmeyer, S. E.; Nguyen, A. *J. Chem. Eng. Data* **1997**, *42*, 1052-1066.
291. Chen, C. J.; Bozzelli, J. W. *J. Phys. Chem. A* **1999**, *103*, 9731-9769.
292. Connett, J. E. *J. Chem. Thermodyn.* **1975**, *7*, 1159-1162.
293. McCullough, J. P.; Pennington, R. E.; Smith, J. C.; Hossenlopp, I. A.; Waddington, G. *J. Am. Chem. Soc.* **1959**, *81*, 5880-5883.
294. Mehrpooya, M.; Vatani, A.; Gharagheizi, F. *Int. J. Mol. Sci* . **2007**, *8*, 407-432.
295. Podlogar, B. L.; Raber, D. J. *J. Org. Chem* **1989**, *54*, 5032-5035.
296. *Heats of Formation of Organic Free Radicals by Kinetic Methods in Energetics of Organic Free Radicals*; Tsang, W., Ed.; Martinho Simoes, J.A.; Greenberg, A.; Liebman, J.F., eds. Blackie Academic and Professional: London, 1996, 1996, pp 22-58.
297. Pittam, D. A.; Pilcher, G. *J. Chem. Soc. Faraday Trans. 1* **1972**, *68*, 2224-2229.
298. Fletcher, R. A.; Pilcher, G. *Trans. Faraday Soc.* **1971**, *67*, 3191-3201.

299. Ferguson, K. C.; Okafo, E. N.; Whittle, E. *J. Chem. Soc. Faraday Trans. 1* **1973**, *69*, 295-301.
300. Kudchadker, S. A.; Kudchadker, A. P. *J. Phys. Chem. Ref. Data* **1979**, *8*, 519-526.
301. Knobel, Y. K.; Miroshnichenko, E. A.; Lebedev, Y. A. *Bull. Acad. Sci. USSR, Div. Chem. Sci.* **1971**, *20*, 425-428.
302. *Energetics of Organometallic Species*; Martinho Simões, J. A., Ed.; Proceedings of the NATO Advanced Study Institute: Curia, Portugal, 1991.
303. Lee, J. H.; Timmons, R. B.; Stief, L. J. *J. Chem. Phys.* **1976**, *64*, 300-305.
304. Hassanzadeh, P.; Irikura, K. K. *J. Phys. Chem. A* **1997**, *101*, 1580-1587.
305. Denis, P. A. *Chemical Physics Letters* **2005**, *402*, 289-293.
306. Denis, P. A.; Ventura, O. N. *Chem. Phys. Lett.* **2001**, *344*.